ANNUAL·REPORT·93

Safety Technology Institute

JOINT RESEARCH CENTRE

EUROPEAN COMMISSION

EUR 15669 EN

ANNUAL·REPORT·93

Safety Technology Institute

JOINT RESEARCH CENTRE
EUROPEAN COMMISSION

EUR 15669 EN

Published by the
EUROPEAN COMMISSION

Directorate-General XIII
Telecommunications, Information Market and Exploitation of Research

L-2920 Luxembourg

Cataloguing data can be found at the end of this publication.

Luxembourg: Office for Official Publications of the European Communities, 1994

Printed in Italy

CONTENTS

EXECUTIVE SUMMARY

NUCLEAR ACTIVITIES

Reactor safety

The research programme on Reactor Safety was successfully continued during the year 1993. The STI activity was completely focused on the study of severe accidents in LWRs. Even if these accidents are highly unlikely, it is very important to improve the knowledge of the complex physical phenomena which could occur in a number of accident scenarios and the methodologies for the evaluation of possible consequences.

Two themes particularly important on which the research is concentrated are the evaluation of the Source Term, that is the quantity and quality of radioactive products which could be released to the environment and the study of the interaction of molten corium with the coolant or the reactor structures during the core melt progression.

In the area of Source Term the STI participation in the international programme Phebus-FP, under way at Cadarache (F), saw a crucial phase because the first test FPT-0 with fresh fuel was executed in December 1993, after more than 5 years of preparatory work. Immediately after the second part of the CEC-CEA agreement (Block B of the Convention) for the execution of 5 in-pile tests with irradiated fuel was signed. In 1993 the STI contribution in this programme concerned the follow up of the project activities (by the STI team detached to Cadarache), the participation in test precalculations and the coordination of partners contributions as well as the work for updating the test matrix, which was substantially modified with the approval of the partners (by the Ispra team). The results of the FPT-0 test will have to be analysed in depth. However, we know that the test was successfully completed, that the melting of part of the fuel is very likely and that the fission product release was larger than anticipated.

In close relation with the Phebus-FP programme is the ongoing development and validation of the informatic system ESTER which has been designed as an advanced mechanistic code package for Source Term evaluation and will be available to the Member States for Phebus-FP and severe accident sequence calculations. ESTER will include in a modern informatic structure a number of modules already developed and validated at national level or still under development. A number of Shared Cost Action (SCA) contracts, which are now almost completed, have given essential support to this project and made the cooperation with the European Partners easier. In 1993 a number of new modules have been included in the system and in 1994 a new version will be released to the partners. Maintenance, validation and improvement of the code package are assured by the STI team.

As in the past, the work on model development and validation brought the STI to launch a number of international benchmark calculations related to ongoing activities or to be involved in ISPs (International Standard Problems) organised by the OECD/CSNI. These exercises are very useful to better understand code/model weaknesses and to reach common views among the experts.

In order to investigate aspects of the aerosol physics that due to the scale will not be covered by the Phebus-FP project, the STI decided at the end of 1991 to start the design and construction of a large-scale experimental facility called STORM for the investigation of aerosol deposition and resuspension in primary system components. This project is jointly sponsored by the JRC and ENEL (I) and is open to the cooperation of other institutions.

In 1993, in addition to the intensive work for component and instrumentation procurement, thermohydraulic and aerosol calculations have been started. Two international meetings have been organised at Ispra (in April and December) to present the project and to launch benchmark calculations. The construction of the STORM plant will be terminated in 1994 and scoping tests will then be performed.

Concerning the second theme of research, which is the study of the interaction of molten corium with the coolant and reactor structures during a severe accident, the FARO experimental programme on in-vessel melt quenching was actively continued. After the solution of many technological problems, a successful test (Base Case Test) was performed in December, with the release of a large amount of

molten material (160 kg), considerable increase of the pressure in the test section and consequently venting of steam into the condenser due to the opening of safety valves. From the preliminary analysis no steam explosion took place and a large amount of quenched material was found on the debris catcher.

The debate and the interest on these tests and those which could be performed in future was very large during 1993. A number of discussions on this subject took place with the European and US partners.

Considerable effort has been made to complete a detailed documentation of the second melt quenching test and to analyse the results. Precalculations and post-test analysis have been performed using TEXAS III, while the 2D IFCI code (USNRC) is being implemented. A new code called COMETA, coupling thermalhydraulics and melt-water interaction, which allows to describe the overall behaviour of the FARO plant is being developed at the STI and has already been successfully applied for test preparation and analysis. Some of the European Partners participated in the test analysis with their codes.

The small-scale KROTOS test programme for FCI investigation, was also successfully continued. The tests with Aluminium Oxide with and without trigger have been completed and documented. New tests with Uranium Oxide to which USNRC is contributing started in 1993 and will be completed in 1994.

The STI team which has been charged to complete the documentation of the LOBI tests has almost finished its work and started to work in support of the DG XI safety activities aiming at the harmonisation of safety rules in the EU. The main contribution of this group is in the thermalhydraulics area.

Safeguards and waste

Safeguards scientific and technical activities performed in the frame of the programme R&D for Safeguards and Fissile Material Management illustrated below are tightly coordinated with and complementary to the Support to the Commission activities described in section 2. The main Safeguards activities performed at the Safety Technology Institute (STI) of the JRC Ispra are executed within the Safeguards PERformance LAboratory (PERLA) and in the TAME facility of the Institute. PERLA deals in particular with Non-Destructive Analysis (NDA) methods for the determination of U and Pu isotopes in bulk and itemised form by active and passive neutron measurements, gamma spectrometry, calorimetry, used either individually or in integrated systems.

In 1993 activities on NDA-PERLA were very much focused on improving solid plutonium bulk material monitoring, employing neutron or combined neutron-gamma-calorimetry techniques and testing a new infrared methodology. PERLA laboratory has continued to support ESARDA by hosting an International Workshop on Passive Neutron Counting. In 1993 the strong effort, initiated in 1992, was continued to finalise and start up the new facility TAME, which is now ready to be used for tank volume measurements for Safeguards applications.

A second User Group meeting was held in October 1993 for TAME, resulting in strong international support to the laboratory by laboratories, plant operators and Safeguards Authorities. The support to the Commission activities by the STI are subdivided in two parts:

- Support to ESD,
- Support to IAEA (through DG I).

The Safeguards Support Programme aims at assisting the Euratom Safeguards Directorate (ESD, DG XVII, Luxembourg) and the International Atomic Energy Agency (IAEA) in the implementation of safeguards instrumentation required in the frame of both the Euratom and the Non-Proliferation-Treaties for Special Nuclear Material. The objectives of this work are:

- to develop, test and implement reliable non-destructive assay (NDA), instruments, associated data acquisition systems, interpretation models and software for user friendly applications of the various techniques,
- to provide after sale services and training to the inspectorates of both institutions.

Both support programmes are structured following specific task sheets describing the activities pertinent to each task and the relevant mile stones to be achieved. In 1993 the most important activities in support to Euratom consisted in realising a functional study for an Unattended Monitoring System (UMS) for Low Enriched Uranium (LEU) fuel elements. The outcome of the study was a detailed project for a station integrating a supporting structure for the fuel element, a newly designed active neutron collar system and surveillance cameras. A highly integrated user-oriented software package has been specified to manage both data collection and evaluation, and

inspection functions. Training and calibration in PERLA, as well as field support have continued. The design and realisation of Head Quarters Destructive Analysis (DA) and Non-Destructive Analysis data bases has been continued.

The final aim of this work will be to provide ESD with a high level integrated data evaluation and storage package, that integrates verification and accountancy. As far as IAEA support is concerned, the TAME facility has been enlarged with a new tank (the so-called "D" or "Harp" tank) and with new instrumentation in order to have the possibility of calibrating and giving training on the most commonly used tanks and instruments.

The aim of the PETRA programme during the year has been focused on the completion of the second "nuclear test" as agreed with the Italian Licensing Authority (ENEA-DISP). The main activities carried out in the PETRA facility can be summarised as follows:

- the third phase of the second nuclear test, the so-called "uranium solidification" process started in January 93,
- the fission product free uranyl nitrate solution, which was stored as final "product" at the end of the previous "1st extraction cycle", has been utilised for the solidification process.

On the basis of results of "nuclear tests" performed up to this stage, it can be concluded that:

- the five PETRA plant safety systems have successfully met the requirements,
- radioactive aerosols have been completely trapped in the Vessel Off-Gas System,
- aqueous liquid wastes have been properly managed within the imposed plant requirements. Discharged radioactive contaminants have been well below the acceptable plant limit,
- all the functional systems involved in the nuclear test have demonstrated their capability to implement the research programme.

PETRA operations have been mothballed in June 1993. At the present time a decision is pending on the (eventual) utilisation of PETRA as a tool for testing instrumentations and validate mass/volume calibration procedures, as foreseen by the Safeguards Programme. For intermediate storage, transport and final disposal of radioactive waste, the waste package has to fulfil the waste acceptance criteria, as defined by the nuclear regulatory institutions of the various countries. Important, especially for storage or final disposal, is the radiochemical content of the waste package.

The fulfilment of the waste assay criteria concerning radiochemical content can be verified by the execution of a quality assurance programme from the waste production up to the waste package, ready for final disposal, complemented by computations and/or measurements at the beginning during and at the end of the waste treatment. A programme to develop measurement systems, instruments and analysis methods is executed in order to enable an experimental assay of waste packages with enough accuracy.

Relative to the measurement methods waste is subdivided in waste containing fissile and non-fissile radionuclides. The fissile isotopes can be either plutonium or uranium (or possibly other minor fissile isotopes) or both.

Plutonium containing waste is assayed by passive neutron interrogation possibly complemented by gamma interrogation to measure the isotopic composition. The time correlation method (TCA) consists of analysing a measured pulse train, and derive therefrom the neutron multiplets due to spontaneous fission of the ^{240}Pu. Two analysis techniques are used. A first method is based on a Monte Carlo calculation and comparison between measured and calculated multiplets. A second method analyses the moments of the multiplets analytically. From this the plutonium quantity in the waste can be determined.

The problem for uranium containing waste is much more difficult. The measurement is based on active neutron interrogation with an external neutron source. Two factors define the correct determination of ^{235}U: the matrix with its moderating properties and the distribution of uranium in the matrix. An R & D project is in execution to attack this problem with the final goal to produce an instrument to assay uranium in waste.

Non-fissile waste is measured by gamma-scanning. Again two factors determine the precision with which the content of gamma contaminants in waste is determined: the absorption of the matrix and the source distribution. A gamma- scanner and adapted software is currently used.

Fusion

Following provisional acceptance of ETHEL (European Tritium Handling Experimental Laboratory) from

the architect-engineer, the majority of the 1993 activities has been associated with: collating of project documentation, in-house testing of the various systems and modifying the systems where necessary. Such activities have simultaneously supported the training of operations and maintenance personnel serving the laboratory.

As part of its on-going cooperation with its German sister facility, Tritium Laboratory Karlsruhe (TLK), the third JRC-Ispra - KfK workshop was held at which the fusion research programme activities involving tritium of the two organisations were presented. Further collaboration between ETHEL and TLK was also reflected in the facilities' common tritium control methodology document presented to the European Safeguards Direction. Finally, progress has been made on a number of fronts with regard to the Fifth Topical Meeting on Tritium Technology in Fission, Fusion and Isotopic Applications scheduled for May 1995.

Turning towards fusion research activities, one of the first applications will be the use of advanced chromatograph packed columns developed and manufactured within STI for accurately determining the composition of hydrogen isotope mixtures. Such an analytical technique will be employed with pressure-volume-temperature and weight measurements for quantifying tritium flows to and from the laboratory's magazine. In addition, the ETHEL tritium calorimeter, which has undergone successful field testing in Canada and Germany, will reinforce the existing laboratory expertise in tritium control techniques.

Another area of research which has attracted interest from external organisations is the development of tritium permeation barriers for fusion application as well as the use of the experimental apparatus for the measurement of permeabilities on prospective fusion materials. In this area progress has been made in reducing possible leaks due to tritium permeation from waste packages by the use of multilayer metallised polymers. This material, commonly used in the food industry, has the advantage of reducing by several orders of magnitude the permeation of hydrogen isotopes in both elemental and oxide forms and will therefore reduce potential tritium losses to the environment.

One final research activity of immediate benefit to ETHEL and other fusion facilities is the development of a compact tritiated water reducer capable of supplying, as an end-product, pure hydrogen isotopes. The process, based on an iron bed reactant for reducing the water followed by the removal of hydrogen isotopes through a Pd permeator, will help to maximise the recycling of tritium in ETHEL and thereby reduce both tritiated wastes and operating costs. The testing of zeolite-type packing material for gas mixtures purification was continued with the aim to identify substrates not showing "tritium memory" effects.

NON-NUCLEAR ACTIVITIES

Industrial hazards

The activities in the field of industrial safety focus on assessment, improvement and harmonisation of safety methodologies for chemical plants, and are carried out for the benefit of chemical industry, technical institutions and public authorities.

The FIRES facility, designed to study safety of batch chemical reactors, has been modified to accomodate requests of chemical industry to perform experiments simulating operation failures (e.g. stirrer failure) in polymerisation reactors. A cooperation agreement with a large chemical industry serves to enhance the industrial relevance of the venting code RELIEF. This code with a sophisticated user interface is operational on workstations and a PC version is near compilation. Two new venting facilities have been constructed: the large-scale facility DRACULA and the

medium-scale facility COLUMBUS (for venting of long horizontal vessels).

In the area of dense vapour cloud dispersion a 1-D shallow layer model has been completed and validated. The computer code for reacting gas flows simulating explosions under confined and unconfined conditions (REAC FLOW) is in an advanced stage of development. It has been implemented on UNIX workstations and PCs. The Commission has accepted the proposal for a collaboration network "Network on Safety Problems resulting from Runaway Reactors", in which the Safety Technology Institute participates.

Reference methods for the evaluation of structural reliability

The new reaction-wall facility-ELSA of the Safety Technology Institute is being used for prenormative research in support of EUROCODE 8, the provisional European standards for the design of civil engineering structures in seismic areas. This activity is performed in close cooperation with 18 research organisations in the Member States grouped into a scientific network under the Human Capital and Mobility programme. The research covers the major priority topics needing resolution to enlarge the current field of application of EUROCODE 8 and improve its reliability.

As part of the above prenormative research, a 4-storey reinforced concrete structure has been constructed and tested at the ELSA reaction wall under simulated severe earthquake loading. In parallel, preparatory work has been performed to test large-scale models of irregular bridges using the so-called substructured pseudo-dynamic technique. This technique allows to limit physical testing of a complex structure to its critical parts (i.e. those which are expected to undergo severe deformations), the rest of the structure being modelled by a computer code running in parallel with the pseudo-dynamic experiment.

In the area of computational mechanics, activities have concentrated on further development of local and global models for predicting the non-linear cyclic behaviour of steel, concrete and masonry structures. This also included work on special solution procedures for non-linear structural analysis, with particular reference to overcoming limit points, bifurcations, snap-throughs and snap-backs. Further developments have also been made with the PLEXIS-3C code for fast dynamic fluid-structure problems developed in collaboration with CEA-Saclay. In particular, a new automatic and general 2- and 3-D algorithm, based on the method of Lagrange multipliers, has been implemented to treat fluid-structure interaction in a more user friendly manner. Other PLEXIS-3C activities were performed in the framework of a third-party work contract.

As a part of the ongoing research in collaboration with the European Association of Structural Mechanics Laboratories, a large steel/concrete composite structure is being designed according to EUROCODE 8. It will be tested in 1994 with the view of comparing its actual behaviour against the intended design behaviour.

In the area of dynamic material properties, the Large Dynamic Test Facility (LDTF) has been used for studies on behalf of industry. In addition, a new experimental technique, based on a bundle of Hopkinson's bars, has been investigated to allow dynamic testing of concrete into the softening range of behaviour resulting from progressive cracking of the material.

Working environment

Working Environment is a new research programme which was introduced in 1992. The STI works on Ventillation and Pollutant Transport Modelling. The general objective which is pursued by this activity is the improvement of working conditions through a more clean, comfortable and healthy environment at the work place, that can be reached with better and more efficient ventilation systems.

The development of accurate and efficient Computational Fluid Dynamics codes to deal with such problems is a prerequisite to fulfil these objectives. To this purpose the finite element code TRAFLU for treatment of laminar and/or turbulent compressible flow problems is being extended to represent forced ventilation conditions and pollutant transport.

1 SPECIFIC PROGRAMMES

1.1 REACTOR SAFETY

The Reactor Safety Programme of the STI is devoted to the study of phenomena which characterise accidents, especially to so-called Severe Accidents in Light Water Reactors (LWR). Also in 1993 the programme was subdivided into the following main chapters:

- *Source Term, where the main effort is concentrated on the participation in the Phebus FP programme, including the development of the European source term code ESTER and the experimental project on the investigation of aerosol resuspension phenomena STORM;*
- *FARO, an international programme on the interaction of molten corium with coolant water and reactor structures;*
- *Thermalhydraulics which in addition to the conclusion of LOBI test analysis.documentation, includes support activities to the previous subjects.*

The relevant results are described below.

1.1.1 SOURCE TERM

Introduction

The STI research in the Source Term area is being performed through a large cooperation scheme which in the past was stimulated by the existence of Shared Cost Actions and at present by the existence of the international Phebus-FP programme.

Research on Source Term has the objective of improving and making more accurate the methodologies and the calculation tools for the evaluation of the quantity and quality of radioactive products which could potentially be released to the environment in the case of severe accidents. The importance and the difficulty of the problem makes international cooperation and efforts to reach a consensus essential.

The participation in the international Phebus-FP programme remains the most important effort in this area, due to the resources involved, the ambition of the overall programme and the number of partners. In addition to the financial participation, defined by the CEA-CEC "Convention" signed in 1988, the STI staff is directly involved in the project work, particularly in advanced instrumentation and material problems through the small group at Cadarache (F), and in the test definition and analysis as well as in the co-ordination of the partners work through the analyst team at Ispra.

The Phebus-FP programme is managed by a Steering Committee which met twice in 1993 and discussed the new test matrix and other decisions concerning the test execution (FPT-0, FPT-1). A very important role is played by the SAWG (Scientific Analysis Working Group) and the TG (Technical Group) where with four meetings per year all the partners are represented and cooperate in all analysis aspects and in the solution of technological problems.

In close relation with STI participation in Phebus-FP the decision was taken in 1990 to develop a code package called ESTER for severe accident calculations. ESTER has the special features of being constructed at an informatic environment which facilitates the coupling of modules coming from different organisations. To this purpose the support of the SCAs existing in the previous programme was essential because it allowed the contribution of many national teams to the realisation of the first pilot version for Phebus-FP calculations which is already available for the Member States and will be extended and validated in the future. ESTER allows the comparison and coupling of different modules, is fully portable, offers a database management system, a user interface, graphics and other output facilities, ample documentation and has been subjected to quality assurance procedures. Unfortunately in the programme 1992-1994, due to a reduction of resources, the SCA programme has not been extended and puts an addi-

tional load on the STI which has to take over a part of the work previously performed outside.

Among the activities on aerosol physics related to the Phebus-FP programme, an experimental test programme, which foresees the construction of large-scale separate effect test facility called STORM, for the study of aerosol deposition/resuspension, has been started by the STI in collaboration with ENEL(I) in 1991. Resuspension phenomena could have an important impact on source term and up to now the data and models available are very unsatisfactory.

The STORM project has made considerable progress in 1993. The assembly of components has been started and the first tests are expected in 1994. Two international meetings have been organised with a large participation of experts in order to present the project (April 1993) and to launch a series of benchmark calculations (December 1993).

Phebus-FP Programme

Preparatory Activities at Cadarache (F)

1993 was marked by the final preparation of the first experiment of the Phebus Fission Product Programme. FPT-0, and the test execution. The last controls/ modifications of the facility testing and commissioning (T&C) phase and the detailed analysis of the experiment operating plan by the Safety Authorities took considerably more time than anticipated. Development and design of equipment for the second test was started, on the basis of the test objectives defined by the Analytical group and of an overall planning diagram.

Testing and commissioning of buildings and ventilation systems was completed early in the year. The first criticality of the new Phebus reactor core was reached on February 22, 1993, followed by an extended series of low power nuclear calibration tests. In August, the reactor power was gradually raised to 21 MW.

Auxiliary and experimental circuits were under T&C during a large part of the year, including extended thermal-hydraulic tests in the containment vessel REPF 502. At the end of this phase, the sampling instruments of FPT-0 were installed (September-October). The in-pile section (test train) was loaded into the in-pile cell on October 17, 1993.

Two major post-test examination facilities became available by the middle of the year: the radiography and gamma scan pool-side station "PEC", for non-destructive testing of the test train, and the "CECILE" hot cell for disassembly and preliminary analyses of FP samplers. Simultaneously, a specific post-test analysis (PTA) working group prepared detailed flow sheets for handling and analysis of the FP samplers to be recovered from the first test. Eight laboratories in EU member countries will participate in the sample analysis work.

All shielded handling and transport devices were supplied and tested. The last container (radioactive waste container "DEDA") arrived in December, just in time for removing waste from the first test. An extended period of time was spent (July-November) for final testing, modification, and qualification of all planned remote handling operations inside the experimental caisson.

The overall safety report was discussed with the authorities in two formal meetings on January 7 and June 3, 1993, and accepted after a number of amendments. Discussions then focussed on phenomena and management of late phase fuel bundle degradation and on possible molten fuel - water interactions. Additional calculations in the region of possible pressure spikes due to this interaction turned out to be necessary, resulting a.o. in a new test train retention plate avoiding the missile hazard under vapour explosion conditions. These issues were finally concluded, with the support of numerous calculations by IPSN analysts and by US experts, early in November.

The experiment operating manuals for FPT-0 were written on several levels, i.e. from general to more and more detailed instructions:

- "test protocol", a general guideline by the analysts,
- general test plan, followed by the "programme détaillé",
- "fiches d'essai".

The Data Book for FPT-0 was completed, and a major part of the FPT-1 book compiled. The General FPT-1 Test Plan and its instrumentation plan were edited in November. Following the approval of a new programme Test Matrix in March, feasibility aspects of the consecutive tests were examined, and discussed by the Technical Group. Major development requirements for the novel proposals (debris bed - molten pool, and air ingress tests) were identified.

Execution of the first experiment FPT-0

The pre-irradiation of the test train was started on November 21, 1993. The total test fuel bundle power was kept constant at 240 kW during 9 days. Apart from a number of spurious reactor scrams of short duration, this phase was accomplished according to plan. During the "xenon override" stop after this phase, all planned operations and verifications were carried out. The reactor was made critical again early on the 2nd of December. The transient then took place between 10 a.m. and 3 p.m. that day. It ended by the manual reactor scram, upon instruction by the experimenters, following fuel slump and another burst of FP release.

On-line instrument readings were coherent with the conclusion that the two major test objectives, i.e. partial fuel melting and significant FP release, have been achieved. The overall instrumentation and controls performance during the transient was very satisfactory. After the four-days period of containment vessel observation and sampling, the experiment was completed on December 8 by replacing steam with nitrogen, cooling down, and draining of liquid waste. Remote recovery of the FP samplers started on December 13, 1993, and will be pursued during the first months of 1994.

Specific support by the JRC team at Cadarache

The following tasks have been under the responsibility of the JRC staff on site:

- Data Book: compilation, quality control and assurance, and users' services,
- Instrumentation plan and connected R&D management,
- Fuel bundle post-irradiation examination (PIE),
- Post-test analysis pre-calculations (in collaboration with NUPEC, Japan),
- Test train thermal shroud R&D, manufacture of the FPT-1 shroud components,
- BR 3 fuel characterisation and connected operations.

Major contributions have been supplied in the following areas:

- Programme management, including working group organisation, international relations, etc.,
- FP sample post-test analyses (PTA),
- Remote handling of FP samplers,
- decontamination techniques and procedures.

Analytical Activities at Ispra

Test matrix revision

In 1992 the Phebus-FP Steering Committee assigned to a joint team from CEA and JRC the task of proposing a revised form of the Phebus-FP test matrix. Consultations were held with experts in the various EC member countries and also with representatives of the other Phebus Partners, and a series of SCA contracts were established to clarify the main severe accident phenomena affecting the safety of BWRs and advanced reactor designs (the previous test matrix had concentrated on PWRs of current design). The upshot of the discussions and expert evaluations was a draft revised test matrix [1] which radically changes the emphasis of the Phebus tests.

This revised test matrix was accepted by the Steering Committee in October 1992 as a basis for feasibility studies and exploratory calculations, and work in this direction has been executed by STI (as well as by IPSN and other organisations) in 1993. A progress report was made at the end of the year. It is planned to present to the Steering Committee a more formal evaluation in mid-1994, after discussions within the SAWG and the TG.

The previous test matrix reported in [2] used the fuel rod bundle largely as a source of fission products, and tried to represent on a reduced scale the main phenomena affecting fission product transport and retention in the primary circuit. Hence the various tests included in the circuit a steam generator tube (hot or cold), a volume representing the pressurizer (dry or water-filled), complex structures similar to the steam driers, and a pipe simulating the LPIS line. Reflecting current trends in severe accident research, the revised test matrix gives more emphasis to the degradation and release processes taking place in the bundle. The circuit aspect is simplified, recognizing the difficulty of simulating in a representative way the phenomena taking place in pressurizers, complex structures etc. in a small-scale facility such as Phebus. Hence only two circuit configurations are proposed at present: a steam generator tube as in FPT-0, and a long thermal gradient tube, for the investigation of fission product chemistry. The containment vessel expensive to replace, has been retained unchanged in the new tests, but is used in a manner which focuses more upon the chemistry resulting from the different fission product sources which are created by the various bundle scenarios.

The main features of the draft revised test matrix may be seen from ***Table 1.1.*** Tests FPT-0 to FPT-2 are

Table 1.1a Phebus-FP test matrix - main objectives

N°	Identif. lable	Fuel bundle	Prim. circuit	Cont. vessel
FPT-0	**Fresh fuel in oxidizing environment**	FP release and speciation from fresh/preconditioned fuel under steam flow during: – heat up – fuel degradation – fuel melting (up to 20%) – cooling down at low steam flow rate Fuel degradation in oxidizing environment	FP retention in the primary circuit of a S.G. with secondary hot Chemistry of deposits Resuspension scoping study	Aerosol behaviour and deposition during FP injection Radiochemistry of I in gas and acqueous phase at pH=5 Iodine partitioning and formation of organic compounds FP reentrain. at slow depressurization
FPT-1	**Preirradiated fuel in oxidizing environment**	As FPT-0	As FPT-0 Coupons for thermal resuspension	As FPT-0 but: – ph 7 with natural evolution – high humidity
FPT-2	**Preirradiated fuel in reducing environment**	As FPT-1 under oxygen starvation conditions Specifically: – fuel candling and relocation – cooling down at high steam flow rate	Chemistry of deposits Retention on Inconel/SS Pipe section for thermal resuspension	As FPT-1 but: – pH 9 with natural evolution – interm. humidity Single droplet spray
FPT-3	**Open test** **Options:** **1. Back up test** **2. High pressure** **3. BWR and/or advanced fuel**	See Table 1.1b	See Table 1.1b	See Table 1.1b
FPT-4	**Rubble bed**	FP release and speciation during late phase of fuel degradation Fuel degradation from rubble bed to molten pool	Deposition and retention of less volatile FPs and transuran. elements	Deposition and retention of low volatile FPs and transuran. elements FP chemistry with low volatile FPs
FPT-5	**Air cooling**	FP release and speciation from degrading fuel under highly oxidizing conditions Fuel degradation under highly oxidizing conditions	Chemistry of deposits Pipe section for thermal resuspension	As FPT-2 Single droplet spray

Table 1.1b Objectives of the open test FPT-3

N°	Main object.	Fuel bundle	Prim. circuit	Cont. vessel
FPT-3A	**Back-up test**	To be defined	To be defined	To be defined
FPT-3B	**Advanced reactors and BWR phenomena**	Fuel degradation with typical Ad. Reactors & BWR materials* FP release and speciation with slow heat-up and oxidizing conditions	FP retention in minimum line configuration** Chemistry of deposits Thermal resuspension	Containment radiochemistry Effect of thermal resuspension DF and chemical transformation in water pool
FPT-3C	**High pressure conditions**	FP release and speciation under high pressure conditions Fuel behaviour during rapid cooling FP-release under rapid cooling	FP retention in minimum line configuration** Chemistry of deposits Thermal resuspension	Radiochemistry at high Iodine concentrations Iodine partitioning Formation of organic I compounds

* Materials utilized in this tests would be typical of Advanced Reactors and in some cases also of BWRs
** Pending of results of FPT-0 and FPT-1

almost unchanged (except for some questions connected with the pH and buffering of the sump water, discussed in later sections), but the later tests are quite new in concept. FPT-3 is an "open" test with three options:

- repetition of one of the previous tests,
- investigation of advanced reactors and BWR phenomena,
- high pressure conditions.

FPT-4 now concerns degradation and the release of low-volatile FP from a rubble bed such as formed in the TMI-2 accident as a result of severe degradation of the fuel rods. An important question is whether this test should start from an intact rod bundle, which would be allowed to form a debris bundle in a natural but not necessarily representative way, or from a prefabricated debris bed, such as was used in the (out-of-pile) MP tests at Sandia in the US. This is linked directly with questions of safety and feasibility - the only previous in-pile debris bed tests have been conducted for fast breeder reactor safety evaluation, and proved experimentally troublesome.

A second feasibility question concerns the transport of the released FP. It is as yet unclear how they can be transported from the debris bed deep in the Phebus reactor core and through the circuit into the containment vessel without heavy retention on the colder parts of the circuit in the core region. In-pile sampling instruments would be an alternative, but they would require significant development effort.

JRC research for FPT-4 [3] has consisted so far of thermal studies to determine the power necessary to maintain the debris bed in the desired temperature range and then to melt it down into a fuel pool, and exploratory calculations of the flow field above the pool which should transport the FPs up into the circuit. Some first results will be reported in 1994.

The second innovative test is FPT-5, in which the effects on degradation, and more importantly, on FP release and transport of air ingress into the bundle will be investigated. It has yet to be decided whether the target reactor scenario is a vessel bottom melt-through with the formation of a "chimney", or an accident during reactor shutdown e.g. a station black-out. Both degradation and release models are weak in conditions of air ingress, and work so far has concentrated on looking at the conditions expected in the reactor during accidents of the two types mentioned (a relatively new field), and reviewing the results of the few out-of-pile release experiments performed in strongly oxidizing atmospheres. The recent ORNL test VI-7 should be particularly helpful.

Contribution to FPT-0 test preparation

The 1992 STI Annual Report explained at length the objectives and design details of the first Phebus-FP test, FPT-0. In 1993 the work focused on confirming the choices of the Test Protocol both through code benchmarks constructed around the test conditions, and through studies looking at more specific details of execution or of modelling. There was considerable consultation with CEA and, in the SAWG meetings, with the other European and non-European Phebus partners.

This work culminated in a final version of the test protocol [4], which also specifies the schedules for sampling operations. Unsurprisingly, some review of the detailed schedule was necessary later on, to ensure that it correctly translated the specifications of the test protocol, and several corrections were introduced at this stage. These concerned in particular the thermal-hydraulic conditions for the containment vessel (see sections below).

There have been some important conclusions regarding these, supported by information arriving both via experiment (see § on FPT-2 scoping calculations) in the thermal-hydraulics tests, and via 2-d calculations of the flow and temperature distributions in the vessel performed by various partners. Very briefly, it appears that the assumption of a homogeneous distribution of temperatures and concentrations in the vessel made in previous calculations using a range of codes (JERICHO, CONTAIN, MELCOR etc) is not justified. Instead there is a distribution of temperature and concentration, causing differences in local relative humidity, condensation rates on cool surfaces etc. As a second point, the correlations employed to calculate condensation rates upon cool surfaces and the sensible heat transfer to them, based on small-scale tests, appear not to be suitable for Phebus. They overestimate the sensible heat transfer considerably. Hence the final specification of the condenser temperature during the aerosol injection and settling phase of FPT-0 had to be established on the basis of experimental results rather than on calculations.

Thirdly, it seems that the sump region in the containment vessel is nearly stagnant, so that condensation on the sump water and transfer of radiolysis products from sump water to atmosphere are more difficult than had been assumed. The interpretation of the results of the containment portion of FPT-0 is therefore expected to be a significant analytical challenge. All the preparation work for FPT-0 culminated in the

performance of the test on 2nd-5th December 1993. The raw results from on-line measurements, on the basis of which interpretation will start, are expected in February 1994.

BUNDLE CALCULATIONS FOR FPT-0

The objectives of the bundle part of the FPT-0 test are twofold. Firstly, and most importantly, it is planned to measure the release of fission products from fresh fuel in an oxidising environment. Secondly the thermal and mechanical behaviour of degrading fuel rods will be studied under more severe conditions than have been attempted in any bundle experiment before. The objective is to melt 10-20% of the uranium dioxide and for this to happen the temperature in the hottest part of the bundle will need to be around 3050K.

The boundary conditions to achieve these objectives were defined in 1992 by analysts from CEA and checked by JRC, Ispra. A pre-test calculational exercise was then organised by JRC so that other Phebus partners could benchmark their codes against each other and prepare themselves and their codes for the demanding task of post-test analysis that will follow the experiment. The results are reported in [5] and this was the fifth pre-test exercise for the bundle part of Phebus organised by Ispra.

Both Ispra and CEA used ICARE-2 for their calculations. CEA used the latest version (2V2mod1) and Ispra used the version that had been implemented into ESTER. The University of Stuttgart had participated in the previous benchmark exercises with their KESS code and for this exercise they used the latest version - KESS-III. There were two RELAP5-SCDAP calculations - one from the Consejo de Seguridad, Spain and one from ENEA Bologna. This was the first time that these organisations had participated in a benchmark exercise and indeed the first time that calculations from the SCDAP code had been sent to Ispra. The University of Madrid performed MELCOR calculations.

The two ICARE calculations were rather similar and were used as a reference for the others. ICARE was able to play this role because it contains rather detailed models for some Phebus-specific components that are not found in reactors. For instance it contains a model to account for the thermal expansion of the shroud and the closure of the gaps that separate the various layers (see ***Fig. 1.1***). Since KESS did not model this effect the University of Stuttgart submitted two calculations - one with the gap closed and one with it open. Another reason for choosing ICARE as the reference code was that it had been extensively checked and calibrated against Phebus-SFD results.

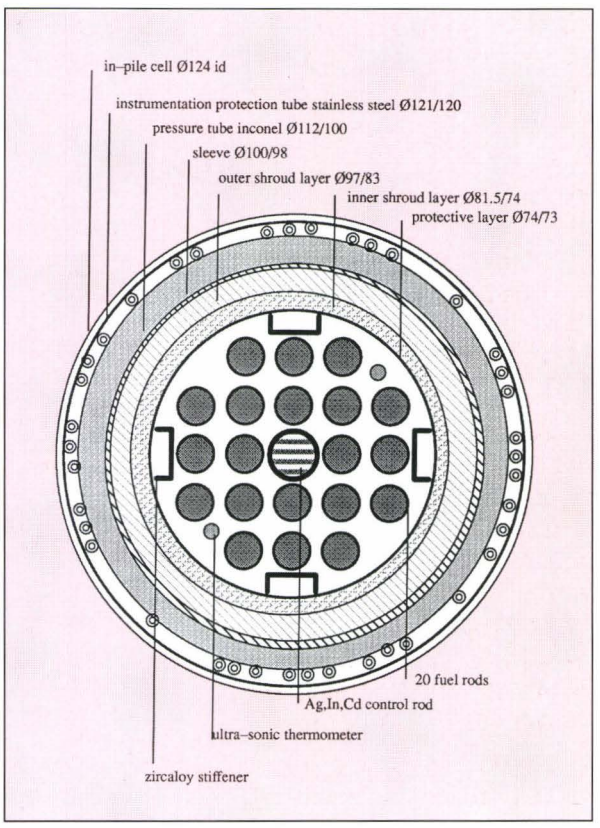

Fig. 1.1 Cross-section of Phebus-FP in-pile test train

In fact the codes predicted a similar thermal behaviour during the test; at least for the first part of the transient. All codes predicted that positive feedback from the exothermic zirconium oxidation would produce a temperature escalation and this is the peak that we see in ***Fig. 1.2*** at around 11 000 seconds. After the zirconium in the centre of the bundle has been completely consumed the temperatures fall again. In some bundle experiments (CORA, PHEBUS-SFD) molten zirconium has been seen to react with the uranium dioxide fuel forming eutectics. These dissolve the uranium dioxide at temperatures depending on the exact composition but, in any case lower than that of pure uranium dioxide. The codes agree that this precocious fuel melting is unlikely in FPT-0 because the zircaloy cladding will be fully oxidized before a significant quantity can melt.

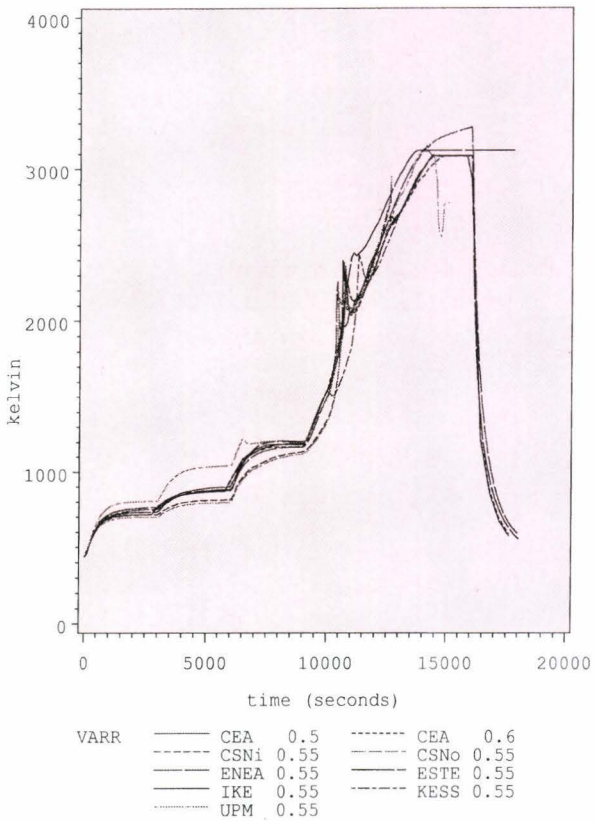

Fig. 1.2 Fuel temperature - 0.55 metre elevation

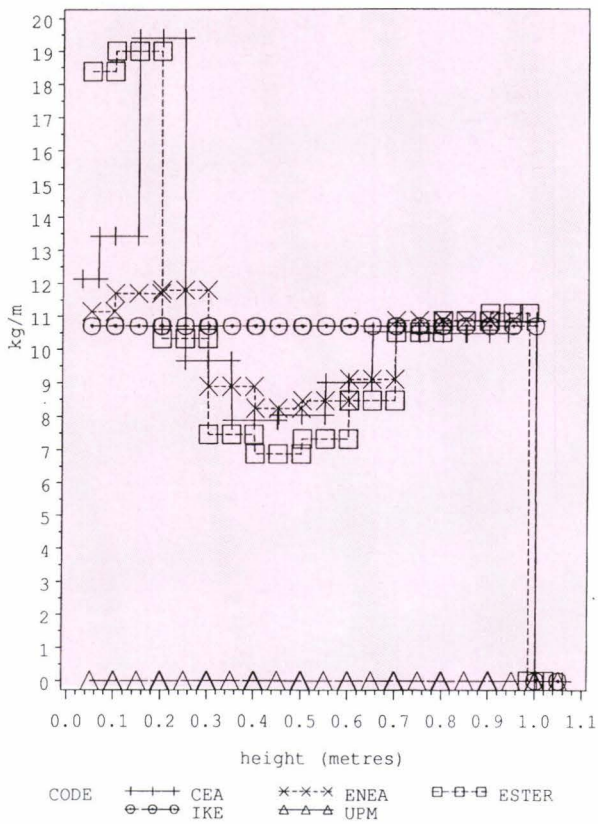

Fig. 1.3 Mass of UO_2 16 000 seconds - FPT-0

The codes all predict that fuel melting temperatures will be reached and that the fuel will relocate downwards but the mass that relocates and the behaviour of the relocated material cannot be predicted with confidence. The codes used have not been assessed for such severe conditions. ***Fig. 1.3*** shows the final profile of uranium dioxide expressed as kilograms per metre height as predicted by the codes.

At a meeting to discuss these calculations all the participants agreed that, with the present state of knowledge of core degradation, the boundary conditions chosen were the best possible and that no modifications to the test procedure would increase the likelihood of achieving the test objectives.

Fission product release benchmark exercise

The Safety Technology Institute in collaboration with the Transuranium Institute (TUI) organized an international benchmark exercise on fission product release. The aim of the benchmark was to compare code predictions for fission product release from fresh fuel (FPT-0) and high burn-up fuel (FPT-1). The benchmark exercise addressed one of the weak links in the Phebus-FP pre-test exploratory calculations.

Participants in the first part of the exercise, which is based on the FPT-0 fuel transient, include organisations from Europe: IPSN Cadarache (France), CRTN/ENEL Milano (Italy), AEA Winfrith Technology (UK), JRC/TUI (Germany); and outside Europe: JAERI (Japan), AECL (Canada), and Argonne National Laboratory (USA). Preliminary results suggest that there is a large discrepancy in code predictions. Specifically, codes that are based on FASTGRASS predict considerably lower release of fission products, whereas predictions from the other codes are in reasonable agreement for the release of volatile fission products and noble gases. Larger uncertainties remain in the release of non-volatile elements (e.g. molybdenum, lanthanum, strontium, ruthenium) and in the timing of the release. The large uncertainties that still remain to be resolved are shown in ***Fig. 1.4*** where percentage iodine release for the FPT-0 transient is shown.

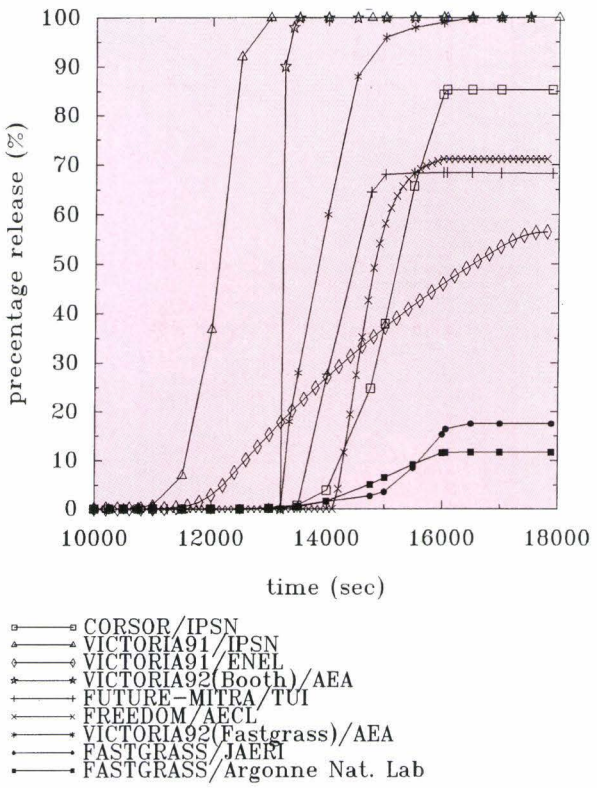

Fig. 1.4 Comparison of predicted FPT-0 iodine percentage release

Circuit calculations for FPT-0

Thermalhydraulics and circuit retention

The exploratory primary-circuit pre-test calculations that had been performed in earlier years were collected and analyzed in [6, 7]. The aim of the pre-test calculations was to calculate the amount and speciation of the release to the containment and to assist in the operation of numerous instruments along the Phebus primary circuit. Retention was deemed an important measurable quantity. The emphasis of the analytical work was on identifying the origin of differences in code predictions.

Earlier studies have shown that the circuit thermalhydraulics calculated by ICARE and CATHARE were similar. CATHARE values were used for all the primary circuit calculations. The circuit nodalization used in CATHARE was the following (232 axial nodes concentrated in the regions of steep thermal gradients):

- 8 nodes in the unheated vertical hot-line (0-0.136 m);
- 129 nodes in the hot-line (0.136 - 12.458 m);
- 72 nodes in the steam generator (12.458 - 21.902 m);
- 23 nodes in the cold-line (21.902 - 26.961 m).

Steam and hydrogen mass flow rates and gas temperatures at the circuit inlet were obtained from ICARE 2 version 2 code results. In the present calculation, the containment response was ignored (as in the ICARE calculation), and the system pressure was assumed constant (and equal to 0.22 MPa).

Fig. 1.5 and *1.6* show respectively:

- the evolution of gas temperature along the circuit at t = 11 000; 12 500 and 16 000 seconds;
- the evolution of gas velocity along the circuit at t = 11 000; 12 500 and 16 000 seconds.

These results indicate that:

- sharp changes of gas temperature occur above the fuel bundle and at the entrance to the steam generator;
- gas velocities (and accelerations) are high, especially at the entrance to the steam generator (from 5 to 20 m/s).

During the test (from 9 000 to 16 000 seconds), the flow regime will change through the circuit as follows:

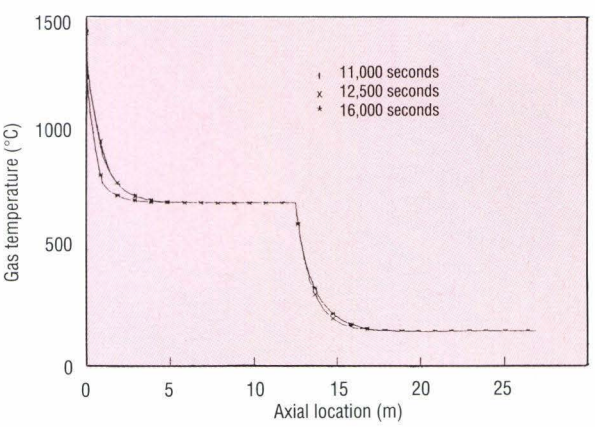

Fig. 1.5 Evolution of gas temperature along the circuit at t = 11 000, 12 500 and 16 000 seconds

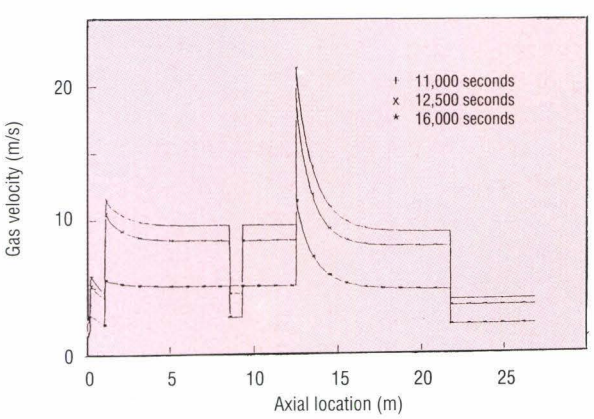

Fig. 1.6 Evolution of gas velocity along the circuit at t = 11 000, 12 500 and 16 000 seconds

- in the vertical hot-line, transitional or laminar;
- in the horizontal hot-line, turbulent or transitional/ laminar;
- in the steam-generator, turbulent;
- in the cold-line, turbulent.

The above calculated flow regimes need to be compared to those existing in reactor scenarios, when considering representativity.

Circuit retention

JRC collected the results of pre-test calculations that had been performed with the following codes:

- TRAPF (version April 1991) at IPSN Cadarache;
- VICTORIA (version May 1991) at JRC Ispra;
- RAFT (modified version of July 1990) at JRC Ispra;
- MACRES (version January 1993) at NUPEC, Japan;
- ATHLET-CD (version January 1991) at GRS Munich;
- VICTORIA (version 1992) at Sandia National Laboratories.

Results for circuit retention are shown in ***Fig. 1.7***. There is general agreement that most retention of volatile fission products (caesium and iodine) occurs at the entrance of the steam generator, where thermalhydraulic calculations show a large temperature gradient. Specifically, the wall temperature abruptly decreases from 973 to 423 K at the entrance of the steam generator. The main deposition mechanisms are predicted to be thermophoretic deposition and wall condensation. Whereas most codes predict a 30 to 40 percent retention in the steam generator, RAFT predicts considerably higher retention (approximately 80%). This important difference will be explained in the § "transport and retention". It will be shown that differences in predicted circuit retention arise from different thermophoretic deposition models and from different calculations of the wall condensation flux.

The results obtained show that the volatile fission products (iodine and caesium) are transported as vapours up to the entrance of the steam generator and then are retained by vapour condensation and aerosol deposition in the remainder of the circuit (i.e. steam generator and cold line) - ***Figs. 1.8*** to ***1.11***.

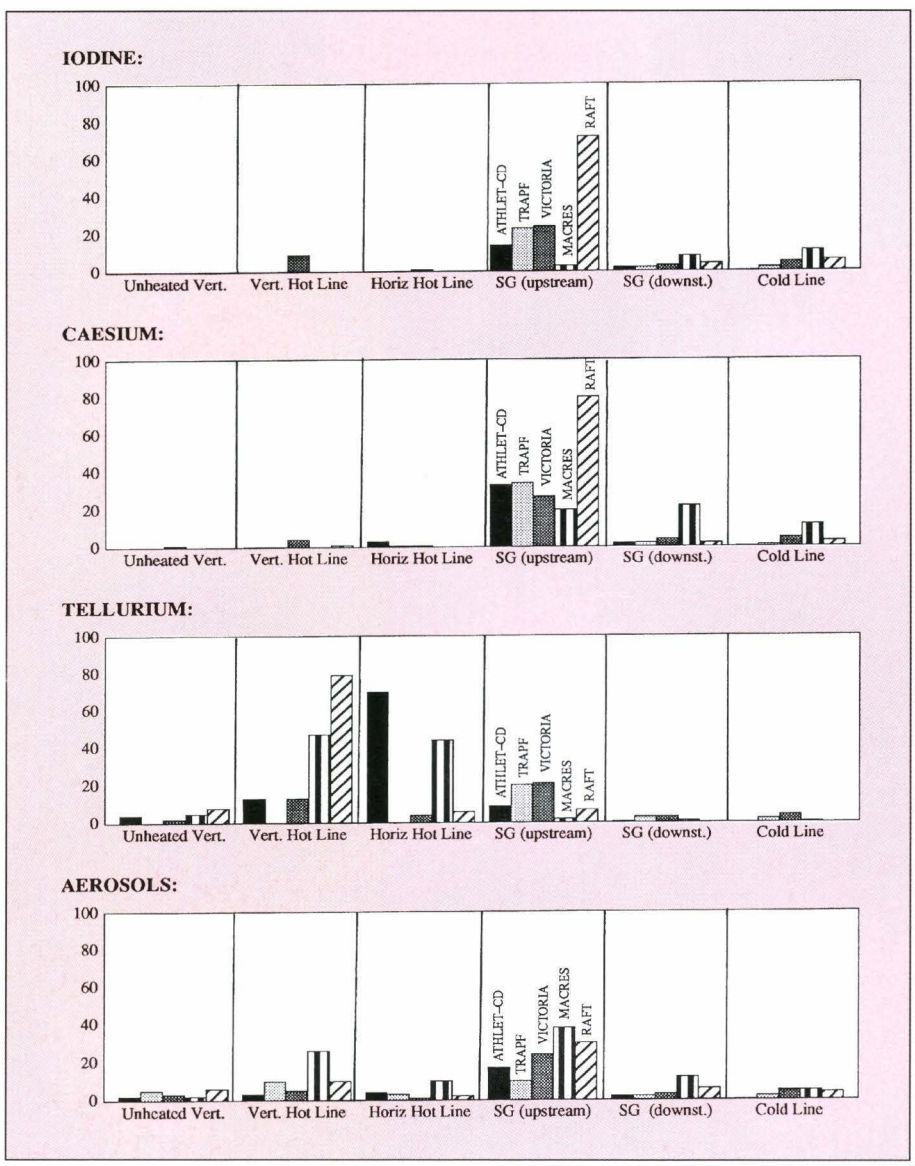

Fig. 1.7 Predicted percentage retention in the FPT-0 primary circuit

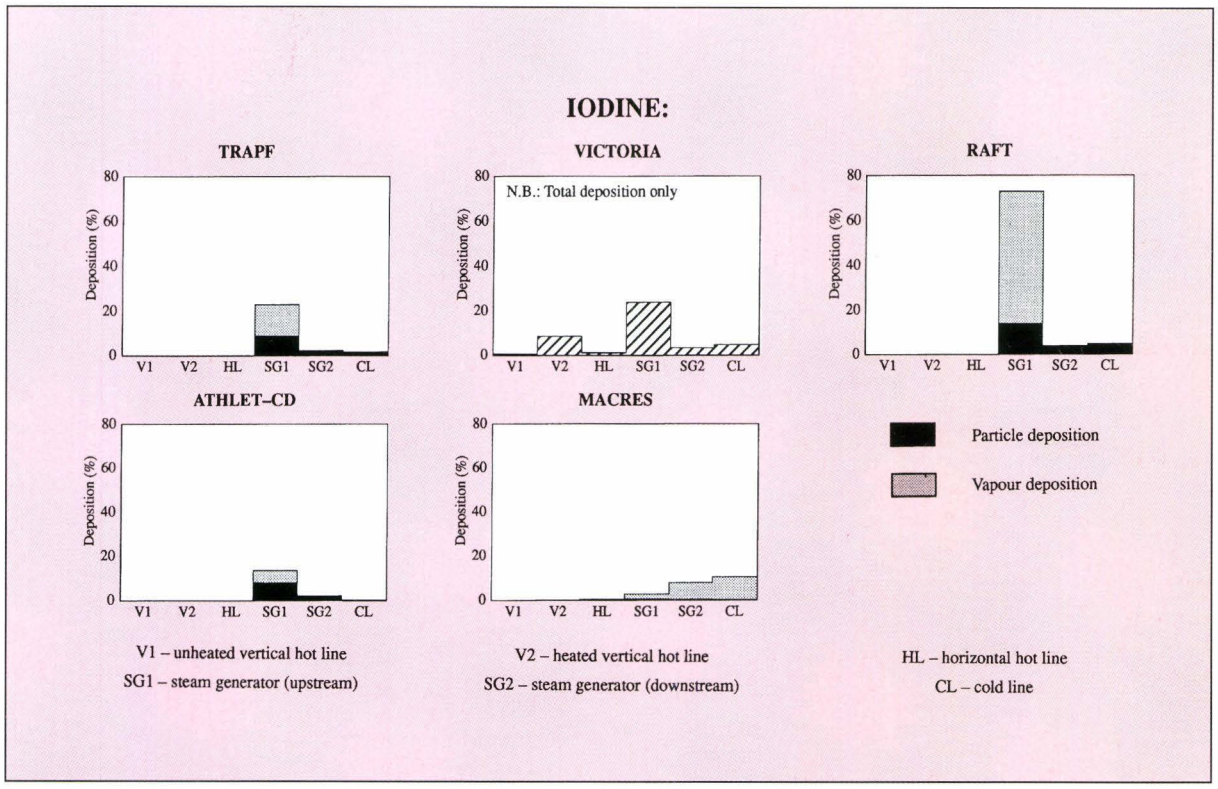

Fig. 1.8 Iodine depletion along the circuit at t = 16 000 seconds

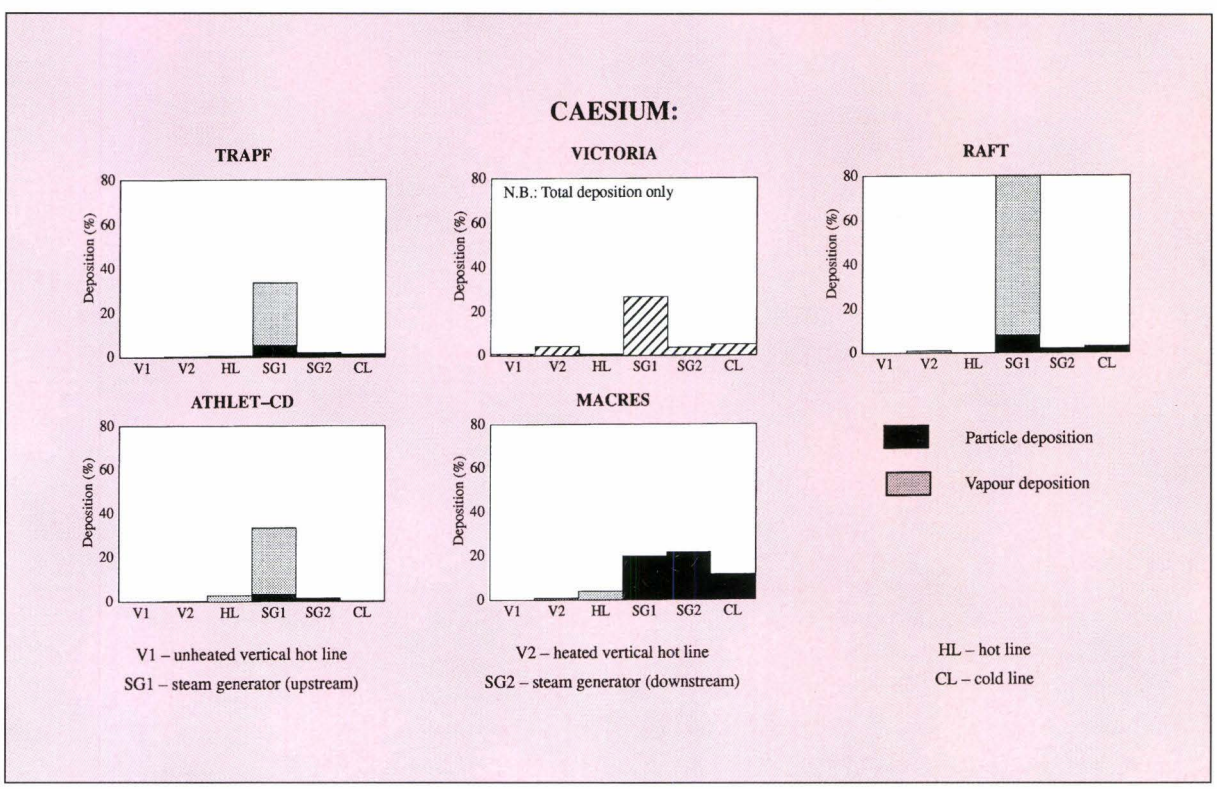

Fig. 1.9 Caesium depletion along the circuit at t = 16 000 seconds

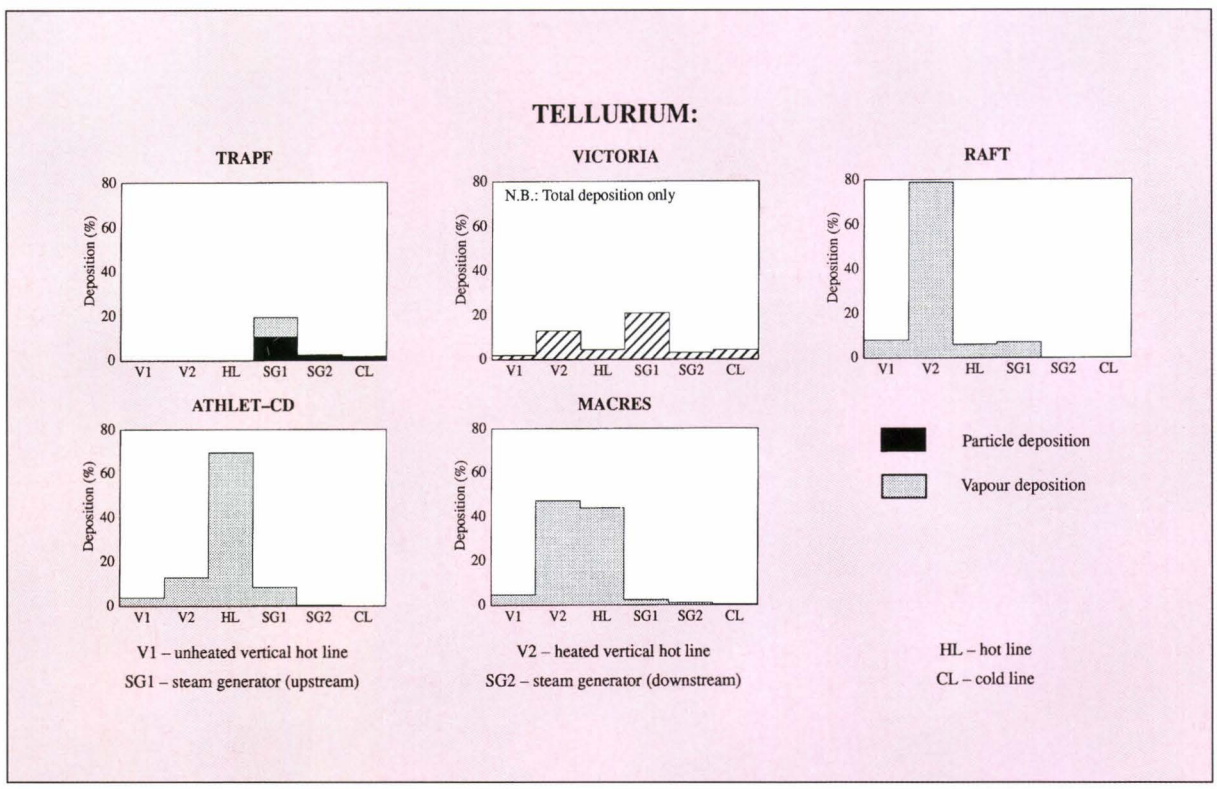

Fig. 1.10 Tellurium depletion along the circuit at t = 16 000 seconds

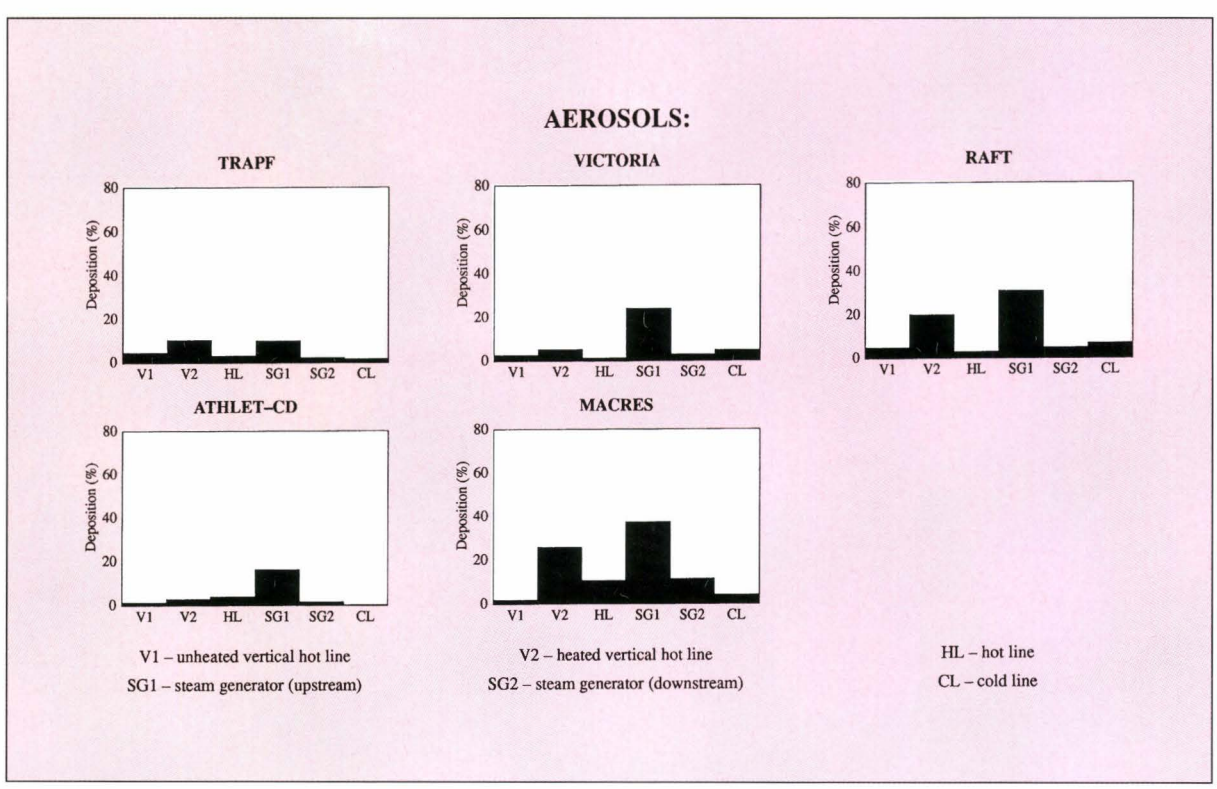

Fig. 1.11 Aerosol depletion along the circuit at t = 16 000 seconds

The values of the transmission factor (mass at the circuit outlet/mass at the circuit inlet) for aerosol and fission products differ greatly from one code to another (***Table 1.2***): from 18 to 84% (iodine), from 14 to 62% (caesium), from 0 to 76% (tellurium) and from 8 to 73% (aerosols). By neglecting the RAFT results, the agreement between code results is better for iodine and caesium: more than half of the release at the circuit inlet is transferred to the containment.

Significant differences in tellurium deposition are attributed to different models for tellurium chemisorption onto the primary circuit walls. Aerosol deposition is predicted to occur (at varying degrees) throughout the circuit. The fission product quantities that are predicted to be released into the containment were considered sufficient for a meaningful study of aerosol behaviour in the containment.

Future work will focus on optimization of code modelling and validation against separate effect tests, and of course again on forthcoming results from the Phebus experiments.

CONTAINMENT CALCULATIONS

Thermalhydraulics tests

It is not a primary objective of Phebus to validate thermalhydraulic codes. In each test target atmosphere conditions are specified that will produce the desired boundary conditions for the aerosol particles and the chemistry. During the injection period steam and hydrogen enter the containment together with fission products and structural material from the degrading core. It is expected that particles containing those fission products that are soluble, caesium hydroxide for instance, will grow due to the condensation of water vapour. Larger particles will settle faster and so after a certain time the atmosphere will contain mostly insoluble aerosol particles. The rate of this condensation depends on the relative humidity and so different humidity targets are set for the different tests. The first test FPT-0 had a target humidity of between 50 to 75%. The second test, FPT-1, will have a higher humidity.

Various attempts were made by Ispra and partner organisations [8, 9, 10] to specify the vessel temper-

Table 1.2 FPT-0 exploratory circuit calculations: transmission factors

$$\text{Transmission factors (\%)} \ldots \frac{\text{Mass at the circuit outlet}}{\text{Mass at the circuit inlet}} \times 100$$

Elements	Computer Codes				
	TRAPF (CEA)	**VICTORIA (JRC)**	**MACRES (NUPEC)**	**RAFT (JRC)**	**ATHLET-CD (GRS)**
Iodine	73	58	78	18	84
Caesium	62	59	42	14	61
Tellurium	76	52	0	0	4
Silver	–	60	96	–	72
Indium	–	64	90	–	–
Cadmium	75	65	95	–	72
Zirconium	–	58	49	–	–
Tin	76	57	46	–	72
Aerosols	68	59	8	29	73

ature, the condenser temperatures and sump temperatures that would produce the desired relative humidity for a given steam injection rate. These scoping calculations highlighted the sensitivity of the results to the heat and mass transfer correlations used in the codes. Although some correlations such as Uchida [11] depend only on the steam content of the atmosphere, these were shown to be insufficiently precise for these purposes [12]. Other correlations, such as that of Collier [13] depend on fluid velocities near the fluid surface but these velocities depend by themselves on the circulation patterns within the vessel and these patterns are difficult to calculate.

It was therefore decided to run a series of "thermal-hydraulic tests" in the actual Phebus vessel where the humidity could be measured and the codes calibrated. Before the test took place a number of double-blind calculations were made of the tests. "Double-blind" means that not only did the participants conduct the calculations with no knowledge of the test results, but also that they had performed no previous calculations on this facility. This can be guaranteed because the calculations were performed before the facility was tested and so the calculations do provide a real indication of the predictive power of the codes for vessels such as the Phebus-FP containment vessel.

The codes were those used for reactor calculations (CONTAIN, JERICHO, CONTEMPT and MELCOR) plus one written specially for Phebus calculations (CONT). The organisations concerned in the calculations were from Europe (JRC Ispra and CIEMAT, Madrid) and also Japan (NUPEC). All these codes were zero-dimensional; they assumed that the atmosphere properties were uniform everywhere. The results were summarised in [14].

The tests were run during the early part of 1993. It is difficult to compare the pre-test calculations directly to the experiments for three reasons. Firstly the experimental results received so far are only preliminary; secondly they are only steady state and thirdly the experiments were run with 1, 2 and 4 grams per second steam injection rates whilst the calculations had used 0.5, 1.5 and 3 grams per second. Nevertheless some comparisons are possible. ***Fig. 1.12*** shows the steady state temperatures in the vessel and ***Fig. 1.13*** shows the saturation temperatures for the case where the vessel wall was 100°C. They are both expressed as functions of the condenser temperature.

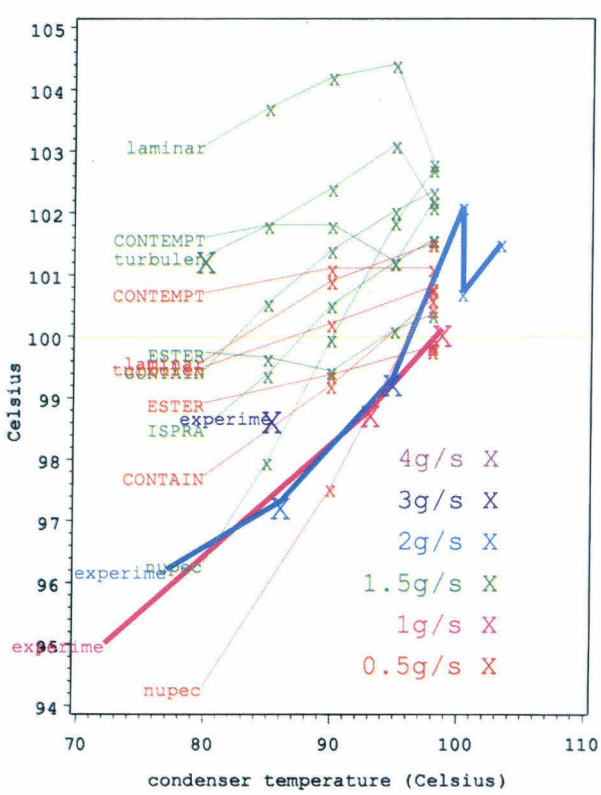

Fig. 1.12 Thermalhydraulic tests - atmosphere temperature (wall temperature = 100°C)

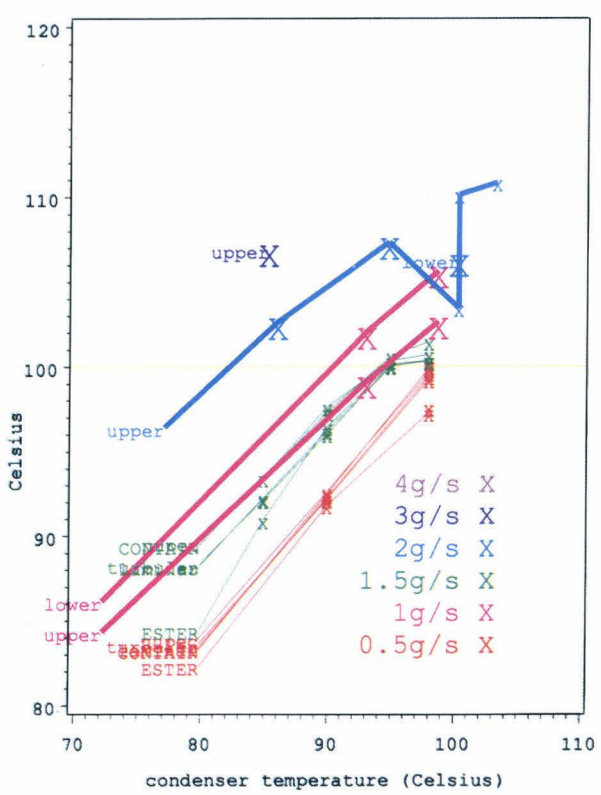

Fig. 1.13 Thermalhydraulic tests - saturation temperature (wall temperature = 100°C)

The figures look rather complicated and require a little explanation. The thick lines are experimental measurements, the thin ones are code calculations. The saturation temperature was measured in the lower and upper parts of the vessel. They are significantly different so both values are given. Each colour marks a different flow rate. As the flow rate rises the temperature, saturation temperature and humidity rise. *Fig. 1.14* shows the humidity. In the case of the experimental values this was derived from the two measured saturation temperatures, so there are two values for each case; one from the upper half of the vessel and one from the lower. *Fig. 1.15* shows the condensation rate on the condenser expressed as a fraction of the injection flow rate.

The steam content of the upper part of the vessel is lower than in the bottom part in the experiment. This is to be expected because injection is in the lower part and most of the condensation is towards the top. The codes predict a lower steam content than was measured even in the upper part of the vessel. Because they also predict a higher temperature the humidity they calculate is significantly lower than was observed.

GRS, Garching, did not participate in this exercise but it too performed a blind calculation with their multi-compartment code FIPLOC. By splitting the containment into separate compartments it was able to reproduce rather well the magnitude of the humidity measured at the bottom and top of the containment vessel. Other attempts have been made using two and three-dimensional codes such as the French code TRIO and the Japanese code ALPHA-FLOW. But these codes are essentially steady-state and cannot yet calculate the phase of the Phebus transient when steam is being injected and condensing on the walls or in the atmosphere.

We intend to use these tests to choose appropriate heat and mass transfer correlations for the Phebus calculations. Unfortunately these correlations will be scale-dependent and cannot be extrapolated to a reactor scale. But the uncertainties in present models, that are shown here, will also be present in reactor calculations. Phebus is not a-priori more difficult to calculate than a full-size reactor. The relative humidity is a sensitive parameter because it depends on both heat and mass transfer. The uncertainties, that are shown here, should be borne in mind when trying to predict the probable thermalhydraulic conditions in the containment following a severe accident.

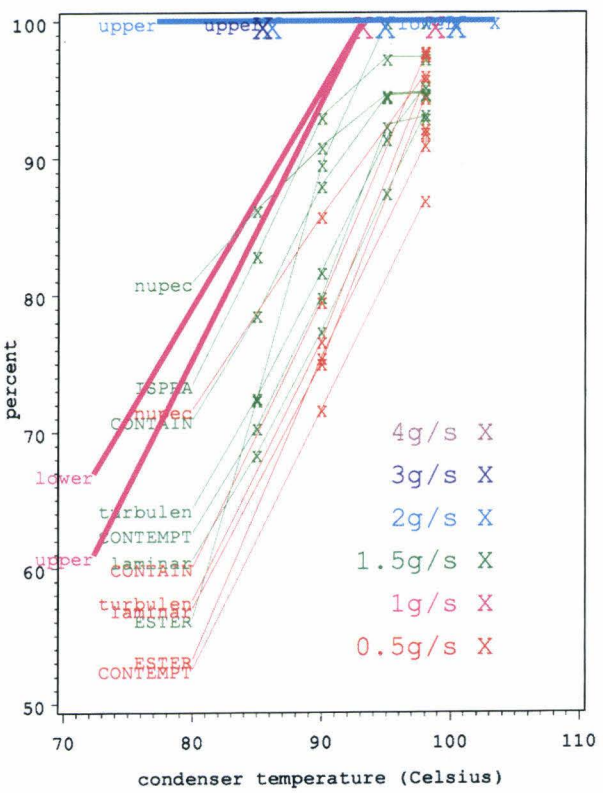

Fig. 1.14 Thermalhydraulic tests - humidity (wall temperature = 100°C)

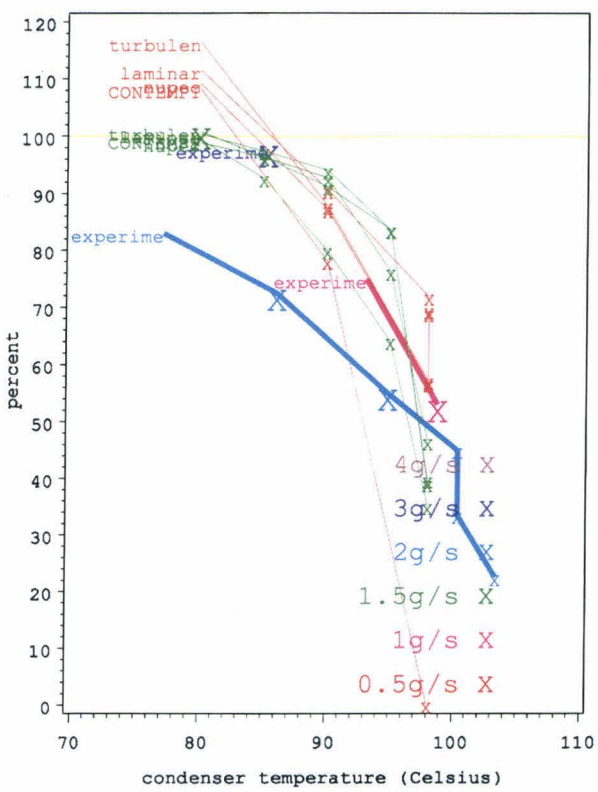

Fig. 1.15 Thermalhydraulic tests - condensation on condenser as percentage of injection (wall temperature = 100°C)

Thermalhydraulics and aerosols

The thermalhydraulic and aerosol behaviour calculations for the FPT-0 test protocol have been performed at Ispra using the CONTAIN 1.12 code. The test protocol includes five different phases [15]:

- Preparatory phase of approximately one day (~100 000 sec, in the calculation 150 000 sec) to establish the initial conditions of the containment before the test itself. The walls are heated to 383 K and the sump water to 363 K. The condenser is kept at 363 K so that in the steady state and without condensation the relative humidity is 55%.
- Aerosol inlet phase (1 800 sec) during which steam, hydrogen and fission products are injected into the containment. The fission product input is taken from VICTORIA predictions and amounts in total to 127 g. Soluble and insoluble components are analysed. The walls are maintained at 383 K and the sump water at 363 K, while the wet condenser temperature is adjusted to get a relative humidity between 55 and 75%.
- Aerosol deposition phase (ten hours). The wall temperature is kept at 110°C and sump water at 363 K. The relative humidity is expected to be around 60%.
- Chemistry phase (3 days) during which the wall temperature is increased to 403 K and the condenser temperature to 383 K.
- Depressurization phase (3 hours) with a depressurization of 5 m^3/h STP. The condenser no longer operates (same temperature as the walls).

The CONTAIN results are shown in ***Figs. 1.16-1.19***.

The atmosphere, wall, sump and condenser temperatures are given in ***Fig. 1.16***. The atmosphere temperature, after the inlet phase where it reaches a peak of 383 K, is constant around 380 K till the chemistry phase where it increases up to 400 K. During the depressurization phase it decreases about 2-3 degrees. ***Fig. 1.17*** shows that the pressure increases during the injection period from 0.2 MPa to a maximum of 0.25 MPa. Then it is almost constant around 0.23 MPa until the depressurization phase, where it decreases very quickly. The relative humidity (***Fig 1.18***) is 54% in the preparatory phase, between 60% and 75% in the inlet phase and 60% in the deposition phase, as wanted. During the chemistry phase it is about 30%.

The results also show that the condensation on the wet condenser during the injection phase is less than 90% of the incoming steam. Then at the beginning of the deposition phase the condensation still keeps increasing for the first 4000 sec, reaching a maximum value of 25.5 kg (total steam input 27.2 kg), and hence evaporation occurs. At the end of the deposition period the wet portion of the condenser is still wet with 0.4 kg of water on it. Undesired condensation on the dry portion of the condenser is predicted to be prevented by its high temperature (393 K). No condensation on the walls occurs in the calculation.

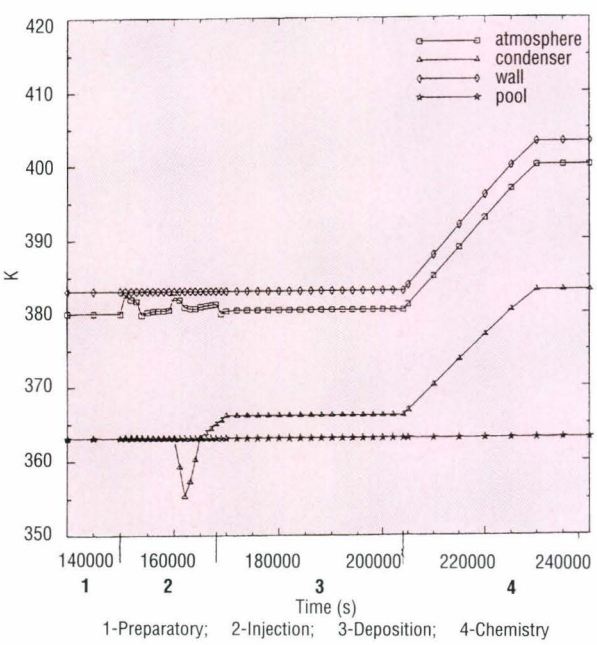

Fig. 1.16 Atmosphere, condenser, walls, pool temperature FPT-0

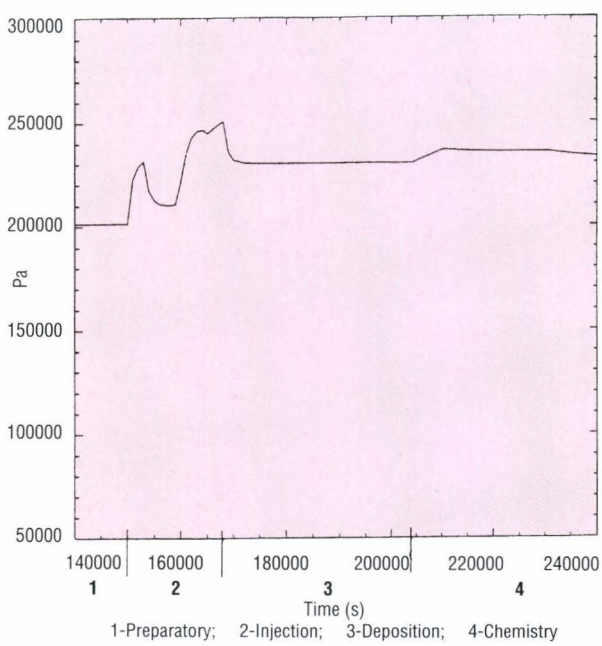

Fig. 1.17 Pressure FPT-0

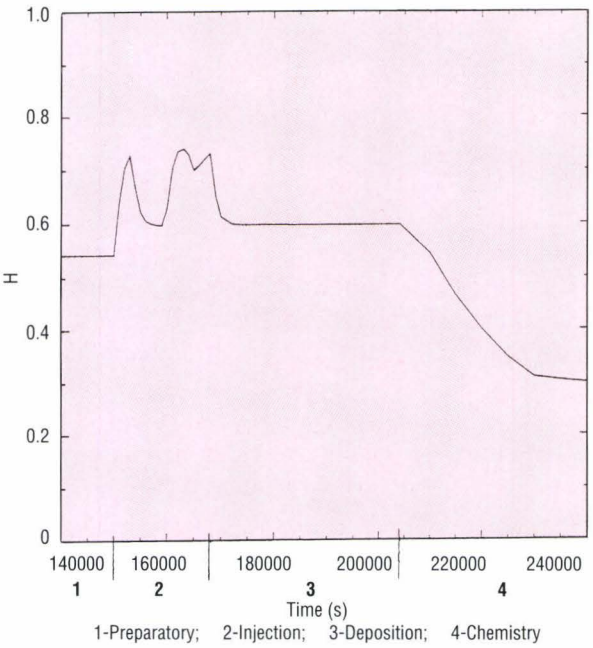

Fig. 1.18 Relative humidity FPT-0

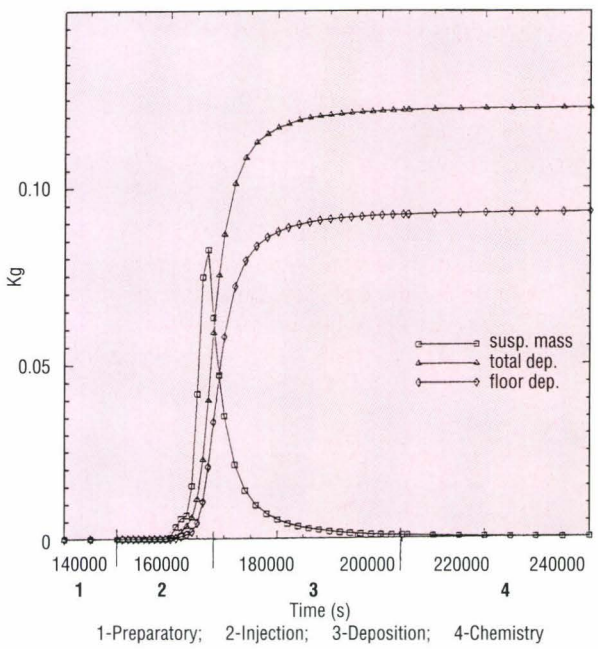

Fig. 1.19 Aerosol suspended and deposited masses FPT-0

Fig 1.19 describes the aerosol behaviour. 6 000 seconds after the isolation of the containment, 90% of the injected aerosol has been deposited, mainly by gravitation and thermophoresis towards the colder sump. The CsI and CsOH masses in the atmosphere reach a maximum of 0.02 g and 0.04 g respectively.

Chemistry

Calculations for the chemistry phase of the FPT0 test protocol were performed by the following partners [16]:

- IPSN/CEA, Cadarache, IODE code;
- CIEMAT, Madrid, IODE code;
- GRS, Köln and SIEMENS/KWU, Erlangen, IMPAIR code;
- OH, Toronto/AECL, Whiteshell and University of Toronto, LIRIC code;
- AEA, Harwell, INSPECT code.

The source assumed was estracted from AEROSOLS/B2 code results (CsI aerosol deposition rate in the sump water) while the thermalhydraulic conditions during the chemistry phase were taken from JERICHO code results [17].

IODE and IMPAIR are empirical codes which use correlations to model the system. INSPECT and LIRIC are mechanistic codes which describe the chemistry in terms of the fundamental reactions which are involved. These codes model chemical reactions in the aqueous and gaseous phases, and also mass transfer effects between aqueous and gaseous phases.

Code results show that the iodine mass distribution in the containment differs from one code to another, but all codes predict that the iodine concentration in the gaseous phase is high enough to be detected by the instrumentation provided (***Fig. 1.20***).

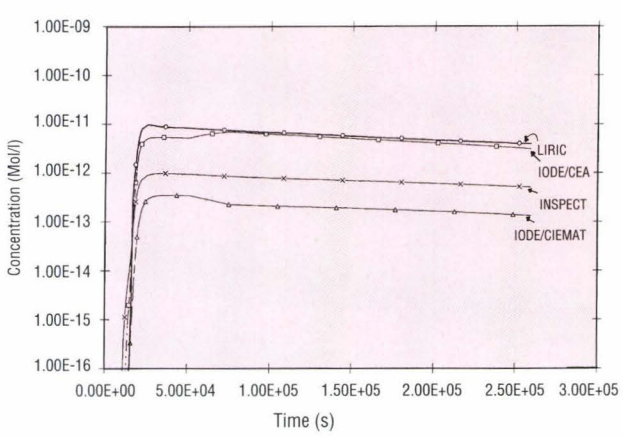

Fig. 1.20 Realistic case FPT-0 - gas I_2

Contribution to FPT-1 test preparation

The objectives, geometry and operating conditions for the bundle and the circuit of the second Phebus-FP experiment are very similar to those of FPT-0. The principal differences concern the containment vessel, where a high humidity (sufficient to cause significant condensation upon aerosol particles) and neutral, unbuffered initial sump water chemistry conditions are specified by the test matrix. It has, however, been necessary to recalculate the bundle conditions to take advantage of the probable introduction of a more insulating shroud in this test. The shroud will be protected internally by a thoria liner, which should remove problems of shroud erosion. The shroud material is however porous, and there are still uncertainties as to the extent to which the shroud will compact (and its internal gaps will grow or close) during the transient. It should be recalled from the previous Annual Report that the unheated section of the circuit just above the bundle was a source of considerable constraint on the steam injection rates in FPT-0. Too high a flow when the bundle was hot would burn out the heaters in the sections above, too low a flow when the bundle was cooler would result in a cold spot, causing local deposition and nucleation of FP.

In the new test train design the unheated section has been made shorter and is better insulated, while the heaters above it are more resistant to temperature transients. It therefore could be considered for sure that FP release conditions remain oxidising throughout, even during the oxidation runaway, while keeping the flow rate to a lower (more representative) value during the period of maximum FP release. Both JRC and CEA have made bundle calculations to arrive at a proposed set of operating conditions for the FPT-1 bundle taking advantage of the more relaxed constraints on the flow rate, and this was approved at the SAWG meeting in November [18].

JRC is now organising benchmark problems for the Partners using these conditions for the bundle, and the predicted bundle outlet conditions as input to circuit thermal-hydraulics and aerosol transport calculations. A set of sensitivity studies has been agreed with CEA [19] in which the main tool for the JRC will be ESTER. They will be performed in the first half of 1994. Meanwhile, the conditions for the containment remain to be specified. The JRC will continue its analysis of the thermalhydraulics tests results in an effort to arrive jointly with CEA at a provisional specification of the containment protocol for the next SAWG in March 1994.

Bundle calculations for FPT-1

During 1993 a set of boundary conditions for FPT-1 were defined by CEA. These aimed to produce the same fuel temperature at the mid-plane and the same coolant temperature at the bundle outlet as in FPT-0. Because the shroud is made of a more insulating material than in FPT-0 the power required and the steam flow will both be lower. It is expected that the high burn-up of the fuel will influence the core degradation but the codes do not at present take this parameter into account. CEA's results for this test are therefore almost identical to those from FPT-0. JRC is in the process of organising a benchmark exercise for this test in order to avoid to rely overmuch on the predictions of a single code.

Circuit calculations for FPT-1

Thermalhydraulics and circuit retention

Exploratory circuit calculations for FPT-1 consisted in identifying a primary circuit geometry that would minimize retention. A series of calculations for a minimum retention line were performed at JRC Ispra (with VICTORIA and RAFT) and at IPSN Cadarache (with TRAPF and RAFT). As ***Table 1.3*** shows RAFT predictions follow the trend that was identified in the FPT-0 pre-test calculations, i.e. it predicts volatile fission product (caesium and iodine) deposition that is almost a factor of two higher than the predictions of VICTORIA or TRAPF for both thermophoretic deposition and wall condensation. These differences are investigated in § "transport and retention".

Pre-test calculations showed that the minimum retention line would result in circuit retention that is slightly lower (in terms of percentage deposition of the introduced source) than the FPT-0 predicted retention. Hence, it was decided that the FPT-1 geometry would be a compromise between the FPT-0 geometry and the minimum retention line. The FPT-0 steam generator will be retained in FPT-1 but a number of bends in the cold part of the circuit, where high deposition is expected, will be removed.

Contribution to FPT-2 scoping calculations

FPT-2 was originally planned as a test in which fission product release takes place with a reducing atmosphere and, in order to ensure that this was the case, it was planned that the inlet flow should be a mixture of hydrogen and helium. However, from the point of view of degradation phenomena a test in which steam starvation is induced at some level in the bundle is most representative.

In this case steam is introduced at the inlet with a flow low enough so that, at times, it is all consumed by the zircaloy oxidation reaction. Helium is also introduced in order to increase the heat capacity of the coolant and thus prevent the outlet temperature of the coolant dropping to unacceptable levels. The flow at the outlet then consists of only hydrogen together with helium. However, it may be difficult to ensure that the fission products, the release and transport of which are the main focus of the experiment, are actually released from the fuel at locations where reducing conditions hold.

Some scoping calculations with ICARE-2 and CORSOR-M have been made for postulated conditions to investigate this question. In this transient the calculation indicated that steam starvation was induced for a considerable period and that the flow at the outlet was pure hydrogen. Clearly there is some uncertainty in this calculation because relocation of cladding away from the hot zone is difficult to predict and could cause a premature ending of the oxidation.

Fig. 1.21 shows the release of caesium in one of these calculations expressed as a function of the temperature and hydrogen mole fraction at the point where it is released. The helium is not counted when

Table 1.3 Comparative percentage deposition along the proposed FPT-1 minimum retention line

	20 mm, Abrupt Temperature Transition				20 mm, 3 m Temperature Transition			
Elements	**RAFT/ JRC**	**VICTORIA -91**	**RAFT/ CEA**	**TRAPF***	**RAFT/ JRC**	**VICTORIA -91**	**RAFT/ CEA**	**TRAPF***
Cs	57	23	50	22	65	20	60	40
I	55	23	46	20	59	21	53	42
Te	91	23	90	18	91	20	93	36
Cd	–	26	88	44	–	26	70	42
Aerosols	43	23	33	16	43	23	31	13

* TRAPF considers only the following species: CsOH, CsI, SnTe, Cd, and inert aerosols

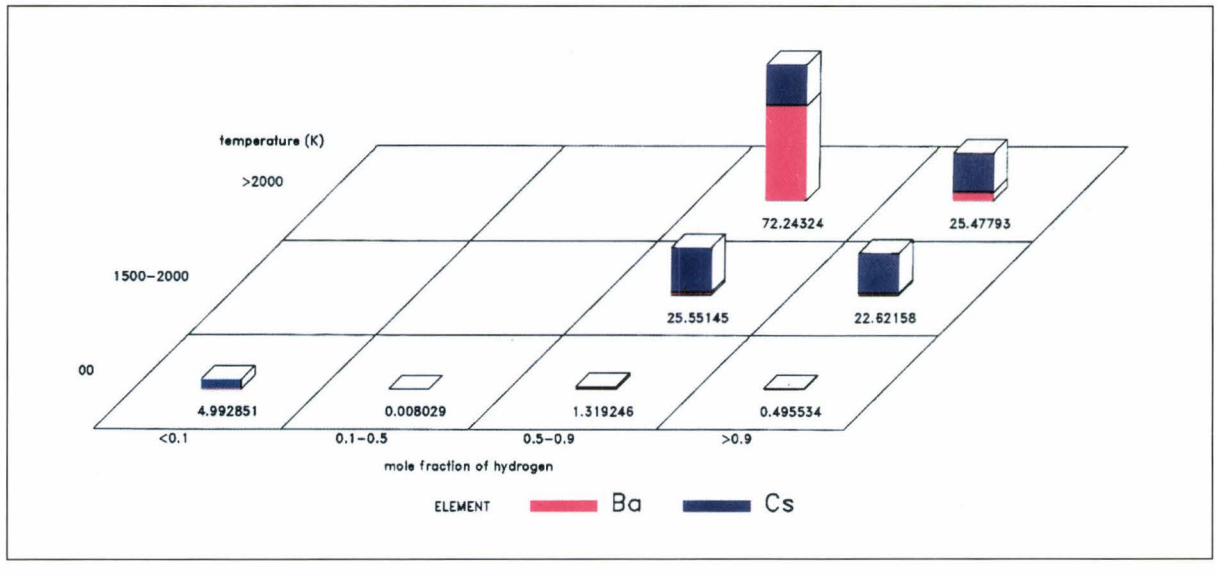

Fig. 1.21 Release of caesium and barium as function of temperature and hydrogen mole fraction

the mole fraction is calculated. Release of volatile elements such as caesium thus tends to take place under oxidising conditions despite the steam starvation. The situation is still more clearly marked for less volatile elements such as barium. The predominantly oxidising conditions are partly a result of the temperature profile in the Phebus bundle. In the upper regions of the bundle where the coolant is reducing, radial heat losses mean that the fuel rods are too cold to release large amounts.

Code Developments

Modelling Studies

State of the art reviews

Following the successful state of the art report on core degradation [20] the CSNI commissioned in 1992 a SOAR on fission product release and transport, a draft version of which is now available [21]. This report is concerned with releases from the core and transport through reactor circuits. The initial chapters cover the experimental and theoretical status of fission product and associated materials release from fuel (and control) rods in their various failure states through to debris beds and molten pools, while later chapters survey the same items for transport through the reactor circuits (excluding pool scrubbing, which is analysed elsewhere). Phenomena considered under the latter heading include vapour and aerosol deposition mechanisms as well as revaporisation and resuspension. The SOAR ends with conclusions regarding the areas where further research is needed in the light of present knowledge and safety needs. They confirm rather well the orientations of Phebus-FP and of STI's source term research in general. Two STI members contributed to the preparation of the SOAR, including the writing of an important chapter comparing the predictions of FP transport models with all the available experiments. A major source of difficulty in modelling in this area is the complex interplay of chemistry, vapour transport and deposition mechanisms, including reactions with structural surfaces, and aerosol transport and deposition mechanisms. Experiments such as Falcon are of great assistance in identifying the most appropriate modelling routes and on providing validation information.

In a second activity, performed in collaboration with interested staff of the ISEI Institute, a review was performed of a compilation of descriptions of reactor safety research activities in the various EC member states [22]. The reviewers commented upon the whole array of activities, pointing out where JRC research complemented that done elsewhere, what fields attracted the most attention, areas apparently neglected, and overlaps or possibilities of collaboration with work performed outside the EC, particularly in the US, Japan and Canada. The resulting report [23] is a useful guide to reactor safety research in EC countries and the Commission's own efforts.

ICARE AND CHIP

ICARE, a code for calculating core degradation and thermalhydraulics in the core region, was the prototype for ESTER and still provides an example of the advantages of the ESTER concept. ICARE is also capable of calculating the flow in pipes provided that there are no loops or branches. During 1993 a new version of ICARE2 (V2mod1) arrived together with a new set of modules (CHIP) that enable the calculation of two phase flow. As well as modelling liquid and vapour the new modules allow the tracking of two incondensable gases which is specially useful because many experiments (Falcon, Phebus-FP) use a mixture of hydrogen and helium as carrier gases. Another feature of CHIP is that it is possible to couple the core modelling implicitly to a circuit thermalhydraulics code. This has been tested for CATHARE but could be extended fairly easily to other codes such as ATHLET.

ICARE is the best integrated code within ESTER because not only does it use the "reader" and "checker" but nearly all communications within the code use the RSYGAL database management library. The code has been tested on different testcases (Phebus B9+ and CORA5 for CHIP and CORA13, CORA5, PBF-SFD 1.4, PBF scoping test, Phebus FPT-0, Three Mile Island) and on different computers. Documentation is copious, both for the new version of ICARE and for the CHIP modules. It includes model descriptions, database descriptions, user manuals and validation test manuals [24, 25, 26]. Data for the test cases are included with the code as is the documentation in the form of TeX.

These codes are the only ones, except ICARE-VICTORIA, to be supplied with a set of standard "analyser" files that read database dumps and convert them into vectors for graph plotting. This is preferable to allowing the code to dump the vectors directly. It is only feasible to dump a limited set of variables on disk. Adding another variable to the list

of dumped variables involves modifying a file with the database dumping method, but would involve modifying the program if the vectors were dumped directly. The other advantage of this method is that the "analyser" allows extensive manipulation of the data. For instance it allows variables to be plotted against time, against position and against each other.

KESS

At first sight there appears to be little scientific justification for integrating both ICARE and KESS into ESTER. Both calculate core degradation behaviour and there are few models in one code that are not included in the other. Nevertheless it was always planned that as a quality control there should be alternative calculational paths for ESTER. IKE from Stuttgart University, have modified ESTER to use RSYGAL tools for data transfer. A post-processor has been written to transform the KESS database to an equivalent standard ICARE/ESTER database so that common output processing techniques can be used. A Phebus FPT-0 test problem has been successfully run on a VAX computer at Stuttgart and a SUN in Ispra.

Circuit models

Transport and retention

Most of the modelling work concentrated on understanding differences of code predictions for primary circuit retention in FPT-0 and FPT-1 pre-test calculations. Differences arise from different models for thermophoresis and for wall condensation in [28].

Thermophoretic models in VICTORIA, TRAPF and RAFT were analysed by calculating a simple analytical experiment in the CEA-sponsored TUBA series. These experiments were designed to test thermophoretic models. The analysis of TUBA 28 showed that the main difference between RAFT on one hand and VICTORIA, TRAPF on the other is in the calculation of the mean free path: RAFT calculates the mean free path using the classical kinetic theory expression, whereas VICTORIA and TRAPF calculate it from the dynamic viscosity. The two expressions give similar results for experiments performed in air, as TUBA 28 does, but they differ greatly for experiments conducted in steam, as is FPT-0.

The three codes also differ in the thermophoretic expressions they use: VICTORIA uses the Talbot expression, TRAPF the Brock equation, and RAFT the Springer equation. Differences between these expressions were investigated in [27, 28] where it is shown that the Talbot and Springer equations agree only over a limited range of Knudsen numbers. Moreover, the Springer equation is a steep function of the Knudsen number, a behaviour that is not supported by experimental results. Hence, even though the Talbot expression is a good interpolation over the whole range of Knudsen numbers, the best choice for the thermophoretic expression depends on the Knudsen number associated with the experimental conditions.

Wall condensation was studied by analyzing an experiment in the DEVAP programme. The DEVAP programme whose objective was the study of fission product vapour deposition by condensation and chemisorption is sponsored by IPSN. The analysis showed that for scenarios with large temperature differences RAFT incorrectly calculates the diffusion flux to the wall, and hence it overpredicts wall condensation. The RAFT expression is questionable because it evaluates the diffusion flux using a mixture of wall and bulk gas temperatures. Moreover, the TRAPF expression for the diffusion constant leads to acceptable results as a result of fortuitous cancellation of two inconsistencies.

Pool scrubbing models - BUSCA

The BUSCA code, developed by AEA in collaboration with other organisations, is the main tool used in Europe for the analysis of pool scrubbing problems. The chief focus in early developments was on scrubbing in open pools, i.e. in those in which the influence of the confining walls was small. The flow regime was assumed to be bubbly, with single bubbles or bubble clouds rising freely. This situation is appropriate for some scenarios in the suppression pool of BWR designs. In Phebus-FP (old test matrix) and in PWRs scrubbing in the circuit (pressurizer or relief tank) is also important, but the physics are somewhat different. The confining walls do affect the flow, and a churn flow regime is common.

Hence the models of a code like BUSCA must be extended to cope with the new situation. Under SCA the Polytechnic University of Madrid (UPM) has made several studies of the phenomena expected in PWR pool scrubbing and of the adequacy of current BUSCA models to handle them. It is concluded that wall effects are not very important for real-size (not model) pressurizers, but that more published experimental investigation is needed of scrubbing under

churn flow conditions. Some models are however available in the literature, which could be integrated into BUSCA without great difficulty [29]. The unmodified BUSCA code [30] has been integrated into ESTER, and the test cases run with satisfactory results.

LACE- ESPAÑA EXPERIMENTAL PROGRAMME ON THE RETENTION OF AEROSOLS IN WATER POOLS

On completion of the phase of participation in the international nuclear safety project LACE (LWR Aerosol Containment Experiment), an experimental project was initiated within the framework of the activities undertaken in 1987 by the LACE-España Consortium with participation of 6 Spanish organisations. The project was partially funded by the European Shared Cost Action Programme on Reactor Safety 1988-91.

The programme consisted of a matrix of 11 experiments on aerosol retention behaviour in submerged beds and suppression pools in water-cooled reactors under severe accident conditions. For performance of these experiments an intermediate scale, multipurpose facility was set up at the CIEMAT installations. The facilitiy includes various systems: aerosol generation (CsI), mixing section, injection line and pool vessel (8 m^3), as well as the corresponding aerosol instrumentation and a process control and data acquisition system. The eleven experiments were successfully carried out between October 1991 and July 1992, the main thermal-hydraulic magnitudes were reproduced and correct operation of the aerosol instrumentation was achieved [31].

The decontamination factor values obtained demonstrate the retention capacity of the pools for series of different scenarios and conditions: particle size, single and multiple orifice injectors and different bubble, jet and steam fraction regimes. The database obtained is intended to contribute to validation of retention models and codes. First code validations with these data carried out within the Consortium by the Polytechnic University of Madrid (UPM). UPM performed pre- and post-test calculations for the 11 tests with the pool scrubbing codes SPARC and BUSCA [32].

It also developed a bubble breakup model which based on experimental studies of gas-liquids hydrodynamics conducted by Battelle Columbus. The model was implemented in the BUSCA-JUN90 code and validated against the ACE Phase A experiments. A sensitivity analysis has been performed for the AA1, MnO test [33].

VALIDATION: FALCON TESTS

The Falcon experiments, conducted at AEA Technology's laboratory at Winfrith, examine various aspects of fission product chemistry but the part considered at Ispra is deposition within a thermal gradient tube, 48cm long and 2.5cm in diameter, through which pass fission products and structural material from fuel rods and control rods. The tube is colder at the outlet than the inlet and, at any position along it, the walls are colder than the bulk gas. Most of the fission products that enter the tube as vapours pass through to the outlet. Most of those that enter as aerosols deposit on the tube walls by thermophoresis and a smaller proportion settle on the bottom of the tube under gravity.

JRC's work has concentrated on two series of experiments. Fal-17 and Fal-18 were designed to investigate the influence of boric acid on fission product transport and were partly financed by the Commission's Shared Cost Actions. The other two experiments, ISP-1 and ISP-2, form the basis of an International Standard Problem. Each pair of experiments are described below in turn.

FAL-17 and FAL-18

These two experiments were essentially the same except that boric acid was injected in Fal-17 and in Fal-18 it was not. Both experiments were analysed with the ESTER version of VICTORIA and with RAFT and reported in [34]. The deposition deduced from the experiment was compared to that calculated by the codes. ***Fig. 1.22*** shows the deposition of caesium measured in Fal-17 and Fal-18 compared to the VICTORIA and RAFT predictions. ***Fig. 1.23*** shows the analagous result for iodine. Analysis of the measurements cannot usually confirm the chemical species of a particular element but it can be seen whether the codes can predict the temperature at which a particular element condenses. Sometimes the speciation can be inferred from this. For instance in Fal-17 it was observed that the maximum vapour deposition of caesium occurred at the same place in the tube as for boron. This indicates that it was caesium borate that condensed.

The experimental results of both experiments showed that caesium, tellurium, cadmium, silver and molybdenum entered the tube as vapour and condensed somewhere along the tube both onto the tube internal walls and onto aerosol particles. Iodine exhibited this behaviour as well in Fal-18 (the test without boric acid) but in Fal-17 it may have already

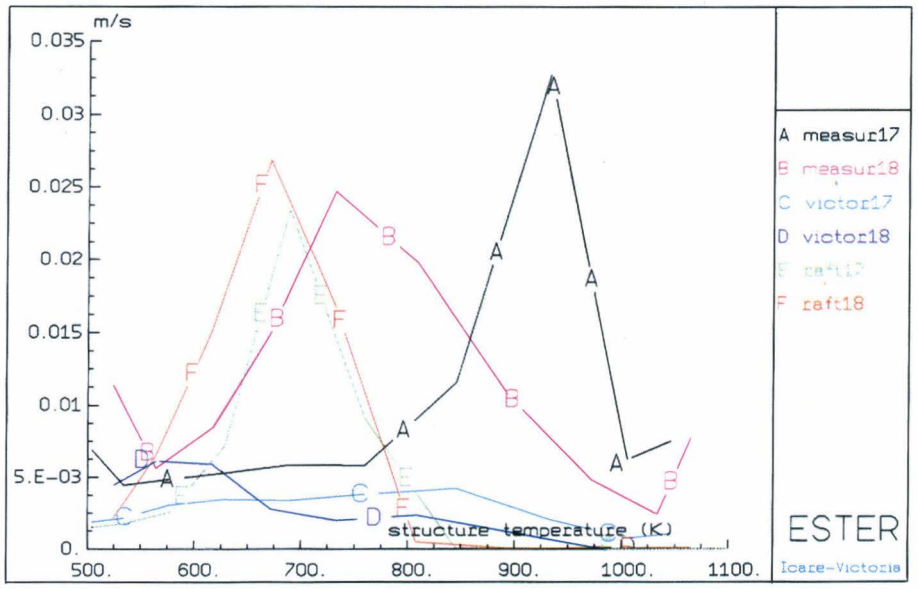

Fig. 1.22 Deposition velocity for caesium in Falcon measurements compared to VICTORIA and RAFT predictions

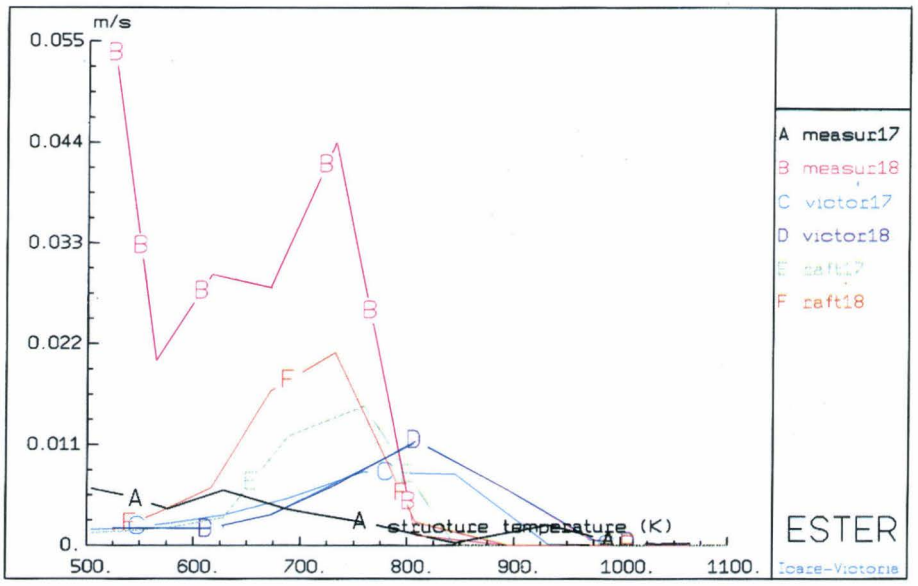

Fig. 1.23 Deposition velocity for iodine in Falcon measurements, VICTORIA and RAFT predictions

been an aerosol when it entered the tube. Strontium, barium, zirconium and uranium were expected to enter the tube as aerosols but the experimental measurememts did not confirm this.

Most elements showed very similar behaviour in the two experiments. The exceptions were caesium and iodine. Caesium was probably mostly in the form of caesium hydroxide in Fal-18 and the less volatile caesium borate in Fal-17. The iodine was probably present as caesium iodide in Fal-17 but not Fal-18. Both RAFT and VICTORIA predicted the deposition of aerosols by thermophoresis adequately. They were less satisfactory for the vapours.

RAFT does not model any species involving boron and in the experiment without boric acid (Fal-18) it made a reasonable calculation for the caesium and iodine deposition. For tellurium it was less successful. RAFT predicted a large amount of chemisorption that was not observed in the experiment.

VICTORIA underestimated the volatility of most elements. It suggested that indium and silver entered the tube as aerosol particles whereas the measurements showed that they were mostly vapour at these temperatures. The condensation temperature for tellurium was likewise overestimated. The deposition of caesium and iodine were not quite so well predicted as by RAFT in Fal-18, the test without boric acid. When boric acid was used, VICTORIA predicted, correctly as is believed, that caesium was associated with caesium borate but overestimated the temperature at which it condensed. As well as the difficulties in predicting the condensation temperature, VICTORIA in general underpredicted the magnitude of vapour condensation.

Some suggestions for the codes' poor prediction of condensation phenomena have been made. The thermodynamic data in VICTORIA are different to

those in RAFT and a comparison of the saturation pressure for caesium iodide showed that the difference was consistent with the observed difference in deposition profiles. Another possibility is that VICTORIA's assumption of ideal solutions in the liquid phase on the aerosol particle and on the pipe wall may not be justified. Any changes to this assumption would favour the experimental evidence that the volatility, particularly of species present in small concentrations, would be increased.

RAFT, on the other hand, assumes that each species condenses onto a particle or surface containing only that species. Modifications to the code have been made to enable it to treat ideal solutions of caesium iodide and caesium hydroxide. The results, reported in [35], did not show a large difference from the standard case but further work is in progress to investigate more complex assumptions.

International standard problem 34

The CSNI-sponsored International Standard Problem (ISP) 34 was based on two experiments that were performed at the Falcon facility in AEA Technology, Winfrith. The first experiment was a low humidity, high aerosol concentration experiment, while the second one was a high humidity, low aerosol concentration experiment. The JRC submissions consisted of three calculations for the primary circuit fission product transport and retention; calculations for both experiments were submitted. The calculations were performed with VICTORIA/ESTER [36], VICTORIA-92-01 [37], and RAFT [38].

VICTORIA predicted that control-rod tellurides determine the behaviour of tellurium, while control rod iodides might be important in understanding the behaviour of iodine. Boron and caesium behaviour were coupled in ISP-1, where equal molar quantities were introduced in the Falcon silica tube and they reacted to form caesium borate, while their behaviour was decoupled in ISP-2, because boron was in excess.

Both VICTORIA analyses showed that deposition in the Falcon facility was strongly time-dependent. In particular, they showed that revaporization determines the boron deposition profiles, while changes in the carrier gas composition resulted in significant deposition speciation changes. The experimental procedure was criticized because it introduced abrupt changes in the carrier gas composition, e.g. the flow of steam and boric acid was simultaneously terminated in ISP-1. Moreover, the experimental results were considered very limited to validate the codes.

The VICTORIA code predictions were in reasonable agreement with experimental results for most species that behaved as aerosols (e.g. silver, uranium, barium, strontium). More significant differences were noted for species that condensed in the 48cm Falcon primary circuit. Typical results for caesium are shown in ***Fig. 1.24*** for VICTORIA/ESTER and in ***Fig. 1.25*** for VICTORIA-92-01. Both VICTORIA versions predicted correctly the overall magnitude of deposition, but the caesium deposition peak is shifted downstream: VICTORIA-92-01 predictions are in better agreement than VICTORIA/ESTER. ***Figs. 1.26*** and ***1.27*** show predicted and experimental deposition profiles for cadmium in ISP-1. The location of the deposition peak is correctly predicted, but the amplitude of the peak is underestimated. The experimental results and the calculations show that cadmium deposits by vapour condensation.

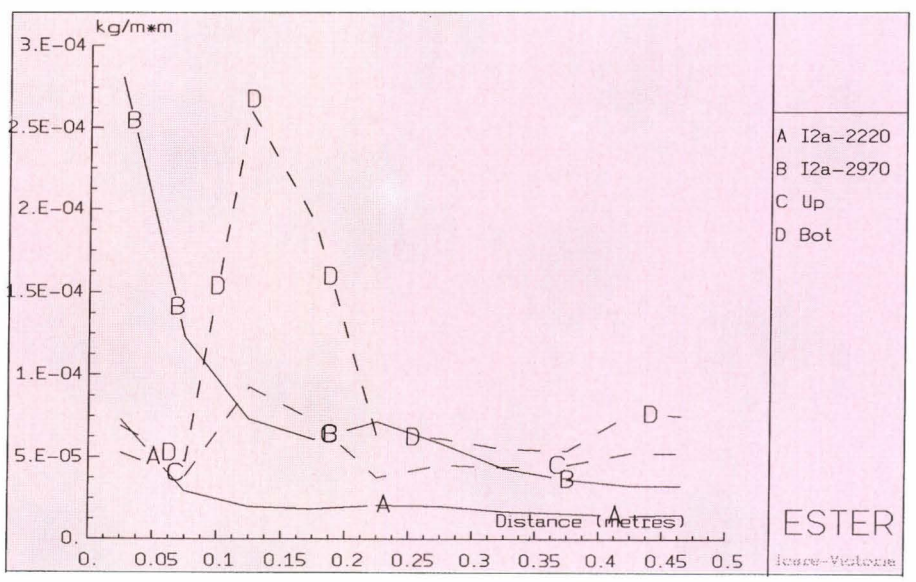

Fig. 1.24 Experimental caesium deposition values (dashed lines) and VICTORIA/ESTER calculated values (solid lines) for Falcon ISP-2

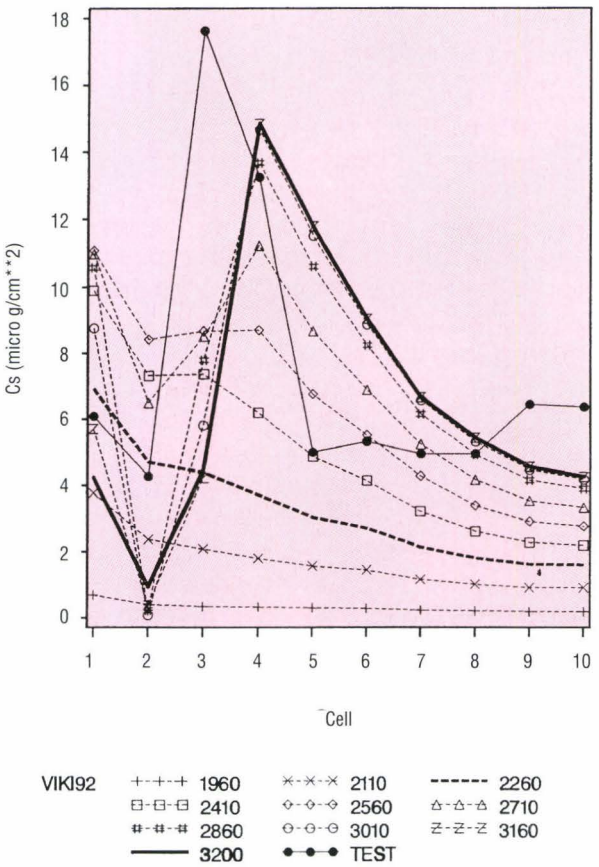

Fig. 1.25 Experimental caesium deposition values (dots) and time-dependent VICTORIA-92-01 calculated values for Falcon ISP-2

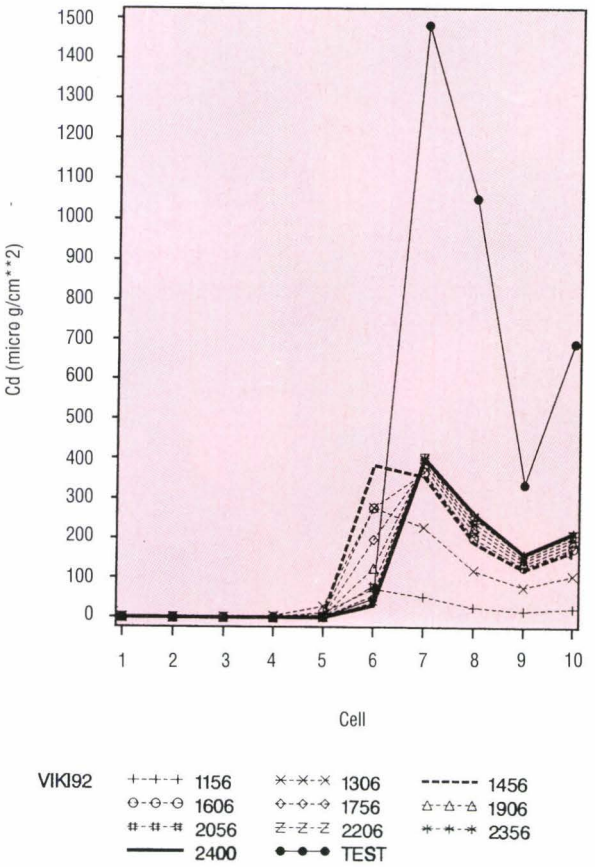

Fig. 1.27 Experimental cadmium deposition values (dots) and time-dependent VICTORIA-92-01 calculated values for Falcon ISP-1

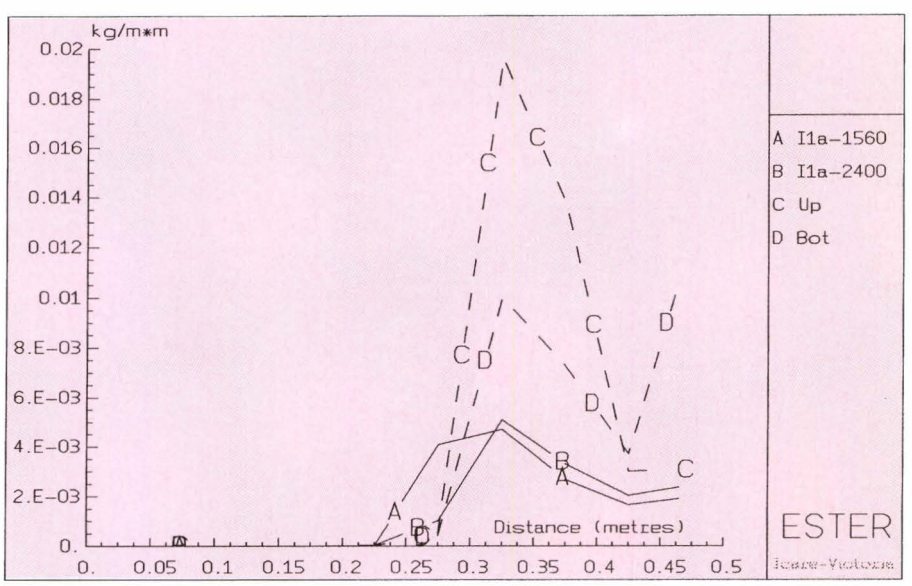

Fig. 1.26 Experimental cadmium deposition values (dashed lines) and VICTORIA/ESTER calculated values (solid lines) for Falcon ISP-1

Some differences between experimental measurements and VICTORIA predictions were attributed to inaccurate low-temperature approximations of the Gibbs free energies. In particular, it was suggested that the Gibbs free energy for boron species, caesium iodide (gas monomer and dimer, and condensed phase) is to be assessed.

RAFT has a much smaller thermodynamic data base than VICTORIA. In particular, it does not

contain data for caesium borate that dominated the behaviour of caesium in both experiments. Nevertheless, predictions for overall retention in the silica tube were of the right order of magnitude as *Fig. 1.28* attests for ISP-1. RAFT, as was the case with VICTORIA and the experimental results, predicted that cadmium deposited by vapour condensation towards the exit of the silica tube. Predicted cadmium deposition for ISP-1 is shown in *Fig. 1.29*. RAFT overpredicted silver and tin deposition at the entrance wall because in the calculation they were introduced as gases in the silica tube which would condense on the entrance walls.

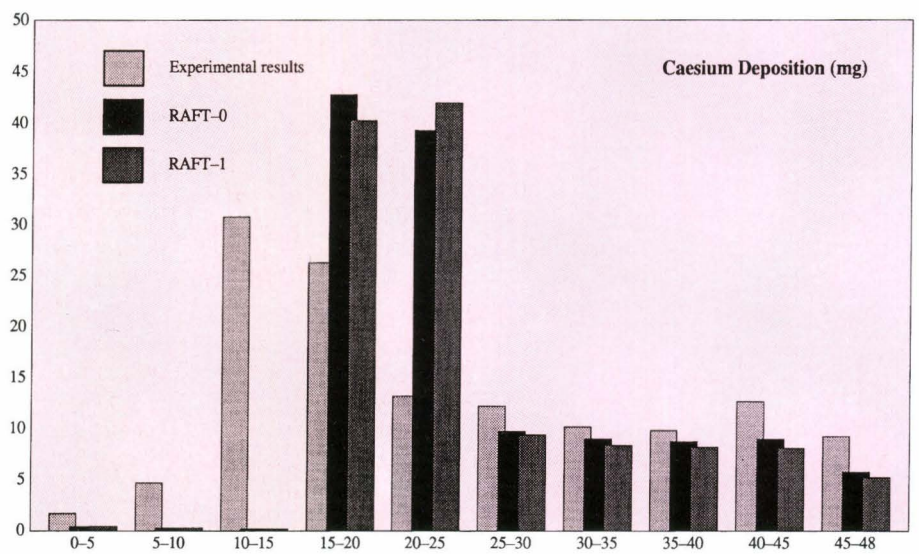

Fig. 1.28 Comparison of experimental measurements and RAFT calculated values for caesium in Falcon ISP-1

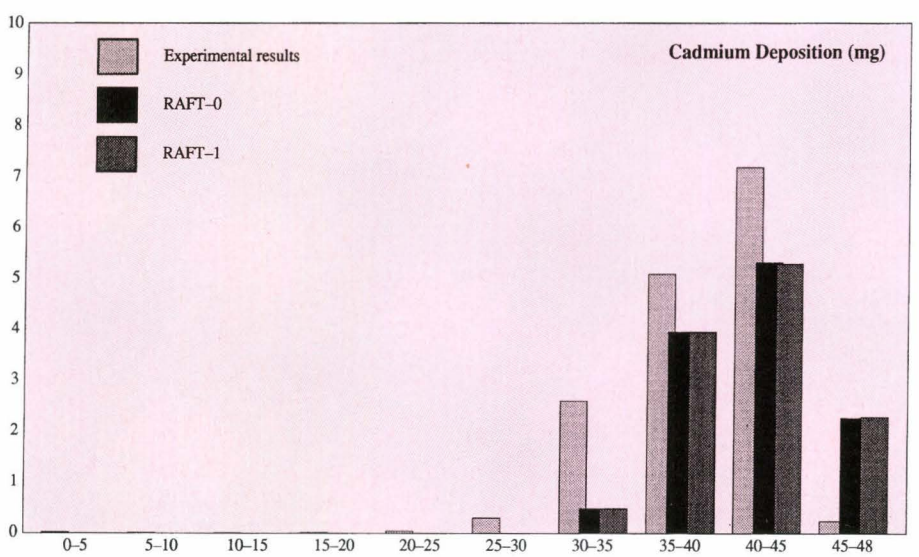

Fig. 1.29 Comparison of experimental measurements and RAFT calculated values for cadmium in Falcon ISP-2

Fundamental studies

A study performed by the University of Cambridge on the fundamentals of aerosol transport and deposition has been completed, and a final report received [39]. It begins by surveying the problem of the transport and deposition of small particles in large and medium-diameter pipes and in other geometries (bends, flow restrictions), under flow velocities ranging from 1-2 m/s to 100 m/s and more. Currently used models are criticised for not taking account of the structure of the turbulent flow, but at most only of its intensity. Turbulence structure effects may be very important in cases where secondary flows exist, where turbulent impaction is important etc.

It is shown that in many problems one can separate the treatment of particle transfer to surfaces into three parts: transport in a turbulent "core" flow, transfer from the core to a thin boundary layer, and finally deposition from this boundary layer to the surface. Classical models can handle the first and last parts quite well, but seem inadequate for the intervening transfer process. In this process an important role is played by "crossing trajectories" i.e. the particles do not follow the paths of the fluid elements because of their inertia, and so have a different "diffusivity" to the fluid.

The (directional) particle diffusivity in turn depends on the turbulence

structure. The report reviews techniques for simulating turbulent flow fields, and notes that few of them display a realistic structure (or appropriate spectral characteristics). Some results from the very few existing calculations of particle interactions with structured turbulence are given. The report also includes some wind tunnel experiments which attempt to verify the calculations. It proves experimentally difficult to produce values for the appropriate non-dimensional parameters which fall within representative ranges. Nevertheless, if the theory could be validated in some neighbouring parameter range one would have more confidence in its extrapolation.

CONTAINMENT MODELS

Thermalhydraulics

The ESTER version of the applications JERICHO-AEROSOLS-IODE and RALOC, developed respectively at CEA (France) and GRS (Germany), have been successfully installed and tested at Ispra. Hence the user of ESTER now has a choice of thermalhydraulics code. JERICHO [40] from CEA, CONT [41] from MATEC, Milan, RALOC [42], from GRS, Garching, and FIPLOC [43] from GRS Munich. The advantage of ESTER for these codes is that it provides a means whereby the results from the thermalhydraulics can be applied as boundary conditions to codes that calculate other containment phenomena. JERICHO can be coupled with ESTER tools to the aerosol code AEROSOLS-B2, the iodine chemistry code IODE and the Franco-German core-concrete interaction code WECHSL. CONT can be coupled to NAUA, RALOC is coupled to models for hydrogen behaviour and FIPLOC also models fission product behaviour.

The prediction of thermalhydraulic behaviour in reactors and experiments depends crucially on the modelling of heat and mass transfer processes. The University of Pisa [44, 45, 46] has made a literature study of all available correlations and compared the results of lumped parameter models with finely nodalized models of condensing films.

Thermalhydraulics validation (ISP 35)

Ispra participated in the CSNI International Standard Problem (ISP) No. 35, a blind calculation for the NUPEC containment test M-7-1, with the objective of validating the CONTAIN 1.12 code with respect to hydrogen behaviour and spray effects on the thermalhydraulics [47].

The test M-7-1 used a 1/4 scaled PWR containment with 25 inner compartments and 66 connections between them. It simulates a Primary Cooling System break with, for the duration of 30 min, steam and helium (for hydrogen) injection in one SG foundation and spray activation in the dome. The steam flow is at 438 K and decreases linearly from 0.08 to 0.03 kg/s, while the helium flow rate is supposed to increase from zero to 0.03 kg/s during the first 15 min and then to decrease again down to zero in the following 15 min. Simultaneously the spray is activated with a constant flow rate of 19.4 kg/s at 313 K.

Thirteen organisations participated in the exercise using 8 different codes (CONTAIN 1.12, RALOC, FUMO, WAVCO, MAAP, COMPACT, MELCOR and WGOTHIC). CONTAIN has been used by AEA, JAERI and SNL besides JRC. The participants had to provide the temperatures, as function of time, in the numerous compartments of the building and in many external walls and internal partitions, the time-varying helium concentrations, and the fluxes between compartments.

Experimental results have now been released [48]. ***Fig. 1.30*** shows the temperature distributions for the various compartments, while the calculated values with CONTAIN at JRC, SNL, AEA, JAERI and those obtained with WAVCO at PSI are represented in ***Figs. 1.31***, ***1.32***, ***1.33***, ***1.34*** and ***1.35*** respectively.

As can be seen, the experimental temperatures converge all in a rather narrow range compared with the CONTAIN calculations, which give a wide spread of temperature distributions. The reason might be that CONTAIN does not allow a realistic description of the spray features in a complex configuration such as the M-7-1 test (compartments located in more than two floors). In the early phase the temperatures tend to be lower than the experiment maybe because of the more effective insulation than specified.

Besides the CONTAIN calculations (mainly SNL, AEA and JAERI) show a remarkable atmosphere temperature rise after the mixture gas injection ended. The rise might be due to the convective heat transfer from the wall surfaces which maintain a relatively high temperature, because the spray impact on the walls is neglected in the CONTAIN spray modeling. A similar but much less accentuated trend is observed in the experimental results. The temperature distributions obtained with WAVCO (***Fig. 1.35***)

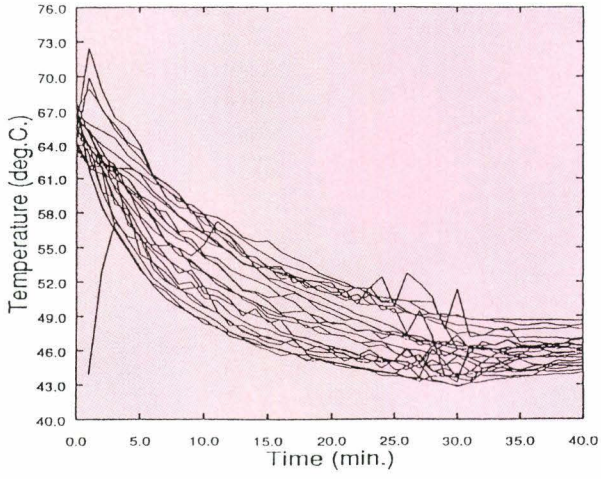

Fig. 1.30 ISP-35: Temperatures-experim.

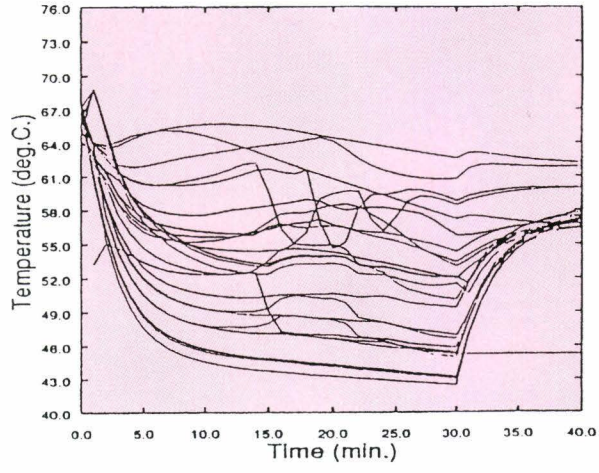

Fig. 1.33 ISP-35: Temperatures-AEA

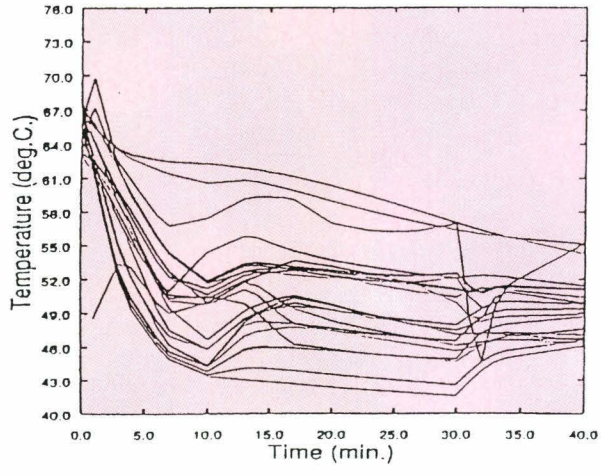

Fig. 1.31 ISP-35: Temperatures-JRC

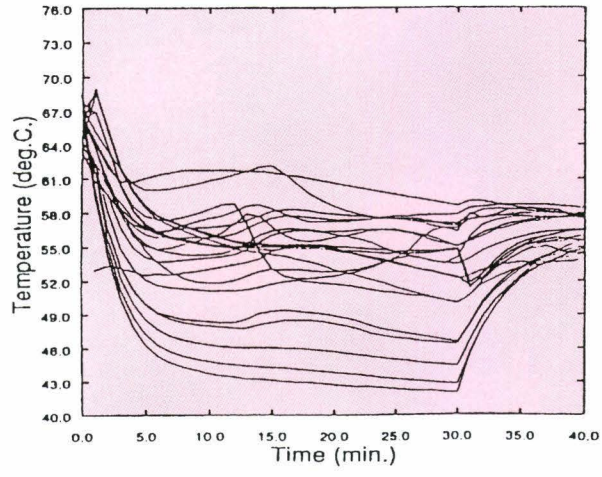

Fig. 1.34 ISP-35: Temperatures-JAERI

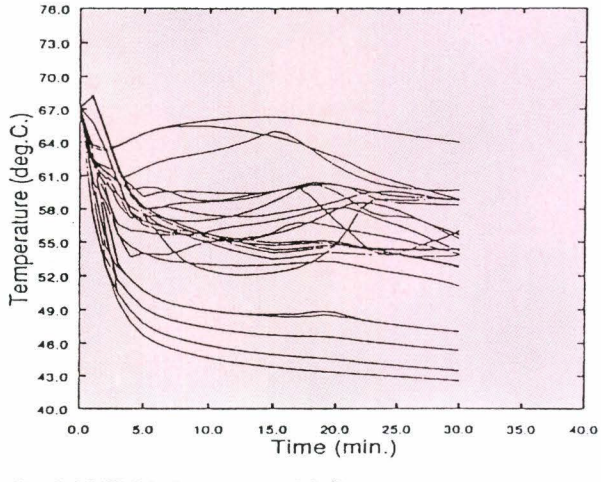

Fig. 1.32 ISP-35: Temperatures-JRC/SNL

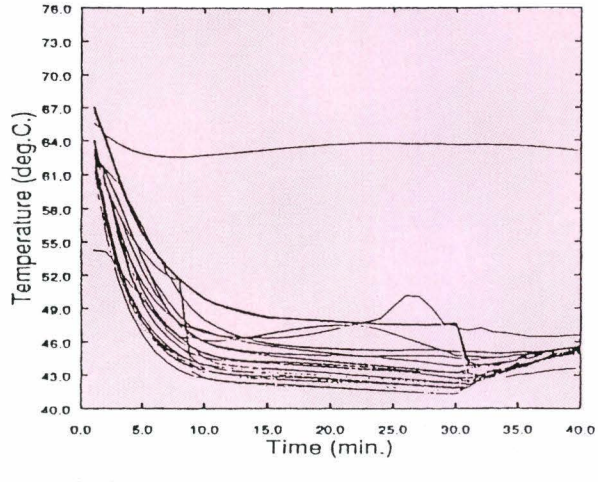

Fig. 1.35 ISP-35: Temperatures-PSI

show a very narrow spread, the results being on the other hand somewhat underestimated.

The measured helium concentrations (*Fig. 1.36*) were almost the same for all rooms except for those immediately above the injection room, showing a good mixing induced by the spray. The CONTAIN calculations, especially at JRC (*Fig. 1.37*) describe rather well the experiment. Other code predictions, such as RALOC and FUMO, deviate significantly.

Concerning the flow loops inside the containment, large discrepancies have been found in the various calculations, sometimes performed also with the same code. Further investigation is required.

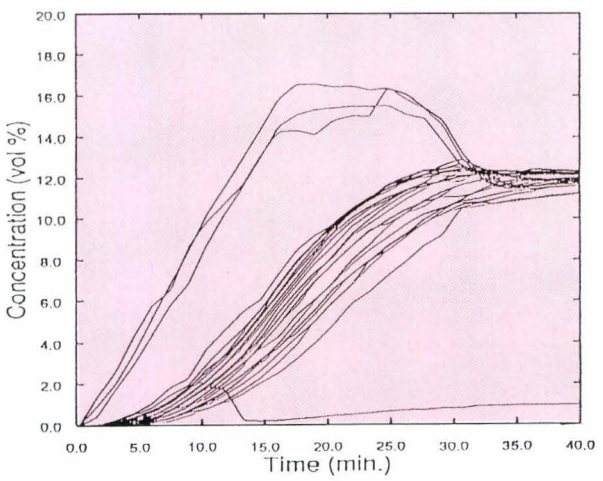

Fig. 1.36 ISP-35: He concentrations-experim.

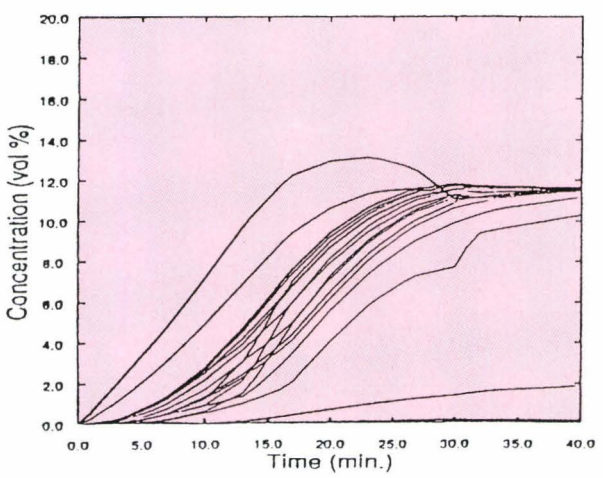

Fig. 1.37 ISP-35: He concentrations-JRC

Aerosol physics

Containment aerosol physics models available and tested in ESTER include FIPLOC from GRS and AEROSOLS-B2 from IPSN, while the USNRC code CONTAIN is available separately. AEROSOLS-B2 is coupled to the thermal-hydraulics code JERICHO within ESTER. CONTAIN has been applied to a large number of Phebus problems (although no experimental results are yet available for validation), some of the results being given in previous sections. For FIPLOC and AEROSOLS only the test problems supplied by the code developers have been run. Once some problems associated with the transfer from one type of computer to another had been resolved the supplied results were satisfactorily reproduced.

Chemistry models (IODE,INSPECT)

Two ESTER applications are concerned with the computation of iodine chemistry in the containment, the codes IODE and INSPECT. The ESTER versions were released during 1993, successfully installed and correctly tested at Ispra, at least with the test problems. The first code was developed by CEA, France and the latter by AEA, Harwell. IODE is one module of the coupled application JERICHO-AEROSOLS-IODE.

Core-concrete interaction models

ESTER has models for the interaction of corium with concrete (WECHSL) and for heat transfer in the resulting cavity (CALTHER). Both are coupled with the containment thermalhydraulics code JERICHO, and were adapted to ESTER jointly by CEA and KfK [49]. They have been successfully ported to Ispra and tested.

ESTER Development

A version of ESTER containing a very few physical models but with a fairly complete set of tools and services was issued at the end of 1992 (version P1). A recent publication on the status of ESTER is given in ref. [50]. It is planned to issue a new version, P2, early in 1994 to a limited number of users for independent testing and assessment, after which a formal version, v1, will be released at the end of 1994. In 1993 all the modules which will go into version P2 were received (largely from SCA contractors), and the newly set up Maintenance Team performed the arduous task of testing them all, verifying the documentation, and incorporating some recent updates of the models. One of the problems with the develop-

ment of a code system such as ESTER is that in the severe accident area the component models and codes are continually being improved and extended.

One important example arose when new versions of the bundle degradation module ICARE and of the circuit FP transport module VICTORIA were received. Thanks to the flexibility of the ESTER data structure it proved possible to create a fully updated version of the coupled ICARE-VICTORIA application described in the previous Annual Report. The basic RSYGAL library has been updated by CISI Ingenierie under a contract. JRC tests have shown that the improvements are mostly transparent to the various ESTER applications. A meeting of the User Club was held in June, where several valuable suggestions for the improvement and extension of ESTER facilities were received. ESTER applications are now the preferred STI tools for Phebus test and Falcon test analysis in several areas, so contributing to ESTER validation.

In the new year it is planned to equip ESTER with portable and easy to use installation procedures, and to create the drivers and data interfaces necessary to support the applications which will comprise the P2 version of the code.

RSYGAL toolkit and RPCs

The new RSYGAL toolkit version 1.3 has been released in September by the contractor CISI Ingenierie. This version took into consideration some remarks from the Users' Club and fixed some errors. The new tool VISU has been implemented. Its purpose is to visualize graphically specific variables during the execution of an application, allowing an easy control of the run. A graphical driver, compatible with the graphical Lahey library for PC, has also been added. The TPAGE tool was modified in order to accept input data from the user, directly from the TPAGE window. The TMENU and TEVOL tools have not been modified. The routines related to the TGLIB and the "analyser" have been grouped together with the BASE library. This new structure is not particularly well suited in the case of the integration of applications that do not need the graphical libraries. RSYGAL v1.3 is still in a test phase; some errors were found and transmitted to CISI.

A specific tool based on Remote Procedure Calls (RPC), to distribute an ESTER application among different processes was developed by IKE, Institut für Kerntechnik und Energiesysteme, Stuttgart, and released to Ispra during 1993. A distributed ESTER application is mainly justified when there is no possibility to have all the ESTER modules of a code system on the same computer, for portability or license problems or when the computing power is heterogeneously distributed among the modules. Thanks to the RPC routines, modules may be included in ESTER without being ported. RPC routines are based on the SUN/RPC library. Two elementary and one global test implying the distribution of an ICARE2 run, the visualization of some variables during its execution and the use of a database server onto three different computers (SUN, IRIS, CRAY2), were successfully executed. A more representative case should be tested in the future. The ICARE2-VICTORIA coupled code should be a good candidate.

Another tool called 'the reporting system', to trace the instrumented variables in an ESTER application, was developed and released in March 93 by AIB Vinçotte Nuclear, Brussels. The software has been distributed to the various developers and users.

Module integration

The first preliminary version of ESTER, distributed since 1992, contains the RSYGAL tools (version 1.2), the bundle degradation application ICARE2 and the fission product release application FPRATE. During 1993, a large number of new ESTER applications have been released by the SCA contractors and successfully installed and tested at Ispra. They are listed in ***Table 1.4***. Furthermore, the thermalhydraulics ESTER module CHIP (circuit) was released in the second half of the year by the SCA contractor CISI Ingenierie, France.

ICARE/VICTORIA

The ESTER version of the fission product transport code VICTORIA has three main advantages over the stand-alone version. Firstly the input data preparation is easier and less prone to error. Secondly the imposition of thermalhydraulic conditions, calculated by ICARE in this case, to VICTORIA is automatic. Thirdly the user can use a set of macros written in the "analyser" language to post-process the results.

The first version of ICARE/VICTORIA had already been distributed in 1992 and is being heavily used to examine phenomena in facilities such as Phebus, Falcon and STORM. During 1993 the new version of ESTER-VICTORIA was received from Winfrith incorporating many modifications. It now treats 288 chemical species rather than 167. This integration with a new version of ICARE (2v2mod1) was accomplished in a relatively short time because the ESTER concept requires little modifications to the modules

being coupled. Most of the work is done by "interface" modules. These remained practically unchanged even though both ICARE and VICTORIA had been changed. The new version of ICARE-VICTORIA will be distributed when the documentation is complete and some checks have been made to compare the results with those of the old version.

JERICHO/AEROSOLS/IODE

Each module is an "application" in ESTER terminology. More complex applications are combinations of modules which work together to achieve a particular task. An example was mentioned above: ICARE/VICTORIA calculates bundle degradation, circuit thermal-hydraulics, FP release and FP transport in the circuit. Another example is JERICHO/AEROSOLS-B2/IODE, created under contract by CEA [51, 52]. This application calculates containment thermal-hydraulics, aerosol physics and iodine chemistry in a coupled manner.

The driver routine provides considerable flexibility. The codes can be run separately (stand-alone) or coupled. Coupling can be by "chaining" (e.g. run JERICHO, store intermediate thermal-hydraulics results, run AEROSOLS using these intermediate results as input) or by interchange of data every timestep. Some test cases show that the latter is preferable when conditions change rapidly, e.g. when there is a hydrogen burn.

Installation and Users' Club

More then ten new ESTER applications and modules have been successfully installed at Ispra, during 1993. It is a far from straightforward process, but rather an iterative one. In fact, the codes developed by the different partners in the context of the SCA contracts did not fulfill immediately all the requirements. A clear description of the installation of the codes was rarely given and bugs or errors were sometimes present. Very often, the result file corresponding to the test case to verify the correct installation of the code, was missing. A user manual and a model description manual were not systematically distributed together with the software or were distributed only on paper and not on tape or disk. The codes installed at Ispra have at least reproduced the results of the test problem(s). In some case the graphical procedures were also tested (KESS3). The different applications listed in ***Table 1.4*** are now being integrated into the RSYGAL (version 1.3) file structure.

Table 1.4 List of ESTER applications for version P2

Code	Version	Description	Company
ICARE2	2.01	core/bundle degradation and thermalhydraulics, circuit thermalhydraulics	CEA
KESS3	1.7	core/bundle degradation and thermalhhydraulics	IKE
VICTORIA	1992	circuit, transport, retention	AEA
DEIMOS	1.0	circuit, thermalhydraulics	MATEC
BUSCA	1.1	circuit, pool scrubbling	AEA
JERICHO- AEROSOLS- IODE	3.1 3.0 3.0	containment, thermalhydraulics containment, aerosols physics containment, iodine chemistry	CEA
FIPLOC	1.5	containment, aerosols physics	GRS
RALOC	2.2	containment, thermalhydraulics hydrogen combustion	GRS
CONT	1.0	containment, thermalhydraulics	MATEC
INSPECT	1.0	containment, iodine chemistry	AEA
WECHSL- JERICHO	3.3 3.3	containment, core-concrete interactions containment, thermalhydraulics	CEA

During the year, the ESTER preliminary version P1 has been transmitted to three new users: ENEA - Bologna, NNC Limited - Chelford, UK, and AEA Technology - Risley. The application ICARE2-VICTORIA was transmitted to FZR, Institut für Radiochemie - Dresden and CISI Ingenierie - Cadarache. The BUSCA application was distributed to CEA - Cadarache. The number of users is growing and other potential users have shown interest.

At the beginning of June, the second ESTER Workshop took place at Ispra and was followed by a training for beginners on the use of the RSYGAL tools and by the Users' Club meeting. An advanced programming course, foreseen during 1993, was postponed to 1994. The user club meeting pointed out some requirements like the possibility to obtain an ICARE-ESTER version suitable for CORA test calculations. Continuous developments of the TIC graphics library will improve the general presentation and quality of the pictures.

A major contribution expected from the users concerns the testing and validation of ESTER for different applications and different computers, and the discovery of bugs. Cadarache was planning to conduct validation calculations with ICARE2 for PBF, CORA and Canadian tests. It was requested from Ispra to keep members informed about ongoing test calculations and results achieved. It was found essential that validation tests be carried out by different laboratories using identical input data. The Ruhr University (Bochum) is carring out a code comparison study with RELAP, MELCOR, ATHLET and ICARE with CORA test calculations. The results could be made available to Ispra.

MAINTENANCE, DEVELOPMENT

During 1993, the maintenance team, set up in 1992 in order to manage the evolution of ESTER and to help the users and the developers, was operated jointly by Ispra and CISI. CISI assumed the maintenance of the RSYGAL tools, under contract, whilst Ispra was responsible for the maintenance of the ESTER applications. CISI had also to specify the functions of the maintenance team and the rules to follow. They have been formalised in a "maintenance guide" which has to warrant the respect of quality assurance requirements and the consistency of the maintenance work in the future.

The maintenance guide, which should be updated annually, defines the tasks of the maintenance team, the maintenance staff, the computers and informatic supports on which ESTER will be distributed, the management of the versions, the handling of exchanges with the users, the new developments foreseen and the maintenance databases. A one day maintenance team training for JRC staff was provided at the end of the 2nd ESTER Workshop. TMENU and TEVOL are the RSYGAL tools concerning the maintenance of ESTER.

Installation and demonstration procedures must be written in order to integrate the applications and corresponding documentation with RSYGAL. An ESTER user manual must be written and more tests must be made before the release of the new ESTER preliminary version P2 to the users, foreseen during the first months of 1994.

Further versions of ESTER will include the Remote Procedure Calls tested with a more appropriate case, new applications (CHIP) or more recent versions of existing applications (ICARE2 mod1) and more consolidated tests. The software will be ported and tested on computers other than SUNs.

STORM Project

The STORM (Simplified Tests On Resuspension Mechanisms) Project has been initiated in 1991 to study the behaviour of fission products and aerosols in reactor components. The STORM facility, see ***Fig. 1.38***, allows representative experiments under prototypical accident conditions like LWR Station Blackout, PWR V-Sequence, etc. Especially the effect of high gas velocities (up to 200 m/s) on the deposition and resuspension of aerosol particles in pipework will be investigated [53]. The STORM experiments will provide a representative data base that will serve to better understand the mechanisms of deposition and resuspension of aerosol particles. The development and validation of theoretical and semi-empirical deposition and resuspension models to be included in nuclear aerosol codes are the final target of the programme.

In December 1991 a contract between ENEL (Italian Electricity Board) and JRC has been signed for cooperation on the STORM Project [54], whereby ENEL is providing significant financial and technical support. The STORM Project is proposed as an international experimental programme with partners inside and outside the European Community [55].

During 1993, the following tasks have been completed:

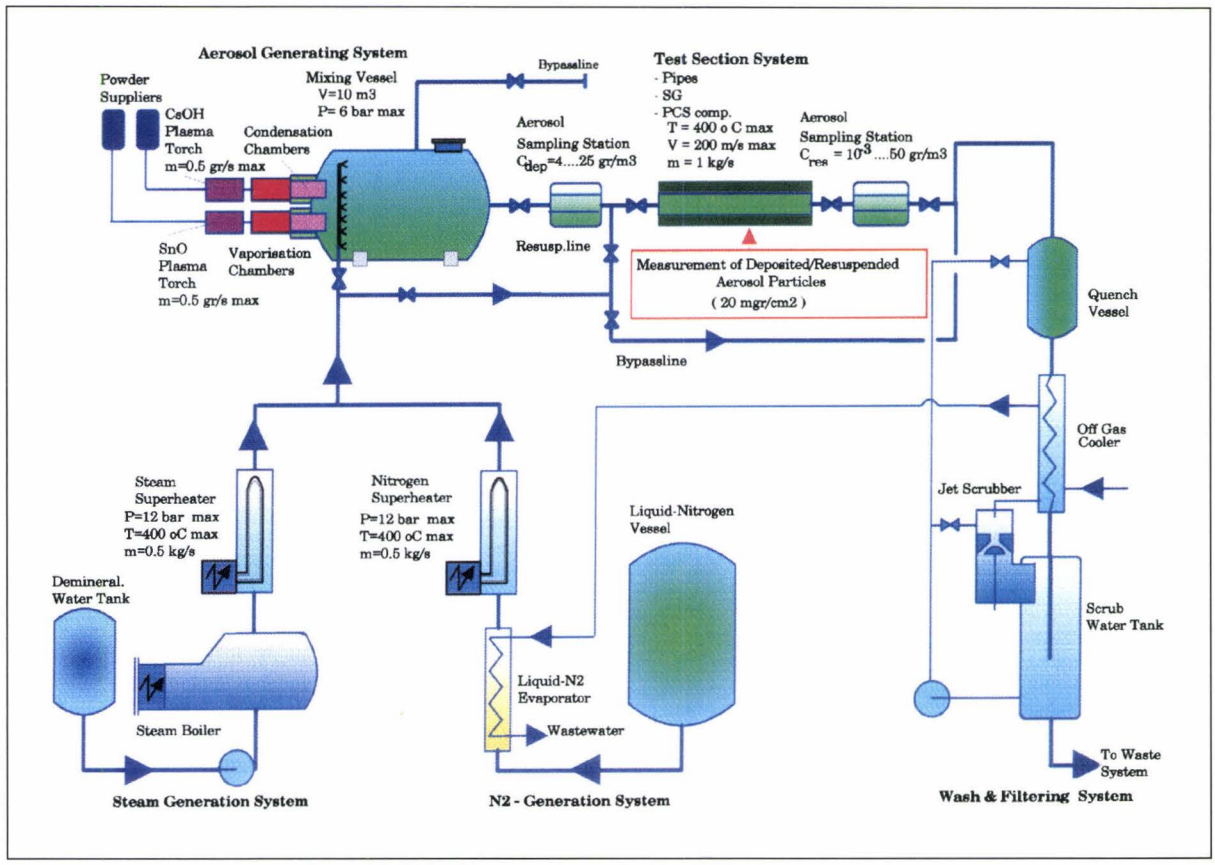

Fig. 1.38 STORM facility

- the design of the facility has been completed and major components have been delivered (the steam and nitrogen supply system, the plasma torches, the mixing vessel, the wash and filtering system). Some very specific components are presently under construction, such as the vaporisation chamber and the condensation pipe. They will be delivered early in 1994;
- the construction of the facility has been started with the installation of all the major components of the facility. The work will continue by assembling the connecting pipeworks, valves, instrumentation, etc. The execution of the first commissioning tests is scheduled for May 1994;
- the control system has been finalised and will be installed in the STORM control room at the beginning of 1994;
- the civil works in the experimental hall have been completed with the preparation of all the foundations for the components and of the channels for piping and electric cables;
- the installations of the main electrical components and of the cables have begun;
- the thermo-hydraulic instrumentation is ready;
- the advanced instrumentation is partly ready (impactors, filters, laser single particle light scattering system, laser extinction system) or under construction (sampling station and radiation system);
- the calibration rig for the on-line optical systems has been designed and build-up. The calibration of the optical instruments has been started and the first results are expected in early 1994;
- thermo-hydraulic calculations have been performed in support of the facility and the aerosol generation system design;
- first aerosol transport calculations have been performed for selected components of the facility;
- a first STORM meeting was held in Ispra in April '93 to present the STORM Project to international organisations [65];
- a second STORM meeting was held in Ispra in December '93 to launch international benchmark calculations on STORM experiments.

The STORM Facility

The Storm facility consists of four main sections, as shown in the schematic representation in *Fig. 1.38*. The first section is the aerosol generation system, which supplies the different condensation aerosols for the experiments. The second is the steam generator and the steam- and nitrogen superheater for the generation of the required carrier flow. The type of carrier will make a considerable difference when using the strongly hygroscopic caesium hydroxide. The generated aerosol (CsOH and SnO_2) is mixed with the carrier gas in the mixing vessel (10m^3). This vessel allows establishment of particle size distributions, typical for the accident scenario. During the propagation of particles through the vessel, they can age and agglomerate. At the same time, the vessel acts as a coarse particle filter due to the deposition of larger particles at low velocities. The third section, the test section (pipe works, valves, components), is mounted downstream of the mixing vessel. The test section is situated within a furnace to maintain defined thermal conditions throughout the test. The final section is the wash and filter system. A central control system (PLC Siemens) controls the facility during the experiments. A workstation (DEC 5000/240) serves as the data acquisition system. All information necessary to document the test, (more than 300 data channels), is being stored. This includes all signals coming from experimental instrumentation as well as measurements characterising the thermo-hydraulic conditions throughout the facility. The most characteristic operating conditions are given in *Table 1.5*.

Table 1.5 Operating conditions for STORM experiments

Carrier gas flows rate: – nitrogen – steam	 up to 0.5 kg/s up to 0.5 kg/s
Carrier gas velocity 63 mm dia. straight pipe	10-200 m/s
Gas pressure	up to 0.4 MPa
Gas/wall temperature	up to 400 °C
Soluble aerosol mass flows rate (CsOH)	up to 0.5 g/s
Insoluble mass flow rate (SnO_2)	
Aerosol mass concentration during the deposition phase	up to 10 g/m^3
Expected aerosol aerodynamic mass median diameter	1.0-2.5 μm
Expected aerosol geometric standard deviation	1.9-2.3
Surface deposit mass loading	grater than 20 g/m^2

The aerosol generation system

Resuspension of aerosol particles will depend on the physical form of the particles. For solid aerosols, the deposit will be formed of agglomerates of particles, of variable dimensions and number of constituent particles. Single particles will be easier to remove by physical resuspension, while large agglomerates where single particles are strongly bound together could be much more difficult to break. If the deposited aerosol particles are liquid, they will tend to form a liquid film lying on the wall that is likely to inhibit physical resuspension. If the deposited aerosol contains a mixture of solid and liquid particles, there might be a threshold value of liquid fraction above which the deposit will behave as in the case of a purely liquid deposit. In order to investigate these different mechanisms and the existence and value of this threshold, there will be STORM tests with different fractions of liquid aerosols, from 0 to 50%.

Plasma torches are used in the STORM facility for the generation of aerosols both because they allow the production of condensation aerosols at high mass flow rates and they offer considerable flexibility of the aerosol species [56, 57, 58, 59, 60]. The aerosols are generated by injecting metal powder (tin) or a solution of liquid caesium hydroxide into the plasma flame (20,000 K), where they are evaporated. This generation procedure simulates the evaporation from the melting core and the subsequent slow propagation through the primary system. Because of the inertia of the evaporation process, a minimum residence time in the hot zone is required. From given transport velocities and the energies for liquefaction and vaporisation, the minimal length of the hot zone can be determined. To extend the exposure time of the powder to high temperatures the spray gun is flanged to a vaporisation chamber, see *Fig. 1.39* This chamber is made of magnesium oxide that resists temperatures of 2 800 K. The geometry of this chamber has been optimised to achieve the temperatures and flow conditions, required to make the aerosol vaporisation highly efficient. In the condensation pipe which is flanged to the vaporisation chamber the vapours are quenched by mixing them with steam and/or nitrogen of 673 K. The vapour condenses forming aerosol, of either droplets of caesium hydroxide or particles of tin dioxide. The SnO_2 aerosol particles will be transported from the condensation pipe to the mixing vessel by a carrier gas. Caesium hydroxide will still be in vapour form when entering the mixing vessel, and it should nucleate inside the mixing vessel.

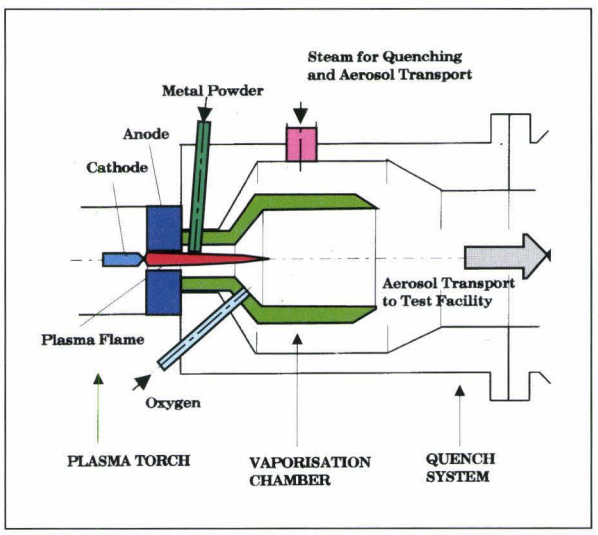

Fig. 1.39 Aerosol generation system

Instrumentation

To fulfil the target of the STORM Project, i.e. to understand the mechanical resuspension, a large reliable data base must be made available. This data base must characterise the process of deposition/resuspension reproduced in conditions typical of nuclear accident scenarios. The instrumentation selected for STORM is based, both on established methods (like those using particle's inertia) and on new advanced real-time techniques like optical and radiation methods, which guarantee a minimum of interference. The airborne aerosols will be characterised during the deposition and the resuspension phase using well established total mass filters and multi-stage cascade impactors [61]. The filters are used to measure the average mass concentration and the cascade impactors to determine the particle size distribution. The particles are separated onto different impactor stages due to their inertia at different velocities, i.e. they follow the streamlines or they impact with the sample plate. The sample flow for the impactors and filters is extracted from the main flow using isokinetic nozzles [62]. This guarantees that the particle size distribution in the sample is identical to the main flow. A set of 10 isokinetic nozzles has been manufactured to accommodate the wide range of velocities of the test matrix of the STORM experiments. To reduce the interference of the extraction nozzles with the resuspension process, and with each other, a sampling station (***Fig. 1.40***) has been elaborated for STORM [63]. This station avoids the extraction of separate sample flows for each impactor and filter by using only one common sample line. From the main extraction line leading into the sampling station fourteen legs branch of. Each of these legs contains either one filter or one impactor. Each leg contains remotely operated valves which allow the control of the timing of each sample taken, and two manual valves to isolate the sample under an inert atmosphere. PC-based software controls the timing of the valves. A separate filter in each leg allows the precise flow rate (without aerosol) to be established through each device before the sample is taken. The sampling station allows full coverage of the whole test with a series of samples, but with minimum interference.

On-line mounted optical systems are especially suited to characterise the aerosol generation and resuspension processes and to observe their temporal evolution. These techniques measure the interaction between particles and light without disturbing the flow. Interaction can be the integral attenuation of the light intensity by a particle collective due to absorption and scattering, or it can be the light scattering by single particles. Two optical instruments are used. The first is a laser extinction instrument which measures particle concentration and the volumetrically averaged particle diameters of small particles (< 2 μm). The second is a single particle laser scattering instrument which determines the particle concentration, the particle size distribution and particle velocity of larger particles (0.7 to 100 μm), see ***Fig. 1.41***. Windows have been mounted shortly before and after the test section and in the sampling line. These allow the observation of the aerosols during the deposition and the resuspension phase. The window in the sampling line allows observation of the aerosols at reduced velocities, and enables better control of the mass loading of the impactors and filters, which are mounted in the sampling station.

A major drawback of optical measurements is that the derived parameters are not mass related, but dependent on particle shape and the refractive index. To derive mass related parameters a test-rig has been built in order to perform the intercalibration of optical and mass related instruments. The test rig consists of a flow channel (d.i. 63 mm) designed to integrate all of the STORM instrumentation. Particles (latex and dust) of different defined size distributions, shapes, refractive indices and concentrations can be used. The performance of each instrument can be established for a wide range of parameters. During the STORM experiments this will allow the real time evaluation of the optical measurements.

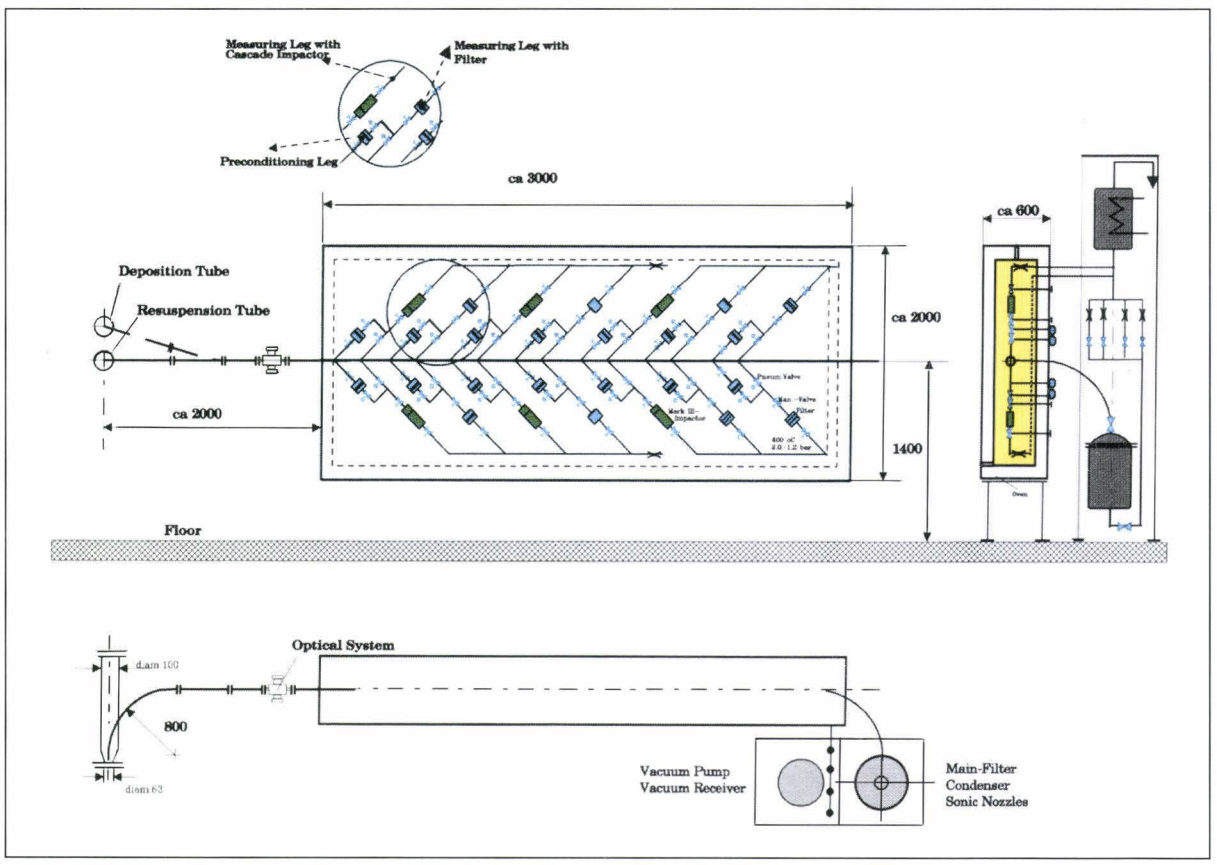

Fig. 1.40 Sampling station

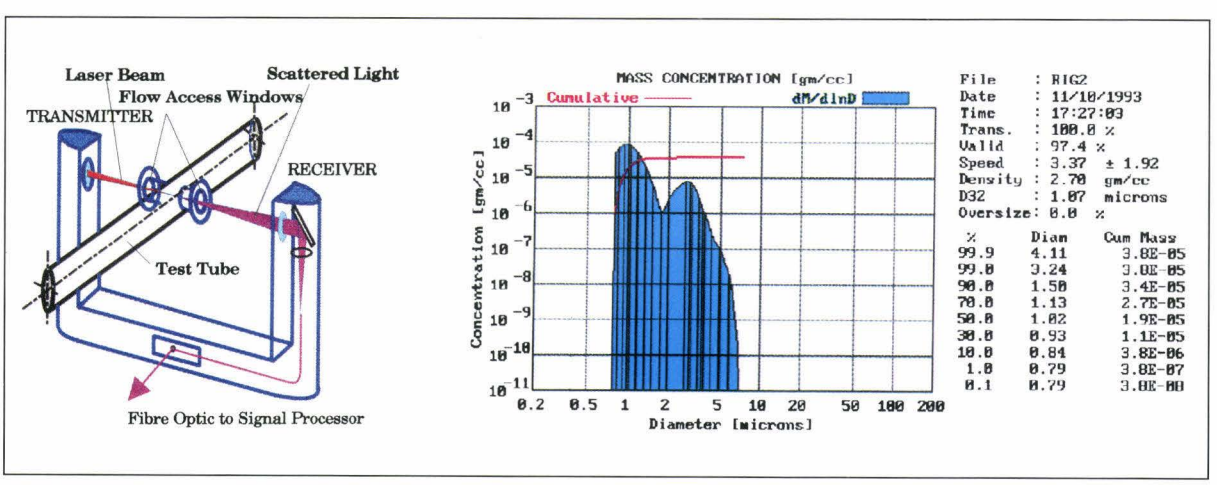

Fig. 1.41 Laser system

The deposition and resuspension process in the experimental pipe is measured using radiation techniques [64]. The deposit thickness as function of density and its evolution in time will be measured by transmission attenuation (*Fig. 1.42*). The gamma radiation from an 500 mCi americium-241 source passes through the test pipe and is attenuated by the tin and caesium in the deposit. Based on a pipe empty calibration the remaining wall effect can be eliminated from the resulting count rate. The film

thickness resolution will be greater than 0.2 mg/cm^2 for CsOH and SnO_2 aerosols. To measure the radial deposit profile in one plane four pairs of radiation windows are foreseen in a 45° arrangement. Chemical composition of the deposit will be obtained measuring the secondary fluorescence radiation. The primary gamma radiation from the americium-241 interacts with the deposit material and secondary fluorescence radiation (caesium 31 keV and tin 25 keV) is released. Using an energy dispersive detector the fluorescence radiation can be clearly distinguished from the scattered radiation. The magnitude of the fluorescence radiation is a mono-tone function of the specific chemical element in the film. To avoid saturation of the detector, the detector is positioned at an angle of 30° from the direct beam. Because the fluorescence measurements allow independent determination of caesium and tin, even lowest count rates can be analysed and film thicknesses down to 2 microns can be resolved.

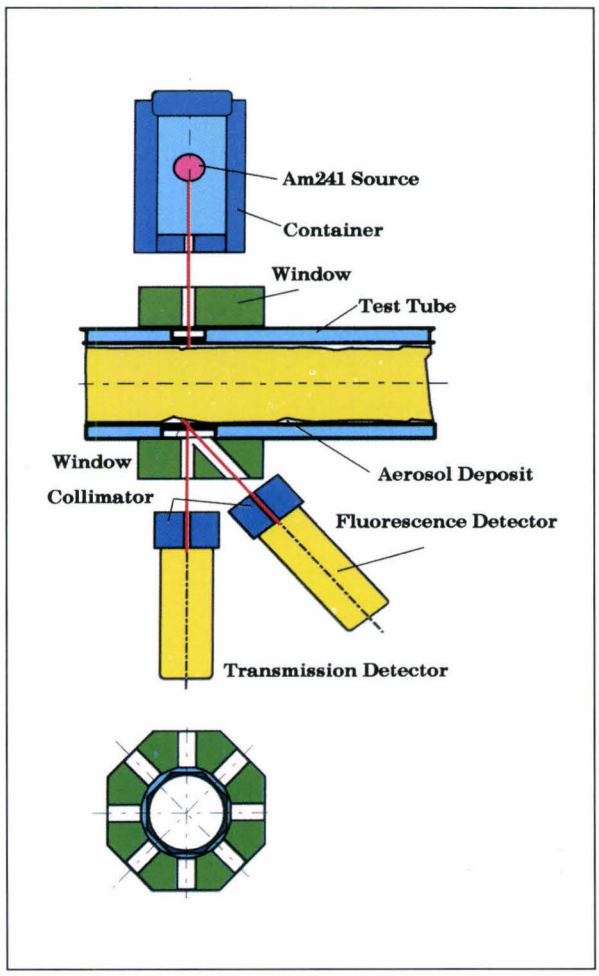

Fig. 1.42 Radiation technique for the deposit characterisation

STORM Experimental Programme

The initiation of the official STORM experimental programme is scheduled by the end of 1994, see ***Table 1.6***. The STORM shake-down tests will start in May 1994 and will be focused on the aerosol deposition mechanisms under different flow conditions. They aim at verifying the correct functioning of the facility and most of the aerosol instrumentation (impactors, filters, cyclones, optical laser system). The advanced instrumentation for the measurement of deposit thickness and chemical composition (based on radiation attenuation and fluorescence techniques), will be progressively installed in the loop, and calibrated. ***Fig. 1.43*** shows the temporal distribution of the measurements throughout the experiment.

In order to ensure that the ambitious and challenging objectives of the STORM Project can be met, a wide international consensus on the STORM Project must be reached. A STORM Consortium of supporting institutions has been proposed at the first STORM Meeting in April '93 [65] as an effective way to manage the project and to coordinate the experimental and theoretical programme. At the second STORM Meeting in December '93, international benchmarks on the thermo-hydraulics and on aerosol deposition/resuspension mechanisms have been proposed and discussed. Fifteen different organisations will participate in the benchmark exercise.

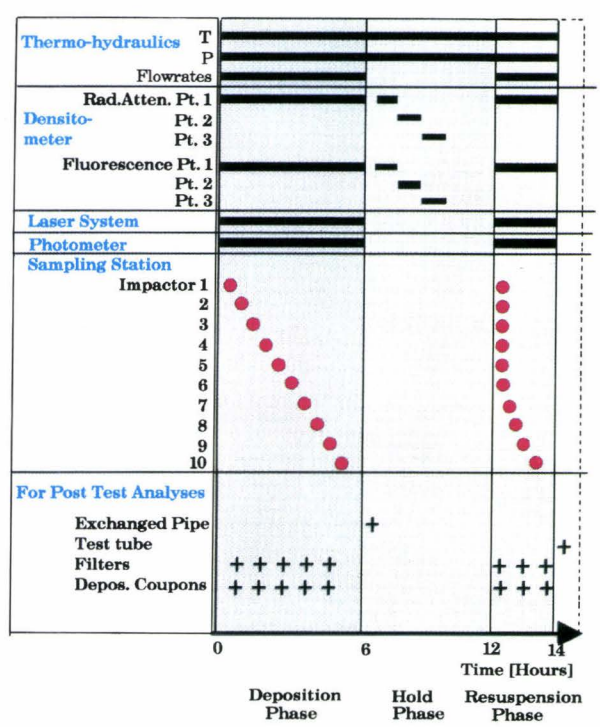

Fig. 1.43 Temporal distribution of the measurements

Table 1.6 Preliminary test matrix of the STORM scoping tests, with test pipe of 63 mm in dia, 5 m long

Scoping Test	Soluble Content (%)	Gas Velocity (m/s)	Resurpension Phase
ST01	–	10	NO
ST02	–	25	NO
ST03	–	50	NO
ST04	–	100	NO
ST05	–	200	NO
ST06	20	10	NO
ST07	20	25	NO
ST08	20	50	NO
ST09	20	100	NO
ST10	20	200	NO
ST11	50	10	NO
ST12	50	25	NO
ST13	50	50	NO
ST14	50	100	NO
ST15	50	200	NO
ST16	–	(*)	YES
ST17	20	(*)	YES
ST18	50	(*)	YES

* To be established on the basis of the previous test results

Computer Code Calculations

Analysis of reactor sequence calculations

The JRC undertook a detailed analysis of a number of severe accident sequence calculations performed in the past, namely a PWR station blackout, a BWR station blackout, a PWR small LOCA and a V-sequence. The calculations had been performed by ENEL with ECART, which includes a resuspension model, in the first three cases, and by the University of Madrid (UPM) with MELCOR (which does not model resuspension) for the V-sequence.

All these calculations show that physical resuspension of aerosol particles previously deposited on sections of the primary cooling circuit pipes might be an important factor in the determination of the source term. In particular, the calculations performed with ECART show that, coinciding with the core slump, there is a steep increase of the carrier gas velocity in parts of the circuit where there is a large concentration of particles deposited during earlier parts of the transient, like in PWR hot legs (***Figs. 1.44*** and ***1.45***).

In the V-sequence calculation with MELCOR, the

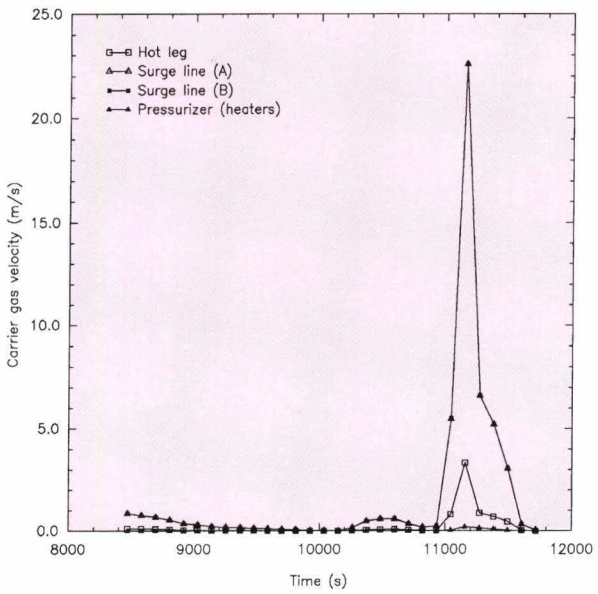

Fig. 1.44 Fluid velocity in PWR hot leg

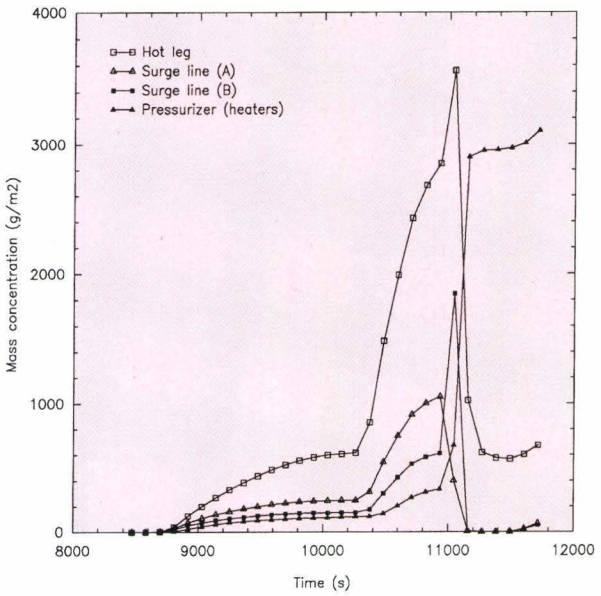

Fig. 1.45 Particles concentration in PWR hot leg

higher concentration of deposited particles is observed in the steam generator tubes, where the velocity is low and stable. A sharp increase of the carrier gas velocity is observed in the LPIS line and in the hot leg of the LPIS loop where deposition concentration is low. It will be important for STORM to determine the relative importance of the pre-existent deposition concentration versus the carrier gas velocity or velocity increase.

Thermohydraulics in the pipework

Preliminary thermohydraulic studies performed in support of the STORM programme have been carried out to provide input data for the aerosol transport codes. The analysis highlights the behaviour of the main flow parameters, such as temperature, pressure and velocity of the carrier gas in may points of the STORM facility, since those variables define the boundary flow conditions for the deposition and resuspension mechanisms.

A total of sixteen thermohydraulic calculations, which encompass the whole range of gas velocities expected in the STORM facility during deposition and resuspension, have been performed with the ICARE2 computer code, developed by the IPSN-CEA. The nodalisation of the circuit is shown in *Fig. 1.46*. Stationary conditions during three different periods were assumed:

- heat-up,
- aerosol deposition and
- particle resuspension.

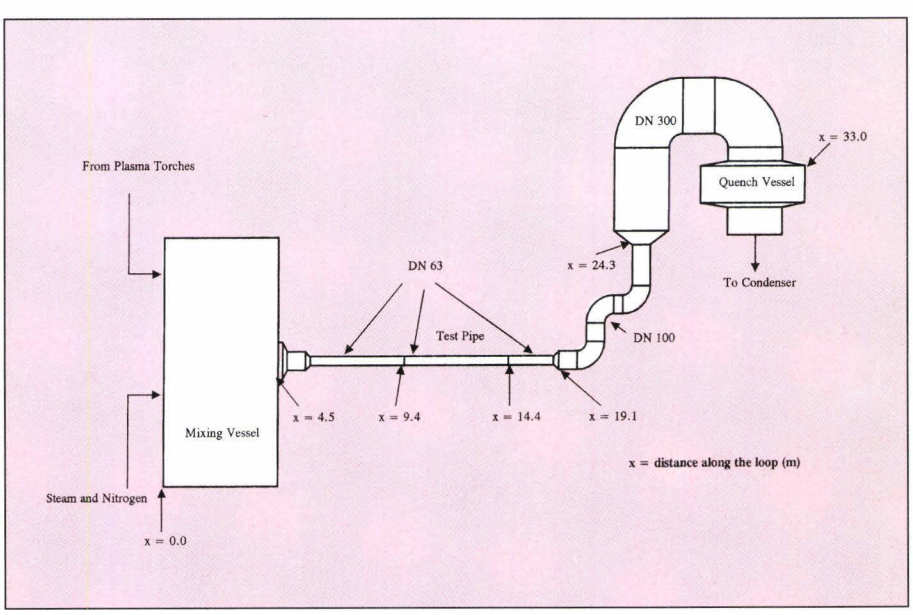

Fig. 1.46 Nodalisation of the STORM facility

The most remarkable results of the calculations are shown in ***Figs. 1.47*** to ***1.50***; from such results it can be concluded that prototypical flow conditions can be reached in the STORM facility with a fluid velocity ranging from 280 to 10 m/s and a pressure from 0.25 to 0.1 MPa. Therefore, the deposition/resuspension mechanisms can be studied under turbulent flow conditions, similar to those expected in the reference scenarios during severe accidents.

In addition, a number of three-dimensional thermal-hydraulic calculations were performed to evaluate the circulation and temperature patterns inside the 10 m^3 mixing vessel. A very strong buoyancy effect is predicted, due to the high temperature (and low density) of the gas leaving the condensation pipe. Higher velocities are predicted upstream from the inlet to the top of the vessel and along the top, with considerable recirculation along the bottom of the vessel. The temperatures drop rather quickly near the inlet, with most of the wall remaining close to the temperature imposed by outside heating.

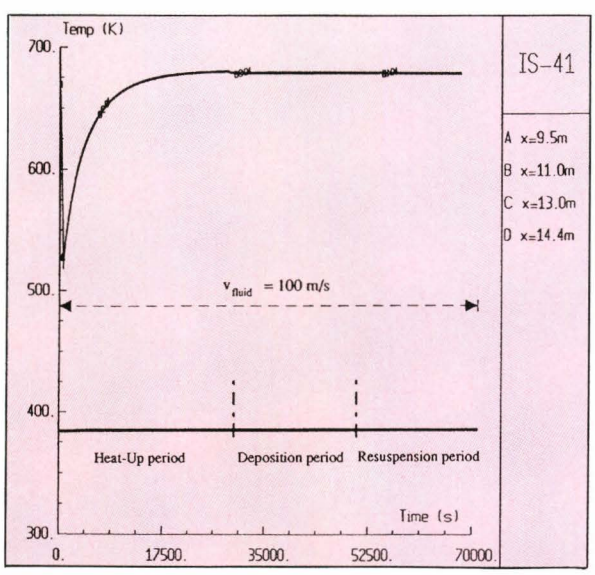

Fig. 1.47 Temporal evolution of temperature IS-41

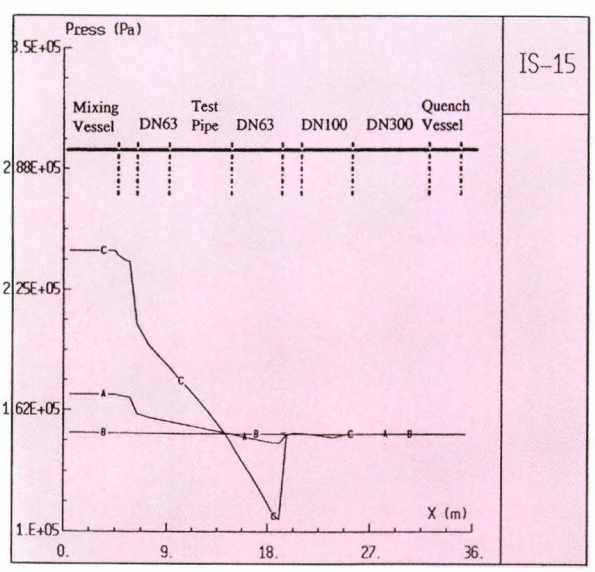

Fig. 1.49 Spatial evolution of pressure IS-15

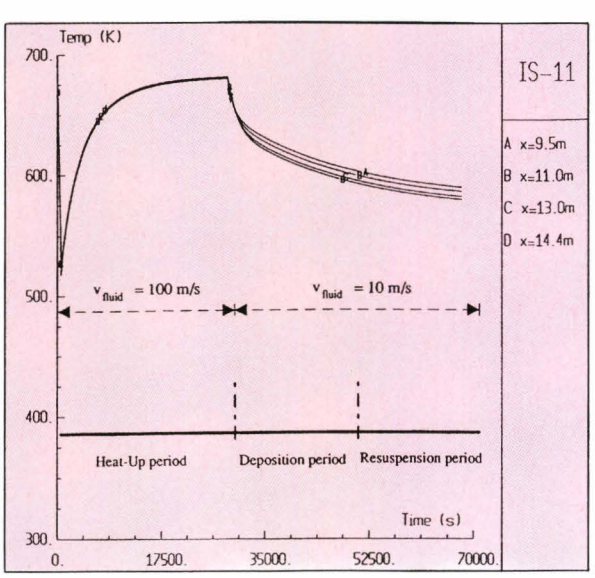

Fig. 1.48 Temporal evolution of temperature IS-11

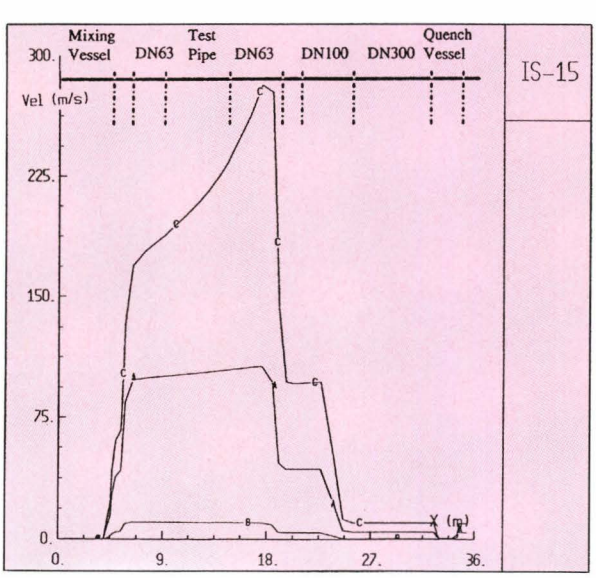

Fig. 1.50 Spatial evolution of velocity IS-15

Aerosol formation in the condensation pipe

Even if the temperatures at the entrance of the condensation pipe are too high for the usual aerosol codes to handle (over 7000 K), some calculations were performed with RAFT 1.1 and VICTORIA 92, to look at the nucleation and condensation process in the condensation pipe. The expected temperature at the outlet is more than 1000 K and, therefore, CsOH is expected to leave the condensation pipe still as a vapour. Tin oxide, however, is predicted by the two codes to start nucleating when the gas temperature reaches around 1700 K. RAFT also predicts a significant amount of condensation directly on the pipe walls, in accordance with previous results which show that RAFT over-predicts vapour condensation for large temperature differences.

The tin oxide particles leave the condensation pipe, according to the codes, with a mass mean radius of 0.25 (VICTORIA) to 0.35 micron (RAFT) and a geometric standard deviation of 1.8 to 2.1. It should be taken into account that VICTORIA models aerosol nucleation by assuming that nucleated particles get into the smallest particle size bin and grow from there. Since the time for growth is very short it is likely that, in this case, VICTORIA underpredicts the mean particle size.

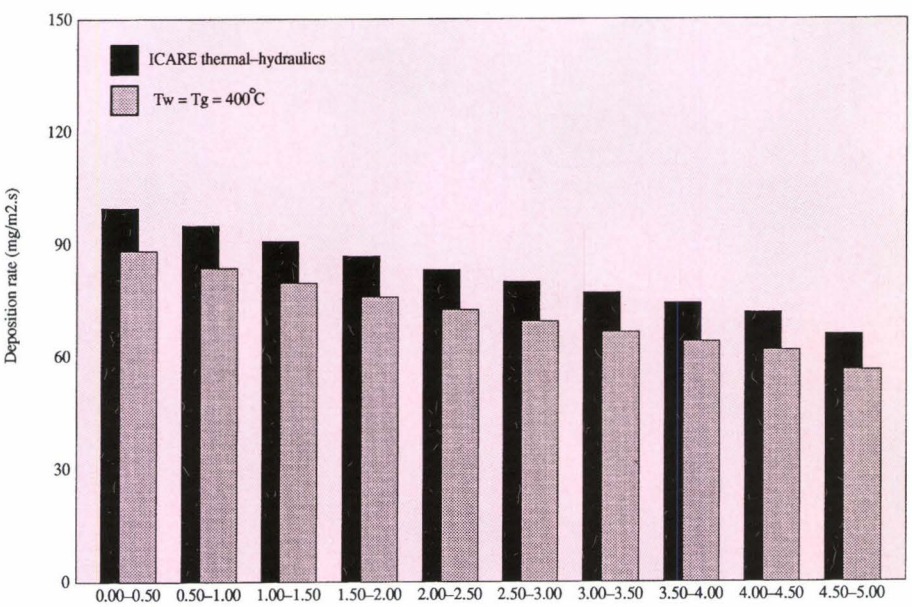

Fig. 1.51 Deposition profile in the test pipe

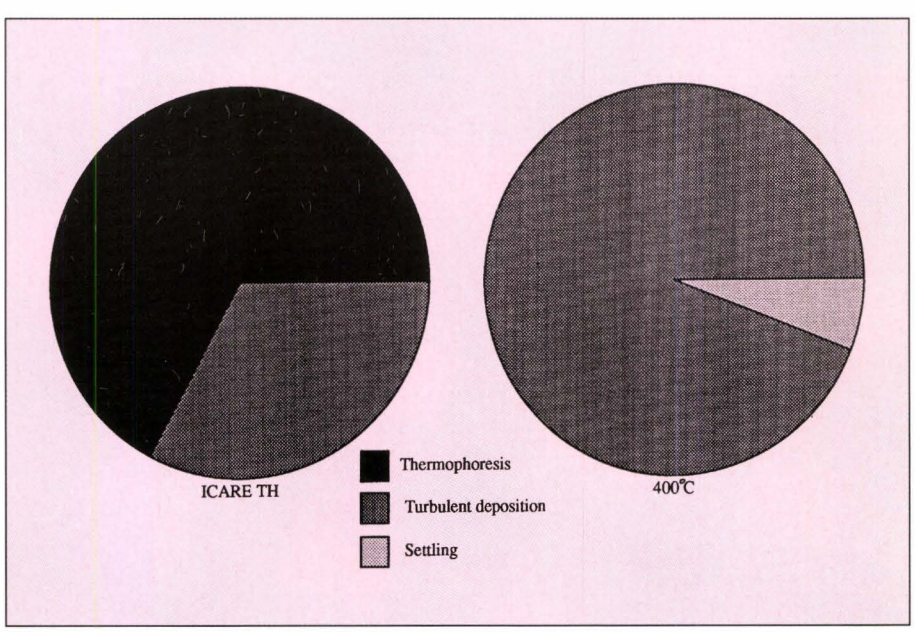

Fig. 1.52 Deposition mechanisms in the test pipe

Aerosol depositon in the test tube

A number of calculations of aerosol deposition in the test tube were performed using RAFT 1.1 under steady-state thermal-hydraulic conditions given by ICARE2 or with constant and uniform temperatures (at 400° C) for both the gas and the pipe walls. These calculations predict a very limited amount of gravitational settling, with turbulent deposition being the dominant mechanism in the absence of a temperature gradient, and thermophoresis taking over when a thermal gradient is imposed, this mainly for the cases with low mean particle sizes (***Fig. 1.51***). The fact that gravitational settling is not an important

deposition mechanism, we can expect a well distributed film in the pipe cross section, without a preferential deposition on the bottom of the pipe. The RAFT results also show a slight decrease of deposition rates along the test tube, as shown in ***Fig. 1.51***. If an hypothetic target of a deposit concentration of 500 g/m^2 is desired in the deposition phase, the time needed to reach this target will be, according to RAFT, between 1.4 and 72 hours.

References

[1] ARNAUD A., JONES A.V. - Lessons from the Analytical Preparation of the First Phebus-FP Test - Workshop Severe Accident Research in Japan, Tokyo, 1-2 November, 1993

[2] KRISCHER W., RUBINSTEIN M.C. (eds) - The Phebus Fission Product Project. EUR 13520 EN (1992)

[3] BIASI L. - Private Communication (1993)

[4] MAILLIAT A., JONES A. - Final Test Protocol for the Phebus FP Test FPTO, version 0, SAWG document 93.11/0 (April 1993)

[5] SHEPHERD I., SERRE F., HOCKE K., BANDINI G., MARTINEZ J., MARTIN FUERTES F. - Phebus FPTO: Bundle Calculations for the Reference Scenario - EUR 15639 EN (1994)

[6] M.P. KISSANE, B. FABRE - Thermalhydraulic calculations for FPT-0 using CATHARE2 Version 1.2E - Private communication (May 1992)

[7] FERMANDJIAN J., AKAGANE K., AREIA-CAPITAO J., DROSSINOS Y., DUMAZ P., KISSANE M.P, TRAMBAUER, K. Exploratory circuit calculations for the first test of the PHEBUS-FP Project, 12th Annual Meeting of the American Association for Aerosol Research, Oak Brook, Illinois (USA), 11-15 October 1993 - EUR 15702 EN (1994)

[8] SHEPHERD I., HERRANZ L., ALCAMI M., AKAGANE K., SMITH P., ELLICOTT P. - Scoping Calculations to Examine a Strategy for the Thermalhydraulic Control of the Phebus-FP Containment Vessel during High Humidity Transients', EUR 14984EN (1993)

[9] SHEPHERD I., JONES A.V., VON DER HARDT P., GAILLOT S. The Quest for Prototypical Conditions in the Phebus-FP Containment Fourth International Conference on Simulation Methods in Nuclear Engineering June 2-4, 1993, Montreal

[10] LAYLY V., TIRINI S. - Containment Thermalhydraulics for Test FPT-1. CEA Proposal Note Technique SEMAR 92/76, Document Phebus PF 92/159 (December 1992)

[11] UCHIDA H., OYAMA A., TOGOY. - Evaluation of Post-Incident Cooling Systems of LWRs. Proc. Int. Conf. Peaceful Uses of Atomic energy. 123 pp. 93-102, (1965)

[12] DE ROSA F., MANFREDINI A., ORIOLO F., PACI S., VILLOTTI A. - An Assessment of Analytical Models for the Simulation of Condensation Heat and Mass transfer University of Pisa Report number RL 586(93), (1993)

[13] COLLIER J.G. - Convective Boiling and Condensation, McGraw-Hill, London 1972

[14] SHEPHERD I., HERRANZ L., ALCAMI M., AKAGANE K., BONANNI E. - Pre-Test Calculations for the Thermal-hydraulics Tests to be Carried out in the Phebus-FP Containment Vessel - EUR 15638 EN (1994)

[15] MAILLIAT A., SERRE F. - Recommendations for the test FPTO performance associated to the Final Test Protocol, N.T.SEMAR 93/58, Doc. PHEBUS-FP IP 93/186

[16] FERMANDJIAN J., DICKINSON S., EDWARD J.B., EVANS G.G., RODRIGUEZ-MAROTO J.J., SIMS E.H., WREN C. - Presentation of the results of exploratory containment iodine chemistry calculations for PHEBUS FPT-0 (Benchmark exercise and realistic calculation) - EUR 15701 EN (1994)

[17] LAYLY V., TIRINI S. - FPT-0 Test Containment thermal-hydraulic calculation with JERICHO, Containment aerosol behaviour with AEROSOLS/B2, Report SAWG N° 92-088/1, October 1992

[18] MAILLIAT A., JONES A.V. - Provisional Test Protocol for the Phebus FP Test1 - Rev. 1 SAWG document 92.077/1 (November 1993)

[19] SCHWARZ M., JONES A.V - Proposal of Sensitivity Studies for the FPT1 Test - SAWG document 93-47/0 (November 1993)

[20] KINNERSLY S. et al. - In-Vessel Core Degradation in LWR Severe Accidents: A State of the Art Report to CSNI - Report NEA/CSNI/R (91)12 (November 1991)

[21] WRIGHT A. et al. - Primary System Fission Product Release and Transport: A State of the Art Report to the CSNI. Draft report NEA/CSNI (June 1993)

[22] DELLA LOGGIA E. (Ed) - National and Communities Research Policies and Programmes on Reactor Safety - Minutes of CGC5(93)-06 (March 1993)

[23] JONES A.V. et al. - Review of National and Communities Research Policies and Programmes on ReactorSafety - To be issued as a Technical Note

[24] CHATELARD P., LAPLAGNE-MALET V. - Integration of Two-Phase Thermalhydraulics Model - User's manual Report for Contract 4592-91-12EL ISP F (1993)

[25] CHATELARD P., LAPLAGNE-MALET V. - Integration of Two-Phase Thermalhydraulics Model - Description of Useful Sub-Databases for Coupling with Other Codes, Report for Contract 4592-91-12EL ISP F (1993)

[26] DE MAGISTRIS F., LAPLAGNE-MALET V. - Integration of Two-Phase Thermalhydraulics Model - Validation Tests Report for Contract 4592-91-12EL ISP F (1993)

[27] DUMAZ P., DROSSINOS Y., CAPITAO J.A., DROSIK I. - Fission product deposition and revaporization phenomena in scenarios of large temperature differences, Proceedings of the 1993 National Heat Transfer Conference, ANS Proceedings, Vol. 7, pp 348-358, August 8-11, 1993, Atlanta Georgia (USA)

[28] CAPITAO J.A., HONTANON E., DROSSINOS Y. - Modelling of thermophoresis in the VICTORIA and RAFT computer codes, submitted to Journal of Aerosol Science (November 1993)

[29] CALVO M., ALONSO A. - Basic hydrodynamics and pool scrubbing, UPM Madrid, EUR 15342 EN, 1993

[30] BAMFORD G.J., BRADLEY S.J.K., RAMSDALE S.A. - Integration of BUSCA into ESTER, AEA Technology Reactor Services, SRD Culcheth, AEA RS 5444 - To be published as EUR report

[31] MARCOS-CRESPO M.J., GOMEZ-MORENO F.J., MELCHES-SERRANO I., MARTIN-ESPIGARES M., LOPEZ-JIMENEZ J. - LACE-España experimental programme on the retention of aerosols in water pools, Proyecto LACE-España, Madrid, EUR 15454 EN, vol. 2, 1993

[32] CALVO M., ALONSO A. - LACE-España pre-test and post-test calculations, Proyecto LACE-España, Madrid, EUR 15454 EN, vol. 1, 1993

[33] CALVO M., ALONSO A. - Bubble break-up model, implementation in the BUSCA (JUN 90) code, Proyecto LACE-España, Madrid, EUR 15454 EN, vol. 3, 1993

[34] SHEPHERD I., AREIA CAPITAO J., DROSSINOS Y. - Post-Test Calculations with ESTER-VICTORIA and RAFT for the Integral Tests Fal-17 and Fal-18 - To be published as EUR report

[35] LAZARIDIS M. - Post-Test Calculations with an Extended Version of RAFT for the Integral Tests Fal-17 and Fal-18 - To be issued as Technical Note

[36] DROSSINOS Y. - VICTORIA/ESTER analyses of the Falcon ISP-34 Experiments, manuscript

[37] HONTANON E. - VICTORIA-92-01 analyses of the Falcon ISP-34 Experiments, manuscript

[38] A. CAPITAO J. - RAFT analyses of the Falcon ISP-34 Experiments, in preparation

[39] PERKINS R.J., VASSILICOS J.C., HUNT J.C.R. - Aerosol Transport, Deposition and Resuspension in the LWR Circuit and Containment - final report, 1994

[40] RENAULT C., TARABELLI D., PUAUX B. - Adaptation of JERICHO, AEROSOLSD-B2 and IODE to ESTER stucture, CEA Note Technique SEMAR 92/38 (1992)

[41] BIASI L. - Development and application of Models and Codes for LWR Fission Product Transport with Particular Reference to Phebus-FP, CEC Contract Number 4258-91-03 EP ISP I, first interim report MTC/PR40/91, July 1991

[42] KLEIN-HESSLING W., KULLMANN T.H, SCHWINGES B. - Integration of the Multi-Compartment Codes RALOC and FIPLOC in ESTER - User Manual GRS-2007 January 1993

[43] KLEIN-HESSLING W., KULLMANN T.H., SCHWINGES B. Integration of the Multi-Compartment Codes RALOC and FIPLOC in ESTER - adaptation of RALOC-FIPLOC-M to ESTER Structure, GRS-A-2006 January 1993

[44] DE ROSA F., MANFREDINI A., ORIOLO F., PACI S., VILLOTTI A. - An Assessment of Analytical Models for the Simulation of Condensation Heat and Mass Transfer, University of Pisa Report number RL 586(93), (1993)

[45] DE ROSA F., MANFREDINI A., ORIOLO F., PACI S. - Models for the Simulation of Condensation heat and Mass Transfer in the Presence of a Noncondensable Gas, University of Pisa Report number RL 585(93), (1993)

[46] DE ROSA F., MANFREDINI A., ORIOLO F., PACI S. - A State of the Art of Heat and Mass Transfer Condensation Models and Experiments suitable for Validation Models University of Pisa Report number RL 557(92), (1992)

[47] BONANNI E. - Analysis of the Hydrogen Mixing and Distribution Test ISP-35 with the CONTAIN 1.12 Code, Second Workshop on ISP-35, Tokyo, 4-5 Nov. 1993

[48] HIROSE T. - NUPEC Hydrogen Distribution Test M-7-1. Test Results, Second Workshop on ISP-35, Tokyo, 4-5 Nov. 1993

[49] COMMANDE A., RENAULT C., FOIT J.J. - Adaptation of the WECHSL-Mod3.3 Code to ESTER Structure - Note Technique SEMAR 93/43, CEA/IPSN Cadarache, KfK Karlsruhe

[50] SHEPHERD I., JONES A.V., JACQ F., SCHMIDT F. - Ester: A new Approach in Source Term Modelling - Fourth Intern. Conf. on Simulation Methods in Nuclear Engineering, June 2-4, 1993, Montreal

[51] TARABELLI D., RENAULT C. - Adaptation of JERICHO, AEROSOLS-B2 and IODE to ESTER Structure Application of the Coupled Codes to Containment Analysis, User Manual, Note Technique SEMAR 92/37, CEA/IPSN Cadarache

[52] RENAULT C., TARABELLI D., PUAUX B. - Adaptation of JERICHO, AEROSOLS-B2 and IODE to ESTER Structure - Note Technique SEMAR 92/38, CEA/IPSN Cadarache

[53] EUSEBI M., PAROZZI F., VALISI M., CAPITAO J.A., DE SANTI G.F. - Preparatory Calculations for a New Experimental Project on Dry Aerosol Resuspension Mechanisms (STORM Project) - Paper presented at the European Aerosol Conference, Oxford (UK), September 1992

[54] AGRATI G., PAROZZI F., SANDRELLI G., VALISI M., MARKOVINA A. - Simplified Tests on Resuspension Mechanisms, Preliminary Description of the Project - ENEL, Milano, 1991

[55] DE SANTI G.F., HUMMEL R., VALISI M., DE LOS REYES A. STORM Project: A Study on Aerosol Resuspension Mechanisms under Prototypical Severe Accident Conditions - Proceedings - Tokyo, 1-2 Nov. 1993

[56] RUHMANN H. - Aerosol Generation System for the STORM Project, Final Report - Siemens KWU, 1993

[57] MATEJKA D., BENKO B. - Plasma Spraying of Metallic and Ceramic Materials - Eds. J. Wiley&Sons, 1989

[58] SCHÖCK W. - DEMONA Jahresberichte - Kernforschungszentrum Karlsruhe, 1984 + 1985 + 1986

[59] VALISI M. - Aerosol Generation at Marviken, Personal Communication - ENEL Milano, 1990

[60] RAHN F.J. - The LWR Aerosol Containment Experiments (LACE), Summary Report - Electric Power Research Institute, Palo Alto, 1988

[61] LODGE J.P.,CHAN T.L. - Cascade Impactor, Sampling and Data Analysis - American Industrial Hygiene Association, 1987

[62] VDI Kommission: Reinhaltung der Luft - Staubmessungen in strömenden Gasen, Gravimetrische Bestimmung der Staubbeladung, VDI Richtlinie - VDI 2066 Blatt 1, 1975

[63] BOOKER D.R., MITCHELL J.P. - STORM Project: Aerosol Sampling Station, Executive Design - AEA, UK, 1993

[64] FORTESCUE T. - Feasibility of Radiation Techniques for the Measurement of Deposited Aerosol on the Surface of a Tube, Final Report - Löffel Verfahrenstechnik GmbH, 1993

[65] SANDERS J., DE SANTI G. - First STORM Meeting, 21-22 April 1993 - CEC-JRC, Technical Note I.93.60, Ispra, Italy, 1993

1.1.2 THE FARO LWR PROGRAMME

The FARO plant

The JRC-Ispra FARO plant is a large multi-purpose test facility in which phenomena related to severe accidents in Nuclear Reactors can be simulated. Basically, a maximum quantity of the order of 150 kg of oxide fuel type melts (up to 3273 K) can be produced in the FARO furnace, possibly mixed with metallic components, and delivered to a test section of interest (containers up to 1.0 m^3, 10 MPa and 573 K are available). From 1987 to 1990, the plant was used for LMFBR safety problems such as melt relocation and molten fuel/sodium interaction.

Following the recommendations of the EU-Member States experts, a change to LWR Severe Accident problems was decided in 1990. A first series of corium melt water quenching experiments was launched in September 1990 in collaboration with the United States Nuclear Regulatory Commission (US-NRC), the Electric Power Research Institute (EPRI) and the Ente Nazionale per l'Energia Elettrica (ENEL). This test series is part of the 1992-1994 CEC Framework Programme and is discussed at regular intervals with a group of EC national experts.

The reference situation is a postulated core meltdown accident when jets of molten corium penetrate into the lower plenum water pool, fragment and settle on the lower head. There is a lack of data on this issue, and particularly on the water quenching potential that determines whether the thermal loading on the bottom head structures can be mitigated. It has been agreed to perform experiments in the existing test vessel TERMOS to investigate this melt/water mixing and quenching process, and melt/structure interaction. The following unique features of the FARO facility determined this choice:

- large masses of molten corium (up to 150 kg) of prototypical compositions (UO_2-ZrO_2-Zr);
- high pressure, high temperature interaction vessel TERMOS (10 MPa, 573 K) in which high-pressure and full-scale-water-depth (up to 2 m) scenarios can be simulated.

The objective of the present test series is to determine, for different pressures, bottom vessel geometries and number of jets:

- the steam generation rate associated with the melt quenching;
- the hydrogen production associated to the zirconium oxidation;
- the thermal load on the bottom structures;
- the debris structure.

The first part of the test matrix deals with high pressure scenarios. Two tests involving 18 and 44 kg of oxide melt quenched into water with a depth of 1 m were performed respectively in 1991 and 1992.

Summary of work performed in 1993

During 1993 the following main activities have been performed:

- Completion of the analysis of the second quenching test, performed during 1992, and issue of the Experimental Data Report [1];
- Preparation of the facility for the quenching tests with 150 kg of melt:
  - Completion of the installation and testing of the steam venting unit (steam-water separator, venting piping, condenser);
  - Completion of the fabrication and delivery of the new components for the test vessel (release vessel, debris catcher, instrumentation rack, heating unit);
- Fabrication and testing of prototypical probes for continuous measurement of the hydrogen produced during an interaction (due to zirconium oxidation);
- Execution of the Base Case Test involving 150 kg of UO_2-ZrO_2-Zr corium melt at 3023 K quenched in 600 kg of water at 5.0 MPa and 536 K;
- Issue of a preliminary proposal for a future FARO programme on the long term coolability issue in the frame of the collaboration agreement with ENEL [2];
- Precalculations and test analyses with the codes COMETA, TEXAS III and IFCI.

Installation and testing of the venting unit

The purpose of this unit is to vent and condense part of the steam produced during the quenching should

the pressure in the interaction vessel TERMOS exceed 9.3 MPa. A scheme of the venting unit is given in ***Fig. 1.53***. A high pressure steam/water separator is connected to TERMOS by a pipe with an internal diameter of 146 mm. From the separator the steam is distributed to four circuits, each including a full lift safety valve with a discharge diameter of 32 mm and a set pressure of 9.3 MPa. The valves can also be remotely controlled for operational purposes (e.g. test of the unit, see below). Down-stream from the valves the steam is vented to a low pressure (0.8 MPa) condenser. The design of the unit by Siemens-KWU, Offenbach, was made to accommodate the most extreme conditions predicted by several computer models. The unit is capable to condense 200 kg of steam at 1 bar and a rate of 24 kg/s. Non-condensable gases (such as the hydrogen produced by zirconium oxidation or the argon possibly initially present in TERMOS) can be stored up to 0.8 MPa in the 2.5 m^3 free volume of the condenser. The instrumentation includes absolute pressure transducers and thermocouples in the separator, on the downstream side of each valve and in the condenser. Water level measurements are made by differential pressure probes mounted both in the separator and in the condenser. Magnetic indicators show the on/off- positions of the exhaust valves.

The installation of the unit was completed by the end of May. A first series of tests up to 2.0 MPa was performed in June, and a second series up to 7.5

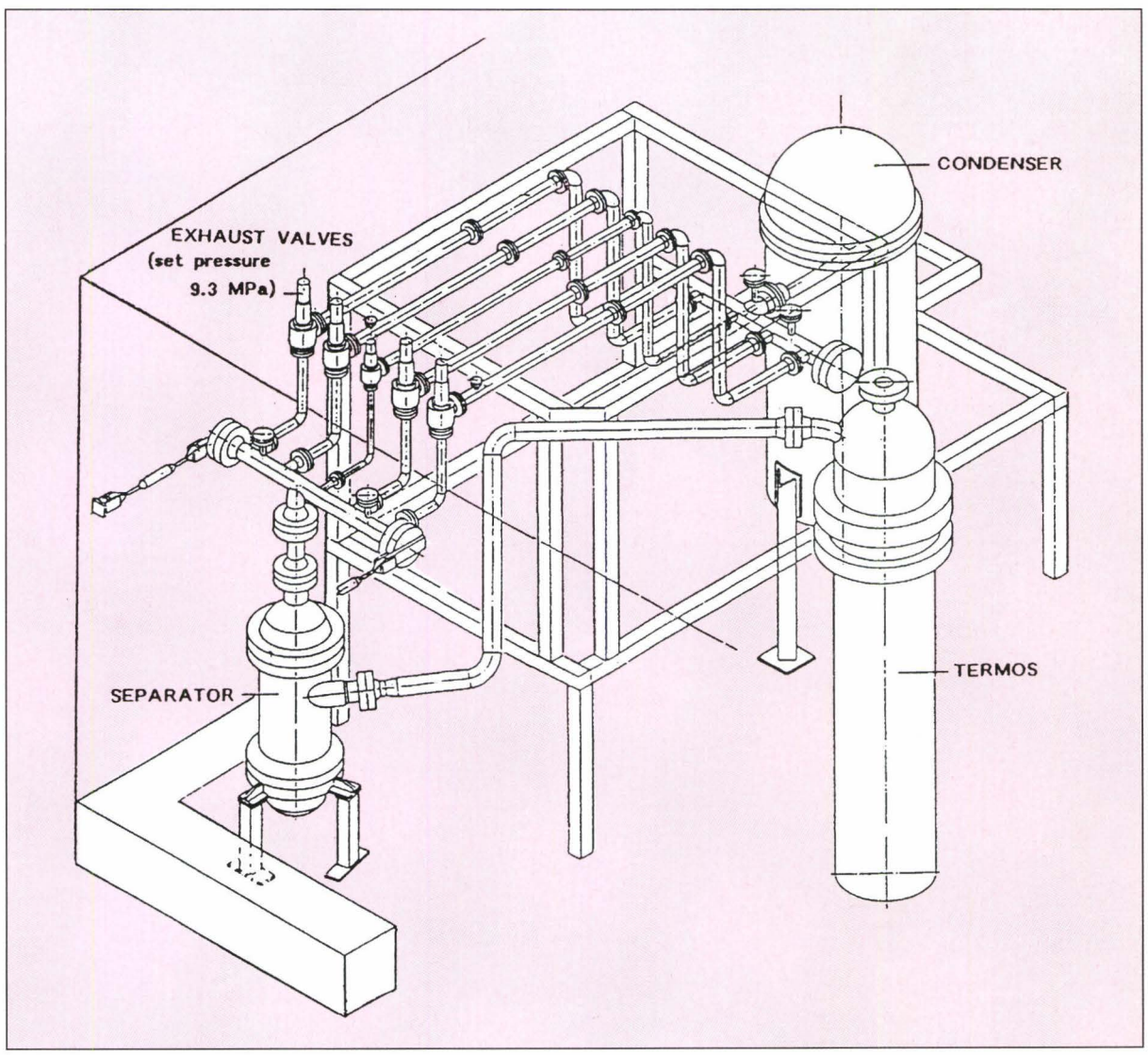

Fig. 1.53 FARO venting unit

MPa in July. The tests consisted in remotely opening and closing one or more valves several times, varying the time they remained open, the opening sequence (logical or random) and the initial conditions of the quencher (prepurged or not). The most challenging test for the unit was opening the four valves at the same time for a duration of seconds without prepurging the quencher. Globally, the unit behaved as expected, but the tests revealed that it would be rather difficult to maintain the pressure in the interaction vessel close to the set point after a first opening of the valves. Due to micro-deposits and/or erosion on/of the valve seats after strong steam flows, the valves exhibited a tendency to work subsequently at lower pressures than the initial set pressure.

Base Case Test (BCT)

The test was performed on 2 December 1993. The objective was to obtain first-of-a-kind information on the quenching of 150 kg of molten corium (76% UO_2-19% ZrO_2 - 5% Zr) when poured into a 600-kg and 2 m high water-pool at saturation and at 5.0 MPa (536 K).

Test arrangement and instrumentation

The test arrangement is shown in ***Fig. 1.54***. The interaction vessel TERMOS was connected to the UO_2-ZrO_2 melting furnace via the release channel and isolated from it during interaction by the valve SO2. It was connected to the condenser via the steam/water separator and the exhaust valves (see ***Fig. 1.53***). After melting in the FARO furnace, the melt was first delivered to the release vessel, and then released into the water. The release vessel contained about 1000 m of 1.2 mm diameter Zr-wire (7 kg) uniformly distributed throughout the whole volume. The super-heated oxide melt coming from the furnace induced the melting of the zicornium and the formation of a homogeneous mixture. Initially, the release vessel was at the same (low) pressure as the furnace (0.2 MPa). After transfer of the UO_2-ZrO_2 mixture to the release vessel, the intersection valve SO1 and the isolation valve SO2 were closed, and the release vessel was pressurised to the TERMOS pressure (i.e. 5.0 MPa) by using an argon supply. Upon pressure equalisation, the two melt catcher flaps automatically opened. The lower flap allowed the melt to be gravity released to the water. The side flap, of the same diameter as the melt release flap, was of use in preventing an under-pressure in the release vessel with respect to the TERMOS pressure throughout the melt release. After mixing with the water, the corium was collected in the debris catcher. Steam/gas venting to the condenser occurs if the pressure upstream to the exhaust valves reaches 9.3 MPa.

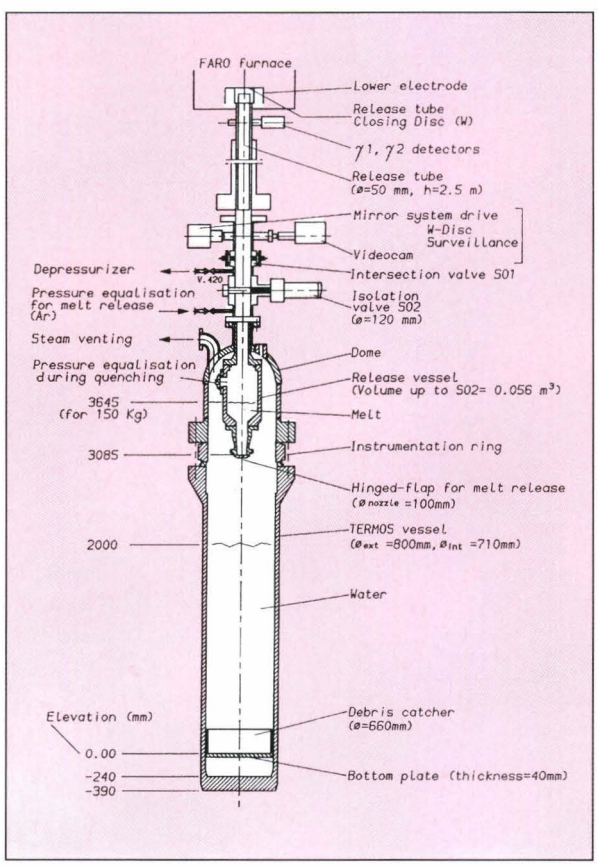

Fig. 1.54 Base Case Test arrangement

The principal quantities measured in the test vessel during the corium quenching were pressures and temperatures both in the gas region and in the water, and temperatures in the debris catcher bottom plate. Pressures and temperatures were also measured at various locations in the venting unit. A total of 250 signals were loaded to 6 different recorders of the data acquisition system. Keller pressure transducers (piezoresistive, 5-kHz frequency response) measured the vessel pressurisation. Vibro-Meter pressure transducers (piezoelectric, 15-kHz frequency response) were located in the water for rapid transient records in case of an FCI. They were protected by stainless steel grids. The steam K-thermocouples were protected from "seeing" the melt jet by ample shells. The water K-thermocouples were essentially sacrificial

thermocouples used to determine the downward progression and radial expansion of the melt jet. Those not destroyed during melt penetration recorded the long-term water temperature history. The centreline thermocouples in the water were sustained by thin (0.2 mm) stainless steel wires crossing the test section. The opening of the melt catcher flaps was indicated by the rupture of two 0.5 mm K-thermocouples (OD1, OD3). Another 0.5 mm K-thermocouple (OD2) was placed on the centreline of the vessel, 250 mm below the lower face of the release flap, for detecting the passage of the melt. The level swell was measured by means of four resistance probes installed every 0.25 m within 1.00 m above the initial water level, and a continuous level-meter based on the time domain reflectrometry method. Experimental probes for testing the capability to quantify the hydrogen produced by the oxidation of the zirconium were mounted. These probes are ultrasonic sensors based on the absorption of hydrogen by palladium.

Experimental conditions

The experimental conditions are summarised in ***Table 1.7***. The melt temperature indicated in the table (~ 3000 K) corresponds to that measured in the release vessel in an earlier test. In that previous test, the melting of the oxides in the furnace and the mixing with the zirconium in the release vessel were performed exactly in the same way as for the present test. ***Fig. 1.55*** shows the response of the ultrasonic temperature sensor (UTS) mounted horizontally in the release vessel outlet channel, 160 mm above the hinged-flap where the channel diameter was 120 mm. Time zero corresponds to the start of release of the oxide mixture from the furnace. The UTS completely crossed the section of the channel and both its ends were attached to the wall. The five measurement zones were each 10 mm long and occupied the 50 mm central part of the UTS. Zone 3 was in the centre of the channel. The melt traces reflect this distribution of the zones with a temperature of zone 3 higher than temperatures of zones 2 and 4, which in turn are higher than temperatures of zones 1 and 5. This decrease from the centre to the periphery is probably due to an influence of the channel walls. The average temperature of the 5 zones is 3000 K.

Table 1.7 Summary of Base Case Test experimental conditions

Melt	
Mass, kg	150
Composition, kg w%	115 UO_2+29 ZrO_2+6 Zr 76.5 UO_2+19.4 ZrO_2+4.1 Zr
Temperature, K	~3000
Delivery nozzle, mm	100
Free Fall in Gas, m	1.085
Water	
Mass, kg	600
Depth, m	2.00
Temperature, K	536
Fuel/coolant mass ratio	0.25
Gas Phase	
Composition, wt%	70 steam +30 Ar
Volume, m^3	1.3
Temperature, K	536
Test Vessel	
Diameter, m	0.71
Initial Pressure, MPa	4.9

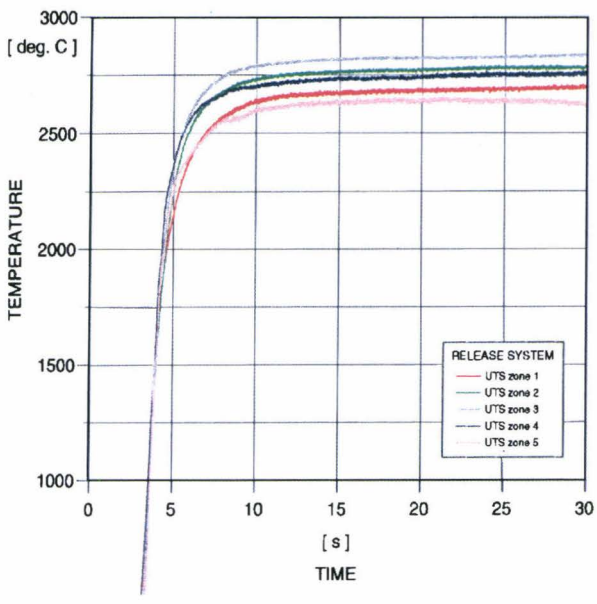

Fig. 1.55 Corium temperature measured by UTS in the release vessel

Results

The results presented below are preliminary. Data reduction should be completed during the first quarter of 1994. After opening of the release vessel, the time the melt front contacted the water was as expected from gravity release, i.e. ~ 0.34 s from release start. The melt first contacted the bottom plate 1.26 s after the melt/water contact, which corresponds to a melt descent velocity of 1.6 m/s through the water. The TERMOS and separator pressure histories are reported in ***Fig. 1.56***. Time zero corresponds to the start of release of the oxide mixture from the furnace. The start of melt to water delivery was 8.76 s. The traces are perfectly identical up to the time at which the gas started discharging to the condenser. The pressure difference between TERMOS and separator indicates the gas flow through the connection pipe. The gas venting started at 9.3 MPa as expected (at 10.2 s), but the pressure continued to increase in TERMOS up to around 10.0 MPa. This overshoot of pressure in the test vessel was due to the fact that the valves did not fully open. The discharge valves were sensitive to the pressure in the second stage of the separator. This pressure never increased beyond 9.7 MPa which was, according to the manufacturer, the lower limit for a full opening of the valves. The discharge of the steam to the condenser completely stopped at the time of 13.8 s when the pressure had reached 7.4 MPa. The steam released to the condenser amounted to 52 kg approximately.

Temperature histories in the gas phase and in the water are presented in ***Fig. 1.57***. The temperature distribution was rather uniform for both the phases. The maximum increases were 42 K for the gas and 29 K for the water, respectively. The temperatures in the bottom plate did not exhibit significant increases (around 5 K) which is strongly in contrast to the previous preliminary tests (Scoping Test and Quenching Test-2, [3]) in which increases up to 275 K were observed. Contrarily to the previous tests, the debris was found to be completely fragmented. The particle size distribution is given in ***Fig. 1.58***. A few kilograms of particles (size of the order of 1 mm) were entrained into the separator during the gas discharge.

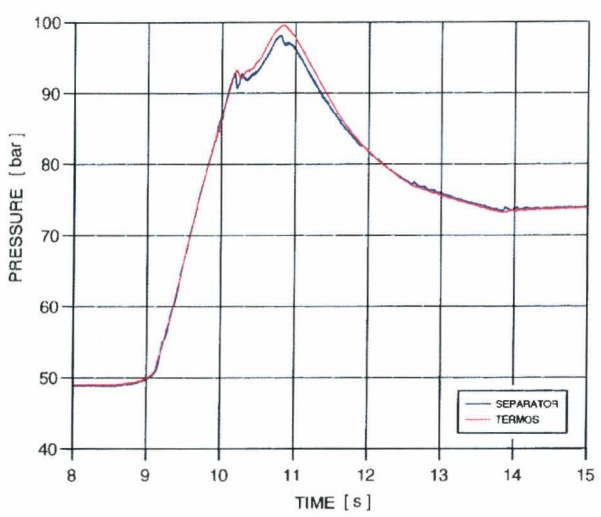

Fig. 1.56 Base Case Test: pressure histories in the test vessel and in the separator

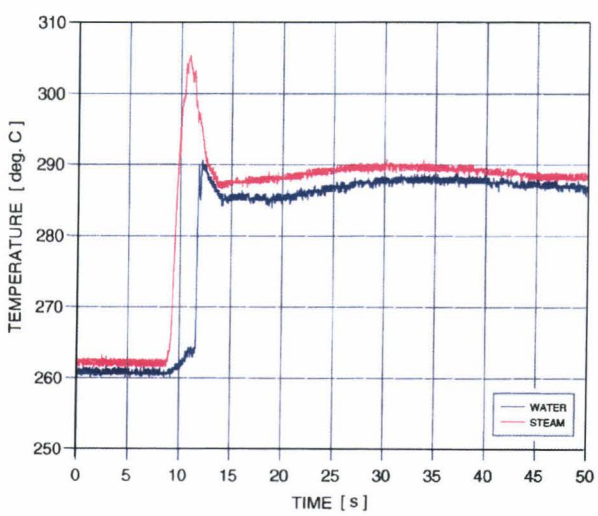

Fig. 1.57 Base Case Test: temperature histories in the gas phase and in the water

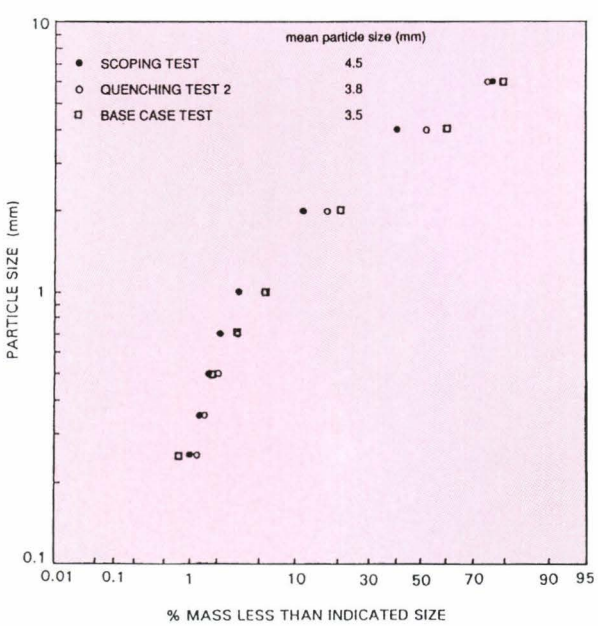

Fig. 1.58 Particle size distribution

A maximum level swell of 0.8 m, i.e. up to 0.2 m below the release vessel outlet, was measured. The mass spectrometer of the condenser qualitatively indicated that significant hydrogen production occurred. Analysis of the hydrogen probe responses and x-ray analysis of the debris are in progress to determine the quantity.

A first estimate of the energy released to the steam/water system from the start of melt to water delivery (time = 8.76 s) to the end of the discharge to the condenser (time = 13.8 s) gives 170 MJ. This value is high with respect to the energy of the 150 kg of melt (225 MJ), but includes also the energy released due to the zirconium oxidation (45 MJ correspond to a complete oxidation of the 7 kg of zirconium).

Conclusions

A more efficient quenching was observed than in the previous tests made with reduced quantities of melt, 1 m water depth and no Zr. The influence of these parameters will be analysed during1994. An enhancement of the jet break-up due to the opening of the discharge valves may also be possible.

COMETA a computer code for melt quenching analysis

In 1993 a new computer code was started to be developed that is the COMETA (COre MElt Thermal-hydraulic Analysis). The objective of this code is the prediction of the thermal-hydraulic behaviour of the FARO facility for design verification, definition of operational procedures and tests interpretation.

The initial configuration of the FARO facility was represented by a vessel of 0.6-0.7 m^3 in which a UO_2/ZrO_2 mixture was released. With this configuration two tests have been performed in which 18 and 44 kg were released [4, 5, 6]. The tests preparation and analyses were performed inside JRC using the TEXAS-II code [7] and outside JRC using codes like TRIO-MC [8] and others.

The configuration foreseen for the Base Case Test, where 150 kg are poured into saturated water at 5.0 MPa is somewhat more complicated because a relief line, a separator and valves (*Fig. 1.53*) are necessary in order to control the vessel pressure. The need for a thermal-hydraulic code that could analyse also complicated networks, as foreseen for the FARO test was identified. The initial choice was to use RELAP5/MOD3 [9] but it was soon dropped because detailed models for fuel fragmentation are not represented, not even in the SCDAP version.

The availability of a code that could analyse with sufficient detail both the thermal-hydraulics and the fuel fragmentation phenomena of melt quenching tests as executed and/or planned in the FARO facility, including all the facility components, was considered necessary. The immediate objective of the COMETA code is the prediction of the thermal-hydraulic behaviour of the FARO facility for design verification, definition of operational procedures and tests interpretation. The validation of the code is being performed by comparison with the available FARO tests as far as regards the fragmentation models and with LOBI tests for the thermal-hydraulic models verification.

Description of the COMETA code

The code has been written to run both on a PC and on a UNIX workstation and it produces on-line plots and automatic nodalization drawing schemes showing volumes void fractions, or fluid temperatures.

The COMETA code is a two field code: the water/steam field and the corium field. The water/steam field is described in an Eulerian 6 equation model including mass, momentum and energy conservation equations for each phase. The interface relations are represented by interface momentum exchange, or interface friction and interface energy exchange. Correlations depending on the actual flow pattern are present in the code.

The nodalization describes a network of fluid volumes that can be connected at their top or bottom or on one of two sides, externally or internally. Specific macrovolumes and macrojunction structures are present in the code (*Fig. 1.59*) with which it is possible to build 2-D noding schemes. The corium field is represented with 3 sub-components (*Fig. 1.60*): the jet, the droplets and the fused-debris bed, which are calculated with a Lagrangian model. The jet is released from a tank through an orifice and is fragmented during its free fall keeping the L/D - ratio constant. This is the ratio between the distance L from the injection orifice to the point at which the jet disappears over its initial diameter D. Experimental correlations are available that describe this quantity, called Jet Break-up Length (JBL).

The heat exchange between jet, droplets, fused-debris bed and the steam water mixture is controlled by heat-transfer coefficients which are dependent on

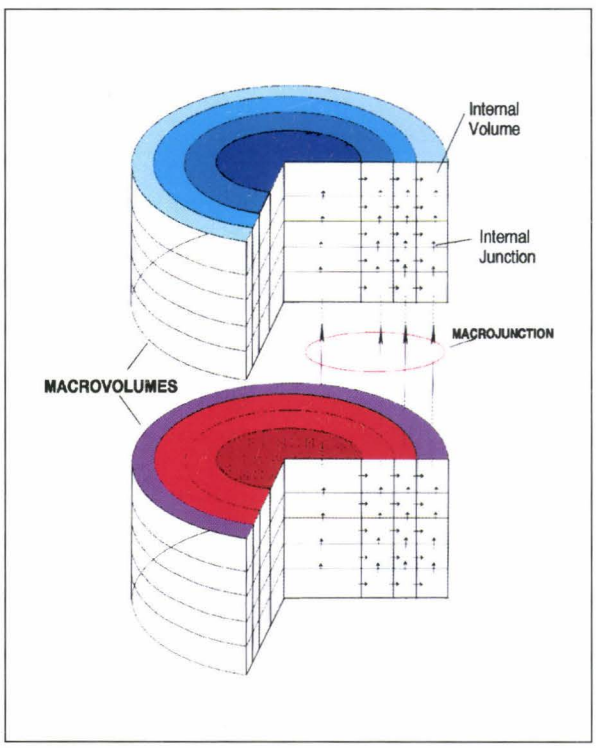

Fig. 1.59 COMETA code macrocomponents

the local thermal-hydraulic conditions. Heat slabs can be specified which represent the vessel walls or any heater. In this case a temperature distribution within the slabs is calculated to take into account the conductivity of the material. Major limitations of version 0.4 of the code, with specific reference to the FARO application are:

- the heat transfer coefficient correlations and the interface correlations (mass and momentum) are to be verified for corium conditions,
- the fuel and slabs properties are constant at each temperature,
- non-condensable gases or chemical reactions are not accounted for.

THERMAL-HYDRAULIC AND FUEL FRAGMENTATION MODELS VALIDATION

The coupling between the fragmentation models and the thermal-hydraulic models is explicit, but the time step chosen is the minimum between the requirements of both fields. In particular, the thermal-hydraulic models use as boundary condition the power transferred by the fuel fragments into the coolant, while

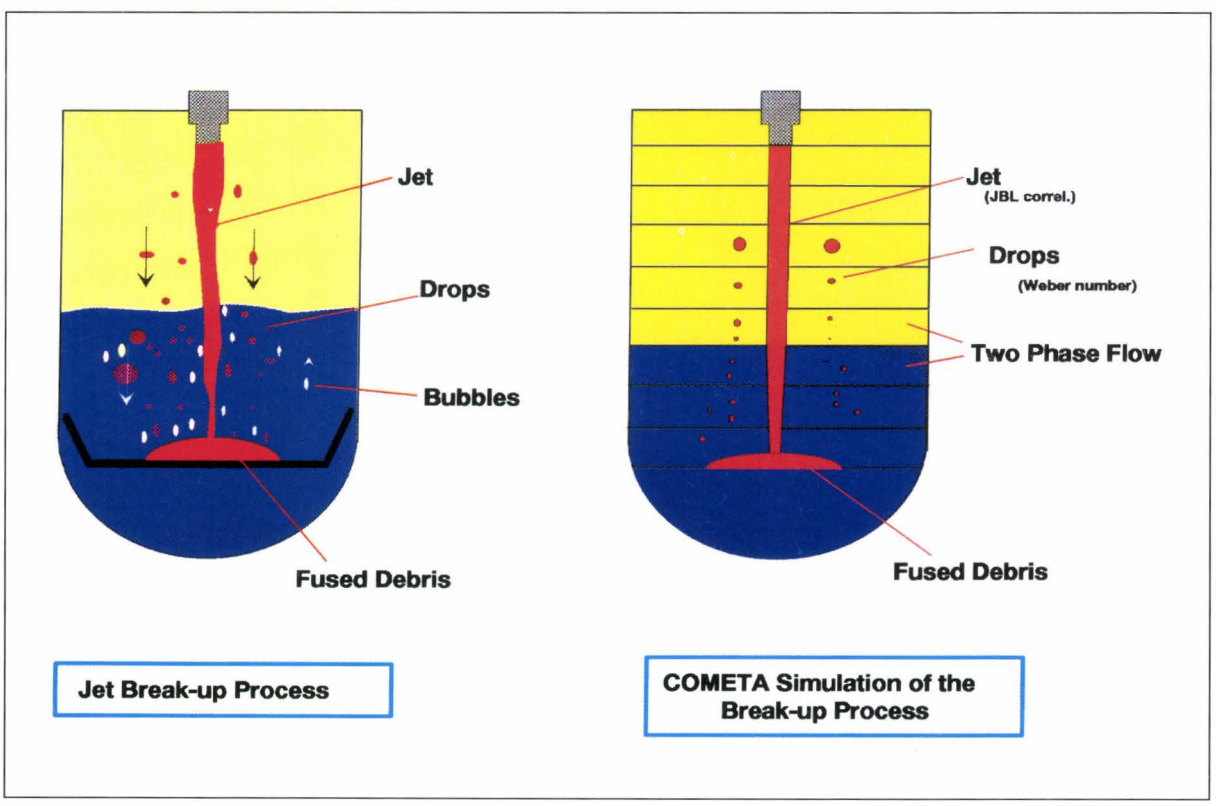

Fig. 1.60 COMETA presentation of the jet break-up process

the fuel fragmentation model use the local density, temperature and void fraction to calculate the fragmentation rate and the heat transmitted to the coolant. The volume occupied by the fuel is generally small compared to the coolant volume and therefore no volume reduction is taken into account. However, some particular circumstances (as for example some KROTOS tests) could require to take into account the volume reduction.

FUTURE COMETA CODE DEVELOPMENTS

Future developments of this code should overcome some limitations present in the actual version of the code. A separator model will be introduced into the code in order to describe the behaviour of the FARO facility. Non-condensable gas field or fields will be introduced in order to account for the initial presence of Ar in the FARO facility and for the production of H_2 during the tests.

The fuel fragmentation will be extended in the radial direction in order to analyse more complex situations. The melt composition is assumed constant with physical properties not depending on the temperature. Therefore it will be necessary to extend the properties database including different melt composition and properties which vary with temperature. A better debris model should be introduced into the code. The internal temperature distribution will be determined for larger drops. Finally the graphical system will be improved including the melt field in the nodalization drawing.

Validation of COMETA code

The COMETA code validation is being performed in parallel with the development of the code. In particular tests from the FARO facility are used to assess the fragmentation models [11] while some tests from the LOBI facilij51ty are used for the validation of the thermal-hydraulic models.

Fuel fragmentation validation

This test is represented by an injection of 18 kg of melt in a almost saturated environment. The nodalization scheme is presented in ***Fig. 1.61 a***. The calculation was performed with a mixed correlation for the Jet-Break-up Length including the Saito correlation and the Epstein-Fauske correlation with a interpolation between the two as the Weber number increases,

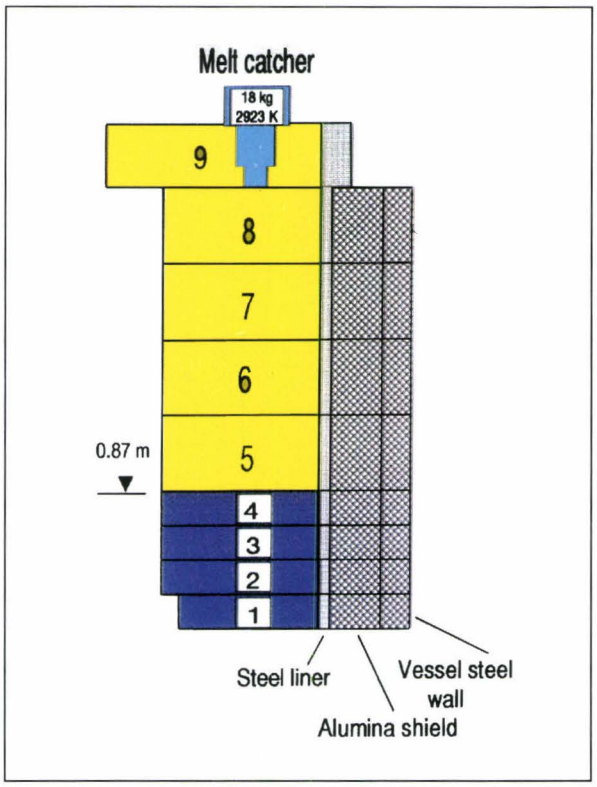

Fig. 1.61a L-06 post-test nodalization

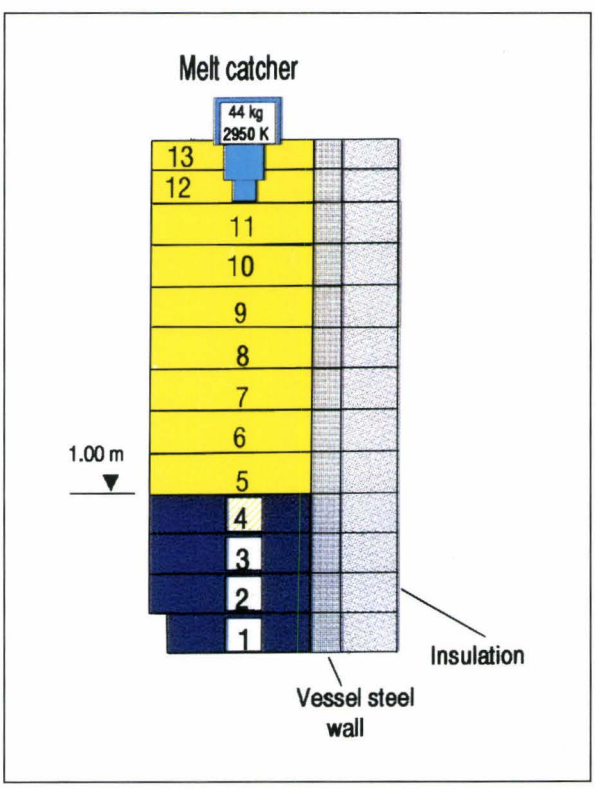

Fig. 1.61b L-08 post-test nodalization

and taking into account the ΔP across the melt catcher that was deduced experimentally, determined by the sudden connection of the TERMOS volume (at about 54 bar) with the melt catcher volume (at atmospheric pressure).

With these conditions the TERMOS pressure is quite accurate (*Fig. 1.62*). In the calculation without the ΔP, the Weber number at the injection point remains well below the value of 50. The application of the ΔP increases the Weber number, thus causing an increase of the L/D-ratio and a reduction of the fragmentation. The liquid temperature, measured at three different radial positions at elevation 350 mm (from the bottom vessel), is compared with experimental results in *Fig. 1.63*. The behaviour is satisfactory on the long-term while it gives an average in the first 2 s, for which a more detailed 2-D noding would be necessary.

This test was characterized by a greater melt quantity (44 kg) released in the TERMOS vessel, which was slightly subcooled due to argon addition (about 8 bar of partial pressure). Since the code does not yet allow non-condensable gases, the initial pressure was the real total pressure while the liquid temperature was taken as derived from the test. In the steam phase, however, saturation conditions are assumed by the code. In *Fig. 1.61b* is the nodalization used in the COMETA code.

In this test, a greater pressurization occurred with a peak at 1.2 s of about 76 bar. In this test the ΔP over the melt catcher was greater than in the previous case, up to 3 bar at the beginning and up to 1.7 at 0.08 s. Again the better calculation is obtained with the same correlation as before and includes the effect of the pressurization (*Fig. 1.64*). The fluid temperatures, measured at two different radial

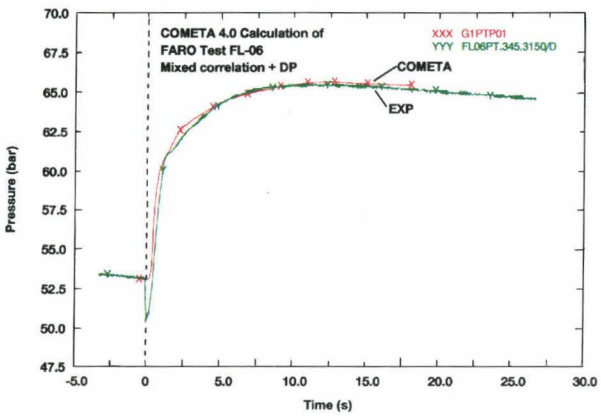

Fig. 1.62 Pressure in TERMOS in L-06 test compared with COMETA calculation

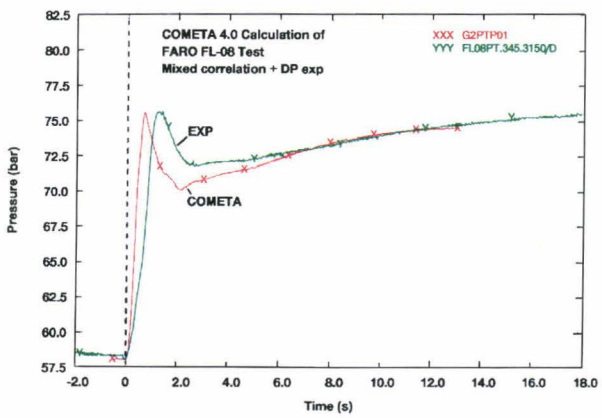

Fig. 1.64 Pressure in TERMOS in L-08 test compared with COMETA calculation

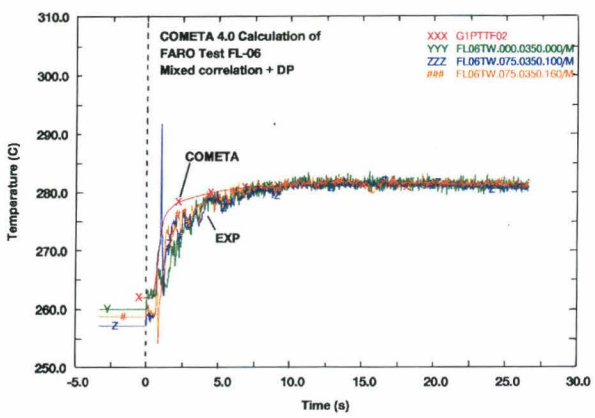

Fig. 1.63 Liquid temperature in TERMOS vessel during test L-06

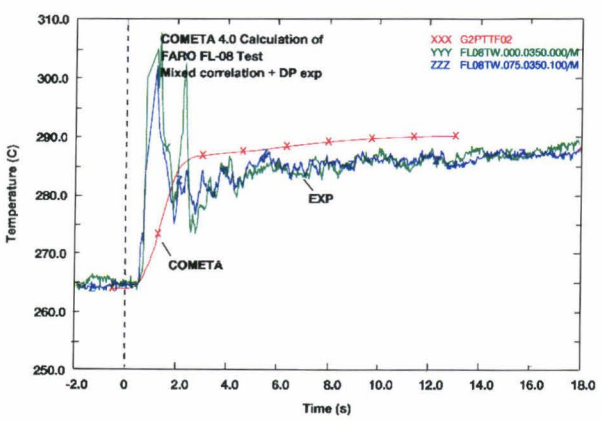

Fig. 1.65 Fluid temperature in TERMOS vessel compared with COMETA calculation

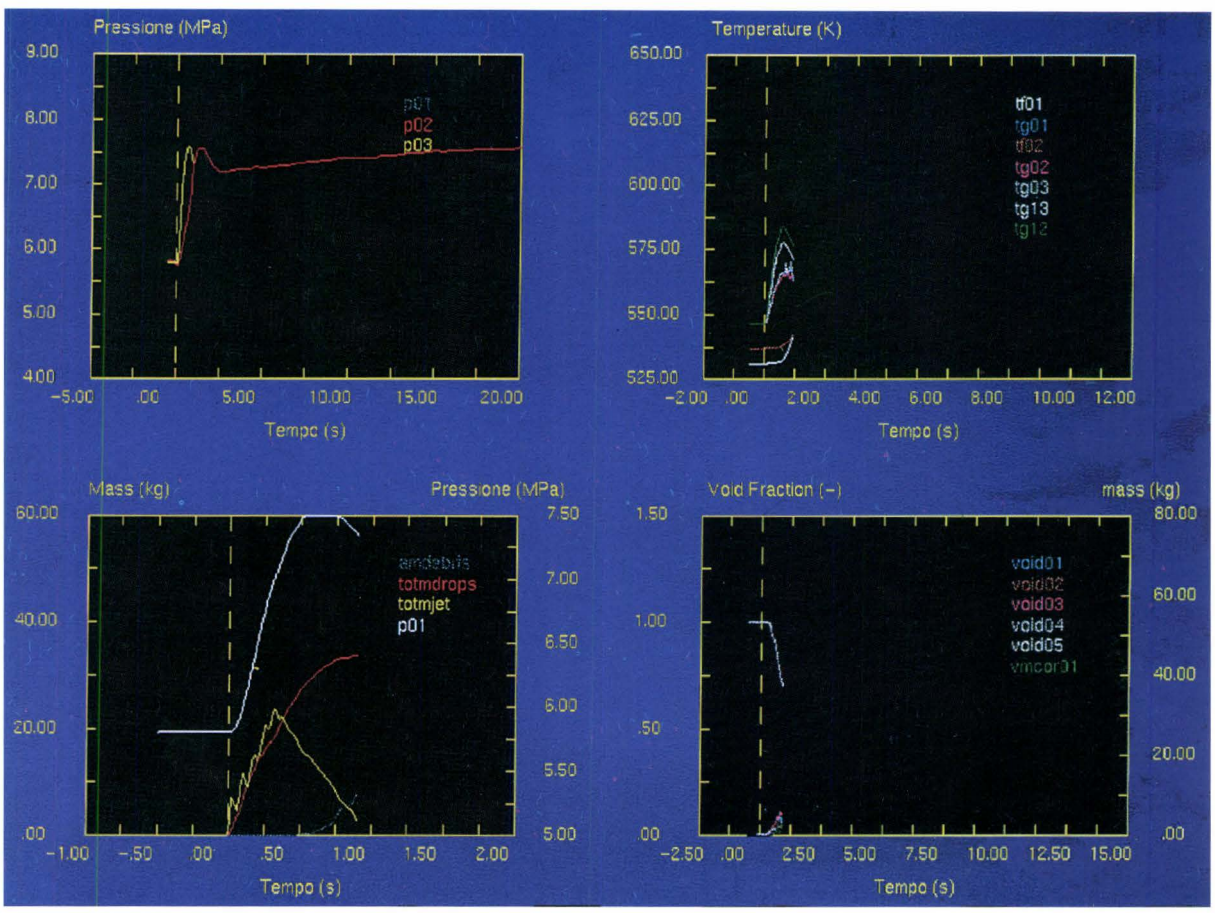

Fig. 1.66 Example of COMETA on-line plots

positions at elevation 300 mm, are compared in ***Fig. 1.65***. The liquid temperature at elevation 350 mm is difficult to compare because the melt fall-down effect is strongly affecting the thermocouples. However, considering the signal after 2.5 s, representative of the liquid temperature, the final value seems too high, even if it is very similar to the measured saturation value. In ***Fig. 1.66*** an example of the on-line plots produced by the code is presented. It is possible to specify up to 9 plots on the same window each with 2 axes and up to 30 curves, which are plotted during the calculation.

Thermal-Hydraulic Validation

Some LOBI tests are used for the validation of the thermal-hydraulic models. An example of a 6% cold leg break, the LOBI test BL-34 [10], simulated by the COMETA code is presented. All the important phenomena occurring experimentally were well predicted by the code. This test was characterized by an initial power of 14% of the nominal power. In this case no HPIS is present and only one accumulator injecting in the cold leg was used. Three dryouts and rewettings occurred in the test: a first dryout at 135s, caused by loop seal formation/clearout; a second dryout at 362s due to low inventory, terminated by accumulator injection; a third dryout occurring at 1705s after the accumulators emptying, terminated by LPIS injection.

The COMETA prediction is indicated in ***Figs. 1.67*** to ***1.69***. The primary system pressure is well predicted, see ***Fig. 1.67***. The depressurization after the loop seal clearing is slightly greater than experimentally. The primary inventory is shown in ***Fig. 1.68***. The code predicts rather well the whole inventory behaviour, even if the accumulator injection is too strong, due to high interphase heat-transfer coefficients that determine a too high condensation at the injection point. The core surface temperature, measured at three axial levels (10, 11, 12), is shown in ***Fig. 1.69*** compared with the corresponding COMETA slabs (4, 5, 6

respectively). The code tends to predict too high temperature peaks but the key phenomena are correctly simulated.

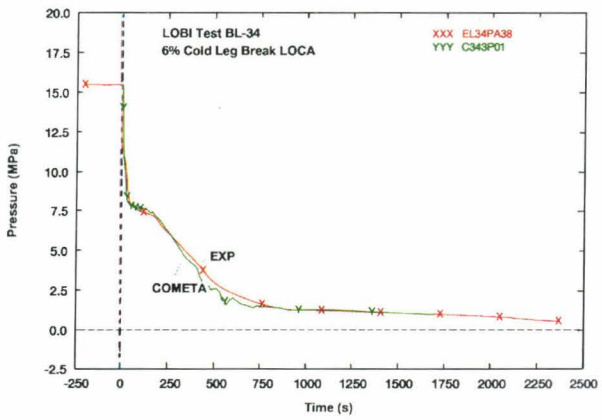

Fig. 1.67 Pressure in LOBI test BL-34 compared with COMETA calculation

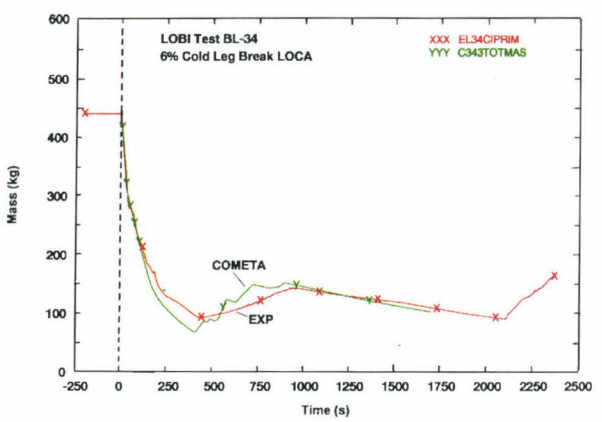

Fig. 1.68 Primary mass inventory in LOBI test BL-34 compared with COMETA calculation

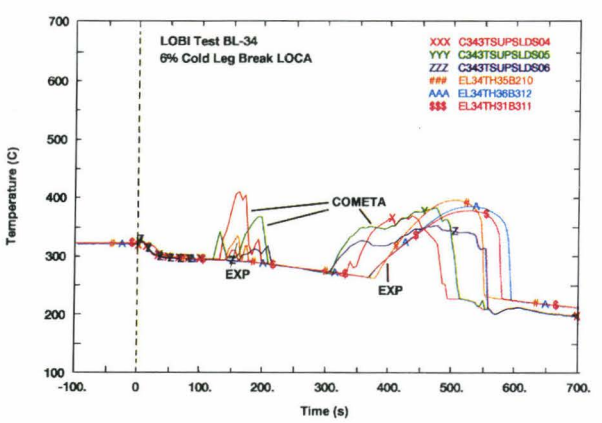

Fig. 1.69 Surface temperature in LOBI test BL-34 compared with COMETA calculation

Application of the COMETA code for the prediction of the FARO Base Case Test

The adopted COMETA nodalization is given in ***Fig. 1.70***. This test is represented by a release of 150 kg of melt in a saturated fluid at 50 bar. No pressure control is adopted in the calculation but the test facility design pressure is 100 bar. In the calculation, (***Fig. 1.71***), the pressure reaches a maximum at about 3 s of 114 bar [12]. Therefore the pressure becomes greater than the TERMOS maximum pressure and the regulation valves, that will be set in the test at 93 bar, should open. Another case was run including the valves opening. It was found that they are sufficient to control the pressure, see ***Fig. 1.71***.

A strong energy release occurs due to the great quantity of material released in the test vessel. About 130 kg of material is transformed in drops while the

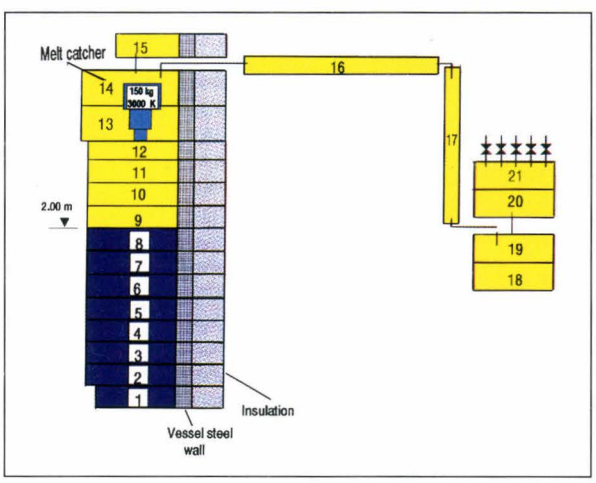

Fig. 1.70 Base Case pre-test nodalization

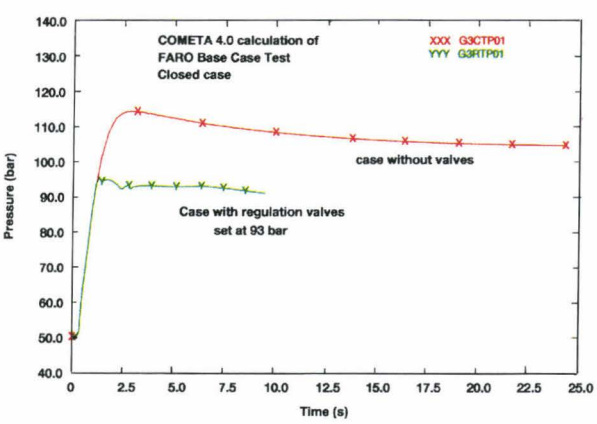

Fig. 1.71 Pre-test prediction of pressure in the FARO Base Case Test

remainder accumulates on the bottom as melt debris (*Fig. 1.72*). Sensitivity analyses were performed on the amount of injected material, its initial temperature, initial subcooling, presence of cold heat structures and the computer used for the calculation (IBM RISC 6000, HP 750, PC-DOS). As a result of the sensitivity analyses a bounding range for the pressurization expected for the test can be indicated. In *Fig. 1.73* this range is indicated with a shadow curve which enclose all the pressurization curves obtained. The maximum pressure should be therefore between 89 and 114 bar. This test was in reality executed on Dec. 2, 1993, and the pre-test calculations were confirmed. The 93 bar valves opened and controlled the pressure. A complete analysis of the test is still underway.

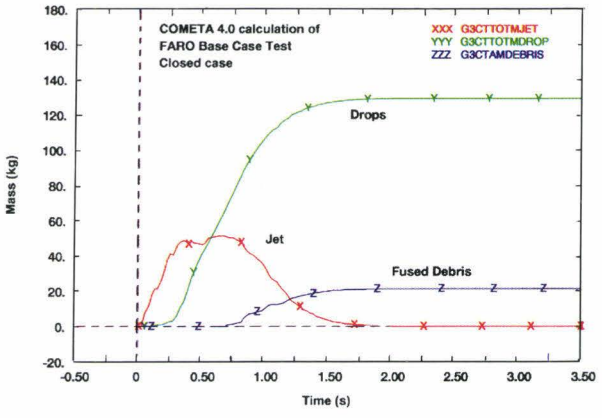

Fig. 1.72 Jet drops and fused debris behaviour in pre-test prediction of the FARO Base Case Test

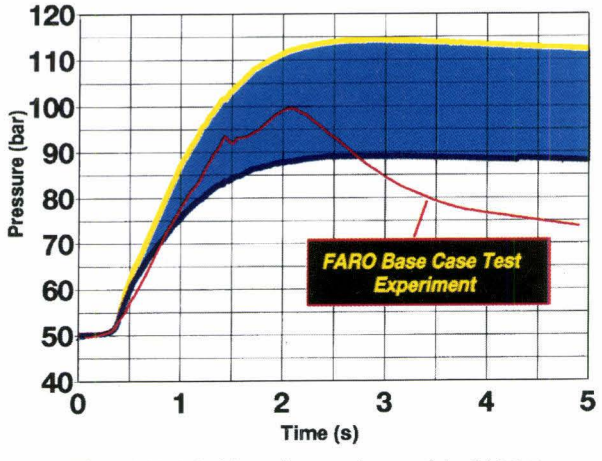

Fig. 1.73 COMETA 0.4 bounding prediction of the FARO Base Case Test

TEXAS-III Developments

A new version of the TEXAS computer code, named TEXAS-III, has been developed in collaboration with the University of Wisconsin [13]. This code solves one-dimensional, three-field, conservation equations for multiphase flows. Two Eulerian field represent the coolant as liquid and vapour. The third field is Lagrangian and deals with discrete particles (representing the molten fuel) moving through the other two fields. Separate partial differential equations for each of the three fields express conservation of mass, momentum and energy for each individual component. This fluid dynamic formulation allows thermal and mechanical non-equilibrium between the fields. A hydrodynamic model to describe fuel liquid particle fragmentation, based on Rayleigh-Taylor instabilities, is included.

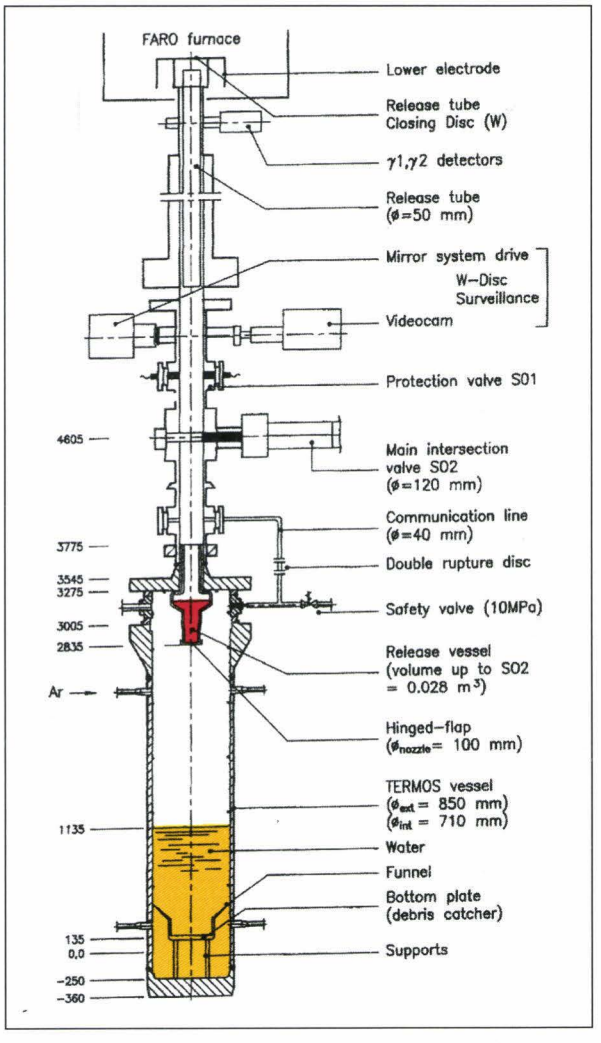

Fig. 1.74 Quenching test 2 arrangement

Several improvements have been added in this version of the code including new pre- and post-processor, new numerical and model developments such as the radiation heat transfer from fuel to vapour and a more realistic kinematic description of the fuel jet free fall.

TEXAS-III has been used for the interpretation of the FARO-LWR test L-08 in which 44 kg of molten fuel have been released in the TERMOS vessel (at initial pressure of 5.8 MPa), partially filled with water slightly subcooled due to the preliminary addition, in the free-board, of argon (about 0.8 MPa of partial pressure). The lay-out of the test L-08 is shown in *Fig. 1.74* [3].

Representative calculational results obtained with the TEXAS-III code are illustrated in *Fig. 1.75*. On the left hand side of the figure, the calculated vapour void fraction distribution at 9.49s is depicted. In addition, the positions where pressure (G1), vapour temperature (G3) and liquid temperature (G6) histories are recorded during the calculation, are indicated. Since the code does not yet consider non-condensable gases, initial saturation conditions corresponding to the measured initial vapour temperature, have been assumed. Therefore, the initial pressure for the code calculations was 5 MPa instead of the measured initial value of 5.8 MPa due to the addition of argon. Furthermore, the calculations have been performed assuming adiabatic vessel walls and neglecting vapour condensation on the vessel walls. It is planned to make the improvements necessary to remove the above mentioned model inadequacies. Taking into account these limitations, the TEXAS-III calculations reproduce reasonably the experimental values.

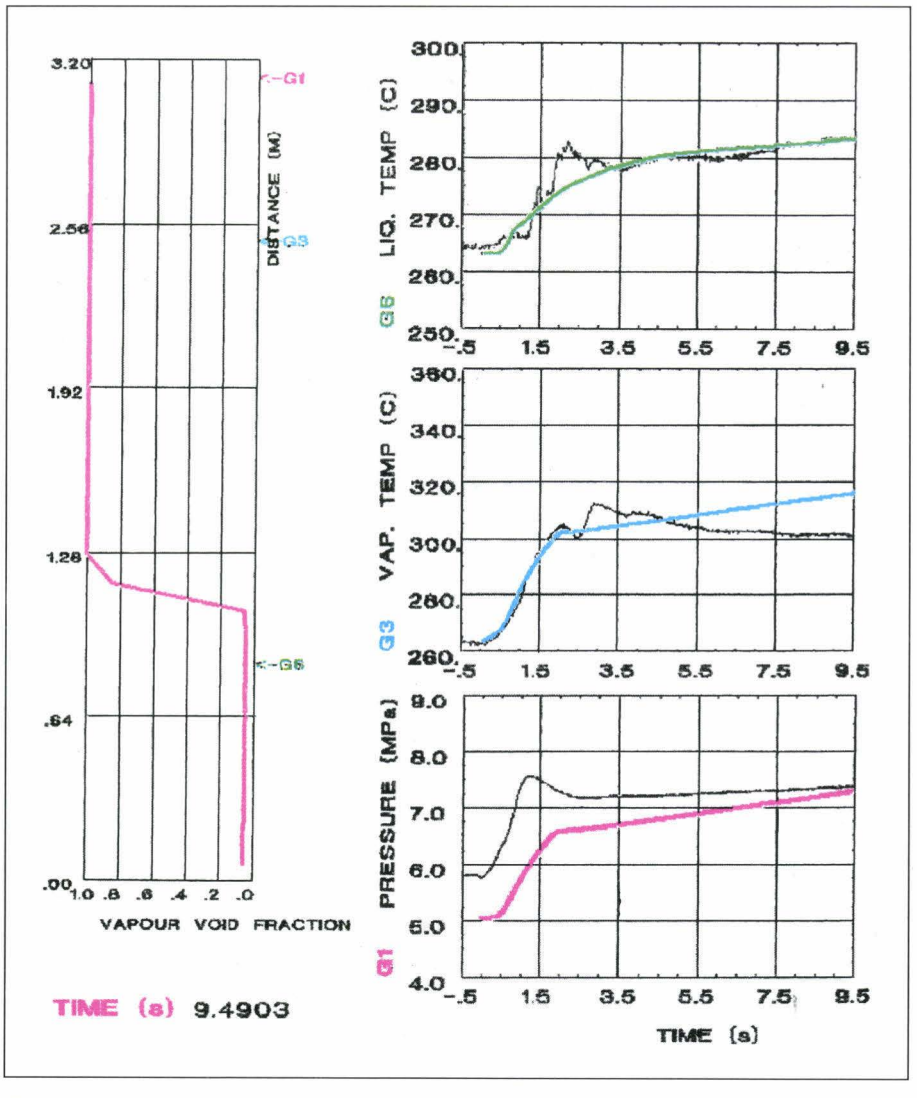

Fig. 1.75 FARO-LWR second Quenching test; TEXAS-III calculation results

IFCI Activities

The Integrated Fuel-Coolant Interaction computer code developed at Sandia National Laboratories (SNL) [14] is submitted to an assessment performed in collaboration with the University of Wisconsin, ENEL and ENEA, in view of its possible use for FARO-LWR pre - and post-test calculations. This code can deal with FCIs in a mechanistic way, considering coarse fragmentation and mixing of the molten fuel with water, triggering, propagation and fine fragmentation and expansion of the melt-water system.

IFCI is based on MELPROG's two-dimensional, cylindrical geometry, four field hydrodynamic method [15] with separate mass, momentum, and energy equations for each field. The constitutive relations required for the interfield coupling terms (heat transfer, momentum exchange and phase change) include the bulk boiling model, a subcooled surface boiling model, a three-field flow regime map, adaptations of standard heat transfer and momentum transfer correlations.

Several calculations on FARO-LWR tests and detailed analysis of the models employed have been performed during 1993. In spite of a satisfactory agreement reached in the first phase (~1 second) of the fuel mixing process, some model limitations, mainly concerning the interphase surface area tracking procedure, have been identified. Additional work is needed to remove model inadequacies and to complete the code assessment activity.

Safety assessment of the FARO-LWR plant

In some tests of the FARO-LWR experimental programme it is foreseen to investigate the interaction of a mixture of 150 kg molten $UO_2/ZrO_2/Zr$ (76 wt%/19wt%/5 wt%) with water (pressure ~5 MPa, temperature ~536 K). Under these conditions the 7 kg of Zr give rise to a production of ~4 m^3 of H_2 due to the complete Zr oxidation in presence of steam. Considering the hypothetical and extremely unlikely event of a leakage in the test section containment barriers, it is important to verify the effects on the upper containment building (FARO furnace bunker) of a H_2 detonation triggered by a hypothetical ignition event. To calculate the load on the walls and on the lid of the FARO bunker, 2-D calculations have been performed using REACFLOW ([16] to [21]), a code for the numerical simulation of reactive gas flows, which is under development at JRC-STI. In the worst case all the hydrogen accumulates at the top of the bunker right under the lid with the critical mass fraction of 2.8% H_2 and 97.2% air (stoichiometric detonation relation). The dry air is composed of 21% O_2 and 79% N_2.

The bunker has a dimension of 7.5x7.5 m and a height of 6.5 m. It is assumed that the 4 m^3 of hydrogen are located as a cloud under the lid of the bunker (see ***Fig. 1.76***). The bunker is assumed to be adiabatic and rigid. The ignition point has been set at the bottom of the hydrogen cloud. The initial temperature has been set to 295 K.

The calculations have been performed with a second order accuracy in space and time using an explicit approximate Riemann solver combined with the implicit calculation of the chemical kinetics based on a scheme with 8 elementary reactions involving 6 active chemical species which describe the chemical reaction between hydrogen and air [17]. Since the turbulence model is not yet implemented a laminar flow field has been applied. Diffusion processes are not taken into account.

In the following figures the results are briefly explained. The pressure and combustion front reaches the lid after about 0.7 ms (see ***Figs. 1.77*** and ***1.78***; ***1.79*** and ***1.80***). It hits the lid with about 1.5 MPa but after 1.5 ms the pressure time histories for some

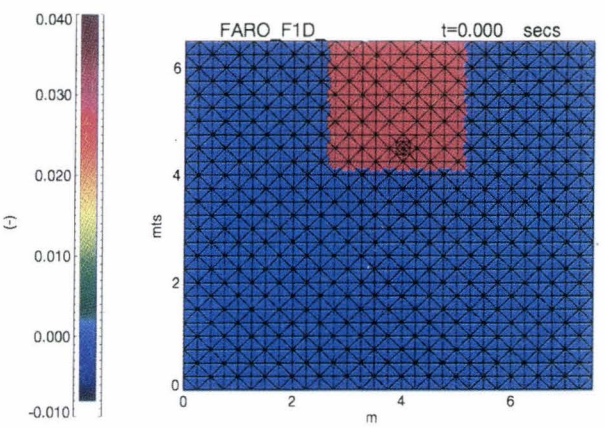

Fig. 1.76 Initial hydrogen distribution with overlaid coarse grid

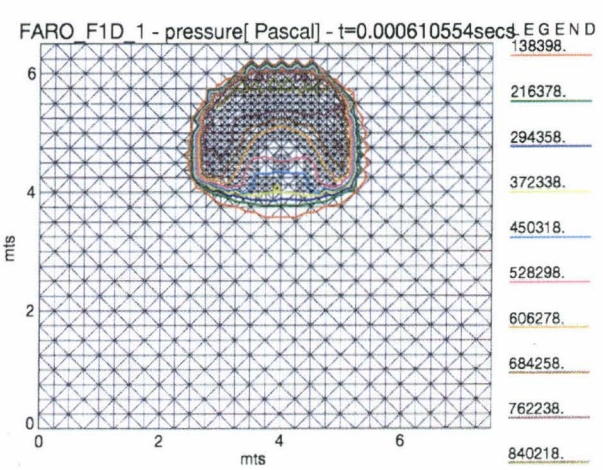

Fig. 1.77 Lines of constant pressure at time = 0.61 ms

points on the upper boundary show a significant pressure decay. The temperatures after the ignition of the hydrogen are about 2900 K due to the strongly exothermic burning process. In *Figs. 1.81* and *1.82* the temperature fields are shown at different times. In *Figs. 1.83* and *1.84* the temperature time histories for some points on the upper boundary are given.

The main conclusion of these REACFLOW calculations is that the transient peak pressure remains well below 2 MPa and the maximum temperature immediately after ignition is about 2900 K. As a consequence of the calculated pressure peak the lid would be lifted of a negligeable amount (~1.6 mm).

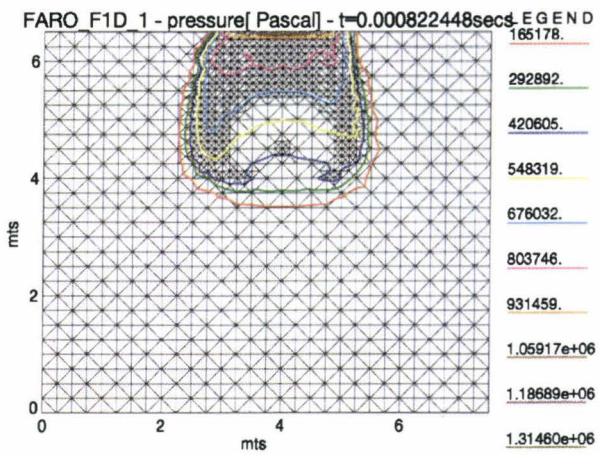

Fig. 1.78 Lines of constant pressure at time = 0.82 ms

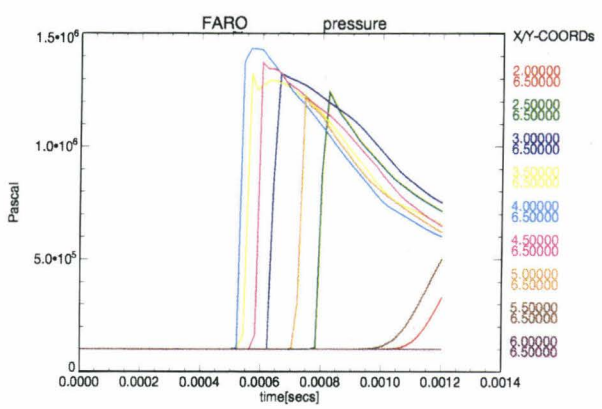

Fig. 1.79 Pressure at various nodes on the top boundary (fine grid) for the first 1.2 ms

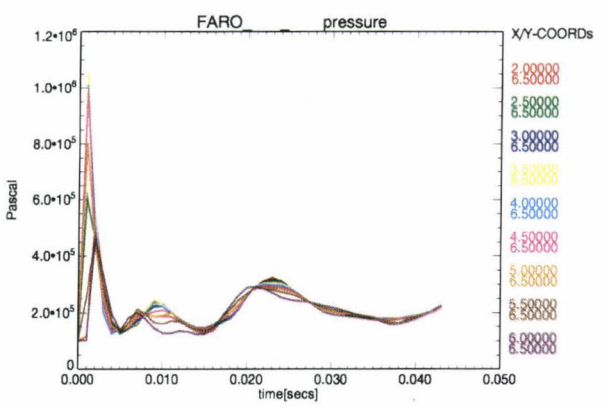

Fig. 1.80 Pressure at various nodes on the top boundary (coarse grid) for the first 43 ms

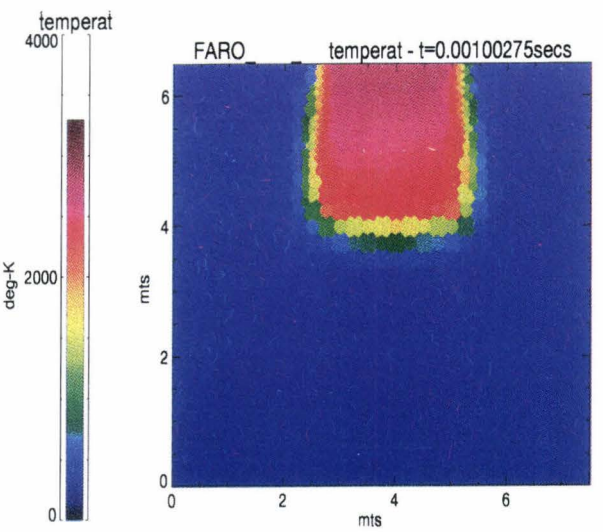

Fig. 1.81 Temperature field at time = 1.0 ms

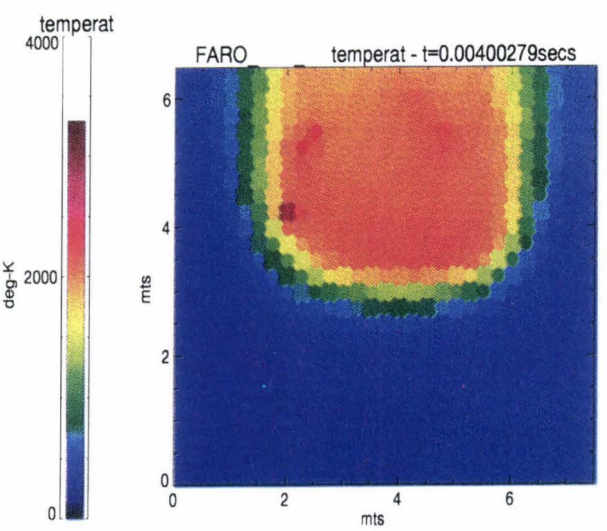

Fig. 1.82 Temperature field at time = 4.0 ms

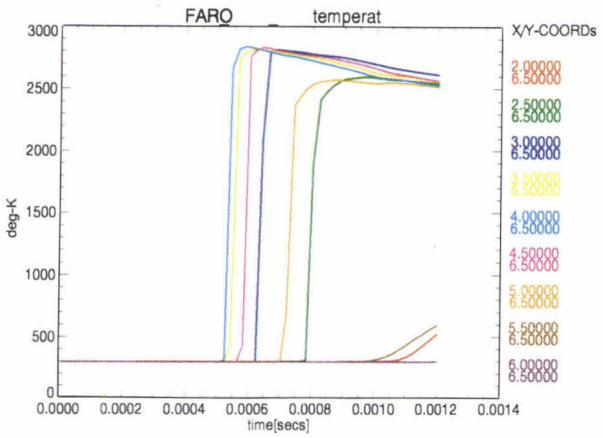

Fig. 1.83 Temperature at various nodes on the top boundary (fine grid) for the first 1.2 ms

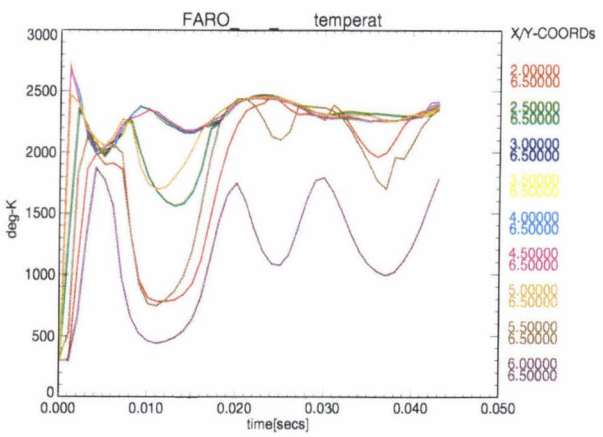

Fig. 1.84 Temperature at various nodes on the top boundary (coarse grid) for the first 43 ms

KROTOS tests

In support of the large-scale FARO tests the KROTOS facility was used during 1993 for FCI studies in the molten uraniumoxide-zirconiumoxide/water system. The objectives of these tests were to investigate in a 1-D geometry the premixing of molten fuel jets with nearly saturated and subcooled water.

The experimental set-up and procedures were already described in the Annual Report 1992 (see also [22]), as well as the test results for the Al_2O_3/water tests, performed during 1991/92. A view of the KROTOS test facility is shown in ***Fig. 1.85***. A general arrangement of the KROTOS test section is given again in ***Fig. 1.86*** (here for KROTOS 32) which also shows the experimental instrumentation, mainly consisting of pressure transducers and thermocouples.

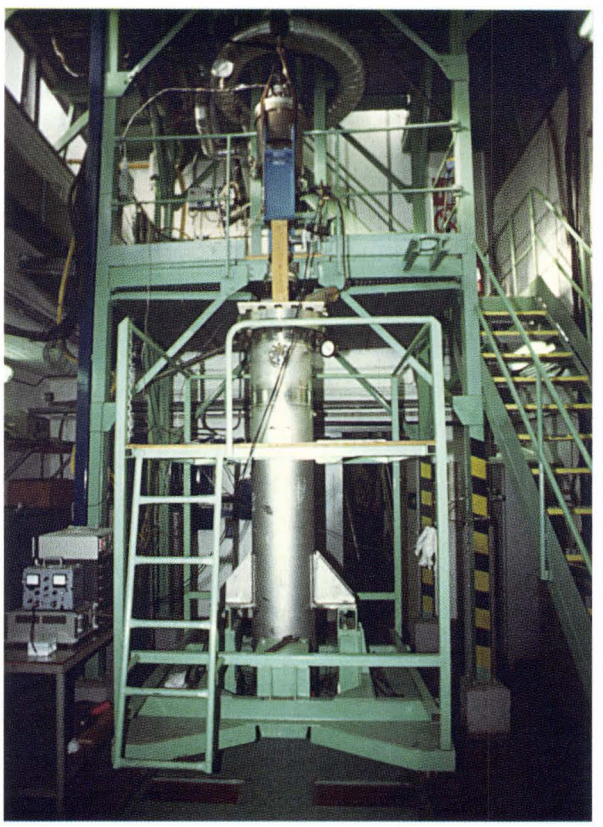

Fig. 1.85 View of the lower part of the KROTOS test facility

A pre-test series with UO_2/ZrO_2 melts showed that some modifications of the facility were required with respect to the previous test series with molten tin and aluminiumoxide. The high temperatures (up to 3273 K) involved in the UO_2 melting using graphite heaters caused material problems due to unexpected chemical reactions. For these reasons the graphite heater elements were replaced by tungsten heaters. The pre-test also demonstrated that helium was better suited as furnace cover gas than argon. Furthermore, due to the high temperatures in these tests only tungsten could be used as the material for the melt crucible and the puncher (the device for destroying the crucible bottom). Extensive work had to be done to refine the sophisticated fabrication techniques to machine the bottom membrane of the tungsten crucibles according to the required dimensions (0.2-0.3 mm thickness).

In both tests, KROTOS 32 and 33, about 3 kg of melt composed of 80 w% UO_2 and 20 w% ZrO_2 (density 8.0 cm^3/g) at 3073 K was used. The melt was contained in the W-crucible of 3 mm wall thickness and dropped from the furnace onto the W-

puncher where the bottom membrane was ruptured (*Fig. 1.87*). In these tests the tin brake disk was not used because the pre-tests showed that the UO_2/ZrO_2 melt would develop a crust upon touching it. This crust was observed to block the melt injection into the test tube (KROTOS 31). The nozzle exit was positioned 0.46 m above the water free surface in the test tube. The initial water temperature was 351 K in KROTOS 32 and 298 K in KROTOS 33. The tests were performed at an initial pressure of 0.1 MPa. The height of the water column in the test tube was 1.08 m and its diameter 95 mm. At the upper

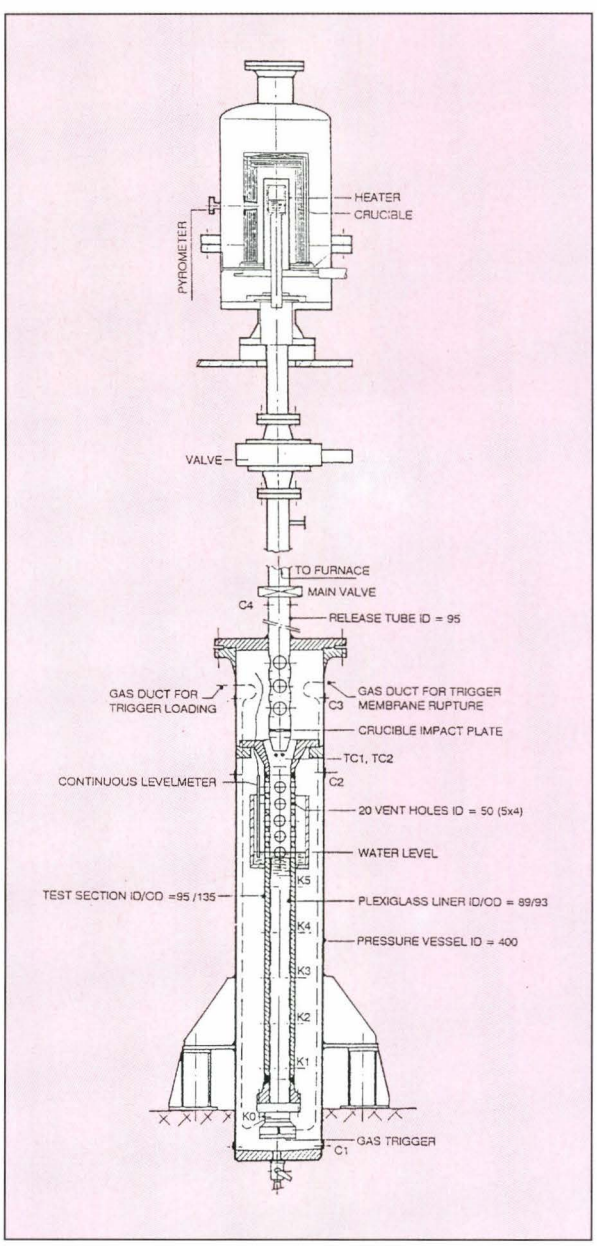

Fig. 1.86 KROTOS test facility

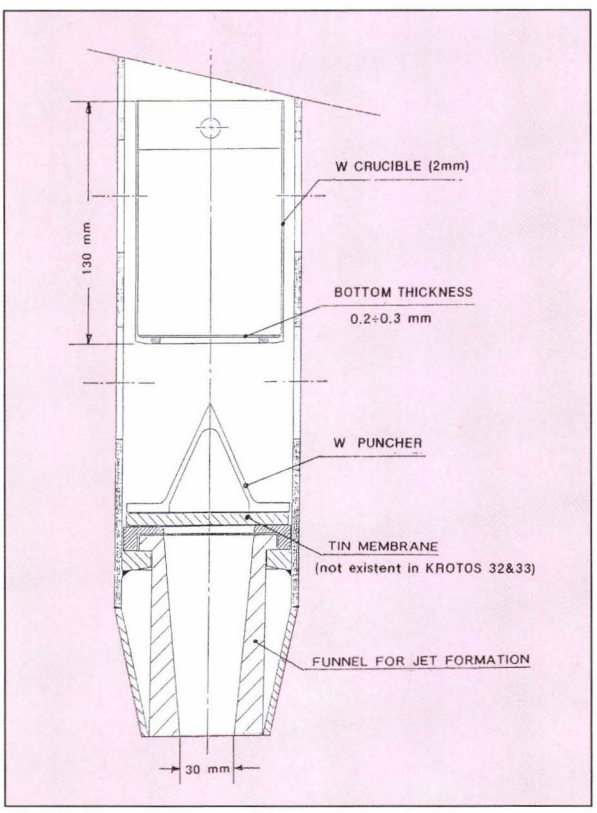

Fig. 1.87 Crucible with puncher for uraniumoxide/zirconiumoxide - water tests

Table 1.8 Summary of KROTOS UO_2/ZrO_2 initial conditions

	32	33
Melt composition, wt%	80.8 UO_2 19.2 ZrO_2	81.2 UO_2 18.8 ZrO_2
Melt mass, g	3033	3170
Melt temperature, K	3073	3073
Water mass, kg	7.45	7.65
Water depth, cm	1.08	1.08
Water volume, liters	9.5	10
Water temperature, K	351	298
System pressure and cover gas	1 bar Helium	1 bar Helium
Tin plate brake	no	no
Test section liner	plexiglass	no
Debris catcher	Al_2O_3	Stainless Steel
Release nozzle diameter, mm	30	30
External trigger	no	no

part of the test tube a steel vessel of 205 mm inner diameter was mounted and filled up with water to the test tube water level. In this vessel, levelmeters were placed to measure the water level swell during melt-coolant mixing. Levelmeter data allow to estimate the integral vapour void fractions in the test volume. The initial conditions are summarised in ***Table 1.8***. The zero-time signal for the data acquisition was generated by the falling crucible fracturing a copper wire in the release tube. This signal is the time reference for all measurements.

KROTOS 32 test

The objective of this test was to study premixing of UO_2/ZrO_2 melts with water at low subcooling (22 K) and to determine if an energetic FCI could take place under such conditions. A plexiglass liner was used in the test section to reduce the risk of a spontaneous steam explosion upon the melt contacting the walls of the test section. Approximately 3 kg of UO_2/ZrO_2 was heated up to 3073 K in a tungsten crucible. After the test sequence initiation, the crucible was released and fell down onto the puncher. Since the test was performed without a brake disk, the melt was free to stream out through the punctured crucible bottom and funnel into the water without any time delay.

The thermocouple data shown in ***Fig. 1.88*** give an estimate of 4.2 m/s for the leading edge velocity using the thermocouples TC6 and TC7 as melt arrival indicators. This value is significantly lower than the value considering a gravity release of the melt from the furnace. Evidently, the puncher and funnel assembly slowed down the release rate. Thermocouples in the water allowed for the estimation of the melt velocity after penetration into the water. The estimated velocity of the melt jet between TC5 and TC6 was approximately 1.5 m/s. The thermocouple data demonstrate that the coherent jet penetrated at least down to TC5. ***Fig. 1.89*** shows the arrival time of the quenched material at each thermocouple location down the tube.

No energetic interactions occurred, and the pressurization of the expansion volume was only due to the steam generation of the quenching melt (see ***Fig. 1.90***). The initial steam spike reaches approximately 2.3 bar and then the pressure falls quickly to the quasi steady-state value of about 0.5 bar due to condensation heat-transfer onto the cooler test section walls.

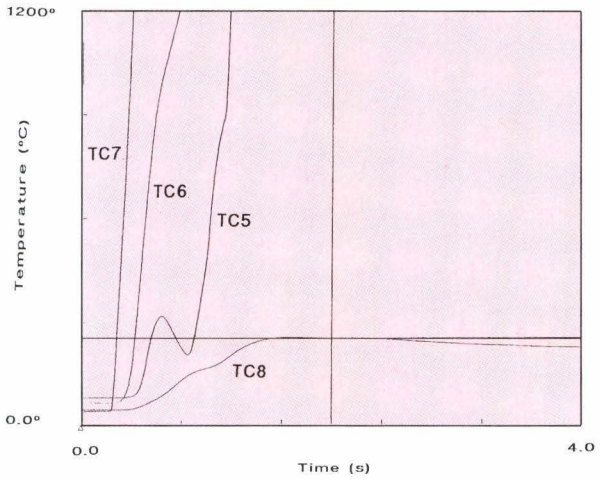

Fig. 1.88 Measured temperature histories in KROTOS 32 test

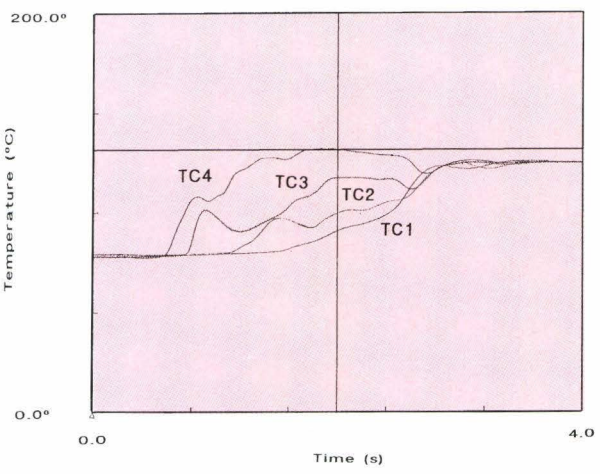

Fig. 1.89 Measured water temperatures in KROTOS 32 test

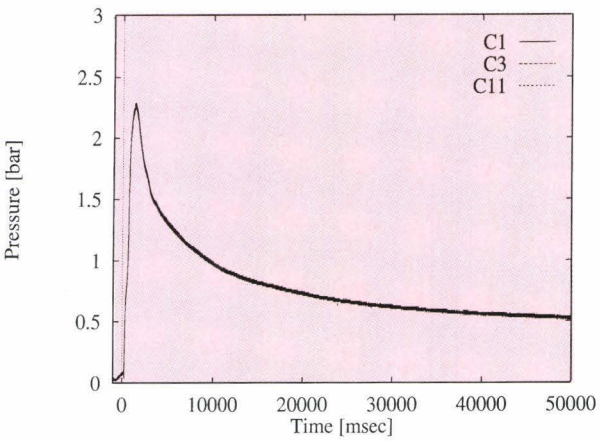

Fig. 1.90 Pressurization of the expansion vessel in KROTOS 32 test

KROTOS 33 test

The KROTOS 33 test was essentially a repeat of the KROTOS 32 test except that the water subcooling was higher (75 K) and that the plexiglass liner was removed from the test section. A similar estimate to KROTOS 32 for the leading edge velocity was obtained (see ***Figs. 1.91*** and ***1.92***). The TC6 and TC7 data indicated a somewhat higher velocity of 8 m/s prior to melt penetration into the water. Once in the water, the jet decelerated rapidly from the average velocity of 4.4 m/s between TC6 and TC5 to 0.9 m/s between TC5 and TC4. Due to the higher subcooling, the pressurization of the expansion volume is less than in KROTOS 32 with a maximumof about 1.4 bar and a quasi steady-state level of about 0.25 bar (see ***Fig. 1.93***).

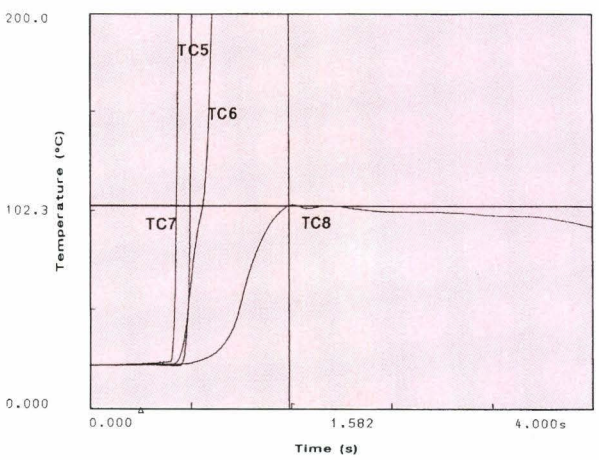

Fig. 1.91 Measured temperature histories in KROTOS 33 test

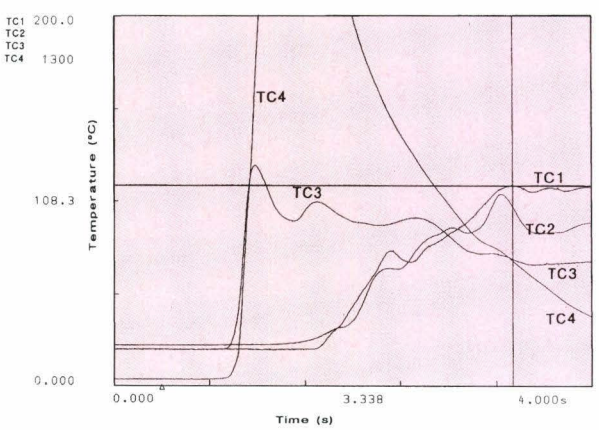

Fig. 1.92 Measured water temperatures in KROTOS 33 test

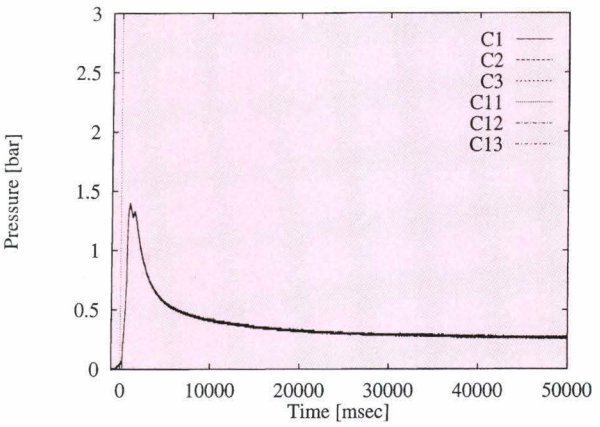

Fig. 1.93 Pressurization of the expansion vessel in KROTOS 33 test

Summary of KROTOS 32 and 33

Table 1.9 summarises the experimental results. In the following the main observations have been listed:

- no steam explosions,
- initial melt/water contact gives rise to some early water expulsion with debris sweep-out into the levelmeter container and pressure vessel,
- molten jet penetration at least 35 cm down into the water column,

Table 1.9 Summary of KROTOS UO_2/ZrO_2 results

Description	32	33
T_{sub}, K	22	75
Water temperature, K	351	298
Leading edge velocity at water surface, m/s	~4.2	~8.0
Confirmed penetration depth of the jet	TC5	TC4
Spontaneous explosion	no	no
Total debris, g	2607.9	2802.4
Debris mass in catcher, g	1401.7	1704.7
Debris smaller than 0.1 mm, g	20.9	37.4
Post test water level and volume	H=90.5 cm V=5.9 l	H=95.5 V=6.3 l
Max pressure increase in the expansion volume, bar	2.3	1.4

- more than 50 percent of the melt mass settled in the bottom of the test tube (initial water column 108 cm),
- the higher melt jet velocity along with the higher subcooling may have contributed to slightly enhanced fragmentation in KROTOS 33, see *Table 1.9*.

In 1994, the KROTOS test series with UO_2/ZrO_2 is continuing with tests to investigate the potential of steam explosions by using external triggers (strong gas trigger, see [22]). Furthermore, the effects of 2-D flow field on mixing are going to be examined with a larger diameter test section and with higher amounts of melt.

Analysis of KROTOS experiments with TEXAS-III

The TEXAS-III computer code has been used to analyse the KROTOS 26 test (see ***Fig. 1.86*** where the experimental arrangement is illustrated). The conceptual picture of the model adopted to describe the vapour explosion in TEXAS-III is represented by vapour film collapse due to Rayleigh-Taylor instabilities generated by a "trigger" pressure pulse and subsequent penetration of coolant microjets into the molten fuel. The rapid vaporization of these microjets within the fuel drop, produces local pressure growth and fuel fragmentation thus increasing the fuel surface area of heat exchange and hence vaporizing more coolant with subsequent additional pressure increase. This mechanism enhances the process of film collapse in the surrounding fuel drops leading to a spatial explosive-like propagation phenomenon.

The objective of the KROTOS 26 test was the triggering of a steam explosion at 0.1 MPa system pressure. From a mass of 1.4 kg Al_2O_3 at 2573 K, less than 1 kg was drained from the Mo-crucible and poured into a pool of 7.2 kg of water at 333 K. The trigger pulse of an amplitude of 10 MPa, was fired 2 s after zero-time but at that instant the melt front was at most above the K4 transducer. Nevertheless, a steam explosion did occur. The strong pressure wave generated exceeded the upper limit of the pressure transducers (25 MPa).

The TEXAS-III capabilities to model such explosion phenomena are shown in ***Fig. 1.94***, where the experimental pressure time histories recorded by the transducers KO, K1, K2, K3, K4 and K5 are compared with the results calculated by the code. The agreement is considered satisfactory for all the positions except for transducer K4. However, the transducer K4 was considered unreliable because its pressure signal is too low compared with that of other transducers.

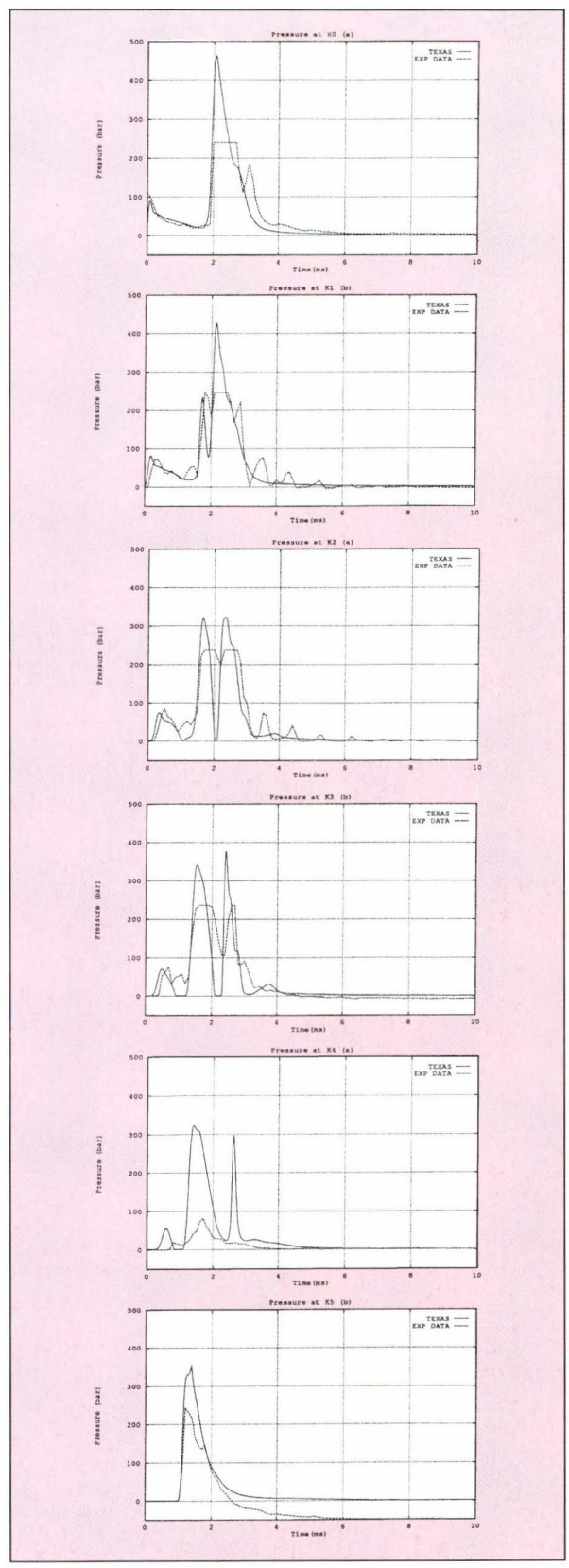

Fig. 1.94 Comparison of transient pressure histories in KROTOS 26 test and TEXAS III predictions

References

[1] MAGALLON D. et al. - Quenching Test-2 Data Report, JRC-Ispra Technical Note I.93.154, Nov.1993

[2] MAGALLON D. - Preliminary Proposal for a FARO Experimental Programme on the Core Retention Issue for Advanced Nuclear Power Plants, Internal Report made in the frame of Accordo di Collaborazione N. 4549-91-11 TG ISPI con ENEL, May 1993

[3] MAGALLON D., HOHMANN H. - High Pressure Corium Melt Quenching Tests in FARO, CSNI Specialist Meeting on Fuel Coolant Interaction, Santa Barbara (CA), 5-8 Jan.1993

[4] MAGALLON D. - Scoping Test Data Report, JRC-Ispra, Technical Note I.92.135, Dec.1992

[5] WIDER H., BENUZZI A., HOHMANN H., MAGALLON D., YERKESS A. - Quick Look Report on the Scoping Test, JRC-Ispra, Technical Note I.92.139, Dec.1992

[6] WIDER H. - Quick Look Report on the Quenching Test, JRC-Ispra, to be issued as Technical Note

[7] CHU C.C., CORRADINI M.L, MURPHY J., TANG J. - A Code Manual for TEXAS-II; Nucl. Eng. and Eng. Physics Dept., Univ. of Wisconsin, 1991

[8] BERTHOUD G.,VALETTE M. - Calculations of the Premixing Phase of an FCI with the TRIO-MC Code, CSNI Specialist Meeting on Fuel Coolant Interaction, Santa Barbara (CA), 5-8 Jan. 1993

[9] CARLSON K.E. et al. - RELAP5/MOD3 Code Manual (DRAFT)- NUREG CR 5535 -EGG 2596, 1990

[10] ANNUNZIATO A. - Quick Look Report on LOBI-MOD2 Test BL-34 -LQC 91-60, COM 4538, 1991

[11] ANNUNZIATO A. - COMETA vO.4: Post-Test Calculations of FARO Tests L-06 and L-08, JRC-Ispra, Technical Note I.93.115, 1993

[12] ANNUNZIATO A. - COMETA vO.4 Pre-Test Calculation of FARO Base Case Test, JRC-Ispra, Technical Note I.93.114, 1993

[13] TANG J. - Modeling of the Complete Process of One-Dimensional Vapour Explosions, PhD Thesis, Univ. of Wisconsin, 1993

[14] YOUNG M.F., GIGUERE P.T. - The IFCI (Integrated Fuel Coolant Interaction), Code: Models, Correlations and Quality Assurance, Sandia Innovative Technology Applications Division, SNL, Albuquerque, NM, 1990

[15] DOSANJH S.S. (ed). - MELPROG-PWR MOD1: A Two-Dimensional, Mechanistic Code for Analysis of Reactor Core Melt Progression and Vessel Attack under Severe Accident Conditions, SAND88-1824, NUREG/CR-5193, Albuquerque, NM, 1989

[16] RUEL F. - Numerical Simulation of Reacting Gas Flows: Basic Models and Algorithms, Presentation of a Preliminary Code Version, JRC-Ispra Technical Note I.91.109, Sept. 1991

[17] HULD T. - An Implicit Chemical Kinetics Solver for Multi-dimensional Reactive Flow Simulations: Application to Hydrogen Combustion Schemes, JRC-Ispra Technical Note I.91.155, December 1991

[18] DONEA J., RUEL F., SORIA A. - On the Numerical Simulation of Hyperbolic Problems, Deuxième Congrès Methodes Numériques en Ingénierie, La Coruña, Espagne, 7-11 June 1993

[19] PEGON P., SORIA A., LAVAL H. - A Review of Finite Element Solvers for the Compressible Navier-Stokes Equations, EUR 14987 EN, 1993

[20] SORIA A., PEGON P. - Semi-Implicit Conservative Upwind Schemes for Transient Compressible Flows, EUR 14986 EN, 1993

[21] PETER G., HULD T. - Calculation of a Hydrogen Detonation in the FARO Bunker using REACFLOW, a Code for Numerical Simulations of Reactive Gas Flows, JRC-Ispra Technical Note to be published Jan. 1994

[22] HOHMANN H., MAGALLON D., SCHINS H., YERKESS A. Experiments in the Aluminumoxide/Water System, CSNI Specialist Meeting on Fuel Coolant Interaction, Santa Barbara (CA), 5-8 Jan. 1993

1.1.3 THERMALHYDRAULICS

The activities in the field for reactor thermal-hydraulic safety research and development have been concentrated on the analysis and documentation of the LOBI test data and on the coordination of the LOBI Data Users Club assembling experts from EU as well as Central and East-European countries research organisations.

LOBI test analysis and documentation

A comprehensive experimental data base, pertinent to a wide range of postulated accident conditions in Pressurized Water Reactors (PWRs), has been established in the framework of the LOBI (LWR Off-normal Behaviour Investigations) experimental programme carried-out from December 1979 to June 1991. In its final form, the LOBI Data base comprises the test data of 70 experiments (***Tables 1.10*** and ***1.11***) performed in the LOBI test facility, a 1:700 scale model of a 4-loop 1300 MWe PWR.

As for the programmatic objectives of the LOBI research programme, the acquired data base provides a valuable set of reference information for the evaluation of PWRs loss-of-coolant accidents (LOCAs) and other risk dominant sequences such as anticipated

Table 1.10 LOBI-MOD1 experimental programme

Test	Sponsored by	Date	Description
			Large Downcomer 50 mm
A1-04	Germany	12.12.79	200% CL Break LOCA, CL ECC
A1-01	Germany	29.01.80	200% CL Break LOCA, CM ECC
A1-02	Germany	14.02.80	200% CL Break LOCA, CM ECC
A1-03	Germany	19.03.80	200% CL Break LOCA, CL ECC
A1-05	Germany	06.05.80	200% CL Break LOCA, CM ECC
SD-SL-01	Germany	04.06.80	10% CL Break LOCA
SD-SL-02	Germany	18.06.80	1% CL Break LOCA
SD-SL-03	Germany	24.09.80	0.4% CL Break LOCA
A2-59	Germany	27.10.80	100% CL Break LOCA, CL ECC
B-101	France	26.11.80	2x50% CL Break LOCA, CL ECC
A2-55	Germany	19.01.81	50% CL Break LOCA, CL ECC
A2-59R	Germany	11.02.81	100% CL Break LOCA, CL ECC
B-R1M	Germany	17.03.81	25% CL Break LOCA, CL ECC
			Small Downcomer 12 mm
A1-66	Germany	03.07.81	200% CL Break LOCA, CL ECC
A1-07	Germany	09.07.81	200% CL Break LOCA, no ECC
A1-06	Germany	21.07.81	200% CL Break LOCA, CM ECC
A1-67	Germany	30.09.81	25% CL Break LOCA, CM ECC
A1-68	Germany	28.10.81	50% CL Break LOCA, CM ECC
A1-10A	Germany	25.11.81	200% HL Break LOCA, CM ECC
A1-10B	Germany	10.12.81	200% HL Break LOCA, CM ECC
A1-70	Germany	13.01.82	200% PS Break LOCA, CM ECC
A1-73	Germany	04.02.82	25% HL Break LOCA, CM ECC
A1-72	Germany	24.03.82	200% CL Break LOCA, CM ECC
A1-69	Germany	06.04.82	100% CL Break LOCA, CM ECC
A1-74	Germany	21.04.82	200% CL Break LOCA, CM ECC
B-222	France	05.05.82	2x50% CL Break LOCA, CL ECC
B-302	Italy	16.06.82	2x50% HL Break LOCA, CL ECC

Table 1.11 LOBI-MOD2 experimental programme

Test	Partner Country	Date	Description
A1-76	D	12.04.84	SG Performance
A2-81	D	27.09.84	1% CL Break LOCA, 2/4 HPIS in CL
A1-82	D	28.09.84	1% CL Break LOCA, 2/4 HPIS in HL
A1-78	D	24.10.84	2% CL Break LOCA, ECC in CM
A2-77A	D	28.11.84	Natural Circulation, 90 and 75 bar
A1-83	D	19.12.84	10% CL Break LOCA, ECC in CM
A2-90	D	27.03.85	LONOP-ATWS "Station Blackout"
A1-85	D	07.05.85	0.4% Pressurizer Break, 2/4 HPIS in HL
BL-00	F	03.07.85	0.4% CL Break LOCA, 1/3 HPIS in CL
A1-84	D	14.10.85	10% HL Break LOCA, ECC in CM
BT-00	UK	30.11.85	LOFW+Bleed and Feed
BT-01	B	24.01.86	Small (10%) Steam Line Break+PTS
BL-02	UK	22.03.86	3% CL Break LOCA, 2/4 HPIS in CL
A1-79	D	15.05.86	1% CL Break LOCA, 4/4 HPIS in HL
A1-88	D	11.06.86	0.4% CL Break LOCA, as. Cooldown
BL-01	D	20.09.86	5% CL Break LOCA, HPIS+ACCU in CM
BC-01	WG-B	18.10.86	SG Secondary Inventory
BC-02	WG-B	26.11.86.	SG Heat Losses
BL-21	I	24.01.87	0.4% SGTR+'SSN' Recovery
BL-12	F	19.02.87	1% CL Break LOCA, no HPIS, no Cooldown
BT-02	F	09.05.87	LOAF+Feed and Bleed
BT-12	UK	17.06.87	Large (100%) Steam Line Break
A1-91	D	26.09.87	1% CL Break LOCA, 1/4 HPIS in HL
BT-03	I	24.10.87	LOFW-ATWS+'SSN' Recovery
A1-92	D	30.11.87	Natural Circulation, 40 bar
BL-16	D	19.03.88	0.4% CL Break LOCA, as. Cooldown
BC-03	WG-B	15.04.88	SG Heath Losses
A1-93	D	30.04.88	2% CL Break LOCA, no HPIS
A1-94	D	27.05.88	4% CL Break LOCA, 40 bar
BC-04	WG-B	07.02.89	Core Bypass Measurement
BL-30	WG-B	15.04.89	5% CL Break LOCA, HPIS+ACCU in CL
BL-22	B	17.06.89	0.4% SGTR+Cooldown
A1-87	D	11.11.89	PCS Cooldown, MCP off
BT-04	F	10.02.90	PCS Cooldown, MCP on, 1-SG isolated
BL-34	WG-B	22.03.90	6% CL Break LOCA at Low Power, BETHSY CPT
BL-44	JRC	26.04.90	6% CL Break LOCA at Full Power, no HPIS
BT-56	UK	03.07.90	Multiple Failures
BT-15/16	UK	22.11.90	LOFW with SG Boiloff and Refill, MCPs on/off
BT-17	D	07.02.91	LOFW with SG Bleed and Feed
BT-06	F	21.03.91	Small (10%) Feed Line Break
BL-40	E	16.05.91	SGTR in 1-Loop PWR
BL-06	F-UK	21.06.91	1% CL Break LOCA, HPIS off, MCP on

and abnormal transients. The test data are of specific relevance for:

- identification and/or verification of basic thermal-hydraulic phenomenologies governing the evolution of PWR accidents with emphasis on the performance of the engineered safety systems and on the effectiveness of accident management strategies,
- development and/or validation of analytical models and the assessment and/or improvement of the predictive capabilities of system codes used in water cooled reactors safety analysis.

The LOBI test data constitute an integral part of the reactor safety research and code assessment programmes of several EU member countries. LOBI data are systematically used being included in the assessment matrices of the French code CATHARE and of the German code ATHLET. Various research organisations are also using the data for the assessment of other system codes such as RELAP and TRAC.

Through a special arrangement with the Organisation for Economic Cooperation and Development (OECD),

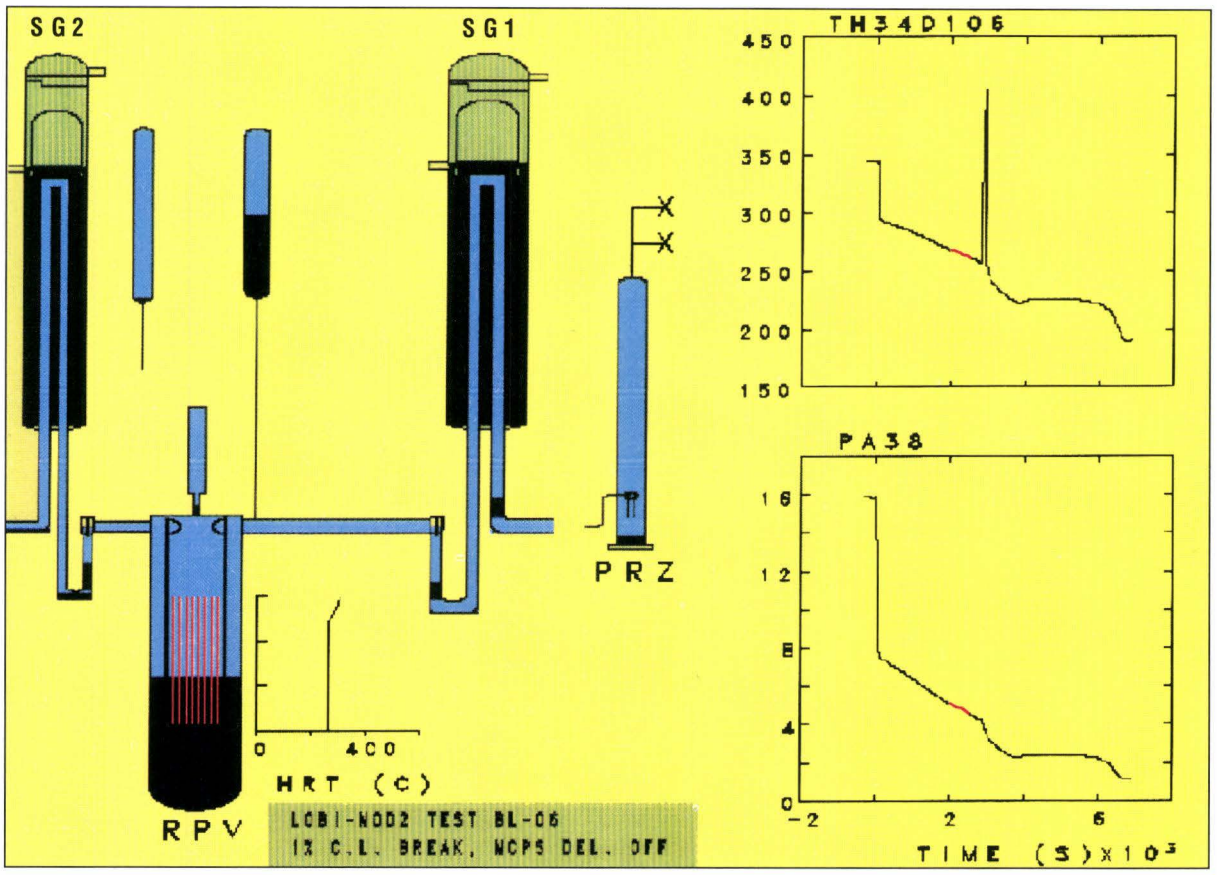

Fig 1.95 Display of fluid distribution in LOBI-MOD2 test BL-06 at 2500s after rupture

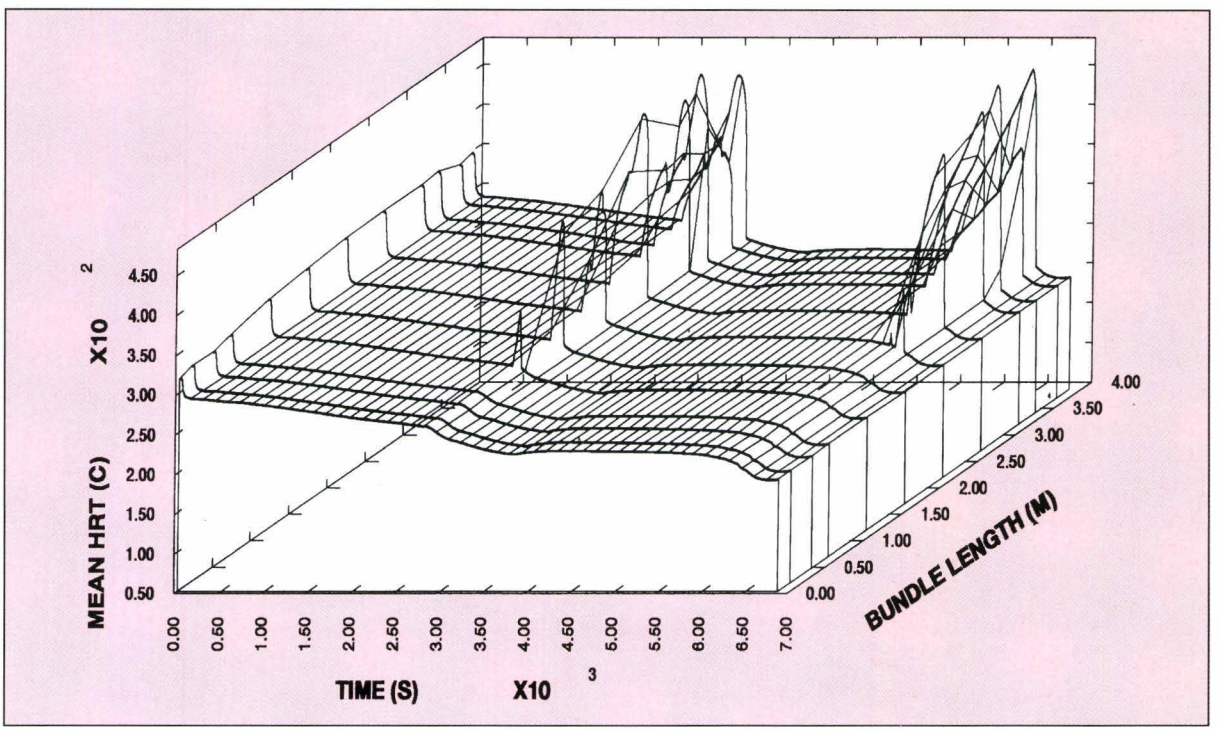

Fig. 1.96 3-D plot of core temperature response in LOBI-MOD2 test BL-06

several LOBI tests have been included in the international code assessment programme of the OECD Committee on the Safety for Nuclear Installations (CSNI) and are thus available also outside the EU context. Some research organisations from Central- and East-European countries have requested the access to and the use of the LOBI Data Base. In view of the emerging cooperation in science and technology with non-EU member countries, the data are being released to requesting organisations following the establishment of collaborative agreements in the frame of Article 10 of the EURATOM Treaty.

During the reporting period a considerable effort has been devoted to the analysis and documentation to provide prospective users with the required reference information [1-11]. Accident management strategies alternative to conventional emergency operating procedures are being considered to enhance the safety margins of reactors of current design or are being integrated in the conceptual development of advanced reactor configurations within this context, the effectiveness of secondary system feed and bleed in the LOBI test facility has been assessed through a detailed post-test analysis of the results from Test BT-17 [6].

The influence of the main coolant pump operation during the evolution of a small break LOCA has been evidenced by the post-test analysis of LOBI-MOD2 test BL-06 [8]. Specifically, it has been shown that pump operation mode is clearly coupled to primary system mass depletion and distribution and thus, to core thermal response, ***Figs. 1.95*** and ***1.96***.

Table 1.12 LOBI Data Users Club

Country	Institutions
Germany	GRS, Siemens-KWU, Battelle
France	CEA, FRAMATOME
UK	Nuclear Electric, AEA Technology, Rolls Royce
Belgium	TRACTEBEL
Italy	ENEA, PISA UNIVERSITY
Spain	CIEMAT, UPC, Union FENOSA
Hungary	KFKI Atomic Energy Research Institute
Poland	Institute of Atomic Energy
Russia	Science and Engineering Safety Centre Electrogorsk Research and Engineering Centre
Czech Republic	Nuclear Research Institute

LOBI data user's club

In line with the tradition of an effective approach to international collaboration in the field of water cooled reactor safety research, the LOBI Data Users Club established upon request of several EU member countries, has been convened. The terms of reference of such a Club is to provide the framework for a continuing collaboration among experts from institutional and industrial organisations from EU as well as Central- and East-European countries (***Table 1.12***). Specifically, the LOBI Data Users Club aims at providing:

- an open forum for the presentation and discussion of significant results deriving from the application of the LOBI data, including test analyses, code assessment, evaluation of counter part tests and accident management strategies,
- a scheduled opportunity to LOBI data users for the exchange of related experience and expertise as well as for interfacing with the JRC staff to obtain information and clarification for the interpretation of the data,
- the bases for the phenomenological classification of the LOBI tests to direct the selection of the test cases for code application and assessment.

As structured, the LOBI Data Users Club intends to follow-up the activities previously carried out in the LOBI Working Group B as well as in the LOCA and Special Transients Task Forces. Such a club will contribute to the promotion of international collaboration in the field of water reactor safety research and will be open and, as appropriate, enlarged to research organisations from Central and East-European countries to enhance the establishment of a common safety culture on a pan-European level.

References

[1] ADDABBO C., LEVA G., ANNUNZIATO A. - Experimental Data Report on LOBI-MOD2 Test BT-15/16; CEC-JRC, COM 4346, March 1993

[2] ANNUNZIATO A. - Quick Look Report on LOBI-MOD2 Test BT-15/16; CEC-JRC, COM 4347, April 1993

[3] ADDABBO A., LEVA G., ANNUNZIATO A. - Experimental Data Report on LOBI-MOD2 Test BT-06; CEC-JRC, COM 4348, May 1993

[4] PRETEL C., REVENTOS F. - Post-Test Analysis of LOBI Test BL-30 using RELAP5/MOD2.5; CEC-JRC, Technical Note I.93.64, May 1993

[5] SEIGNEURET-GABORIT N. - Analysis of Typical LOBI Test Results Relevant to PWR Safety Analysis; CEC-JRC, Technical Note I.93.70, June 1993

[6] ANNUNZIATO A. - Phenomena Influencing Secondary Side Feed and Bleed Effectiveness in Pressurized Water Reactors; NURETH-5, Grenoble (F), October 1993

[7] ADDABBO C., LEVA G. - Quick Look Report on LOBI-MOD2 Test BT-06; CEC-JRC, COM 4249, June 1993

[8] ADDABBO C., LEVA G., ANNUNZIATO A. - Experimental Data Report on LOBI-MOD2 Test BL-06; CEC-JRC, COM 4350, October 1993

[9] ADDABBO C., LEVA G., ANNUNZIATO A. - Experimental Data Report on LOBI-MOD2 Test BL-40; CEC-JRC, COM 4353, November 1993

[10] ADDABBO C., LEVA G., ANNUNZIATO A. - Experimental Data Report on LOBI-MOD2 TEST BT-04; CEC-JRC, COM 4351, November 1993

[11] ADDABBO C., LEVA G., ANNUNZIATO A. - Experimental Data Report on LOBI-MOD2 Test BT-56; CEC-JRC, COM 4352, December 1993

1.2 MANAGEMENT AND STORAGE OF RADIOACTIVE WASTE

After the decision taken at the beginning of the year, not to proceed with the studies on waste management alternatives, the activities of the PETRA facility have been focused on the completion of the second "nuclear test" as agreed with the Italian Licensing Authority (ENEA-DISP), limited to the utilization of depleted unirradiated Uranium and Fission Products simulants. On the basis of the results the facility was declared suitable for starting hot operation by the Safety Authorities.

PETRA operations have been mothballed in June 1993. At the present time a decision is pending on the (possible) utilisation of PETRA as a tool for testing instrumentation and validate mass/volume calibration procedures, as foreseen by the Safeguards Programme.

For intermediate storage, transport and final disposal of radioactive waste, the waste package has to fulfil the waste acceptance criteria, as defined by the nuclear regulatory institutions of the various countries. Important, especially for storage or final disposal, is the radiochemical content of the waste package.

The fulfilment of the waste assay criteria concerning radiochemical content can be verified by the execution of a quality assurance programme from the waste production up to the waste package, ready for final disposal, complemented by computations and/or measurements at the beginning, during and at the end of waste treatment. A programme to develop measurement systems, instruments and analysis methods is executed in order to enable an experimental assay of waste packages with sufficient accuracy.

Plutonium containing waste is assayed by passive neutron interrogation using the time correlation method (TCA) possibly complemented by gamma interrogation to measure the isotopic composition. The problem for uranium containing waste is much more difficult. The measurement is based on active neutron interrogation with an external neutron source. An R&D project is in execution to attack this problem with the final goal to produce an instrument to assay uranium in waste. Non-fissile waste is measured by gamma-scanning. Again two factors determine the precision with which the content of gamma contaminants in waste is determined: the absorption of the matrix and the source distribution. A gamma-scanner and adapted software is currently used.

1.2.1 THE PETRA FACILITY

PETRA is a hot cell facility designed to produce various types of fully active waste such as they will arise from any kind of present and future spent fuel processing with high and ever increasing burn-up. The reference research programme places specific emphasis on processes suitable to minimise waste (and to improve the quality of the conditioned waste product). The facility can also be seen as a tool for customers and central bodies associated with the quality and characteristics of the final product for performing independent verification and control. In addition Safeguards Authorities can utilise PETRA for testing under realistic conditions instrumental and analytical methods and procedures for fissile material flow control in processes and waste streams at reprocessing facilities.

Activities

The aim of the PETRA programme during the year has been focused on the completion of the second "-nuclear test" as agreed with the Italian Licensing Authority (ENEA-DISP).

The main activities carried out in the PETRA facility can be summarised as follows:

- The third phase of the second nuclear test, the so-called "Uranium solidification" process started in January. The fission product free uranyl nitrate solution which was stored as final "product" at the end of the previous "1st extraction cycle", has been utilised for the solidification process. About 27 dm^3 of solution (with 280 g/dm^3 nitrate concentration) have been transfered through a reciprocating pump (delivery rate 1,5 dm^3/h) from the storing vessel located in cell 4306 into the solidification crucible located in cell 4305. Temperature of the crucible has been regulated at about 300° C during the above feeding phase and dry nitrates have been produced. Temperature has then been raised up to 550° C for nitrate decomposition. A "yellow cake" including mixed Uranium oxides and nitrate residues has been the final process "product". Steam leaving the crucible has been condensed and analysed to evaluate the decontamination factor during the process. Condensate has been recycled, concentrated and then transferred to the crucible in order to solidify all uranyl nitrates residues. After solidification completion, the crucible has been weighed on a balance located in cell 4304. A content of 3585g non-irradiated uranium has been measured. *Fig. 2.1* shows a photographic view of cell 4304 during weighing operations. NOx output has been recordered during the whole process.
- As complementary activity a campaign for treating all aqueous liquid wastes which were produced in the second nuclear test, has been performed in the period March - May. Process vessels have been rinsed by flooding them through the decontamination system. Small quantities of disseminated uranyl nitrates have been recovered and then solidified. About 578 dm^3 of aqueous distillate including only a few grams of uranium have been transferred to the JRC centralised liquid waste treatment facility.
- All the circuits involved in solidification process and in liquid waste treatment have worked in a proper manner.
- After solidification completion the absolute filters installed in the Vessel Off-Gas-System have been inspected. No traces of uranium have been detected on the last stage filter.

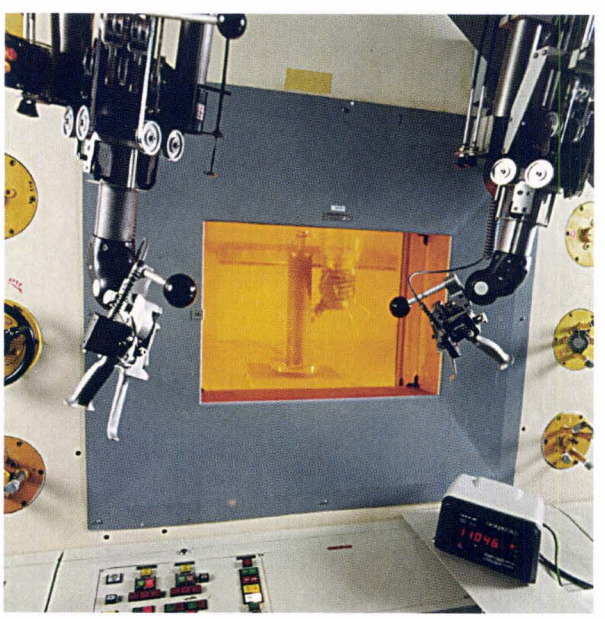

Fig. 2.1 View of cell 4304 during weighing operation

On the basis of results of "nuclear tests" performed up to this stage it can be concluded:

- The five PETRA plant safety systems have met the imposed requirements. No defects have been detected during the entire series of nuclear tests runs. The organisation which was set up for the test programme has achieved the proposed objectives. The Process Computerised System, telemanipulators and remote operated cameras, have successfully been utilised by the operating team.
- Radioactive aerosols have been completely trapped in the Vessel Off-Gas-System.
- Aqueous liquid wastes have been properly managed within the imposed plant requirements. Discharged radioactive contaminants have been well below the acceptable plant limit.
- All the functional systems involved in the nuclear test have demonstrated their capability to implement the research programme.

Since June the plant is in a rest condition. A few liters of concentrated uranyl nitrate are available for further tests. Chemical additives simulating the fission products as well as organic solvents have been collected in separate single vessels.

Planning 1994

PETRA operations have been mothballed in June 1993. At the time being a decision is pending on the (possible) utilisation of PETRA as a tool for testing instrumentation and validate mass/volume calibration procedures, as foreseen by the Safeguards Programme.

1.2.2 MONITORING OF RADIOACTIVE WASTE

The research activity in the field of waste monitoring has been developed and applied according to:

- active neutron interrogation methods for determining uranium content,
- passive neutron correlation methods for determining plutonium content,
- gamma interrogation methods for characterizing gamma-active waste.

Two factors make a measurement difficult and the application of special techniques mandatory. They are:

- the presence of a mostly unknown and inhomogeneous waste matrix,
- the random location of the radioactive contaminants in this matrix.

Measurement of uranium waste by active neutron interrogation

Existing active neutron interrogation devices like PHONID, AWCC, Cf shufflers, DDA are sensitive to matrix material and heterogeneous distribution of the fissile content. For this reason measurements with these devices need complex calibration campaigns for each individual class of material. Measurement accuracy sufflers since a proper classification of samples with respect to their calibration is very difficult.

An active neutron interrogation device with limited calibration requirements needs to determine the moderation and absorption characteristics of the matrix and to localize lumps of fissile material within the sample. This could be done accurately with a proper combination of transmission and emission measurements using position sensitive neutron specrometers. Before neutron spectrometry and position sensitive detectors can be used their response functions, especially energy and resolution calibration, have to be determined.

Neutron spectrometry development has been started, in collaboration with PTB, Braunschweig (Germany) for the classical NE 213 liquid scintillator. The work will be extended to gas-filled detectors, ^{3}He, ^{4}He and H. A NE 213 detector has been calibrated fully for gamma detection. The neutron calibration has started. The search for the spatial resolution of position sensitive ^{3}He tubes is being continued.

Assay of plutonium in waste by passive neutron correlation techniques

The activity in the field of Pu waste monitoring was subdivided in the following main actions:

- construction of an industrial waste barrel monitor,
- determination of an analytical dead time correction,
- development of a new time correlation analyser,
- field tests in collaboration with ENEA.

Construction of an industrial waste barrel monitor for Pu assay

A prototype waste barrel monitor for the assay of Pu in radioactive waste has been designed and build, and is undergoing final testing [1]. The design of the

Fig. 2.2 The new waste barrel monitor for passive assay of Pu

monitor is based on previous experiences from measurements with simulated waste at JRC Ispra and from measurement campaigns in nuclear facilities. The in-house experiments [2] served first of all to optimize design parameters such as the detection probability, decay constant of the time response function, external source shielding etc. The in-field campaigns [3,4] provided experience concerning the instrument requirements when applied to an industrial environment such as measures against fire hazard, criticality, contamination etc. Attention was paid as well to operator requirements for safe handling of standard radioactive waste containers. *Fig. 2.2* shows the barrel monitor in it's final configuration at JRC Ispra. A series of measurement campaigns utilizing the monitor at various nuclear facilities throughout Europe will be initiated early next year.

Analytical dead time correction of the signal pulse train

A theoretical treatment of updating dead times in signal pulse trains was needed for the analysis of Pu assay data from passive neutron detector systems. The theoretical treatment derives the dead time corrected correlated signal multiplets of first, second and third order from measured signal frequency distributions [5]. This technique has recently been programmed for three different observation interval trigger methods and a single data line. The technique is currently being tested on simulated measurement data.

The dead time correction is essential when the correlation analysis is applied to safeguards inspections of large Pu masses. However, esperiences from measurements on both real and simulated waste, has shown that the influence of dead time is significant even for Pu masses in the gram range when the (α,n) reaction rate is very high. This is, for example, the case for residues of spent reactor fuel with a large ingrowth of ^{241}Am.

The new dead time correction algortithms were first tested on the simple case of Poisson distributed neutron pulse trains. The simulated pulse trains of various dead times and count rates were corrected perfectly within the statistical uncertainty by the various algorithms.

At present, tests are carried out on Monte Carlo generated pulse trains simulating PuO_2 and ^{252}Cf neutron sources. *Table 2.1* shows for various masses of

Table 2.1 Effect of analytical dead time correction on the correlated doublets R_2 and correlated triplets R_3 for large Pu samples

Mass $^{240}Pu_{eq}$	R2 [s^{-1}]			$(R_{2.corr}/R_{2.theo})$ -1
[g]	Theoretical	Un-corrected	Corrected	[%]
500	113,459.3	91,234.3	112,967.7	-0.44
250	56,729.6	51,032.0	56,699.2	-0.05
125	28,364.8	26,978.5	28,468.9	0.37
72.5	14,182.4	13,813.9	14,200.6	0.13
36.25	7,091.2	6,989.5	7,094.8	0.05
	R_3 [s^{-1}]			$R_{3.corr}/R_{3.theo}$) -1
500	26,003.7	-1,688,321.1	23,419.8	-9.94
250	13,001.8	-266,442.9	12,081.1	-7.08
125	6,500.9	-31,833.6	6,500.0	-0.01
72.5	3,250.5	-2,361.9	3,062.0	-5.80
36.25	1,625.2	748.7	1,609.7	-0.96

The measurement parameters were:
Observation interval: 19.2 μs Detection probability: 0.50
Decay time 45.0 μs (α, n) neutrons/spont. fiss. neutrons=1.0
Dead time 0.1 μs

^{240}Pu equivalent, the dead time correction of the correlated doublets R_2, and the correlated triplets R_3, using the signal trigger method. The singlets R_1 were corrected perfectly, and are not included in the table. It can be seen that the R_2 rate, which is used in the shift register technique, is corrected satisfactorily. The error is within the statistical uncertainty arising from the limited number of pulses generated with the Monte Carlo code. For the R_3 rate, the large error for large Pu masses may be due to the influence of higher order multiplets. This is still being investigated. For both R_2 and R_3 the error without dead time correction is unacceptably large. It can be seen that the rates of un-corrected triplets could even be negative for large Pu masses.

Development of a new time correlation analyser (TCA)

A new TCA has been specified according to the acquired experiences at the JRC Ispra during the last decade. The analyser is presently being built under license by A.N.Technology Ltd, and is expected to be commercially available beginning of the new year. It is realised with modern programmable microchips (DSPs and FPGAs) which will give the instrument exceptional resolution and count rate capabilities. The analyser was presented at a joint A.N. Technology and JRC Ipra trade stand at the INMM annual meeting [6]. During the year the new analyser and the correlation analysis technique were described in several publications [3,4,6,7,8,9].

Collaboration with ENEA, Casaccia (Italy)

A measurement campaign, aimed at monitoring the Pu content in 15 litres primary containers of low density solid waste, has been carried out at the ENEA Casaccia IPU pilot plant at the predecommissioning stage during 1993 [4]. Two indipendent measuring systems and techniques have been used, namely:

- ENEA developed a fully automated system, based on the detection of specific gamma signatures of Pu isotopes: the technique is particularly suited for detection of low amounts of Pu in small containers,
- JRC Ispra developed a neutron measurement system, based on the TCA for monitoring Pu in both primary and secondary (220 l) waste containers: this technique is also suited for detection of high Pu content in waste containers.

The methodological approach for both systems is described. Experimental data, comparison of the results obtained by the different systems as well as a discussion of the achievable performance are also reported.

In preparation of the planned decommissioning measurement campaign, a sensibility study has been carried out. A well counter of 1000 mm height and 200 mm internal diameter has been applied for the sensibility study. The 32 ^{3}He tubes ordered in two rings provide for a high detector efficiency of 27%. The waste items provided for final disposal are contaminated by a small quantity of strong diluted plutonium. The multiplication effect (induced fission) is therefore neglected. Similarly, no matrix effect was considered for the 15 litres drums. The 1mg ^{240}Pu (corresponding to 10 nCi of total Pu in conditioned waste) can still be measured with sufficient precision. However, these measurements are characterized by long measurement periods.

Characterization of gamma active waste

An instrument and a method [10] were developed to assay low active waste produced during the decommissionig and operation of 'hot' installations (e.g. 'hot' cells). The system is in use since one year with good results. The extension to a tomographic method is under development.

References

[1] PEDERSEN B., BONDAR L. - Characterization of the new JRC waste barrel monitor, JRC Ispra, 1993, EUR report in preparation

[2] PEDERSEN B. - Experience with neutron correlation techniques for the assay of Pu in simulated waste barrels, JRC Ispra, 1993, Technical Note in preparation

[3] HAGE W., PEDERSEN B., BONDAR L., SWINHOE M., LEDEBRINK F.W. - Triple neutron correlation for MOX waste, American Nuclear Society, 1993 annual meeting, San Diego, June 20/24,1993

[4] VICINI C., RESTI P., ELEMENTI R., SARDO I., BONDAR L. - Measurement of low plutonium contaminated solid waste in 15 litre containers from Casaccia MOX pilot plant, ESARDA 15th annual symposium of safeguards and nuclear material management, Rome, Italy 11/13, 1993

[5] HAGE W., CIFARELLI D.M. - Correlation analysis with neutron count distributions for a paralyzing dead time counter for the assay of spontaneous fissioning material, Nucl. Sci. Eng. 112, 136 (1992)

[6] BONDAR L., HAGE W., LEDEBRINK F.W., MASON J.A., PEDERSEN B., SWINHOE M. - Assay of Pu by neutron multiplicity counting using periodic and signal triggered methods, INMM 34th annual meeting, Scottsdale Arizona July 18/21, 1993

[7] MASON J.A., BONDAR L., HAGE, PEDERSEN B. - The advantages of neutron multiple correlation analysis, ESARDA, 15th annual symposium of safeguards and nuclear material management, Rome, Italy, May 11/13, 1993

[8] HAGE W., PEDERSEN B., OCINO V., MASON J.A. - Development state of the triple neutron correlation technique by the factorial moment method at JRC Ispra, ESARDA international workshop on passive neutron coincidence counting, Ispra, Italy 20/23 April, 1993

[9] BONDAR L. - Passive neutron assay by the Euratom time correlation analyser, ESARDA international workshop on passive neutron coincidence counting, Ispra, Italy, 20/23 April, 1993

[10] BINDA F., DIERCKX R., DONGIOVANNI S., GRITTI R., REMORINI B. - JRC Ispra, Technical Note IST/NFC NE 40.1800.A.001

1.3 SAFEGUARDS AND FISSILE MATERIAL MANAGEMENT

At the JRC a specific programme is being developed which is intended to provide improved technical tools suitable for verification activities. The basic justification for this R & D activity performed within the Commissions Frame Work Programme is laid down in its legal obligations.

- *Safeguards on non nuclear material is performed in nuclear installations within the European Union (EU) in the framework of the Euratom Treaty (Chapter VII, articles 77-85) and Supply Agreements. The control activities are carried out by inspectors from the Euratom Safeguards Directorate (ESD, DG XVII Luxembourg).*
- *In the frame of the Non-Proliferation Treaty (NPT) and the Verification Agreements the International Atomic Energy Agency (IAEA) is performing verification activities worldwide including the EU.*

Safeguards scientific and technical activities performed in the frame of the programme R&D for Safeguards and Fissile Material Management illustrated below are tightly coordinated with and complementary to the Support to the Commission activities described in paragraph 2.

The main safeguards activities performed at the Safety Technology Institute (STI) of the JRC Ispra are executed within the Safeguards PERformance LAboratory (PERLA) of the Institute. They deal in particular with Non-Destructive Analysis (NDA) methods for the determination of U and Pu isotopes in bulk and itemized form by active and passive neutron measurements, gamma spectrometry, calorimetry, used either individually or in integrated systems.

In 1992 and 1993 a large effort has been dedicated to finalize and start up the new facility TAME which is now ready to be used for tank volume measurements for safeguards applications. In the field of safeguards the STI nuclear facilities constitute a tool unique in the world and perfectly aligned with the subsidiarity mandate of the Commission.

1.3.1 LABORATORY RESEARCH

Fissile mass multiplication factor correlation for Pu measurements

An empirical correlation between the fissile mass and the leakage multiplication factor as determined by High Level Neutron Coincidence (HLNC) counting, was developed based on available measurement data. This correlation has been used successfully for the simulation of the HLNC counting. With the singles countrate (totals) the correlation can be used to obtain a quick estimate of the plutonium mass of the sample in less time than required to measure the real coincidence countrate. The correlation can also be used to evaluate samples contaminated with alpha-n sources such as fluorine [1-6].

Concentrator synchronizer derandomizer

In the measurement made by the commercial instrumentation often used by Safeguards inspectors and plant operators to verify with the neutron coincidence counting technique [7, 8] the plutonium weight of a sample, the dead time of the electronic chain is a large source of errors. In these systems the TTL pulses collected by each electronic chain, are mixed together with a number of 'OR' gates equal to the number of the electronic chains. When two pulses arrive simultaneously, only one pulse might be detected. This effect is sensible above all to high pulse rate. To avoid these counting losses a new logic was studied to collect pulses coming from all electronic chains and in such a way that if two pulses come together, they should have a fixed time interval (derandomizer).

The first prototype will have the following characteristics:

- board clock: TTL oscillator max freq = f_{osc} 40 MHz
- synchronizing clock: frequency = $f_{osc}/4$
- derandomizing period: TD = 4 f_{osc}/(>100 ns)
- single channel dead time: min TD max 2 TD
- input: input number 18

TTL compatible logic pulses
(width = 20 ns min)
- output: output number 1
TTL compatible logic pulses
width = $2/f_{osc}$
- power supply: +5 VDC 200 mA
- max dimensions: 45x100x20 mm

Combined measurements on Pu (neutron + gamma + calorimetry)

The isotopic composition of ^{242}Pu, the alpha factor and the multiplication factor, are normally calculated in NDA analysis with an empirical correlation. Sometimes this leads to high errors in their evaluation. The experimental data from high resolution gamma spectroscopy, passive neutron and calorimetry were used to determine the plutonium weight , the isotopic weight percentage and the ^{241}Am content without resorting to correlation. The use of this method can be applied also to get an estimation of the alpha factor (alpha-n reaction rate) or of the multiplication factor in the case of samples with known abundance of ^{242}Pu. The data were collected in the JRC PERLA facility and the results are compared to nominal values. The accuracy is always better than 0.5% on the total plutonium mass [9]. The PERLA standards are pure, therefore the alpha factor can be evaluated rather accurately also with the correlation: however, the accuracy achieved with the new method is better than with the correlation.

A programme NEutrons GAmma CAlorimeter (NEGACA) has been developed under mathematical environment to evaluate with the combined NDA techniques, the weight of the main isotopes of plutonium (^{238}Pu up to ^{242}Pu), ^{241}Am, the alpha-n reaction rate and the multiplication factor. ***Fig. 3.1*** shows the experimental set-up.

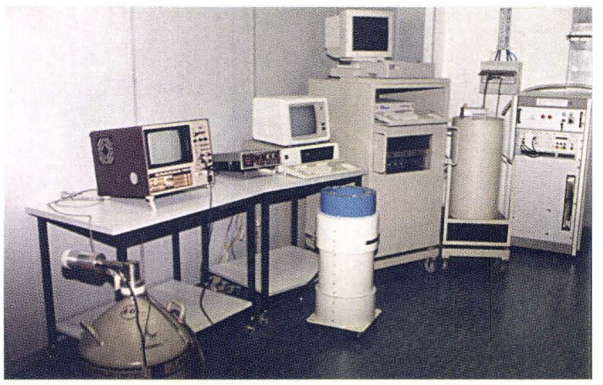

Fig. 3.1 Experimental set-up for contemporary gamma, neutron, calorimetry measurements on Pu samples

First approach to use a thermal video system for safeguards applications

The new generation of infrared detection systems with high performance level could possibly be used for Safeguard applications. In 1993 in the PERLA facility one of the most advanced infrared detectors has been tested on the plutonium PERLA samples. The nominal weight of bulk samples under evaluation was about 1.0 kg of PuO_2 of low, medium and high burn-up. The experiment was focussed on the observation of three main parameters related to the container/cladding of the Pu samples: emissivity, axial thermal profile and temperature stability.

Emissivity (double canned samples)

In order to increase its emissivity the stainless steel canning the sample was surrounded by a painted black copper cylinder. The Thermogram of the Pu samples reported in ***Fig. 3.2*** shows the system's precision close-up capability and a high resolution video image.

Thermal profile

This parameter could be interesting for quality control relative to the PuO_2 blended oxide and MOX powders or fuel pins. The measurement system is suitable to define any 'hot -cold point' with differences in thermal patterns as small as 0.01°C. The temperature measurements have been taken simultaneously on three different positions along the vertical axis of the Pu sample. ***Fig. 3.2*** shows the position of the three

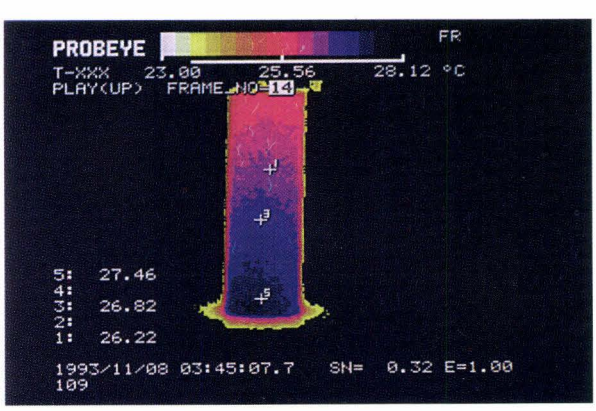

Fig. 3.2 Thermogram of a PuO_2 sample

markers on which temperature values have been detected which are reported at the left side of the image. As it can be seen from the figure, the mass of the Pu powder and its distribution in the inner container is clearly identifiable. *Figs. 3.2* and *3.3* show the thermograms of 2 different bulk Pu samples.

Measurements have been taken in the PERLA Pu storage in order to see the thermal distribution and to verify the effective presence of the samples. *Figs. 3.4* and *3.5* show a partial view of the storage of bulk samples, and a rack of fuel pins containing few grams of Pu respectively. *Fig. 3.6* shows the measurement taken on two short pins containing only one pellet with nominal weight of 1 g of Pu and different isotopic composition. This last image points out the high sensitivity of the instrument being the maximum temperature difference with respect to the environment (marker 1 and 2) of about 0.3°C.

Temperature stability

The temperature measurements have been taken on three double canned samples belonging to the family of low medium and high burn-up Pu. The environmental temperature was monitored by a precision thermometer and by a thermograph in order to evidence some eventual temperature perturbations. Results are given in *Table 3.1*.

Contribution to ESARDA

The STI contributes to ESARDA (European SAfeguards R & D Association), amongst others, with the convenorship of the NDA Working Group. Under the next chapter, Progress in PERLA, the outcome of an International Workshop on Passive Neutron Counting organized at PERLA by the ESARDA NDA Working Group is reported.

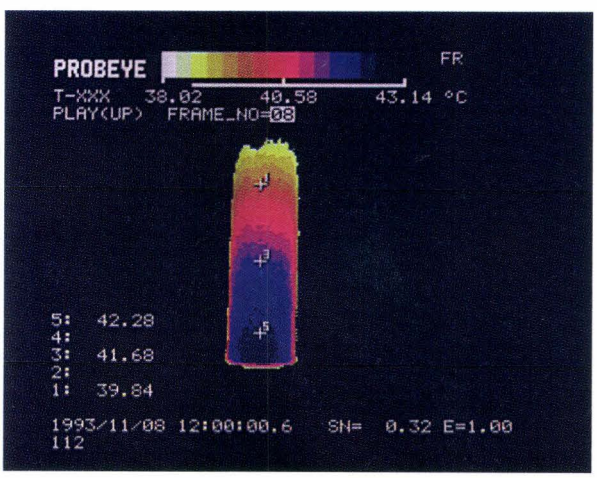

Fig. 3.3 Thermogram of a PuO_2 sample

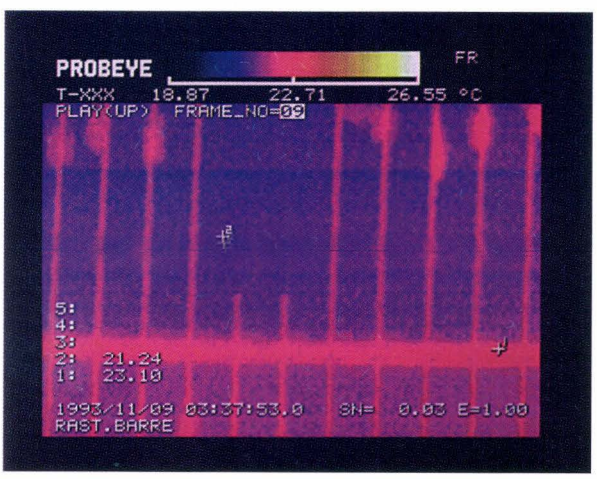

Fig. 3.5 A rack of fuel pins

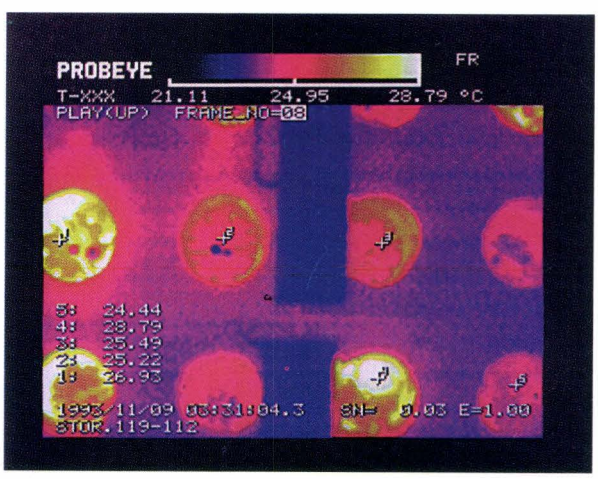

Fig. 3.4 Partial view of the storage of PuO_2 samples

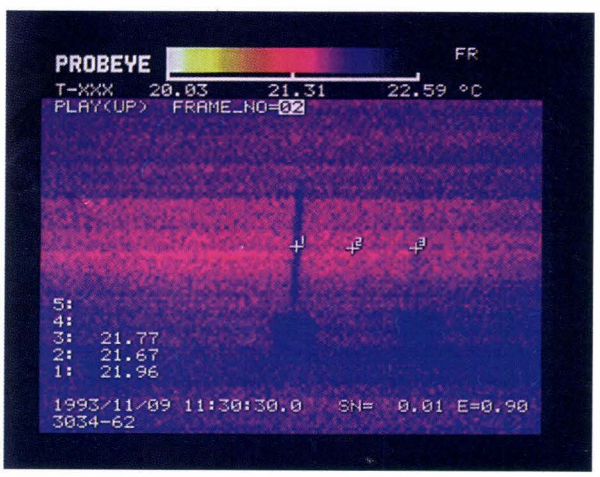

Fig. 3.6 Thermograms of 2 short pins

Table 3.1 Temperature profiles detected on PERLA samples

	Sample					
	H.B. Pu	**Mean Value**	**S.D. %**	**L.B. Pu**	**Mean Value**	**S.D. %**
Temperature °C posit. marker 5	43.25 43.56 43.66 43.54 43.62 43.58 42.16 42.20 42.28	43.54 42.22	0.3 0.5	26.80 26.96 27.18 27.32 27.46	27.14	1.0
Environment temperature °C	23.2 23.3 23.3 23.4 23.5 23.5 23.5 23.5 23.5	23.4 23.5	0.5 0.0	23.5 23.5 23.5 23.5 23.5	23.5	0.0

1.3.2 PROGRESS IN PERLA

The ESARDA Working Group on Techniques and Standards for Non-Destructive Analysis (NDA) has organized at the PERLA (***Fig. 3.7***) laboratory of the Commission of the European Communities an International Workshop on Passive Neutron Counting as an Accountancy and Verification tool for Plutonium bearing materials (***Fig. 3.8***).

The workshop has reviewed the current status of passive neutron assay and made recommendations for further development efforts. Developers and users of passive neutron assay instruments together with national and international inspectorates have conducted a three day workshop on the passive neutron assay of plutonium.

The workshop consisted of presentations, demonstrations and measurements by participants and discussion periods. Basic technology topics included radionuclides nuclear data, shift register based instruments as well as multiplicity counters, high resolution gamma spectrometry (HRGS) measurements, uncertainty propagation models and performance evaluations of various instruments and techniques. Particular attention has been given to ESARDA NDA Performance Values and to IAEA International Target Values. The measurement sessions have been performed on the well characterized PuO_2 and MOX PERLA standards.

The workshop was focused mainly on discussion sessions which provided the opportunity for the participants to evaluate the current status of performances

Fig. 3.7 The PERLA laboratory

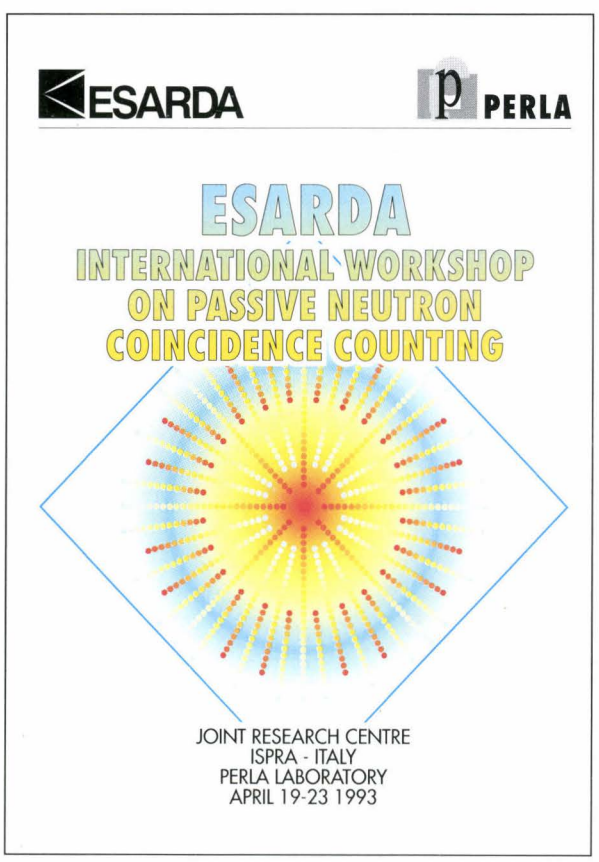

Fig. 3.8 International Workshop on Passive Neutron Counting

of passive neutron assay and to develop conclusions and recommendations which have been included in the workshop proceedings. The workshop evaluations, the nuclear constants recommended by the ESARDA NDA working group and the list of contributions are reported in the following.

Workshop evaluation of the status of passive neutron coincidence counting

The conventional shift register technique

- The two-parameter shift register technique has been used for a number of years and is satisfactory for many applications. It will remain the principal passive neutron measurement method for most materials. The number of unattended applications will increase. Containment and surveillance methods can also be combined with NDA to produce integrated systems. More use of operators passive neutron equipment by the inspectorates would lead to cost savings if suitable authentication measures can be applied.
- The performance of the method is described in a number of publications for a range of detectors and material types. The typical uncertainties for pure material are of the order of 1-2% without including the uncertainties on the isotopic composition values.

- For the interpretation of all neutron techniques it is essential that the isotopic composition is known. At the very least the measured ^{240}Pu eff. must be converted to Pu total.
- HRGS (often combined with MGA) plays an important role in the verification of the declared isotopic composition and has been extremely valuable. However, if HRGS values are used for the analysis of the neutron results, there is a significant bias in the case of high burn-up material caused by the error in the ^{242}Pu values which are obtained from the existing correlation. Other correlations, including the proposal described in [10] should be tested with available data.
- In order to determine the capability of the technique, performance values are needed. The definition of these values should be established. The working group took note of the fact that the error models of [11] could lead to enhanced understanding of error performance and suggested that this approach should also be explored. Once this method is proven with available data, the errors derived from historical performance can be compared with propagated error values. An algorithm for propagating the isotopic counting statistics and other errors has been developed and can be applied for such evaluations [12,13].
- The measurement of small samples using the two-parameter shift register technique is currently being improved. This is done by improving the design of the detector, careful background monitoring and reproducible sample handling.
- The analysis of neutron coincidence measurements should use an agreed set of nuclear data for the calculation of ^{240}Pu effective and alpha values wherever possible. Currently used constants are given in the annex.
- In order to use the technique to its best advantage, the results from all evaluation techniques should be examined, i.e. the results from all known alphas, Ms and uncorrected Rs should be consistent (in some circumstances not all methods apply).
- In the 'known M' technique, the value of the multiplication is taken from empirical correlations between multiplication and effective fissile content. The method has been shown to work with assemblies and rods. Further work is required to validate the method for powders, pellets and MOX materials.
- The conventional shift register technique has limitations when it is used to measure inhomogeneous and/or impure materials, particularly scrap and waste. For these materials alternative techniques are necessary.

Multiplicity analysis

- The multiplicity analysis method gives more information, and can be used to determine the plutonium mass when the alpha values or efficiency are unknown (in addition to the unknown multiplication).
- Several types of electronics have been developed which essentially generate a histogram of multiplicity values. Several manufacturers are beginning to supply electronic units.
- The analysis is commonly based on the equations of [14]. The values of nuclear data currently used are given in annex 1. Two semi-empirical corrections are required [15]. One is concerned with deadtime correction and the other is due to the effect of multiplication varying within the sample. An analytical solution for deadtime [16] has been produced and should be tested on available data.
- This multiplicity analysis method has reached a significant stage of development, and is used in the field. The uncertainty of the technique was estimated to be 3-5% for impure scrap and heterogeneous material (with uniform isotopic composition) over a wide mass range.
- Another application of the technique is for waste (when the multiplication is small). Measurement of MOX waste drums with unknown alpha values (around 1.0) and efficiency gave an estimated uncertainty of 5-10% with a measurement time of about 1 hour.
- An alternative analysis technique, which may have advantages in some circumstances, is to calculate the multiplicity distribution to be expected from known sample properties (verification).
- Recording the raw pulse train information provides a good opportunity for testing alternative data processing methods.
- In order to test and compare different data acquisition and analysis systems it is recommended that benchmark experiments be carried out. This would allow the measured values to be compared between systems and would also provide data which could be used to investigate alternative analysis methods.
- To test the capability of the system fully, characterized samples with a range of high alpha values are essential.

For further details see also [17,18].

ESARDA neutron workshop

Recommended nuclear constants

taken from KRICK LA-UR-88-1301 (1988)

α

K_1	=	134
K_2	=	0.381
K_3	=	1.41
K_4	=	0.013
K_5	=	0.020
K_6	=	26.900
K_7	=	10.200
K_8	=	2.54
K_9	=	1.690
K_{10}	=	2.062

Pu 240 eff

K_{11}	=	2.52
K_{12}	=	1.68

Halflife (y) IAEA currently used values

Pu 238	=	87.74
Pu 239	=	24120.0
Pu 240	=	6560.0
Pu 241	=	14.35
Pu 242	=	376300.0
Am 241	=	433.6
Cf 252	=	2.643

KRICK LA-UR-93-1394 (1993) used in multiplicity analysis

fast neutron induced fission

spontaneous fission

SF 1st moment	=	2.154
SF 2nd moment	=	3.7890
SF 3rd moment	=	5.2110

fast neutron induced fission

IF 1st moment	=	3.1630
IF 2nd moment	=	8.2400
IF 3rd moment	=	17.321
SF/g/s	=	473.500

List of contributions

(1) GUARDINI S. - ESARDA-NDA Working Group Workshop structure

(2) KULIKOV Y. - IAEA Vienna Current Status of NCC techniques at the IAEA Safeguards

(3) BIGNAN G., ROMEYER-DHERBEY J. - CEA Cadarache - Neutron detection: advantages and disadvantages of the 'charge collection' mode and of the 'current collection' mode

(4) KRICK M.S. et al., LANL, Los Alamos - Passive thermal neutron multiplicity counting developments at Los Alamos

(5) HAGE W. et al., JRC Ispra - Development state of the triple neutron correlation technique by the factorial moment method at JRC Ispra. Deveopment state of the triple neutron correlation technique by the factorial moment method at JRC Ispra

(6) CROFT S. et al., UKAEA Harwell - Topics in neutron multiplicity counting at Harwell

(7) FRANKLIN M., JRC Ispra - Quantification of measurement uncertainty

(8) STEWART J.E., LANL, Los Alamos - A generalized assay mass sensitivity limit for passive neutron coincidence counting

(9) BONDAR L., JRC Ispra - Passive neutron assay by the EURATOM time correlation analyser

(10) RONALDSON J.P., WHITEHOUSE K.R. - BNFL Sellafield - Special radiometric measurement systems on THORP

(11) DORLET J., TAUREL B. - CEA Fontenay-aux-Roses - Compteurs de multiplicites: un essai d'utilisation d'une modelisation exponentielle sur un ensemble de detection pour lequel cette hypothese est peu realiste

(12) RUHTER W.D. et al., LLNL Livermore - MGA and passive neutron measurements

(13) HEVILLON J. et al., CEA Bruyeres-le-Chatel - Comparison of three electronic units for the detection of fission neutrons by passive counting

(14) SWINHOE M.T., VERRECCHIA G.P.D. - EURATOM Luxembourg - Euratom's view of recent developments in neutron coincidence counting

(15) ABEDIN-ZADEH R., IAEA Vienna - Practical Experience with NCC performance

(16) DE RIDDER P., IAEA Vienna - NCC performance results in the IAEA safeguards

1.3.3 PROGRESS IN TAME

The TAnk MEasurement laboratory TAME, has been installed at the JRC Ispra and is currently undergoing extensive commissioning and performance testing of equipment. TAME has been installed with a view to investigate the techniques of volume and mass determination of liquids in medium and large tanks of the type associated with the back-end of the nuclear fuel cycle. The construction and operation of large throughput industrial reprocessing plants, comprising large volume input (10 to 70 m^3) and output (700 dm^3) tanks propose a new challenge to the performance of weighing and volume measurement techniques. These measurements are the basis for process control, quality control of intermediate and final products and for material accountancy and its verification. Application of such techniques are used in parts of the nuclear fuel cycle which have a very high strategic importance and where the measurement uncertainty has to be low. The Safeguards Inspectorates are indeed facing increasing responsibilities particularly on the verification capability of maintaining an effective safeguards role. The problems are many and varied but are generally linked to phenomena affecting verification accuracy, instruments and equipment, calibrations, data acquisition, analysis and evaluation. The TAME laboratory has therefore been constructed in order to address these problems and provide means or supporting the Inspectorates in R&D training and calibrations of volume/mass measurement techniques.

The activity carried out in the TAME laboratory project has concentrated on the installation of equipment, particularly instrumentation, related to the following main components:

- an input accountancy tank of 12.5 m^3 resting on 3 load cells (***Fig. 3.9***),
- an output product tank of 250 dm^3,
- 'mini TAME' which is the ex-IAEA facility of 200 dm^3,
- a dosing station for calibrations of the tanks,
- 3 storage vessels of combined volume 14 m^3,
- an off-gas system for maintaining and controlling tank under pressure,
- recycling and homogenisation systems of all tanks,

Fig. 3.9 Input accountancy tank, showing load cells and Paar densitometer (0 meter level)

- ejector air-lift systems for remote sampling,
- instrumentation for measuring, temperature, pressure, humidity, density, air and liquid flow,
- series of differential pressure measurements for determining volume and mass of tank contents (Ruska, Diptron, industrial type electromanometers),
- a 'D' shaped product tank of volume 400 dm^3 equipped with pneumercator tubes and weighing scales purchased from the AEA (UK) (***Fig. 3.10***). This tank is currently undergoing installation and will be incorporated into the existing facility, making use of the ancillary equipment, like service and feed lines, off-gas system, process control and data acquisition system.

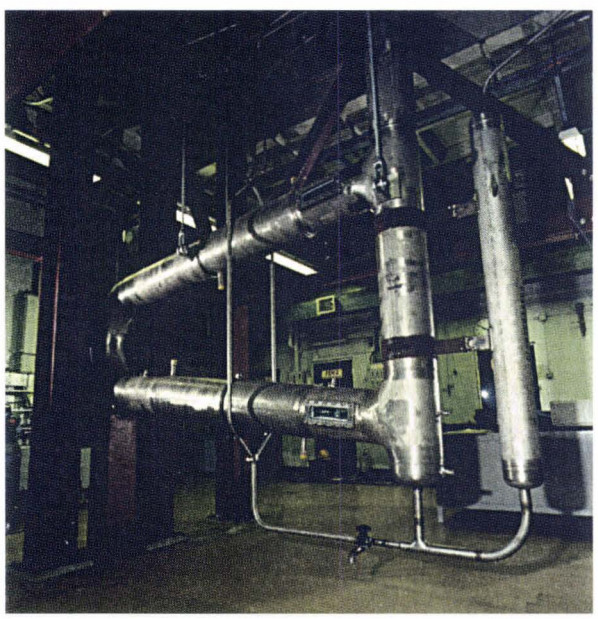

Fig. 3.10 'D' shaped output product tank (400 litres)

- a process control and data acquisition system. This system allows the automatic calibration of the tanks, either in a continuous or an incremental mode.

The facility is now undergoing a series of tests, including the calibration of the vessels in both the continuous and incremental mode and at the same time checking the performance of the various installed instrumentation of the sub-systems (off-gas, pneumercators, etc).

References

[1] VOCINO V., MAUCQ T. - Experiments on Neutron Coincidence Counting, Technical Note I.93.44, April 1993

[2] MAUCQ T., VOCINO V. - Setting up of the Neutron Electronic Chain Used for the HLNCC Family, Technical Note I.93.45, April 1993

[3] VOCINO V., FARESE N., MAUCQ T. - PECC Algorithms and Procedures, Technical Note I.93.46, April 1993

[4] VOCINO V., FARESE N., MAUCQ T., VERRECCHIA G.P.D. Active Euratom Coincidence Counter (AECC), part 1, User's Manual, April 1993, to be published as EUR report

[5] LU M.S., TEICHMANN T., VOCINO V., VERRECCHIA G.P.D., CHARE P. - Fissile Mass-Multiplication Factor Correlation for Pu Measurements, ESARDA, May 1993

[6] VOCINO V., FARESE N., MAUCQ T., CALDON L. - Plutonium Pin Assay (PUPA), Technical Note I.93.43, April 1993

[7] VOCINO V., MAUCQ T. - Pulse Interval Analysis (PIA), Technical Note I.93.47, April 1993

[8] HAGE W., PEDERSEN B., VOCINO V. - Development state of the triple neutron correlation technique by the factorial moment method, at JRC Ispra, ESARDA, International workshop on passive neutron coincidence counting, April 1993

[9] VOCINO V., BINDA F., CARAVATI G., D'ADAMO D., FARESE N., MAUCQ T., REMORINI B. - Assay of Plutonium by the use of Passive Assay Technique, ESARDA May 1991

[10] RUHTER W. et al. - MGA and Passive Neutron Measurements, Proc. of the Passive Neutron Workshop, JRC Ispra, April 1993

[11] FRANKLIN M. - Statistical models of NDA measurements, Technical Note I.91.160, JRC Ispra, December 1991

[12] GOLDMAN et al. - LA-U-R 91, 2505 (1991)

[13] LU M.S. - Nuclear Technology, Vol. 102, No 2, H 196209, May 1993, LU M.S., Nuclear Instruments and Methods, Phys. Res. A, A327, pp 544-550

[14] HAGE W., CIFARELLI D.M. - Correlation analysis with neutron counting distibutions in randomly or signal triggered time intervals for assay of special fissile materials, Nucl. Sci. and Eng. 89, pp 159-276 (1985)

[15] KRICK M.S., HARKER W.C. - User Manual for MULTIPLICITY COUNTER, LANL 3479 (1992)

[16] HAGE W., CIFARELLI D.M. - Correlation analysis with neutron counting distribution for a paralyzing dead-time counter for assay of spontaneous fissioning material, Nucl. Sci. and Eng. 112, pp 136-158 (1992)

[17] DERON S. et al. - 1993 international target values for uncertainty components in fissile isotopes and element accountancy for the effective safeguarding of nuclear materials, IAEA, STR 294, 1993

[18] GUARDINI S. (editor) - Proceedings of the ESARDA international workshop on passive neutron coincidence counting, EUR 15102 EN, 1993

1.4 FUSION TECHNOLOGY AND SAFETY

In the frame of the European Union's Fusion Programme, the JRC as a technically fully integrated Associated Laboratory concentrates its efforts and contributions to the demonstration of the safety and environmental feasibility of fusion power.

The identification of the quality and quantity of source term under normal and abnormal operating conditions is indispensable as input for a reliable safety analysis by facility design teams as well as for providing confidence to Regulatory and Radiological Protection Authorities in their assessment of the acceptability of envisaged protection systems, for any future tritium burning device.

The activities refer to a common "Leitmotiv" which is:

- *Minimization of the hazard, i.e. of the radioactive inventory at any time of the life of a plant;*
- *Minimization of the routine releases, i.e. containment of the radioactive products during the normal operation and routine maintenance phases;*
- *Minimization of the accidental releases, i.e. containment of the radioactive products during possible accidents occurring during the operational and the shut-down phases;*
- *Minimization of the doses to the operators during the life cycle of the plant;*
- *Minimization of the wastes and of the doses to the population before and after the decommissioning of the plant.*

They intend to cope in a complementary manner to other Associations with "non-functional specifications", i.e. with problems associated with the behaviour of the plant outside the limits fixed for its normal operating conditions and with the side effects on the population of this new type of energy. As such it can be the most reasonable response to the social and political demand of safety assurance.

As the boundaries between functional and non-functional specification are not rigid, this "mission" of the JRC has to be understood in terms of a general orientation, and does not exclude involvement in functional problems, where economically convenient for existing investments, competences, etc.

The European Tritium Handling Experimental Laboratory (ETHEL) will become fully operational during 1994. Research in ETHEL will focus above all on tritium by identifying its transfer mechanisms, mitigating its propagation, minimising its dilution and optimising its confinement by studying:

- *Loss mechanisms such as adsorption/desorption rates, permeation rates, leakages and the effects of potential remedies like permeation barriers;*
- *Multiple containment systems and fluid clean-up concepts under normal and accidental conditions;*
- *Methods for solid waste handling, treatment, conditioning and eventual disposal;*
- *Tritium control, monitoring and surveillance over the whole concentration range during both normal/abnormal operating conditions and maintenance activities.*

These items are of specific and primary interest for the NET/ITER Tritium Technology Programme as well as, in the shorter term, directly assisting JET operations.

In view of tritium experiments in ETHEL and to provide information on the basic processes involved in order to define final process schemes, preparatory experimental studies are being performed at the JRC-Ispra laboratories using protium, deuterium and small quantities of tritium. Experiments performed in the frame of the various preparatory studies are described below.

1.4.1 HYDROGEN ISOTOPES - MATERIAL INTERACTION

Transport of hydrogen isotopes in fusion reactors

LIBRETTO-3 (Liquid Breeder Experiment with Tritium Transport Option)

As part of the Liquid Metal Blanket Programme [1], the in-pile irradiation LIBRETTO series of experiments has been carried out within the European Fusion Technology Programme on Blanket Technology as a joint project between the Institute of Advanced Materials (IAM, JRC-Petten), CEA, Saclay and the Safety Technology Institute (STI, JRC-Ispra) (tasks LMB-BAR-J and LMB-PER-J). The irradiations are performed in the High Flux Reactor (HFR) at Petten.

The aim of the irradiation of the LIBRETTO-3 [2] capsules was the in-pile testing of the efficiency of proposed tritium permeation barriers. The experiment employed four bubbled capsules (***Table 4.1***) including one capsule without any permeation barrier coating (blank capsule). Of the three coated capsules, one was coated with Al_2O_3 (by pack cementation) performed by the CEA (France) while JRC-Ispra coated the other two with Al_2O_3 and TiC using CVD (Chemical Vapour Deposition).

Table 4.1 Test matrix and irradiation conditions for LIBRETTO-3

Capsule No.	**9**	**10**	**11**	**12**
Supplier	JRC Ispra			CEA
T release, optional	extraction and/or permeation			
Cladding material	AISI 316L			
Permeation barrier	None	TiC (CVD) Outside	Al_2O_3 (CVD) inside	Al_2O_3 (PC) inside
Pd-17Li weight [g]	28.97	27.69	28.75	27.4
Irradiation time [d]	76.57 or 3 HFR cycles			
Temperature [°C]	280, 330, 370, 420 and 450			
Gas composition of primary and secondary containments	pure He or He + 0.1 vol% H_2 or He + 1 vol% H_2			
T release rate [3] [mCi/min]	0.094 [1] 0.03 [2]	0.052 [1] 0.03 [2]	0.055 [1] < 0.02 [2]	0.067 [1] 0.033 [2]
T production rate [3] [mCi/min]	0.101 [1] 0.057 [2]	0.095 [1] 0.054 [2]	0.098 [1] 0.056 [2]	0.091 [1] 0.052 [2]
Lithium burnup [%]	0.99	0.98	0.97	0.95

[1] Beginning-of-life

[2] End-of-life

[3] Theoretical T production rate for a solid alloy cylinder of 8 cm length positioned in the maximum neutron flux

Table 4.2 Steady-state measurements and calculated results

Capsule No.	9	10	11	12
Measured data				
Temperature [°C]	333	344	331	340
Bubbling flow rate, Q [cm^3/min]	21.0	21.5	19.5	17.1
T extraction rate, J_e [mCi/min]	0.0134	0.0213	0.0225	0.0545
T permeation rate, J_p [mCi/min]	0.0806	0.031	0.032	0.0127
Calculated data				
T production rate, P_t [1] [mCi/min]	0.101	0.095	0.098	0.091
Extraction efficiency [%]	13	22	23	58
T partial pressure in Pb-17Li [hPa]	30.3	47.1	54.9	151.3
Relative permeation reduction factor	1	3.24	3.39	14.7
T recovery rate [%]	93.1	55.1	55.6	73.8

[1] Theoretical production rate for a solid alloy cylinder of 8 cm length, positioned in the maximum neutron flux

In the conditions of the LIBRETTO-3 irradiation, the pack cementation aluminisation seems to be the better performing barrier (see *Table 4.2*). However, permeation reductions of 100 or more, as reported previously in an out-of-pile experiment, could not be confirmed in the in-pile or by later out-of-pile experiments (see paragraph on Influence of Coating on Permeation). It is not clear yet if this is due to differences in aluminisation batches, poor coating of welds or irradiation effects. Important progress will be required concerning suitable barriers or T extraction. In future experiments small-scale effects such as capillarity and gas inclusions should be avoided and measures of liquid metal evaporation and condensation should be improved. The T partial pressures in the LIBRETTO-3 experiment were also much higher than in the blanket which limits the applicability of the experiment. Cooling water on the outside of the capsule will have no effect when the barriers efficiency is limited by diffusion of tritium through the material and not by surface effects.

Calculation of tritium inventory, permeation and recycling in fusion reactor first wall

The source of hydrogen isotopes in the first wall of a fusion reactor is due to the unavoidable interaction between the plasma and the materials facing the plasma. A fraction of the hydrogen atom flux reaching the first wall surface will be reflected (backscattered) and another fraction will diffuse in the lattice and may be trapped in lattice defects caused by neutron irradiation, forming as such the inventory of the wall, or might reached the back surface and be desorbed (i.e. permeation). A fraction of the implanted flux will reach the plasma side of the first wall combining with other atoms to form hydrogen molecules (surface molecular recombination) producing the phenomenon of recycling. All these phenomena form the basis of the model for the transport of the hydrogen isotopes in the first wall of a fusion

device. The mathematical formalism associated with the model is quite complex and a computer code (TIRP) has been developed for calculating the above processes.

During this year the code has been transferred from the version running in the old central computer of JRC-Ispra to a work station. The new version has been tested with results obtained previously. In parallel, a compilation of data on tritium materials interaction properties for fusion reactors materials has been produced [3,4,5] including calculations of tritium inventory, permeation and recycling using the code.

Recycling of hydrogen isotopes from first wall materials of fusion reactors

Plasma-wall interaction prediction and control are key issues in thermonuclear fusion. Particle and energy confinement in a tokamak fusion reactor is not perfect in spite of the strong magnetic fields applied to the plasma. Therefore, a certain amount of ionized particles leaves the core of the plasma, moves towards the edge, crosses the last closed magnetic flux surface (LCFS) and eventually impinges on one of the structures surrounding the plasma. Ions escaping from the plasma may also be neutralized by charge-exchange reactions before striking a solid material in a region called the scrape-off layer (SOL).

The particles bombarding the first wall structures might be suddenly backscattered after suffering one or more collisions with the target atoms or they might be slowed down to thermal velocities within the subsurface layer. These implanted particles, which have been neutralized on their very first impact with the surface, diffuse in the material, following the direction of the existing concentration and temperature gradients.

A fraction of the total impinging flux remains in the bulk of the material, building up the so-called inventory, while some of the atoms permeate through it to the outer surface. Most of the diffusing atoms reach the plasma-facing surface, where recombination with other atoms takes place and a hydrogen molecule is released with a thermal energy in equilibrium with the surface temperature. Both this and the backscattering process constitute the so-called recycling, which is a particle re-emission from the first wall structures to the plasma.

The comprehension of the recycling behaviour of hydrogen isotopes from the first wall structures is a crucial task in plasma-wall interaction research because both plasma performance and safety aspects strongly depend on the time-scale and the magnitude of this phenomenon. Moreover, in order to avoid any influence on the plasma density and composition at the beginning of a burn time in ITER, the outgassing rate at the end of dwell time between two reaction phases must be smaller than 10^{14} $cm^{-2} \cdot s^{-1}$.

The physical parameters that mainly influence the recycling process are particle flux density at the surface, ion energy and target temperature. Calculations for ITER operation give as an estimated value for the impinging flux some 10^{16} $cm^{-2} \cdot s^{-1}$, with an energy distribution peak around 200 eV. Temperature may vary between 575 K and 875 K, depending upon the breeding blanket design solution adopted.

The recycling of deuterium and tritium in a fusion reactor should reach steady state in a short time. However, pulse duration in present day machines is too short compared to that of ITER to be able to study the hydrogen isotopes recycling behaviour under steady state conditions. Therefore, this study can be better performed using plasma simulators able to operate at particle flux densities and ion energies similar to those of ITER. Consequently, an experiment has been designed to study the hydrogen isotopes implantation, uptake and release from material used as first wall in a fusion device. A detailed description of the experimental apparatus for tritium recycling measurements from metallic surfaces has been presented somewhere else [6,7,8].

The study of the operating parameters of the plasma and a general calibration of the experimental procedure, as well as testing the control philosophy (-mainly the development and test of the control software) has been carried out in this facility that is much more flexible than its hot counterpart (see paragraph on ETHEL-001) due to the use of hydrogen and deuterium only. This feedback procedure of cold testing allows to change previously established configurations of ETHEL-001 in real time, i.e. during the assembly phase, avoiding possible drastic changes at the end of the assembly (during the cold commissioning) which might not always be possible. The multipole ion source typically works with a gas pressure in the range 0.05 to 0.5 Pa and at a discharge potential of 80 V, where a high ionization probability is observed.

Due to the presence of the magnetic field, the electrons emitted from the cathode and accelerated by the discharge potential towards the anode follow a spiral path, hence considerably increase their path length and the probability of ionization. When the ions are accelerated towards the target, thus starting implantation, a sudden pressure decrease in the ion chamber is observed. Therefore, pressure must be kept constant in the experimental chamber. This task is accomplished by a pressure control system which allows the necessary amount of gas to enter the ion source volume. Moreover, as a result of increasing temperature in the chamber due to ion and electron bombardment as well as heat flux, an increase of the overall outgassing rate has to be expected in spite of the cooling systems. For these reasons, a continuous gas flow is needed in order to keep a high hydrogen isotope purity in the ion source.

Work has been carried out on this matter, with the purpose of optimising the gas flow as a function of gas pressure in the ion source under operating conditions. The aim was to minimize gas consumption for a given acceptable hydrogen isotope concentration, in view of the tritium operation phase where only a limited amount of gas will be allowed for the experiment. As was expected, the impurity content is much more significant at lower pressure operation. However, it can be kept at reasonably small values by supplying a suitable gas flow. Working on the low pressure side of the ion source operating range, a lower limit of about $5 \cdot 10^{-3}$ Pa·m^3·s^{-1} has been obtained for an impurity content around a few percent. This limit can be reduced up to 10^{-3} Pa·m^3·s^{-1} if the gas pressure is raised above 0.3 Pa. A comparison between the gas spectra obtained at the limits of the pressure range is presented in ***Figs. 4.1*** and ***4.2***.

A second important effort was made in the characterization of the plasma composition during a discharge. As can be expected, both the atomic flux density at the target surface and the energy carried by each atomic particle entering the material are strongly affected by the type of the ions being produced in the source. After the solution of some problems related to the tuning of the plasma analyzer, which had been intentionally modified by the manufacturer for our purposes, a comprehensive study of plasma composition in the ion source has been performed. The gas used was high purity deuterium (D_2>99.4%) supplied by SIO Company Milan. Our measurements confirmed that the ratio high-to-low

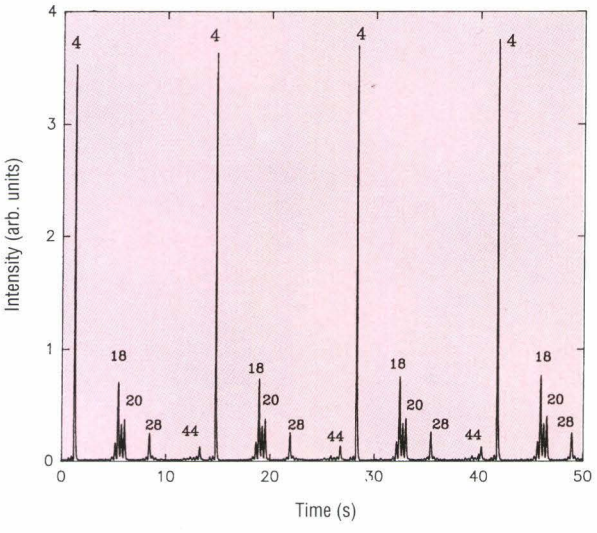

Fig. 4.1 Gas spectrum during implantation at p=0.05 Pa with Ø=0.05 mbar·l·s^{-1}

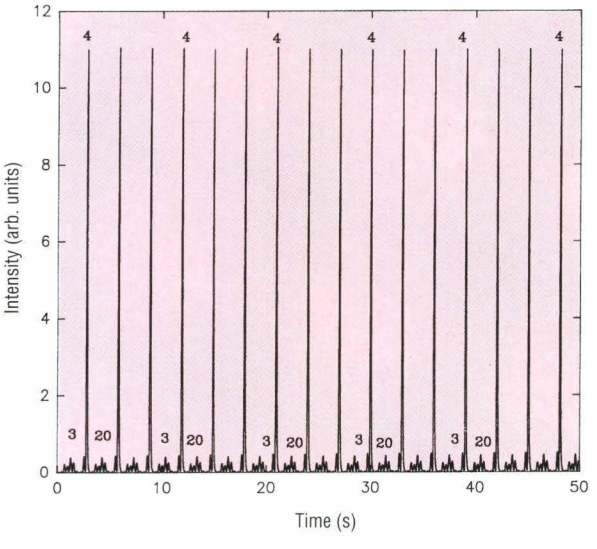

Fig. 4.2 Gas spectrum during implantation at p=0.3 Pa with Ø=0.01 mbar·l·s^{-1}

masses D_3^+ is increasing with pressure [9,10,11], varying within the limits of almost 100% D_2^+ at about 0.05 Pa and 100% D_3^+ when the pressure is higher than 0.3 Pa. Monoatomic ions D^+ are detected only at the lowest pressure and in a very small quantity. The plasma composition as a function of gas pressure in the ion source is shown in ***Fig. 4.3***.

It can be defined in the intermediate pressure range what was called the "transition region", where there is the inversion of the relative abundance of the two main ionic species, i.e. the ratio D_3^+/D_2^+ changes from values lower than 1 to values greater than 1. In

this region, approximately between 0.1 and 0.2 Pa, the plasma composition is not very stable and we observe periodic fluctuations probably induced by the variation of macroscopic parameters such as pressure (due to the gas puffing of the pressure control system) and temperature. From these discussions, three different operating pressure regions have been delimited and are presented in *Table 4.3*.

The following considerations can be made: below 0.07 Pa, where almost only D_2 is present, one can have the highest energy per implanted atom but a low atomic flux at the target surface, a higher impurity content and some measuring problems due to the low pressure; above 0.3 Pa, where we have again a monoenergetic ion flux composed of D_3^+ ions, the atomic particles impinging on the target can reach the largest amount but with only two third of the energy carried by each atom in the preceding case; finally, in the transition region around 0.1 Pa both D_2^+ and D_3^+ are present, producing a more complex and slightly varying atomic energy distribution and flux at the target. Further experiments performed in the transition region showed that no significant variations in the plasma composition occur when ion energy or ion current are changed.

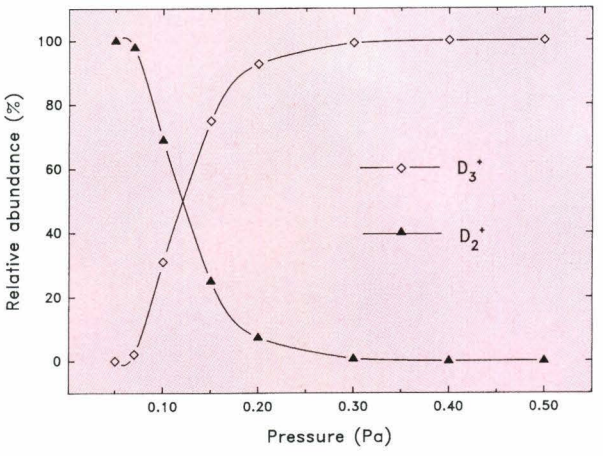

Fig. 4.3 Plasma composition as a function of neutral gas pressure

Table 4.3 Operating pressure regions

p (Pa)	p < 0.07	p ≈ 0.1	p > 0.3
main ionic species	D_2^+	$D_2^+ + D_3^+$	D_3^+
atomic flux	low	medium	high
atom energy % total	50%	33 - 50%	33%

Solubility, diffusivity and permeability in fusion reactor materials

Low activation martensitic steels LA 12 TALC, LA 12 TALN and LA 7 TALN

Irradiation of the first wall and blanket components of a fusion reactor will lead to the activation of structural materials. This activated material will make up the majority of the solid radioactive waste produced during operations. Low and/or reduced activation martensitic steels (LAMs) are of great interest for fusion reactor applications as structural and first wall materials because their reduced activation will lower the radioactive waste produced during reactor operations and simplify its handling, storage and final disposal. The development of low activation martensitic and ferritic steels has been pursued by substituting molybdenum and niobium (the primary producers of long lived activity) by tungsten and vanadium, and by the use of lower carbon and nitrogen contents.

Continued development of some 9 and 11% CrWV steels has been achieved by the addition of a small amount of tantalum and the use of lower carbon and nitrogen contents [12,13]. Although mechanical properties of these steels have been previously studied [14], nothing was known about their hydrogen behaviour (diffusivity and solubility) that governs their tritium retention and permeability characteristics with consequences in the safety of the reactor and its environmental impact.

The chemical compositions of the studied LAM's are shown in *Table 4.4*. Each of the steels used in the study was produced on a laboratory scale by vacuum melting, followed by hot rolling of the ingot into 19 mm diameter bars [13]. The LAM samples were fabricated by cutting cylinders from the original bar using electro-erosion. A post-fabrication vacuum heat treatment (1375 K for 1 hr and 1025 K for 2 hr) was applied to all the specimens to produce a fully martensitic structure.

The experimental method used was a gas release technique. A single experimental run consisted of two phases: first, the sample was loaded with hydrogen at a given temperature and pressure until saturation was reached and then, after a short pump down to less than 10^{-4} Pa, the pressure increase due to gas release from the sample and from the inner walls was measured in a calibrated volume until a new equilibrium was obtained. Each run was followed by a blank run under the same experimental conditions

but without the sample. The contribution of the inner wall surface thus obtained was then subtracted from the total pressure increase to give the net contribution due to the sample alone. The solubility was determined from the final pressure in the calibrated volume and the diffusivity from the time dependence of the release pressure curve by a non-linear least squares fitting process to a diffusion controlled gas release model.

Sievert's constants and diffusivities of hydrogen in the three LAMs studied are presented in ***Figs. 4.4*** and ***4.5***. Further heat treatment of the LAM samples at 900 K showed nearly no change of hydrogen solubility, but a strong decrease of hydrogen diffusivity (indicated as "heat treated" in ***Figs. 4.4*** and ***4.5***). As it was the case for MANET (see STI Annual Progress Report 1992), hydrogen diffusivity was similar when the additional heat treatment was carried out at a temperature below 740 K.

The strong decrease of the diffusivity is explained by the increase in importance of surfaces effects. This hypothesis is substantiated by a reversal to the virgin material (non-heat treated) diffusivity when a 1 μm slab is machined out of the surface. On the other

Table 4.4 Chemical composition of the experimental low activation martensitic steels (wt%)

Steel	Fe	C	Si	Mn	Cr	V	W	N	Ta
LA7TaLN	Balance	0.18	0.04	0.70	11.1	0.24	2.95	0.005	0.10
LA12TaLC	Balance	0.09	0.03	1.01	8.9	0.39	0.76	0.019	0.09
LA12TaLN	Balance	0.17	0.02	0.74	9.1	0.25	0.77	0.004	0.10

Other element content typical for LAM casts: 0.005 P, 0.005 S, <0.01 Mo, 0.02 Ni, 0.0005 B, 0.005 Al, 0.01 Co, 0.01 Cu, <0.01 Nb, <0.005 Sn, <0.001 Ti

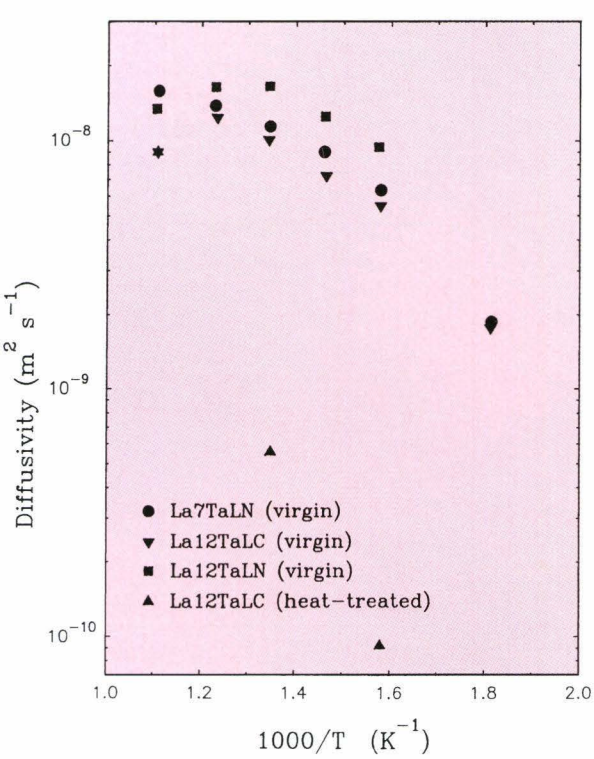

Fig. 4.4 Diffusivity of hydrogen in the virgin and heat-treated low activation martensitic steels

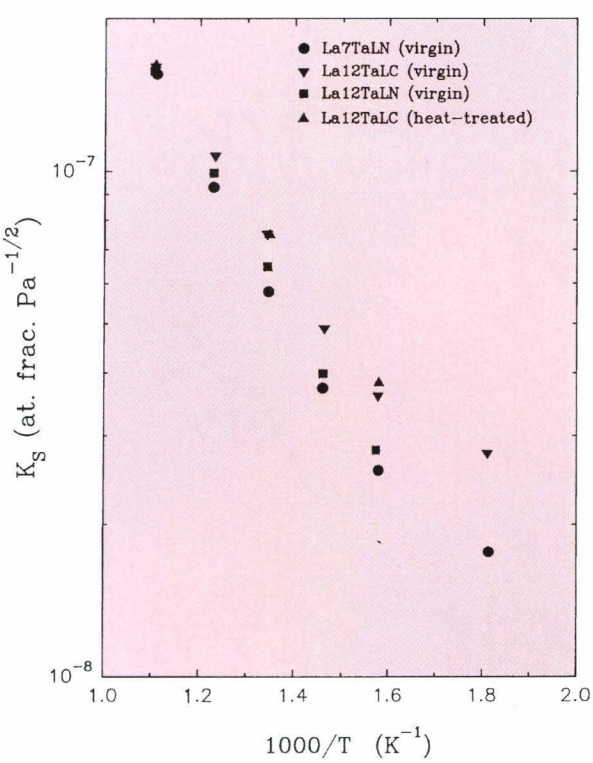

Fig. 4.5 Sieverts' constant of hydrogen in the virgin and heat-treated low activation martensitic steels

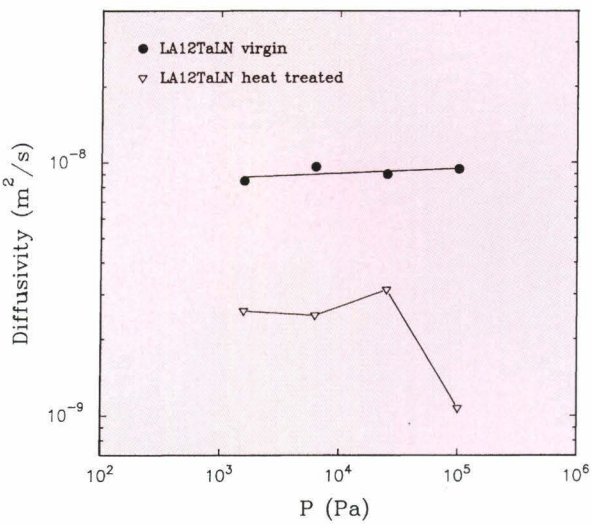

Fig. 4.6 Pressure dependence of the diffusivity before and after heat-treatment

hand a study of the dependency of the diffusivity with the loading pressure shows that in the case of virgin material, the diffusivity is independent of the pressure while in the case of treated material there is a strong dependence on pressure (***Fig. 4.6***). This fact indicates a change from the diffusion-limited controlled gas release regime to a surface-limited one, where surface effects play a strong role in hydrogen interaction with the material.

Influence of coating on permeation

The tritium permeation rate through structures such as the first wall and breeder blanket containment is a critical factor in the determination of fusion reactor viability [15]. Most current fusion reactor designs such as NET or ITER envisage breeding tritium from a lithium compound (Pb-17Li, for example). It is intended that the breeder material will be contained in steel tubes, forming a blanket around the vessel where the fusion reaction takes place. The breeder blanket will also contain many coolant tubes to remove heat generated by the fusion reactions. Thus, there is the possibility of the loss of tritium from the breeder material to the coolant by permeation through the steel containers.

The objectives of the investigation were, firstly, to reduce the permeation rate of hydrogen isotopes through fusion reactor materials by the application of surface layers, and secondly, to investigate the effects of liquid Pb-17Li on the permeation rate through coated samples. The first results on CVD coated and aluminised discs have already been reported [16]. The present report describes the measurements on tubes with and without Pb-17Li.

The present measurements were made on samples of the same dimensions and type as for the LIBRETTO (Liquid Breeder Experiment with Tritium Transport Option) in-pile tritium permeation experiment. The present capsules are designated for LIBRETTO-3, following on from the LIBRETTO-1 and 2 experiments [17]. The advantage of the experimental method employed here over the in-pile experiment is the improved control of the critical parameters such as hydrogen isotope concentration and temperature.

Previous papers have shown that aluminised layers can form effective permeation barriers [18] and can also resist corrosive attack by lithium lead. However, it has been unclear if the permeation barrier, which is almost certainly due to the thin oxide formed on the aluminised layer rather than on the iron-aluminium alloy itself, will be stable in the presence of lithium lead.

Since Al_2O_3 is one of the most promising materials to form permeation barriers, it was decided to investigate a CVD (Chemical Vapour Deposited) layer of alumina during the current research project. To improve the adhesion of the layer, it was applied onto an interlayer of CVD TiC. Some previous authors have suggested TiC could form an effective permeation barrier [19] although in our recent experiments the effect was shown to be modest. However, it was also decided to measure the permeation through CVD TiC coated tubes. For all the tube samples, the base material was 316L stainless steel with the dimensions (220 mm length x 10 mm O.D. x 1 mm wall thickness). The CVD coatings, produced by Wolframcarb in Castellamonte, Italy, of TiC and Al_2O_3 were applied as follows:

- An internal CVD layer of 3 μm Al_2O_3 on 1 μm TiC.

The exact coating procedure is proprietary. However, in the case of the TiC coating, the CVD was carried out at approximately 1275 K for around 2 hours.
In addition, the following layer was produced by the pack-cementation at the Heurchrome Company, France:

- An internal aluminised layer of 80 μm thickness.

For comparison with the above coated samples a control sample was included:

- An uncoated 316L stainless steel tube.

Fig. 4.7 shows a schematic view of one of the LIBRETTO tubes sealed into the permeation apparatus.

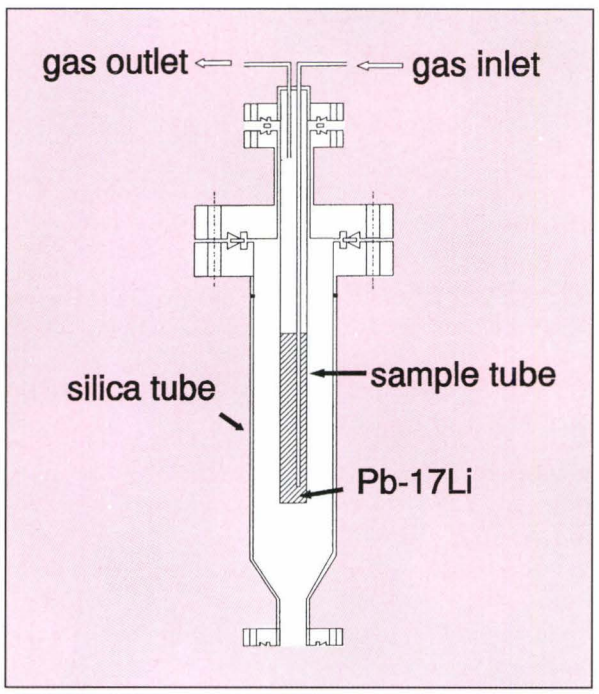

Fig. 4.7 Schematic view of the LIBRETTO tube sealing system

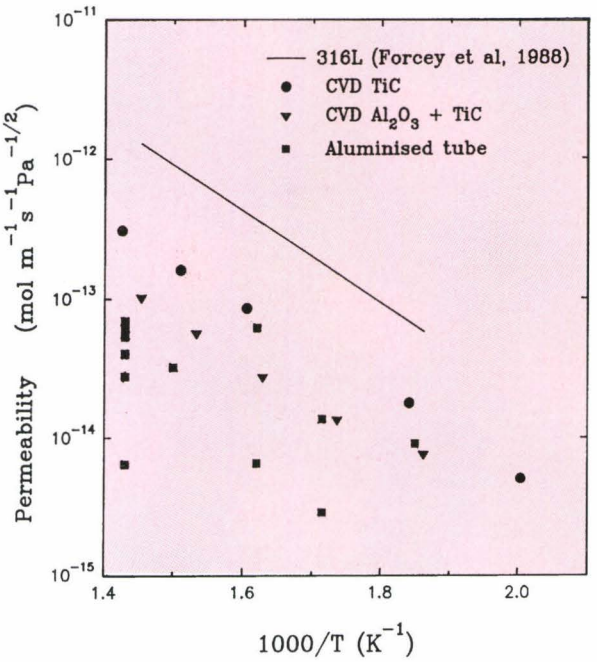

Fig. 4.8 An Arrhenius plot of the permeability of the LIBRETTO stainless steel tubes with CVD and aluminised coatings compared to uncoated stainless steel

All permeation measurements described in this section were performed with deuterium gas. Measurements were first made on tubes without Pb-17Li and then on breeder filled samples. The results are presented in Arrhenius plots and plots of permeation rate against high pressure.

Permeation measurements were carried out on the LIBRETTO tube-shaped specimens (without Pb-17Li) over the temperature range 500-700 K and for pressures in the range 5.5-100 kPa. The results from the LIBRETTO tubes with CVD coatings (shown in ***Fig. 4.8***) are broadly similar to measurements on CVD coated discs reported previously [16]. For comparison data from ref. [20] for the permeability of uncoated stainless steel is shown. Permeation reductions of up to around one order of magnitude were observed in both cases with the Al_2O_3/TiC coating being slightly more effective. The activation energies of the effective permeabilities of the CVD coated specimens were the same as for the substrate stainless steel, suggesting that the permeation barrier acted by restricting the amount of surface area of the substrate available for permeation.

The results from the aluminised tube, also shown in ***Fig. 4.8***, reveal that the permeation rate was reduced by up to two orders of magnitude, although the data points are scattered. There was a general trend for the results from this sample of an increasing efficiency of the permeation barrier as the experiment proceeded, probably due to in-situ oxidation. The pressure dependence of permeation through gas-filled tubes revealed the expected half-power dependence, typical of diffusion limited permeation.

Some results from the permeation tests on the LIBRETTO tubes in the presence of Pb-17Li are shown in ***Fig. 4.9*** and ***4.10***. It can be seen that the Pb-17Li completely removes the permeation barrier in the case of the aluminised tube (presumably by removing the surface oxide). In the case of the CVD Al_2O_3+TiC layer, the effectiveness of the permeation barrier was unaffected by lithium-lead. The permeation rate through the uncoated steel tube was also found not to change after Pb-17Li was added. The pressure dependence of permeation through the Pb-17Li filled aluminised tube and CVD coated tube was measured and, as expected, diffusion limited permeation was observed.

In addition to the work on LIBRETTO tubes, an investigation was carried out on the permeation of deuterium through packaging materials for tritiated waste. This involved measuring the permeation rate through two types of materials: High Density Polyethylene

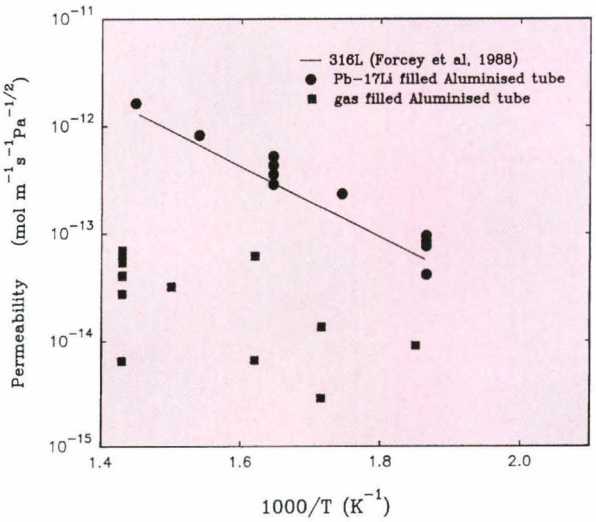

Fig. 4.9 An Arrhenius plot of the permeability of the aluminised LIBRETTO stainless steel tubes with and without Pb-17Li. The permeability of uncoated stainless steel is shown for comparison

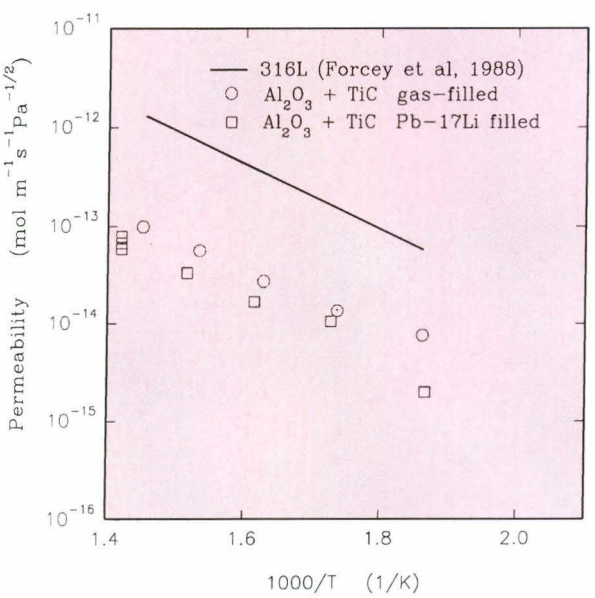

Fig. 4.10 An Arrhenius plot of the permeability of LIBRETTO stainless steel tubes with the CVD Al_2O_3+TiC coating with and without Pb-17Li

(HDPE) and a sheet consisting of 3 layers: HDPE, aluminium foil, and polyester. The measurements showed that the permeation rate of hydrogen isotopes through the material containing the thin aluminium foil was a factor of at least 10^4 times less than the HDPE of similar thickness [21]. Thus the tri-layer packing material would appear to be vastly superior to the conventional packing material HDPE.

Measurements were performed on an oxidised 316L stainless steel specimen provided by the Institute for Advanced Materials. This material had been given a special oxidation at a low oxygen partial pressure in order to cause the preferential growth of chromium and manganese oxide rather than iron rich oxides. The treatment was originally devised to produce a corrosion-resistant coating on steel exposed to Pb-17Li, but it was also hoped that the oxide would reduce the permeation of hydrogen isotopes. However, measurements revealed that, at least on the specimen supplied by IAM, the oxide did not reduce the permeation rate.

In addition, measurements were performed on the vanadium alloy V-3Ti-1Si, which is a candidate fusion reactor structural material. Compared to materials such as stainless steel, this alloy has both a high diffusivity and a high exothermic solubility for hydrogen isotopes. Interpretation of the experimental data was complicated by the strong dependence of the diffusivity and solubility of deuterium on the concentration of dissolved deuterium itself. Since this concentration was time-dependent, the usual equations applied to permeation through steel specimens, for example, were no longer applicable. It was decided that further studies on this material would have to be carried out at relatively low deuterium pressures (below 100 Pa).

Tritium permeation through engineering components

Permeation of tritium through components of a fusion reactor poses a safety problem. Although studies exist of the permeability of hydrogen through several materials of interest for fusion technology, little data are available on the permeation of tritium through engineering components working in a realistic environment, where mechanical stresses might be of importance when quantifying the tritium permeation through them. The objective of this experiment is to obtain data on the permeation of tritium through engineering components typical of those to be used in a large-scale fusion reactor. Presently the study is focused on Inconel 625 and AISI 316L bellows which are engineered components employed at JET to accommodate thermal movements, allow fine alignment of components, reduce mechanical shocks and permit large movements within some systems. The measurement of permeation rate on Inconel bellows has already been reported in the previous STI

Annual Report, therefore here only the values for the AISI 316L bellows are reported.

An experimental facility has been constructed (see STI Annual Report 1991) and operated to obtain the required data on tritium permeation rates. Parallel to this, a theoretical model to interpret the data has been developed. The rather simple model developed is a surface-limited model, i.e. it assumes the diffusion, much more rapid than the recombination at the surface, cancels the concentration gradient within the membrane. The permeation rate is proportional to the pressure and independent of the thickness, depending purely on the surface parameters. The permeability of the bellows has been obtained by fitting the experimental data to the model ***Fig. 4.11***. Although good fits are obtained, the simplified surface model assumption, that the upstream pressure is kept constant throughout the length of the experiment, is not satisfied by the experimental setup since no continuous feed of tritium is applied to the upstream volume (bellows volume). However, the use of this approximation is justified in a time region where the upstream pressure (P_h) is much larger than the downstream pressure (P_l), i.e. the tritium loss from the high pressure side by permeation is insignificant. It should be kept in mind that the upstream pressure is of the order of 10^{-2} Pa (10 GBq·m^{-3}) while the downstream pressure at the highest temperature investigated is of the order of 10^{-6} Pa (4 MBq·m^{-3}), that is Ph is three to four orders of magnitude larger than P_l.

The experimental results, ***Fig. 4.12***, show that, at the contrary to the case of the Inconel bellows, flexing of the bellows does not change the permeation rate. This might be due to a more stable surface oxide in the case of the steel in contrast to that of the Inconel. From the safety point of view, the permeation rate is around 1000 times lower than the one expected in the case of the diffusion limited regime [18].

The project has been successfully terminated and the installation decommissioned. Part of the installation with due changes will be used for other experiments with tritium (see paragraph ETHEL-009: Interactions between tritium and wall surface materials).

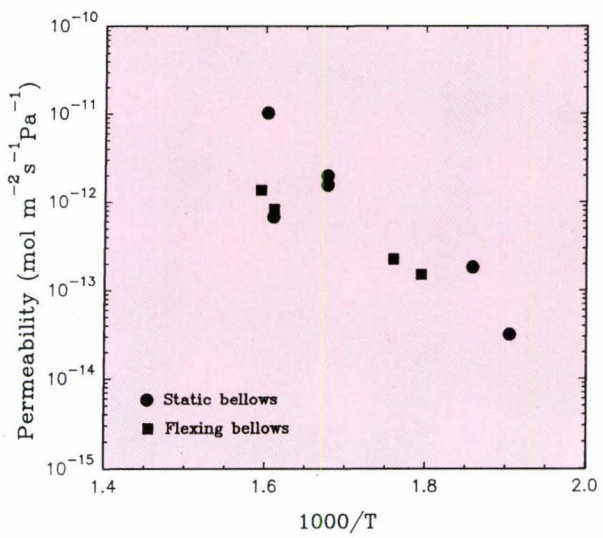

Fig. 4.11 Temperature dependence of the permeability of tritium through SS 316L bellows

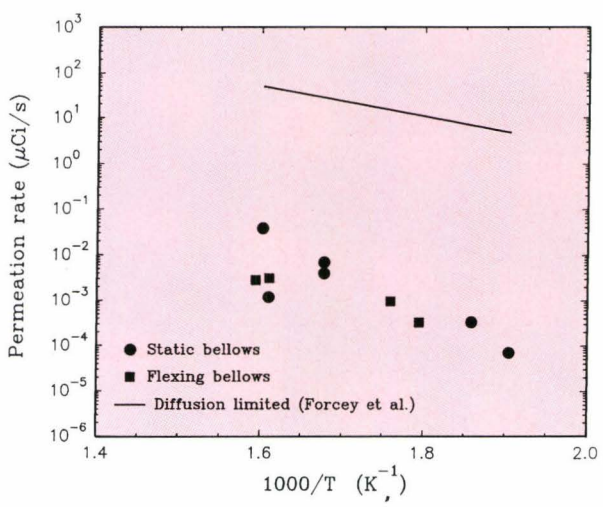

Fig. 4.12 Permeation rate of tritium through the SS 316L bellows compared with values obtained by diffusion-limited permeability (Forcey et al.)

1.4.2 GAS SEPARATION PROCESSES ON SOLID SUBSTRATE

Scaling-up of plasma exhaust purification process by cryosorption: determination of multicomponent adsorption equilibria

Adsorption-based separation processes can be successfully applied in the field of the thermonuclear fusion reactor technology as a valid and advantageous alternative to other traditional separation techniques such as cryogenic distillation, membrane permeation and catalytic conversion. On this basis, particular emphasis has to be devoted to the possible use of the adsorption-based separation processes to solve some problems related to fusion technology such as:

- purification of the exhausted plasma stream pumped out from the toroidal chamber during the burn - and dwell - time and recovery of tritiated components;
- tritium extraction from the reactor blanket;
- purification of tritiated atmospheres;
- hydrogen isotopes separation for both diagnostic and quantitative purposes.

The theoretical design of a gas separation adsorption process using pressure or thermal swing requires the following informations:

- the thermodynamic limits of adsorption of each component of a gas mixture present within an adsorber at the prevailing local conditions of pressure (P), temperature (T) and gas-phase mole fraction (y_i) of the i-th component;
- the driving forces for ad(de)sorptive mass transfer of the i-th component from the gas to the adsorbed phase or vice versa at the local conditions within the adsorber;
- the isosteric heat of adsorption of the i-th component at the local conditions inside the adsorber which is required for taking into account local heat generation (consumption) during the ad(de)sorption process.

The knowledge of multicomponent gas adsorption equilibria, from which the above informations are deduced, is crucial in the design of the adsorption process.

In this context, adsorption equilibrium models can be very useful to provide the multicomponent adsorption equilibria at the conditions of interest from a limited number of experimental adsorption equilibrium data. Different adsorption equilibrium models existing in literature have been, therefore, taken into consideration to test them in predicting the adsorption equilibria against experimental adsorption equilibrium data. In particular this work has been addressed to the scaling-up of a cryosorption process for plasma exhaust purification [22,26]. Experimental measurements of adsorption equilibrium for the pure gas, binary, ternary and quaternary mixtures of O_2, CH_4, NO_2 and CO have been carried out in a wide range of temperature, pressure and composition by using different experimental techniques [23]. The single component, binary and multicomponent data have demonstrated a satisfactory degree of thermodynamic consistency [24]. Thus, these data are useful to test mixed gas adsorption models. The experimental single component data have been correlated according to a model of ideal adsorbed solution (IAS) model for the prediction of the adsorption equilibria of the six binary mixtures of the above mentioned gases.

The experimental binary data have been compared with the predictions of the IAS model and it was observed that all six binary mixtures exhibited deviation from the ideal behaviour. These non-idealities have been interpreted in terms of activity coefficients describing the adsorbate-adsorbate interaction in a real adsorbed solution (RAS) model. The experimental activity coefficients have been obtained from the experimental binary data and then correlated according to a suitable model for the activity coefficients of the adsorbed phase. The activity coefficient model has therefore been used for the application of the RAS model. In the second approach the adsorbent is assumed to have energetic heterogeneities. The non-idealities of the binary data are ascribed to specific interactions between the adsorbent surface and the adsorbed molecules, whereas the adsorbate-adsorbate interactions have been ignored. These specific interactions are described by means of the site-matching conditions (HIAS) model which specifies the energetic state of a local set of adsorption sites with respect to each of the components of the

adsorbed mixture. The site-matching conditions have been determined by minimising the deviations between the experimental binary data and the HIAS predictions as a function of a site-matching parameter. Both the models have been able to correlate the experimental binary data (***Figs 4.13*** and ***4.14***) and the results of this correlation have been used for the application of the two models in predicting the multicomponent adsorption equilibria [23,25].

The predictions of the RAS and HIAS models for the four ternary systems and for the quaternary mixture of the above mentioned gases have demonstrated a good agreement with the experimental data for these systems (***Fig. 4.15, a*** and ***b***). Therefore, both RAS and HIAS models are able to predict the multicomponent adsorption equilibria from single component and binary experimental data, even when high non-idealities are involved. However, the HIAS model is preferred because it is simpler to apply than the RAS theory and, moreover, it better describes the physical reality of the system.

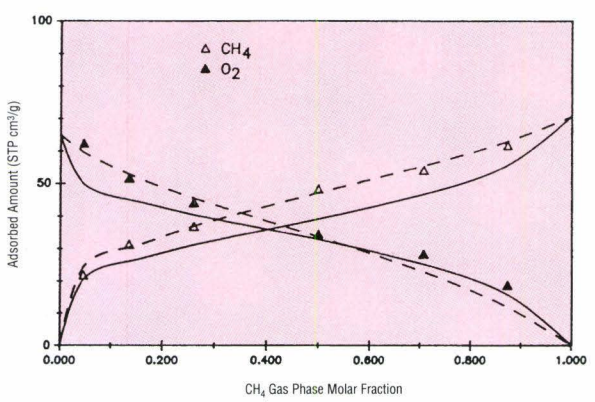

Fig. 4.13 CH_4 - O_2 binary data correlation at 153 K and 450 torr (—— RAS Model; - - - - HIAS Model)

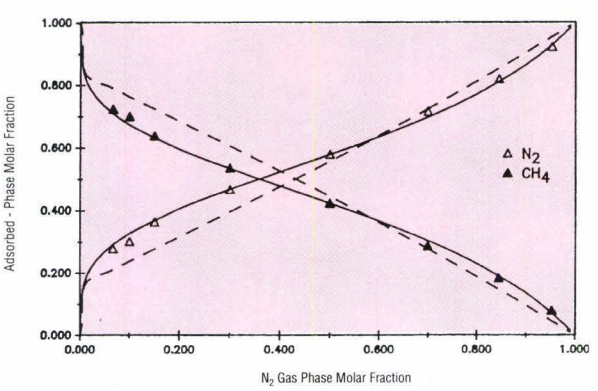

Fig. 4.14 CH_4 - N_2 binary data correlation at 153 K and 450 torr (—— RAS Model; - - - - HIAS Model)

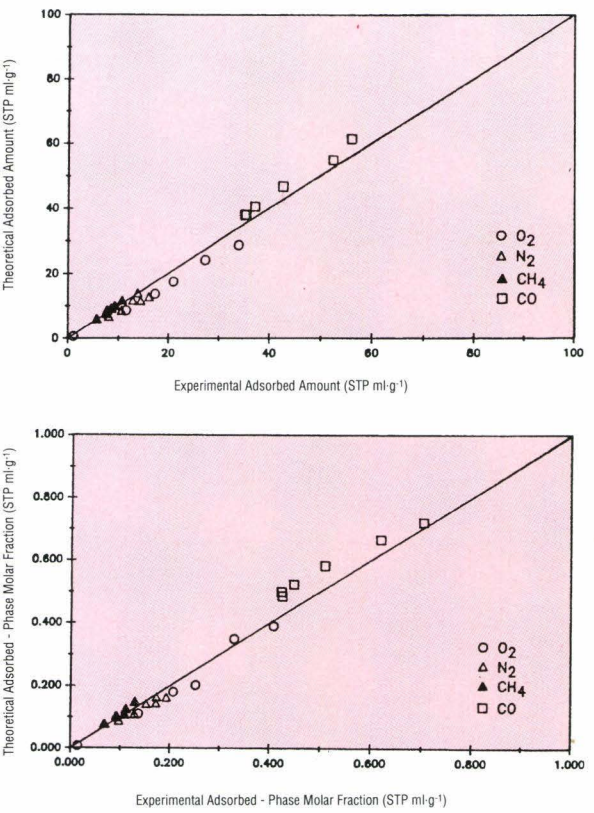

Fig. 4.15 Experimental data and HIAS model prediction for the adsorption equilibria of the quaternary mixture O_2 - N_2 - CH_4 - CO at 153 K and 450 torr

Near real-time diagnostic analysis of hydrogen isotopes by gas-chromatography

When selecting operating conditions for an analytical gas chromatography it is generally required to maximise the resolution between the components to be analysed, with some restrictions on the maximum acceptable retention time.

This restriction is strongly marked for the analysis of the six isotopic forms of hydrogen in the fuel cycle processing of a D-T fusion reactor. In effect, the main requirement for tritium diagnostic apparatuses is to perform the quantitative analysis of the hydrogen isotopes mixtures in real time (less than 10 min). In the past, good resolution between the isotopic forms of molecular hydrogen was obtained, but the time of a complete analysis was too long to satisfy the above mentioned requirement. In this context, an extensive research was carried out at JRC-Ispra laboratories in order to select suitable adsorbent material.

A Na-Ca mordenite LP pelleted with 30% alumina binder has been chosen as adsorbent material since it is characterised by low values of the H_2 and D_2 Henry adsorption constants, which provide short retention times, and a high ratio between them [26]. This allows high selectivity (***Fig. 4.16***) at relatively high temperatures (168-183 K). The best operating conditions of the adsorbent column, i.e. temperature, pressure, granulometry and gas carrier flowrate, have been studied by means of the analysis of the eluted peak moments and of the height equivalent to a theoretical plate HETP [27]. The results have been tested with a ternary equilibrated mixture H_2-HD-D_2 using He as carrier at different temperatures with 3 m and 4 m long columns (***Table 4.5***).

As far as the separation factors are concerned, it is evident that the separation factors are improved by reducing the temperature while the time of the analysis remains relatively short, at maximum nearly three minutes for the 4 m long column at 168 K.

One can also observe a reduction of the separation factor from the 3m to the 4m long column at the same temperature. This is due to the fact that the higher average partial pressure of the adsorbable components in the 4 m long column removes the system from the Henry adsorption region. Furthermore, the higher pressure drop along the 4 m long column distorts the peaks from their ideal symmetrical form so that the ratio between the retention times at the maximum of the peaks (these are values obtained experimentally) can differ from the ratio between the mean retention time which gives the true value of the separation factor. These effects on the separation factors are more pronounced when a sample volume larger than 0.05 ml is used.

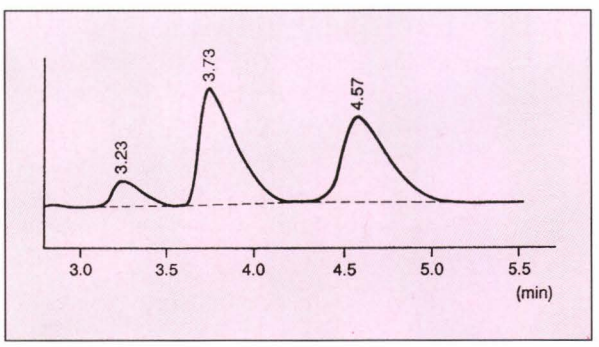

Fig. 4.16 Chromatogram of H_2-HD-D_2 on Na-Ca mordenite LP; temperature = 178 K, column length = 3 m, He carrier flowrate = 46 ml·min^{-1} STP

Table 4.5 Results of experimental chromatographic tests on Na-Ca mordenite LP

Column length, m	**3.0**				**4.0**			
T, K	168	173	178	183	168	173	178	183
t_{H2}, min	3.86	3.16	2.33	1.75	5.74	4.25	3.38	2.57
t_{HD}, min	4.64	3.76	2.75	2.03	6.78	4.94	3.89	2.92
t_{D2}, min	6.08	4.80	3.46	2.50	8.59	6.11	4.73	3.48
SF (HD/H_2)	1.20	1.19	1.18	1.16	1.18	1.16	1.15	1.14
SF (D_2/HD)	1.31	1.28	1.26	1.23	1.27	1.24	1.22	1.19
SF (D_2H_2)	1.57	1.52	1.48	1.43	1.50	1.44	1.40	1.35
RF (HD/H_2)	1.78	1.75	1.44	1.34	1.88	1.68	1.67	1.35
RF (D_2/HD)	2.56	2.23	2.03	1.69	2.98	2.65	2.39	2.08
RF (D_2/H_2)	4.50	3.97	3.40	3.10	5.10	4.47	4.18	3.46

Adsorbent: Na-Ca mordenite LP;
Column int. diameter: 1.9 mm;
He carrier flowrate: 46 STP ml/min;
Mixture: H_2/HD/D_2;
Sampling volume: 0.05 STP ml.

A strong increase of the resolution factors by reducing the temperature and, at the same temperature, for the longer column can be observed. Also, under the selected operating conditions, the chromatograms exhibit small peak tails. Therefore, the increasing difference of the retention times between the peaks is more significant than the increasing spread which occurs at lower temperatures (higher mass transfer resistance) or for longer columns (higher pressure drops).

In *Table 4.6*, the best results obtained on a Na-Ca mordenite LP 4 m long column are reported in comparison to those of other researchers. It can be seen that the results presented in this work are characterised by the very small retention and analysis time, although a longer column and lower carrier gas flowrates are used. In particular, with respect to the precedent work of Pierini [28] a great improvement of the resolution factors has been obtained. Yoshida carried out a fast separation using alumina at liquid nitrogen temperature but informations about the resolution are not indicated in his paper [29]. Conti [30], Vogd [31] and Genty [32] obtained good separation but the retention and analysis times are not as fast to satisfy the requirements of a close to real time analysis.

Development of new adsorbents

A good adsorbent for isotope separation has a high adsorption capacity and a high selectivity between the isotopic species. The selectivity is a result of:

- steric factors such as difference in the shape and the size of adsorbate molecule;
- equilibrium effects: when the adsorption isotherms of the components of the gas mixture differ appreciably;
- kinetic effects, when the components have substantially different adsorption rates.

Zeolites are the best known materials for separating the six molecular isotopic species of hydrogen isotopes by molecular adsorption. Structurally, zeolites

Table 4.6 Comparison among the experimental results from different laboratories

	This work	[28]Pierini	[29]Yoshida	[30]Conti	[31]Vogd	[32]Genty
t_{H2}, s	344	598	623	900	1518	840
t_{HD}, s	407	712	725	1080	1710	960
t_{D2}, s	515	833	937	1482	2088	1320
RF (HD/H_2)	1.88	1.95	-	2.23	1.26	-
RF (D_2/HD)	2.98	1.18	-	3.98	2.04	-
RF (D_2/H_2)	5.10	3.13	-	6.21	3.30	-
Column length, m	4	2.5	2	2	3	3
Column int. diam., mm	1.9	2.1	2	2	2	4
Column temp., K	168	168	77	127	123	77
Carrier gas	He	He	He	He	He	He
Carrier flowrate, STP ml/min	46	40	67	28	60	200
Hydrogen isotopes mixture	H_2,HD,D_2	H_2,HD,D_2	H_2,HD,D_2	H_2,HD,HT, D_2,DT,T_2	H_2,HD,D_2	H_2,HD,HT D_2,DT,T_2
Packing material	CaNaMLP	CaNaMLP	Al_2O_3	4A	5A	Al_2O_3+ Fe $(OH)_3$

are crystalline aluminosilicates with a framework consisting of an open three-dimensional network of AlO_4 and SiO_4 tetrahedra. The AlO_4 tetrahedra in the framework have a net negative charge. This is balanced by cations (mainly alkaline and alkaline earth cations) which do not form part of the framework.

The open structure of the framework is veined by connected pores and cavities of molecular dimensions. This means that molecules can diffuse right inside the crystals, and have access to an enormous internal area, giving a very high adsorption capacity. Because the pores are part of a regular crystal, the size, shape and adsorption characeristics of the pores are homogeneous throughout. This maximises the selectivity of the adsorption for different gases. *Fig. 4.17* shows the differential pore size distribution of some sorbents, calculated from the adsorption isotherms for nitrogen at 77 K by a method developed at JRC Ispra [33]. It demonstates the uniform pore structure of zeolite materials.

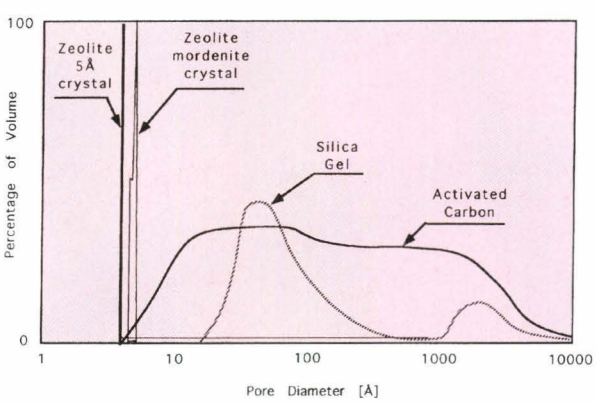

Fig. 4.17 Differential pore size distribution of some adsorbents

The pore size can be chosen by selecting from the 140 natural and synthetic zeolite structures so far reported [34, 35]. The selective adsorption properties can then be tailored, as follows [36, 37]:

- exchanging the extra-framework cations tunes the selectivity by changing the charge at the adsorption sites;
- pre-adsorption of polar molecules modifies the local electric field;
- external surface modification of the crystal by silanation or chemical vapour deposition reduces the size of the pore openings;
- high temperature steaming increases the size of the pore openings.

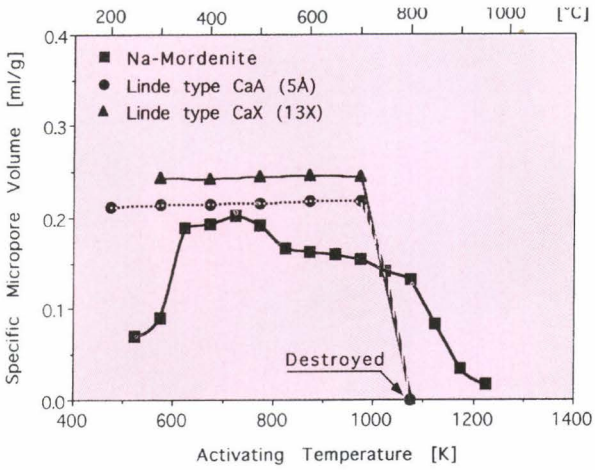

Fig. 4.18 Activation study of different zeolite types. Activation is performed in vacuum for 24 hrs at different temperatures.

Before one can use zeolites as adsorbants, one needs to activate them by heating to drive off the adsorbed water. Fortunately, most zeolites are stable up to several hundred degree Celcius, allowing very thorough outgassing. To illustrate this, *Fig. 4.18* shows the effect of high temperature activation on the volume of micropores of three different zeolites. The volume was calculated from the adsorption isotherms for nitrogen at 77 K using the Dubinin-Raduschevich relationship. It is hardly changed after heating up to about 875 K.

Thermal activation procedures can be critical. This does not only mean using a high enough activation temperature: if water cannot escape from inside the zeolite during heating, it can become incorporated in the strucure permanently as hydroxide groups. This has been demonstrated on zeolites CaY [38] and 5Å [39], and on mordenites in our laboratory. When using zeolites for hydrogen isotope separation, retained water can isotopically exchange and cause tritium memory problems. The effect is probably responsible for the undesirable tritium retention in the dryer of an air detritiation plant reported recently by the Chalk River laboratory [40].

The solution to the problem is to keep the gas around the zeolite as dry as possible during heating, and to use a slow heating rate: 2 K per minute was satisfactory. Infrared spectroscopy work done by Professor Vansant in collaboration with our laboratory [41] has shown that under these conditions mordenite did not retain measurable amounts of hydroxide. Differential scanning calorimetry confirmed that mordenite gave

up the last of its water at about 710 K, giving rise to an endothermic peak in *Fig. 4.19*.

Table 4.7 shows some recent results which are obtained in a study of tritium retention. Mordenite was activated under ultra high vacuum for 48 hours at 725 K, using a slow heating rate; i.e. 2 K per minute. It was then exposed to the saturated vapour from water tritiated to 37 TBq•m^{-3}, for two weeks at room temperature. Subsequently it was activated again using the same procedure as before. Finally the pellets were left under water for a few days to exchange the residual tritium, which was measured with a scintillation counter.

The first column of the table shows that, on pure mordenite, only traces of tritium were retained. On the other hand, the second and third columns show that if the pellets are prepared using a binder, the tritium retention increases. In fact this is not surprising, because the binder usually used is gamma alumina, a material which is known to retain water (in the form of hydroxyl groups) up to very high temperatures.

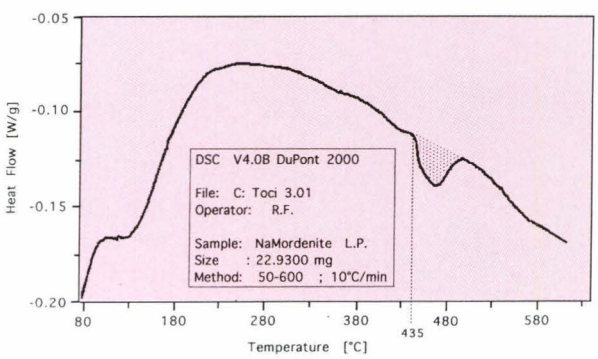

Fig. 4.19 Differential Scanning Calorimetry (DSC) of a microsample of Na-mordenite LP showing an endothermal peak starting at 435°C

Table 4.7 Tritium retention study

Type	Unbound mordenite crystals	Mordenite crystals bound with γ-alumina	Commercial extrudate of mordenite (unknown binder)
Dubinin surface area m^2/g	560	555	360
tritium retention Bq/g	45	560000	900

New research is required on making zeolites into pellets either using a binder which does not retain water, or not using a binder at all [42].

The engineering of gas-solid exchange processes can still be improved, especially by using comprehensive codes to model the separation process, but the major gains in process economics in the future are likely to come from the development of new and improved adsorbents. There have been major advances in the synthesis of new zeolite-like structures, particularly for the use in catalysis. These synthetic structures include silicalite [43], silicoaluminophosphates (SAPOs) [44], aluminophosphates (ALPOs) [45], metalloaluminophosphastes (MeAPOs) [46]; and the recent development of VPI-5 [47], aluminoborates [48], beryllophosphates [49], and pillared clays (PILCs) [50] show that the field is still wide open. But for adsorbant applications, industry is so far only using A, X and Y type mordenites, and some natural zeolites. The commercial potential of the newer types of zeolite materials are yet to be explored and extensive studies from the adsorption point of view are needed.

European tritium handling experimental laboratory

Status of facility

Following provisional acceptance of the laboratory from the architect-engineer, the majority of 1993 has been associated with three activities: collating of project documentation (at the insistence of the Regulatory Authority), in-house testing of the various systems and, finally, modifying the systems where necessary. With regard to the first, a major review of all project documentation has been performed such that the history of the project, from a quality assurance viewpoint, is totally transparent to the Regulatory Authorities. Unfortunately, the quantity of documentation to be reviewed (100 000+ pages, 4 000+ drawings) and the corresponding effort required in the review process has far exceeded that initially envisaged, especially as much critical documentation was only provided by the architect-engineer in the second half of the year. Concerning in-house testing, this activity has allowed future operators to gain experience of the plant while proving the systems under numerous conditions. As a consequence of this work, many plant alterations including

major modifications have been identified and, where possible, implemented with the general aim of improving the safety and operability/maintenance of the laboratory. The list of modifications already completed include the installation of a Heating & Ventilation plenum fire barrier to maintain the integrity of the building in the case of an internal or external fire, the substitution of the halon control room fire protection system with a halogen free system in accordance with applicable EC directives and, finally, the installation of a monitored access system into the controlled areas of ETHEL as part of the laboratory's safeguards requirements. The maintenance sector, which has been heavily involved in the execution of such activities, has also commenced to create a data base regarding routine and unprogrammed maintenance activities, spare part requirements etc. for improved managing and resource usage.

In the area of licensing and in view of the delay to the project, progress has focused on completing the initial series of documents with regard to overall system testing and cold commissioning of the facility. In contrast, no work has been undertaken on developing the future quality programme and procedures of ETHEL, although the training of operation and maintenance personnel in specific topics, e.g. vacuum technology, has commenced.

Also related to ETHEL was the third JRC-Ispra - KfK workshop at which fusion research to be conducted in ETHEL and its support facilities was presented together with the complementary programme of research activities at its German sister facility, Tritium Laboratory Karlsruhe (TLK). The fourth workshop is tentatively scheduled to be held at Ispra in May 1994.

Finally, progress has been made on a number of fronts with regard to the Fifth Topical Meeting on Tritium Technology in Fission, Fusion and Isotopic Applications scheduled for May 1995. The (home) general steering committee and international technical programme committee for the conference have been established and preliminary agreement reached with the Journal of Fusion Technology for refereeing papers and publishing the proceedings. In addition, co-sponsorship has been obtained from various national and international nuclear societies including Canada, Europe, Italy, Japan, US. Finally, a tentative conference location has been identified and the first announcement regarding a call for papers prepared for issue early in 1994.

Tritium control

On the basis of preliminary discussions with the Luxembourg Authorities (Direction Contrôle de Sécurité - DCS), ETHEL and TLK completed the development of a common tritium control methodology [51] for application in the two tritium facilities. The methodology reviews the physical and chemical characteristics of tritium and then describes a typical tritium facility and the likely distribution of tritium in a process plant. Later, practical and theoretical tritium quantification techniques and their advantages/drawbacks are discussed and used to separately quantify tritium inventories likely to be distributed within ETHEL and TLK. On this basis, proposals regarding the number of mass balance areas, frequency of physical inventory verifications and values for material unaccounted for are substantiated. Formal approval of the methodology document is awaited from the DCS.

Continuing in the area of tritium control and following an intensive test programme using calibrated electrical and Pu sources from PERLA, the tritium calorimeter was field tested with tritium in Canada (AECL-Chalk River) and Germany (KfK), the tests being attended by an international audience. Calorimetry represents a non-intrusive means of determining tritium inventories and will play a major role in ETHEL's tritium accountancy techniques. The results of the laboratory and field tests demonstrated the excellent accuracy and precision of the ETHEL calorimeter especially when quantifying large tritium amounts (*Fig. 4.20*), where the error has been defined as the difference in % with the value measured by the PVT-c method.

Work has also been started on the design and construction of the analytical glovebox equipment for the high resolution mass spectrometer (Omegatron) and a gas chromatographic system, to be located in ETHEL's Tritium Magazine (*Fig. 4.21*). With both

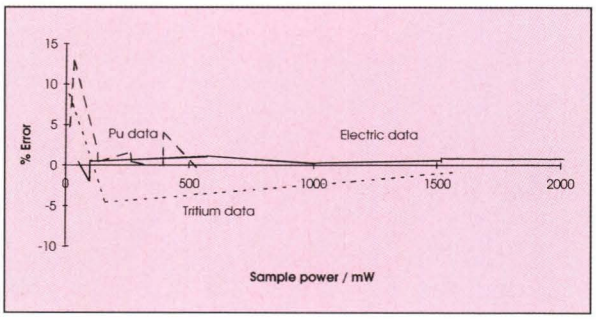

Fig. 4.20 ETHEL calorimeter field tests

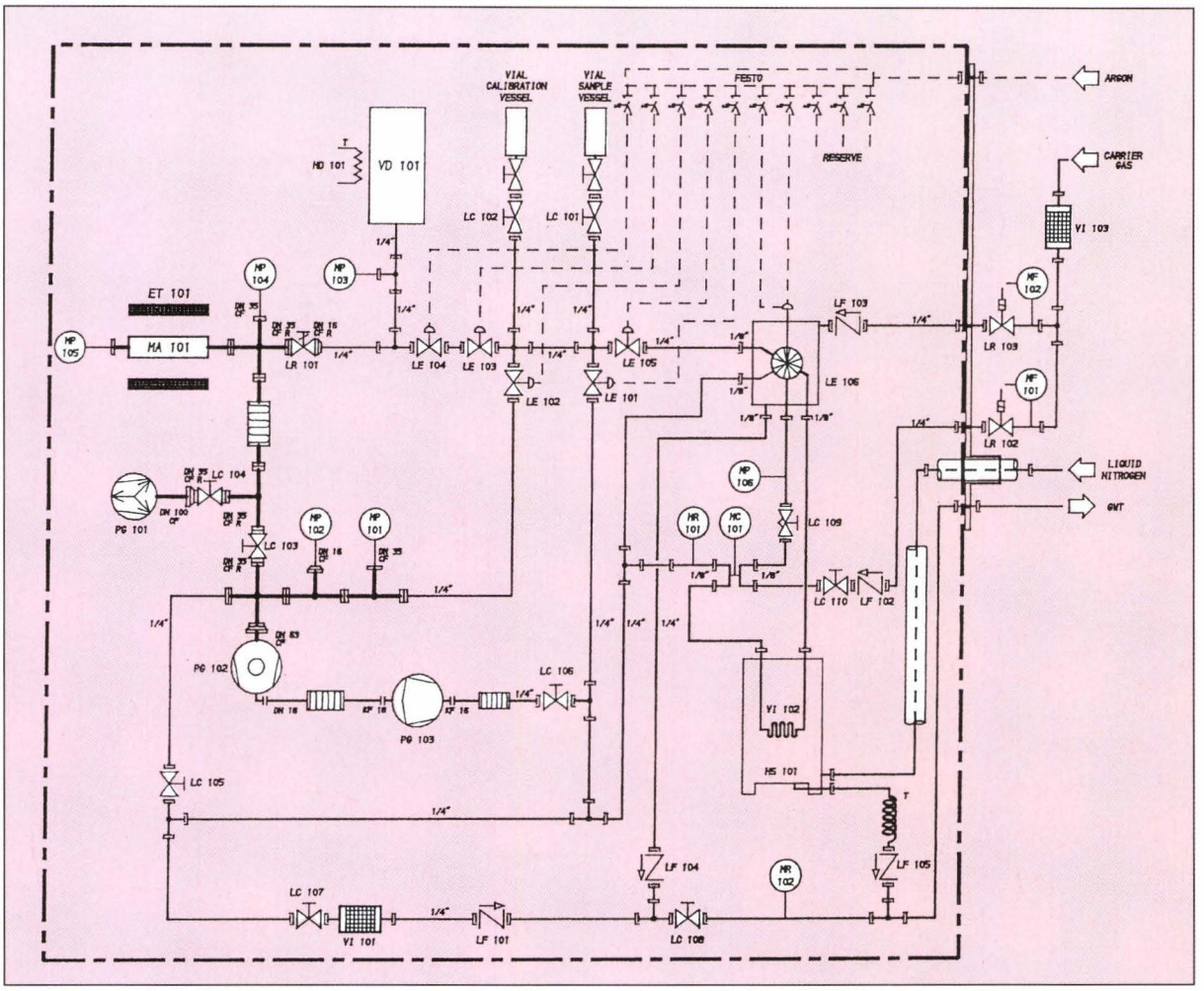

Fig. 4.21 Equipment for the analytical glove-box (ETHEL)

instruments the quantitative analysis of all six hydrogen isotopes and impurities like helium and argon has already been demonstrated. This ability is requested because these impurities are expected to appear due to the production process of tritium, where deuterium is usually predominant. Protium and the heteronuclear isotopes are commonly found in conjunction. The glovebox atmosphere is argon gas and helium is the decay product of tritium.

The process plant set-up consists for routine analysis. Easy maintenance of the system has been considered. The Omegatron includes the Omegatron tube itself, a permanent magnet, an electrometer, a high frequency synthesizer, an exkoll (a modified ionisation vacuum gauge), a tritium compatible pumping system and a specially constructed inlet system. It is believed that this is the first time an Omegatron with a permanent magnet will be used for the routine analysis of tritium. The advantage of using the permanent magnet is that no cooling water is required which leads to a more simple plant design and safer operation. The gas chromatographic system consists of several components: a cryostat, a packed column with Ca-Na-mordenite, a thermal conductivity detector and a flow-through ionisation chamber as detector system, as well as a six-way valve for the gas inlet. The sample coming from the TRSS is attached to the inlet system, which is coupled to both instruments. For the analysis with the gas chromatograph the working temperature range is between 193 K and 153 K with neon as carrier gas. Chromatograms of the mixtures containing different hydrogen isotope compositions are shown for various parameter sets.

The two analytical methods allow a comparison between the results and therefore a higher degree of certainty of the gas composition. The Omegatron

due to this resolution power, which is inversely proportional to the atomic mass, is particularly suitable for hydrogen isotopes. The tube is manufactured out of tungsten covered with gold to guarantee inertness and operated at higher temperatures to minimize memory effects. The separation of the $^3He^+$peak and the T^+ peak is not possible. With the GC a baseline separation of all hydrogen isotopes can be achieved and the helium detected without any interference with the hydrogen, although the helium isotopes themselves can not be separated. Due to their complementary nature the two analytical tools will be used for the correct assignment of all different components. On the basis of initial investigations an accuracy of 1% is envisaged for tritium as the major component.

Likewise, a precision mass comparator has been acquired for large tritium quantities. All of these efforts and equipments will enable ETHEL to take a lead role in the fusion community with respect to the control of tritium in laboratories and research reactors such a ITER.

Tritium experiments in ETHEL

ETHEL-001: Tritium recycling and outgassing of first wall material under fusion reactor conditions

This is the tritium compatible version of the cold facility dedicated to the study of recycling of hydrogen isotopes from first wall materials of fusion reactors. The comprehension of the recycling behaviour of hydrogen isotopes from the first wall structures is a crucial task in plasma-wall interaction research because both plasma performance and safety aspects strongly depend on the time-scale and the magnitude of this phenomenon. Moreover, in order to avoid any influence on the plasma density and composition at the beginning of a burn time in ITER, the outgassing rate at the end of the dwell time between two reaction phases must be smaller than 10^{14} $cm^{-2} \cdot s^{-1}$.

The primary design philosophy for the installation is the efficient and effective containment of the tritium needed for the experiments and the minimization of maintenance requirements for tritium contaminated components. For the containment of tritium, a multi-level containment scheme has been adopted in ETHEL. The first level is made up of the experimental components (i.e. ultra-high vacuum (UHV) experimental chamber, etc.). The second level is provided by a glove box suite of around 7 m^3 placed in the LER of ETHEL. Finally the tertiary containment is provided by the ETHEL laboratory itself.

The restrictions imposed by having an installation for the handling of tritium which is mounted inside an ETHEL glove-box (secondary containment) have led to a design where possible hands-on operations has been eliminated. Considerable effort has been spent in designing the various components to make the facility compatible with the presence of tritium. In particular, the plasma simulator and the UHV pumping system.

The UHV system has been designed to operate in two modes depending upon the levels of tritium present in the installation. In the "low-level mode", gas is removed from the system and exhausted to the inlet of the gas detritiation system of ETHEL. This mode is used when the system is pumping only H and D, as is the case during the installation commissioning period, or when the system is pumped down from atmosphere, i.e. when the only tritium present is the small amount on the walls due to exposure during previous experiments. During experiments with tritium, the system is isolated and pumping occurs in the so called "high-level mode". In this case the gases being pumped, including tritium, are contained within the isolated part of the UHV system.

The assembly of the facility can be divided into two parts: the mechanical and the electrical/control assembly. The mechanical assembly inside of an ETHEL glove box is completed. All the components are in their position and the pumping units are attached. The status of the mechanical assembly can be better seen in ***Fig. 4.22***, where a general view of the present status is given.

The electrical/control part of the facility has been more problematic to accomplish. While the control philosophy of the installation has been clear from the beginning, the complications, cost and work-load involved in connecting the different gauges, pumps, valves, etc. to their controllers sitting outside of the glove box have been completely underestimated. In particular, the preparation of the glove-box service panels to accommodate all the necessary passages and the choice of feedthroughs for the different components have been a continuous design effort during the last year to match properly the large amount of signals and power requirement of the facility. This has been translated into a delay of our project schedule. The assembly of the electrical/control side of the ETHEL-001 facility has now been completed.

Parallel to the assembly of ETHEL-001, work is being

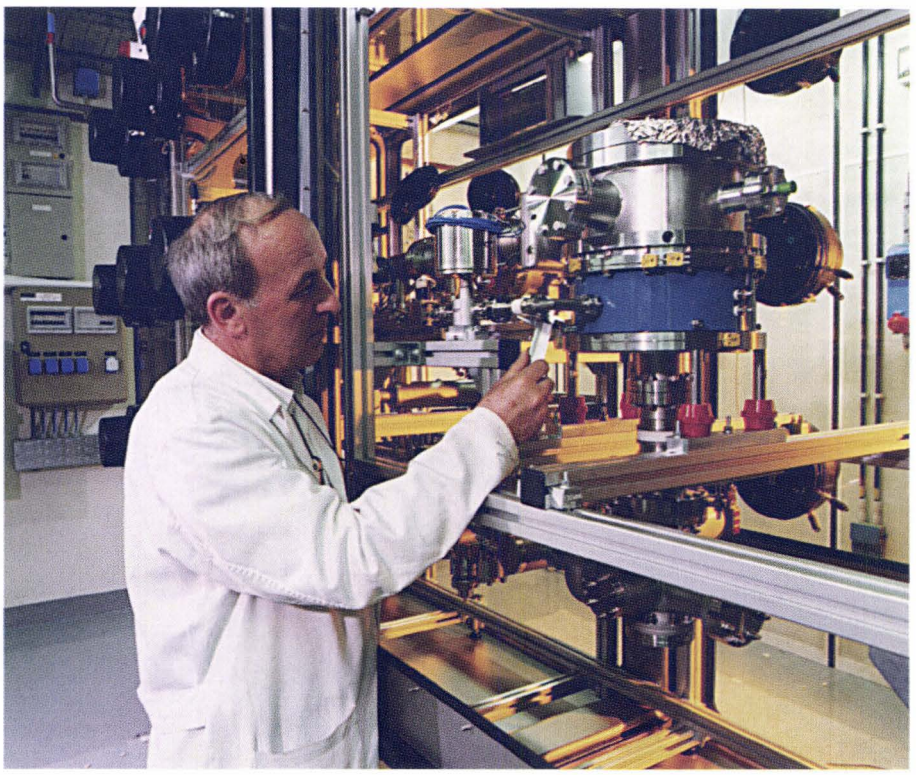

Fig. 4.22 Assembly of ETHEL-001

carried out in its sister cold installation (see paragraph on recycling of hydrogen isotopes from first wall materials of fusion reactors) in order to define the operating parameters of the plasma and to carry out a general calibration of the experimental procedure, as well as testing the control philosophy (mainly the development and testing of the control software). This cold facility is much more flexible that its hot counterpart due to the use of protium and deuterium only. This feedback procedure of cold testing allows to change previously decided configurations of ETHEL-001 in time, i.e. during the assembly phase, avoiding possible drastic changes at the end of the assembly (i.e. during the cold commissioning) which not always might be possible.

ETHEL-002: Large-scale gaseous detritiation

In 1985, during preliminary discussions on the design of the future tritium laboratory with fusion experts, the need to incorporate into the facility a gaseous detritiation system for the working environment, was expressed. The Tritium Systems Test Assembly (TSTA) at Los Alamos, USA, has such a system although it essentially remains unproven. In the case of ETHEL, it was argued by JRC-Ispra staff that, in accordance with the Regulatory Authority, the impact on the public of losing the laboratory's entire tritium inventory of 100 g to the ambient would be tolerable. Nonetheless, it was suggested that the study of such detritiation systems could become an integral part of future research to be conducted in ETHEL. This argument may not be plausible for fusion devices such as ITER where kilograms of tritium are to be handled rather than the gramme quantities as in ETHEL. Indeed, it is possible that without an adequate capability to meet emergency conditions where notable quantities of tritium risk of being discharged into a working area or to the environment, no large scale fusion device will be licensed by the relevant Regulatory Authorities. With this in mind, two stainless steel containments or caissons were included in the basic laboratory design. The Small Caisson is a 5 m^3 vessel employed for bench scale studies. In contrast, the Large Caisson, a 350 m^3 double-skinned containment, is envisaged for demonstrative pilot plant tests and is considered large enough for the scaling of processes and plants serving fusion reactor halls.

The present JRC-Ispra experiment, code-name ETHEL-002, relates to activities to be performed using the Small Caisson and is part of the NET research activities. However, the initial scope of detritiating large volumes of humid air has been extended to also encompass dry, inert atmospheres, both in normal and abnormal, i.e. accidental conditions. This expansion of the research programme reflects the various needs of fusion reactors such as glove-box atmosphere processing, room emergency clean-up or torus detritiation.

The research employs an experimental loop located in two glove-boxes and built around the Small

Caisson. The loop will have typical process parameters of:

- Operating pressure 125 to 900 kPa (a);
- Operating temperature of bed 100 to 775 K;
- Operating process gas flowrate 4 to 16 $m^3 \cdot hr^{-1}$;
- Dry and humid air, N_2, Ar and He atmospheres;
- Tritium quantities up to 37 TBq.

During 1993, the assembly of the loop outside of the glove-box was completed and mounting of the inside of the secondary containments started (***Fig. 4.23***). In parallel, the electrical control and instrumentation rack was completed and the interconnecting cabling to the experiment laid and the glove-box electrical and fluid service panels prepared (***Fig. 4.24***). Cold testing and commissioning of the loop will start in early 1994.

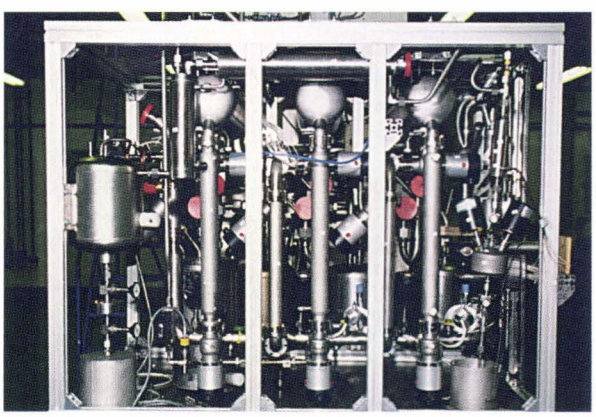

Fig. 4.23 Pre-assembly of a part of ETHEL-002

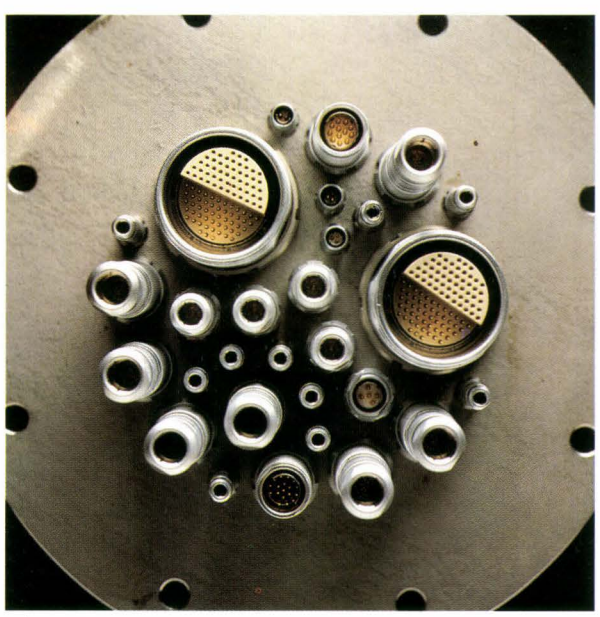

Fig. 4.24 Glove-box service panels for ETHEL-002

ETHEL-004: Tritium permeation through fusion relevant structural material

ETHEL-004 is being designed and constructed with the aim of allowing the direct investigation of tritium permeation through materials such as fusion reactor steels. The apparatus to measure the permeation of hydrogen and deuterium through materials has been constructed and is operating in the cold laboratory of ETHEL [52]. In order to construct the "tritium compatible" version of this equipment (ETHEL-004), it is clear that a number of important changes to the existing design will have to be incorporated. It is intended to keep the basic division of the apparatus into the "upstream side" where gas is introduced onto one side of a sample and the "downstream side" where the gas which has permeated through the sample is collected and measured. The main alterations as compared to the hydrogen prototype are the relatively low pressures of tritium gas which will be used (much less than 100 Pa). This means that a different method to establish and measure the pressure of the permeating gas should be employed. At low pressures, adsorption of tritium onto the walls of the apparatus during measurement has a relatively greater effect on the measured tritium pressure than at high pressures. This effect will have to be considered in the design of ETHEL-004. Other important points are: the pumping system must operate without oil to avoid tritium contamination; the system will operate in a glove box with limited accessibility; leakage of tritium from the parts of the apparatus at elevated temperatures by permeation into the surroundings is to be avoided. The proposed design of ETHEL-004 takes into consideration the previous tritium permeation apparatus as well as the existing apparatus in the ETHEL cold laboratory.

During 1993 the detailed design of the installation and the initial procurement of materials have been realized. The assembly and cold testing of the installation is foreseen for 1994.

ETHEL-006: Tritium recovery from plasma-facing materials

The plasma-facing materials of a fusion reactor become tritiated during operation and their replacement, will form a large part of the waste. Furthermore, experience from JET shows that tritiated graphite powder can be formed during operation. From both the economic and environmental standpoint the tritium should be recovered, and the waste conditioned in a form suitable for disposal. One way to dispose of

solid waste is to incorporate it in a stable, low-cost, metallic matrix.

The aim of the experiment ETHEL-006 is to build a pilot plant designed to heat tritiated graphite, beryllium or other plasma-facing materials in a carrier gas, or in vacuum, and to monitor the amount of tritium evolved. The specimens may be in the form of blocks or dust. The same plant can be used to dissolve the material in liquid metal (typically iron) which is then solidified to immobilise the waste.

The plant is being installed in a new low-level tritium laboratory outside the confines of ETHEL. It comprises two major components: a radio frequency (r.f.) furnace for heating the specimens, and a tritium analysis loop to study the progress of outgassing. The system is designed to allow outgassing at pressures between 1 bar and 10^{-3} Pa. The rate of outgassing can be measured as a function of temperature and pressure, using carrier gases such as pure He, humidified He, He-1% H_2 and humidified He-1% H_2, to examine the effects of isotope swamping.

The r.f. furnace has a dual function: as a detritiation chamber and as a furnace for dissolving materials in molten metal. For incorporating graphite, matrix materials such as iron (m.p. 1807 K), iron-4%carbon (m.p. 1420 K) or an iron-manganese-carbon eutectic (m.p. 1373 K) are under consideration. As well as reducing the melting point, the matrix materials decrease the solubility of tritium in the melt, allowing more efficient outgassing. Preliminary runs were aimed at testing the crucibles: two materials have been found which allow heating to ~2300 K.

ETHEL-007: A reactor-permeator for the reduction of tritiated water

The fuel cycle of fusion reactors, as well as some operations in laboratories, produce streams of tritiated water. For safety and economic reasons the tritium must be separated and recycled. Isotope separation is much more efficient when the hydrogen isotopes are in the elemental form, hence the tritiated water must first be decomposed. Two methods for doing this are being developed elsewhere although both have problems:

- electrolysis lacks materials which are tritium compatible, and has a high tritium inventory;
- the water-gas-shift reaction requires a large and complex installation.

JRC-Ispra has demonstrated that the reduction of water on activated iron can be achieved in a simple, compact apparatus with a low tritium inventory. The aim now is to make an apparatus capable of meeting ETHEL's needs and demonstrating the viability of the concept for ITER.

Activated iron granules were chosen as the most promising reactant. Initial tests showed that such a material could not only decompose water rapidly, but could also be repeatedly regenerated without loss of reactivity. Important is that the oxide formed is not hydrated and hence retains very little tritium. Significant reaction conditions were found to be:

$$3Fe + 4H_2O \underset{<<regeneration\ 755K<<}{\overset{>>decomposition\ 655K>>}{\rightleftharpoons}} Fe_3O_4 + 4H_2$$

The shift in equilibrium caused by temperature cycling is not sufficient to produce pure hydrogen by water decomposition, so the iron granules are contained in a palladium alloy tube, which only allow spure hydrogen to permeate into an outer chamber. Regeneration of the oxidised iron is done by shutting off the supply of water vapour and then passing hydrogen through the bed: water vapour is continuously removed in a cold trap.

The design of the first reactor-permeator prototype was shown in the last annual report. The first test showed an excellent water decomposition rate: 9.5 g of water in 8 hr using 210 g iron. However, it took more than 48 hr to complete the regeneration; the rate being limited by diffusion of water vapour into the cold trap. In the second test a metal membrane pump was used to circulate the gas through the reactor chamber and cold trap. The regeneration time was reduced to 16 hrs, which allows a complete decomposition/regeneration cycle in 24 hrs.

The reactor-permeator was then subjected to further cycling. There was no loss of performance, but on the fourth cycle the internal heater failed. The cause was found to be distortion of the palladium alloy tube. A second, improved prototype is now being installed in the new low-level tritium laboratory outside ETHEL: the thermocoax heater is separated from the palladium alloy tube. At present, the amount of tritium carried over into the regeneration stage is being assessed. The next experimental tasks are to examine possible improvements from using a smaller granulate size and the tolerance of the system to impurities. Satisfactory results would allow a simplification of the rest of the clean-up system.

Meanwhile a tritium-compatible reactor-permeator for use in the ETHEL gas detritiation system is being designed. This is based on an advanced, high-reliability permeator capable of passing 15$dm^3 \cdot hr^{-1}$ of hydrogen at one bar differential pressure. It should decompose 35 kg of water per year, with a maximum hydrogen isotope inventory of 20-60mg. Particular attention is being paid to minimize the tritium carryover in the structural materials. Up-scaling the same design using a single permeator could increase the throughput to cover any likely needs of ITER.

ETHEL-009: Interactions between tritium and wall surface materials

There is a safety requirement to better understand the parameters and physics/chemistry controlling the uptake, oxidation, and re-emission of tritium from wall surface materials likely to be encountered in future fusion reactor buildings. An experiment is being undertaken, code name ETHEL-009, with the objective of performing small scale exposure tests concerned with in-building tritium behaviour. The experimental loop, shown in *Fig. 4.25*, is placed in a fume hood that is used as a dynamic containment. The intent is to utilize for this experiment an existing experimental loop which recently became available (the installation for performing the JET bellows permeation tests). Accordingly, although compatible with the specific requirements of the present experiment, the design of the set-up was purposely constrained to be as close as possible to the JET bellows set-up.

The basic aspects that will be studied are the conversion of tritium gas to tritiated water under room temperature conditions as well as tritium absorption by the wall surface. With respect to the exposure conditions it is foreseen to apply concentrations over the range of $3.7 \cdot 10^8$ to $3.7 \cdot 10^{10}$ $Bq \cdot m^{-3}$ (10^{-2}-1 $Ci \cdot m^{-3}$). According to previous investigations, these are typical values for the tritium concentration in a commercial-sized fusion reactor hall, covering chronic and accidental room contamination patterns. Owing to the very low tritium quantities involved, the experiment can be effectively undertaken within the existing ESSOR regulatory framework. The project is on schedule. The necessary procurement has been made, and now the set-up is being commissioned. Effective experimental work will start at the beginning of 1994.

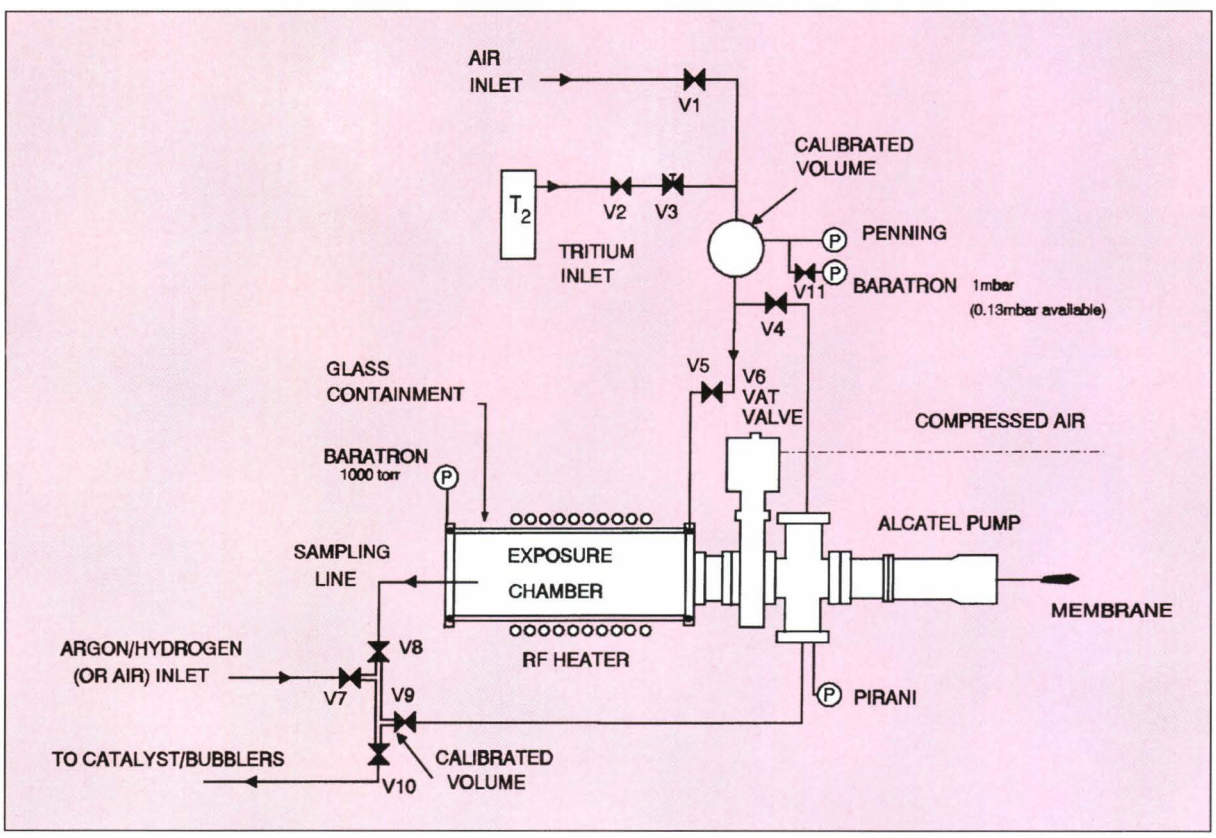

Fig. 4.25 ETHEL-009 flowsheet

References

[1] GIANCARLI L., BARBIER F.T., FLAMENT-FÜTTERER M., LEROY P., PROUST E., SANNIER X., RAEPSAET J., TERLAIN A., COEN V., PERUJO A., SAMPLE T., AGOSTINI P., BENAMATI G. - European Research and Development Programme for Water-Cooled Lithium-Lead Blankets. Present Status and Future Work, Fusion Technology, 21 (1992), pp 2075-2080

[2] CONRAD R., FÜTTERER M., GIANCARLI L., MAY R., PERUJO A., SAMPLE T. - LIBRETTO-3: Performance of Tritium Permeation Barriers under Irradiation at the HFR Petten, presented at the ICFRM-6, Stresa, Italy 27/9 - 1/10, 1993

[3] REITER F., FORCEY K.S., GERVASINI G. - A Compilation of Tritium Material Interaction Parameters in Fusion Reactor Materials, EUR 15217 EN

[4] REITER F., FORCEY K.S., GERVASINI G. - Tritium-Material Interaction Properties in Fusion Reactor Materials, Proc. XII Conf. on Vacuum Science and Technology, Bolzano, 23-26 March 1993

[5] GERVASINI G., REITER F. - Tritium-Materials Interaction in First Walls and Plasma Facing Components of Fusion Reactors to be published in Journal of Fusion Technology

[6] PERUJO A., CAMPOSILVAN J., CAORLIN M., PIOSCZYK B., REITER F., TOMINETTI S. - Proc. of the Course and Workshop on Tritium and Advanced Fuels in Fusion Reactors, Varenna, Italy, September 6-15, 1989, Ed. by Bonizzoni G. and Sindoni E., EUR 12540 EN

[7] REITER F., CAMPOSILVAN J., CAORLIN M., PERUJO A., TOMINETTI S. - J. Nucl. Mater 316, pp 179-181 (1991)

[8] PERUJO A., CAMPOSILVAN J., AGOSTINI P., REITER F. - Proc. of the Second ETHEL-TLK Workshop on Tritium Technology and Safety in Thermonuclear Fusion, Ispra, Italy, February 6-7, 1992., Ed. by Mannone F. and Penzhorn R.D. - S.P.I. 93.12

[9] PIOSCZYK B. - KfK-Primärbericht 11/04/02 P 12 M (1980)

[10] LEUNG K. N. et al. - Rev. Sci. Instrum. 49(3) (1978) 321

[11] EHLERS K. W., LEUNG K. N. - Univ. of California, LBL 14956 (1983)

[12] TUPHOLME K.W., DULIEU D., BUTTERWORTH G.J. - J. Nucl. Mater 650, pp 155-157 (1988)

[13] TUPHOLME K.W., DULIEU D., BUTTERWORTH G.J. - J. Nucl. Mater 684, pp 179-181 (1991)

[14] SAMPLE T., KOLBE H., ORECHIA L. - Prod. of SOFT 17, Rome, Italy, Sept. 14-18 (1992)

[15] BASKES M.I., BAUER W., Wilson K.L. - J. Nucl. Mater 663, pp 111&112 (1982)

[16] FORCEY K.S., PERUJO A., REITER F., LOLLI-CERONI P.L. - J. Nucl. Mater 417, p 200 (1993)

[17] PROUST E., LEROY P., FRANENBERG H.W. - J. Nucl. Mater, 186, pp 191-194 (1991)

[18] FORCEY K.S., ROSS D.K., WU C.H. - J. Nucl. Mater. 182 (1991), p 36

[19] CAORLIN M. - Ph.D. thesis, The Open University, Oxford, UK, 1992

[20] FORCEY K.S., ROSS D.K., SIMPSON J.C.B. and EVANS D.S. - J. Nucl. Mater 117, p 160 (1988)

[21] VASSALLO G. et al. - Improved Permiation Barriers for Tritiated Waste Packaging, to be published in Journal of Fusion Technology

[22] MALARA C., RICAPITO I., SPELTA B., TOCI F., VIOLA A. - Adsorptive Removal of the Impurities from the Exhausted Plasma, Paper presented at the 9th Int. Zeolite Conference, Montreal (Canada), July 5-10, 1991

[23] MALARA C. - PhD Thesis, University of Antwerp (UIA), Antwerpen (Belgium), September 17th, 1993

[24] MALARA C., MENCARELLI T., PIERINI G., RICAPITO I., TOCI F. - Determination of Multicomponent Adsorption Equilibria on Microporous Adsorbents, paper presented at 3rd International Symposium on Separation Technology, Antwerpen (Belgium), August 22-27, 1993

[25] MALARA C., PIERINI G., RICAPITO I., TOCI F. - Contribution of JRC-STI to the 3rd TLK/ETHEL Workshop, Karlsruhe, May 24-25, 1993, edited by H. Dworschak, Technical Note I.93.78

[26] MALARA C., PIERINI G., RICAPITO I., SPELTA B., TOCI F., VIOLA A. - Progress in Quantitative Analysis of Hydrogen Isotopes, paper presented at 3rd TLK/ETHEL Workshop on Tritium Technology and Safety in Thermonuclear Fusion, Karlsruhe (Germany), May 24-25, 1993

[27] RICAPITO I., MALARA C., PIERINI G., SPELTA B. - Near Real-Time Diagnostic Analysis of Hydrogen Isotopes by Gas-Chromatography, paper presented at 3rd International Symposium on Separation Technology, Antwerpen (Belgium), August 22-27, 1993

[28] PIERINI G., SPELTA B., MALARA C., RICAPITO I. - Hydrogen Isotopes Separation, paper presented at 2nd ETHEL/TLK Workshop on Tritium Technology and Safety in Thermonuclear Fusion, Ispra (Italy), February 6-7, 1992

[29] YOSHIDA et al. - J. Nucl. Sc. and Tech., 19, (1982)

[30] CONTI M., LE SIMPLE M. - J. Chromatog., 29 (1967)

[31] VOGD R. - ISSN0366-0885 (1988)

[32] GENTRY C., SCHOTT R. - Anal. Chem., 42, 1, (1970)

[33] MALARA C., MENCARELLI T., RICAPITO I., TOCI F., VANSANT E.F. - Characterization of Porous Solids by Analysis of Gas-Physisorption Measurements, paper presented at 9th International Zeolite Conference, Montereal (Canada), July 5-10, 1992 and accepted for publication on Microporous Solids

[34] BRECK D.W. - Zeolite Molecular Sieves, Wiley-Interscience, N.Y. (1978)

[35] BARRER R.M. - Zeolite and Clay Minerals as Sorbents and Molecular Sieves, Academic, N.Y. (1978)

[36] BARRER R.M., VANSANT E.F., PEETERS G. J. - Chem. Soc., Faraday Trans., 1, 74, p.1981 (1983)

[37] VANSANT E.F. - Innovation in Zeolite Material Science (P.J. Grobet Ed.) Elsevier, Amsterdam (1988)

[38] COE C.G., KUZNICKI S.M. - European Patent 109,063 (1984)

[39] JASRA R.V., CHOUDARY N.V., BHAT S.G.T. - Separation of Gases by Pressure Swing Adsorption, Separation, Sci. and Tech., 26(7), p.913 (1991)

[40] ALSOP P.J., SENOHRABEK J.A., MILLER J.M., ROMANISZYN E.F. The Effects of Residual Tritium on Air-Detritiation Dryer Performance, Fusion Technology, 21, pp 599-603, 1992

[41] VANSANT E.F. - Controlled Permeabilization of Zeolite, contract n° 2541-84-12 EDISPB, Antwerp

[42] PROF. AIELLO, personal communication

[43] FLANIGEN E.M. et al. - U.S. Patent 4, 104, 294

[44] LOK B.M., MEZZINA C.A., PATTON R.L., GAJEK R.T., CANNA T.R., FLANIGEN E.M. - U.S. Patent, 4, 440, 871 (1984)

[45] WILSON S.T., LOK B.M., FLANIGEN E.M. - U.S. Patent, 4, 310, 440 (1982)

[46] WILSON S.T., FLANIGEN E.M. - U.S. Patent, 4, 567, 029 (1986)

[47] DAVIS M.E., SALDARRIGA C., MONTES C., GARCES J., CROWDER C. - Zeolites, 8, p 362 (1988)

[48] WANG J., FEN S., XU R. - J. Chem. Soc. Chem. Comm., (5), 265 (1989)

[49] HARVEY G., MEIER W.M. - Zeolites: Facts, Figure, Future (Jacobs P.A. and Van Santen R.A., Eds.) Elsevier, Amsterdam, p 41 (1989)

[50] BURCH R., Ed. - Pillared Clays, Catalysis today, Vol. 2, Nos.2-3 , ISNN 0920-5861 Elsevier, Amsterdam (1988)

[51] KRAEMER R., BESSERER U., JOURDAN G., HOUSIADAS C., PERUJO A., VASSALLO G. - Proceedings of the 15th Annual Symposium on Safeguards and Nuclear Material Management, Rome, Italy 11-13 May, 1993, EUR 15214 EN, pp 147 -151

[52] FORCEY K.S., PERUJO A., REITER F., LOLLI-CERONI P.L. - The Permeability, Diffusivity and Solubility of Deuterium in TZM, J. Nucl. Mater 203 (1993), pp 36 - 42

1.5 INDUSTRIAL HAZARDS

The general objective of the work is the assessment, improvement and harmonization of safety methodologies, focusing on the key areas:

- *control of chemical reactions with a potential for thermal runaway,*
- *emergency pressure relief of batch chemical reactors and storage vessels,*
- *prediction of the dispersion of dense vapour clouds,*
- *gas cloud explosion hazards.*

1.5.1 BATCH CHEMICAL REACTORS

The optimisation of batch chemical reactors, from safety and quality points of view, is the only way to reduce the number of accidents leading to considerable human and material losses and strong environmental impact. Research on process dynamics of discontinuous chemical reactors, in conditions close to runaway, is carried out in the FIRES Project (Facility for Investigating Runaway Events Safely). The main objective of FIRES is the study of off-normal behaviour of batch and semi-batch processes in a scale closer to industrial practice. Specifically, this study intends to:

- check and develop criteria for the safety of processes by studying the characteristics of reactive mixtures and determining the critical operating conditions;
- test and develop measures for the prevention of uncontrolled thermal excursions and the associated over pressurisation phenomena, including control and early detection systems, and interlocks;
- develop and validate experimentally models for the numerical simulation of discontinuous chemical reactors under normal and off-normal operating conditions;
- integrate these models into advanced methodologies for process optimisation and prevention of uncontrolled thermal excursion, process design and process control by developing an intelligent tool to assist in these tasks.

The FIRES project is divided in three different parts:

- A calorimetric laboratory which is used to gain basic knowledge of the chemical processes prior to their investigation in the FIRES reactor. The laboratory has been equipped with a differential scanning micro-calorimeter, a small scale reactor and an adiabatic calorimeter for venting studies. Furthermore, Gas Chromatography, IR and UV spectroscopy are used for chemical analysis.
- A mathematical simulator of FIRES (FISIM = FIres SIMulator) that serves as an aid and a complement to experiment design, and subsequent data analysis [1]. Furthermore, a special version of the simulator is applied on-line for the estimation of non-measured variables and main parameters of the process, such as kinetics and heat transfer characteristics [2].
- A fully automated 100 l pilot plant reactor installed within a bunker, equipped with sensitive measuring devices, and provided with an early warning detection system, shut- down systems, and emergency pressure relief, so that hazardous chemical reactions can be investigated safely [3-4].

Simulation of batch chemical processes (FISIM)

The main simulation activity has concentrated on the extension of the mathematical model developed for toluene nitration to other aromatic compounds [5-6]. A comparison between the experimental and simulated results demonstrates that the model providcs accurate results by modifying the appropriate parameters that depend on the aromatic compound being nitrated, i.e. the reaction rate constant, the solubility of the aromatic species in mixed acid and the physical properties. As an example, the comparison

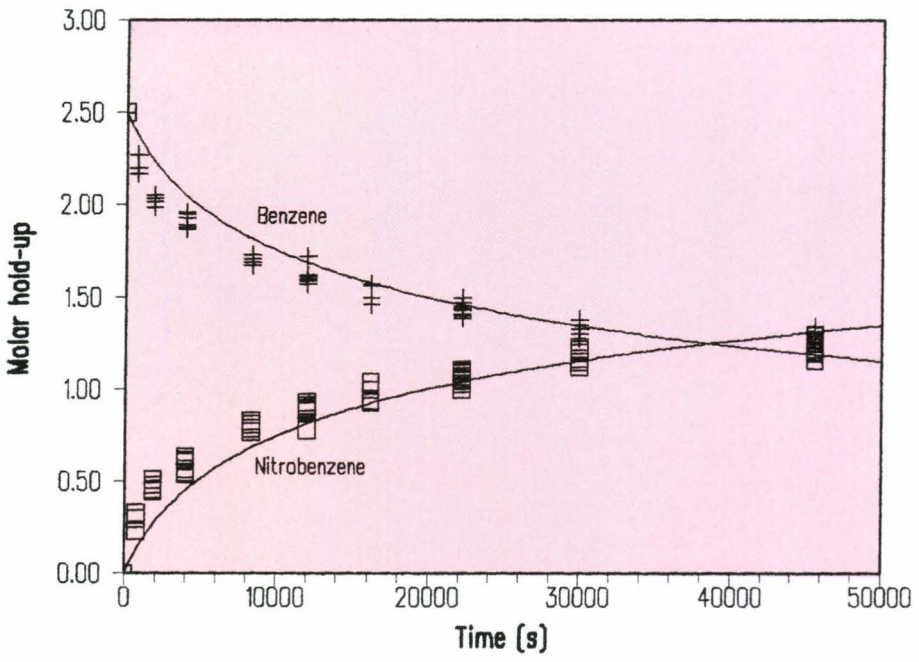

Fig. 5.1 Experimental versus simulated molar hold-ups as a function of time for benzene mononitration using the Mc function. 195 g of benzene added batchwise to 868 g of mixed acid (H_2SO_4 strength 62.0 wt%). Tmset-point = 298.16 K and Na=6.67 s-1

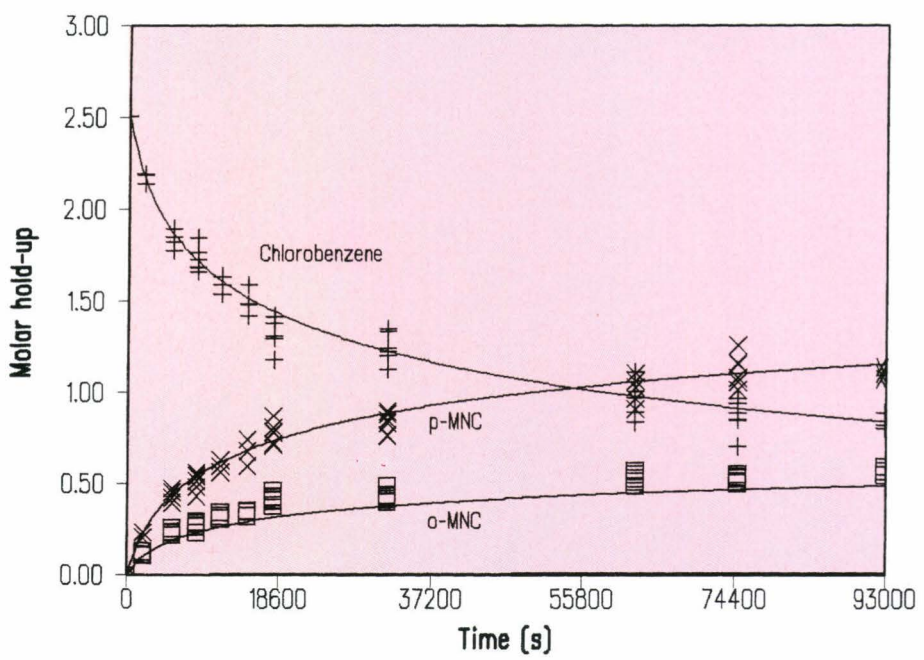

Fig. 5.2 Experimental versus simulated molar hold-ups as a function of time for chlorobenzene mononitration using the HR function 281g of chlorobenzene added batchwise to 851 g of mixed acid (H_2SO_4 strength 62.0 wt%). Tmset-point = 328.16 K and Na=6.67 s-1

between experimental and simulated molar hold-up profiles for chlorobenzene and benzene versus time is shown in *Figs 5.1* and *5.2*. The work has demonstrated that mathematical modelling and numerical simulation are an efficient tool for the scaling-up of chemical processes, for its design and its optimisation. Furthermore, a special version of the simulator has been used for testing the performances of new adaptive control schemes with constraints in the design, not only in the control variables but also in their derivatives [7-8].

Small-scale studies

The work has focused on the extension of work carried out during 1992 regarding the toluene mononitration to other aromatic nitrations, i.e. benzene, chlorobenzene and mesytilene in order to validate experimentally the developed model. The work subdivides in two parts:

- Preparatory experiments: In order to identify separately different characteristics of aromatic nitrations, a preparatory experimental programme was set-up. The objectives were: to determine the heat transfer coefficient in mixtures of organic

compounds (benzene and chlorobenzene) and sulphuric acid solutions; to calculate the phase inversion point and to calculate the solubility of organic species in acid mixtures as a function of temperature and composition. Furthermore, adiabatic nitration experiments have been carried out using the PHI-TEC experiments to study the heat of reaction and the thermal stability of the reacting mixtures.

- Reaction Calorimeter experiments: A series of chlorobenzene and benzene nitration experiments was performed in the RC1 reaction calorimeter with the aim of studying the influence of the operating conditions: temperature, sulphuric acid strength, stirrer speed and feeding rate (see ***Figs. 5.1*** and ***5.2***).

The experiments were supported by chemical analysis using Gas Chromatography [9] and Ultraviolet Spectroscopy.

Application of neural networks in chemical reaction engineering

The use of Artificial Neural Networks, a last years' Exploratory Research action, has been taken up in the programme, focusing on three different activities:

- Identification of thermo-kinetic parameters from laboratory data: traditional methods of kinetic identification have been compared with the neural networks approach [10]. The results indicate that the back-propagation neural network can be used to produce an accurate kinetic expression from experimental data when there is no knowledge about the kinetic pathway and when the time to determine it is limited.
- Early warning detection of runaway initiation: Kohonen maps have been used for pattern recognition to distinguish between normal and dangerous states in the reactor, based on the measurements of reactor and jacket temperatures. The results indicate that the problems of noise in the OLIWA system could be solved by this approach.
- Temperature control of discontinuous chemical reactors: dynamic back-propagation neural networks are used to replace the identification and control blocks in the indirect adaptive control scheme. The first results indicate promising possibilities.

Stability analysis of chemical reactors using chaos theory

This work relates to a last years' Exploratory Research action now taken up in the research programme. It is well-known that for certain values of the parameters in the mass and energy balance equations that represent the dynamic behaviour of batch reactors, the system becomes very sensitive to the values of the initial conditions. This sensitivity to initial conditions is a well-known characteristic of chaotic phenomena. To study such a systems researchers have developed powerful methods to extract physical quantities from experimentally obtained irregular signals. Between them, Lyapunov exponents are the average exponential rates of divergence or convergence of nearby orbits in phase space. Since nearby orbits correspond to nearly identical states, exponential orbital divergence means that systems whose initial differences have not been resolved will soon behave quite differently: in this case the predicting ability is rapidly lost. This definition is related to the sensitivity of the temperature with respect to several input variables along the trajectory, corresponding to nominal operating conditions introduced in the context of chemical reactor theory. In consequence, the sensitivity has been used to identify critical regions by calculating the Lyapunov exponents [11] (see ***Fig. 5.3***).

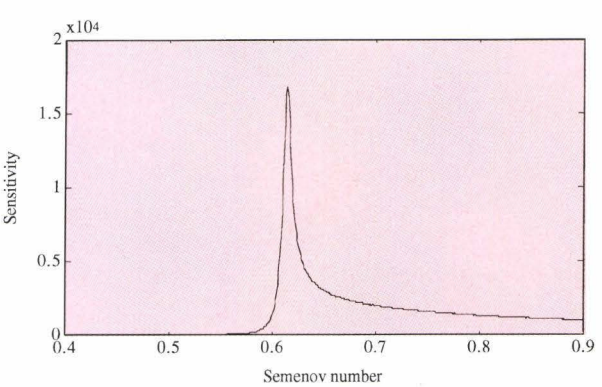

Fig. 5.3 Sensitivity calculated using Lyapunov exponents as a function of the Semenov number. $\varepsilon = 0.05$, $n = 1$, $Ti = 1$, $B=20$. $\psi_c = 0.614$ (reported value from Morbidelli and Varma (1988), $\psi_c = 0.616$)

FIRES

After evaluation of the nitration experiments in the 100 l reactor the temperature control was improved. A modification in configuration of the controllers

improved the temperature stability of the heating/cooling jacket. With smaller fluctuations in temperature calorimetric measurements using the temperature differences between jacket in- and outlet are feasible. Kalman filtering techniques have to be applied to achieve this.

A study was made on how to improve the data acquisition and control system of the facility, allowing the implementation of advanced applications; more precise: how to increase reliability of data transfer to and from the main computer, how to improve capacities of rate and storage of acquisitions and how to perform independent and standard data acquisitions at VME level. Using up-to-date hardware and software developments, it was decided to replace the main computer by a workstation SUN-spark10 and to use user-friendly LABVIEW software for data acquisition and control of FIRES.

From a market study experimental failure simulation is identified as the most promising application of the facility. Direct requests of chemical companies and proposed projects within the network on runaway reactions confirm this. Examples of experimental failure simulation are stirring and cooling failure of suspension or emulsion polymerisation, followed by injection of an inhibitor to stop a possible runaway. For these purposes the facility was modified and completed further. The cooling lines for the condensation unit were connected to the central cooling system. From an existing industrial polymerisation plant a condenser was down scaled and installed, as well as a foam pot and a pressure vessel for handling chemicals. These modifications allow to study the polymerisation, the failure of the process, the stopping of a runaway and the safe handling of gaseous monomers. For two different polymerisation processes these unique experiments will be carried out in 1994.

1.5.2 EMERGENCY VENTING OF REACTOR VESSELS

Investigation of multiphase flow phenomena in reactor relief systems during venting (MPMC project)

When the pressure in a process vessel such as a chemical reactor threatens to rise above a safe limit (e.g. as a result of external fire or runaway chemical reaction), the pressure must be reduced by discharging some of the vessel contents through a pressure relief system. This system often comprises a safety valve or rupture disc together with associated piping, the design problem being to determine the appropriate sizes of these components in order that the flowrate of liquid-vapour mixture through the system removes sufficient energy from the vessel to prevent the pressure rising to unsafe levels.

The objectives of this experimental project are:

- provide consultancy/test services to industry and public authorities,
- obtain experimental data on various aspects of two-phase venting,
- use these data for validation of the JRC computer code RELIEF (design of venting systems),
- assess the implication of these experimental findings for the design of industrial pressure relief systems,
- ensure the transfer of these findings to industry.

Experimental work

This year, attention has been focussed on the construction of two new venting facilities, namely DRACULA (**D**epressuration, **R**elief **A**nd **C**ontainment **U**sing **L**arge **A**pparatus) and COLUMBUS (venting of long horizontal vessels). The design of these facilities and the test programmes have been discussed with industrial working groups [12, 13].

DRACULA facility. This large-scale venting facility is shown in ***Figs. 5.4*** and ***5.5***. The reactor vessel and catch-tank have volumes of 6 m^3 and 20 m^3 respectively and there are two sizes of vent-pipe, 82.5 mm and 160 mm diameter with overall length of 24 m. A number of commissioning tests have now been performed (see ***Fig. 5.6***) and the test programme is expected to commence in Summer 1994 once the specially-designed gamma-densitometer mass flowmeter is constructed and installed. The test programme will concentrate initially on the transient two-phase flow characteristics of large safety valves and rupture discs under a variety of conditions using high-viscosity fluids and fluids with polymer suspensions.

COLUMBUS facility: This medium-scale facility is shown in ***Fig. 5.7*** and is concerned with the venting characteristics of long horizontal vessels. The horizontal vessel (4000 mm x 2500 mm) and the catch tank have volumes of 0.3 m^3 and 1.7 m^3 respectively and there are two sizes of vent-pipe 20 mm and 50 mm diameter with an overall length of 4 m. Objectives here include determining how the venting characteristics of horizontal vessels are different from those of vertically-orientated vessels and to formulate these observations into design guidelines for industry. In addition, there will also be complementary studies of safety valve performance (the COLUMBUS catch-tank can be pressurised whereas the DRACULA catch-tank cannot). Commissioning tests on this facility are likely to start in February 1994.

A venting test with a high-viscosity foamy fluid was recently reported [14] and, at present, the perfor-

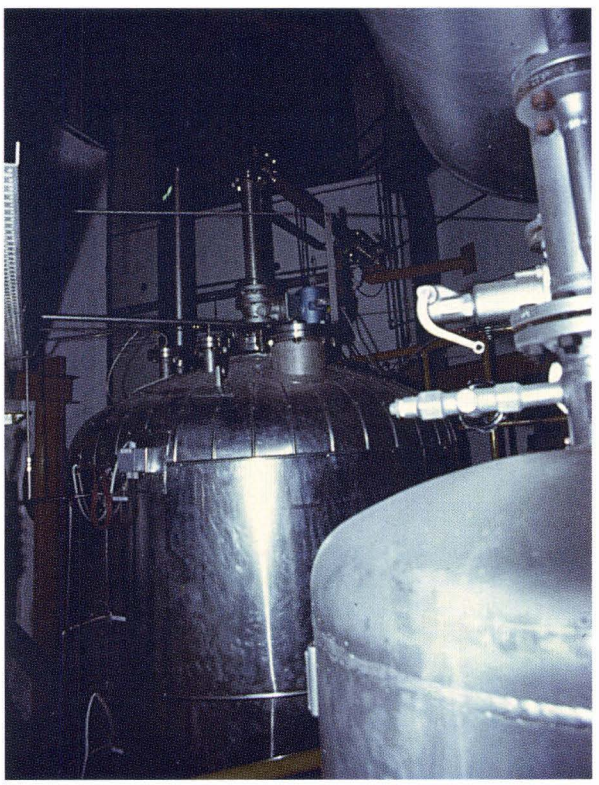

Fig. 5.4 DRACULA facility: 6 m^3 reactor vessel (vent-pipe at top vessel)

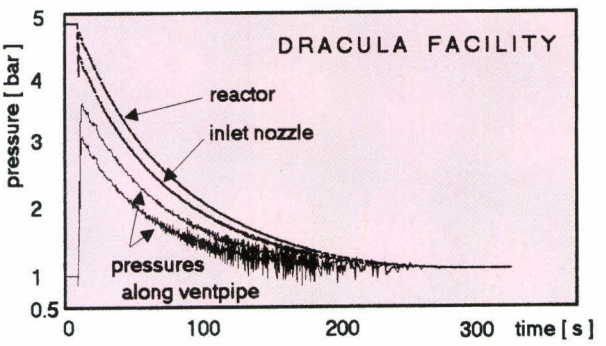

Fig. 5.6 Typical pressure traces during venting of the DRACULA facility

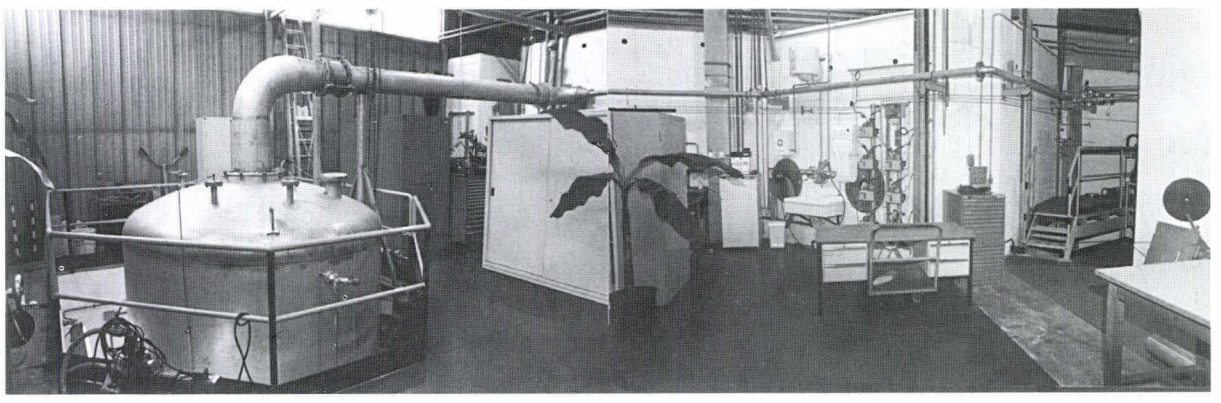

Fig. 5.5 DRACULA facility: vent-pipe and catch-tank

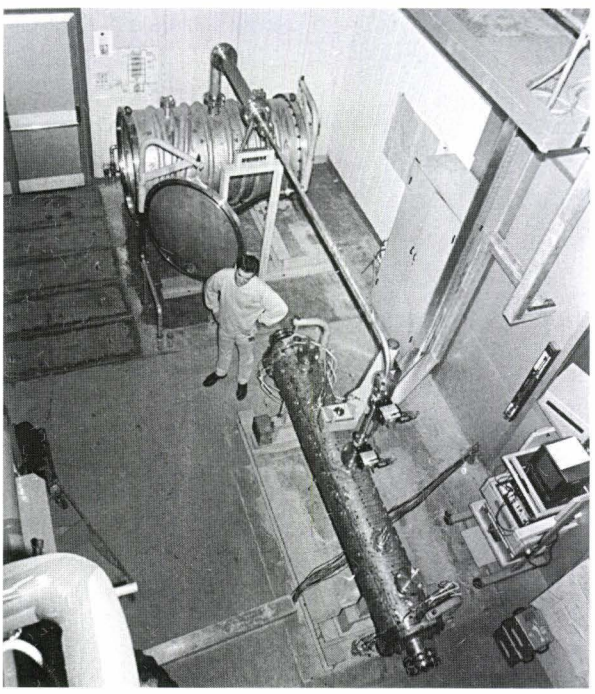

Fig. 5.7 COLUMBUS facility: horizontal vessel, vent-pipe and catch-tank

mance of the gamma-densitometer mass flowmeter for the COLUMBUS facility is being assessed on the old MPMC facility for which flow conditions are known. In support of the above experimental activities, a number of analytical studies have been completed and discussed at meetings of industrial working groups [15 - 19]. In June 1993 a Collaboration Agreement was signed with the Explosion and Flame Laboratory of the Health & Safety Executive, U.K. (see Section 3.2).

Nuclear Magnetic Resonance (NMR) mass flow measurements

NMR mass flow measurements have been carried out in water-nitrogen two-phase flow. Reliable measurements, which compare with the loop input values, are only possible if one is in a pseudo-stationary two-phase flow. This limits our measuring range. The velocity v_{NMR} of the water is obtained straight forward by the efflux time T_e [46]. Calculating the velocity v_o, which would be obtained at the same mass flow without gas, the liquid fraction $\varepsilon_v = v_o/v_{NMR}$ by the continuity equation was obtained. On the other hand one gets an NMR amplitude $A_{NMR}(v)$ at velocity v in the two-phase flow. If this is compared with the amplitude $A_o(v)$ without gas at the same velocity, again the liquid fraction $\varepsilon_{NMR} = A_{NMR}/A_o$ is obtained. For the evaluation of A_{NMR}, A_o and v_{NMR} careful and lengthy calibration procedures are necessary [47]. In ***Fig. 5.8*** the liquid fraction ε_{NMR} versus ε_v is shown.

The accuracy is well within ±5%. The NMR mass flow MF_{NMR} is obtained by the product of ε_{NMR} and v_{NMR} and the inner cross-section of the loop tube. It can easily be shown [47] that

$$\frac{\varepsilon_{NMR}}{\varepsilon_v} \quad \frac{\dot{M}F_{NMR}}{MF_0}$$

where MF_o is the mass flow measured by the turbine at the water input into the loop. This ratio gives the accuracy of the NMR mass flow measurement. It is plotted in ***Fig. 5.9*** versus liquid fraction ε_v (for comparison with ***Fig. 5.8***). The mass flow obtained by NMR can thus be claimed to be accurate to within ±6%.

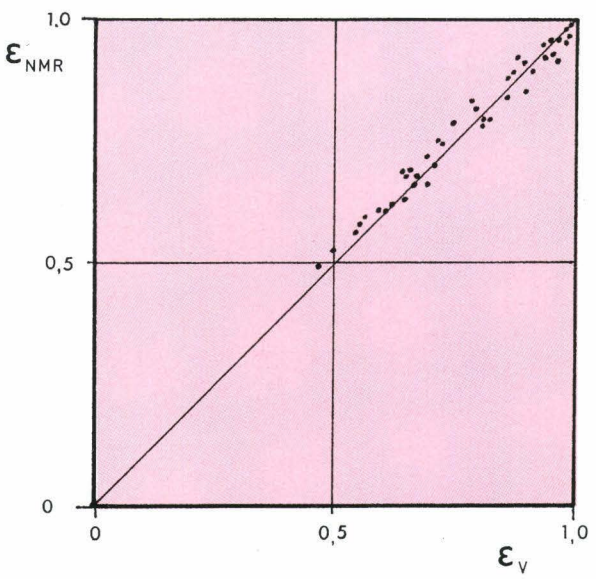

Fig. 5.8 Liquid fraction ε_{NMR} obtained from NMR-amplitude vs. ε_v obtained from velocity and continuity equation

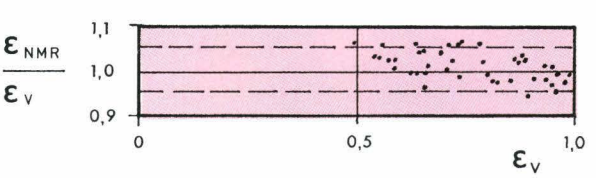

Fig. 5.9 Ratio MF_{NMR}/MF_o vs. ε_v, showing the accuracy of the NMR mass flow determination

Fig. 5.10 Screen layout

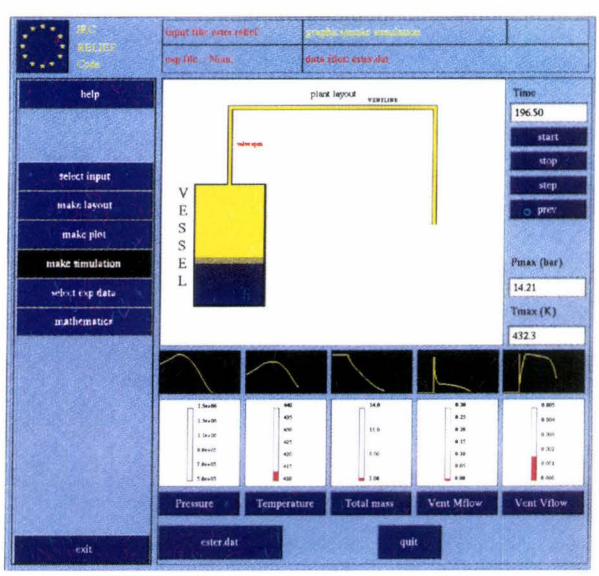

Fig. 5.11 Simulation option esterification runaway reaction

The emergency relief system code RELIEF (20, 21, 22)

RELIEF is a computer code package that has been specifically designed to model the transient, one-dimensional, two-phase flow behaviour of a multi-component, chemically reacting fluid mixture. Its function is to simulate batch type chemical reactors and storage vessels prior to and during accidental thermal runaway events leading to emergency pressure relief. The physical model that describes the above phenomena is coupled to a sophisticated input and output processor in such a way that a complete self-contained package is created. The working environment that results from this enables the user, in a very convenient way, to interactively set up a problem definition, execute the computation and interrogate the results. A comprehensive on-line help facility gives the user guidance and recommendations to further ease the task of input of data. There are also consistency, limit and syntax checks so that unrealistic data cannot be entered. Due to the high computational speed of RELIEF the package is an ideal tool for performing parametric studies and for investigating different design strategies.

The main aim of this work is to provide chemical industry, technical institutions and public authorities with a validated computer code that will help create harmonised rules for the design of emergency pressure relief systems at a European level. In some more detail, RELIEF is able to model up to ten chemical species (both inert and reactive), up to ten parallel irreversible chemical reactions, the mass transfer between the component liquid and vapour phases, the two-phase fluid dynamics and the interactions among these processes. A variety of vessel shapes can be modelled together with the vessel wall thermal capacity and heat transfer. It is possible to specify up to ten vent lines which can be located anywhere on the vessel, with each vent line having an independently controlled safety valve or bursting disc. The results of the calculation are displayed graphically (with the option of a postscript hard copy),and an additional animation feature allows the user to visualise the transient in faster than real time. Examples of the screen layout, the simulation option and the pressure response for an esterification runaway reaction are shown in ***Figs 5.10***, ***5.11*** and ***5.12***.

An underlying feature of emergency pressure relief design is often the lack of data regarding component physical properties and chemical kinetics, so for this reason where possible predictive features have been incorporated into RELIEF. These include vapour pressure behaviour, surface tension and non-ideal liquid and vapour specific volume behaviour as the critical region is approached. A user generated physical property database is also included in the system.

During 1993 much effort has been devoted to the validation of the physical models within RELIEF, and

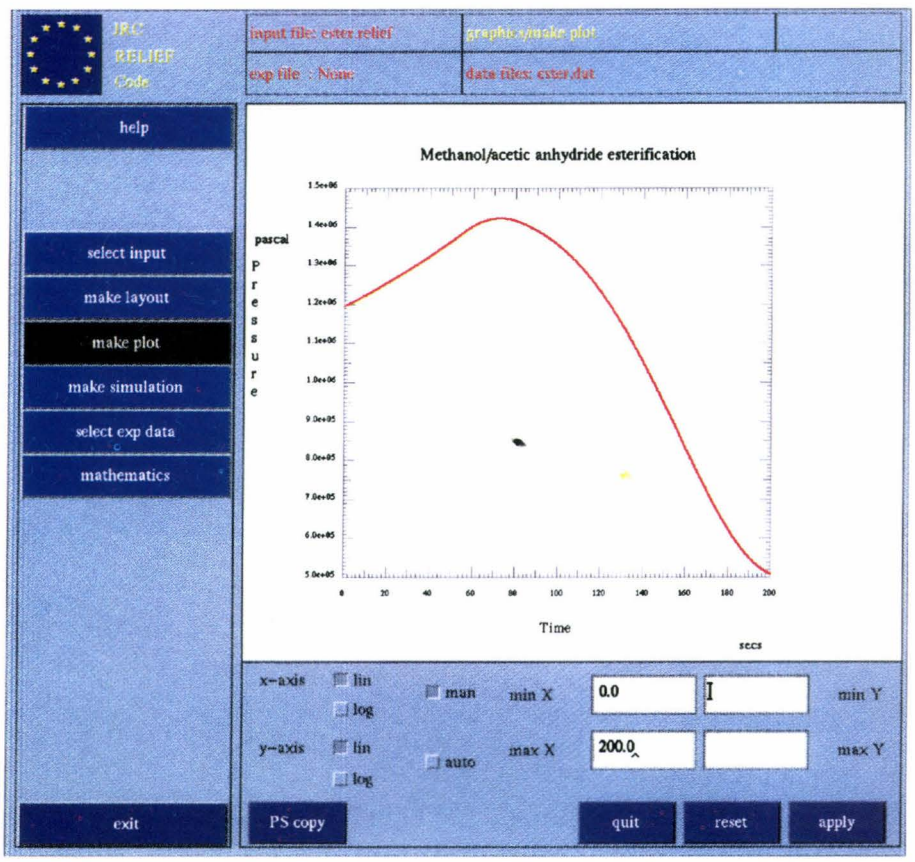

Fig. 5.12 Pressure history of esterification runaway reaction

to extending the capabilities of the package. For the validation exercise experimental results from the JRC venting facility MPMC, from the work performed by the DIERS group and data from the open literature have been used. A cooperation agreement has been signed with an industrial partner from the petrochemical industry, and the package has been implemented in its research laboratory. Further cooperation agreements with other partners from the chemical industry are in preparation. In this way preliminary evaluation of the package will be performed against industrial problems prior to the commercialisation of the package.

RELIEF is operational on a general workstation platform and a PC version is very near completion. The modelling work aimed at simulating the transient behaviour during emergency pressure relief of a liquid full catalyst bed reactor, operating at near critical pressure, is near completion too. A special treatment was made for the fluid expansion and chemical conversion processes. A critical flow model capable of describing highly subcooled conditions in a vent line containing a safety control valve has been written. These models are to be implemented into the RELIEF code.

Advanced two-phase flow modelling

The major objective of this activity is the development and verification of a general code module for the numerical simulation of multidimensional two-phase flow. The project is based on a new modelling concept for inhomogeneous, nonequilibrium two-phase flow and takes advantage of recent developments in numerical techniques for solving hyperbolic flow equations. As such, it represents a well-posed initial-boundary value problem that admits to apply modern computational solution techniques.

The study of multiphase flow conditions is of large interest in many industrial applications where process optimisation or plant safety is of primary concern. Although specific techniques are available for the design of process equipment or the study of particular plant transients, many situations call for a more general analytical approach. The present work, building on previous experience in the area of nuclear reactor thermal-hydraulics analysis, aims at providing a reliable and efficient computational tool for the numerical simulation of dynamic two-phase flow processes where strong thermal nonequilibrium effects and inhomogeneous flow conditions are particularly important. A multidimensional capability will eventually allow complex 1-, 2-, or 3-D simulations to be made.

Specific applications envisaged include:

- analysis of depressurization and discharge phenomena in chemical or nuclear reactors in case of pipe failures or intentional relief processes,

- analysis of transients in thermal-hydraulic networks,
- design and transient analysis of process components, e.g. boilers, steam generators, cryogenic systems of rocket engines or fusion reactors. Emphasis could be given to design optimisation or safety studies depending on the problem. The code structure will be set up in a way that allows easy adaptation to various applications with regard to the required degree of modelling detail and geometrical complexity.

Following the concept of a 'two-fluid' representation of two-phase flow, a new approach [23, 24] has been adopted based on the macroscopic formulation of the phasic conservation equations for mass, momentum and energy. The highly non-linear non-hyperbolic field equations for the case of two-phase flow preclude the direct use of existing solution methods so that the system of governing equations is rendered hyperbolic by the introduction of additional terms in the momentum equations, representing space and time derivatives of the major flow parameters.

The initial emphasis of this project was directed towards the development of the basic modelling approach for one-dimensional flow processes and to numerical techniques which were developed originally for high speed gas flows [25, 26, 27]. These include:

- the Split Coefficient Matrix method, a finite difference upwind technique,
- the Flux Vector Splitting method, a finite volume scheme based on the approximate Riemann solver.

Various benchmark problems have been run to test the basic modelling concept and numerical techniques for one-dimensional flow conditions including:

- sedimentation problem,
- oscillating U-tube manometer,
- boiling oscillations in a narrow vertical pipe heated at the bottom,
- fast blowdown of a straight pipe, initially filled with subcooled water (Edward's pipe).

All these test cases confirmed the advantages of the Flux Vector Splitting (FVS) technique that has the intrinsic property of conserving mass, momentum and energy. Compared with present standard techniques, an improved prediction has been achieved with respect to wave propagation phenomena, critical flow conditions, resolution of local flow parameters, phase separation, and the formation and tracking of mixture levels. As an example, results for the oscillating manometer are shown in ***Fig. 5.13***, comparing

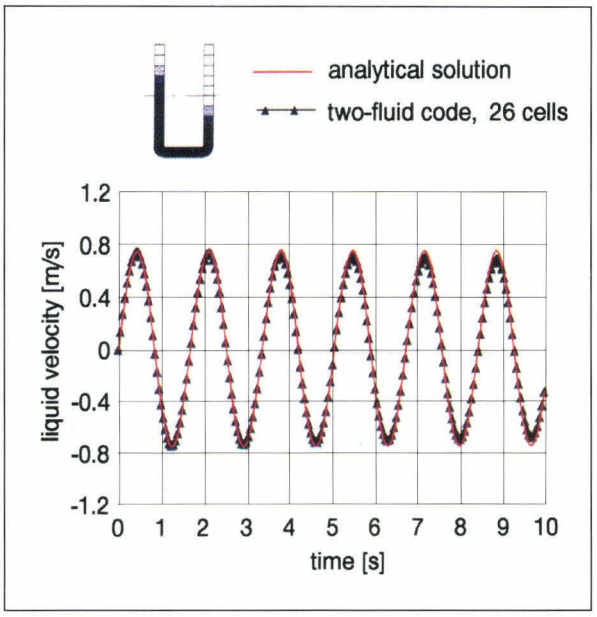

Fig. 5.13 Oscillating manometer problem: liquid velocity at bottom of U-tube

the predicted fluid velocity at the bottom of the U-tube with the (in this case) known analytical solution. The perfect agreement with respect to the oscillation frequency, the very low damping of the amplitude, and the rather good resolution of the void gradient at the liquid level, indicates the quality of the present approach.

The major emphasis during 1993 was directed to further improve the numerical technique to obtain second order accuracy in space and to extend the general modelling to two-dimensional flow conditions. The second order accurate scheme is based on the 'Monotonic Upwind Scheme for Conservative Laws' (MUSCL), together with slop limiters which provide the 'Total Variation Diminishing' (TVD) property. An example is shown in ***Fig. 5.14*** for the sedimentation problem using the 'superbe' slope limiter which resulted in the best resolution of steep void gradients. The figures clearly indicate the propagation of two void fronts:

- a rising front between the liquid and the two-phase regions, and
- a falling mixture front separating the two-phase region from the pure vapour at the upper part of the vessel. The figures show a clear distinction between the two separation fronts and the high resolution of the steep void (density) gradient that could not be achieved with the standard techniques having inherent large numerical diffusion properties.

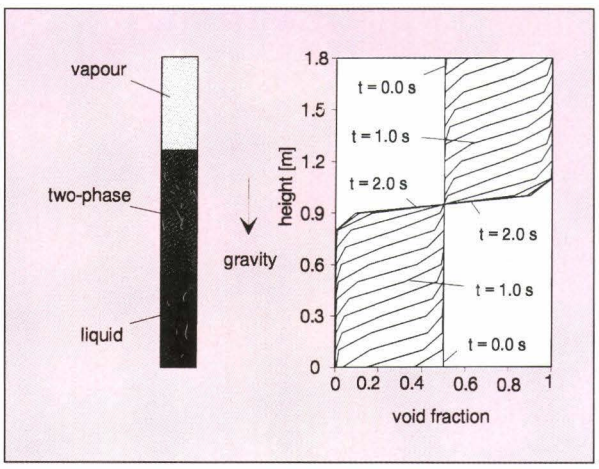

Fig. 5.14 Sedimentation problem, second order scheme: void distribution at different time values

Further effort was directed to the extension of the basic modelling and numerical techniques to multidimensional flow conditions using structured (Cartesian) grids and a decomposition of the signal propagation into one-dimensional wave pattern. First verification calculations have been performed for various two-dimensional flow problems, including:

- two-dimensional sedimentation problems,
- sudden collapse of a vertical liquid cylinder,
- natural circulation of an externally heated/cooled vessel,
- depressurization of a tank with top or side venting. An example is given in ***Fig. 5.15***, which show the velocity field for the vapour phase and the associated void distribution during the first phase of the depressurization of a pressure vessel initially filled (partially) with subcooled liquid.

The major activities planned for 1994 will be related to increase the robustness of the calculation by an improved implicit treatment of the interfacial exchange processes (source terms) and an implicit treatment of the pressure wave propagation processes in order to avoid the present time-step size limitation on the basis of sound velocity. However, the main emphasis will be placed on the implementation of a new, highly modular code structure, having a large flexibility for the solution of varied two-phase flow problems. This would provide, within a common framework, the means of analysing and comparing single and two-phase flow situations with varying degrees of sophistication with respect to the treatment of thermal non-equilibrium effects or inhomogeous flow conditions, the principal use of unstructured grids, and the capability to connect 1-D components with multi-dimensional domains.

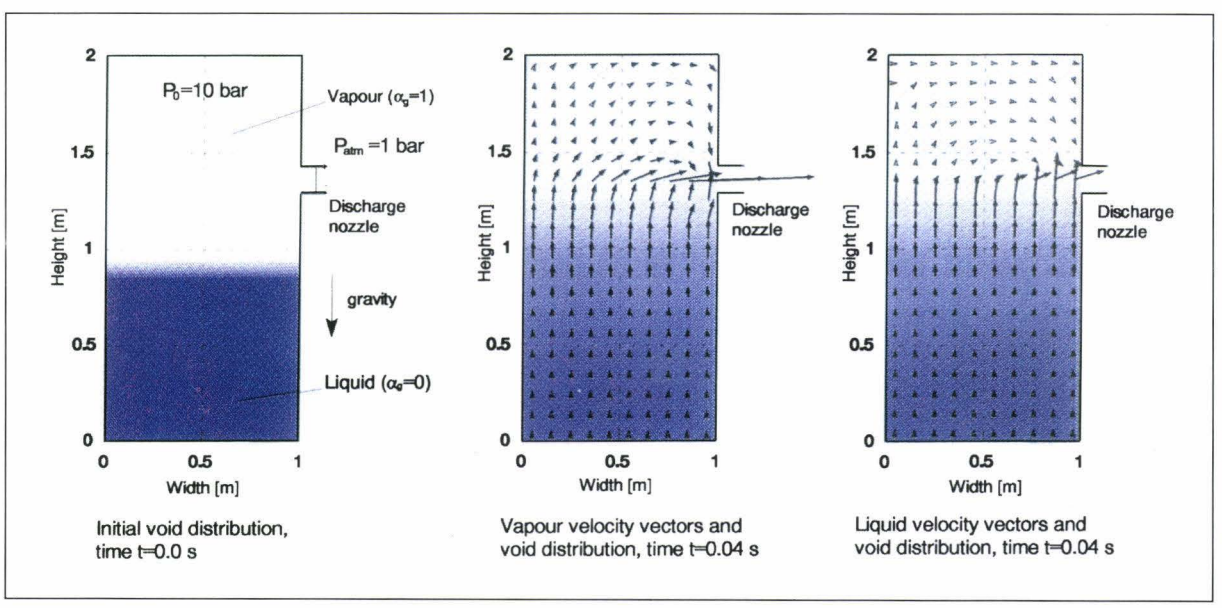

Fig. 5.15 Depressurisation of a 2-D pressure vessel, second order scheme, 10x20 cells

1.5.3 DISPERSION OF DENSE VAPOUR CLOUDS

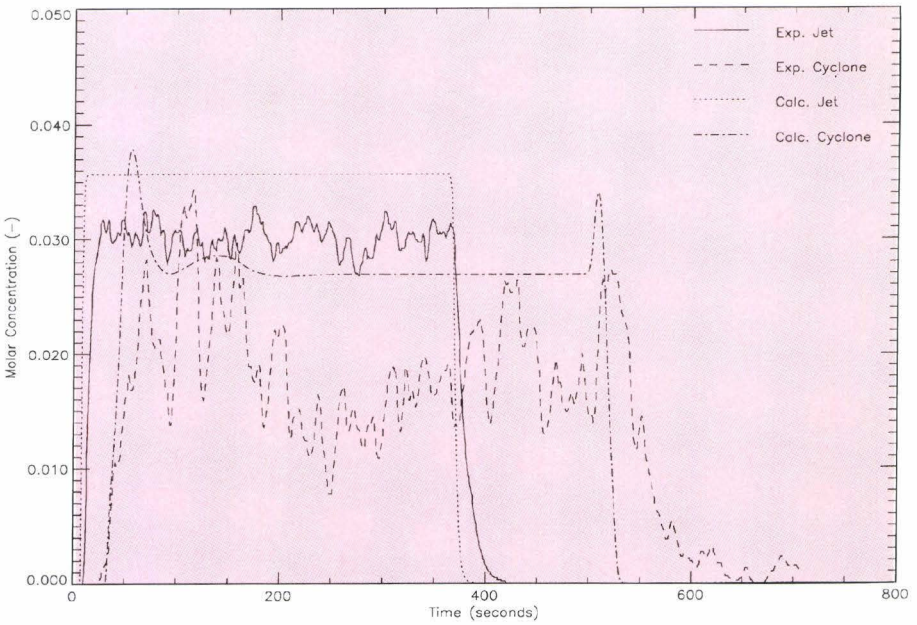

Fig. 5.16 Comparison between experimental and calculated concentration histories for the EEC propane experiments 55 (jet) and 57 (cyclone). The sensor was positioned at ground level ca. 30 m downwind the source. The calculations were performed with the 1-D shallow layer model.

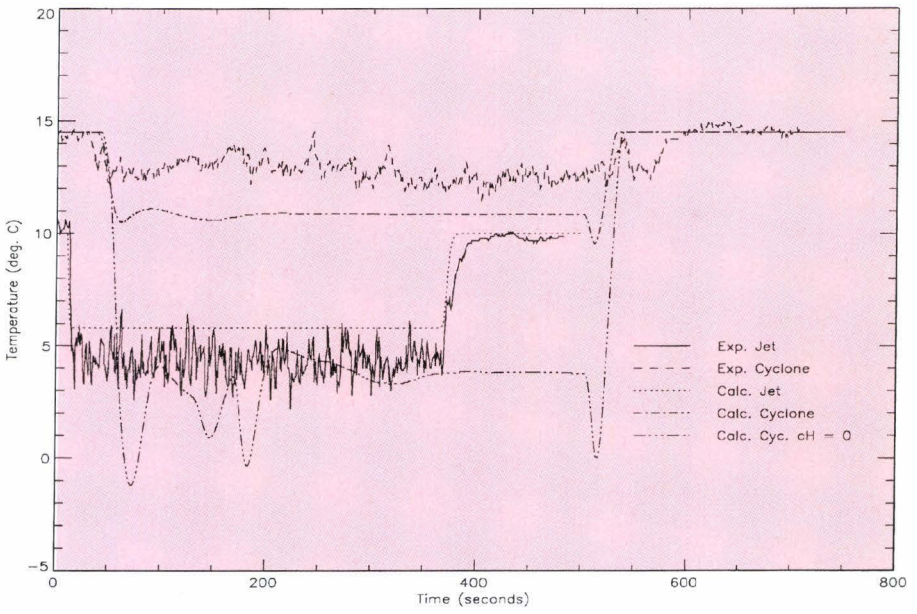

Fig. 5.17 Comparison between experimental and calculated temperature histories for the EEC propane experiments 55 (jet) and 57 (cyclone). The sensor was positioned at ground level ca. 38 m downwind the source. The curve indicated with cH = 0 results from a calculation without ground heat transfer. The calculations were performed with the 1-D shallow layer model.

The objective of this project is to develop and validate computer models describing dispersion of denser-than-air vapour clouds in irregular terrains with obstacles. The two main applications are assessment of accident consequences in terms of damage to the public and installations, and optimisation of safety engineering features for accident mitigation. Due to the diversity in the model application areas, it is desirable to have access to models with different levels of detail in the description of the dispersion phenomena. The work consists of development and improvement of a code package comprising three models: a detailed fully three-dimensional model ADREA-HF and two simpler models based on the shallow layer concept. The research is carried out in the frame of a collaboration contract with the Demokritos Research Centre in Athens and in association with the CEC sponsored project FLADIS on two-phase flashing releases under the STEP programme.

The 1-D shallow layer model, describing a 3-D

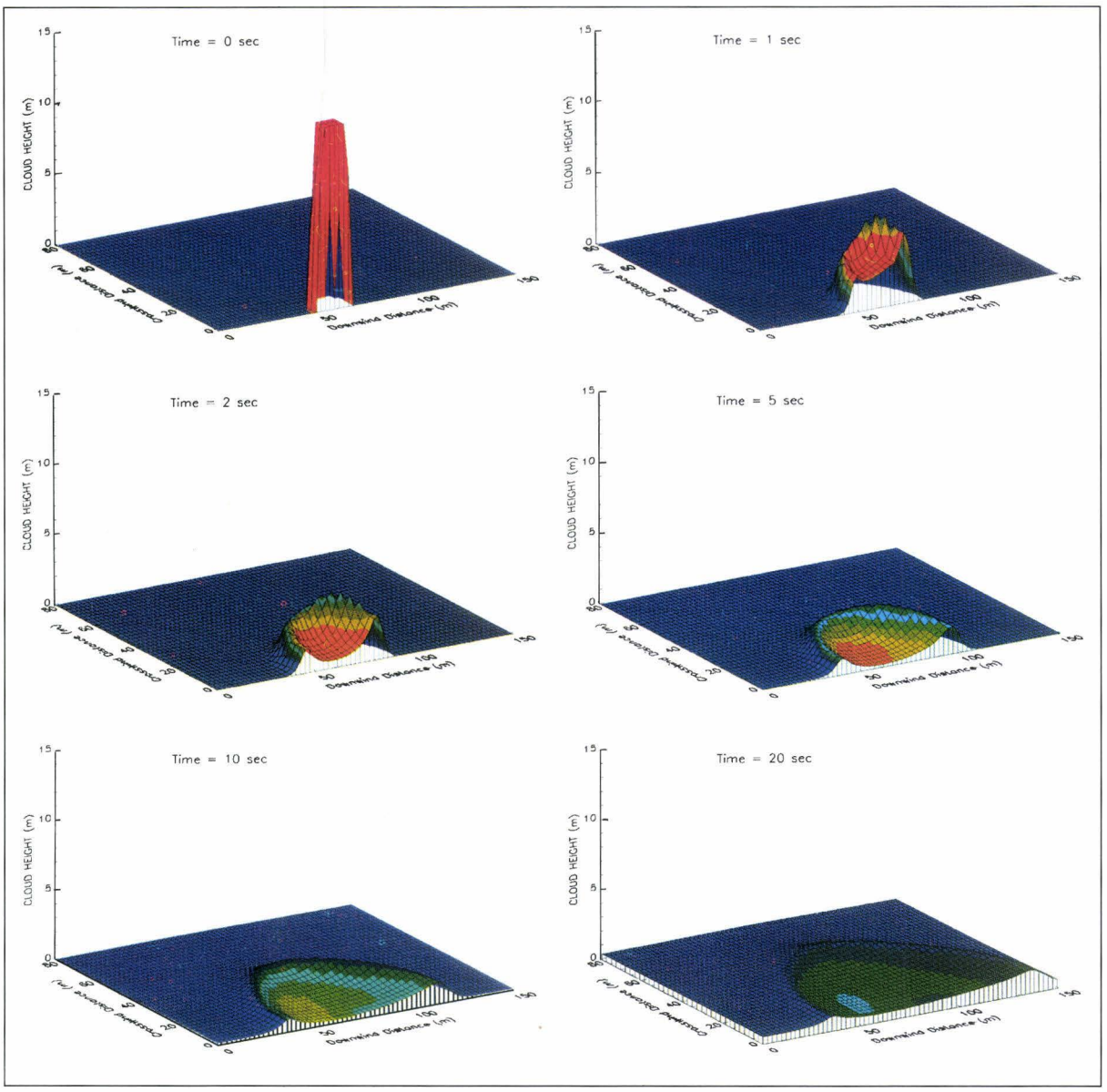

Fig. 5.18 Simulation of the Thorney Island Trial 8 by the 2-D shallow layer model. The initial height of the cloud is 13 m and diameter 14 m. The wind velocity at 10 m height is 2.4 m/s. Red corresponds to a concentration greater than 0.70 and blue to a concentration less than 0.01.

cloud by integration over the cloud height and width, has been validated and documented [28 - 30]. By application of several field test and wind tunnel data it was demonstrated that the model is able to predict concentration and temperature histories with an accuracy close to the experimental variability, under a large range of conditions. These include releases with and without momentum (jets and cyclone releases), non-isothermal conditions, and the presence of obstructions. The capabilities of the model are illustrated in ***Figs. 5.16*** and ***5.17*** where measured and calculated results are compared for two different releases, with and without momentum. The field experiments were the EEC propane releases 55 (jet) and 57 (cyclone). They were continuous, flashing releases of liquified propane, with a release rate in the order of 3 kg/s. In ***Fig. 5.16*** the experimental and calculated volumetric concentration histories are compared for the two tests. It is seen that the influence of the jet momentum (ca. 200 N) is well predicted. Both the earlier cloud arrival time and the immediate occurrence of a steady-state for the jet

case is accurately calculated by the model. A similar comparison of the temperature histories is shown in ***Fig. 5.17***. In order to illustrate the importance of taking the heat transfer from the ground into account, the result of a calculation without ground heat transfer (cH = 0) is included for the momentum-free release.

The work to extend the model to two dimensions, where integration only takes place over the cloud height, has been continued. This development work is partly based on the 1-D model, and partly on the 3-D ADREA-HF code [30] - [32]. In ***Fig. 5.18*** is shown a prediction of the field experiment Thorney Island No. 8 where 2000 m^3 dense gas was released instantaneously. The above mentioned calculations are performed as a part of a comparison study between the present model and a 2-D shallow layer model under development at the Cambridge University.

The intercomparison exercise on Thorney Island trial 21 (with a semi-circular fence) between ADREA-HF and MERCURE-GL (developed by EdF and GdF) has been completed [33 - 34]. The study revealed a few minor weak points in the turbulence models applied by the two codes. However, the general conclusion drawn was that both codes are able to predict with adequate accuracy the dispersion phenomena in the presence of obstacles. The implementation of a model for concentration fluctuations in the ADREA-HF code has been completed. Validation is in progress by application of wind tunnel and field test data.

1.5.4 NUMERICAL SIMULATIONS OF REACTIVE FLOWS

The code development activity regarding the numerical simulations of flows including chemical reactions has to deal with the difficulties associated to flows whose characteristic speeds are spread over a large range. This makes it difficult to track simultaneously all the waves correctly. Typical situations of this kind are subsonic, almost incompressible flows in which the thermodynamic characteristics (that include also the chemical aspects) become more and more uncoupled with the mechanical characteristics of the flow. Another class of problems are phenomena with very different time scales, so called 'stiff' problems. Dealing with these issues typically requires the use of a certain degree of implicitness for the time integration in the numerical discretization of the wave propagation. Doing so, one necessarily renounces to simultaneously and exactly capture all the phenomena, but at least can hope to resolve one single phenomena with the desired accuracy [36], [38]. The code REACFLOW, which is under development in CPA/PED, does address these types of problems. The major activities in the year 1993 are described in the following.

In addition to the existing semi-implicit time integration scheme [35], [39], that was designed to accurately track the convective signals, a *fully implicit, second order time integration scheme for the multi-component inviscid equations of gas dynamics has been implemented*. The conservation of species, momentum and total energy are discretized in time by means of a linearisation of the numerical fluxes, formulated according to the Roe approximate Riemann solver. The resulting numerical procedure, being unconditionally stable, allows to select the time step in such a manner as to follow the propagation of any traveling signal. The price to pay for this flexibility is that a large system of equations must be solved at each time step, whose size increases quadratically as the number of species increases. The scheme tends also to show numerical viscosity effects for the convective waves slightly superior to those observed for the previously existing semi-implicit time integration procedure. On the other hand, the scheme has proven a robustness far beyond the semi-implicit scheme.

In order to be able to deal also with fully incompressible cases, a *multi-component Navier-Stokes solver has been set up*. The multi-component character of the flow introduces some particular properties that

should be underlined. Even if discontinuities in the pressure field are no longer expected, discontinuities can be present in the density fields, as well as in the energy field. Although the density of each component is a constant, the density field is not uniform due to spatial variations coming from different mass fraction distributions, thus preventing the writing of the Navier-Stokes equations in its kinematic form. The numerical approach adopted is an extension of the well-known ICE (Implicit Continuous Eulerian) method, to deal with unstructured volumes and multi-component flows. Viscous and inviscid flows are treated simultaneously within this module, and natural convection effects (i.e. the feedback from the energy equation to the momentum equation) are simulated by including a Boussinesq momentum source term. As within many projection methods, it requires the solution of a Poisson-like equation for the pressure. For the classical Navier-Stokes single-component case, and also for those formulations treating the chemical species as passive scalars convected by the flow, the matrix associated with the Poisson problem depends only on the grid. On the contrary, in the multi-component case, this matrix needs to be calculated at each time step, and thus the overall computational cost of the procedure increases. However, since the implicit system of equations concerns only a scalar variable, the incompressible treatment of a problem is, if possible, always faster than an implicit treatment of the compressible equations.

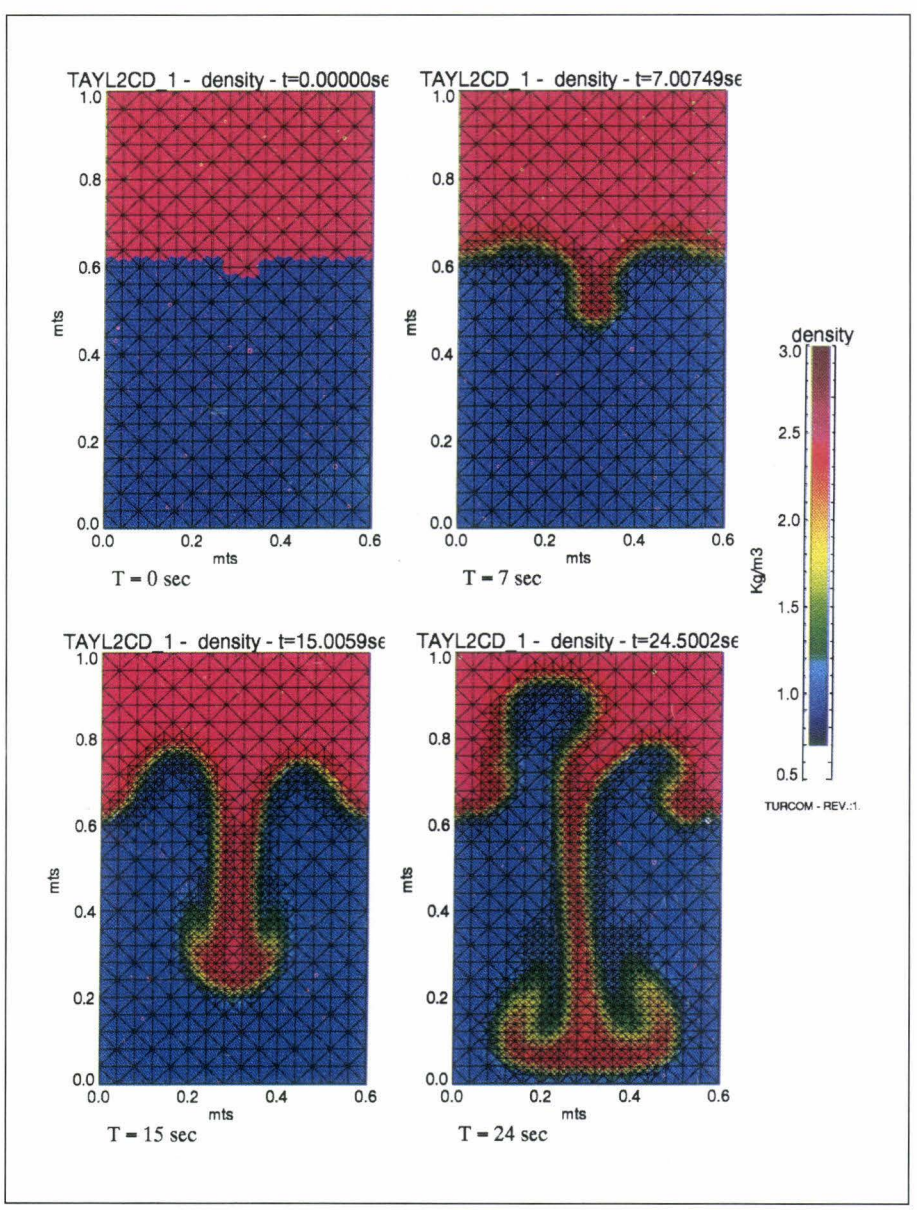

Fig. 5.19 Color fields which represent the density for the calculation of the Taylor instability with two components at different times using the incompressible module of REACFLOW

An example of a fully incompressible calculation is shown in ***Fig. 5.19*** as a time sequence of a density field represented by different colors in a calculation of the Taylor instability. Two liquids are in a closed adiabatic container where no slip on the walls is assumed. The heavy liquid (density = 2.5 kg/m^3) is in the upper part, and the lighter liquid (density = 1.0 kg/m^3) is in the lower part. The separation between the two liquids has a slight disturbance, which causes the heavy liquid to penetrate into the lighter liquid. The gravity is set to - 0.1 m/s^2. The calculation

has been performed with two components with a second order numerical scheme in space and time. The light component is inviscid, whereas the heavy component has a viscosity of 2.0 E-3 m^2/s.

In the course of 1993 *the simulation of the diffusive processes* (heat conduction, viscosity, molecular diffusion) *has been further refined* and put on a more rigorous mathematical basis [37]. Assessment of the diffusive processes by the solution of purely parabolic problems has demonstrated that the solver is able to accurately reproduce exact solutions to the test problems. A possibility has been introduced of relaxing the requirement of a conservative pointwise reconstruction of the volume-averaged data. This gives the possibility of solving the linear system of equations rising from the implicit treatment of the equations together with the linear system of the fully implicit hyperbolic solver described above. That leads to a saving of computation time and an increase of stability of the solver.

The diffusive solver has also been tested against realistic problems. ***Fig. 5.20*** shows a 1-D calculation of a premixed flame in a one-dimensional simulation of a deflagration in a one-meter region. The deflagration takes place in a uniform mixture of hydrogen and air, with $[H_2]=[O_2]$, at ambient pressure and temperature. Ignition takes place at the closed left end of the region by imposing a temperature above the ignition point in a small region. The temperature and density at time t=0.06 s after the ignition are shown over the domain. The right end of the region is open, allowing the precursor wave to escape. The temperature and density fields show the classic features of a deflagration: low flame speed (about 7 m/s) and an expansion of the air across the flame front. The flame speed is not as previously only determined by the grid geometry and the flow solver, but is fully controlled by the heat conduction coefficient (and thus, given a Lewis number of unity, the molecular diffusion coefficients). In this the heat conduction coefficient acts as a sort of very primitive turbulence model, directly supplying the anomalous diffusion, term that arises from a true turbulence model. In the future, when the turbulence modelling will be operative, the need for such "tweaking" of the heat conduction will no longer be necessary. Work on implementing a model for the turbulence (in the first instance, the k-epsilon model) is in progress at the turn of the year.

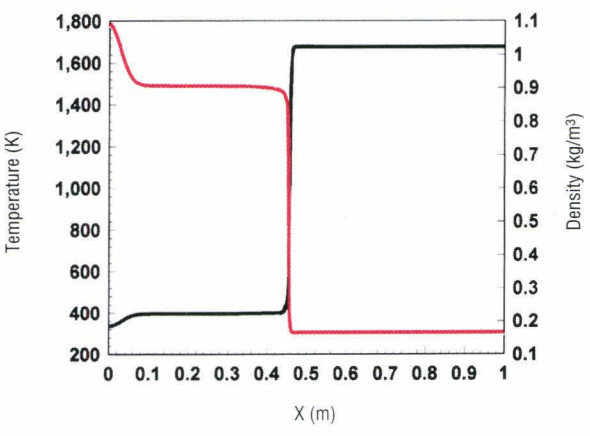

Fig. 5.20 1-D flame calculation

The *automatic and reversible grid adaptation system SANGRIA has been further improved* and is now used systematically for every day work [41]. The *animation system ISOLDA has been extended* and improved, so that it has become a useful tool to check on-line the ongoing calculation. A demonstration tool has been developed from ISOLDA, which can replay the plotting files, without doing the calculations. This has been very useful for presentations showing fast-moving on-line animation, without having to pass to a VCR.

The code has been implemented on different UNIX platforms (DEC Alpha, SUN Sparc, HP-700) and on MS-DOS PCs and runs on all these systems without modifying the sources. This includes also the graphics [40] and means that REACFLOW and the ISOLDA graphic system are fully portable. The Post-Processing system TURCOM, originally developed at ISEI, has been taken over by the team REACFLOW and was further improved.

Documentation and Assessment is an ongoing activity and will be addressed also in 1994. A major activity for next year will also be to finish the implementation of the turbulence model. This will then complete the development phase of the 2-D code version. A thorough validation and verification must then follow, in order to assure that the results of the code are reliable and to prove the robustness of the code. Looking forward to the next framework programme, where safety research may have less emphasis, the activity "Reactive Flows" could also be shifted to other applications (e. g. clean combustion, etc.). Further investigations will, however, be necessary in this regard (possible research fields and customers, code capabilities, etc.).

1.5.5 ENVIRONMENTAL PROTECTION: FLUID DYNAMICS AND TRANSPORT PROCESSES

The general objective of the work related to environmental fluid dynamics and transport processes is to contribute to the understanding of the phenomena related to man made environmental problems and climate change. The related activities are an integral part of joint research activities with the other institutes of the Ispra establishment. The work in STI deals with numerical-mathematical modelling of 3D dynamics of ocean and atmosphere, of the related transport of seawater - and air - components and of the 3D characteristics of physico-chemical/bio-chemical reactions between these components, supposing that the process models of the respective reactions are provided by the partner institutes or from outside.

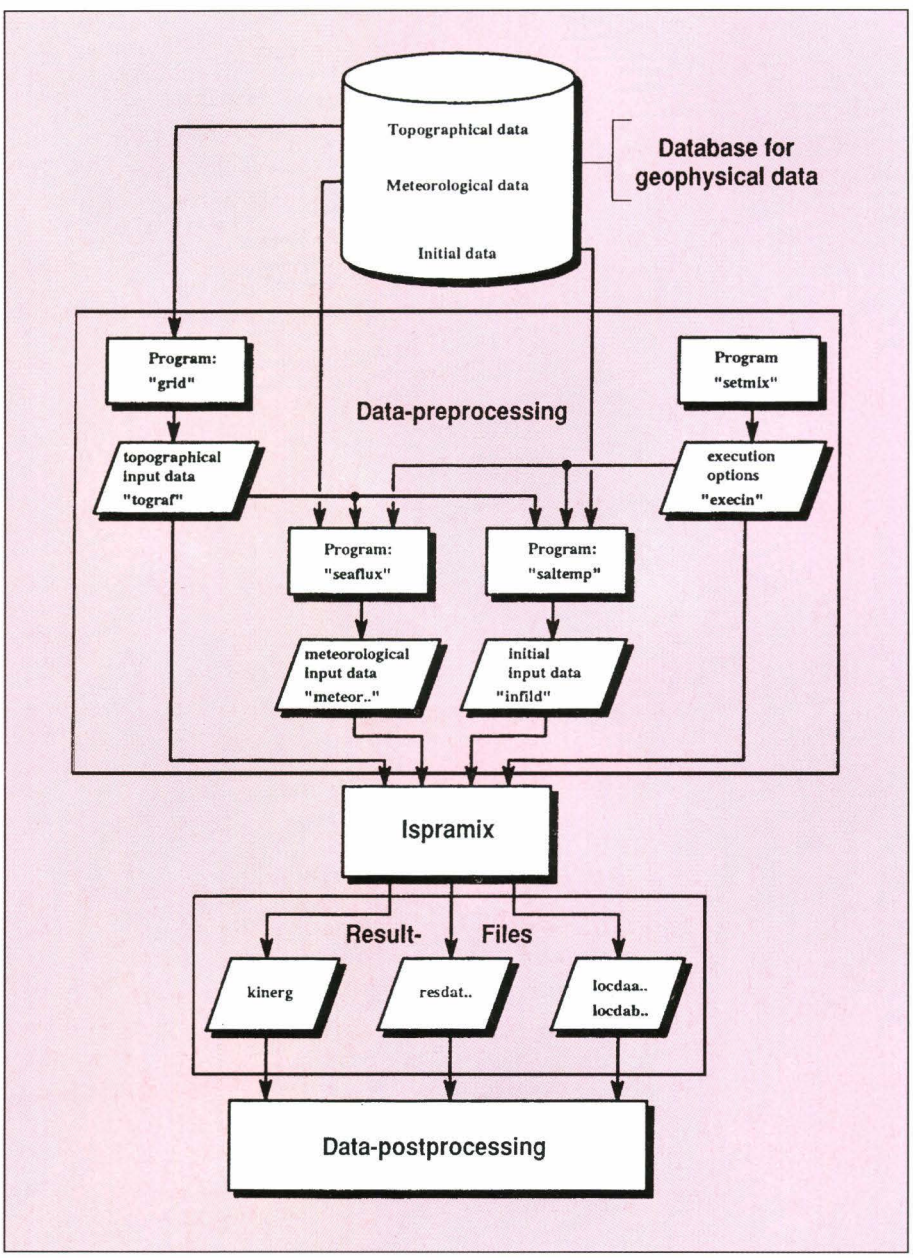

Fig. 5.21 Data-flow-chart of the ISPRAMIX model system

The following activities have been defined via inter-institutes contracts with the partner institutes:

- Modelling related to marine processes and remote sensed data assimilation (with IRSA);
- Modelling of marine water quality (with EI);
- Modelling of the global 3D aerosol dynamics in the atmospheric sulphur cycle (with EI).

The first two activities make use of the model system Ispramix [44].

Extension of the model system "Ispramix"

Fig. 5.21 shows the data-flow-chart of our model system. Starting

from a database comprising topographical data, meteorological data for given time periods, and climatological temperature and salinity fields needed as initial conditions, a number of subsequent preprocessors represent the interface providing the necessary input data for the model ISPRAMIX. Main emphasis during this year was given to the preprocessors GRID and SEAFLUX. Specifying the minimum and maximum longitude and latitude for the considered window, the preprocessor GRID [42] helps, in dialog with the user, to define the space discretisation grid and all related parameters. The resulting data file (TOGRAF) serves as input for ISPRAMIX as well as for the other preprocessors. Based on the stored meteorological data furnished by ECMWF (European Center for Medium Range Weather Forecasts) in Reading (UK), the preprocessor SEAFLUX [43] furnishes the meteorological driving forces (surface boundary conditions) for ISPRAMIX.

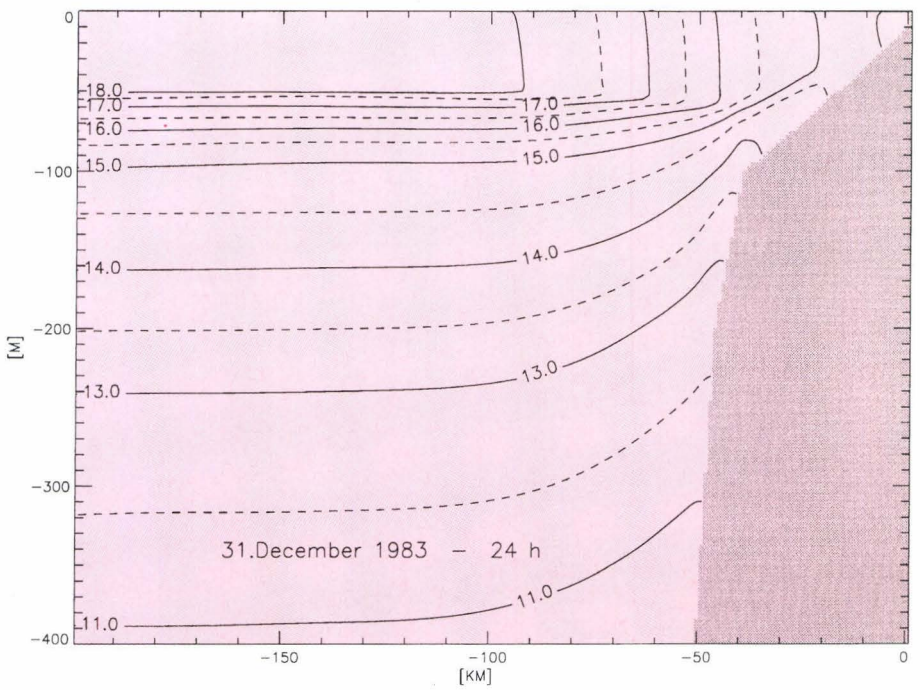

Fig. 5.22 Temperature-isolines (in °C) in wind-driven upwelling (near Cap Blanc, West-African coast)

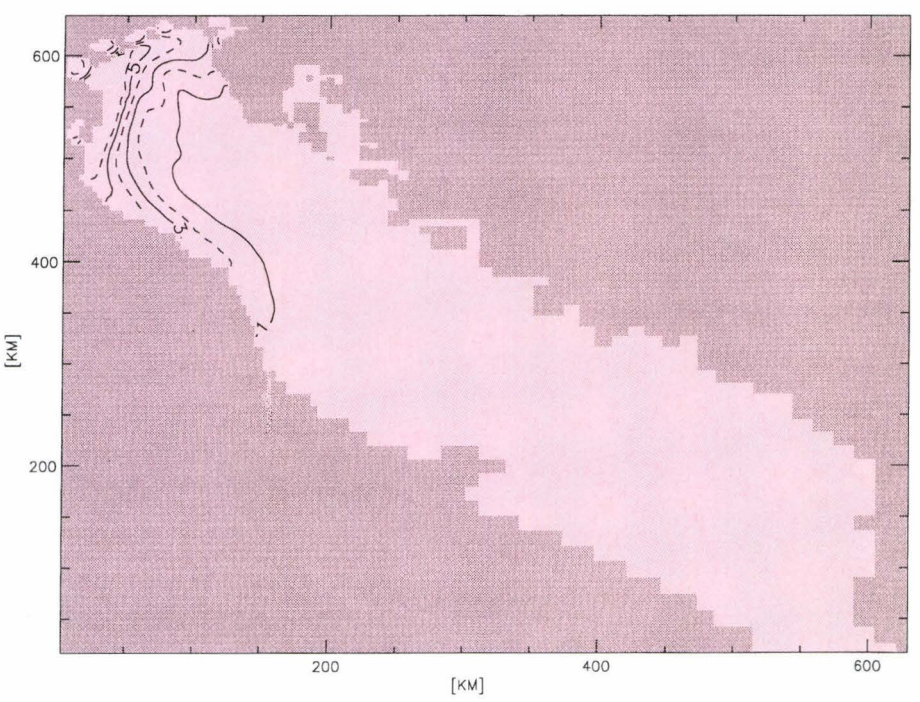

Fig. 5.23 Phytoplancton blooming due to the outflow of nutrients via the Po river

Modelling related to marine processes and remote sensed data assimilation

The model ISPRAMIX was applied to typical two-dimensional cross-sections in the Atlantic, the results of which are described in [44]. *Fig. 5.22* shows a computed temperature distribution represented as isolines in the offshore-depth-plane near the Cap Blanc (Mauritania) at the West-African coast. The trade winds cause upwelling of the cold deep water, a fact which is well traced by the isoline behaviour near the coast. The wind induced turbulence leads to a thorough mixed

upper layer traced by the vertical isolines near the sea surface.

Modelling of marine water quality

The model ISPRAMIX (supplemented by a suitable biological model) has been applied to the Adriatic sea with the intent to demonstrate the feasibility of such simulations of biological dynamics. Since the area of main interest is the Northern Adriatic, a relatively fine horizontal grid was chosen (3,2 km x 3,2 km), increasing southward the grid size to a maximum of about 16km. The total number of grid points is about 500 000, of which however only 70 000 are "wet", i.e. computational points. On our Alpha-DEC workstation the CPU time is less than 1% of the simulated time. *Fig. 5.23* shows isolines of phytoplancton. Nutrients are flowing in the Adriatic via the Po river, and - under typical weather conditions at the beginning of the year - phytoplancton blooming occurs mainly along the coast of Emilia Romagna.

Modelling of the global 3D aerosol dynamics in the atmospheric sulphur cycle

Main attention was focused on the aerosol model AERO2 of EI with the intention to reduce the required computer time. AERO2 has been developed as box-model without any requirement for computational efficiency, using a fourth order Runge-Kutta numerical procedure. For applying AERO2 in combination with a global transport model, the CPU time has to be drastically reduced with respect to that of the original model. *Fig. 5.24* shows a comparison of computations with the original model and of computations using new algorithms. It is shown that for the case considered, and keeping the number of particle size classes constant, the computations are speeded up by a factor of more than 20, without losing precision. Further CPU time may be gained by reducing the number of six classes, provided that the physicists accept the corresponding deviation of the results from those obtained for the reference case. The new algorithm for the aerosol model is described in [45].

References

[1] ZALDIVAR J.M., HERNANDEZ H., BARCONS C. - Development of a Numerical Simulator for a Reaction Calorimeter, FISIM, RC1 version, JRC Ispra, Technical Note I.90.109, 1990

[2] HERNANDEZ H., ZALDIVAR J.M., BARCONS C. - Development of a mathematical model and a numerical simulator for the analysis and optimisation of batch reactors, Computer Chem. Engng. 17S, pp 45-50, 1993

[3] ZALDIVAR J.M., HERNANDEZ H., NIEMAN H., MOLGA E., BASSANI C. - The FIRES project: experimental study of thermal runaway due to agitation problems during toluene nitration, J. Loss Prev. Process Ind., 6, pp 319-326, 1993

[4] NIEMAN H., ZALDIVAR J.M., HERNANDEZ H., BASSANI C. The JRC FIRES project for investigations on runaway reactions, Proceedings of the 11th International Congress of Chemical Engineering, Chemical Equipment Design and Automation, Praha (Czech Republic), 1993

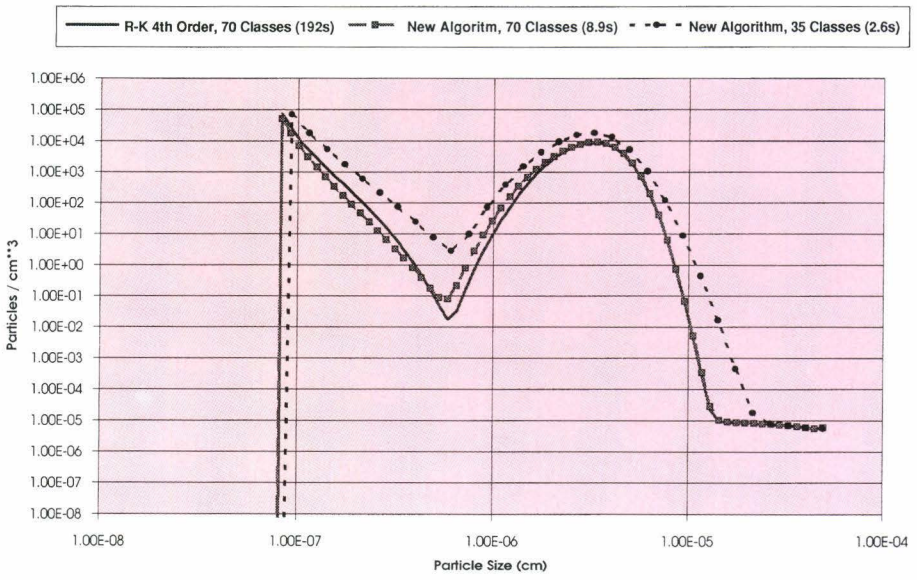

Fig. 5.24 Comparison of aerosol particle size distributions computed with different algorithms

[5] ZALDIVAR J.M., HERNANDEZ H., MOLGA E., ALOS M.A. Mathematical Modelling and Simulation of Aromatic Nitrations by Mixed Acid in discontinuous reactors, Part I: Slow Liquid-Liquid Reactions, JRC Ispra, Technical Note I.93.162, 1993

[6] ZALDIVAR J.M., BARCONS C., HERNANDEZ H., MOLGA E. Safety Aspects of Aromatic Nitrations by mixed acid in discontinuous reactors, Proceedings of the 11th International Congress of Chemical Engineering, Chemical Equipment Design and Automation, Praha (Czech Republic), 1993

[7] MOUSSAS C., BITSORIS G. - Generalized One-Step-Ahead Control subject to Input Constraints: A linear time-varying system approach, accepted for publication in Control-Theory and Advanced Technology, (Mita Press), 1993

[8] MOUSSAS C., BITSORIS G. - Adaptive Constrained Control subject to both Input-Amplitude and Input-Velocity Constraints, IEEE Systems, Man and Cybernetics Conference, 17-20 October, Touquet (F), 1993

[9] MOLGA E., BARCONS C., ZALDIVAR J.M. - Mononitration of Toluene and Quantitative Determination of the Isomer Distribution by Gas Chromatography, Afinidad, 50, pp 15-20, 1993

[10] ZALDIVAR J.M., HERNANDEZ H., MOLGA E., GALVAN I.M., PANETSOS F. - The use of neural networks for the identification of complex reactions, Procc. of ESCAPE-3, Graz (A), pp 42-46, 1993

[11] STROZZI F., ZALDIVAR J.M. - A General method for assessing the thermal stability of batch chemical reactors by sensitivity calculation based on Lyapunov exponents, requested to be published in Chem. Engng. Science

[12] MORRIS S.D. - The new venting facilities at JRC Ispra: DRACULA and COLUMBUS, European DIERS Users Grup Meeting, Lyon, France, 4/5 May 1993

[13] MORRIS S.D. - The DRACULA venting facility: design of the relief system, US DIERS Users Group Meeting, Albuquerque, USA, 11/13 May 1993

[14] MORRIS S.D. - A venting test with a high-viscosity foamy fluid, European DIERS Users Group Meeting, Lyon, France, 4/5 May 1993

[15] MORRIS S.D. - Maximum void fraction in vessel: some comments and further developments, European DIERS Users Group Meeting, Lyon, France, 4/5 May 1993

[16] MORRIS S.D. - Luviskol Round-Robin problem, US DIERS Users Group Meeting, Albuquerque, USA, 11/13 May 1993

[17] MORRIS S.D., KUHN H.G. - Some simplified design equations for gas vent sizing, US DIERS Users Group Meeting, Albuquerque, USA, 11/13 May 1993

[18] MORRIS S.D. - 4P6 safety valve Round-Robin problem, US DIERS Users Group Meeting, Albuquerque, USA, 11/13 May 1993

[19] MORRIS S.D. - The bubbly flow model, European DIERS Users Group Meeting, The Hague, Netherlands, 14/15 October 1993

[20] DUFFIELD J.S., FRIZ G., NIJSING R. - The venting of peroxide solutions, 29th European Two-Phase Flow Group Meeting, Stockholm, May 1992

[21] DUFFIELD J.S., FRIZ G., NIJSING R. - Critical flow in a chemically reacting two-phase multicomponent mixture; Accepted: International Journal of Mutliphase Flow, 1993

[22] DUFFIELD J.S., NIJSING R. - Computer simulations describing the emergeny pressure relief of hybrid and gassy systems, to be presented at HAZARDS X11, European Advances in Process Safety, Manchester, April 1994

[23] STÄDTKE H., HOLTBECKER R. - A Hyperbolic Model for Inhomogeneous Two-phase Flow, 29th Meeting of the European Two-phase Flow Group, Stockholm, June 1-3, 1992

[24] STÄDTKE H. - On the Hyperbolic Nature of Two-phase Flow Equations, to be published as EUR Report

[25] HOLTBECKER R. - Untersuchung Physikalischer und Numerischer Modelle für Inhomogene Zweiphasenströmungen, University of Stuttgart, PhD thesis, 1993

[26] STÄDTKE H., HOLTBECKER R. - A Hyperbolic Model for Inhomogeneous Two-phase Flow, International Conference on Multiphase Flows, '91 Tsukuba, Sept. 24-27, 1991, University of Tsukuba, Japan

[27] STÄDTKE H., WORTH B. - Numerical Simulation of Two-phase Flow based on Hyperbolic Flow Equations, Sixth International Topical Meeting on Nuclear Thermal Hydraulics, NURETH-6, Grenoble, October 5-8, 1993

[28] WÜRTZ J. - A Transient One-Dimensional Shallow Layer Model for Dispersion of Denser-than-Air Gases in Obstructed Terrains under Non-Isothermal Conditions, EUR 15343 EN, 1993

[29] WÜRTZ J. - Shallow Layer Model Simulations of Dispersion of Propane Released with and without Momentum in an Obstructed Terrain; Submitted for publication in Journal of Hazardous Materials

[30] WÜRTZ J., BARTZIS J.G., VENETSANOS A., ANDRONOPOULOS S., STATHARAS J.C., NIJSING R. - A Dense Vapour Dispersion Code Package for Applications in the Chemical and Process Industry, To be presented at the symposium on Heat and Mass Transfer in Chemical Process Industry Accidents, September 15-16, 1994, Rome

[31] ANDRONOPOULOS S., BARTZIS J.G., WÜRTZ J., ASIMAKOPOULOS D. - Simulation of the Thorney Island Dense Gas Trial No.8, Using the Code ADREA-HF, Process Safety Progress Vol. 12, No.1, January 1993

[32] STATHARAS J.C., BARTZIS J.G., VENETSANOS A., WÜRTZ J. - Prediction of Ammonia Releases Using the ADREA-HF Code, Process Safety Progress, Vol. 12, No. 2, April 1993

[33] ANDRONOPOULOS S., BARTZIS J.G., WÜRTZ J., ASIMAKOPOULOS D. - Modelling the effects of obstacles on the dispersion of denser-than-air gases; Accepted for publication in Journal of Hazardous Materials

[34] CARISSIMO B., ANDRONOPOULOS S., BARTZIS J.G., WÜRTZ J. - Intercomparison on Heavy Gas Dispersion Between the Three Dimensional Models MERCURE and ADREA, Part II: Instantaneous Release with a Semi Circular Wall, EdF Report HE-33/93-05, 1993

[35] RUEL F., SORIA A. - A Semi-Implicit Solution of the Multicomponent Euler Equations in Subsonic Regime, JRC-Ispra, Technical Note I.93.76, June 1993

[36] DONEA J., RUEL F., SORIA A. - On the Numerical Simulation of Hyperbolic Problems, Deuxième Congrès Methods Numériques en Ingeniérie, La Coruña, Espagne, 7 - 11 June, 1993

[37] HULD T. - Numerical Simulation of Reacting Gas Flows: Explicit and Implicit Solvers for Diffusive Processes, JRC-Ispra, Technical Note I.93.104, July 1993

[38] PEGON P., SORIA A., LAVAL H. - A Review of Finite Element Solvers for the Compressible Navier-Stokes Equation, EUR 14987 EN, 1993

[39] SORIA A., PEGON P. - Semi-Implicit Conservative Upwind Schemes for Transient Compressible Blows, EUR 14986 EN, 1993

[40] PETER G. - DIGLIB: A Device Independent Graphics Library, JRC-Ispra, Technical Note I.93.102, July 1993

[41] PETER G. - A System for automatic, dynamic, fully reversible grid adaption, JRC-Ispra, to be issued as Technical Note

[42] CARUSO S. - GRID: An Ispramix processor which allows a quick and easy preparation of a tridimensional topographic discretisation model, to be issued as Technical Note

[43] DEVOS J. - The fluxes at the sea-atmosphere interface: a pre-processor for Ispramix, to be issued as Technical Note

[44] EIFLER W., SCHRIMPF W. - A model for computing the hydrodynamics in combined shelf/deep sea areas and its application to typical coastal upwelling (1993), submitted to J. Applied Mathematical Modelling

[45] SKOULOUDIS A.N., EIFLER W. - Fast algorithms for simulating the time evolution of the size spectrum characterizing aerodisparse particles (1993), to be issued as Technical Note

[46] KRÜGER G.J., HAUPT J., WEISS R. - A nuclear magnetic resonance method for the investigation of two-phase flow - Measuring techniques in gas-liquid two-phase flows, IUTAM Symposium Nancy, France, 1983, pp. 435-454, DELHAYE J.M. COGNET G., Eds. Springer, Berlin Heidelberg, 1984

[47] KRÜGER G.J., BIRKE A. - Nuclear Magnetic Resonance (NMR) two-phase flow measurements, submitted for publication

1.6 REFERENCE METHODS FOR THE EVALUATION OF STRUCTURAL RELIABILITY

The new reaction-wall facility ELSA of the Safety Technology Institute is being used for prenormative research in support of Eurocode N° 8 (EC8), the provisional European standard for the design of civil engineering structures in seismic areas. This activity has been set up in close collaboration with the Directorate General III of the European Commission and the EC8 expert group of CEN.

The research is performed jointly with the European Association of Structural Mechanics Laboratories (see section 3.1) and a number of research organisations in the Member States grouped together in the scientific network PREC8 under the Human Capital and Mobility programme (see section 1.8). Progress in the execution of the above integrated programme is described in the following sections which cover both the experimental research and the computational mechanics activities. Also included are new developments in the area of fast transient dynamics.

1.6.1 LARGE-SCALE PSEUDO-DYNAMIC (PSD) TESTS

During the year 1993 the experimental sector in charge of the ELSA reaction-wall laboratory has conducted a series of PSD tests on a three-storey steel frame and a four-storey reinforced concrete frame. In parallel, preparatory work has been performed to test large-scale models of irregular bridges using the so-called substructured PSD technique.

Pseudo-dynamic tests on a full-scale three-storey steel moment resisting frame

A full-scale three-storey one-bay steel frame has been constructed and tested pseudo-dynamically in the European Laboratory for Structural Assessment (ELSA) of the Safety Technology Institute. The structure has welded beam-to-column connections and shear panel zones, without flange continuity plates in the joints. The frame joints and connections were capable of resisting the girder plastic moment.

The objectives of this research were on the one hand to study the seismic behaviour of a realistic steel frame structure, designed according to the relevant Eurocodes for steel construction, and on the other hand to compare the experimental results with the analytical predictions from the available computer models and subsequently to identify up-dating needs. In addition, these tests have been used to commission the ELSA pseudo-dynamic testing set-up (see STI annual report 1992).

The structure constructed in the ELSA laboratory consisted of two steel frames placed parallel to each other and connected with reinforced concrete slabs. The loads were introduced at the floor center-line. At each storey level two hydraulic actuators were placed in order to introduce the loading on the frame. All tests were displacement controlled using the horizontal displacement of the concrete slab at each storey level, derived from the dynamic equilibrium equation, as the control parameter.

Pseudo-dynamic tests on the steel frame were executed using an explicit time integration scheme. The steel frame has been subjected to the Kalamata-Greece earthquake ground motion. Additionally, one artificially generated accelerogram has been used in the tests, having the same characteristics (response spectrum) as considered in the steel frame's design. For the first tests, the earthquake ground motions, both Kalamata and Artificial, have been scaled down to a level insufficient to cause yielding in the steel frame structure. The earthquake intensity has been progressively increased until yielding of the steel skeleton has been identified. Subsequently, the intensity of the ground motions has been increased, in order to introduce yielding in the structure. The frame's inertia loads and associated floor horizontal displacements, as well as the internal force/moment distribution in the girders and columns has been continuously recorded. Additionally, the beam-to-column connection and shear panel rotations were recorded. These data were used in order to verify the design concept from Eurocode N° 8 (strong column-weak beam).

Computer model for the three-storey one-bay steel frame and comparison with pseudo-dynamic test results

The numerical simulations of the steel frame seismic behaviour were performed using the DRAIN-2DX computer code [4]. Herein, the frame girders and columns were simulated using "beam-column elements" where plastic hinges were allowed to appear at the element-ends [1,2,6], following a bilinear hysteretic rule. These elements were capable of capturing Moment-Axial Force interaction. The beam-to-column welded connections and shear panel zones were modelled using equivalent moment-rotation springs (*Fig. 6.1*). These springs had bilinear hysteretic behaviour. The stiffness properties of these springs were selected using an analytical method developed in [2,6].

The "beam-column elements" and moment-rotation springs were assembled together to form the steel frame computer model (*Fig. 6.1*). To perform dynamic time-history analysis to capture the frame non-linear seismic behaviour, the structure masses were assumed to be lumped at the floor levels. The steel frame computer model was subjected to the Kalamata and Artificial seismic base excitations.

A comparison of the numerical results with the PSD-experimental behaviour showed that the computer model captured accurately the time-histories of the floor inertia loads and horizontal displacements (*Fig. 6.1*). On the other hand, the distribution of bending moments, axial forces in the girders and columns as obtained from the computer model, were in agreement with the experimental data measured [6]. Correspondingly, the hysteretic behaviour of the beam-to-column joints and connections was captured accurately by the computer model (*Fig. 6.1*).

The results from the experimental and analytical studies have shown that beam-to-column joint and connection flexibility should be considered in the frame design using Eurocodes 8 and 3. Additionally, it is proposed to size the joint shear panel zone (column web in the joint) on an Allowable Stress Design basis [1,2,3,6]. Actual Eurocode 8 design provisions

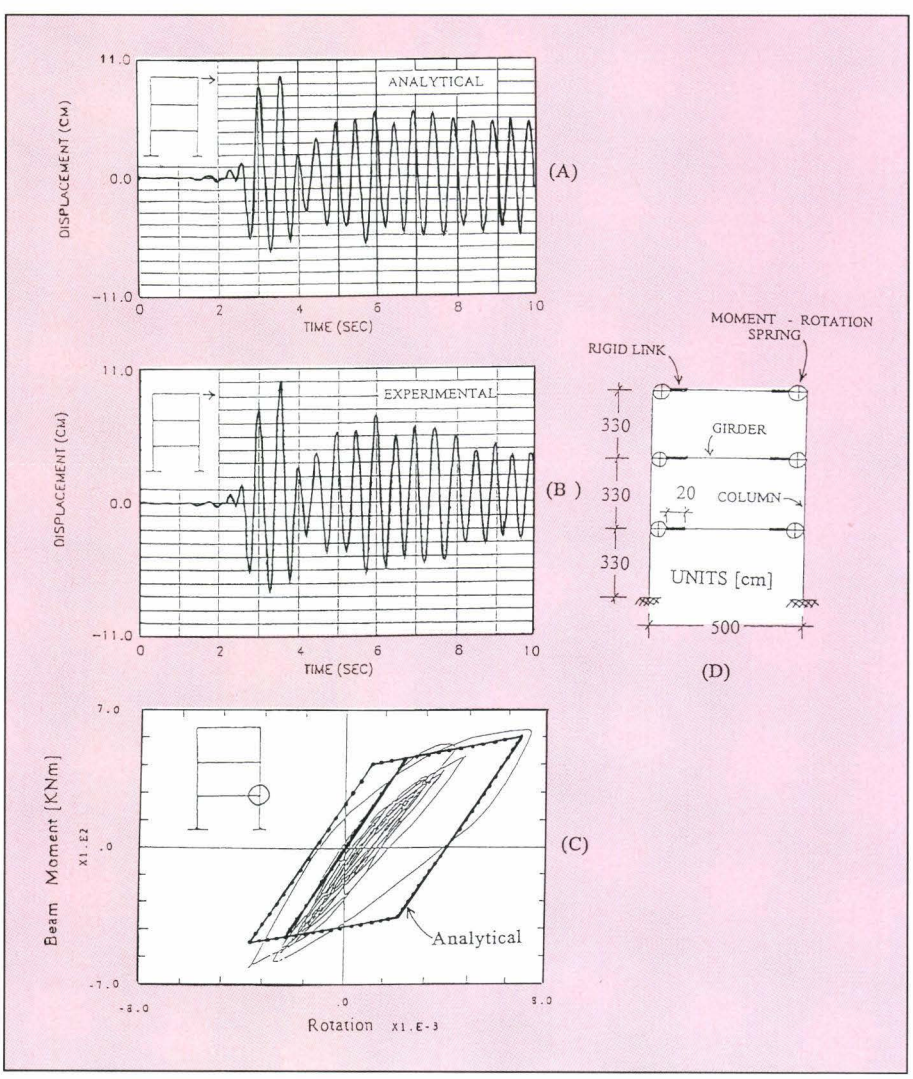

Fig. 6.1 Steel Frame Seismic Response, subjected to Kalamata Earthquake Intensity 1.5
A) Response of third floor horizontal displacement - experimental result
B) Reponse of third floor horizontal displacement - analytical result
C) Moment rotation seismic behaviour of first floor joint
D) Steel frame computer model

for the beam-to-column joints recommend a Capacity Design for that zone. During all experiments performed, it was identified that following Eurocode 8 design, the frame joints become plastic under seismic loads and hence, the strong-column/weak girder design concept as proposed in Eurocode 8 cannot be fulfilled in the present case [5,6].

Pseudo-dynamic testing of a four-storey reinforced concrete frame

The testing campaign is being performed in the framework of the European Association of Structural Mechanics Laboratories.This research represents the continuation of a previous activity of the Association on the seismic design of reinforced concrete structures according to Eurocode 8. During the first phase, the scope was to check the applicability of the code to real structures, to enable a comparison of the computer codes used in seismic analysis in different countries and to identify the research needs and priorities to make progress on the solution of specific problems still open in seismic design. The purpose of the current phase is the definition of damage indicators and failure criteria. This is based on a testing activity which culminates in the full-scale pseudodynamic test at ELSA.

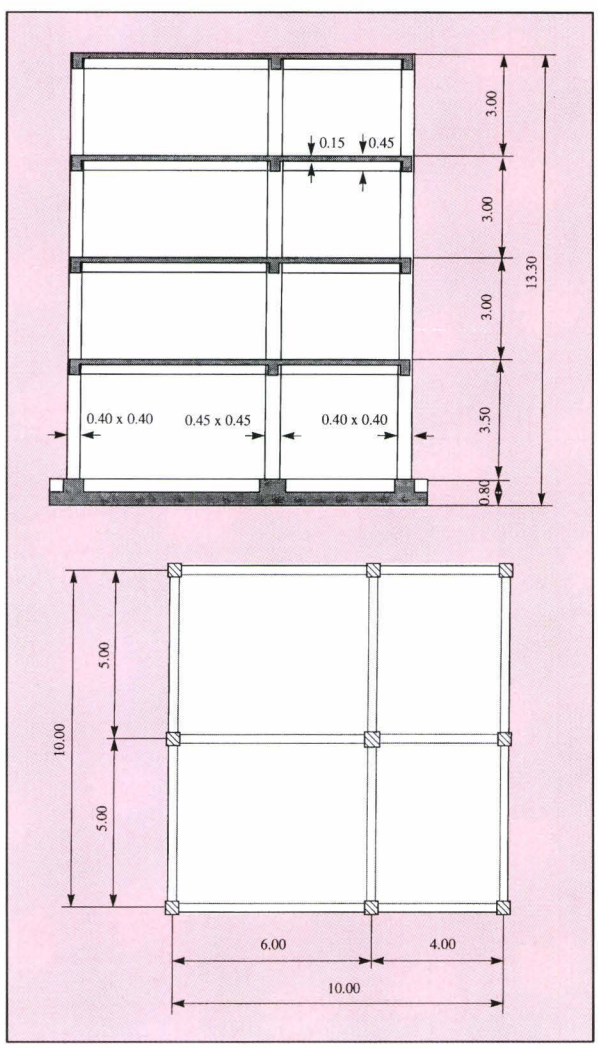

Fig. 6.2 Lay-out of 4-storey reinforced concrete framed structure

The specimen building is a four-storey framed structure (see ***Fig. 6.2***), with plan dimensions of approximately 10 x 10 m and a total height of 12.5 m. The plan is symmetrical with respect to the direction of testing, but eccentric in the orthogonal direction. The building has been designed for typical live loads and for severe seismic actions (ground acceleration = 0.3 g, medium soil conditions). The design actions have been defined as for "Ductility Class High" in the Eurocode 8, thus significant inelastic deformation is expected during the test.

The materials have been defined as ordinary C25/30 concrete, whilst for the reinforcing bars Tempcore B500 steel has been selected. This steel, originally not included in Eurocode 8 provisions, is becoming dominant in some European countries, so the importance to assess the adequacy of this material for earthquake resistant constructions has been recognized.

Construction of the specimen

The design of the test structure has included all the necessary provisions and checks for the transportation of the specimen and the introduction of loads. The specimen has in fact been constructed in the working area outside the laboratory (***Fig. 6.3***) and has been raised from the floor by hydraulic jacks and moved inside by means of plastic tube rollers.

These transportation procedures had to be studied in great detail due to the weight of the specimen (more than 400 tons), however, this has greatly reduced the construction problems and has allowed other tests to be conducted during the construction phase. After the major test, it will be possible to move the specimen back to the working area for repair.

A grid of 800 mm deep foundation beams, with a 400 mm slab has been designed to ensure the spec-

imen could have been raised and transported without any structural damage to the upper part. The specimen has been raised for 150 mm by means of 8 pairs of hydraulic jacks, connected in such a way to send to all of them the same oil flow. A special hydraulic apparatus has been designed for this purpose, in order to avoid the formation of cracks during the procedure. Great care has been placed on the design of the rollers: these consist of high density polythene tubes connected by a steel frame ("ladder"). The tube material is stressed at a level which allows any subsequent deformation due to irregularities of the floor to be accommodated by plastic deformation of the rollers. Extensive numerical simulations have been performed to seek the most efficient layout. The complete procedure of transportation and positioning (***Fig. 6.4***) of the specimen took two days, and the system proved to be very effective. During the lifting and transportation phase, the relative displacements of the base of the columns were continuously monitored. The maximum relative displacement was found to be less than 0.5 mm, i.e. that the integrity of the specimen has been assured.

Fig. 6.3 Construction of R/C framed structure in the working area outside the ELSA Laboratory

Load introduction and instrumentation

The loads are applied by pairs of hydraulic actuators laterally attached at each floor slab (***Fig. 6.5***). One additional actuator attached to the third floor controls

Fig. 6.4 Transportation of R/C framed structure from the construction area to the reaction-wall

Fig. 6.5 Hydraulic actuators and load introduction system into floor slabs of R/C frame

the out-of-plane movement of the structure, to prevent secondary sway deformations. The storey displacements are measured with respect to two steel reference frames placed in front of the specimen.

Measurements include, besides the floor displacements which are controlled by the pseudodynamic algorithm, the acquisition of the rotations of all the beam and column base joints of the interior frame and of one exterior frame. Pairs of displacement transducers have been placed at each joint at a distance of one element height. At the second floor, and at the base of the columns, another pair of displacement transducers has been placed to achieve an experimental assessment of the curvature distribution in plastic hinge regions. A typical arrangement of transducers is shown in ***Fig. 6.6***. Additional instrumentation has been placed to measure the collaborating slab width and the amount of rotation due to the slippage of the bars in the joint.

Concrete blocks have been placed on the floor slabs to account for the weight of the non-structural elements (partitions and floor finishing) and for the factorized live loads. This was not done to reproduce the inertial properties, since in the pseudo-dynamic test method the masses are included in the numerical algorithm, but to reproduce the stress levels in the members of the structure.

Fig. 6.6 Typical arrangement of transducers to measure curvature in plastic hinge regions

Tests performed so far

The preliminary testing activity included dynamic snap-back tests, pseudo-dynamic reproductions of the snap-back tests and direct stiffness measurements. The importance of the dynamic low level tests is twofold:

- they allow the dynamic characterization of the specimen, by measuring its main initial frequencies and damping,
- they provide a reference signal for calibrating the pseudo-dynamic algorithm and its implementation before the main non-linear tests.

The dynamic snap-back tests were performed by pulling the structure against the reaction-wall by means of a steel bar. Two different tests were performed, with the steel bar placed either at the third and fourth storey, to capture the contribution of the different vibration modes. The steel bars were calibrated in such a way that they would have broken for a load of 150 kN at the third storey and of 85 kN at the fourth. These values were supposed not to lead to significant cracking inside the structure, a requirement which was necessary to compare the behaviour with the pseudo-dynamic simulation.

After mounting the actuators, the snap-back tests were reproduced pseudo-dynamically. The displacements corresponding to the dynamic and pseudo-dynamic tests are depicted in ***Fig. 6.7***. The comparison is considered to be quite accurate, the differences being due to a slightly different damping value and to the unavoidable uncertainties in the evaluation of the storey masses.

The direct stiffness matrix measurement has been obtained by imposing prescribed structural displacements at each storey, constraining the remaining ones, and measuring the corresponding restoring forces. Again, the displacements to be imposed were selected in such a way to avoid cracking inside the structure. The procedure has been made automatic, so that the prescribed displacements have been imposed to the four storeys in sequence. The measured stiffness matrix is reported in ***Table 6.1***. The measurement of the initial stiffness matrix is important in assessing the adequacy of the assumptions adopted in modelling the structure. In ***Table 6.2*** the frequencies obtained with the three different experimental techniques are compared.

The testing sequence includes the pseudo-dynamic simulation of the effect of an artificial earthquake, scaled to different values. The accelerogram has been generated to approximate the response spectrum given in Eurocode 8, starting from the real 1976 Friuli Earthquake. The accelerogram is shown in ***Fig. 6.8***, and in ***Fig. 6.9*** the corresponding elastic response spectrum is compared with the Eurocode 8 spectrum assumed in the R/C frame design. The nominal base acceleration is 0.3 g.

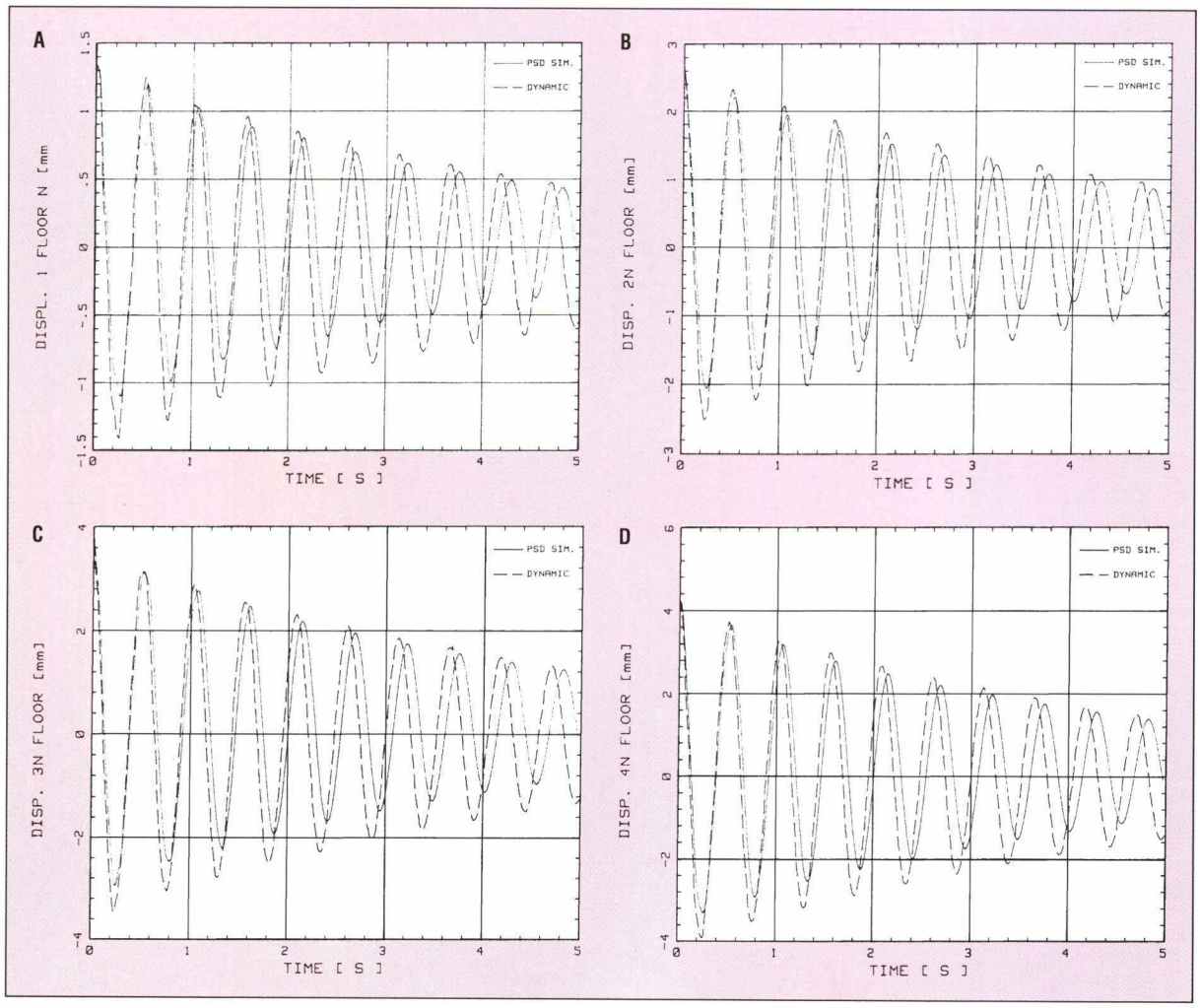

Fig. 6.7 Comparison between floor displacements obtained in a dynamic snap-back test and its pseudo-dynamic reproduction

Table 6.1 Average measured stiffness matrix (kN/m)

0.28328×10^6	-0.16648×10^6	0.22225×10^5	-0.16875×10^4
-0.16648×10^6	0.25920×10^6	-0.13124×10^6	0.14290×10^5
0.22225×10^5	-0.13124×10^6	0.21257×10^6	-0.99450×10^5
-0.16875×10^4	0.14290×10^5	0.99450×10^5	0.86110×10^5

Table 6.2 Measured frequencies log.

Mode	Dynamic snap-back	PSD snap-back	Stiffness measurement
1	1.90	1.85	1.78
2	5.95	5.54	5.12
3	10.4	9.94	8.65
4	16.3	13.5	12.0

The storey displacements obtained in the pseudo-dynamic test, corresponding to the effect of the earthquake scaled to 40%, are depicted in ***Fig. 6.10***. The results of this test are of great importance for the final calibration of the apparatus, but they also represent a useful piece of information for the behaviour of the structure up to the yield level. The scatter in the numerical predictions of the results was in fact much higher for this relatively low-level test than for the final 1.5 scale factor test.

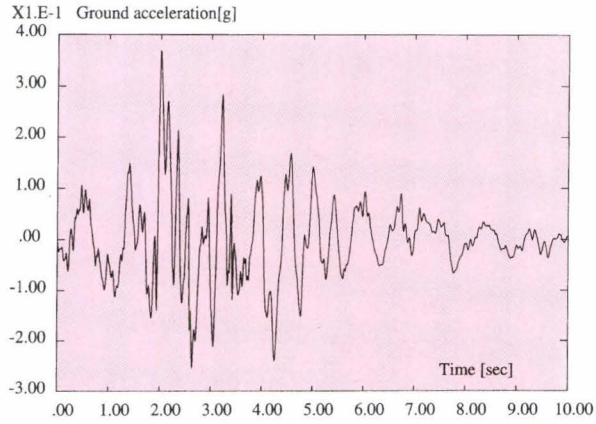

Fig. 6.8 Accelerogram from the 1976 Friuli Earthquake

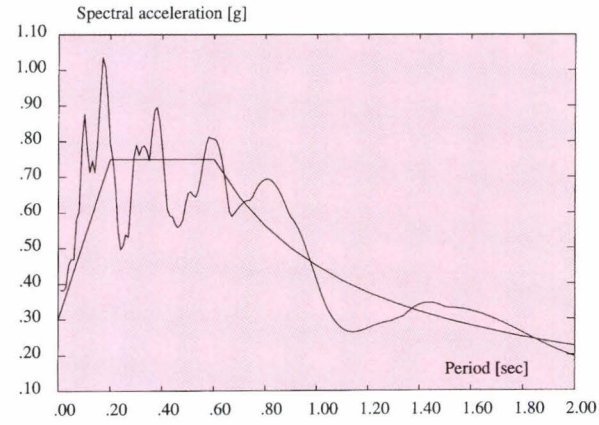

Fig. 6.9 Comparison between elastic response spectrum corresponding to the Friuli Earthquake and the Eurocode 8 spectrum assumed in the R/C frame design

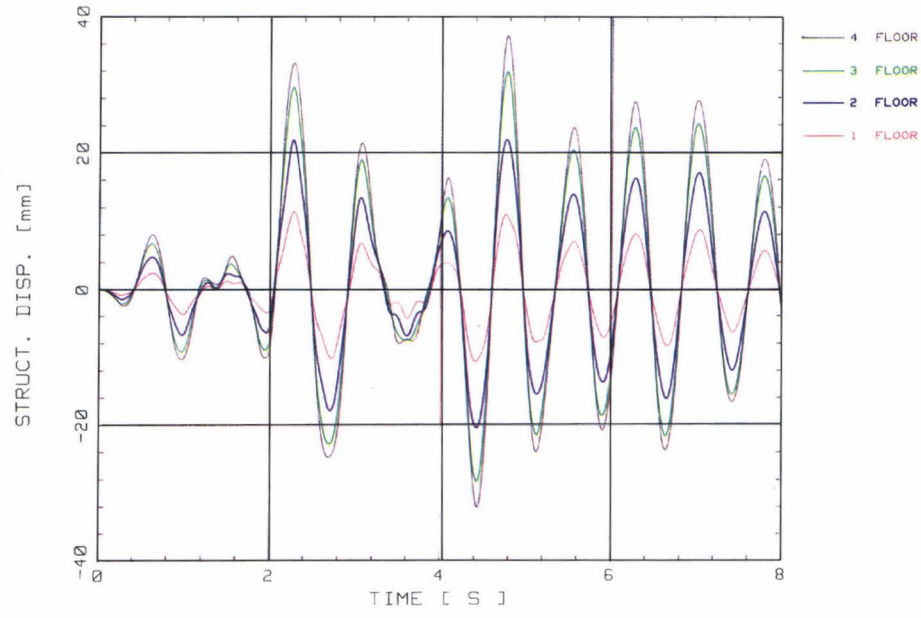

Fig. 6.10 Storey displacements obtained in the PSD test corresponding to the Friuli Earthquake scaled to 40%

The test for the reference earthquake scaled to 1.5 has been conducted for the first few cycles. The experiment had to be interrupted due to an unexpected vibration of the system. The reason for this problem has been identified in the sensitivity of the reference frames to environmental vibrations. The frequency of the reference frames is in fact close to the main frequency of the building, so that small amplitude vibrations can be excited, particularly at low values of the restoring forces. The members of the reference frames are being filled with sand. This will shift the fundamental frequency of the frames, and moreover will increase the damping of the reference structures. The need for more redundant control checks and for quick re-starting procedures has also been recognized. These features are being incorporated in the control algorithm.

Lifting and transportation of the four-storey reinforced concrete building

The four-storey reinforced-concrete frame was built in the area outside of the laboratory in front of the large entrance door. It was therefore necessary to move the structure to the testing area in front of the Reaction-Wall. This was obtained by means of the following actions:

Lifting of the structure

To lift the structure, use was made of a system of eight independent pressurized circuits acting on sixteen hydraulic actuators. The total weight of about 420 tons has been distributed in such a way to minimize the stresses and the global deformation of the structure. ***Fig. 6.11*** shows the eight circuits and the position of the actuators and ***Table 6.3*** lists the forces acting in each circuit.

Entrance into the laboratory

To move the structure into the laboratory it was necessary to design a transportation system

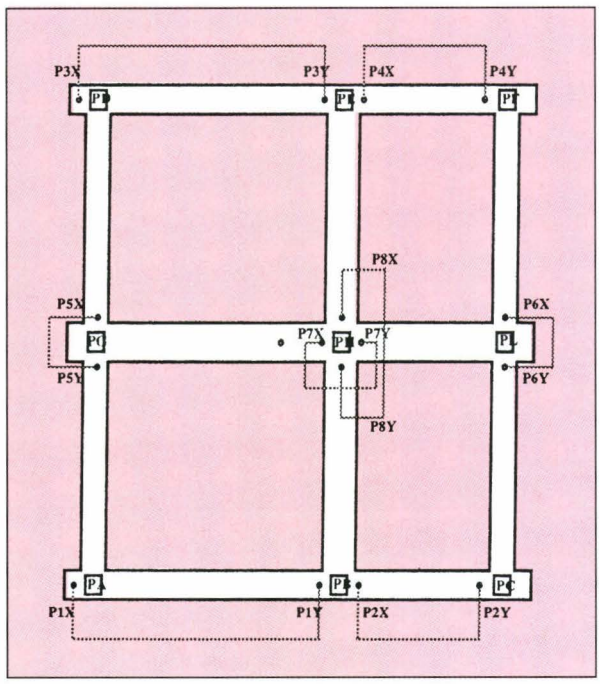

Fig. 6.11 Hydraulic circuits and actuators for transportation of 420t R/C frame

able to distribute the reactions to the building weight in such a way as to avoid damage to the structure itself. The transportation system designed in-house consists of four frames with rolling tubes placed under the base of the building; the quantity. The distribution and the size of the rolling tubes have been assessed after a parametric study and the asymmetry of the structure has been taken into account.

Positioning in front of the reaction wall

The positioning of the structure in front of the reaction wall has been obtained by means of a specific transportation system. The building was symmetric for this action, so that the frames and the rolling tubes were also symmetrically disposed. The transportation has been realized by the cyclic repetition of the following actions:

Pulling of the building by means of hydraulic actuators for a length of one meter, lifting of the structure, repositioning of the frames, lay down of the structure on the frames and pulling of the building again. The two movements related to the entrance of the structure into the laboratory and its positioning in front of the reaction wall are schematically shown in ***Fig. 6.12***.

Table 6.3 Lifting forces

Circuits	Force for Actuator (8 circuits)	
	Force	
	[kN]	[ton]
P1X=P1Y	267.7	27.3
P2X=P2Y	227.8	23.2
P3X=P3Y	267.7	27.3
P4X=P4Y	227.8	23.2
P5X=P5Y	307.9	31.4
P6X=P6Y	215.8	22.0
P7X=P7Y	279.3	28.5
P8X=P8Y	268.3	27.3
P17	–	–
total	2 * 2062.3	~ 420.5

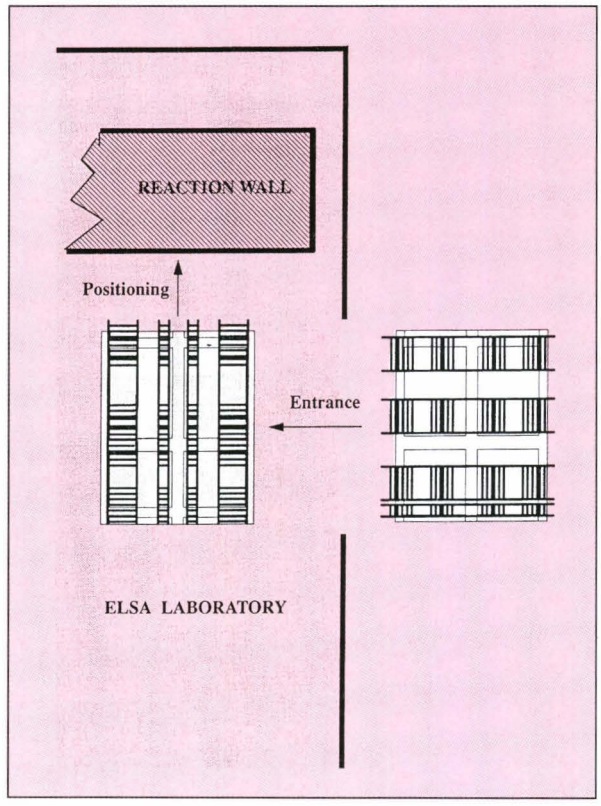

Fig. 6.12 Schematic of the transportation and positioning of the R/C structure

Experimental files management system and data bases

The experimental files of the ELSA laboratory are based on a standard named EEDF (ELSA Experimental Data Files) not compatible with the experimental files from other laboratories of the Safety Technology Institute and with the stress analysis computer codes. In the Institute there exists a system of Data Bases whose standard is named EDF (Experimental Data Files). This standard has been adopted to store in Data Bases the most interesting data or results for or from the laboratory. A computer program named WDB (Working on Data Bases) has been developed both for the handling of the binary ELSA files (EEDF) and to interface the Data Bases based on the EDF standard.

The stress analysis computer programs of the Applied Mechanics Unit have been interfaced with the Data Bases so that data and results can be exchanged between the Experimental Group and the Computational Group. The program WDB can also read or write ASCII files of various formats. By that way there is no problem of data exchange also with external laboratories. At present four Data Bases are installed on the server of the computing system and five local Data Bases are installed on peripheral work stations. The experimental files management system, the actual situation of the Data Bases and the main interfaces made effective by WDB are shown in *Fig. 6.13*.

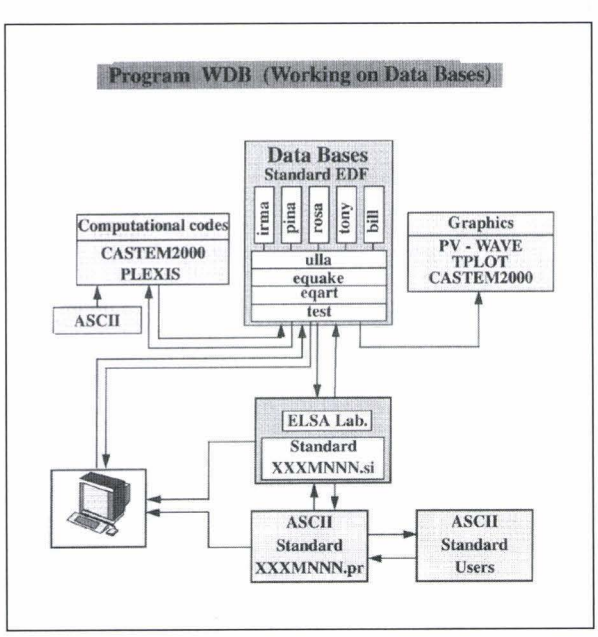

Fig. 6.13 Data bases and experimental files management system of the ELSA laboratory

The main functions of the program WDB are the following:

- put ELSA Lab. files in the Data Bases (from EEDF to EDF standard),
- get a file from the Data Bases (from EDF to EEDF standard),
- copy one file from a Data Base to another one,
- list the contents of both EEDF and EDF files,
- delete a file from a Data Base (only if owner),
- execute a large number of manipulations and mathematical operations on the ELSA Lab. files (standard EEDF).

Supporting activities in experimental mechanics

Research was conducted on the strain rate sensitivity of rubber compounds using alternate strain-rate testing. It was thought judicious to acquire some knowledge of the behaviour of such materials as they are essential components of many base isolation systems. It was found that the strain-rate sensitivity is not particularly pronounced (about 10% in our field of interest). It was also possible to ascertain the qualitative nature of the rate mechanisms on the material properties, and so, a numerical correction was devised to correct, during a PSD test, the effective load that would have been measured had the material been deformed at the real time scale (see references [7] and [8] and *Fig. 6.14*). In this figure the less inclined

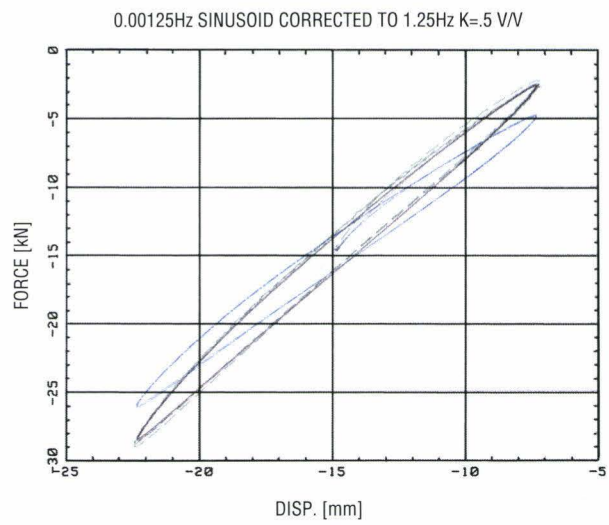

Fig. 6.14 Force-displacement loops for rubber compound under slow and fast strain rate cycles showing efficiency of proposed numerical correction method for PSD tests

loop corresponds to the slow strain rate cycles ; the more inclined, superimposed, loops correspond to the fast cycles and the slow cycles after having been corrected for rate effects.

Research was also conducted on explicit time integration algorithms. The algorithm is based on the principle of virtual work and energy conservation. The idea is to perform tentative (arbitrary displacements) paths so as to quantify a work function. The work increment is equated to the change in kinetic energy and, hence, the velocity of the associated mass particle at a given instant in time. The recursive algorithm then uses this velocity value to draw a new path during the next time step. The method has been adapted to the PSD technique. A single-degree-of-freedom system snap-back test on a non-linear specimen has been conducted using a revised PSD control procedure.

The method seems to work well for multi-degree-of-freedom systems and could be used for solving numerical structural dynamics problems. Also, by decomposing the particle velocity into fast and slowly varying terms, it has been possible to obtain an enhanced stability with respect to the more standard central difference method. The response of a two-degree-of-freedom system with distant eigenfrequencies was solved numerically using a sampling frequency ($\omega\Delta t$) of 2.5. The response is shown in *Fig. 6.15*. Under these conditions the standard central-difference scheme would have exploded. It can be seen that the results agree well with the central-difference scheme having a sampling frequency of 1. Although the stability has been heuristically proved to extend to very high sampling frequency ratios, considerable work has still to be conducted on the general stability and accuracy of this method.

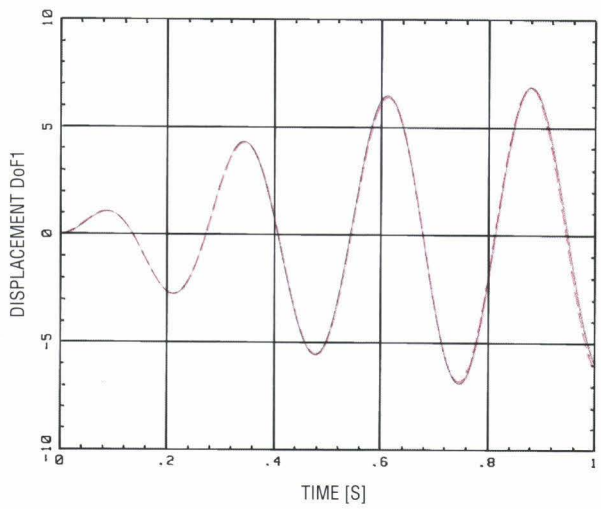

Fig. 6.15 Response of a 2 D.o.F. system with distant eigenfrequencies indicating improved stability properties with respect to the explicit central difference method

1.6.2 MODELLING AND STRUCTURAL ANALYSIS

During 1993 the computational mechanics activities were mainly directed to the further refinement, calibration and exploitation of analytical models for simulating the earthquake response of steel, concrete and masonry structures. This also included work on special solution procedures for non-linear structural analysis and support to the development and use of the PSD method. Further developments have also been made in the PLEXIS-3C code for fast dynamic fluid-structure problems developed in collaboration with CEA-Saclay.

Analysis of structures/assessment of design code provisions

The computational mechanics activity in the field of earthquake engineering was mainly directed towards the calibration and exploitation of analytical models. In addition, participation in national and international research programmes was pursued. Special reference shall be made to the activities of the working groups of the European Association of Structural Mechanics Laboratories (EASML) in general and to

the activity of the Reinforced Concrete Working Group (RCWG) in particular. The ELSA participation in the "HCM - Network on Pre-Normative Research in support of EC8" research programmes, including the study of irregular buildings and bridges and the effects of infills, has been defined both regarding the analytical and experimental aspects.

The analytical models developed and implemented in the reference computer code CASTEM 2000 [9] were used to perform the second phase of the dynamic non-linear analysis of the R/C structure to be tested at the Reaction-Wall. Design and analysis of this structure were included in the research programme of the RCWG. This second phase already included the results from the material tests (concrete blocks and steel bars used in the construction). The calculations have been performed assuming alternatively mean and variable values of material properties leading to the results shown in ***Fig. 6.16***. In addition, studies on the adequate testing sequence (intensity of earthquake ground motion) have been performed. Results of this study are illustrated in ***Fig. 6.17***, indicating that a gradual increasing of the intensity (0.4, 1.0 and 1.5 times the nominal) could be used without major changes of the results, allowing thus to obtain intermediate results, very useful for model calibrations. More detailed information can be found in the contribution to the RCWG final report [10].

Definition of the global member model parameters used in the above mentioned work is a difficult task due the large number of variables and physical phenomena involved (e.g. cracking of concrete, yielding of steel, pull-out effects). Consequently, this task is often based on empirical relations derived from experimental results and so are valid only for similar cases. This becomes very inconvenient when a wise and general approach is envisaged. Thus, a mechanistic procedure was adopted, in which the three main points of the moment-curvature curve, namely cracking, yielding and ultimate points, are determined on the basis of steel and concrete stress-strain models. The considered material models consist of a linear elastic-plastic diagram for the steel and a parabolic-linear one for the concrete, as shown in ***Fig. 6.18***, with common defining parameters easily understandable in the same figure. Criteria for the establishment of the referred points are: cracking is attained when the most stressed fibre reaches the tensile concrete strength; yielding point occurs as soon as tensional steel enters the plastic "plateau"; finally, the ultimate point is associated with the concrete crushing, i.e. the attainment of pre-defined maximum compressive strain. The referred points could be defined

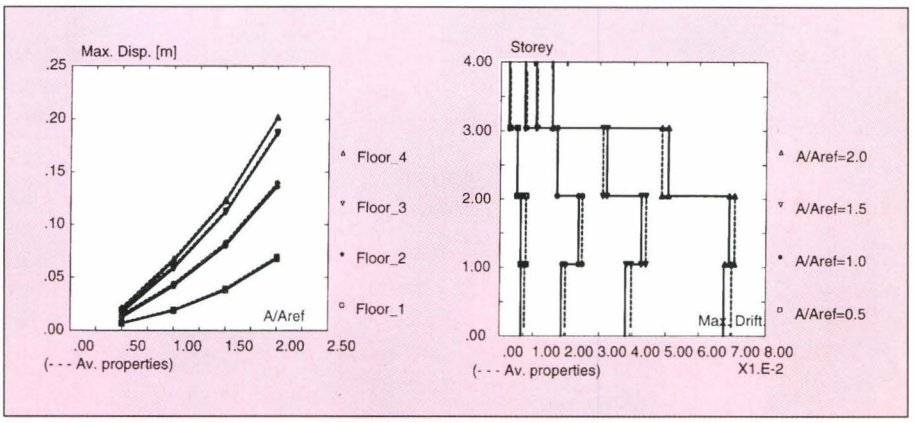

Fig. 6.16 4-Storey R/C building - vulnerability functions: displacement and drift profile (average and variable properties of the materials)

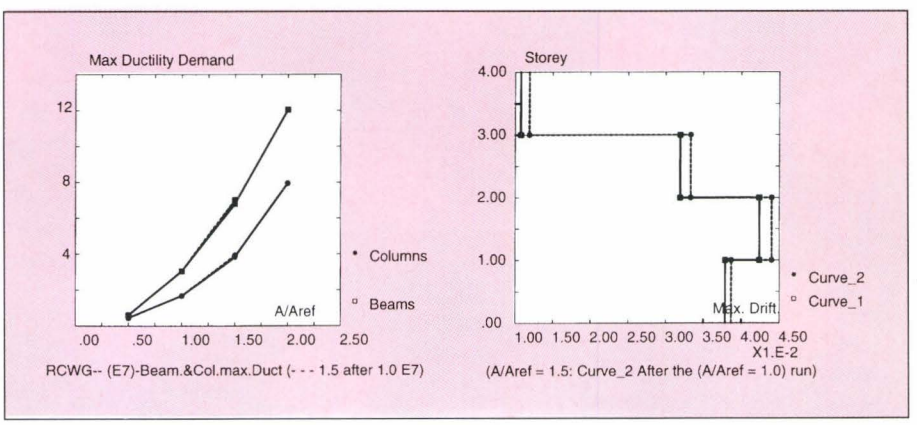

Fig. 6.17 Drift profiles and "real and apparent vulnerability functions" for ductility: ground motion (1.5xE7) applied subsequently to the (1.0xE7) ground motion

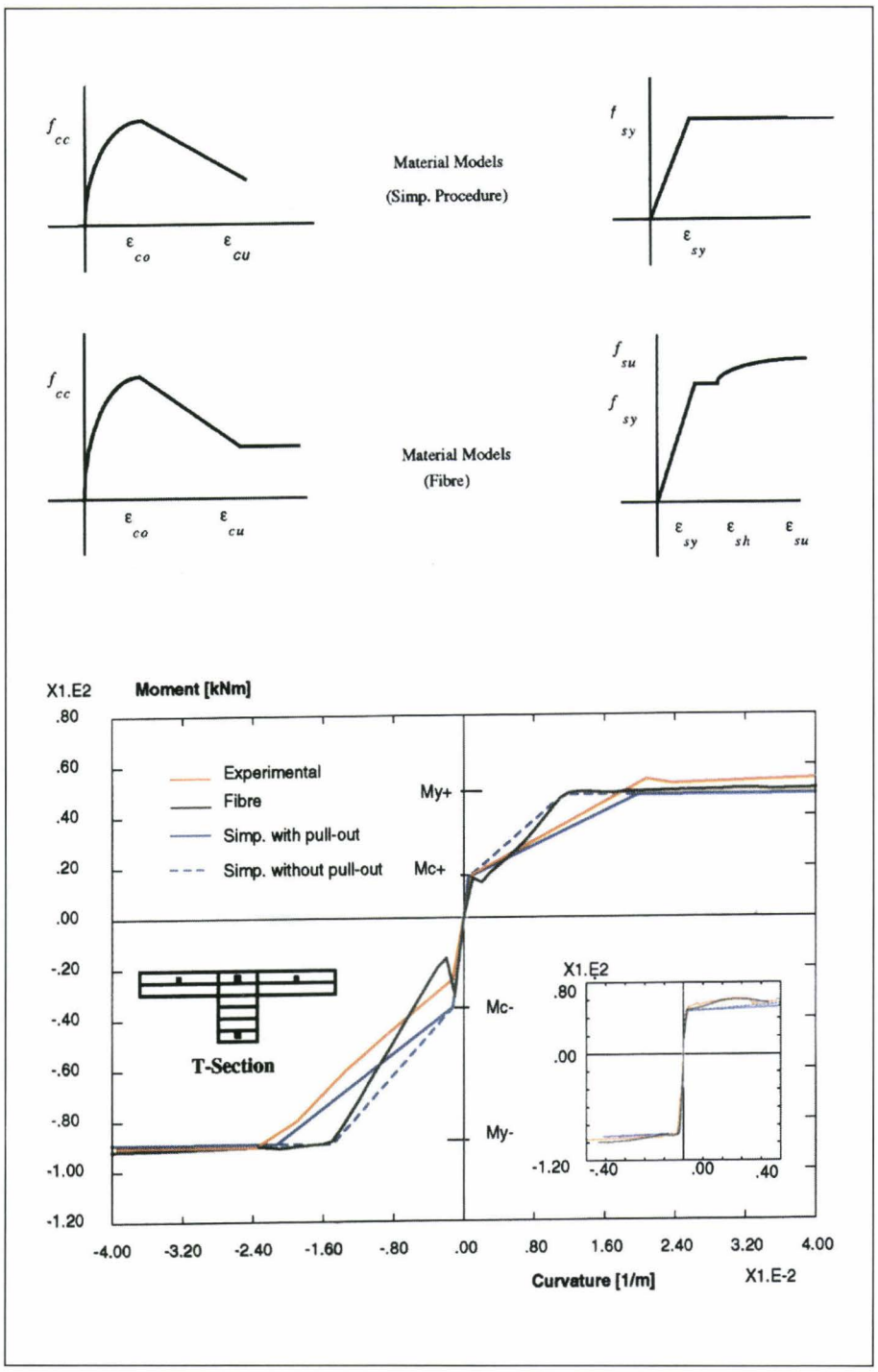

Fig. 6.18 Moment-curvature diagrams: experimental, fibre model, simplified identification procedure without pull-out, simplified identification procedure with pull-out

by means of a fibre-type discretization of the section, thus enabling a general section procedure, but being rectangular and T-sections of interest, analytical expressions have been deduced to obtain an efficient scheme implemented in CASTEM 2000. The pull-out effect in structural joints has been included, by means of the Morita's proposal [11] slightly modified, and thus affecting both yielding and ultimate curvatures. An example of a moment-curvature diagram is plotted in ***Fig. 6.18***, referring to an experimentally analysed T-section [12], in which is also shown the obtained curve when the pull-out effect is neglected (dashed line).

Studies on the seismic behaviour of irregular structures are to be undertaken during 1994 under the HCM-Network programme. For this purpose, simplified global models (storey shear/drift and torsion moment/rotation) are being implemented and calibrated in order to allow extensive calculations to be performed (parametric studies and different seismic inputs).

In order to represent the behaviour of bridge piers, fibre type models have been implemented and the corresponding constitutive relationships are being improved in order to take into account the cyclic effects, the tensile behaviour of concrete and the buckling of the reinforcement bars. ***Fig. 6.19*** compares the fibre results with the experimental testing performed in ELSA.

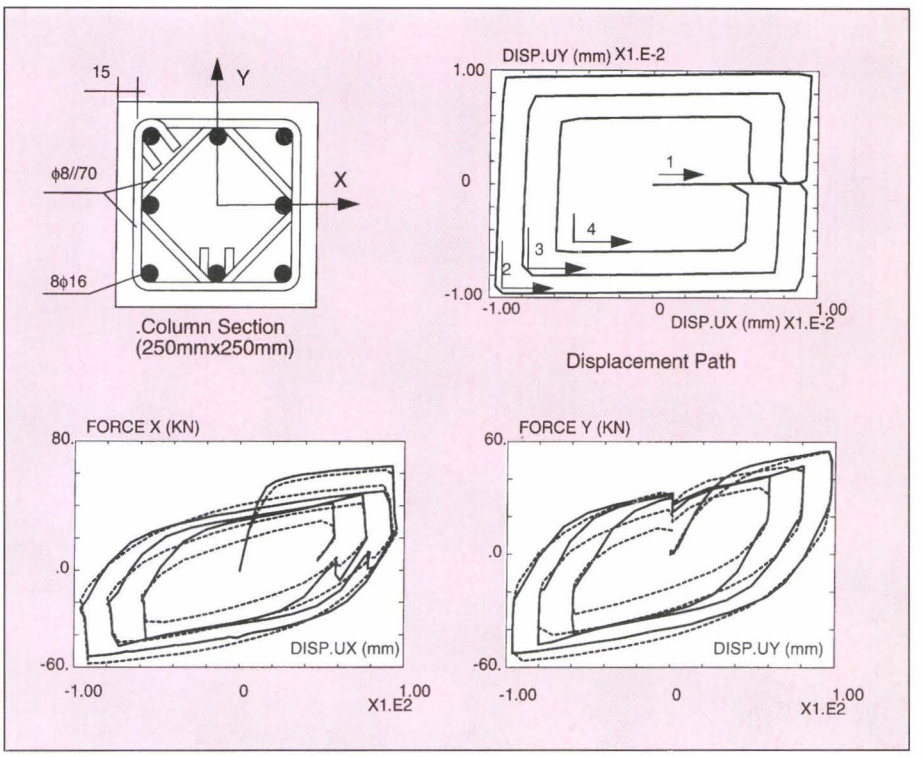

Fig. 6.19 Biaxial bending of R/C cantilever column with constant axial force (100 kN) - Results from fibre analysis and testing (broken line)

The final version of the Seismic Working Group research programme has been jointly prepared by the coordinator and the working group members and was approved by the COST-C1 Management Committee. Two meetings have been organized (in Ispra on June, 4, 1993 and in Lausanne on December, 9, 1993) and the first working group report will be available by February, 1994. In addition to the coordination of the working group activities, ELSA is participating actively in the research programme namely with the testing and analysis of the 3-storey steel frame and the 4-storey R/C building. The main conclusions of this activity have been presented during the WG meetings and will be included in the WG report. A joint research programme (ELSA - University of Bogazici, Turkey) on the strengthening and repair of R/C elements has been set-up. It includes the testing of R/C assemblages (beam/column) in ELSA.

The COST-C1 project (semi-rigid joint behaviour)

COST-C1 is a project intended to study the behaviour of semi-rigid civil engineering structural connections. It is mainly a framework for R&D cooperation in the field, allowing for both the coordination of national research projects and/or the participation of third countries in Community programmes, taking the form of pre-competitive or basic research or of activities of public utilities. In addition to the EC Member States, six of the EFTA countries are now participating in the project (Austria, Finland, Iceland, Norway, Sweden, Switzerland) as well as the Czech Republic, Slovakia, Hungary, Poland, Turkey and Slovenia.

ELSA participates in this project with two main aims, namely:

- to promote and extend the participation of Member States, EFTA countries and other European countries in cooperative research and development specially related to the ELSA activities,
- to promote the laboratory to industry for qualification of innovative design concepts and advanced manufacturing technologies.

Support to the development and use of the PSD method

The support to the development and use of the Pseudo-Dynamic (PSD) Test Method has been organized along the following lines:

- Study of an accurate implicit non-iterative integration scheme: the α-Operator-Splitting (OS) method,
- Implementation of the substructuring technique.

The Operator-Splitting method

The experimental study by the PSD test method of civil engineering structures involving several degrees of freedom (D.o.F.) may raise the following problem:

the lowest and the highest natural frequencies of the test structure may be different by, say, two orders of magnitude, while the seismic excitation may activate only the natural modes associated with the lowest natural frequencies. In this situation, the use of an explicit time integration scheme is not effective since the time step imposed for reasons of numerical stability (dictated by the highest natural frequency), is significantly lower than what is required for accuracy in implicit schemes.

The introduction of implicit time integration methods into PSD algorithms has been performed in the US and Japan along two distinct axes: use of implicit schemes involving subcycling at each time level for reaching equilibrium (US, see e.g. [13]), use of linearly implicit and non-linearly explicit non-iterative schemes (Japan, see e.g. [14]).

Even if the use of a non-iterative scheme seems to be the only effective alternative to the use of an explicit scheme, the Operator Splitting (OS) method proposed and used in Japan was not fully convincing, maybe for the two following reasons: first the experimental results often showed spurious oscillations associated with the highest frequencies reachable with the chosen time step, second no in-depth analytical study of the impact of the experimental errors, similar to the ones performed in the US for developing and improving the iterative schemes had been published.

Such an in-depth analytical study has been performed and, as a result, a slight modification of the OS method has been proposed: use of the OS method in conjunction with the α-modified Newmark scheme which tends to damp numerically the undesired spurious oscillations.

In order to check the validity of the results of this analysis, the computer code environment CASTEM 2000 was used for simulating the PSD method: given a complex, possibly non-linear numerical structure, say a frame building, we apply the PSD method, perturbating the setting of the displacement and the measure of the reaction force (experimental errors). It is then possible to show not only that the α-modified Newmark OS scheme effectively removes most of the spurious oscillations, but also that this scheme can compete favourably at the level of the results with the iterative scheme and this in both linear and non-linear situations. A part of this work has been published in a student's project report [15] and presented in a JRC summer seminar [16].

The substructuring technique

The PSD method is a hybrid method which combines the numerical integration of the equations of motion of a complex structure, condensed on a reduced number of D.o.F., and the experimental measurement of the reaction forces which result from this motion. Assuming that the behaviour of a part of a given structure, the substructure, is known, it is possible to numerically simulate the response of the substructure while experimentally testing only the rest of the structure, which is expected to undergo severe damage. This extension of the PSD test method is today applicable only if the connections between the substructure and the physically tested structure are simple. This substructuring technique allows to test specimens such as bridges whose size is even larger than the one of the laboratory: in the present case only the piers are physically tested while the deck is simulated on a computer (see ***Fig. 6.20***). In order to minimize the development effort for the implementation of the substructuring technique, only marginal modifications were introduced in the miniPDTM program controlling the experiments, and the modelling potential of CASTEM 2000 for simulating the substructure was massively used (see ***Fig. 6.20***).

In practice a substructuring test involves two processes running in parallel on two different hardware (miniPDTM on PC and CASTEM 2000 on a UNIX-workstation), using the same integration scheme and exchanging information relative to the D.o.F. connecting the structure and the substructure at each time level. This exchange of information is performed using the standard Berkeley socket library (see ***Fig. 6.20***). For that purpose, some function "call" have been added to miniPDTM while a new operator has been developed in CASTEM 2000.

A basic experimental validation of the substructuring technique has been obtained on a full-scale three-storey building, performing the following elastic tests:

- spring back test using actuators located at each of the three storeys,
- static experiment for identifying the stiffness of this 3 D.o.F. system,
- static experiment for identifying the stiffness of the building tested by only two coupled actuators located at the first storey,
- use of this information to calibrate a virtual substructure, able to complete, at least elastically, the above mentioned 1 D.o.F. (the substructure is virtual in the sense that the upper storeys of the tested structure were not removed),
- spring-back test with one actuator at the first storey and substructuring,
- comparison between the first storey displacement for the two tests is shown in ***Fig. 6.21***.

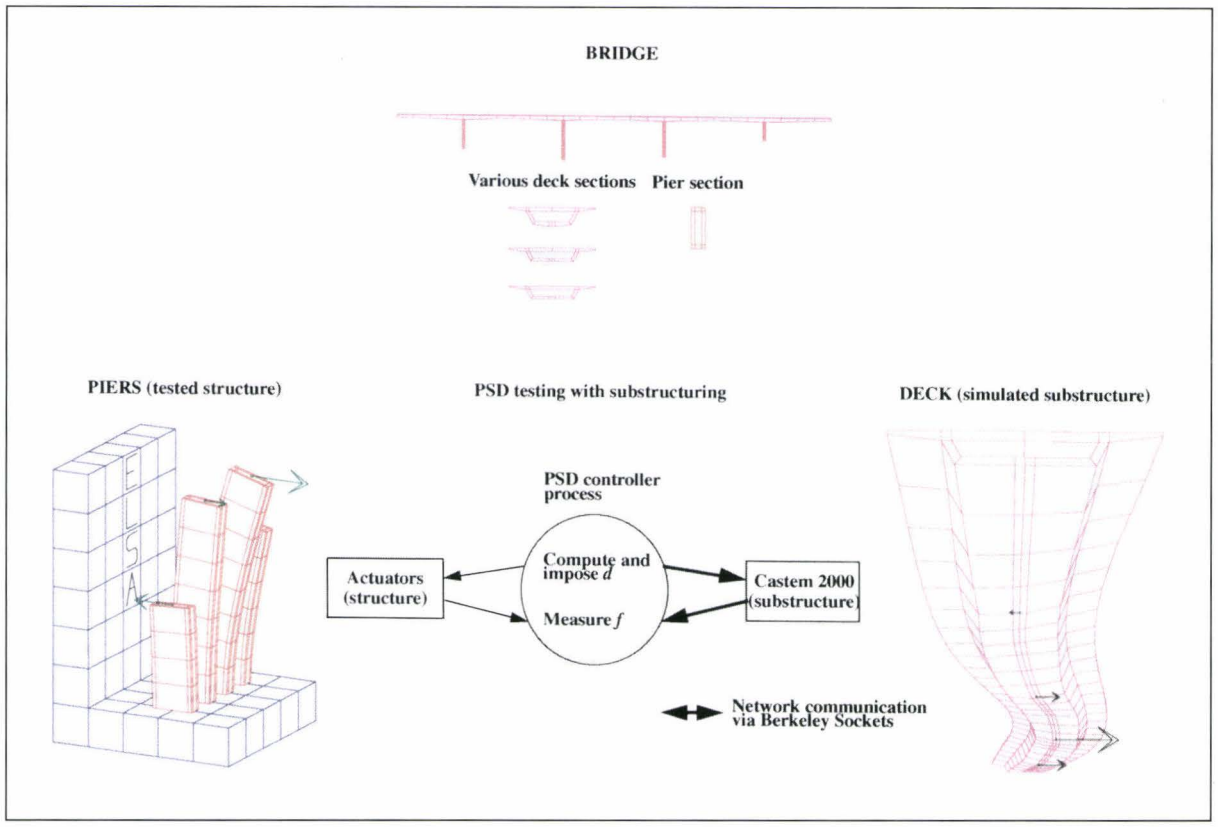

Fig. 6.20 Substructuring technique for bridge PSD testing

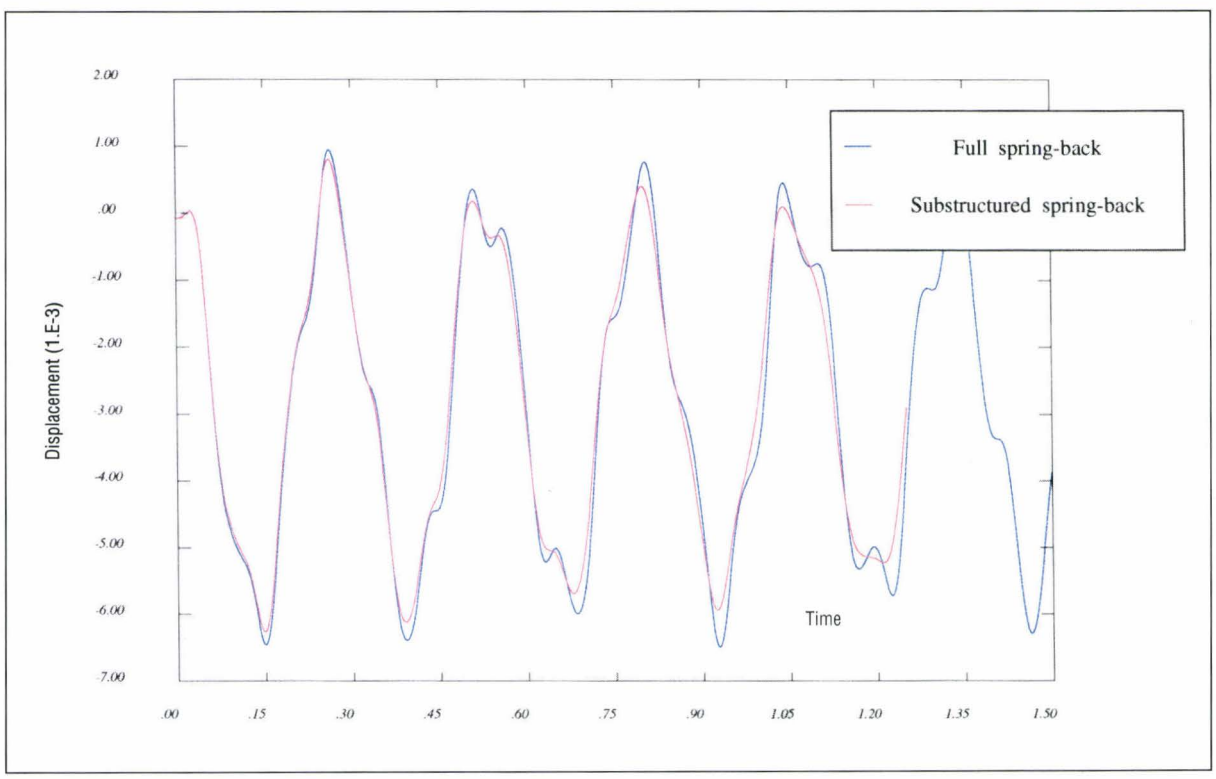

Fig. 6.21 Experimental comparison between two equivalent tests, one being performed with substructuring

During one validation test, the Berkeley communication line blocked at the level of the PC where the implementation is not native. Reviewing carefully the implementation of the exchange of information, some improvements of the robustness of this exchange have been proposed and tested, but the implementation, apparently due to persistent JRC network problems, is not 100% safe yet. The running of the substructuring PSD technique particularly highlights the complementary character of the numerical simulation tools and the experiments:

- Only the resort to simulation tools allows to compare the results between a "true" dynamical analysis and a pseudo-dynamic analysis performed on a reduced set of controlled nodes, in order to optimize the position of the actuators and to check the simplicity of the connection between the structure and the substructure.
- Only the resort to the experiment allows to obtain a fully realistic response of complex R/C structures under cyclic loading.

The implementation of the substructuring technique also underlines the need for a well-understood implicit scheme, such as the α-OS method.

The fibre model

Many frame structures may be modelled using beam elements. However, for reinforced concrete beams with complex steel distribution, it is not easy to provide a simple material behaviour model which would include biaxial bending interacting with normal force load. Instead of assuming a constitutive law relating generalized stress (say the bending moments and the normal force) to generalized strain (say the curvatures and the normal strain) for a section, it may be more convenient to assume that the section is made of fibres which do not interact one with another and which are characterized by a tensile stress/strain scalar relationship.

The implementation of such a model has been performed in CASTEM 2000 so that the description of the sections (shape, material characteristics) is general, easy to generate and to post-process. In fact, in the same way a problem is usually set up in CASTEM 2000, the sections are described by various models (say steel fibre, concrete fibre,...) associated with the meshes of these various components. This description allows in turn to define the beam modelling (see [17] for introducing a new model in CASTEM 2000, and [18] for the Timoshenko beam element used). The resulting model is biaxial for the bending and is naturally eccentric. The evaluation of the stress resultant for each beam element proceeds as follows:

- Evaluation of the generalized strain at the integration points of the beam elements.
- Use of the beam model in order to evaluate the deformation tensor and in particular its tensile component at the level of each fibre, located at the Gauss integration points of the elements describing the section.
- Use of the constitutive relationship in order to evaluate the stress tensor at the level of each fibre and, in particular, its tensile component.
- Integrations over the section of the relevant stress components in order to compute the generalized stress for the section (the use of Gauss numerical integration rules allows to obtain precise evaluations for these quantities).
- Computation of the stress resultant for the beam element. Two fibre laws have been already implemented:
  - the Menegotto-Pinto model for the reinforcing steel,
  - a Hognestad-type model for concrete, including confinement and cyclic behaviour.

This type of modelling is to be used for the piers in the various pre-test calculations required for performing PSD tests on bridges with substructuring.

Non-linear strategies for brittle materials such as concrete

The local modelling of softening materials is an important ingredient of the ongoing identification of the modelling of masonry panels or reinforced concrete beams. However, the simulations involving such type of materials are faced with the following list of connected problems:

- The concrete, the brick and the mortar are assumed to be described by a damage law. In order to account for the brittle character of these materials, the dissymmetry between traction and compression is very large, and the softening behaviour in traction is rather brutal.
- In order to be able to obtain numerical solutions which are not strongly mesh dependent and also to allow the damage to propagate, a non-local regularization of the damage law is used. This

regularization introduces a physical scale in the constitutive behaviour so that any mesh having a mesh size lower than this scale is able to produce convergent solutions, in the usual finite element sense.

- The tangent stiffness associated with the local behaviour is non-symmetric and non-regular. The non-local character of the formulation introduces not only further non-symmetry but also the loss of the conventional element stiffness notion. In practice, the best straightforward matrix to be used for performing the non-linear equilibrium iterations is the secant stiffness matrix associated with the local law. However, this matrix is very different from the tangent stiffness so that, even if it accounts for the non-homogeneous loss of stiffness of the strongly damaged elements, the convergence of the iterations is very slow and sometimes impossible.
- In order to accelerate this convergence process, various now-standard non-linear techniques may be applied, namely Quasi-Newton or Secant Newton accelerations and line-searches: however these techniques, which work very well with plastic materials, were not able to supply a robust framework for our computations. In place of this, an acceleration technique, depending on 4 previous residuals and displacement estimations has been used with success.
- In many situations, the loading path frequently exhibits limit points or unstable branches (snap-through or snap-back pattern). In order to overcome these difficulties continuation methods have to be introduced. The arc-length method limiting the norm of the increment of displacement has first been used. It appears, however, that an arc-length method based on the maximum increment of deformations gives more robust results. These continuation methods have of course to be combined with the above mentioned acceleration technique in order to achieve convergence.
- Since no tangent stiffness is readily available, the specification of the length of the arc is only based on the convergence rate. In case of non-convergence, a bisection process is introduced. Provision has also been made in order to prevent the non-linear iteration procedure from spurious convergence.

The developed numerical strategy in CASTEM 2000 allows to treat a problem involving a strong snap

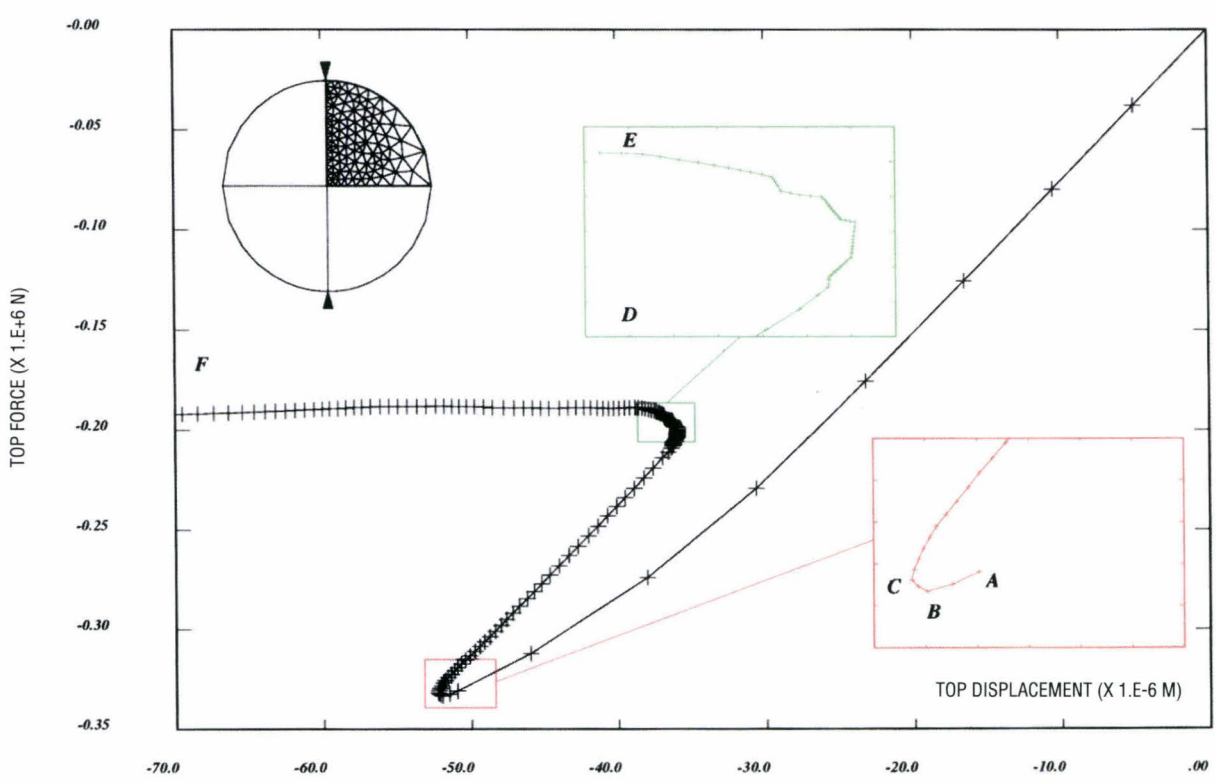

Fig. 6.22 Applied top force versus top displacement for the Brazilian test

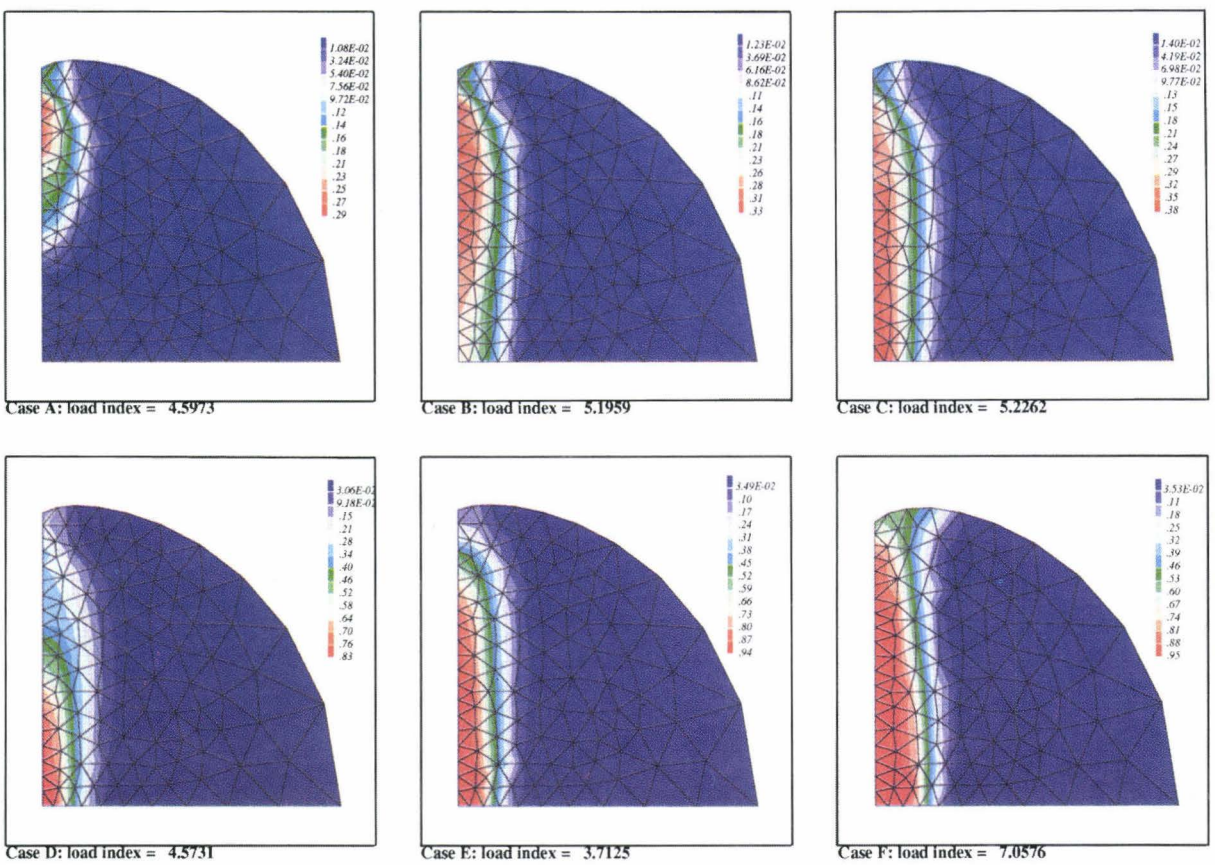

Fig. 6.23 Damage distribution at some selected solicitation levels of the Brazilian test

back and a complex localization pattern: the Brazilian test. This test is used for measuring the tensile characteristics of a brittle material by applying a load on a regular cylinder placed between to parallel plates. This problem was treated introducing the geometry and the material modelling used in previous simulations, which allowed to find only the limit load. ***Fig. 6.22*** shows the top force versus top displacement diagram which is now obtained and ***Fig. 6.31*** the damage state at some selected solicitation points referred to in ***Fig. 6.23***. This last figure clearly shows that the damage initiates under the load point, migrates to the centre (maximum load) and concentrates in the centre (relative maximum displacement and snap back) before expanding from the centre versus the top.

Shear-compression testing and analysis of brick masonry walls

The objective of this research was to investigate, both experimentally and numerically, the seismic behaviour of brick masonry walls subjected to complex loading conditions. Two types of walls have been chosen for being the key-elements of a building prototype to be tested at the Pavia University within the framework of an international cooperative research programme ("Experimental evaluation for the seismic behaviour of structures") promoted by the Consiglio Nazionale delle Ricerche (CNR - Italy).

Five specimens having the same width d = 1m, the same thickness t = 0.25m (two wythes thickness English bond) but different heights h = 1.35m or 2m, have been built. Three of them have been tested quasi-statically whereas the two remaining ones are planned to be tested pseudo-dynamically. The experimental set-up is schematically represented on ***Fig. 6.24***. The loading conditions have been chosen so as to reproduce as close as possible the real conditions undergone by the panels during a seismic event (constant vertical load, double bending moment). A uniform vertical compressive stress of 0.6 MPa was applied first by means of the two vertical actuators, the resulting vertical load being $F_y = F_{y1} + F_{y2} = 150$ kN. The lateral displacement U_x was

imposed by means of the horizontal actuator. At each step, the forces F_{y1} and F_{y2} in the two vertical actuators were adjusted in order to maintain the same value of the vertical load as well as the horizontality of the steel beam; thus, with the notations of *Fig. 6.24*, the forces and the displacements in the two vertical actuators were such that

$$F_{y1} + F_{y2} = F_y = 150 \text{ kN} \quad (1)$$

$$U_{y1} = U_{y2} \quad (2)$$

Alternated lateral displacements U_x of increasing amplitude have been imposed quasi-statically (*Fig. 6.25*). The walls were fully instrumented in order to get a large amount of data susceptible to be compared with finite element results (forces and displacements at the top and also deformed shape of the wall). The results of the quasi-static loading put in evidence the effect of the height/width ratio on the behaviour of the walls (*Fig. 6.26*): the ultimate load and displacement, the ductility, the degradation, the deformed shape and the failure mode are strongly influenced.

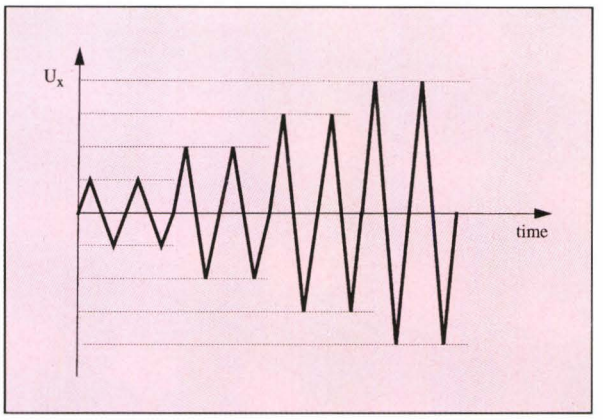

Fig. 6.25 Lateral displacement history

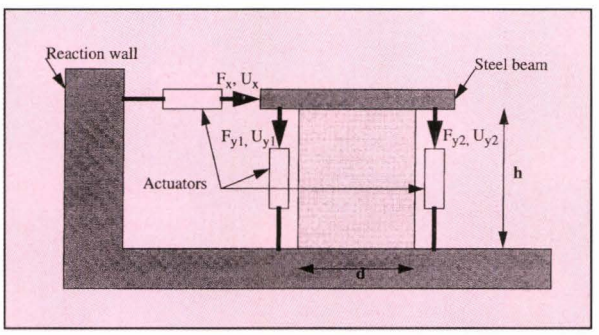

Fig. 6.24 Schematic view of the test set-up for masonry walls

Numerical simulations [19] have been carried out with the finite element code CASTEM 2000: masonry has been modelled as a two-dimensional continuum subjected to isotropic damage. The parameters of the model have been chosen according to preliminary tests performed on small-scale specimens (masonry wallettes). The loading conditions (Eq. 1 and 2) were respected but the lateral displacement was monotonically increased. The numerical results are qualitatively in accordance with the experimental observations. In particular, the failure mode and the crack pattern are well predicted (*Fig. 6.27*), independently of little variations of the constitutive parameters. However, further refinement of the model (cyclic loading, anisotropy) is needed in order to achieve a better accuracy.

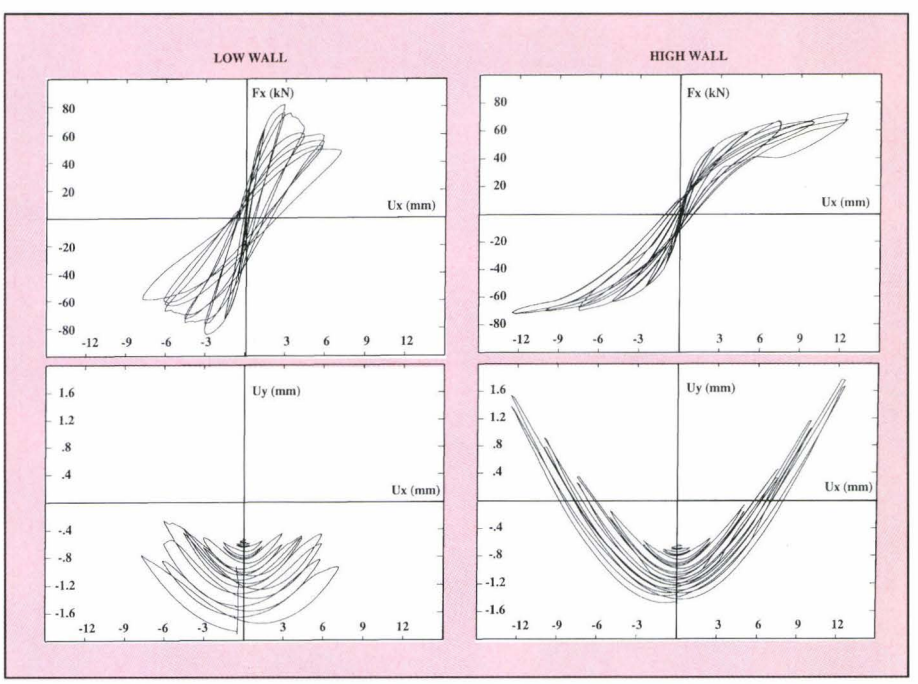

Fig. 6.26 Horizontal force F_x versus lateral displacement U_x (up) and vertical displacement U_y versus lateral displacement U_x (down) for the low wall (left) and the high wall (right)

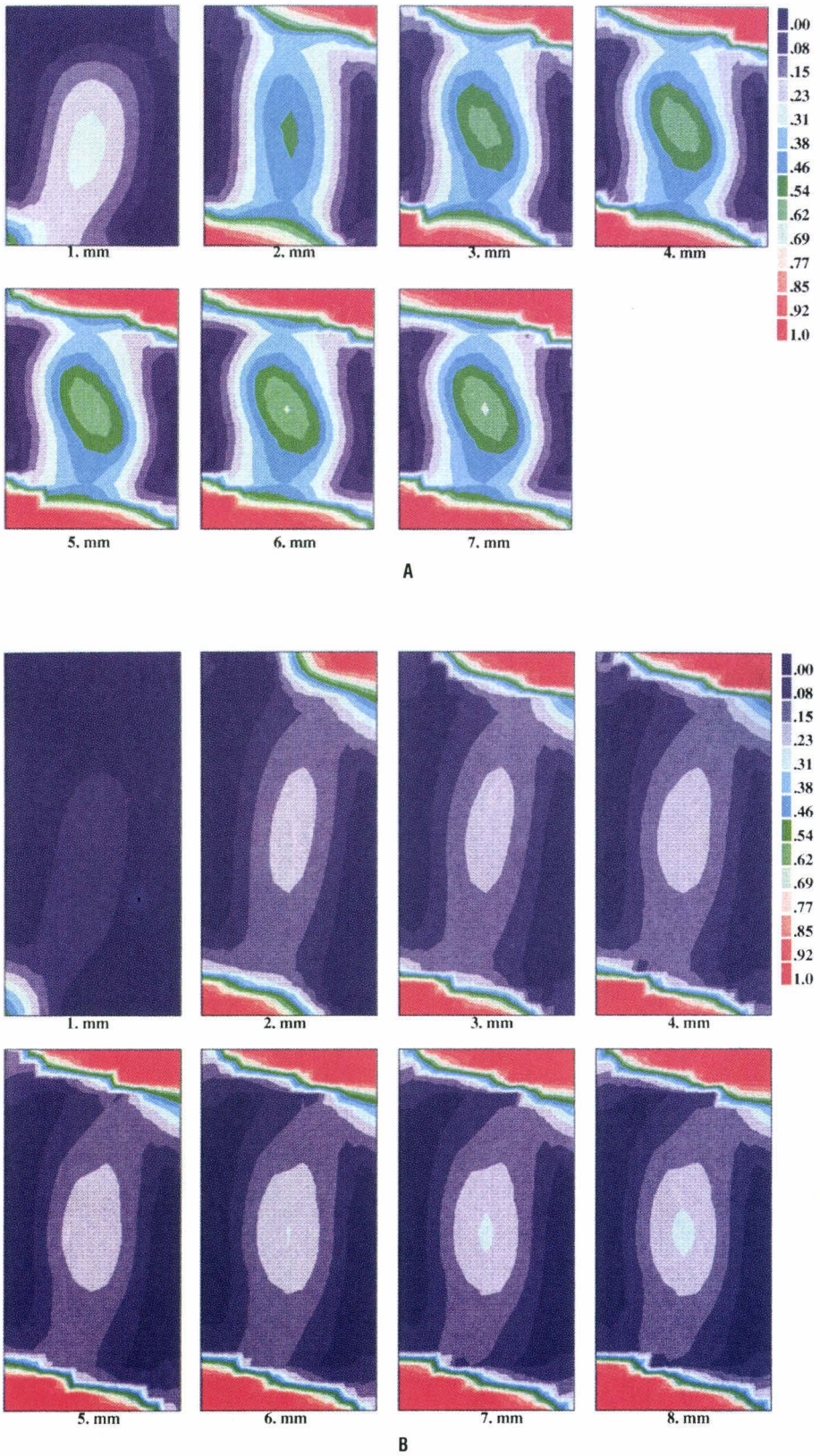

Fig. 6.27 Computed damage index for increasing values of the lateral displacement U_x, for the low wall A and the high wall B

Non-linear modelling of masonry

From the preliminary numerical tests performed in 1992, it resulted that three-dimensional computations were necessary to derive the macroscopic behaviour law of masonry through the homogenization theory. As a matter of fact, two-dimensional calculations under the plane stress assumption were found to give erroneous results in the non-linear range (both brick and mortar being assumed as subjected to isotropic damage). In 1993, further calculations showed that, a good alternative to a time-consuming 3D calculation was a 2D calculation under the generalized plane strain assumption. As shown on *Figs. 6.28* and *6.29*, the results are in excellent agreement qualitatively (mode of failure) as well as quantitatively (macroscopic stress-strain relationship). However, it should be noted that 3D calculations remain necessary as soon as the characteristics of the masonry vary through the thickness of the wall (hollow bricks, composite walls, complex bonds).

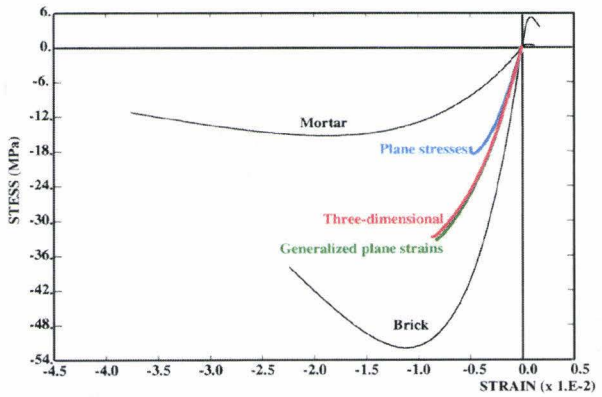

Fig. 6.28 Uniaxial vertical compression curves: contrarily to the plane stress assumption, the generalized plane strain assumption gives satisfactory results even in the non-linear range

PLEXIS-3C project

The activity on the PLEXIS-3C project was continued during 1993 in collaboration with CEA Saclay and with ENEL-CRIS. PLEXIS-3C is a computer program for the finite element modelling of fast transient dynamic problems in fluid-structure systems. The major achievements are documented in references [20] to [34]. In the area of metal forming no new modelling activities were performed, but a new publication, describing work of the previous period not cited in last year's report, was issued, see reference [20]. The main developments in the period of interest were the following.

In the field of structural shell elements, the revision work started in 1992 was completed, verified and documented. The models for two-dimensional shells are described in reference [27]. The three-dimensional triangular plate/shell element is described in reference [30], with various illustrative and validation examples. Finally, the theory for 3D degenerated shell elements is described in reference [22] and an extensive account of their implementation in PLEXIS-3C is given in [26]. Actually, a whole family of elements was implemented in the code, using linear or parabolic in-plane displacement fields (linear or quadratic elements), and with triangular or quadrilateral shapes. Various types of numerical integration are also possible. The report [26] contains also many examples of test problems, complete with input files, and is a first step in a large effort of preparation of program documentation and user's (examples) manual pro-

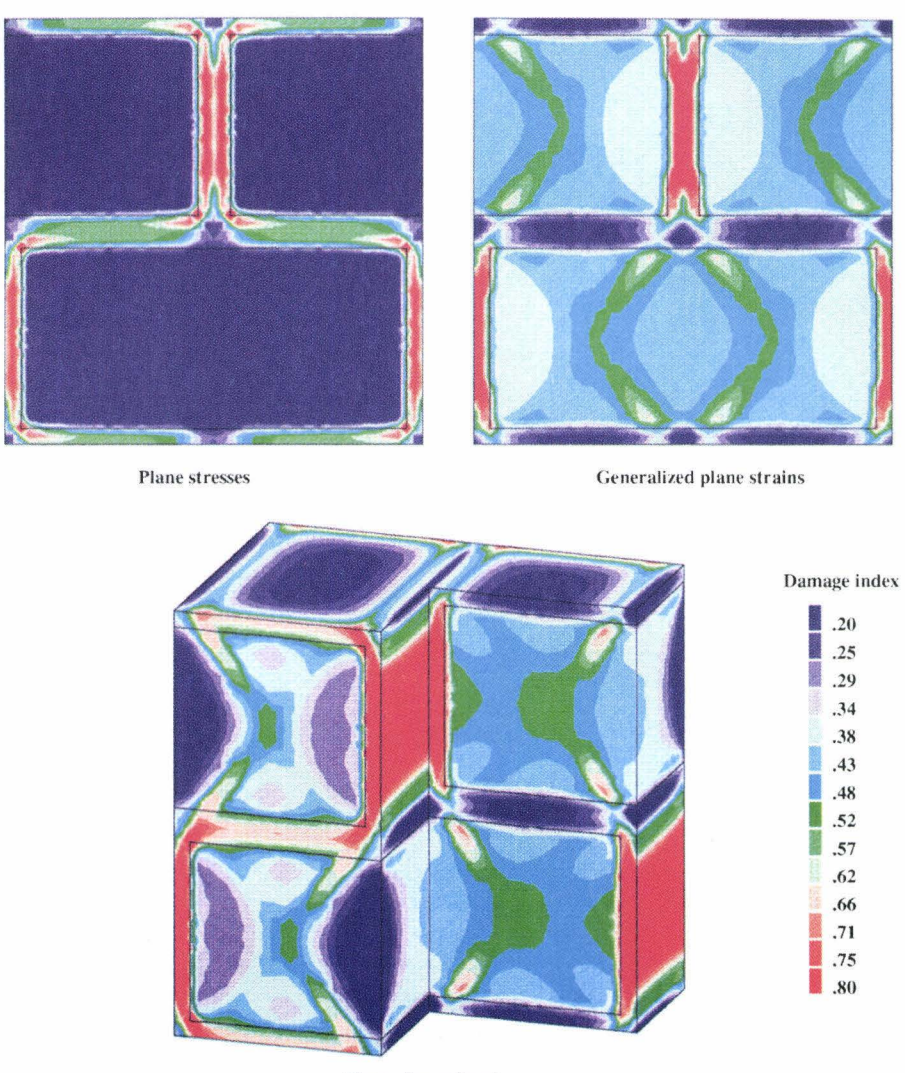

Fig. 6.29 Damage at maximum compression stress: under the plane stress assumption, failure occurs by cracking (vertical joint) and crushing (horizontal joint) of the mortar. The failure mode under the generalized plane strain assumption agrees well with the three-dimensional one (cracking of the vertical mortar joint and of the brick)

duction which is being undertaken in view of a first official release of PLEXIS-3C.

In the field of compressible fluids, reference [25] provides a detailed description of the models currently implemented in PLEXIS-3C. These models have undergone a slow but constant evolution over the years and there was a need for an up-to-date reference. The report includes a description of the ALE mesh rezoning algorithms, for both 2D and 3D geometry. Reference [21] contains a detailed treatment of the classical shock tube test solved by PLEXIS-3C and provides a guide to users for the correct choice of the parameters that are at disposal in the program for the treatment of the fluid domain. The study showed some fine points but also demonstrated that the default values of these parameters, as chosen automatically by the code, provide a reasonable choice, appropriate for most practical situations.

The revision of boundary conditions started last year was continued. Probably, the most important achievement of the current year was the formulation, implementation and validation of a new model for fluid-structure interactions of the permanent (ALE) type. The model is automatic in the sense that it requires almost no effort from the users in the specification of input data even for the most complex cases, and is coupled with CASTEM 2000 for pre- and post-processing. This almost eliminates the possibility of human errors and greatly improves the productivity of the code in complex, 3D coupled fluid-structure simulations. The model is fully general and deals automatically with both 2D and 3D geometries. The strongest feature is that it is able to cope with very complex situations of large practical importance, such as: fluid contact along both sides of a structure, arbitrary structural bifurcations and junctions, submerged structural edges, etc., also in the presence of large displacements, rotations and strains in the structures. Furthermore, being based on the method of Lagrange multipliers and on the use of a matrix of connections, the new sliding conditions are directly combinable with any other boundary condition available in PLEXIS-3C that uses the same method. This particular aspect was documented in reference [29], while a detailed report on the theory of permanent fluid-structure interaction is given in reference [31]. The latter report also includes many practical examples, complete with pre-processing and input files, so that it represents a valid practical guide for the users.

Some further new models and improvements to PLEXIS-3C existing models were documented in reference [28]. These included: a) a modification of the critical time step estimation in 9-node elements, that avoids numerical problems (stability) when dealing with large shear deformations, and b) a new algorithm for the description of sliding along free surfaces in the ALE formulation.

Much effort was devoted in the period of interest to the execution of sample test cases and realistic applications. Besides the shock tube study already mentioned (reference [21]), and the many examples contained in references [26], [30] and [31], two studies of complex applications were performed. The first one was the simulation of a hypothetical gas explosion in a reactor containment and is reported in reference [32]. The geometry was 2D axisymmetric and use was made of the new fluid-structure interaction models. The second application, described in reference [33], was a complex, fully 3D problem of a postulated explosion in an underground cell. The cell is partially open to the outside environment and is surrounded by a cylindrical wall. The goal was the prediction of overpressure distributions in the area around the wall as a function of time. The problem is defined in ***Fig. 6.30*** where the geometry and finite element mesh are shown. In order to give an idea of the extreme simplicity of the PLEXIS-3C input file, even for such a complex, coupled problem, the input file is listed in ***Table 6.4***. Thanks to the new automatic fluid-structure interaction model, the specification of sliding conditions between the fluid and the structure (which has fluid on both sides and contains a circular submerged edge) reduces to just one line: "FSA LECT FSAN TERM", see towards the end of the file. The FSAN object is generated by CASTEM 2000 in the pre-processing phase and is simply used by PLEXIS-3C to extract the list of nodes affected by sliding conditions. As a further example of results, ***Fig. 6.31*** shows the fluid pressure distributions at various instants in the cell, inside the cylindrical wall and (sectioned mesh) in the whole model.

To complete the list of this year's developments in PLEXIS-3C, some advances were also obtained in the area of post-processing, see references [23] and [34]. The new interfacing with CASTEM 2000 for output post-processing described in [34] is especially important, because it allows to produce realistic, full-color plots of the computed results (see examples above), and also includes the possibility of producing animations on the screen. A set of simple, standardized CASTEM 2000 procedures, described in [34], was produced in order to simplify and automatize, as far as possible, the post-treatment of PLEXIS-3C results. Finally, a preliminary version of the PLEXIS-3C user's manual for input preparation was produced, reference [24]. The same documentation is also available on-line.

Table 6.4 PLEXIS-3C input file for the underground explosion simulation

```
cent - 06
$
  ECHO
$VERI
$CONV TEKT
CAST 'cent06.sauv' MESH
TRID NONL ALE
$
DIME
PT6L 90 PT3L 2433 FL38 1674 FL36 408 COQI 120 ZONE
3
  MATE 3 tabl 1 5
  NALE 49 NBLE 1 FSA 150
  BLOQ 3000
  LIAI 2586 173322
  DMAT 43
  ECRO 31398
TERM
$
GEOM
  FL38 MESH8 FL36 MESH6 COQI TUBO TERM
$
COMP
  EPAI 0.001 LECT TUBO TERM
$
GRIL LAGR LECT TUBO TERM
      ALE LECT CELLA CILI ESTER CIELO TERM
$
$ steel
MATE VM23 RO 7800. YOUNG 1.6E11 NU 0.333 ELAS
1.05E8
  TRAC 2 1.05E8 .656256E-3 1.6105E10 1.00066
  LECT TUBO TERM
$ high-pressure perfect gas
  FLUT RO 1.22 EINT 3.046E6 GAMM 1.269 PB 0 ITER
1
  ALF0 1 BET0 1 KINT 0 AHGF 0 CL 0.5 CQ 2.56
  PMIN 0 NUM 1 LECT EXPL TERM
$ same gas at a lower pressure
  FLUT RO 0.1237 EINT 3.046E6 GAMM 1.269 PB 0
       ITER 1 ALF0 1 BET0 1 KINT 0 AHGF 0 CL 0.5
       CQ 2.56 PMIN 0 NUM 1
       LECT ARIA CILI ESTER CIELO TERM
$
LIAI BLOQ 123456 LECT BLOCALL TERM
  BLOQ 1 LECT BLOCX
  BLOQ 2 LECT BLOCY
  BLOQ 3 LECT BLOCZ
  FSA LECT FSAN TERM
$
ECRI VITE TFRE 50.0E-3
$ FICH ALICE 'cent06.alic'    TFRE 1.E-3
  FICH K2000 'cent06.k200'    TFRE 10.E-3 POIN TOUS
                              CHAMELEM
$ FICH TPLOT 'cent06.tplo'    FREQ 1 desc 'cent06'
$                             POIN LECT TPLN TERM
$
OPTI PAS AUTO NOTEST STEP IO
CALCUL TINI 0 TEND 50.E-3 NMAX 100000
FIN
```

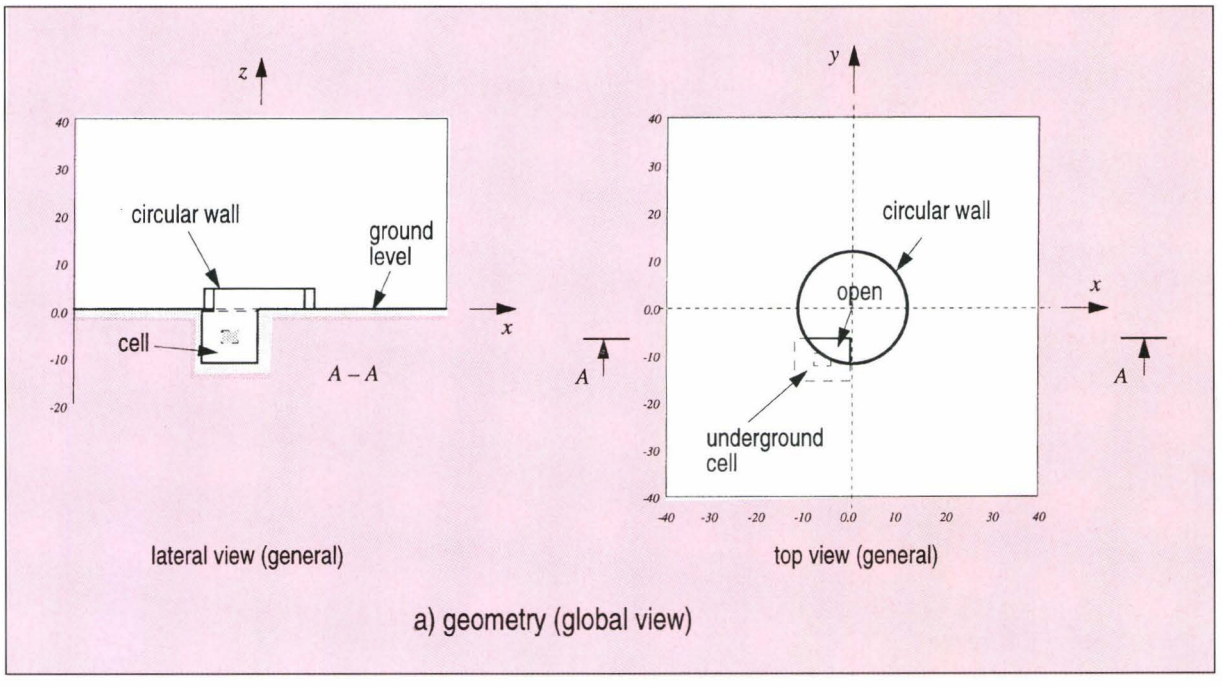

Fig. 6.30a Simulation of an explosion in an underground cell: geometry and finite element mesh

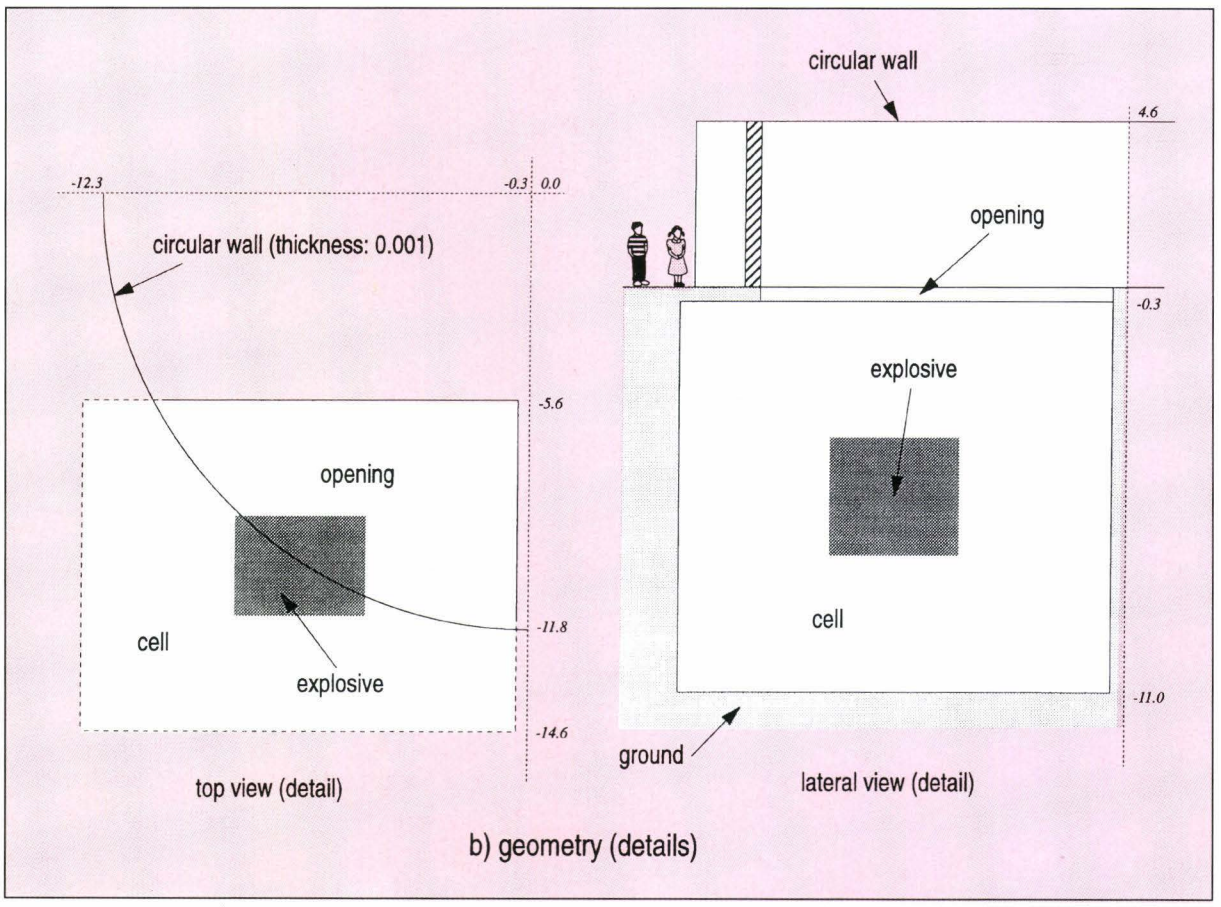

Fig. 6.30b Simulation of an explosion in an underground cell: geometry

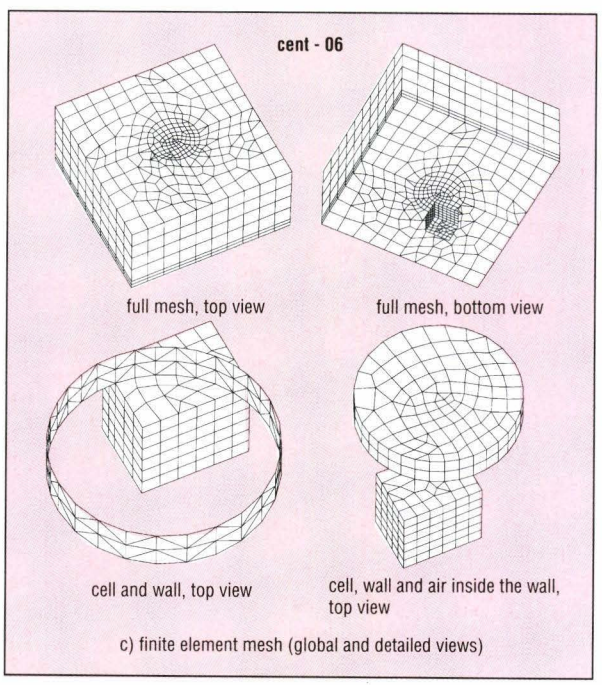

Fig. 6.30c Simulation of an explosion in an underground cell: finite element mesh

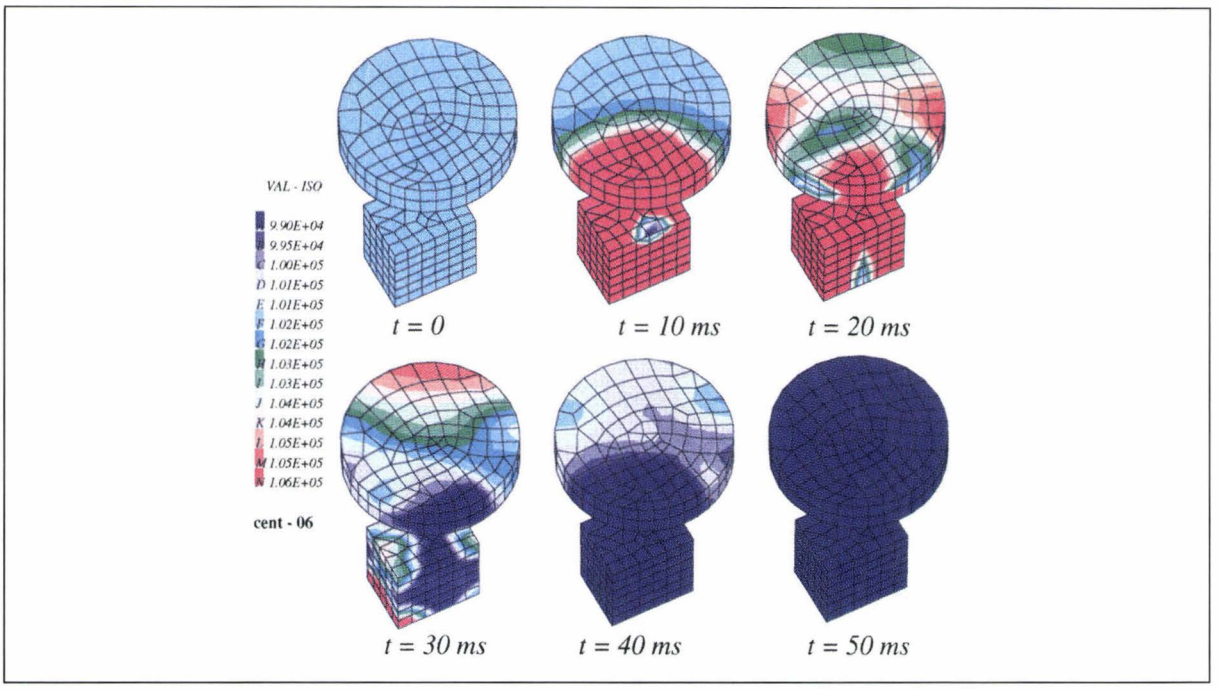

Fig. 6.31a Fluid pressure distributions at various instants in the cell, inside the cylindrical wall and (sectioned mesh) in the whole model

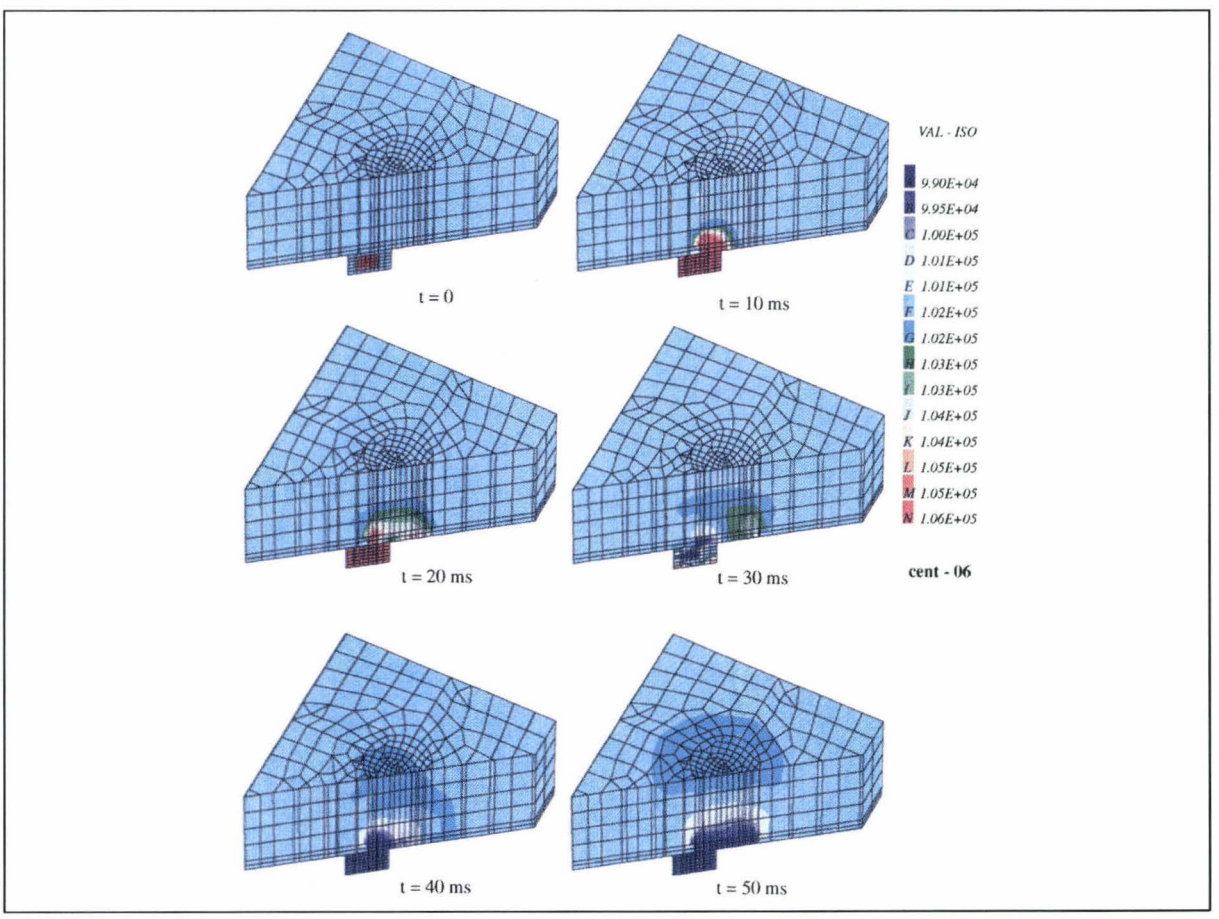

Fig. 6.31b Fluid pressure distributions during the transient (sectioned global mesh)

References

[1] KAKALIAGOS A. - Behaviour of steel frames with semi-rigid joints under seismic induced loads" Dissertation; Technical University Darmstadt, Darmstadt, Germany 1989

[2] KAKALIAGOS A., BOUWKAMP J.G. - Seismic behaviour of a Ten-Storey Steel Moment Resisting Frame with semi-rigid beam-to-column connections; Paper presented in the "1993 National Earthquake Conference", Vol. 2, pp 389-398, May 3-5, 1993, Memphis, Tennessee

[3] KAKALIAGOS A., BOUWKAMP J.G. - Tests on Steel - Composite Beam-Column Connections, Strength and Stiffness Aspects, Earthquake Spectra (E.E.R.I), Vol. 9, number 4, November 1993

[4] PRAKASH V., POWELL G.H. - DRAIN-2DX: a general purpose computer program for dynamic analysis of inelastic structure - January 1992, Version 1.0, NISEE, Computer Applications, Department of Civil Engineering, University of California, Berkeley

[5] KAKALIAGOS A. - Design of Three-Storey One-Bay Full-Scale Steel Frame for Pseudo-Dynamic Testing; Commission of the European Communities, Joint Research Center, Institute of Safety Technology, Report EUR-15103 EN-1993

[6] KAKALIAGOS A. - Pseudo-Dynamic Testing of a Three-Story One-Bay Steel Moment-Resisting Frame. Experimental and Analytical Results; Commission of the European Communities, Joint Research Center, Institute of Safety Technology, to be published as EUR-Report

[7] GUTIERREZ E., MAGONETTE G., VERZELETTI G. - Experimental Studies of Loading Rate Effects on Reinforced Concrete Columns, ASCE, vol. 119, No 5, pp 887-904, May 1993

[8] GUTIERREZ E., VERZELETTI G. - Possibilities of Vibration Isolation Testing at the ELSA Laboratory of the Joint Research Centre, Proc. International Post-SMIRT Conference on Isolation, Energy Dissipation and Control of Vibrations of Structures, Capri, August 1993

[9] CASTEM 2000 - Guide D'Utilization, CEA/Saclay, France, August 1990

[10] PINTO A.V., NEGRO P., PEGON P., AREDE A. - Analysis of the 4 Storey R/C Building to be Tested in the ELSA Laboratory (2nd Phase), Cooperative Research on Seismic Response of Reinforced Concrete Structures, Contract n. 4504 - 91-10 ED ISP P, E.C. Carvalho (Ed.), proc. 135/11/10778, LNEC, Lisbon, 1993

[11] MORITA S., KAKU T. - Slippage of Reinforcement in the Beam-Column Joint of Reinforced Concrete Frames; Proceedings of 8th World Conference on Earthquake Engineering, S. Francisco, Vol. 6, pp 477-484, 1984

[12] PIPA M., CARVALHO E.C. - Cyclic test on RC Cantilever T-Beams With B500 Steel, Cooperative Research on Seismic Response of Reinforced Concrete Structures, Contract n. 4504 - 91-10 ED ISP P, E.C. Carvalho (Ed.), proc. 135/11/10778, LNEC, Lisbon, 1993

[13] SHING B., VANNAN M.T., CATER E. - Implicit Time Integration For Pseudodynamic Tests, Earthquake Eng. Struct. Dyn., Vol. 20, pp 551-576, 1991

[14] NAKASHIMA M., KATO H. - Experimental Error Growth Behaviour and Error Growth Control in On-line Computer Test Control Method, BRI-Report, Japan, 1987

[15] COMBESCURE D. - Etude de l'influence des erreurs expérimentales sur la méthode d'essais pseudodynamique; Rapport de stage de fin d'étude et de D.E.A., ECP Paris, 1993

[16] PEGON P., COMBESCURE D. - Impact of Experimental Errors on the PSD Method, Workshop on Pseudo-dynamic Test Method, ELSA, July 1993

[17] PEGON P. - Model Implementation in CASTEM 2000: Some General Considerations and a Simple Practical Realisation, JRC-Technical Note I.93.06, 1993

[18] PEGON P. - A Timoshenko simple beam element in CASTEM 2000, JRC-Technical Note I.93.05, 1993

[19] ANTHOINE A. - Homogenization of periodic masonry: 2-D (plane stress) or 3-D modelling of the basic cell; Proceedings of the First Forum of Young European Researchers, Liège, Belgium, July 18-23, 1993

[20] HUERTA A., CASADEI F., DONEA J. - An arbitrary Lagrangian- Eulerian stress update procedure for coining simulations; Numerical Methods in Industrial Forming Processes, Eds. Chenot J.L., Wood R.D. and Zienkiewicz O.C., ISBN 90 5410 087 7, Balkema, Rotterdam, 1992

[21] CASADEI F. - PLEXIS-3C Solutions to a Shock Tube Problem, Technical Note I.93.33, March 1993

[22] CASADEI F. - A Non-linear 3-D Shell Finite Element Implementation for Transient Problems, Technical Note I.93.41, April 1993

[23] CASADEI F. - Considerations about a Data Management and Document Production System for AMU, Technical Note N. I.93.55, April 1993

[24] CASADEI F., HALLEUX J.P. (Eds.) - PLEXIS-3C User's Manual (Preliminary Version), Technical Note I.93.83, June 1993

[25] CASADEI F. - Implementation of Compressible Fluid Models in PLEXIS-3C, Part I - Models, Technical Note I.93.86, June 1993

[26] CASADEI F. - Implementation of 3-D Degenerated Shell Elements in PLEXIS-3C, Technical Note I.93.88, July 1993

[27] CASADEI F. - Generalisation of a Two-Dimensional Rectilinear Beam/Conical Shell Element to Large Membrane Strains, Part I - Theory, Technical Note I.93.89, July 1993

[28] CASADEI F. - A Miscellanea of New Models in PLEXIS-3C, Technical Note I.93.90, July 1993

[29] CASADEI F. - Treatment of Essential Boundary Conditions in PLEXIS-3C, Technical Note I.93.91, July 1993

[30] CASADEI F. - A Triangular Plate Element for the Non-linear Dynamic Analysis of Thin 3-D Structural Components, Technical Note I.93.92, July 1993

[31] CASADEI F. - Implementation of A.L.E. Fluid-Structure Interaction Models in PLEXIS-3C, Technical Note I.93.139, November 1993

[32] CASADEI F. - Simulation of a gas explosion in a reactor containment by PLEXIS-3C, Technical Note I.93.148, November 1993

[33] CASADEI F. - Simulation of a gas explosion in an underground cell by PLEXIS-3C, Technical Note I.93.149, November 1993

[34] CASADEI F. - Postprocessing of PLEXIS-3C calculated results by CASTEM 2000, Technical Note I.93.150, November 1993

1.7 WORKING ENVIRONMENT

Working Environment is a new research programme which was started up in 1992. At present, the programme at the STI is limited to the subject "Ventilation and Pollutant Transport Modelling" and involves only a small effort. The general objective which is pursued by this activity is the improvement of working conditions through a more clean, comfortable and healthy environment at the workplace, that can be reached with better and more efficient ventilation systems. The development of accurate and efficient Computational Fluid Dynamics models to deal with turbulent air-pollutant flows is a pre-requisite to fulfill these objectives.

1.7.1 VENTILATION AND POLLUTION TRANSPORT MODELLING

The activity during 1993 on the ventilation and pollutant transport project entailed both further refinements and improvements of the turbulence models implemented in the TRAFLU computer code as well as the consideration of two additional pollutant transport models (gaseous pollutants and solid aerosol particles). The two-dimensional finite element computer code TRAFLU, was developed at the Joint Research Centre, Ispra site, for solving unsteady laminar and/or turbulent incompressible flow problems. The code includes two types of turbulence models: the Van Driest mixing length model and the low Reynolds number two-equation κ–ε model. Several types of finite element schemes have been implemented in the TRAFLU code. These range from the explicit second-order accurate (three fractional steps) Taylor-Galerkin scheme to the implicit second order accurate (two fractional steps) Petrov-Galerkin scheme [1, 2]. TRAFLU is still undergoing development as far as turbulent flows, boundary conditions and aerosol modelling are concerned.

The two-equation, low Reynolds number κ–ε turbulence model implemented in the TRAFLU code has undergone further validation through comparisons with a test case typical of indoor ventilation problems [3,4]. The test case, proposed by Nielsen [5] involves a benchmark calculation of isothermal turbulent flow in a ventilated room (with one inlet and one outlet) whose geometry is illustrated in ***Fig. 7.1***. The shape of the room and the relative size of the inlet and outlet ports are fixed as following:

$$H = 3\ m$$
$$L = 3\ H$$
$$h = 0.056\ H$$
$$t = 0.160\ H$$

A Reynolds number equal to 5000 and a kinematic viscosity of 1.53x10-5 m^2/s are used to evaluate the supply air velocity as 0.455 m/s. The calculations were carried out on a 50x32 non-uniform computational mesh. ***Figs. 7.2*** and ***7.3*** compare the TRAFLU results of velocity profiles and turbulence intensity, ($\sqrt{\kappa}/1.1$), with experimentally measured data at two locations, x=H and x=2H. Satisfactory agreement is generally observed between the TRAFLU predictions and the experimental results. The agreement near the upper solid wall can be improved by increasing the number of grid nodes in that zone.

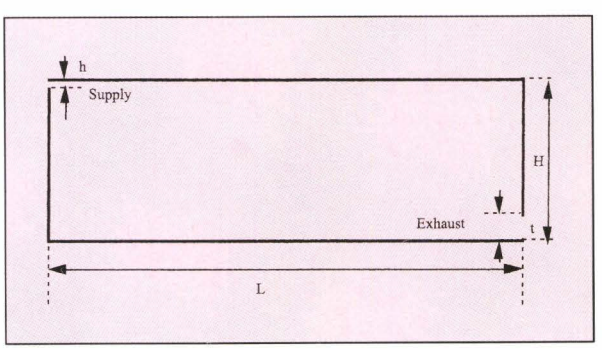

Fig. 7.1 Geometry of the two-dimensional Benchmark test case (Nielsen problem)

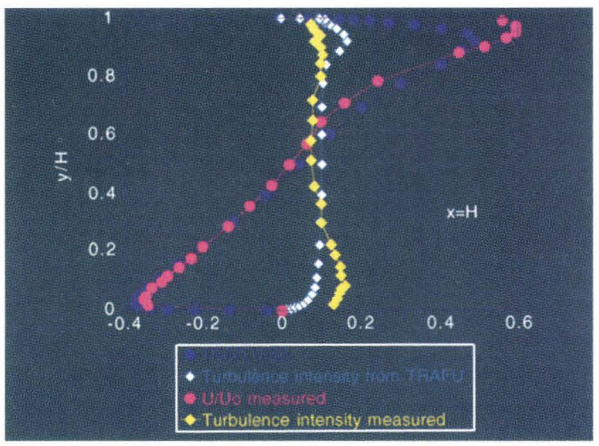

Fig. 7.2 Comparison of the computed and measured mean velocity and turbulent intensity in section x = H

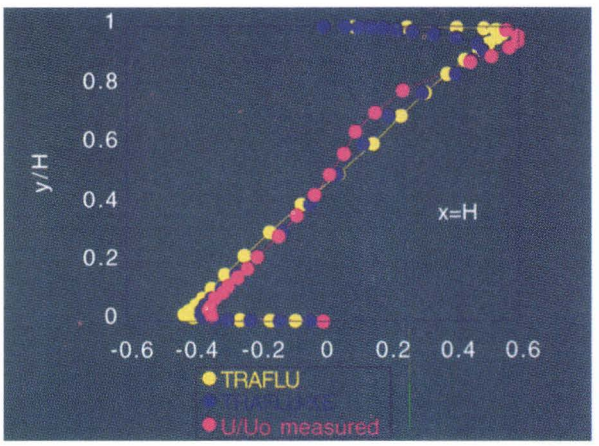

Fig. 7.4 Comparison of the mean velocity at x = H: mixing length versus κ–ε model

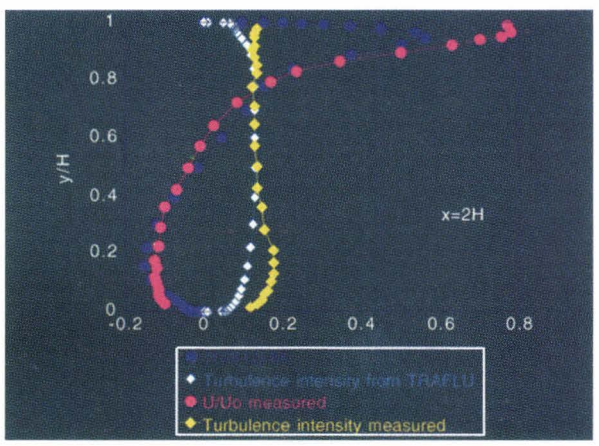

Fig. 7.3 Comparison of the computed and measured mean velocity and turbulent intensity in section x = 2H

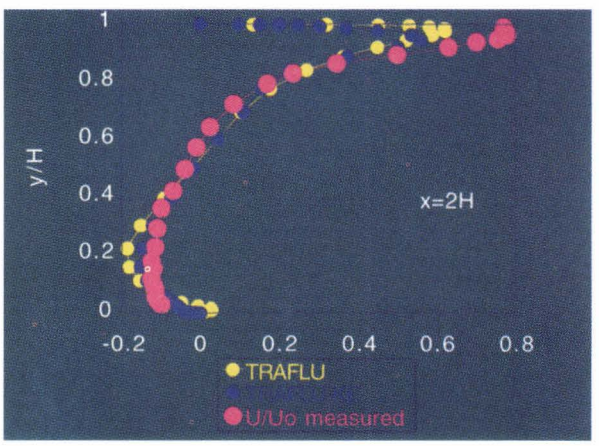

Fig. 7.5 Comparison of the mean velocity at x = 2H: mixing length versus κ–ε model

The Nielsen test case is also used to assess the Van Driest mixing length turbulence model implemented recently in the TRAFLU code [3, 4]. ***Figs. 7.4*** and ***7.5*** compare the velocity profiles obtained using TRAFLU with experimental results at two locations, x=H and x=2H. The TRAFLU results compare surprisingly well with measured data. However, further tests must be carried out before drawing definite conclusions with respect to utilising this model in general ventilation problems.

A simple model describing the transport of a passive gaseous pollutant (both the air and the pollutant have the same velocity) in a ventilated enclosure was developed. This involved implementing an additional transport equation representing the pollutant concentration [6]. A special treatment has been developed to avoid the occurrence of spurious negative concentration values during the calculations. The strategy adopted is similar to the one previously employed for treating negative κ and ε values [4]. At each iteration, the concentration is updated utilising an increment of the concentration value (due to the convection and diffusion treatment). This increment is the sum of the negative and positive components of the concentration:

$$\phi^{\kappa+1} = \phi^{\kappa} + \Delta\phi^{+} - \frac{\phi^{\kappa+1}}{\phi^{\kappa}}\,\Delta\phi^{-}$$

where ϕ^{κ} is the value of concentration at "κ"-th iteration.

$\frac{\phi^{\kappa+1}}{\phi^{\kappa}}$ is equal to 1 when the steady state solution is reached.

Nielsen's test room is used to examine the validity of this model. The two-dimensional enclosure in this case (see ***Fig. 7.1***) is assumed to be uniformly contaminated (clean air has the concentration value = 1.0) with the pollutant of interest whose initial concentration is Co=0. The clean air flows into the room at a velocity of 0.455 m/s. The numerical computation is started at the time t=0 when the air mixture in the room is motionless. The reason being that we are interested in studying the transient removal of a contaminant. ***Fig. 7.6*** shows the flow and concentration patterns for low Reynolds numbers (Re=30). The flow is laminar in this case. Low C values correspond to contaminated fluid, while C values close to 1 represent flow regions that have been effectively cleaned by the through flow. The results compare reasonably well with those of Lage and Bejan (1991); see ***Fig. 7.7***. ***Figs. 7.6a*** and ***7.6c*** show that the jet divides the room into two large corner cells such that the clockwise one (in the lower left region) is stronger. The constant concentration lines reveal a pollutant removal process in which the contaminated fluid (low C values) is displaced to the right. The Nielsen test room is currently being tested for high Reynolds numbers (Re=5000), taking into account two types of turbulence models: the Van Driest mixing length model and the two equation $\kappa-\varepsilon$ model.

The 2D-thermal square cavity with insulated top and bottom walls and vertical walls maintained at different, but constant temperatures, is also employed to test the passive pollutant model. This test case has been previously used to assess the two equation $\kappa-\varepsilon$ turbulence model [4]. The cavity has a hot left vertical wall and a cold right vertical wall. The temperature difference between the vertical walls is 5°C. The Rayleigh number of the fluid mixture (air) is set equal to 5×10^{10}, the Lewis number is 1.4, and the Prandtl number is equal to 0.71. Turbulence is modelled via a low-Reynolds number two-equation $\kappa-\varepsilon$ model. The aim is to study turbulent thermosolutal convection in a

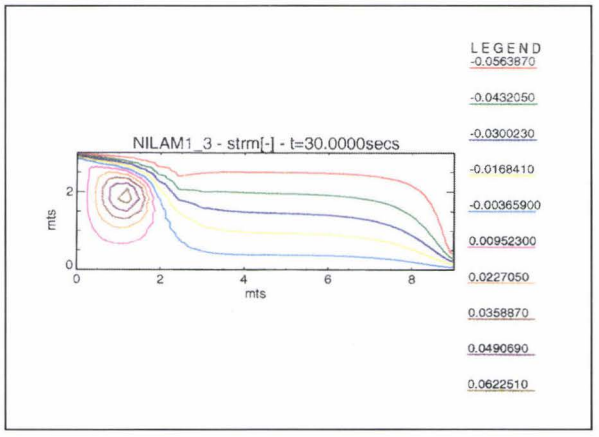

Fig. 7.6a Laminar flow (Re = 30): streamline contours

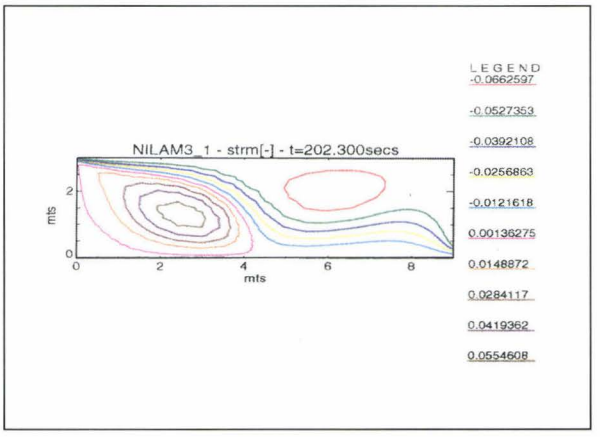

Fig. 7.6c Laminar flow (Re = 30): streamline contours

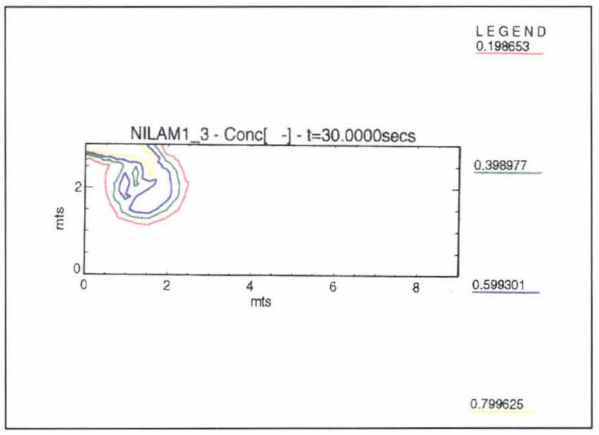

Fig. 7.6b Laminar flow (Re = 30): concentration contours

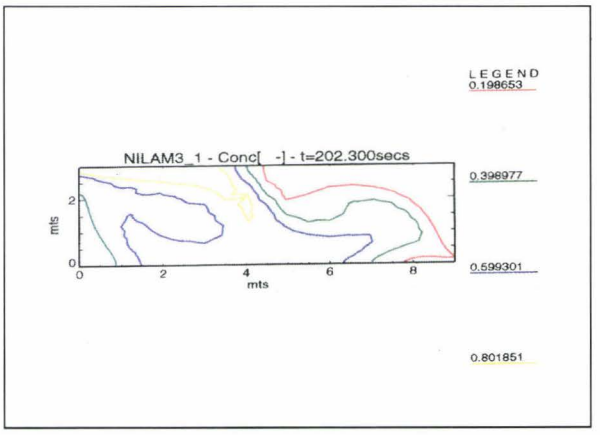

Fig. 7.6d Laminar flow (Re = 30): streamline contours

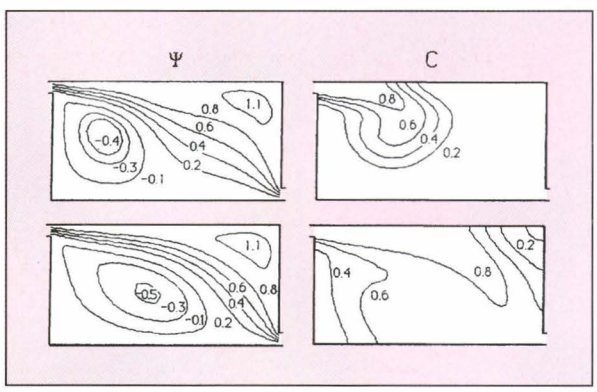

Fig. 7.7 Laminar flow (Re = 30): the evolution of the flow and concentration patterns at t = 70s and 350s respectively

thermally driven cavity whose vertical walls are maintained at different but constant concentration levels. ***Fig. 7.8*** shows the configuration of the thermal cavity. ***Figs. 7.9a-c*** show the streamline, temperature and concentration contours

$$\text{(with } T_{ref} = \frac{T_H + T_C}{2} \quad \text{and } C_{ref} = \frac{C_H + C_C}{2}\text{)}.$$

The pollutant concentration is diffused within the whole cavity through the combined effects of molecular and turbulent diffusions. The isotherm and iso-concentration profiles (***Figs. 7.9b*** and ***7.9c***) have very steep flows within the boundary layers adjacent to the vertical walls. Outside the boundary layers the profiles are almost horizontal. The isotherm and iso-concentration profiles are very similar since the Lewis number is near the value of 1.0. The concentration patterns of different pollutant species such as benzene, emitted by a latex paint on the vertical wall of a ventilated enclosure, are also being studied.

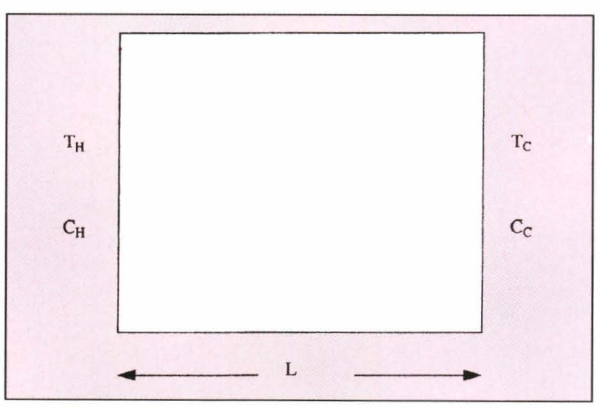

Fig. 7.8 Thermal cavity: the configuration studied ($T_H > T_C$, $C_H > C_C$)

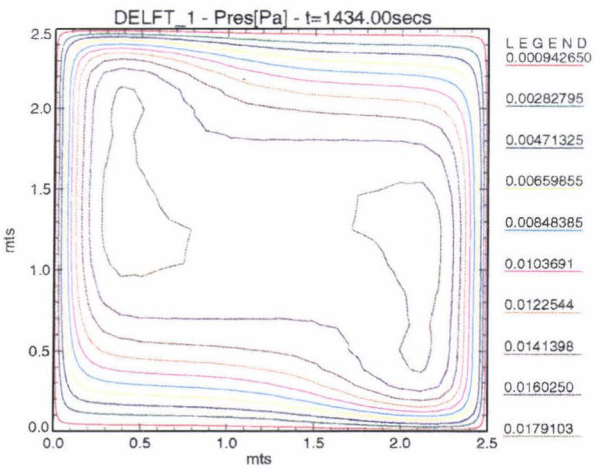

Fig. 7.9a Streamline contours

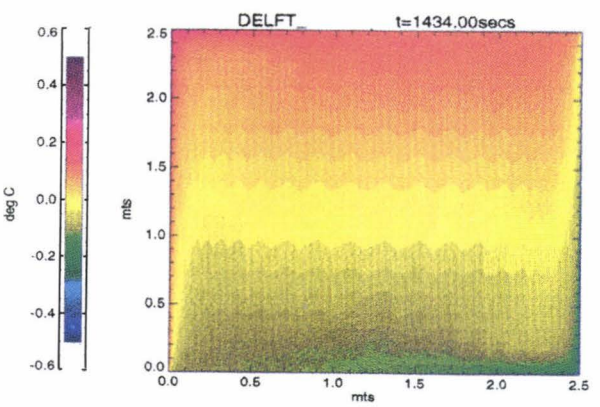

Fig. 7.9b Dimensionless temperature contours ($= \frac{T - T_{ref}}{T_H - T_C}$)

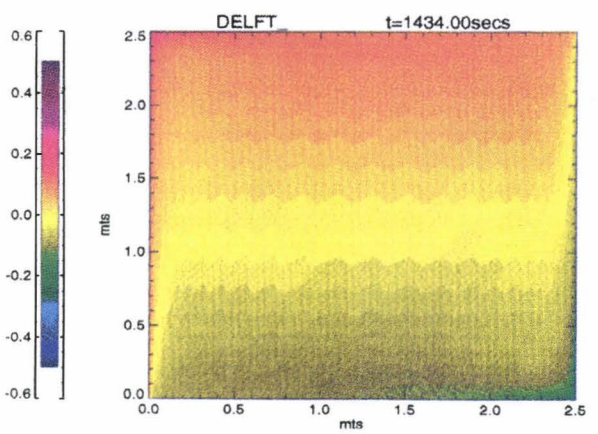

Fig. 7.9c Dimensionless concentration contours ($= \frac{C - C_{ref}}{C_H - C_C}$)

A review of Eulerian and Lagrangian (statistical and deterministic) models that have appeared in the literature for predicting the dispersion of solid aerosol particles in turbulent flows was carried out [8]. After consideration of the advantages and disadvantages of both types of models, the Lagrangian statistical model emerged as the successful candidate for combination with the TRAFLU code to form a new program to describe the motion of solid aerosol particles in confined turbulent flows. Based on the fact that we have at our disposal the atmospheric model (MONTECARLO), which has been developed at the Joint Research Centre [9], committed effort will be spent on applying the underlying strategy utilised in MONTECARLO to form the new TRAFLU-MONTECARLO program.

In the framework of a collaboration established with the French Institut National de Recherche et de Sécurité (INRS), a study to identify possible research topics that could be developed, in the future by the Institute for Safety Technology of the JRC, has been performed. According to the conclusions of the report presented by the INRS [11], the "axis of unification" for the research topics identified can be put under the label:" Towards safer workshops and equipment". In particular, the study recommends the development of a European network on the prediction/modelling of safety in the workplace environment (ventilation, noise, vibrations, lighting, heating,...) the basic objectives of which would be:

- to define standards of communication between design models, data bases and compatibility with classical CAD tools;
- to define a software framework host that will accept other computer programmes for the modelling of the environment of the workplace" via regulations at a European level. In addition the study recommends the development of large scale experimental installations to identify design rules for safe workshops and to permit the validation of the models.

References

[1] DONEA J., GIULIANI S. - A proposed strategy for the numerical simulation of thermal discharges into coastal waters of the sea, Technical Note I.89.84, August, 1989

[2] NGUYEN H. - A Petrov-Galerkin formulation based on the Least Squares finite element concept for multi-dimensional advection-diffusion equations: Application to natural convection problems, Technical Note I.92.25, March, 1992

[3] NGUYEN H., AL-KHUDHAIRY D. - A fractional-step finite element method for the mathematical modelling of turbulent flows in room air motion problems, paper submitted for presentation at Ventilation '94, Stockholm, 5-9 September, 1994

[4] NGUYEN H. - Finite element calculations of incompressible turbulent flows, Technical Note I.93.1710, December, 1993

[5] NIELSEN P.V. - Specification of a two-dimensional test case, Research item I.45, November, 1990, ISSN 0902-7513-R9040

[6] AL-KHUDHAIRY D. - Two-dimensional predictions of Indoor Air Pollutant Transport and Dispersion, Technical Note I.94.51, April 1994

[7] LAGE J.L., BEJAN A. - Efficiency of transient contaminant removal from a slot ventilated enclosure, Int.J. Heat Mass Transfer, 34(10), pp 2603-2615, 1991

[8] AL-KHUDHAIRY D. - Particle Dispersion in two-dimensional confined turbulent flows: A survey of models, Technical Note I.93.152, November, 1993

[9] GRAZIANI G., MOSCA S. - Different schemes for turbulence in a Lagrangian particle model; Computer techniques in environmental studies IV, P. Zannetti (ed.), Computational Mechanics Publications, 1991

[10] NGUYEN H. - A Petrov-Galerkin least squares finite element algorithm for prediction of room air motion: "Indoor Air '93", Int. Conf., Helsinki-Finland, July 1993

[11] ARBEY H., FONTAINE J.R., LOVAT G., CICOLELLA A. - Research axes that could be developed by the STI in the area of the environment of the workplace: Towards safer equipment and workshops; INRS Report D.T. - N/SAE-2092/HAy, July 1993

1.8 HUMAN CAPITAL AND MOBILITY PROGRAMME

Applied mechanics unit

In response to a call for proposals of the new Commission's programme on "Human Capital and Mobility" (HCM), proposals were submitted for the inclusion of the reaction-wall facility ELSA and the Large Dynamic Test Facility (LDTF) in the "Access to Large Scale Facilities" chapter of the HCM programme. Both proposals were accepted by the HCM management committee and access to the ELSA facility has already been offered in 1993 to 3 post-doctoral research fellows and to working parties involved in large-scale structural tests associated with pre-normative research. Funding for the access to LDTF will be available in 1994 and a number of users interested in transient dynamic testing of structural materials and industrial components have already been identified.

Within the framework of the HCM programme, the setting-up of a cooperation network involving 19 European laboratories has been proposed with the aim of covering through experimental and analytical investigations the priority needs for pre-normative research in support of Eurocode 8 identified by Directorate General III of the Commission. The network activity started in June 1993 after signature of the relevant contract with Directorate General XII. As part of the network activity, the ELSA team will be involved during 1994 in the execution of large-scale tests on irregular bridges.

2 SUPPORT TO COMMUNITY POLICIES

2.1 SAFEGUARDS

The Safeguards Support Programme aims at assisting the Euratom Safeguards Directorate (ESD, DG XVII, Luxembourg and the International Atomic Energy Agency (IAEA)) in the implementation of safeguards instrumentation required in the frame of both the Euratom and the Non-Proliferation Treaties for Special Nuclear Material. The objectives of this work are:

- *to develop, test and implement reliable non-destructive assay (NDA), instruments, associated data acquisition systems, interpretation models and software for user friendly applications of the various techniques,*
- *to provide after sale services and training to both inspectorates.*

The support to the Commission activities by the STI are subdivided in two parts:

- *support to ESD*
- *support to IAEA (through DG I).*

Both support programmes are structured following specific task sheets describing the activities pertinent to each task and the relevant programme achieved. The subjects of ESD and IAEA supporting activities are listed in ***Table 8.1*** *and* ***8.2****. Only those for which significant progresses have been achieved during 1993 are illustrated here.*

2.1.1 SUPPORT TO ESD

Training

The complete "menu" of courses held by the STI is reported in ***Table 8.1***.

During 1993 eleven training courses have been held as follows: Each of TRG-1, TRG-2, TRG-3, TRG-8 have been given twice and each of TRG-4, TRG-5 and TRG-10 has been given once.

Table 8.1 PERLA training "MENU"

TRG-1	Verification of uranium enrichment by gamma ray spectroscopy
TRG-2	Determination of plutonium isotopic composition by gamma ray spectroscopy
TRG-3	Passive neutron measurements
TRG-4	Active neutron measurements
TRG-5	Physical Inventory Verification (PIV) at an HEU facility
TRG-6	PIV at a Pu(MOX) facility
TRG-8	PHONID measurement of U235 mass
TRG-9	Introductory applied statistics for safeguards
TRG-10	Basic physics for non destructive assay of nuclear material

TRG-10: basic physics for non-destructive analysis of nuclear material

The subjects of the course were:

- Atoms and nuclei,
- Radioactivity, types of radiation,
- Nuclear reactions,
- Interaction of radiation with matter,
- Attenuation process,
- Radiation detection methods,
- Properties of measurement methods and applications,
- Measurement aims and measurement errors.

The course was provided with extensive demonstrations and experimental exercises.

TRG-3: passive neutron measurement training course

Two courses on Passive Neutron Measurement were held at Ispra during 1993. In each course six participants of ESD Luxembourg attended. The subjects of the course were:

LECTURE: Nuclear properties of uranium and plutonium isotopes. Principles of neutron detection.

Electronic processing of detector signals. Neutron detection heads, neutron pulse train. Principles of coincidence counting.

LABORATORY: Electronic processing of pulses. 3He proportional counter. Neutron slow down and detection. Manual operation of the electronic controller. Characterisation of the HLNCC, PUPA, ISCC. Demonstration of the PECC programme [1]. Assay of Plutonium oxide with PECC. Assay of Plutonium oxide cans and pins with HLNCC, PUPA, ISCC. Effects which influence the measurements.

TRG-4: active neutron measurement training course

One course on Active Neutron Measurement was held at Ispra during 1993 [2]. This course was intended to teach inspectors on the use of the AWCC and PHONID (*Fig. 8.1*) used by Safeguards Inspectors to estimate the uranium 235 content in different uranium samples.

In the PERLA laboratory the following activities were performed: Demonstration of the instruments. Characterisation of the AWCC and PHONID. Demonstration of the AECC programme. Assay of Plutonium oxide with AECC. Assay of Uranium oxide cans, metallic and MTR elements with AWCC in configuration FAST and THERMAL-MTR and PHONID. Effects which influence the measurements.

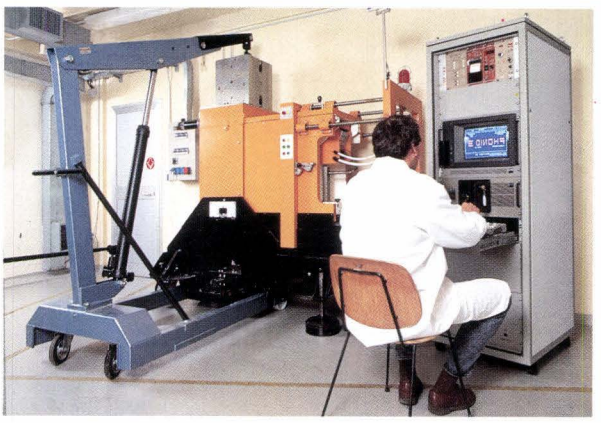

Fig. 8.1 The PHOto Neutron Interrogation Device: PHONID 3b

Support to ESD in the field of NDA and instrument development

Active tasks in progress are listed in *Table 8.2*.

Table 8.2 List of ESD active tasks in progress by December 1993

NDA-3.4	Construction of a PHONID 3bis
NDA-6.3	Consultancy in neutron physics
NDA-7.3	Consultancy in gamma spectrometry and technical assistance
NDA-7.4	Upgrading of enrichment meter software
NDA-10	Improvement of MTR gamma scanners
NDA-16	Software for active and passive neutron correlation instruments
NDA-17	Data base for DA/NDA measurements
NDA-20	Neutron and gamma software support
NDA-22	Advanced Plutonium Pin counter
NDA-24	Unattended measurement station
NMA-6	Application of the D-statistics

NDA-3.4: PHONID 3b

Two PHONID 3b devices are installed for permanent use at BNFL Springfields (GB) and SIEMENS-RBU Hanau (Germany). During 1993 full support has been given to ESD to the PIV measuring campaigns by ENUSA (E), FBFC (B), BNFL (GB) and Siemens (G) entailing installation of the mobile device (*Fig. 8.1*), preparation of Sb-source capsules, loading-unloading Sb-sources and calibration of devices.

NDA-7.3: consultancy in gamma spectrometry and technical assistance

Under this general task two different activities have been carried out:

- A new generation of miniature multichannel analysers is coming on the market: it is the task of STI to test those new products in support to ESD, to show their performances and possible uses for safeguards inspections. Amongst others PERLA staff have tested two new analyser systems from Silena and Canberra with satisfactory results.
- Testing and development of room temperature gamma detectors for safeguards applications.

MTR spent fuel verification

The aim is to allow measurement of important fission products in individual MTR fuel elements under water in a storage pond without moving the elements. The detectors that have been tested and the results obtained are shown in *Table 8.3*.

Table 8.3 Summary of results of tests executed at room temperature by small gamma detectors

Type	Active volume	Weight and size of detection head	Efficiency in arb. units (600/800 keV)	Energy resolution
NaI	30*30*30 mm^3 with photomultiplier tube	8 kg 200 mm	ca 10	6.8%
CsI	10*10*10 mm^3 with Si photodiode + semiconductor preamplifier	< 100 g 20*20*120 mm^3	1	as NaI
CdTe	5*5*1 mm^3 with semiconductor preamplifier	< 200 g 20*50*120 mm^3	0.03	as NaI
CdTe high resolution	5*5*1 mm^3	(prototype)	0.001	4 keV

The conclusion drawn from this part of the study were the following:

One should concentrate on CsI detectors, since NaI are too large and CdTe have too low efficiency. Next steps are:

- choice of an optimum preamplifier of an optimum scintillator size (10*10*10... 15*15*30 mm^3) and photodiode type,
- optimization of a detection head, consisting of an (air filled) collimation tube of a ca. 1200 mm long, 12 mm dia. tube, some lead shielding and detector and preamplifier housing with a total weight of less than 1.5 kg,
- test measurements in spent fuel storage ponds.

First preliminary spectra taken under water in the spent fuel pond with a CsI detector, without any optimization and without special shielding show the possibility of the measurements (^{137}Cs and very weak ^{134}Cs lines). The results are shown in ***Figs. 8.2*** and ***8.3***. A spectrum of ca. 20 years old spent fuel measured in air with the CsI detector shows ^{137}Cs and ^{154}Eu gamma lines (***Fig. 8.4***).

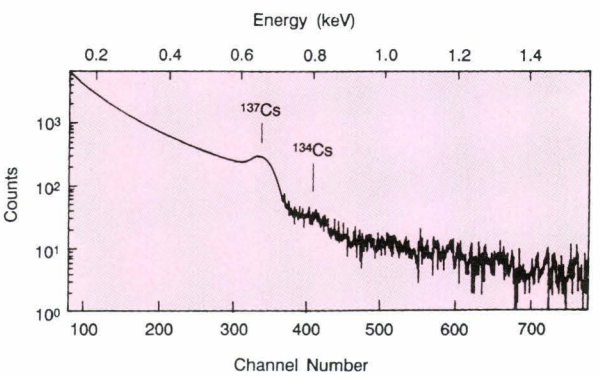

Fig. 8.3 MTR spent fuel

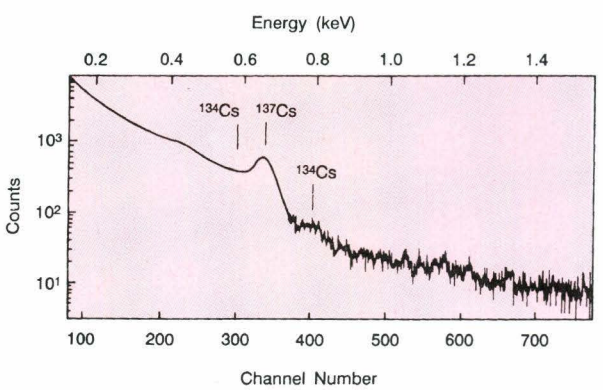

Fig. 8.2 MTR spent fuel, under water, 1st test measurement, without special set-up, no shielding

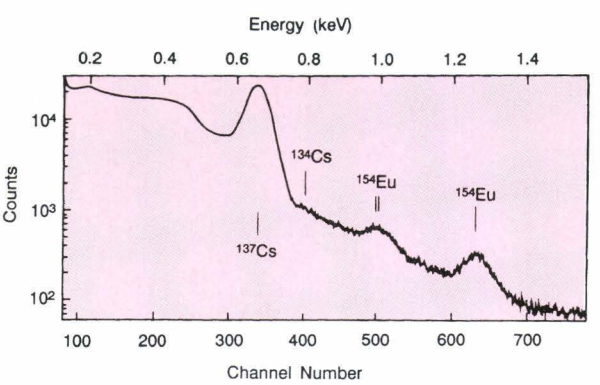

Fig. 8.4 PWR spent fuel, 20 years cooling time, measurement in air

Uranium enrichment measurements

The aim is eventually to replace the heavy NaI detectors at least in some applications. First test results were similar as in *Table 8.3*. Again the conclusion was to look carefully on CsI detectors. Following the work for the spent fuel application and using the experience from there, a small and light detector head could be studied for later replacement of today NaI detectors. Other conclusions were:

- all room temperature detectors cannot replace the high resolution spectrometers for plutonium gamma radiation measurements during the next few years,
- for gamma ray measurements by fixed installations (eg. monitoring spent fuel transport ways) CsI detectors of somewhat larger size (efficiency) seem to have the best properties (electronic stability, low power, low voltage).

NDA-16: software for active and passive neutron correlation instruments

The PECC [1] and AECC version or AWCC software package were successfully used by Euratom inspectors in field, during the training course and in PERLA. A continuous support is provided to Euratom inspectors for difficulties or problems that they can have in the use of these programs, and in the interpretation of the results. A user manual for the AECC version for AWCC has been provided to ESD [2]. The AWCC part 2, for fuel assembly measurements is checked by inspectors in field. Only small modifications were required to better meet their needs.

NDA-17: data base for DA/NDA measurements

Every year the ESD carried out a large number of chemical analyses (DA) as well as gamma and neutron measurements (NDA) of nuclear material throughout the community member countries. The measurement results collected by ESD need to be organised in upgraded databases facilities to permit assessment of equipment, training and measurement procedures. Under this task, STI must provide the database system and the necessary applications as a turnkey system. The system is being implemented as a pair of databases (DA, NDA) linked to a network. As well as communicating with each other for data exchange, each of the two subsystems must be integrated into the routine activities of DA and NDA measurement so that data flow from inspection activities is automatic.

DA system

As well as providing statistical data analysis for performance evaluation, the DA subsystem is also designed to provide complete management of all the administrative activities carried out by Commission inspectors taking samples in plants and sending them to chemical laboratories for analysis. The design of the DA database and its applications has been completed and work is well advanced on the programming of the system. The first version ready for testing is expected to be available in the first quarter of 1994. The final version will be installed for routine use in the ESD by the middle of 1994.

NDA subsystem

Performance evaluation of NDA measurement systems is the primary function of the NDA subsystem. The system is designed to receive inspection results from a wide variety of instruments which store their results on dedicated PCs. The "headquarters" system will also provide the infield systems with the latest versions of calibration curves and estimates of measurement uncertainty. The performance evaluation functions in the system include:

- gamma spectrum analysis tools,
- evaluation and testing of variance matrices for gamma based measurements of Pu isotopic composition,
- testing for bias in gamma based measurements,
- creation and assessment of calibration curves,
- quantification of measurement uncertainty in neutron measurements (ANOVA etc.).

The design of the headquarters NDA database system is being conducted in parallel with a review of the infield software of instruments so as to lead to a fully integrated data management system for NDA. The detailed design of the NDA system will be completed and documented early in 1994 and the first prototype for testing will be available in autumn 1994.

NDA-22: advanced plutonium pin counter

An instrument for Pu mass assay of MOX fuel pins (PUPA: *Fig. 8.5*) has been designed, manufactured, and calibrated at JRC Ispra. The instrument was tested with MOX fuel pins at the PERLA laboratory. During the TRG-3 passive neutron measurement training courses and the Physical Inventory Verification exercise (PIV) the pin counter was used in conjunction with the PECC software in the same manner as the other instruments of the HLNCC family.

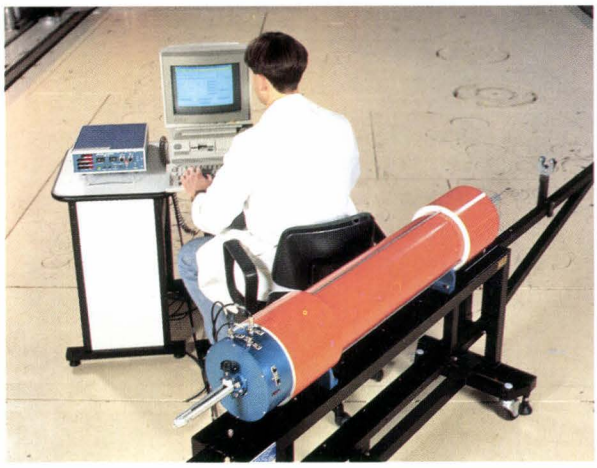

Fig. 8.5 The Plutonium pin counter PUPA

An advanced pin counter is presently being designed. The new design will accommodate an improved detection capability by means of a two ring 3He detector arrangements. A flat axial response is achieved by application of end-plugs and cadmium liners. This feature will allow an absolute determination of the Pu mass in the MOX pins when used together with the latest generation of frequency analysers.

NDA-6.3: consultancy in neutron physics

This task is conceived to give support to ESD and/or to other task sheets as far as neutron physics models or calculations are concerned. During 1993 the work has been concentrated in particular on the calculations of the neutron coincidence collar, an instrument used to monitor low enriched uranium (LEU) fuel assemblies. These calculations are required also by the UMS (Unattended Monitoring System) under elaboration at the STI (see task NDA-24).

The ESD has to determine the amount of fissile material in fuel assemblies by NDA methods. The standard procedure for this purpose is the neutron coincidence counting technique, which allows quantitative conclusions on the amount of fissile material (U235) based mostly on empirically established calibration curves. A Monte Carlo simulation of the experiment could predict the expected counting rates for the TOTALS and REALS. The following procedure was adopted: based on the operator declaration the expected counting rates are calculated, the actual measurement of these counting rates are performed and compared with calculations. A careful error analysis of both quantitites helps eventually in making the decision on the acceptance of the declaration.

The exact theoretical formulas for the relevant counting rates are rather complex, however, it is possible to reduce them to simple. expressions in almost all practical cases. These reduced working expressions contain some parameters characterising the combined detector-fuel system, and the Monte Carlo calculation has to determine the values of these parameters (e.g. time decay constant, average value of the squared sensitivity).

A detailed analysis of the calculations leads to a modification of the standard Monte Carlo procedure. The new aspect is the following. In the standard procedure n-starting points are chosen for the source neutrons from some spatial distribution and from each starting point one neutron is started . In the new approach the total effort of running n- histories has to be divided into spatial starting points and starting histories from each point. This modified starting procedure results in a modified procedure for the calculation of the errors, especially of the errors for REALS.

An example (Passive Case: no external source)

The above mentioned programme was applied to the following configuration (for more details see [3]). A fuel assembly consisting in a square lattice of 17x17 fuel pins was surrounded by 4 detectors banks (see ***Fig. 8.6***).25 fuel pins were initially empty

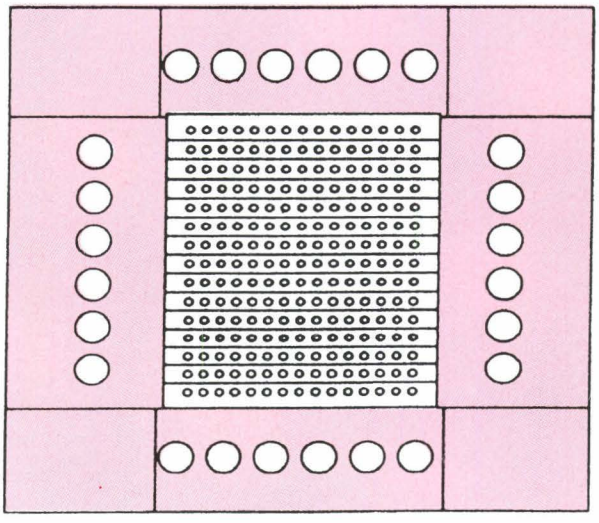

Fig. 8.6 Geometry of the neutron collar (17x17 fuel pin assembly surrounded by 4 detector banks)

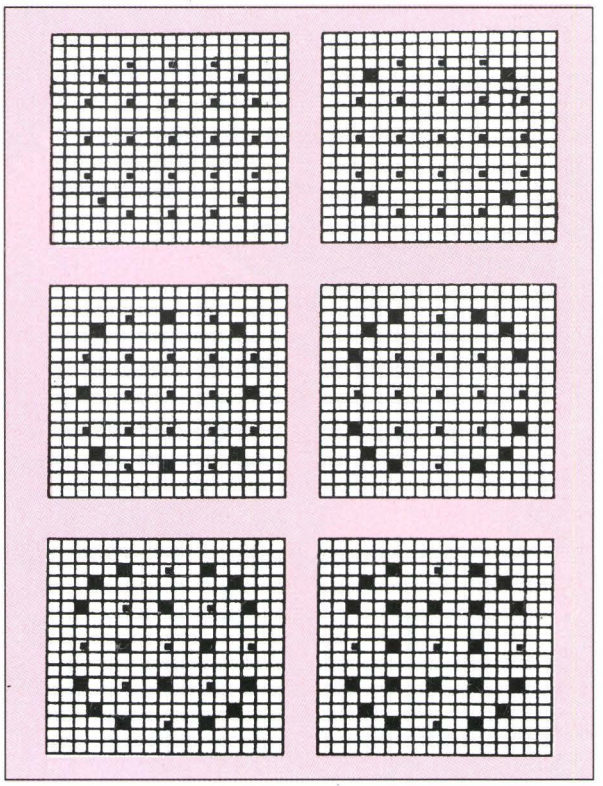

Fig. 8.7 Clusters of Boron-Carbide rods inserted into initially empty pins

and then progressively filled with 4,8,12,16,20 poison rods (*Fig. 8.7*). The fuel was MOX (mixture of 97.3% UO_2 and 2.7% PuO_2) of the isotopic composition is given in *Table 8.4*. The results of the calculations for this configurations are represented in *Table 8.5*.

The results of the calculations for this configuration are represented in *Table 8.5*.

In STEP II 80000 particles were used for the TOTALS and Pu consisted of Pu235, Pu238, Pu239. In STEP III 5000 starting points and 150000 particles were used for the calculation of f and W^2. *Figs. 8.8* and *8.9* show the calculated behaviour of the relative values of the TOTALS "C" and REALS "R" compared with experimental results. The relative errors of the TOTALS are provided directly by the MCNP(Monte Carlo Neutron Photon) run of Step II.

NDA-24: Unattended Monitoring System (UMS)

Modern fuel fabrication plants are becoming more and more automated. This implies that safeguards is progressively based on automated techniques too. The reasons are the following:

Table 8.4 Fuel specification for the VENUS mock-up experiment

isotope	U234	U235	U235	U236	Pu238	Pu239	Pu240	Pu241	Pu242	Am242
(v/w)%	0.016	2.002	0.013	97.97	0.068	79.247	17.1977	3.044	0.445	0.075

Mass loading [$g.cm^{-1}$]: Pu tot. 0.1424, U235 0.1026,
Fuel diameter [cm]: 0.902, cladding SS 304,
Fuel length [cm]: 50.0, diameter [cm]: 0.978, thickness [cm]: 0.038.

Table 8.5 Results of the '3 step' calculational procedure for the VENUS mock-up

STEP I	STEP II					STEP III	
	case	total	Pu 235 10^2	Pu238 10^2	Pu239 10^2	f	W^2 x 10^2
Y tot. = 48.91	1	0.13948	6.483	7.129	1.332	0.625	2.511
	2	0.13853	6.239	7.192	1.288	0.627	2.423
	3	0.13695	6123	7.265	1.271	0.631	2.398
$\Sigma u\ Yu^{SF}$ Pu = 60.331	4	0.13415	5.972	7.336	1.226	0.633	2.366
	5	0.13385	5.878	7.460	1.219	0.632	2.3322
	6	0.13290	5.855	7.537	1.207	0.633	2.332

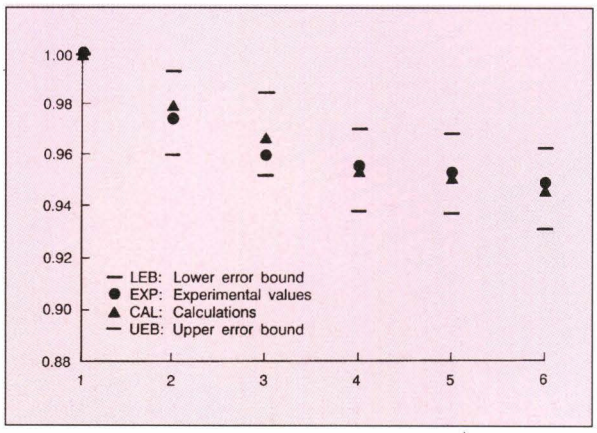

Fig. 8.8 Relative values of the "Totals" for different poison rod-clusters. The indicated error bars give the evaluated uncertainty of the calculations

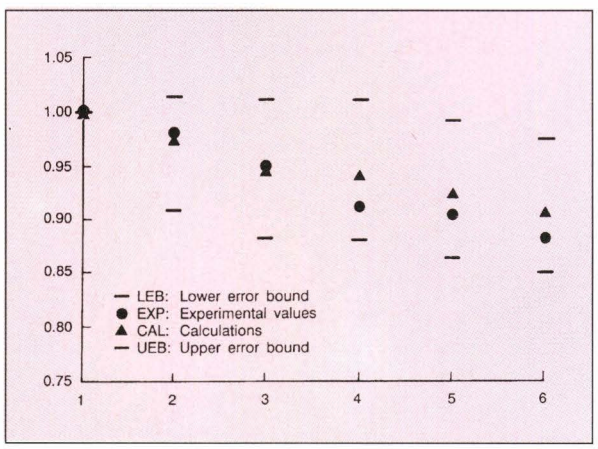

Fig. 8.9 Relative values of the "Reals" for different poison rod-clusters

- savings on resources,
- reduced chance of human errors,
- increased speed,
- integration of NDA and C/S systems,
- reduced radiation doses to inspectors.

Scope of the Unattended Monitoring System project

Low enriched uranium (LEU) fuel fabrication plants are one of the locations in the fuel cycle where increased use of automation can improve cost effectiveness in safeguards. This particular project is aimed at providing a flexible unattended measurement station for verification of fuel assemblies of both PWR and BWR types. This instrument combines neutron coincidence counting for verification measurement with video surveillance to automatically read the fuel assembly identity. The development is being carried out in collaboration with ISEI which provides the video subsystem. The unattended system will allow the Euratom Safeguards Directorate to implement a 100% verification of fresh fuel assemblies in all LEU fabrication plants in the Community with limited manpower costs. The complete project will cover the design, manufacture, testing and implementation of such systems. The work reported here, which was carried out during 1993, refers only to the completion of the detailed design study. The unattended measurement station will consist of a fixed structure supporting the fuel element to be scanned (*Fig. 8.10*), a neutron collar of new design with an automated source loading mechanism (*Fig. 8.11*) and electronic racks holding control hardware along with the control and analysis software.

Functions and software architecture

A general overview of the software architecture is given in *Fig. 8.12*. This shows the unattended station software as four communicating subsystems which are:

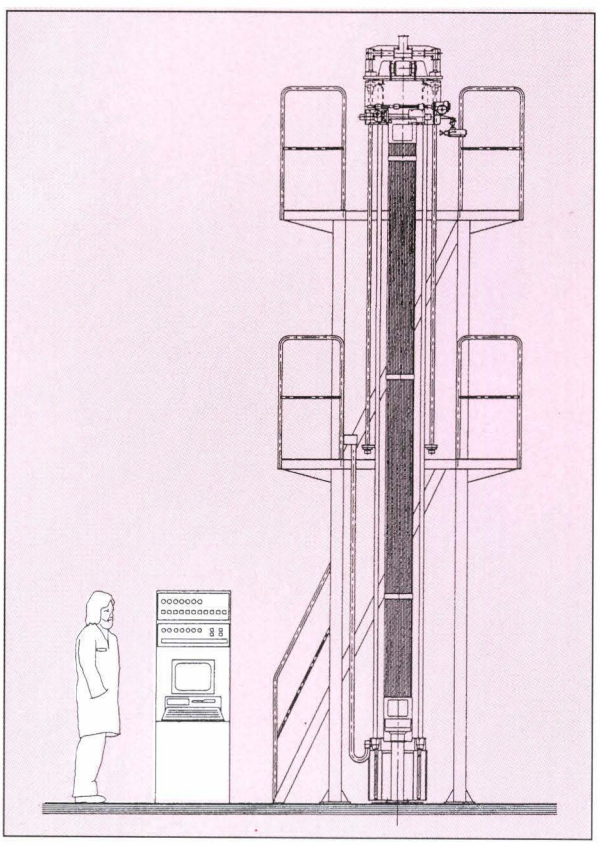

Fig. 8.10 Unattended Monitoring System (UMS) for Low Enriched Uranium (LEU) fuel elements

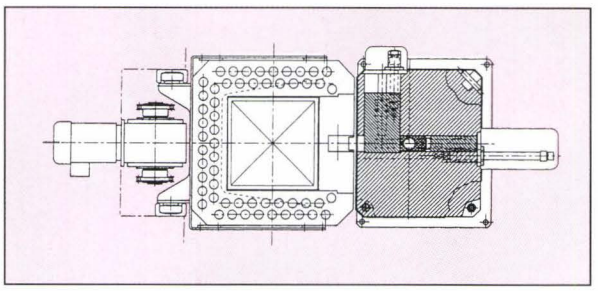

Fig. 8.11 New collar system designed for the UMS

- the video identification system which reads and interprets the assembly identification number, supplies this information to the NDA system and manages the storage of raw video data,
- the mechanical control system which implements and supervises all the activities of collar position and movement source loading and unloading, the functioning of assembly head clasps, as well as the presence or absence of an assembly,
- the neutron measurement system which collects and stores the neutron measurement raw data and carries out realtime evaluation in an automatic mode, if required,

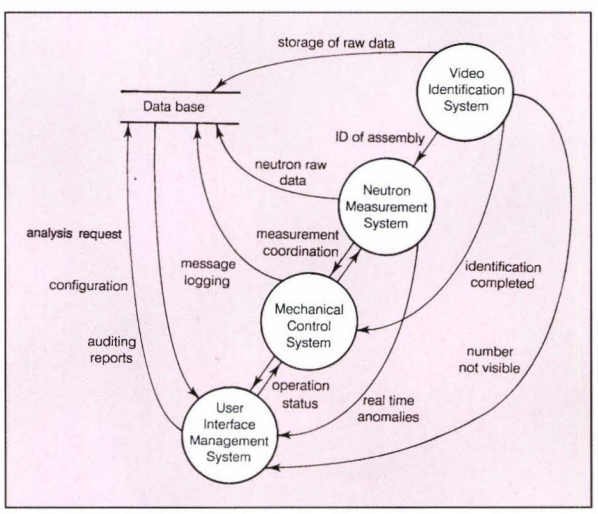

Fig. 8.12 UMS: general software architecture

- the user interface management system which provides communication with the facility operator for loading and unloading of assemblies as well as the inspector user interface for measurement, auditing and configuration activities.

In addition to these four software subsystems, the system employs a database made up of:

- video data archive,
- collar measurement data archive,
- operator declarations archive,
- anomaly message log,
- a variety of libraries specifying measurement interpretation and configuration of the automated functions.

NMA-6: application of the D-statistic

The expression "D-statistic" refers to the types of data evaluation used in nuclear materials auditing to provide an audited estimate of the material balance (Pu or U235). This kind of data analysis combines inspectors verification measurements with the facility operators accountancy declarations to provide an estimate of the material balance and of its uncertainty. The objectives of this task are to provide the ESD with:

- a comparison of different types of approaches, i.e. classical D-statistic, ratio statistic (R),
- specification of algorithms for implementing R&D for a complete material balance taking account of the measurement history of the material,
- consultancy in identifying the most appropriate data processing approach for implementation as a part of routine inspection activities.

A report [4] has been forwarded to ESD covering each of these topics and discussions are continuing in order to define the appropriate data processing strategy. Some of the findings of this task are also published in [5].

2.1.2 SUPPORT TO IAEA

In the field of support to IAEA two NDA tasks, A00515 and TB00388 and two tasks on solution mass verification linked with the TAME laboratory namely OA2-01 and OA2-03 are currently being pursued (*Table 8.6*).

Table 8.6 List of IAEA active tasks by December 1993

TB 00388	Physical inventory verification(PIV) training course in PERLA facility
EUR A 00515	Absolute emitting rates and x-rays from PERLA standards
EUR 91/0A2-01	Solution mass verification technology in TAME laboratory
EUR 91/0A2-03	Nuclear material solution accounting and verification training

TB 00388: PIV course in PERLA facility

The PIV training course was held in Vienna and in PERLA during June 1993 with the participation of eight IAEA inspectors and instructors from IAEA, LANL and JRC. It is expected to repeat the same course in 1994.

EUR A 00515: absolute emitting rates and x-rays from PERLA standards

High resolution gamma spectra of plutonium show prominent fluorescent x-rays. Modern gamma spectrum evaluation codes give the possibility to quantitatively evaluate the peak areas even for the complicated Pu spectrums. Thus, the K x-ray peak of Pu could be included into the characterisation of Pu bearing materials, e.g. for the determination of Pu concentration in solids or solutions.

The excitation of fluorescent x-rays is a rather complex process. K-shell electrons can be excited by alpha and gamma radiation coming from the different radioactive nuclides of the sample. The excitation of atoms depends on their position within the material, since the exciting radiation fields are inhomogeneous, especially close to the surfaces of the materials, where the escaping (and measurable) x-rays are originated. To evaluate the contribution of the alpha particles and the gamma rays in the fluorescence process the K-shell excitation and x-ray emission was calculated.

As a first result it could be stated that the contribution of the alpha radiation to the K-shell excitation can be neglected. The calculation of the gamma ray excitation takes into account all individual gamma lines of each isotope and results in the excitation power if the Pu isotopes 238 Pu, 242 Pu and of 241 Am. Also based on the single gamma lines the K-shell excitation and the x-ray emission in material mixtures are calculated, including special geometric corrections for the case of 'enrichment measurement geometry'.

The results of the calculations have to be compared with experimental data measured at a large variety of Pu samples with different isotopic compositions and in different chemical compositions. Measurements of well characterised PERLA samples showed good agreement with the calculations (*Fig. 8.13*) encouraging further experimental work in this direction especially the extension to solutions.

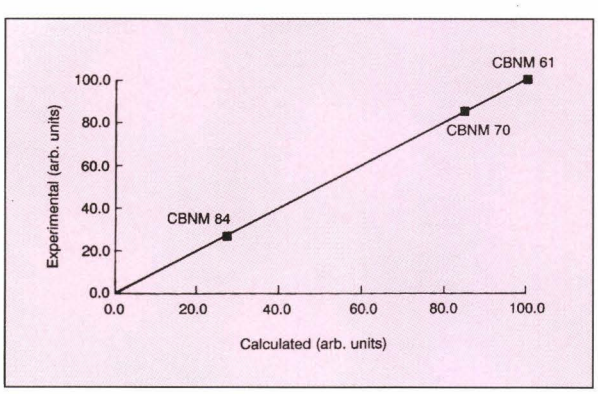

Fig. 8.13 X-ray intensities of Pu-samples

EUR 91/0A2-01: solution mass verification technology in TAME laboratory and EUR 91/0A2-03

Nuclear material solution accounting and verification training

The TAME laboratory currently installed at the JRC Ispra site is dedicated to the safeguards experimental

programme for studying the problems related to the measurement of volume and mass of liquids in the nuclear industry. In cooperation with the IAEA and reprocessing plant measurement experts, validation campaigns of volume/weight measurements for input process and product tanks will be carried out.

Last year the JRC organised a meeting of experts [6] with the scope to review the needs of the nuclear industry in this particular technology area, to collect suggestions to the possible activities of TAME and finally to explore the feasibility of bilateral and/or multilateral collaborations. The information presented by the experts during the meeting, which had been presented in the form of a working document, was very useful for determining the configuration of the laboratory. These suggestions were implemented during the current year and demonstrated to a second meeting of experts and potential users at Ispra, which was convened in order to discuss the future activities of the laboratory [7]. The meeting was well represented by operators, nuclear inspectorates and scientific research establishments. An active demonstration of various features of the Laboratory was given including, in joint collaboration with BNL-DOE, a demonstration of the portable pressure volume authenticator. The results of the meeting will be reported in a working document which will include the areas of interest expressed by the various experts and an indication to what extent they are prepared to contribute. The areas of interest can be summarised as follows:

- operational, process variables,
- methods/instruments testing,
- data evaluation development,
- test of procedure,
- verification procedures,
- training.

A complete and detailed description of the TAME facility and the R&D on volume measurements were presented at the ESARDA [8] and INMM [9] conferences respectively. The facility is now undergoing a series of tests, including the calibration of the vessels in both the continuous and incremental mode and at the same time checking the performance of the various installed instrumentations of the sub-systems (off-gas, pneumercators, etc.).

References

[1] VOCINO V., et al. - PECC Algorithms and Procedures, Technical Note 93,46, April 1993

[2] VOCINO V., et al. - Active Euratom coincidence counter (AECC), User's Manual, April 1993, to be published as EUR report

[3] VERRECCHIA G.P.D., et al. - Calibration of the neutron coincidence collar for the assay of fuel assemblies containing thermal neutron poison, 13th ESARDA Symposium on safeguards and nuclear material management, Avignon, France, 14-16 May, 1991

[4] FOGGI C., HUNT B.A. - The TAME laboratory installation at the JRC Ispra site of the CEC; 15th annual symposium on safeguards and nuclear material management, ESARDA, Rome, Italy, 11-13 May, 1993

[5] FOGGI C., HUNT B.A. - R&D on the volume mesurements of liquids in the TAME laboratory, 34th annual meeting of the Institute of Nuclear Material Management, Phoenix USA, July 1993

[6] FRANKLIN M. - Implementation of Difference Statistics in Safeguards, Technical Note I.93.103, JRC Ispra, 1993

[7] FRANKLIN M. - A Comparison of D Statistic Approaches; Proc. of 34th Annual Meeting of the Institute of Nuclear Materials Management, Phoenix, USA, July 1993

[8] 1st meeting on R&D on volume and mass determination of liquids in tanks used in nuclear materials processing installations, Working Document, SPI 92-27, Ispra, Italy, 25-27 April, 1992

[9] 2nd meeting on R&D on volume and mass determination of liquids in tanks used in nuclear materials processing installations, Ispra, 6-7 October, 1993

2.2 PARALLELISATION OF LARGE COMPUTER CODES

The Safety Technology Institute is applying, developing and modifying a number of large computerised models related to safety technology in support to DG XIII. The models apply various types of numerical methods of which the main groups are based on Finite Elements or Finite Volumes. The algorithms are often iterative with convergence criteria relating various parts of the codes mutually to each other.

The codes have been developed over many years with subunits elaborated by different groups - often in collaboration with external agencies. An enormous amount of resources has been invested in the codes. The present sequential hardware is considered insufficient for the long term requirements of the scientists of the STI. They have an unsatisfiable hunger for CPU power. This is caused by:

- *the models are steadily growing in complexity,*
- *more detailed grid for the definition of the problem geometry is desired,*
- *larger physical space covered by the models (e.g. in ocean modelling),*
- *more parameter studies are desired,*
- *animation and real-time simulations are to be introduced.*

Two methods could provide relatively short execution times for the codes:

- *Port the existing codes to run on parallel machine architecture. This could offer a performance increase to satisfy the short-term requirements.*
- *Rewrite the existing codes to fully benefit from the modern computer architectures. This would be a resource demanding action. Before it would be terminated, the target computer might have changed architecture.*

These possibilities must be considered in view of the following boundary conditions:

- *portability of the codes is of high importance,*
- *minimum change to the existing sequential sources is important as long as many users will still apply the codes on conventional computers,*
- *programming know-how necessary for the porting of the codes to parallel systems is still scarce within the STI.*

Based on the premises above, the STI has chosen, as a first step, to port existing codes to parallel machines. The experience obtained will continuously be applied in the ongoing work with the sequential counterparts of the programmes. New developments will more directly be designed with the parallel architecture as one of the target machines.

As first candidates for parallelisation the codes VICTORIA, PLEXIS-3C and ISPRAMIX are selected. These three codes cover different numerical and modelling methods. In addition, the parallelisation envolve a large number of staff of the STI. This is important for the continuous upgrade of the skills needed. The scopes of the three candidate codes are as follows:

- *VICTORIA is a program for safety analysis of nuclear power plants [1]. It calculates the physical and chemical interactions within the reactor circuit of fission products released as a consequence of a hypothetical accident. The program has been parallelised and a version named VICPAR is described in [2] and [4].*
- *PLEXIS-3C is a code for general analysis of transient dynamic phenomena in fluids and structures [3]. It is a huge modular program system based on the finite element method. A parallel version of a subset of PLEXIS-3C is running on an array of transputers [4].*
- *ISPRAMIX is a code for the modelling of hydraulic aspects of oceans and seas. It is based on finite volume methods [5]. The algorithms are relatively small but repeated many times for an enormous number of volume elements.*

2.2.1 PARALLEL VIRTUAL MACHINE (PVM)

High performance computing hardware is developing fast and without any reference standards. A high performance machine can be applied for a specific application software with strict performance requirements (e.g. daily weather forecast). However, when developing models which should be applicable on various computing platforms a certain common base must be established. Therefore, the work on parallelisation at the STI is addressing the general methodology of the coding rather than a specific high performance parallel machine.

As hardware it was originally decided to apply transputers based machines (T-node and PC hosted Quintek board) and a networked array of UNIX workstations communicating by means of sockets. Software as EXPRESS allows for a high degree of portability. The transputer based machines have been used for the VICPAR [2] and PLEXIS-3C [4]. Networked workstations have been applied for VICPAR and have partly been set up for ISPRAMIX.

To enable HP and DEC workstations to collaborate on a single problem communication routines based on Berkeley sockets were written and tested. However, in the fall of 1993 a new array of HP workstations was installed at the STI. At the same time the PVM 3.2 became available for the project. The PVM is a software developed at Oak Ridge National Laboratories. It facilitates the use of an array of UNIX workstations of various makes and types as a single multiprocessor parallel machine.

The PVM 3.2 has been installed on the HP-network and the DEC-network. Thus, a parallel machine with some 20 nodes is available within the STI. The functionality of the system has been tested and verified. The transputer based version of PLEXIS-3C is at present being ported to the PVM. This requires modification of the communication part of the program. Some functions of the EXPRESS System are being rewritten so that they are based on PVM primitives. This will allow for "backward" compatibility to the transputer based EXPRESS system.

2.2.2 ISPRAMIX

The ISPRAMIX is a result of a collaboration between the STI and the Institute for Remote Sensing Applications (IRSA). The aim of the collaboration is to integrate remotely sensed data, in-situ observations and results of computational models in order to create a comprehensive image of the real world. ISPRAMIX is the computational model for the hydraulic part of the project.

The numerical model for the hydraulics of the sea is searched optimised in order to save computation time. A key feature is a kind of time step splitting. Based on explicit formulations the water elevations are calculated for each micro-time step. Only during each macro-time step all the implicitly formulated vertical variations are treated. The resulting scheme for parallelisation saw the calculations of the micro-time steps distributed to a number of processors each of which should deal with one or more horizontal layers. The inter-processor communication should be performed at each macro-time step when the vertical variations have been calculated.

The program is written in FORTRAN for an ordinary sequential computer. The programmers have exclusively applied named common statements to define

the interfaces for the various subroutines. A first analysis of the program was performed by means of the UNIX profiler. The major CPU consumption was identified to be in a few routines only.

In order to arrange for the inter-processor communication a map of the data flow was needed. Declarations and definitions of variables are normally poor in FORTRAN programs. This is caused by one of the basic features of the FORTRAN language. The usage of named common as basis for the original lay-out of ISPRAMIX turned out to be an advantage when mapping the use of global variables. All global variables where found in the named commons. Tables containing the address of statements where the variables were used and/or assigned values were set up. For this purpose an extensive use of the FORTRAN cross-reference feature was needed. To avoid human errors when reading the cross-references listings utility programs written as awk-scripts were applied (later PERL has become available). The resulting group of awk-scripts could be used to automatically translate the entire program from an exclusively common based code to one which consists of a number of subroutines communicating by means of parameter lists only. Based on the tables of global variables a communication strategy for the parallel version of the program could be established and the modified routines were more simple to place on the various processors.

The program is written in a rather compact way. However, many subroutines to be seen as "fat-coded" by the caller. This is caused by an extended use of condition and status parameters. They are applied in a way that only part of the routines will be activated by each call and the rest remain as inactive ("fat"). To create a smooth flow of control many of the "conditioned" functions of the program have been replaced by "non-conditioned". Routines of the original ISPRAMIX which depend on one or more status parameters (e.g. "is it x-direction?" or "is it y-direction?") have been re-written or duplicated with modifications so that each conditional functionality is accommodated as non-conditional by its own routine.

When the entire ISPRAMIX program was mapped it turned out that a non-foreseen dependency exists between the various horizontal layers on "micro-time step" level. Thus, the original lay-out for parallelisation cannot be applied. Two alternative methods are now being pursued:

- The original parallelisation method with the overhead caused by the need of data transfer after each micro-time step.
- Division of the problem domain into a number of sub-domains. Each sub-domain is calculated on a separate processor and the boundary conditions are common for neighboring sub-domains and are communicated among the processors.

At present the first method is about to be tested on the PVM.

References

[1] HEAMES T.J., WILLIAMS D.A., BIXLER N.E., GRIMLEY A.J., WHEATLEY C.J, JOHNS N.A., CHOWN N.M. - VICTORIA: A mechanistic model of radionuclide behaviour in the reactor coolant system under severe accident conditions; Technical Report NUREG/CR, SAND90-0756, Sandia National Laboratory, 1990

[2] TAUTGES T.J. - Modelling Fission Product Chemistry and Aerosol Physics on a distributed Memory Parallel Computer: The P-VIC Code, The Commission of the European Communities, EUR 14387, 1992

[3] BUNG H., CASADEI F., HALLEUX J.P., LEPAREUX M. - PLEXIS-3C: A computer Code for Fast Dynamic Problems in Structures and Fluids, The 10th International Conference on Structural Mechanics in Reactor Technology (SMIRT10), Anaheim, California, USA, August, 1989

[4] MEHR K., TAUTGES T. - Experience with the Parallelisation of Large Computer Codes", PACTA '92, Barcelona, October, 1992

[5] EIFLER W., SCHRIMPF W. - ISPRAMIX, a hydrodynamic program for computing regional sea circulation patterns and transfer processes, Part 1: Description of the model equations and of the solution procedure, EUR 14856/EN, 1992

2.3 PRENORMATIVE RESEARCH FOR EUROCODE No. 8

In the framework of the European Council directive on construction products adopted in December 1988, Directorate General III of the Commission is involved in the elaboration of harmonized standards at European level. In the particular field of mechanical resistance and stability of civil engineering structures, the proposed harmonized standards are known as the structural EUROCODES.

The objective of the ongoing collaboration between DG III and the ELSA laboratory of the Safety Technology Institute is a major contribution to the prenormative research needed to support the elaboration and validation of design specifications in the structural EUROCODES. The contribution of the ELSA laboratory is concerned, in particular, with the provision of experimental data on the actual performance of various types of civil engineering structures designed according to the EUROCODE specifications. The design of the large-scale experiments to be performed at the ELSA reaction-wall and the specification of the data to be measured are made in close collaboration with DG III and the expert committees of CEN (Comité Européen de Normalisation) involved in the relevant EUROCODES.

The current programme of prenormative research addresses EUROCODE No. 8 which applies to the design of civil engineering structures in seismic zones. The programme concentrates on four major priority topics needing resolution to enlarge the current field of application of EUROCODE No. 8 and improve its reliability. The priority topics identified by DG III and its experts are:

- reinforced concrete frames and walls,
- infilled frames,
- bridges,
- foundations and retaining walls.

A total of 19 European laboratories grouped within a "Human Capital and Mobility" network do take part in the programme together with the ELSA laboratory which is in charge of conducting the large-scale tests.

A research activity on the seismic behaviour of irregular bridges has in fact started as a part of the Prenormative Research in support of Eurocode 8 (PREC8). The main objective of the research is to verify the dependency of the ductility demand on the regularity of the bridge. The behaviour factor value to be adopted for irregular bridges is in fact regarded as an open problem. Moreover, in irregular pier bridges the maximum ductility demand suffers by the shorter piers, but the opportunity to increase the strength of the shorter piers is debatable. The need for large-scale tests to verify the adequacy of different design approaches has been expressed.

The experimental activity will allow the pseudo-dynamic testing of six five-span bridges with piers of different heights. The tests will be conducted on the piers only, since the deck (which will remain almost elastic during the seismic action) will be modelled analytically taking advantage of the substructuring capabilities implemented in ELSA. The piers will have heights varying from 7 to 21 meters, with a box-type rectangular cross section of 4 x 2 m, and will be constructed with a scale factor of 2.5. Six different tests will be conducted, with the following combinations of pier heights:

- 14-21-14, as an example of regular bridge;
- 14-7-21, as an example of irregular bridge, where the traditional design approaches will be adopted;
- 14-7-21, as before, but with an increased strength of the shorter pier; which may reduce ductility demands;
- 14-7-21, as before, but with an increased strength of the higher piers, which should reduce demands on the shorter one;
- 14-7-21, with traditional design but with seismic isolation devices;
- 14-7-21, with traditional design, by applying asynchronous base motion.

The design of the piers has been completed, including all the technical solutions for fixing the specimens to the strong-floor of the laboratory and for applying the loads (a value of the axial load up to nearly 2000 kN is foreseen). A total of 10 piers will be constructed (due to the irregularity of the bridges, the higher piers will suffer relatively low damage, in order that they can be used in more than one test). The hollow piers will be prefabricated, transported in the laboratory and connected to the cast-in-situ bases. The base will be prestressed to reduce size and weight, to reduce costs and problems during the transportation procedures.

The construction of the specimens will start at the beginning of 1994. Great interest on the results of these tests has been expressed by the scientific community. These tests will represent the first pseudo-dynamic tests on a complete bridge model and the first large-scale implementation of the substructuring technique.

2.4 HARMONISATION IN REACTOR SAFETY

The Directorate General XI (Environment, Nuclear Safety and Civil Protection), in line with various resolutions of the Council of Ministers, promotes and coordinates specific actions aimed at the harmonisation of methodologies, criteria, codes and standards adopted in the assessment of thermal reactors safety. Such actions are carried-out in close collaboration with national experts from industrial and institutional organisations of EC as well as EFTA member countries. As appropriate, DG XI also attempts to establish cooperative actions with central- and east-european countries to strive for a progressive harmonisation of reactor safety practices and procedures on a pan-European level.

The scientific and technical support provided by the Safety Technology Institute is mainly aimed at assisting DG XI in the promotion and coordination of those initiatives emphasising a deterministic approach in reactor safety. Specific actions are carried-out in the following fields:

- reactor safety margins and containment performance under severe thermal and mechanical loads,
- severe accident management strategies emphasising molten core coolability and containability aspects,
- safety principles of advanced reactor concepts and innovative safety technologies,
- safety aspects of east-european plants,
- transfer of information and expertise on a pan-european scale.

In addition, it is envisaged to exploit the multidisciplinary competences available within the Safety Technology Institute for the:

- quality assurance of the results of study contracts which DG XI may wish to allocate to external organisations,
- coordination of software and user qualification benchmarks exercises.

In order to account for the work carried-out by other international organisations such as the IAEA and the OECD/CSNI in the field of reactor safety, the scientific and technical support provided by JRC-STI also includes the follow-up of the activities promoted by these organisations.

3 ASSOCIATION OF LABORATORIES

3.1 EUROPEAN ASSOCIATION OF STRUCTURAL MECHANICS LABORATORIES (EASML)

Set-up in 1989 at the initiative of the Institute for Safety Technology, the EASML is an association intended to promote European collaboration in the fields of structural mechanics and earthquake engineering. The University of Wales, Swansea, the University Carlos III of Madrid and the Bundesanstalt für Materialforschung und Prüfung (BAM), Berlin, joined the Association in 1993, bringing the total number of associated laboratories to 32. The picture in ***Fig. 9.1*** was taken during a meeting of the Association.

Four working groups are established within the Association to study reinforced concrete, steel/concrete composite and masonry structures, as well as to promote the further development of testing techniques, in particular the pseudodynamic test method used at the ELSA reaction-wall facility to simulate the earthquake response of large-scale models of structures.

As regards the reinforced-concrete group, the second phase of its programme has been completed. This phase has concentrated on the development of damage indicators and failure criteria for plastic hinge regions, thereby contributing to the advancement of safety evaluation of reinforced concrete structures under seismic actions. Global damage indicators and failure criteria in plastic hinge regions have been implemented in computer codes for non-linear analysis and used in the pre-calculations of the seismic response of the 4-storey reinforced-concrete frame tested in the ELSA reaction-wall laboratory at the end of 1993.

The programme of work for the group on masonry structures should be finalized in early 1994 as a function of the results of current research in the associated laboratories, in particular at Pavia and Lisbon.

The work of the group studying steel/concrete composite structures has been delayed due to difficulties with shaking-table testing of beam-column composite connections. The results of these real-time tests still have to be used to assess the reliability of pseudo-dynamic tests on the same composite specimens. This working group is also involved in the design of a 3-storey composite frame to be tested in the ELSA facility in 1995.

The work performed so far by the group on test method development has been reviewed during a one-day seminar held at Ispra in July 1993. The activity mainly consists of numerical and experimental studies in support of the validation and further improvement of the pseudo-dynamic test method.

Further support and new opportunities for strengthening the collaboration links within the Association were provided in 1993 through the "Human Capital and Mobility" (HCM) programme.

The work of the HCM network on prenormative research in support of Eurocode No. 8 started in June 1993 after signature of the related contract with DG XII. More than 10 laboratories in the Association take part in this cooperative research. The laboratories in the Association now also benefit from the "Access to Large Installations" chapter of the HCM programme which provides funding for the execution of large-scale shaking-table and reaction-wall tests.

Fig. 9.1 Meeting of the European Association of Structural Mechanics Laboratories at JRC Ispra

3.2 COLLABORATION AGREEMENT WITH THE EXPLOSION AND FLAME LABORATORY, HEALTH & SAFETY EXECUTIVE (BUXTON, U.K.)

This Collaboration Agreement was signed by both parties in June 1993 and covers the following technical areas: Runaway Reactions, Venting and Explosions. Initially, a joint action is foreseen on the following specific topics:

- comparison of EFL and STI experimental data on the butyl alcohol/propionic anhydride esterification reaction and eventual recommendations to industry,
- validation of the JRC RELIEF code against the above data,
- complementary tests to be carried out on the EFL medium-scale pilot plant (venting with chemically-reacting fluids) and the STI large-scale DRACULA facility (venting with non-reacting fluids). Subsequent validation of the RELIEF code against these data.

Since the signing of the Collaboration Agreement a number of discussions have taken place to plan the specific details of the above work. More recently, the EFL and STI have become partners in a new EC Shared-Cost Action (CHEERS Project) together with a number of other European organisations.

4 EXPLORATORY RESEARCH

Each year a percentage of funds coming from the Frame-Work Programme (FWP) and from the Support to the Commission Programme has to be allocated in the Institutes to "Exploratory Research" in order to give support for a period of time (usually no longer than 1 or 2 years) to the development of new ideas which could open new routes for future research programmes or for Third Party Work.

In 1993 the mechanism for the proposal selection, which was agreed by the Director General and the Board of Governors was the following:

- 3% of the FWP was allocated by the Board of Governors with a free competition of proposals coming from all the JRC Institutes;
- 3% of the FWP plus 3% of Support Commission funds were allocated by the Institute Directors to their respective Institute.

The following proposals (*Table 10.1*) have been selected at the STI for 1993:

Table 10.1 Proposals for exploratory research selected by the STI for 1993

Paragraph	Title	Responsible
4.1	Physics of actinide and fission product transmutation	Rief H.
4.2	Boron neutron capture therapy studies	Ricchena R.
4.3	NDA detection limits for plutonium in radioactive waste	Pedersen B.
4.4	Iron ore reduction by hydrogen	Dworschak H.
4.5	Unattended material control system for safeguards	Franklin M.T.
4.6	Extension of the pseudo-dynamic method for testing distributed mass systems	Donea J.M.
4.7	Study of the true stress-strain diagram of plain concrete with real size aggregate	Donea J.M.
4.8	High resolution and general circulation models	Cuvelier C.
4.9	Development and qualification of crucibles for high temperature melts	Hohmann H.

4.1 PHYSICS OF ACTINIDE AND FISSION PRODUCT TRANSMUTATION

In the search for transmutation concepts the first candidates were actinide fuelled (critical) reactors. But soon it turned out that they pose a particular problem of control. This is due to the fact that the fissile isotopes of Neptunium, Americium, and Curium have a considerably smaller fraction of delayed neutron emitters (as compared to the more common fuels ^{238}U and ^{235}U), a small Doppler effect and a positive sodium void coefficient. As is well known, the fraction of delayed neutrons is essential for the control of a nuclear reactor in the critical state. To overcome these problems various concepts of accelerator driven systems aiming at the transmutation of actinides and long lived fission products have been proposed in the recent past.

The safety of a multiplying system depends almost entirely on fast transients caused by accidental reactivity insertions. To study the power changes in accelerator driven systems a kinetic model dealing with fast transients as a function of reactivity insertion was developed and programmed. The model allows a comparison with an equivalent critical reactor. It was tested by a comparison with a NEACRP benchmark. As a general tendency it turned out that accelerator driven systems behave quite benignly even if they are only slightly subcritical.

The Kinetic Model: In the following considerations the conventional point kinetics equation to which the term S(t) is added was used. It describes an external source which in this case are the spallation neutrons generated by a proton accelerator.

$$\frac{dN}{dt} = \frac{\rho(t,N) - \beta}{\Lambda} N + \sum_{i=1}^{6} \lambda_i C_i + S(t) \qquad (1)$$

$$\frac{dC_i}{dt} = \frac{\beta_i}{\Lambda} - \lambda_i C_i; \qquad i = 1,2,\ldots,6 \qquad (2)$$

where N = number of neutrons in the system (it is considered to be proportional to the power), C_i = delayed precursor concentration of the i-th delayed neutron group, λ_i = decay constant of the i-th delayed precursor group [s-1], β_i = delayed neutron fraction of the i-th delayed precursor group, β = total delayed neutron fraction (= $\beta_1+\beta_2+\ldots+\beta_6$), $\rho(t,N) = \rho_R(t)+\rho_D(N)$ total reactivity variation caused by the time dependent ramp-rate $\rho_R(t)$ and the power (neutron population) dependent Doppler reactivity $\rho_D(N)$, Λ=prompt neutron lifetime [s], S(t) = rate at which external neutrons are inserted. It is chosen such that a certain power level is maintained in the system.

The coupled equations (1) and (2) are solved by a numerical method employing a variable implicit technique. The method yields an efficient and accurate solution. The general features of the program include time dependence of the total reactivity, prompt neutron generation time and time step size, and a maximum of six delayed neutron precursor groups. Furthermore, the total stored energy is calculated by integrating the reactor power from t = 0 to the time of interest.

The solution of equations (1) and (2) is based on the program of Cheng [1] to which the following features were added:

- The possibility of inserting a linear or quadratic time dependent reactivity ramp. The quadratic time dependent reactivity ramp serves for the simulation of gravity induced accidents like earthquakes, etc.,
- A negative reactivity feed-back mechanism to take the Doppler-effect into account,
- The possibility to shut down the external neutron source by an exponential, τ dependent, decay law of the form $\exp(-t/\tau)$,
- A graphical display of the power and reactivity changes.

The External Source: It can be seen that near criticality a 1 mA current already generates a relatively high fission power. For k=0.97 more than 100MW can be achieved. One can assume that $S(t) \cong -\rho_0 n_{sp}/\Lambda$ is a good approximation since the spectrum of the spallation neutrons is quite similar to the fission spectrum, except for a tail of fast neutrons above 20 MeV. It follows therefore that

$$S(t) = P_{fi} \frac{\rho_o \nu (1-k)}{\Lambda \quad \alpha \cdot k} \frac{C}{IE_f}$$

The Effect of Unprotected Reactivity Accidents: Usually three types of unprotected reactivity accidents are considered:

- Slow reactivity ramp insertion,
- Fast reactivity ramp insertion,
- LOF driven TOP (fast reactivity ramp insertion due to sodium voiding caused by a loss of coolant accident).

Slow reactivity ramp insertions without a scram are for example the inadvertent withdraw of a control rod(s) (few cents/s or 0.0001 k_{eff}/s). A typical fast reactivity ramp insertion occurred in the EBR-I accident which was caused by an inward bowing of the

fuel pins. Other accidents of this category are earthquakes or diagrid failures without a scram (up to a few \$/s or 0.01 k_{eff}/s).

The NEACRP Benchmark Problem: As a first example the KfK benchmark problem defined as a rod ejection accident and proposed by the Nuclear Energy Agency Committee on Reactor Physics is chosen. It consists of a fast reactor made up of a core with a bank of annular control rods, radial and axial blankets and sodium coolant. The essential features of the problem are: Axis-symmetry, two neutron groups and six delayed neutron precursor families and thermal feedback through Doppler effects in capture and fission cross sections.

The transient is obtained through steady control rod bank withdrawal. The reactivity insertion starts at 1 ms and increases at a rate of 170 \$/s for the duration of 16 ms. (The speed of the control withdrawal is adjusted to produce a ramp of 0.548 cm/ms.) After this time the reactivity is kept constant.

The reactivity reduction by the Doppler coefficient was calculated from the sample data obtained from Beauwen's paper [2] as a heat generation coefficient of -0.92108 \$/GJ.

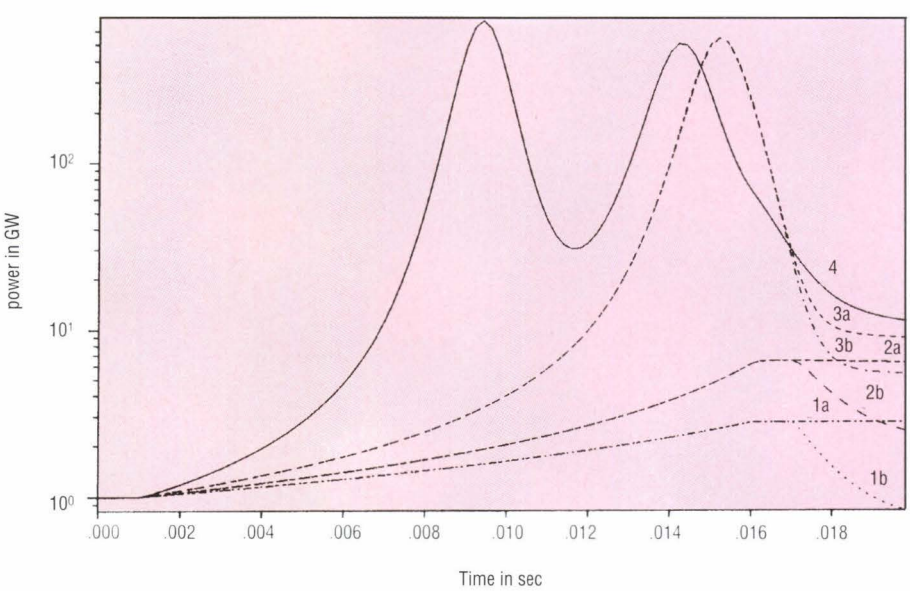

Fig. 10.1 Power excursion after a reactivity insertion accident (170 \$/s during 15 ms); 4: critical reactor, 1 to 3: subcritical accelerator driven systems

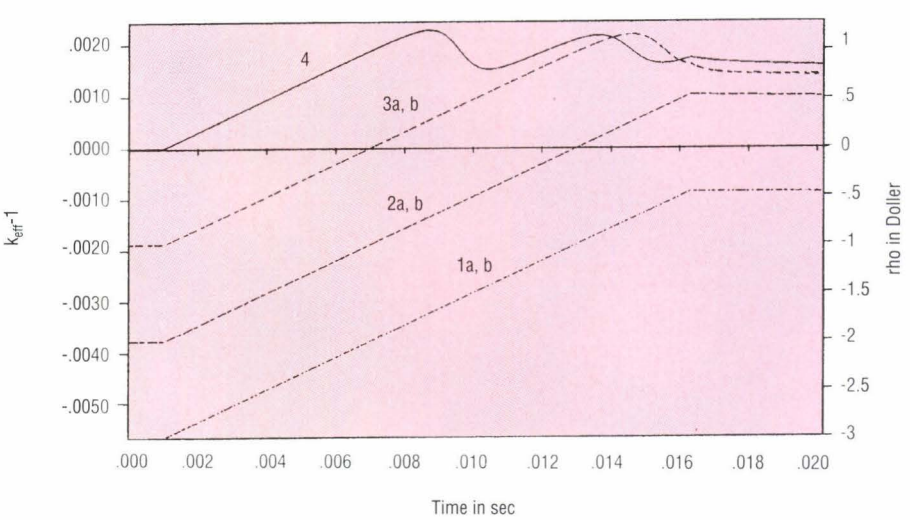

Fig. 10.2 The reactivity behaviour during the accident scenario

The analysis of this problem allows a comparison with transient calculations obtained by others to validate the code used in our analysis. It also gives a first indication of the mitigating effect of using a subcritical, accelerator driven system [3].

Figs. 10.1 and *10.2* show the power and reactivity change in a critical reactor (solid line, curve No. 4) and in systems being sub-critical between -3 \$ and -1 \$ (dotted lines, curves No. 1 to 3). These systems are driven by a spallation source dimensioned such that they generate in steady-state operation the same power as the critical reactor, which is assumed to be 1 GW_{therm}. Curve 4 corresponds to a critical reactor. Its power oscillates and has two peaks in a short time interval. Super-prompt criticality produces these peaks, as can be seen in *Fig. 10.1*. The power rises rapidly during the period of super-prompt criticality and reaches its peak

value at the time when the Doppler effect reduces the reactivity to values below the super-prompt limit.

In the case where the reactor is operated in a subcritical mode the neutron source is determined such that the system generates 1 GW thermal power and this source strength is maintained during the whole time the reactivity is increased. When the time reaches 17 ms, or when the thermal power of the reactor reaches 50 times the initial power (50 GW), the neutron source is reduced by the shut-off function $\exp(-t/\tau)$ where τ = 1 ms.

The case in which the initial sub-criticality is -3 and -2$ respectively, the power increases only to 2.2 GW and 6 GW respectively after 16 ms and after 17ms the power decreases almost proportionally with the neutron source strength of $\exp(-t/\tau)$ (curves 1b and 2b). If on the other hand the neutron source is maintained constant (the accelerator is not shut-off), also the power remains almost constant in this time range (curves 1a and 2a). For a subcriticality of -1$ only a single peak-power of 530 GW was calculated. Even though this value is similar to the peak of curve 4, the integrated power, i.e. the total energy release during the excursion is much less than for a critical system.

An interesting result of this analysis is the fact that the power decreases even between the delayed and prompt critical state. This is due to the long time constant of the delayed neutrons. When the reactor is in an under prompt-critical condition, the neutron flux is controlled by prompt neutrons which decrease for a sub-supercritical condition. For the case of a critical reactor two power peaks (curve No. 4) of 700 GW and 500 GW resp. were calculated which is in good agreement with the results of the NEACRP benchmark.

When the neutron life time and delayed neutron portion becomes half the value of the original case, then the power change as well as the reactivity change in units of dollars (as a function of time) becomes identical to the first case. This means that power and reactivity are time scale invariant in both the neutron life time and delayed neutron portion b. This can be easily verified by an analysis of equation 1, where a simultaneous change of the parameters in the numerator and denominator does not change the numerical value of the coefficients.

When the power change is slow, the reactor can be controlled by a mechanical movement of control rods or by a hydraulic dispersion of liquid neutron absorbers which are dispersed by melting fuel elements like an electric fuse mechanism. In a subcritical reactor operated by spallation neutrons, the power change is much slower than in a critical reactor. This provides a great advantage from the point of view of reactor safety.

It appears that a systems with a keff of around 0.9 ~0.95 (= -30$ ~ -15$ for a FR) would even look more attractive from the safety point of view. But these systems would require an expensive high current accelerator. In addition, they are characterized by an inhomogeneous power distribution with a sharp peak around the target area. On the other hand, as was shown above, accelerator driven slightly subcritical systems behave more benignly than the "classical" reactors. They also have a relatively flat power distribution, and require only a low proton current and therefore much less expensive accelerators.

4.2 BORON NEUTRON CAPTURE THERAPY STUDIES

The installation of the new plant for BNCT was completed at the Petten HFR reactor early in 1991. Since then a great number of measurement and tests concerning physics and biological dosimetry have shown the validity of the neutron beam design which provides the basic characteristics able to assure a satisfactory start of the therapy.

Other plant optimisation studies carried out at Ispra in 1992 (see previous STI Annual Report) demonstrated the difficulty of improving the present beam parameters, without significant modifications of the HFR reactor wall in the zone of the neutron extraction. As these structural changes could affect the general reactor safety, the research for a more advanced BNCT plant in Petten was deferred to a later date, when more experience will be gained on the therapy effectiveness.

The development plan scheduled 1994 as the starting year for the irradiations of human brain tumours and, for this reason, the problems connected with the treatment planning assume a high priority. The treatment planning should be performed in two steps: the radiological doses for the tumour and healthy tissue should be calculated by means of computer simulations in dependence of the tumour location and of the direction, aperture and intensity of the neutron beam. Then, on the basis of a great number of calculations, an optimal treatment should be determined. At present, there is a wide choice in computer programs which perform numerical simulation of radiation space transport (e.g. the MCNP code), but the BNCT pretreatment analysis needs distinctive features on the input data preparation, computer time requirements and dose maps display which the current codes do not have.

In order to simulate a typical BNCT treatment with a good accuracy, the current codes require large computer times even if using the faster workstations available; times as long as 15 hours are normal. This fact prevents the possibility of obtaining an optimisation based on the results of many calculations. In general the preparation of the input data and interpretation of the results are difficult and prone to error operations for these codes which belong to the family of Monte Carlo codes.

To face this situation, at JRC Ispra it was decided beginning of 1993, to develop a new program (DNP-3) tailored to the use in BNCT treatments having the following features:

- Reduced computer time for analysing a single irradiation (15-20 minutes on a fast workstation),
- Simple preparation of the input using also the modern technique of scanning images,
- Dose maps displayed in a clear and exhaustive way.

Progress up to the end of 1993

DNP-3 is a Monte Carlo transport code for neutrons and photons which implements a fast algorithm to track the particles. It was built with the technique of variable dimensioning, in order not to suffer any limitation on the maximum number allowable of energy groups and irradiated subzones in which the radiological doses have to be calculated. The format of the cross sections library is consistent with that of discrete ordinate (S-N) codes and any existing S-N library can be used. Neutron slowing down in hydrogen can be treated with the discrete energy group model or with the classic continuous model.

The work was concentrated on the development of DNP-3. In only 8 months the code was made operative for what concerns the neutron doses calculations. Input and output subroutines require more work mainly for what concerns the coupling of DNP3 with a graphic subsystem. As yet the tests to validate the code were performed by a comparison with the ANISN code in monodimensional cases. *Table 10.2* provides a picture of the more significant comparison so far carried out. It shows an excellent agreement between DNP-3 and ANISN for what concerns the detailed neutron absorption and leakage probabilities in each energy group.

In *Table 10.2* an example of a typical BNCT pretreatment calculation is given. Here the geometry of the irradiated body approximates the form of a human head by an elipsoid for consistency with previous work, even if this simplification for DNP-3 is not necessary. *Table 10.3* shows that the calculation takes a modest CPU time (only 6 minutes for an IBM workstation, model 220), although the number of neutron collisions which are processed is quite large (~3x106). The statistics is good for the neutron absorption in the 4 zones considered. The calculation confirms the importance of the neutron leakage for the BNCT irradiation problems.

A new DNP-3 code to assist the medical team in establishing an optimal BNCT treatment was developed at the JRC-Ispra [4]. This program has shown good performances when applied to the BNCT irradiation analysis and also in comparison with the ANISN code. It needs more development for the input and output subroutines; and probably a coupling with a powerful graphic system such as PV - WAVE will be necessary in the near future. There is a high probability that the code will be ready before the therapy will be started.

Table 10.2 DNP-3 compared with ANISN

Group	Group Energy Boundaries	Source Spectrum	Leakage		Absorption	
			ANISN	DNP3*	ANISN	DNP3*
1	3÷10 MeV	$1x10^{-4}$	$2.00x10^{-5}$	$3.08x10^{-5}$	$9.57x10^{-7}$	$1.4x10^{-6}$
2	1.4x3 MeV	$1x10^{-4}$	$2.38x10^{-5}$	$3.72x10^{-5}$	0	0
3	0.9÷1.4 MeV	$8x10^{-4}$	$3.27x10^{-5}$	$2.50x10^{-5}$	0	0
4	0.4÷0.9 MeV	0	$3.14x10^{-5}$	$3.12x10^{-5}$	0	0
5	0.1÷0.4 MeV	0.985	$7.34x10^{-3}$	$1.11x10^{-2}$	0	0
6	0.017÷0.1 MeV	$4x10^{-3}$	$6.21x10^{-3}$	$6.72x10^{-3}$	0	0
7	3÷17 keV	0	$5.74x10^{-3}$	$7.12x10^{-3}$	0	0
8	0.55÷3 keV	0	$6.16x10^{-3}$	$6.50x10^{-3}$	$8.16x10^{-5}$	$8.12x10^{-5}$
9	100÷550 eV	0	$7.16x10^{-3}$	$7.88x10^{-3}$	$3.25x10^{-4}$	$3.26x10^{-4}$
10	30÷100 eV	0	$5.58x10^{-3}$	$5.86x10^{-3}$	$4.55x10^{-4}$	$4.41x10^{-4}$
11	10÷30 eV	0	$5.53x10^{-3}$	$5.54x10^{-3}$	$7.25x10^{-4}$	$6.93x10^{-4}$
12	3÷10 eV	0	$6.34x10^{-3}$	$7.40x10^{-3}$	$1.38x10^{-4}$	$1.48x10^{-3}$
13	1÷3 eV	0	$6.15x10^{-3}$	$7.20x10^{-3}$	$2.25x10^{-3}$	$2.35x10^{-3}$
14	0.4÷1 eV	0	$5.39x10^{-3}$	$5.89x10^{-3}$	$2.93x10^{-3}$	$2.88x10^{-3}$
15	0.1÷0.4 eV	0	$1.48x10^{-2}$	$1.11x10^{-2}$	$1.69x10^{-2}$	$8.83x10^{-3}$
16	0÷0.1 eV	0	$1.74x10^{-1}$	$1.72x10^{-1}$	$7.22x10^{-1}$	$7.27x10^{-1}$
Total			$2.51x10^{-1}$	$2.54x10^{-1}$	$7.47x10^{-1}$	$7.45x10^{-1}$

- Geometry of the problem: Slab thick 18 cm; Isotropic Neutron Plane Source at the middle plane
- Number of energy groups: 16 (15 epithermal - 1 thermal)
- Neutron Cross Section library: Hansen and Roach/ANISN approxim. S 32 - P1
- Neutron sample size160 000

* CPU time 4 m' on IBM Risc 6000 mod 220

Table 10.3 BNCT irradiation: Probability of neutron absorption in 4 zones of the body separated by 3 parallel planes from the top of the elipsoid

Zone	Boundaries of the zones (cm)	DNP3 Absorption probability	DNP3 Estimated statistical error
1	0÷2.25	$1.65x10^{-2}$	
2	2.25÷6.50	$8.39x10^{-2}$	~6%
3	6.50÷9.75	$3.72x10^{-2}$	
4	9.75÷13.0	$7.01x10^{-3}$	
Total body		$1.44x10^{-1}$	~5%

- Geometry of the irradiated body: Elipsoid (a=6,5; b=6,5; c=9.0 cm)
- Composition in atoms/barn cm
  H=0.06
  O=0.03
  B10=$1.0x10^{-5}$
- Collimated plane neutron source: aperture 2x2 cm; at the top of the elipsoid; energy groups and cross section library as in case of ***Table 10.2***, source concentrated in group 6.
- Neutron sample size: 160 000/mean number of neutron collisions per history 20.6;
- Neutron leakage probability 0.86
  CPU Time = 6.1 minutes for IBM Risc 6000 mod 220

4.3 NDA DETECTION LIMITS FOR PLUTONIUM IN RADIOACTIVE WASTE

The passive neutron correlation technique is the most promising NDA method for the absolute determination of the Pu mass. Neutrons emitted from a Pu containing test item are detected in a detector head consisting of fast neutron detector modules arranged in a 4 π geometry around the test item. A signal pulse train is formed consisting of correlated neutrons from spontaneous fission of the even mass number Pu isotopes, multiplied neutrons from induced fast fission in fissile isotopes, and uncorrelated (α,n) reaction neutrons. From analysis of the signal pulse train the content of spontaneous fissile isotopes can be determined even when the test item contains neutron absorbing and moderating materials.

Some particular problems arise, when the technique is applied to the assay of small Pu masses in radioactive waste. These refer to the influence from cosmic radiation generated neutron bursts and the dead time effects due to high count rates from (α,n) reactions. These problems were dealt with throughout this work and results have been reported earlier. In the following the major achievements from two years of exploratory research in this field are reported.

The aim of the research task was to elaborate a passive neutron correlation technique for the absolute determination of small Pu masses in radioactive waste. The problem was approached in three different ways exploring improvements of the neutron detector heads, the signal pulse train analysis technique and the necessary modifications of the theory.

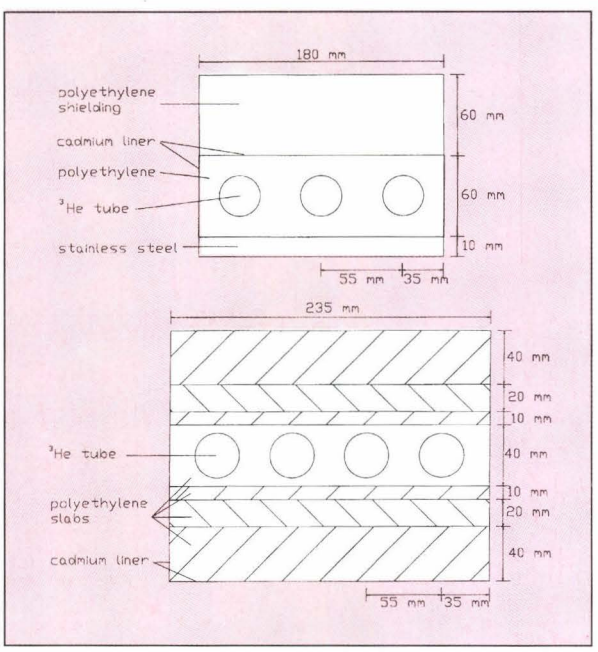

Fig. 10.3 Cross sections of present detector module (top) and the experimental module (bottom)

Modules of the neutron detector head consisting of a polyethylene moderator, ^{3}He neutron counters and Cd-liners (***Fig. 10.3***) were investigated. The task was to find the optimum ratio of moderator to detector volume V_m/V_c (***Fig. 10.4***). This ratio was found to be around 10. The decay constants were measured over the whole range of V_m/V_c and turned out to be a single exponential as a function of time over at least two decades. The results of these measurements are given in ***Fig. 10.5***.

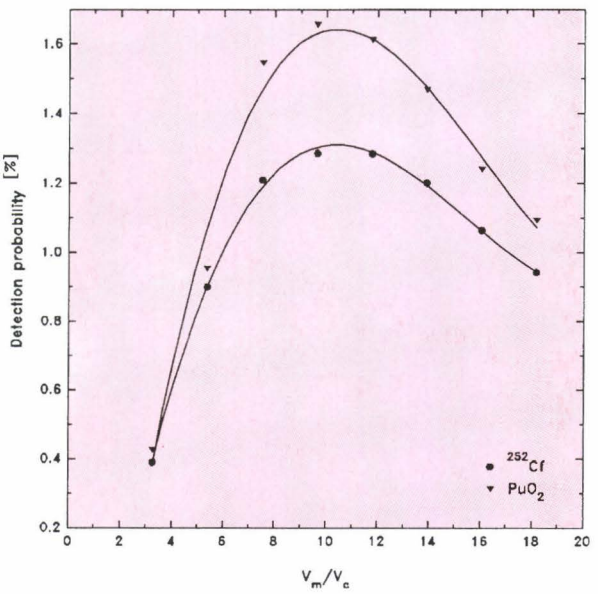

Fig. 10.4 Detection probability ε as function of ratio of moderator to detector volume V_m/V_c

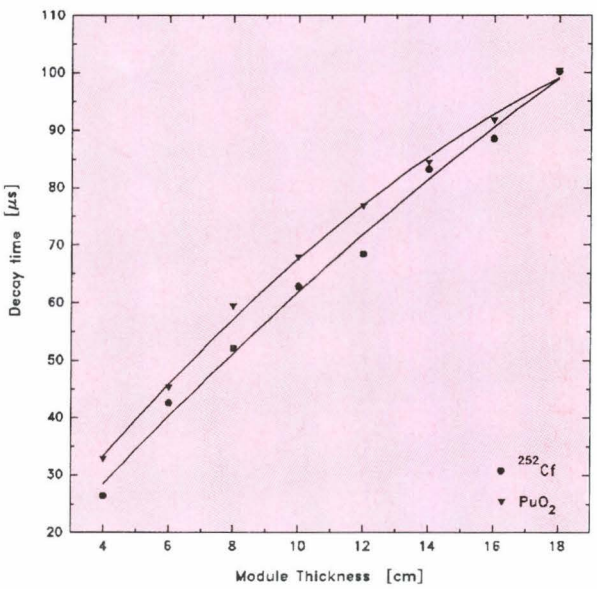

Fig. 10.5 Decay time $1/\lambda$ as function of module thickness

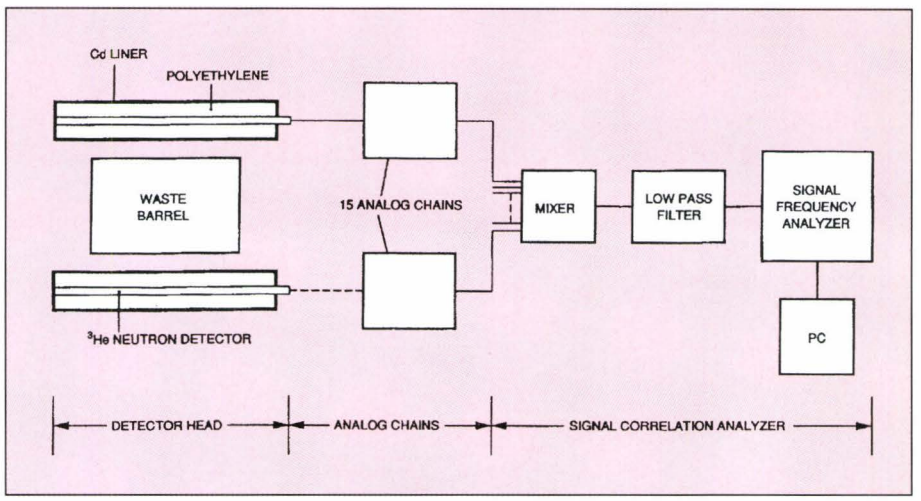

Fig. 10.6 Schematic view of the waste barrel monitor with low pass filter

Improvement of the electronics

In order to reduce the influence of the cosmic radiation a dead time filter with an updating dead time (low pass filter) was built and inserted between the mixer and the signal input to the frequency analyser (*Fig. 10.6*). It was found that a dead time of 2 μs in the low pass filter reduced considerably the influence of the high neutron multiplicites in the cosmic radiation background (*Fig. 10.7*). The experience gained during these measurements led to an improved specification of a new generation of frequency analysers for passive neutron assay.

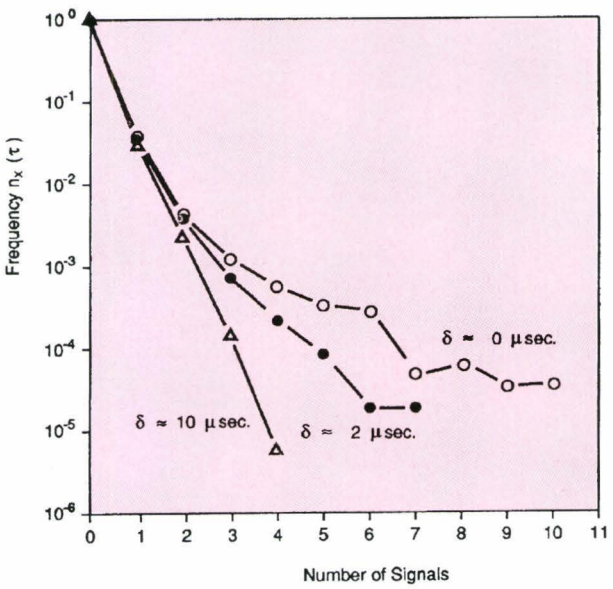

Fig. 10.7 Frequency distribution of background measured with various dead times of the low pass filter τ= 64 μs; T_M=30 hours

Improvement of the theory

For the analysis of the factorial moments of the frequency distribution measured with an updating dead time (*Fig. 10.8*) it was necessary to develop a new theory. This theory has as well applications for Pu waste with a high ^{241}Am build-up and for the assay of large Pu quantities (nuclear safeguards). The final interpretation formulas were derived, tested and published in [6].

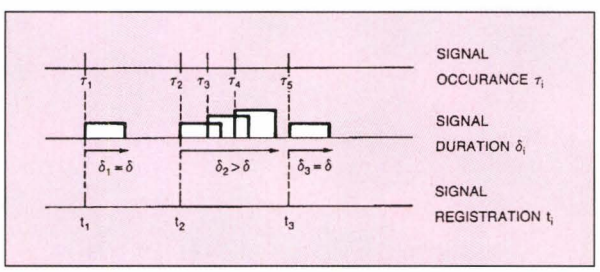

Fig. 10.8 Signal detection with an updating dead time counter for a constant dead time δ

Conclusion

A new detector head was designed and built according to the acquired experiences. It is expected to have a detection probability of 0.2 compared to 0.12 with the present device and the same number of ^{3}He counters. The detection limit will thus be better than 10 mg of ^{240}Pu effective but needs to be confirmed experimentally after the availability of small Pu samples and of the new frequency analyser.

4.4 IRON ORE REDUCTION BY HYDROGEN

The objective of this exploratory work and study is to verify the feasibility of a novel environment-friendly process for iron and steel production. The use of coal for iron and steelmaking is responsible for about 10% of man's carbon dioxide emissions [7], whilst the concentration of the industry in large production sites makes it a prime candidate for measures to reduce emissions. The new iron and steel making process, subject of JRC patents P-2321 and P-2370, uses hydrogen instead of carbon as a reductant. The price of hydrogen would be competitive where excess hydroelectric capacity is available for electrolysing water [8]. The final aim of this work is to eventually convince industry to build a pilot plant to demonstrate its feasibility on a large scale.

The reduction of iron ore by hydrogen is presently carried out in the solid state, using fluidized beds at temperatures between 373 K and 1573 K [9]. The product obtained is a pyrophoric sponge which must be deactivated, before use, by bricketting or melting in an electric arc oven. Another method presently under study reduces powdered iron ore in a hydrogen arc plasma at 2000 K, producing a partially-reduced molten mass [10]. The method proposed in the present work uses hydrogen to reduce a bath of molten iron ore. In a single step pure molten iron is produced, which can be converted directly into steel using only ladle additions. Other advantages are that the particle size of the ore is not critical and that scrap can be incorporated.

Progress up to the end of 1993

The 1992 annual report showed the design of a closed reactor in which the reduction is kept going by the continuous removal of water in a trap connected to the reaction chamber, whilst hydrogen is supplied to maintain a constant pressure. The melt is induction heated using an 80 kW supply. Tests using this reactor showed that the pressure in the reaction chamber makes little difference to the rate of reduction, which is limited by diffusion in the gas. The use of a molecular sieve in the water trap leads to a modest increase in process efficiency.

In order to measure the maximum reaction rate per unit area of melt, it is necessary to flow hydrogen over a small surface area of melt. Generally, the reaction rate is then extremely fast. However, after most of the ore has been reduced, the reaction rate starts to decrease as the iron oxide is diluted by the build-up of oxides from the gangue. Oxide dissolving from the crucible can greatly exacerbate this effect. Crucibles made of alumina, zirconia and magnesia of different densities were tested. Alumina was the worst, and magnesia the best, from both melt resistance and cracking point of view. However, boron nitride proved to be an even better material, being apparently immune to both dissolution attack by the melt and to thermal shock.

In parallel to the above experimental activities, the industrial feasibility of the system is being assessed, in consultation with industry experts. This involves:

- Assessing alternative reactor geometries: bubbling the hydrogen through the melt from below the melt, injecting it at high pressure from above, or simply streaming it over the surface, possibly through an electric arc.
- Selecting a plant configuration to optimise hydrogen and heat recovery. The most promising method still appears to be using the off-gas from the molten ore reduction to heat and pre-reduce the ore in a countercurrent configuration, as specified in JRC patent P-2321.
- Finding a refractory lining which withstands attack by the molten oxide. This is an exacting task because the partially reduced oxide, FeO, is very corrosive. Unfortunately, it is not feasible to produce industrial-scale crucibles using boron nitride. The best choice would appear to be magnesite or chrome-magnesite.
- Assessing the purity of the product: rather clean iron should be produced from many types of ore because no impurities are introduced from coal and others are carried away by the hydrogen. Although the iron will have to be poured into a ladle for degassing, a few additions at this stage should be sufficient to produce useful grades of steel directly.

The conclusion of the final report will give an estimate of the production cost of steel using the new process, based on a plant producing 250 thousand tonnes per year, using hydroelectric power.

4.5 UNATTENDED MATERIAL CONTROL SYSTEM FOR SAFEGUARDS

The future trend of safeguards technology is towards unattended systems. Here unattended means that they are able to do the work of an inspector without the inspector being present. Such systems are usually combinations of radiation detectors, neutron or gamma measurement instruments, video cameras and sensors linked together in a network so as to allow a computer to make inferences based on the raw data being generated by all these sensors. The system is designed to make reliable inferences about material control in some part of a facility. Typically these kinds of systems are used for monitoring storage or monitoring and measuring movements of material between facility locations. In addition, such a system must be tamperproof and this is usually achieved by ensuring that no function of the system can be tampered with, without leaving evidence of some kind. These systems are continuously receiving raw data which are interpreted to evaluate both material control and the systems own integrity.

The other important aspect of such systems is that they have to be sufficiently flexible to allow the facility operator to carry out his work without excessive hindrance. Inevitably however they oblige the operator to structure his work activities in such a way that they can be monitored by the system. The design of a system is usually specific to the activities of a particular plant or location within a plant. The design is the result of a negotiation between the facility and the inspectorate to find a compromise between work procedures which are sufficiently flexible for the operator while at the same time being sufficiently categorisable for an automated inference system. The outcome of this negotiation is that the operator accepts certain limits on his freedom of action because not doing so would create difficulties for automated verification. The system, however, is able to verify that the operator respects the agreement to exclude certain behaviours. The operator will also accept certain obligatory work practises which are essential to allow verification by the unattended system. Once this kind of arrangement is set up, the objectives of the automated system are to:

- verify that excluded behaviours do not occur and that obligatory actions do occur,
- collect appropriate data to characterise the legitimate events, i.e. identify items, measure content of items, record storage locations, record access to storage locations, etc.,
- verify the integrity of its own components in terms of both reliability and tamperproofing.

The use of unattended systems will reduce the manpower cost of inspection work for safeguards authorities. They do, however, give rise to a number of technical design and cost problems. One of these stems from the fact that they tend to be plant specific and hence the hardware configuration as well as the data analysis and inference processes for one application will be different from that of another application. In each application the software to drive the system is complex and costly. The safeguards inspectorate would like to have systems which are assembled from modular intelligent components which could be integrated in a plant specific way while having a great deal of common basic software with a different integration in a different application. This has led to the strategy of having each data generation hardware (e.g. camera, gamma or neutron instrument, sensor etc.) linked to its own local processor providing some local data evaluation and local inference functions. These Data Acquisition Systems (DAS) are linked in a network to a central computer which receives messages (and some data) from the individual DAS. The central computer makes higher level inferences, acts as a central data base for inference results (and selected raw data) and provides the auditing interface for the inspector. With this approach, the design problem becomes how to segment the intelligence of the system into local inferences in the DAS and higher level inferences in the central computer. It also means defining the content of messages which pass between the periphery and the centre. Having a degree of decentralised data analysis, in which local inferences form the basis for messages, offers the possibility of defining modularity and avoids the transmission of huge amounts of raw data to the central computer. It has to be done, however, in a way which avoids having local units make definitive decisions without taking into account corresponding information from other units.

In this exploratory research, the design of such systems are studied from two points of view, which are:

- The design of a software architecture which provides a central database and message handling functions in a way which is configurable to plant specific combinations of hardware in a modular system. The software architecture and database structure should be independent of the plant specific details of the inference processes in any application and the database should provide an adequate platform for the auditing functions which will have plant specific features.
- The use of fuzzy logic as a basis for defining the outputs of DAS data evaluation which are the information content of messages being sent to the host computer. This in turn necessitates starting

from a fuzzy logic representation of the raw data evaluation and inference processes going on inside any kind of DAS.

For brevity the review below covers only the fuzzy logic aspects of this work. The objectives of the software design aspects of this research are to explore how the concepts of object oriented software development can be applied to this problem so as to create flexible modularity in the design. A more detailed discussion of these aspects is given in [5] below.

Fuzzy logic and distributed intelligence

The application of fuzzy logic to distributed intelligence in a multicomponent system is represented as follows:

- Particular sequences of states of the environment being monitored are defined as illegitimate behaviours and other sequences are defined as obligatory behaviours.
- The relationship between the states of the real environment and the partial observation of these states by individual sensors is represented by considering the individual DAS as trying to make inferences about a partition of the global state space. The way in which the inferences of one DAS should be combined with information from other DAS so as to infer the precise state of the real environment, is determined by the set operations with which the different DAS partitions can be combined to discriminate details of the real state. With this process in view, the environment state sequences which represent obligatory behaviours or illegitimate behaviours are analysed to identify sequences of DAS "observations" (partition element sequences) which are corroboratory to verifying obligatory and illegitimate sequences. The credible identification of such sequences is the motivation for a message to the central computer. Note that partition here can mean a crisp partition but can also mean a set of linguistic variables which form a pseudo partition.
- For each DAS, the raw data from each small time interval is evaluated to provide a possibility measure on the elements of the DAS partition of the global environment. The kind of analysis which is carried out on a sequence of such possibility measures represents the systems ability to combine information through time so as to take a decision that a safeguards relevant sequence has been recognised (i.e. make some communication) and assign a credibility to this recognition at the moment of sending a message. The credibility is expressed as a possiblity measure on the set of alternative interpretations of the total interval of time deemed to cover a safeguards relevant activity. The value of fuzzy logic in this regard is that even though the DAS must occasionaly make decisions about whether or not to communicate and even though this decision process is based on the sequence of possibility measures, the possibility measure on the set of interpretations of an interval of time, can be defined in such a way that it is not conditioned by implicit decisions made during the interval of time (i.e. decisions that a particular state transition has really happened).
- The host computer must combine information from differed DAS either to make higher level anomaly related inferences (and perhaps send a message via a modem) or alternatively to recognise an obligatory or acceptable event. The events to be recognised by the host computer are defined as functions of DAS events where the functions are constructed using fuzzy operators on the DAS event fuzzy sets. Given this defining structure, the fuzzy measures representing information from individual DAS are the inputs to the computation of a host fuzzy measure. In this way the host computer combines information to generate a credibility for the host event in the context of alternative interpretations.

The objectives of the fuzzy logic aspects of this research are currently concerned with:

- clarifying which credibility computation operators should be used for different data integration scenarios at the level of the host computer,
- examining how the outputs of traditional statistical estimation and pattern recognition algorithms can be formally represented as fuzzy possibility measures,
- whether DAS messages should be conceived as possibility measures on the DAS state space or whether it would be sufficient to transmit a possibility measure on a linguistic variable partition of the DAS state space,
- providing a fuzzy logic definition of audit trail and assurance of non tampering and analysing its relationship to multiple mode tampering strategies,
- deciding whether any real gains in effectiveness are obtained by using fuzzy rather than crisp logic messages and attempting to quantify these gains, if any.

4.6 EXTENSION OF THE PSEUDO-DYNAMIC METHOD FOR TESTING DISTRIBUTED MASS SYSTEMS

The pseudodynamic test method can be directly applied to structures having masses concentrated in few degrees of freedom. This is the case of multi-storey frame buildings, where most of the mass is concentrated at the floor slabs. In testing framed structures, the actuators are attached to the floor slabs (assumed to be rigid in their plane), so that only three degrees of freedom per storey (two horizontal displacements and rotation about the vertical axis) need to be included in the discrete parameter system.

In many cases the mass distribution is far from being concentrated in few locations. In typical masonry buildings the ratio of distributed mass to the total is typically 50%, due to the weight of the masonry panels. In other structures, such as towers, chimneys or monument buildings, where no horizontal partitions exist (ancient churches quite often have light wooden roofs), this ratio could reach 100%.

Rational techniques to lump the masses at the few degrees of freedom to be controlled during the test are then required. Starting from the consistent mass matrix, the masses could be lumped with the "economizer" techniques used in finite element analyses, assuming the deformation patterns [11], viz. the force distribution patterns [12] do not dramatically change during the test.

However, when dealing with distributed-mass systems where large stiffness changes may occur, no constant mass matrix can represent the inertia forces for the discrete system. As an example, we may consider a typical test arrangement for a built-in cantilever masonry panel [13], with a single actuator on top. If a purely flexural behaviour is expected, the deformed shape is known in advance, so that the mass value for the corresponding single-degree-of-freedom can be found by applying the Hamilton's principle as 24% of the total mass of the panel. Conducting a single-degree-of-freedom pseudodynamic test with this mass value would yield good results, even if the stiffness changes due to cyclic damage, as long as the deflected shape does not change significantly. Should in fact a shear-type behaviour take place, the mass value would take the new value of 40% of the total, whilst the slippage of the bottom mortar layer would correspond to a mass equal to the total mass of the panel.

During the test, the displacements are measured at a number of locations much larger than the number of actuators. The deflected shape can then be continuously monitored. By using this information, it is possible to update the discretised mass properties whenever a significant change in the incremental deflected shape takes place.

A suitable methodology to update the mass values starting from the consistent mass matrix can be found in the numerical techniques developed for nonlinear modal analysis [14]. Numerical simulations have been performed for a set of benchmark problems by using these techniques [15]. The adequacy of the method has been explored by comparing the results which can be obtained with the solution which may be achieved by using a large number of degrees of

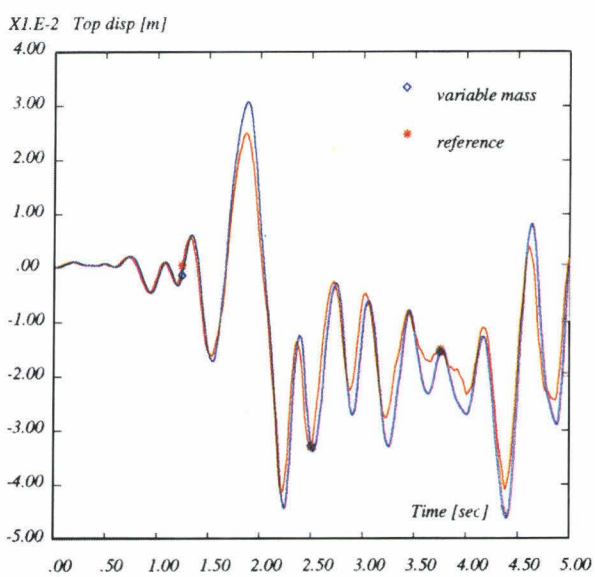

Fig. 10.9 Variable mass vs. reference solution

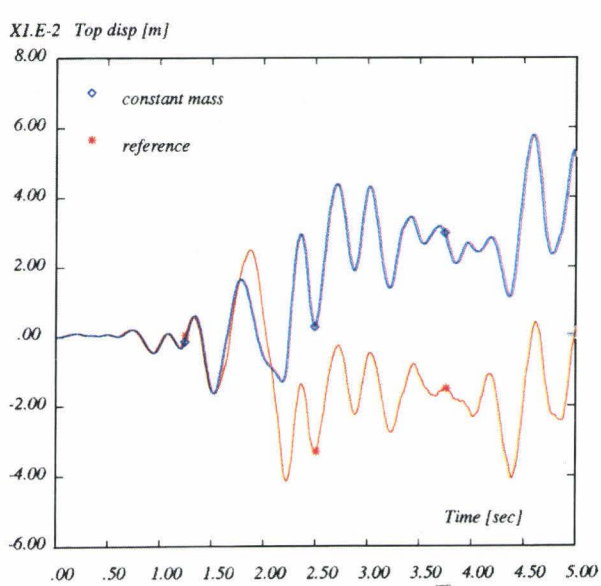

Fig. 10.10 Constant mass vs. reference solution

freedom. In some cases the method yields very accurate results. In *Fig. 10.9* the solution obtained with variable mass techniques (broken line), approximates fairly well the solution obtained with eight degrees of freedom, whilst the solution with a constant mass value (*Fig. 10.10*) is very poor.

In other cases, however, the method seems not to work. This is due to the equilibrium unbalance which may arise from the change of deflected shapes. Additional studies to account for the local equilibrium balance are then required.

4.7 STUDY OF THE TRUE STRESS-STRAIN DIAGRAM OF PLAIN CONCRETE WITH REAL SIZE AGGREGATE

The objective of the work is the measurement of the true energy absorption capability of the unit material volume during fracture of brittle materials (plain concrete). This data is fundamental for structural analysis of failure during service, earthquake, impact loading. The measurement will be performed using concrete with real size aggregate because the data from microconcrete are not transferable to real structures.

Progress up to the end of 1993

The measurement of the true energy absorption capability of plain concrete will be performed with a bundle Hopkinson's bar consisting of two sets of 25 aluminium bars to which a cubic concrete specimen with 20cm side will be glued. This test section will be installed in the Large Dynamic Test Facility (LDTF) as an extension of the devices previously developed for testing thin sheet metal structures [16, 18, 19].

Strain gauges applied to the individual bars in the bundle will provide local information on incident, transmitted and reflected pulses. The analysis of these signals is expected to yield information, instant by instant, on the true resisting cross section of the specimen during crack propagation, hence allowing a study of the true shape of the softening branch of the dynamic stress-strain diagram and of the true energy absorption.

The achievements at the end of 1993 are the following:

- Construction of the bundle Hopkinson's bar test section by electroerosion cuts (October 93) and installation in the LDTF (December 93), as shown in *Fig. 10.11*,
- Design of the mechanical devices to be implemented on the bundle Hopkinson's bar installed in the LDTF in order to realize special loading histories (like half cycle in tension or compression, complete cycle) for the calibration of plain concrete models corresponding to the loading histories of real earthquakes and impacts (December 93),
- Patent proposal of the special loading histories devices (EUR P/2355),
- Signature of a collaboration contract with ENEA, ENEL, Politecnico di Milano, University of Karlsruhe for the characterisation of plain concrete in tension and compression using the Hopkinson's bar bundle and the special loading history devices,
- Other tests on the dynamic behaviour of ductile steels were performed in direct collaboration with industrial partners [17, 20].

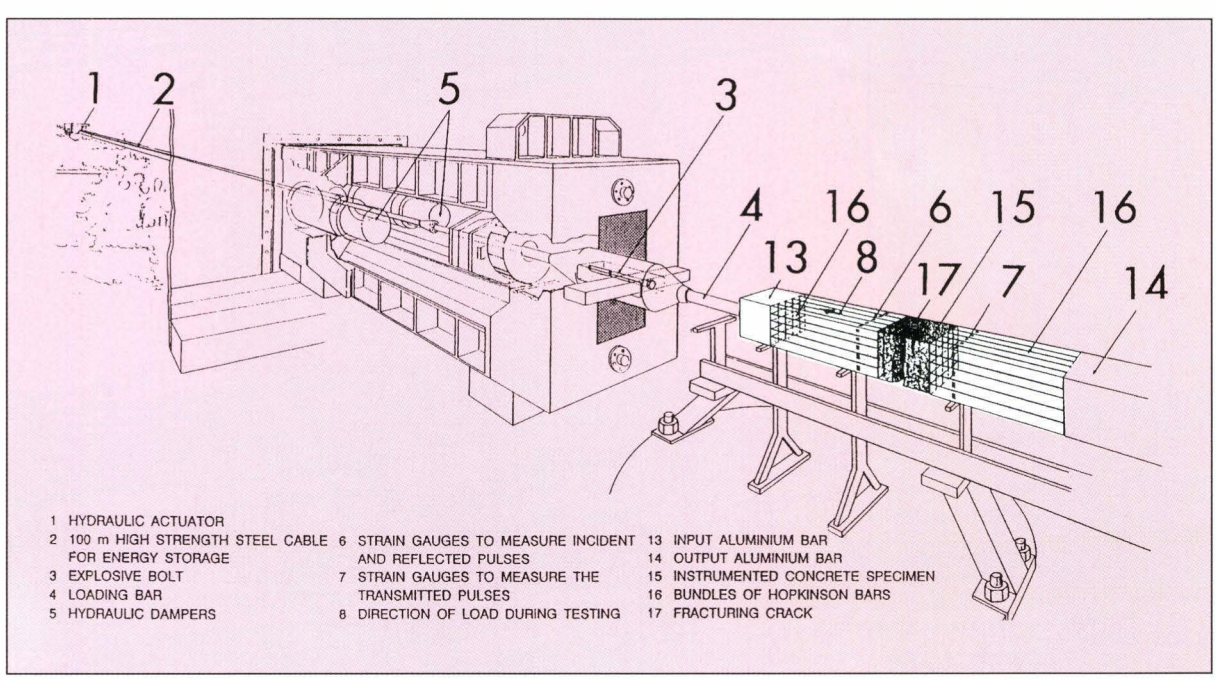

Fig. 10.11 Tension test of large concrete specimens with crack propagation measurement

4.8 HIGH RESOLUTION AND GENERAL CIRCULATION MODELS

The increasing demand by the scientific community, policy makers, and the public for realistic projections of possible regional impacts of future climate changes has rendered the issue of regional climate simulations critically important. The problem of projecting regional climate changes can be identified as that of representing effects of atmospheric and oceanic forcings on two different spatial scales: large-scale forcings, i.e. forcings which modify the general circulation and determine the sequence of weather events which characterise the climate regime of a given region (e.g. greenhouse gas abundance), and meso-scale forcings, i.e. forcings which modify the local circulations, thereby regulating the regional distribution of climate variables [21] (e.g. complex mountainous systems).

Atmospheric and Oceanic General Circulation Models (AGCM, OGCM) are the main tools available today for climate change simulations. However, typical GCMs have a horizontal resolution of around 500 km, whereas significant topographic features and associated local precipitation patterns often occur at smaller scales. Running a GCM at higher resolution is prohibitively expensive and it is unlikely for the next years that global climate simulations can be performed at resolutions high enough to accurately describe the climate at a regional or local scale.

In the regional modelling approach attempts are made to explicitly describe the effects of the meso-scale forcings by increasing the model resolution not globally, but only on specific areas of interest. The high-resolution limited-area model (LAM) is then nested within a (global) GCM. In the one-way nesting approach the global model will determine the large-scale climatology, while the LAM will resolve the regional climate. In the more complex two-way approach, the influence of the regional high-resolution climate on the global climate is also taken into account [22] (i.e. the feedback from the LAM solution to the GCM).

Progress up to the end of 1993

During 1993 contacts were established with the Department of Atmospheric Sciences at the University of Illinois at Urbana-Champaign UIUC (USA), the Centro Svizzero di Calcolo Scientifico CSCS in Manno (Switzerland), and the Hadley Centre for Climate Prediction and Research at the Meteorological Office in Bracknell (UK).

At the UIUC a detailed study was made of the mathematical and physical aspects of the climate models developed at UIUC. These models include:

- Energy Balance Model: This is a 1D model based on the first law of thermodynamics. It predicts the temperature change at the Earth's surface under the condition that the net radiation flux is zero. This model runs easily on a PC.
- Radiative-Convective Model: This 1D model is based on the thermodynamic energy equation and on convective schemes. It evaluates the vertical temperature profile in the atmosphere and the ocean taking into account the heating and cooling effects by solar radiation at various levels of the atmosphere. This model, which runs also on a PC, is very sophisticated and is a simple tool to perform scenario-studies.
- AGCM: This code solves the 3D hydrodynamic equations for conservation of momentum, energy and moisture in the atmosphere. The simplest of these models (with horizontal resolution of 40x50 and vertical layers) can be run on a workstation. The model requires the following input data: orography, sea-surface temperature and surface type. Instead of prescribing the sea-surface temperatures, a model for the mixed-layer in the ocean can be used.
- Coupled AGCM-OGCM: A few runs were performed with the UIUC coupled models on the CRAY supercomputer at the University of California at Los Angeles UCLA.

Contacts with the CSCS were established for the use of the NEC SX-3/24R supercomputer, on which the Max Planck coupled AGCM-OGCM has been implemented.

Through the European Research Community for Flow, Turbulence and Combustion (ERCOFTAC) contacts were established with the Hadley Centre. In 1994 these contacts will be intensified through an exchange of information and the formulation of common research projects. At Hadley portable versions of the UK (atmospheric and oceanic) climate model were developed which can be run on any UNIX-based workstation or larger system and which have been made available for researc purposes.

In the development phase of our future applications it is essential to have access to a workstation version of an AGCM and an OGCM. For more realistic high-resolution limited area simulations the access to GCMs running on supercomputers is of vital importance.

4.9 DEVELOPMENT AND QUALIFICATION OF CRUCIBLES FOR HIGH TEMPERATURE MELTS

A crucial problem in many melting processes is the availability of high temperature crucibles for large charges of metallic materials. These crucibles have to resist temperatures up to 2273 K for times of a few hours and due to high cost they have to be used a number of times. The solution of this problem is essential for extending the capability of the FARO and KROTOS facilities used for the study of severe accidents in LWRs as well as for processes related to waste treatment.

- Corium for FARO tests:
  Future tests in the FARO facility which are related to the investigations of severe accidents in ex-vessel situations require large amounts of *corium* melt. In addition to UO_2 and ZrO_2, the corium mixture also contains metallic components (i.e. stainless steel, zirconium). The problem, addressed by the current research, is to develop crucibles which can withstand temperatures up to 2273 K and contain melt masses up to 200 kg.
- Crucibles for KROTOS tests:
  Steam explosion phenomena have been successfully investigated in the KROTOS facility using simulant materials. For the extension of the test programme to realistic core melts, crucibles are needed for melting oxides or metals at 3273 K and 2273 K, respectively.
- Nuclear waste processing:
  Decommissioning of nuclear reactors produces large volumes of contaminated scrap. For disposal these are best processed to reduce the volume by melting and re-casting. Moreover, molten steel could be used to treat the exhausted B_4C control rods: their tritium content would be released as they dissolve, and the resulting casts would be suitable for disposal. The crucibles used in these processes must resist molten alloys and floating contaminant slags up to about 1973 K. The separation of this slag would be facilitated by a system for draining the melt from the bottom of the crucible.

Progress up to the end of 1993

The research on this topic was already started in 1992 [see former Annual Report] and continued during 1993. The main achievements for the three objectives are briefly summarized below.

- Corium for FARO tests:
  Laboratory scale experiments to study the compatibility of various types of zirconia and magnesia crucibles with metallic melts of 2273 K have been performed during 1992/1993. Furthermore, the capability of boron nitride crucibles (hot-pressed and high-isostatic pressed HIP-BN) to withstand high temperature metallic melts was investigated. In these tests, mixtures of a few hundred of grams of 80 wt% stainless steel and 20 wt% zirconium were melted in inert gas atmosphere and heated to 2273 K using induction furnaces with the power of 25 kW. Both types of boron nitride crucibles were observed to have an excellent thermal shock durability. However, only the HIP-BN crucibles were corrosion resistant to chemical attack.

  Therefore, HIP-BN material would be the best choice for the high temperature melt crucible. However, its application for large melt masses is restricted mainly due to the small crucible dimensions currently available and to the high fabrication costs. Thus, zirconia crucibles were selected for melting larger masses.

  The feasibility study with a 50 kg stainless steel/zirconium melting furnace (for 2273 K melt temperature) was concluded. Based on this study the design and fabrication of components were performed to convert an existing high pressure (2.7 MPa) radiation furnace into an MF induction furnace (3-5 kHz, 250 kWe). The assembly of the furnace components was initiated, the set-up of the auxiliary circuits (i.e. cooling water, inert gas system) was accomplished, the furnace control and measurement system (mainly temperatures and pressures) were installed. Various release systems to drain the melt through the crucible bottom were studied. Finally, a commercially available slide valve was chosen. This valve, designed for 1873 K melt temperature, must be adapted to the furnace requirements (i.e. 2273 K melt temperature). After having performed functional tests, the first melting test with 50 kg stainless steel/zirconium is planned for spring 1994. Based on the results and experience of this intermediate-scale furnace, it is intended to design and order a melting plant for 200 kg by the end of 1994. If the desired goals for the 50 kg melting plant can be achieved during 1994, this furnace will be connected to the FARO facility to allow the execution of a first test series with 200 kg corium containing up to 25% of metallic composites already in 1995.

- Crucibles for KROTOS tests:
  The development and fabrication of tungsten crucibles with special preparation of very thin bottoms were performed during 1992. These crucibles allowed to begin a test series in the KROTOS facility with 3 kg uraniumoxide/zirconiumoxide melts at 3073 K in 1993. The tests to study the potential for steam explosions in the UO_2/ZrO_2-water system are underway.
- Nuclear waste processing:
  Small crucibles of hot-pressed boron nitride and various grades of alumina, zirconia and magnesia were tested in air to 2073 K, using molten steel with and without iron oxide additions. All materials resisted to attacks by molten steel. Iron oxide attacked alumina and zirconia, but magnesia was more resistant. Furthermore, it was not wetted, so that it retained the melt even if cracked. Boron nitride was immune to both chemical attack and thermal shock. Thus boron nitride and magnesia are the best crucible materials. Two melt-release systems were identified: slide-valves and an electromagnetic system with no moving parts. On the basis of these findings, the specification is being prepared of a furnace for making test-melts of 15-20 kg.

References

[1] CHENG H.S. - A Point Kinetics Program, BNL Memo, April 26,1976; Revised -Point Kinetic Solution by VIP-, BNL Memorandum 8/31/90

[2] BEAUWENS R., GUESSOUS N., MUND E. and VAN DE VELDE A. -Intermediate Report on the Development of HEXNODYN-2-, Service de Metrologies Nucleares, Unversité Libre de Bruxelles. 1050, February 21, 1992, Brussels

[3] RIEF H. and TAKAHASHI H. - Control of Accelerator Driven Subcritical Systems Fuelled by Actinides-, Technical Committee Meeting on Safety and Environmental Aspects of Partitioning and Transmutation of Actinides and Fission Products, IAEA, Vienna, Nov.29 - Dec. 2, 1993

[4] RICCHENA R. - DNP3: A code to calculate three-dimensional transport of radiation from a neutron source to a heterogeneous body specialised to treat the BNCT treatment planning, to be issued as Technical Note

[5] FRANKLIN M. et al. - Unattended monitoring and measurement for safeguards, Proc. of ESARDA Symposium Rome (I), May 1993

[6] HAGE W., CIFARELLI D.M. - Correlation analysis with neutron count distributions for a paralizing dead time counter for the assay of spontaneous fissioning material, Nucl.Sci. Eng. 112, p 136, 1992

[7] DOYLE T. - Hydrogen in Steel Production, Ansaldo Hydrogen Symposium, Genova, Italy, Nov. 29, 1991

[8] GRETZ J., KORF W., LYONS R. - Hydrogen in Steel Industry, Int. J. Hydrogen Energy, vol. 16, No. 10, pp 691-693, 1991

[9] OLETTE M., BESSIER J., RIST A., GLEITZER C., FAUCHAIS P. - L'Hydrogene en Siderurgie, Entropie No. 116/117 (1984)

[10] MULLER R. - The Use of Hydrogen Plasma Processes in Petrochemical and Iron-smelting Industries, Proc. of the World Hydrogen Energy Conference IV, Pasadena, California, USA, 13-17 June, 1982, Vol. 2, Permanon Press (1982)

[11] KAMINOSONO T. et al. - U.S.-Japan Cooperative Research on R/C Full-Scale Building Test, Part 1, Single-Degree-of-Freedom Pseudo-Dynamic Test, Proceedings of the 8th World Conference on Earthquake Engineering, San Francisco, vol. 6, pp 595-601, Prentice-Hall Inc., New Jersey, USA, 1984

[12] NEGRO P., JONES P.M., PINTO A.V. - A reduced Degree-of-Freedom Approach in the Pseudodynamic Test Method, Proceedings of the 10th World Conference on Earthquake Engineering, Madrid, vol. 7, pp 3803-3808, Balkema, Rotterdam, 1992

[13] CALVI G.M., NAKASHIMA M. - Sulla Sperimentazione Pseudodinamica di Strutture in Muratura, Ingegneria Sismica, VIII, n.3, 1991

[14] LEGER P. - Non-Linar Seismic Response Analysis Using Vector Superposition Methods", Earthquake Engineering and Structural Dynamics, vol. 21, pp 163-176, 1992

[15] NEGRO P. - Toward a Variable Mass Formulation in the Pseudodynamic Test Method, Pre-print, 1993, to be issued as Technical Note

[16] ALBERTINI C., DEL GRANDE A., DELZANO C., KIEFER R., MONTAGNANI M., MURAROTTO M., PIZZINATO E.V., RODIS A., SCHNABEL W. - New Approach to Crash-Worthiness Studies of Automotive and Aerospace Thin Sheet Metal Structures by a Large Hopkinson Bar Method; Proceedings of EURDYN 93, 2nd European Conference on Structural Dynamics; The Norvegian Institute of Technology Trondheim, Norway, 21-23 June 1993

[17] ALBERTINI C., DELZANO C., PIZZINATO E.V., RODIS A. - Dynamic Mechanical Properties of Ductile Steel to Base Failure Criteria of Advanced Containment Shells, SMIRT-12, Stuttgart, August 1993

[18] ALBERTINI C., DEL GRANDE A., DELZANO C., MURAROTTO M., PIZZINATO E.V., RODIS A. - Large Hopkinson Bar Methods for Advanced Impact Testing of Structural Containment Components in Steel and Concrete, SMIRT-12, Stuttgart, August 1993

[19] ALBERTINI C., PIZZINATO E.V., RODIS A. - Large Hopkinson Bar Experiments for the Validation of Numerical Crash Computations of Car and Road Safety Structures; 26th ISATA Conf., Aachen, Germany, September 1993

[20] ALBERTINI C., MONTAGNANI M., RODIS A., MARIOTTI P., PALUFFI A., PAZIENZA G. - Influence of Strain Rate, Biaxial Loading and Deformation Mode on Fracture Criteria of Ductile Steels, 8th DYMAT Conf., J.R.C. Ispra (Varese) Italy, 12-13 October 1993

[21] CUVELIER C. - Collected Notes on Atmosphere, Weather, Oceans, Climate and General Circulation Models, 1993, to be issued as Technical Note

[22] GIORGI F., MEARNS L.O. - Approaches to the simulation of Regional Climate Changes: A Review; Reviews of Geophysics, 29, 2/May 1991

5 DECOMMISSIONING

The STI is responsible for managing a number of nuclear systems and plants which for safety reasons and following a request by the Italian Regulatory Authority, must be placed in a secure confinement (Protected Passive Custody) in anticipation of their subsequent decommissioning. The plants of concern, and on which 1993 activities have been focused, are the ISPRA 1 Reactor and the Hot Research Laboratory (ex-LMA).

5.1 ISPRA 1 REACTOR

The ISPRA 1 Reactor is of the CP-5 type using a D_2O coolant and moderator, and a graphite reflector. Over the 15 years of its operational life ending 1973, the reactor hosted numerous experiments. To maximise the number of experiments, the reactor core was provided with 40 experimental canals of various configurations, i.e. radial, penetrating, tangential, horizontal and vertical. Several experiments of those configurations are still in the reactor core.

Work during 1993 concentrated on attaining a secure conservation of the plant prior to the successive phases of the Protected Passive Custody and the overall decommissioning process. The principal activities were:

- reorganisation of the numerous experimental and conventional materials left in the controlled zone;
- radiological classification and in-situ decontamination;
- re-grouping and storing of contaminated materials;
- removing of clean materials (~20 t) for eventual re-use or waste disposal;
- general cleaning of the controlled zone and re-dressing of the working areas (~1000 m^2) with an anti-corrosive treatment and final painting.

At the end of the reorganisation and cleaning phase, a maintenance programme for the operating plant features in the reactor containment is envisaged to be set up.

In parallel, another major activity which has to be tackled is the performance of an inventory audit of radioactive materials of the various storage places, including the reactor pool. The material inventory will form an integral part of the Safety Report which must be submitted to the Regulatory Authority in order to obtain the license permitting the reactor to be placed into Protected Passive Custody condition.

5.2 HOT RESEARCH LABORATORY (EX-LMA)

This nuclear plant complex was authorized to start operation in 1978 with the ministerial decree being renewed in 1982. During the period of operation ending in 1984, the following research activities were undertaken:

- high burn-up fuel cutting;
- metallographic examinations;
- gamma-scanning examinations;
- fuel dissolving;
- extraction and separation of actinide elements using chemical processes;
- radioactive waste material vitrification.

The hot-cell complex is composed of an entrance cell fabricated of barytic concrete, followed by 19 lead shielded cells, each of which was appropriately equipped for the above mentioned research activities. To date, two cells have been cleared and decontaminated. Due to limitations arising from the JRC nuclear programme, the STI responsibility has been restricted to place the area of the hot-cells under "stand-by" conditions and declassifying the laboratories for the use of the JRC non-nuclear programme activities.

6 HUMAN RESOURCES

6.1 Structure and distribution

6.1 STRUCTURE AND DISTRIBUTION

Table 11.1 Institute structure

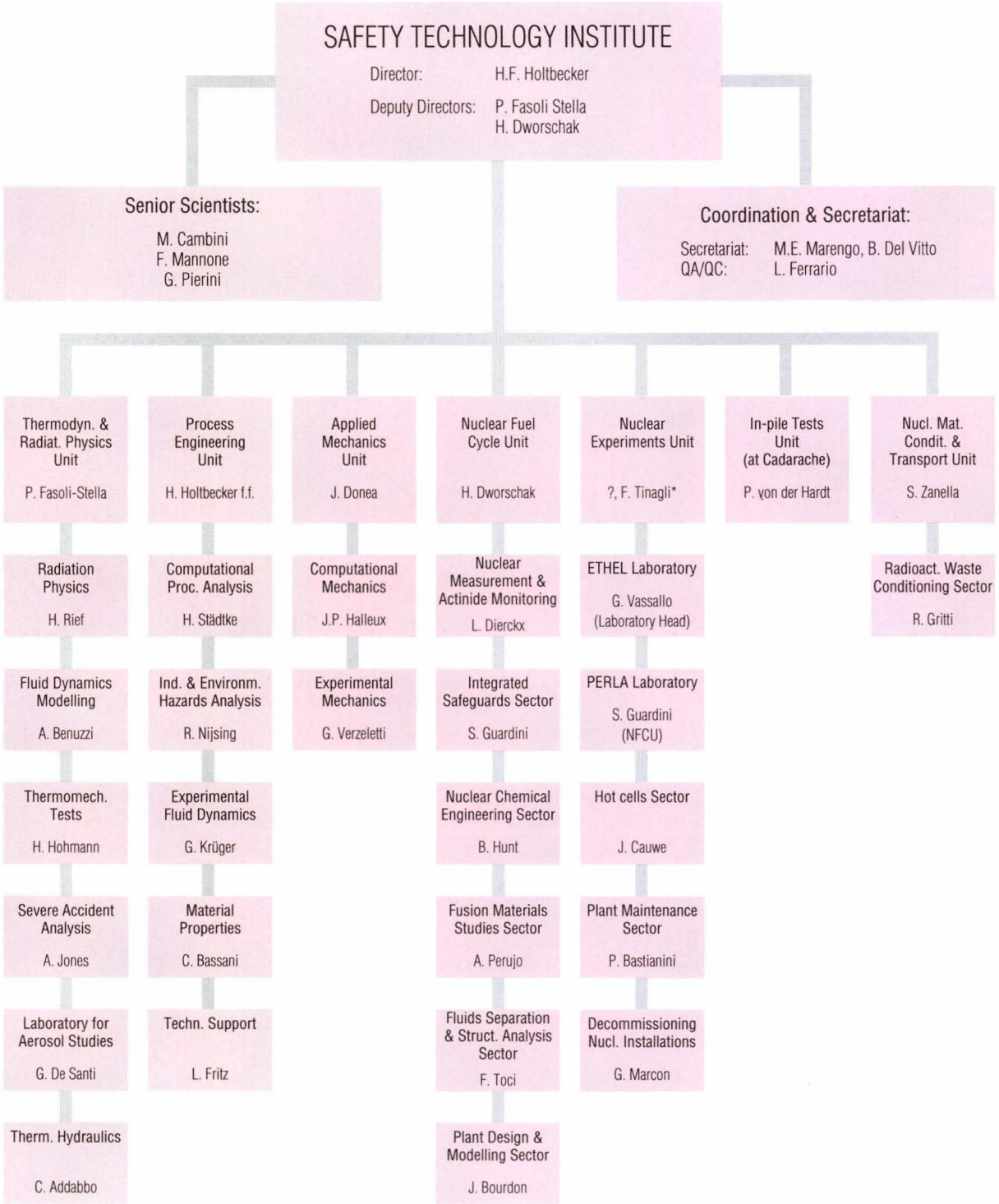

* Responsible for Licensing & Operations

Table 11.2 Institute staff (status 31.12.1993)

	Scient./ Techn. Staff	Admin. Staff	Authorized Recruitm. 1993		People who left in 1993		Grantholders		Visiting Scientists		Experts Seconded		Auxil. Agents
			ST	Adm.	ST	Adm.	present	addit. expected arrivals	present	addit. expected arrivals	present	addit. expected arrivals	
Direction Pers. Attente Affectat.	6 1	2			1				–				
Thermodynamics and Radiation Physics	61	5		–	2	–	8			–	1	–	–
Process Engineering	46	4		–	2		8				–	–	–
Applied Mechanics	28	2	2	–	–	–	6				–	–	3
Nuclear Fuel Cycle	53	4		–	5	–	5				1		–
Nuclear Experiments	38	2	2	–	7	–	–	–	–	–	–	–	3
In-Pile Tests	3	1	–	–	–	–	–	–	–	–	–	–	–
Nucl. Mat. Condit. and Transport Unit	26	10	2	–	3	–	–						3
	262	30	6	–	20		27				2	–	9

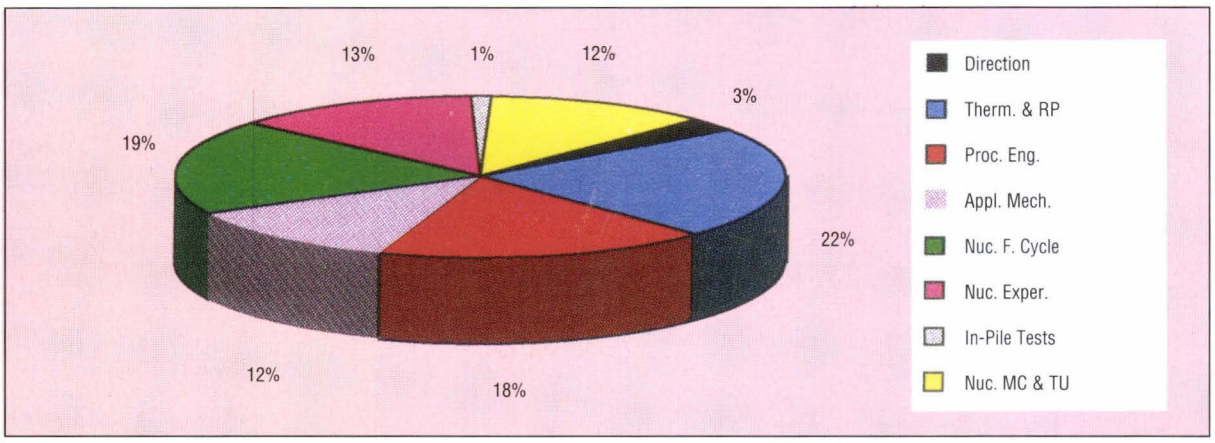

Fig. 11.1 Institute staff (status 31.12.1993), distribution (%)

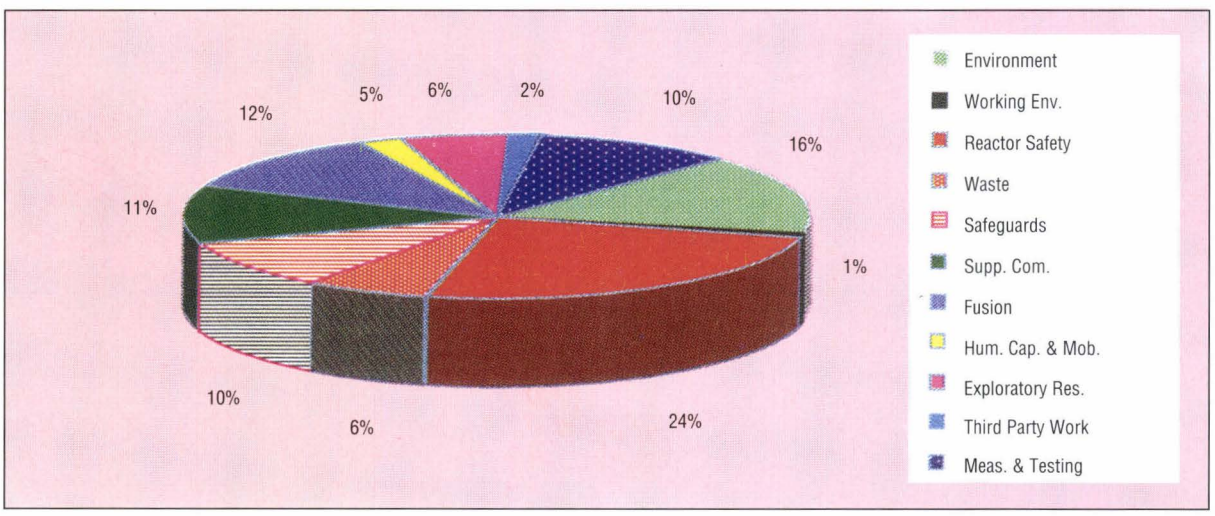

Fig. 11.2 STI - financial resources (1993), distribution (%)

7 PUBLICATIONS AND EVENTS

7.1 PUBLICATIONS

Specific Programmes

Reactor safety

CONTRIBUTIONS TO PERIODICALS AND MONOGRAPHS

CAPITAO J.A., HONTANON E., DROSSINOS Y. - Modelling of thermophoresis in the VICTORIA and RAFT computer codes, submitted to Journal of Aerosol Science (November 1993)

RIEF H. - A Synopsis of Monte Carlo Perturbation Algorithms; Journal of Computational Physics - ART 40561

ANNUNZIATO A. - Secondary Side Feed and Bleed Effectiveness in Pressurized Water Reactors; Journal of Nuclear Technology - ART 40869

ANDRONOPOULOS S., BARTZIS J.G., WÜRTZ J., ASIMAKOPOULOS D. - Simulation of the Thorney Island Dense Gas Trial No.8 Using the Code ADREA-HF; Process Safety Progress Vol. 12, No.1 (1993), pp 61-66 - ART 41052

BOR-JING CHANG, YEN-WAN H. LIU, WUN CIN CHUNG, RIEF H. - Calculations of EURACOS Iron Benchmark Experiment Using the HYBRID Method; Nuclear Science and Engineering - ART 41283

SKOULOUDIS A., WÜRTZ J. - Film-Thickness, Pressure Gradient and Turbulent Velocity Profiles in Annular Dispersed Flows; Journal of Fluids Engineering - ART 41424

PERUJO A., FORCEY K., SAMPLE T. - Reduction of Deuterium Permeation through DIN 1.4914 Stainless Steel (MANET) by Plasma-Spray Deposited Aluminium; Journal of Nuclear Materials - ART 41636

TECHNICAL EUR REPORTS

SHEPHERD I., HERRANZ L., ALCAMI M., AKAGANE K., SMITH P., ELLICOTT P. - Scoping Calculations to Examine a Strategy for the Thermalhydraulic Control of the Phebus-FP Containment Vessel during High Humidity Transients, EUR 14984EN, 1993

FRANCHELLO G., STÄDTKE H., WORTH B. - RELAP5-MF, a System Code for Thermal-Hydraulics Networks - EUR 15141/EN, 1993

SHEPHERD I., HERRANZ L., ALCAMI M., AKAGANE K., BONANNI E. - Pre-Test Calculations for the Thermalhydraulics Tests to be Carried out in the Phebus-FP Containment Vessel - EUR 15638 EN

SHEPHERD I., SERRE F., HOCKE K., BANDINI G., MARTINEZ J., MARTIN-FUERTES F. - Phebus FPT-0: Bundle Calculations for the Reference Scenario - EUR 15639 EN

FERMANDJIAN J., DICKINSON S., EDWARD J.B., EVANS G.G., RODRIGUEZ-MAROTO J.J., SIMS E.H., WREN C. - Presentation of the results of exploratory containment iodine chemistry calculations for PHEBUS FPT-0 (Benchmark exercise and realistic calculation) - EUR 15701 EN

CONTRIBUTIONS TO CONFERENCES

ARNAUD A., JONES A.V.- Lessons from the Analytical Preparation of the First Phebus-FP Test - Workshop Severe Accident Research in Japan, Tokyo, 1-2 November, 1993 - ORA/PRO 37857

FERMANDJIAN J., AKAGANE K., AREIA-CAPITAO J., DROSSINOS Y., DUMAZ P., KISSANE M.P, TRAMBAUER K. - Exploratory circuit calculations for the first test of the PHEBUS-FP Project, 12th Annual Meeting of the American Association for Aerosol Research, Oak Brook, Illinois (USA), 11-15 October 1993 - ORA/POST 37735, EUR 15702 EN

SHEPHERD I., JONES A.V., VON DER HARDT P., GAILLOT S. - The Quest for Prototypical Conditions in the Phebus-FP Containment; Fourth International Conference on Simulation Methods in Nuclear Engineering, June 2-4, 1993, Montreal - ORA/PRO 37334

DUMAZ P., DROSSINOS Y., CAPITAO J.A., DROSIK I. - Fission product deposition and revaporization phenomena in scenarios of large temperature differences, Proceedings of the 1993 National Heat Transfer Conference, ANS Proceedings, Vol. 7, pp 348-358, August 8-11, 1993, Atlanta Georgia (USA) - ORA/PRO 37325

BONANNI E. - Analysis of the Hydrogen Mixing and Distribution Test ISP-35 with the CONTAIN 1.12 Code, Second Workshop on ISP-35, Tokyo, 4-5 Nov. 1993 - ORA 37982

SHEPHERD I., JONES A.V., JACQ F., SCHMIDT F. - ESTER: A New Approach in Source Term Modelling - Fourth Intern. Conf. on Simulation Methods in Nuclear Engineering, June 2-4, 1993, Montreal - ORA/PRO 37333

DE SANTI G., HUMMEL R., VALISI M., DE LOS REYES A. - STORM Project: A Study on Aerosol Resuspension Mechanisms under Prototypical Severe Accident Conditions, Proceedings,Tokyo, 1-2 Nov. 1993 - ORA 37978

MAGALLON D., HOHMANN H. - High Pressure Corium Melt Quenching Tests in FARO, CSNI Specialist Meeting on Fuel Coolant Interactin, Santa Barbara (CA), 5-8 Jan. 1993 - ORA/PRO 37301

ANNUNZIATO A. - Phenomena Influencing Secondary Side Feed and Bleed Effectiveness in Pressurized Water Reactors; NURETH-5, Grenoble (F), October 1993 - ORA/PRO 37733

HOHMANN H., MAGALLON D., SCHINS H. YERKESS A. - Experiments in the Aluminumoxide/Water System, CSNI Specialist Meeting on Fuel Coolant Interaction, Santa Barbara (CA), 5-8 Jan. 1993 - ORA/PRO 37302

AREIA-CAPITAO J., DROSSINOS Y., HONTANON E. - Modelling of Thermophoresis in the VICTORIA and RAFT Computer Codes; Workshop on Phoretic Effects, Inst. Chem. Proc. Fundamentals, 12-15 July 1993, Prag (CS), Journal of Aerosol Science - ORA/ART 37727

RIEF H. - Monte Carlo Perturbation Algorithms Exploit New Computer Architectures; Proceedings of the Conference on Mathematical Methods and Supercomputing in Nuclear Application, KfK, TU, 19-23 April 1993, Karlsruhe (D), ORA/PRO 37316

SCHINS H., CORRADINI M. - Compositions and Energetics of Thermal Explosives; 14th Intern. Colloquium on Dynamics of Explosions and Reactive Systems, 1-6 August 1993, Coimbra (P) - ORA 37619

WIDER U., ANNUNZIATO A., HOHMANN H., MAGALLON D., YERKESS A. - Corium Debris Cooling in the FARO experiments; Proceedings of the SMIRT Seminar on Containment of Nuclear Reactors, KfK, 23-24 August 1993, Karlsruhe (D) - ORA/PRO 37779

HOLTBECKER H., VON DER HARDT P. - PHEBUS PF, ein internationales Projekt der Reaktorsicherheitsforschung; PHEBUS-PF Seminar, FZR, 4. Oktober 1993, Rossendorf (D) - ORA 37942

SHEPHERD I., JONES A.V., GONNIER C. - PHEBUS-FP: Programme and Results of Thermalhydraulic Tests; Proceedings of the 21st WRSM, USNRC, 25-27 October 1993, Bethesda, Md (USA) - ORA/PRO 37951

WORTH B., PELLISSIER M., STÄDTKE H. - Counterpart Testing and Scaling Methodologies: Experience Gained from CATHARE2 Calculations Using LOBI and BETHSY Test Results; Proceedings of NURETH-6, FANS, 5-8 October 1993, Grenoble (F) - ORA/PRO 37359

COMMUNICATIONS*

ADDABBO C., LEVA G., ANNUNZIATO A. - Experimental Data Report on LOBI-MOD2 Test BT-15/16; CEC-JRC, COM 4346, March 1993

ANNUNZIATO A. - Quick Look Report on LOBI-MOD2 Test BT-15/16; CEC-JRC, COM 4347, April 1993

ADDABBO C., LEVA G., ANNUNZIATO A. - Experimental Data Report on LOBI-MOD2 Test BT-06; CEC-JRC, COM 4348, May 1993

ADDABBO C., LEVA G. - Quick Look Report on LOBI-MOD2 Test BT-06; CEC-JRC, COM 4249, June 1993

ADDABBO C., LEVA G., ANNUNZIATO A. - Experimental Data Report on LOBI-MOD2 Test BL-06; CEC-JRC, COM 4350, October 1993

ADDABBO C., LEVA G., ANNUNZIATO A. - Experimental Data Report on LOBI-MOD2 Test BL-40; CEC-JRC, COM 4353, November 1993

ADDABBO C., LEVA G., ANNUNZIATO A. - Experimental Data Report on LOBI-MOD2 TEST BT-04; CEC-JRC, COM 4351, November 1993

ADDABBO C., LEVA G., ANNUNZIATO A. - Experimental Data Report on LOBI-MOD2 Test BT-56; CEC-JRC, COM 4352, December 1993

TECHNICAL NOTES*

SANDERS J., DE SANTI G. - First STORM Meeting, 21-22 April 1993 - CEC-JRC, Technical Note I.93.60, Ispra, Italy, 1993

MAGALLON D. et al. - Quenching Test-2 Data Report, JRC-Ispra, Technical Note I.93.154, Nov. 1993

ANNUNZIATO A. - COMETA v0.4: Pre-Test Calculation of FARO Base Case Test - JRC-Ispra, Technical Note I.93.114, 1993

ANNUNZIATO A. - COMETA v0.4: Post-Test Calculations of FARO Tests L-06 and L-08, JRC Ispra, Technical Note I.93.115, 1993

PRETEL C., REVENTOS F. - Post-Test Analysis of LOBI Test BL-30 using RELAP5/MOD2.5; CEC-JRC, Technical Note I.93.64, May 1993

SEIGNEURET-GABORIT N. - Analysis of Typical LOBI Test Results Relevant to PWR Safety Analysis; CEC-JRC, Technical Note I.93.70, June 1993

VENTURA M., SHEPHERD I., SERRE F. - Sensitivity Calculations for PHEBUS-FP Tests Using the ICARE-2 Code - Technical Note I.93.27

YERKESS A. - TEXAS Calculations for the FARO-LWR Scoping Test, Technical Note I.93.151

YERKESS A. - Pre-Calculations for the FARO-LWR Base Case Test, Technical Note I.93.59

SANDERS J. - Minutes of the 7th Meeting of the Safety Technology Institute Advisory Board, Technical Note I.93.08

SANDERS J. - Minutes of the 8th Meeting of the Safety Technology Institute Advisory Board, Technical Note I.93.127

PETER G., PELLISSIER M. - Implementing the LWR Safety Code CATHARE under UNIX; Progress Report, Technical Note I.93.30

PELLISSIER M., WORTH B., FRANCHELLO G., PETER G., STÄDTKE H. - Application and Assessment of the CATHARE2 Code; Final Report on JRC Ispra Activities, 1990-92, Technical Note I.93.319

WORTH B., FRANCHELLO G., STÄDTKE H. - Generation and Verification of a RELAP5/MOD1-EUR Code Version Running on IBM RISC-6000 Workstations, Technical Note I.93.140

Safeguards and waste management

TECHNICAL EUR REPORTS

GUARDINI S. (editor) - Proceedings of the ESARDA International Workshop on Passive Neutron Counting - EUR 15102/EN, 1993

VOCINO V., MAUCQ T., FARESE N., VERRECCHIA G., NEBULONI N. - AWCC Users' Manual - EUR 15058/EN, 1993

CONTRIBUTIONS TO CONFERENCES

HAGE W., PEDERSEN B., BONDAR L., SWINHOE M., LEDEBRINK F.W. - Triple neutron correlation for MOX waste, American Nuclear Society, 1993 annual meeting, San Diego, June 20/24,1993 - ORA/PRO 37324

* Restricted distribution

VICINI C., RESTI P., ELEMENTI R., SARDO I., BONDAR L. - Measurement of low plutonium contaminated solid waste in 15 litre containers from Casaccia MOX pilot plant, ESARDA 15th annual symposium of safeguards and nuclear material management, Rome, Italy 11/13, 1993 - ORA/PRO 37560

BONDAR L., HAGE W., LEDEBRINK F.W., MASON J.A., PEDERSEN B., SWINHOE M. - Assay of Pu by neutron multiplicity counting using periodic and signal triggered methods, INMM 34th annual meeting, Scottsdale Arizona, July 18/21, 1993 - ORA/PRO 37618

MASON J.A., BONDAR L., HAGE W., PEDERSEN B. - The advantages of neutron multiple correlation analysis, ESARDA, 15th annual symposium of safeguards and nuclear material management, Rome, Italy, May 11/13, 1993 - ORA/PRO 37447

HAGE W., PEDERSEN B., VOCINO V., MASON J.A. - Development state of the triple neutron correlation technique by the factorial moment method at JRC Ispra, ESARDA international workshop on passive neutron coincidence counting, Ispra, Italy 20/23 April, 1993

BONDAR L. - Passive neutron assay by the Euratom time correlation analyser, ESARDA international workshop on passive neutron coincidence counting, Ispra, Italy, 20/23 April, 1993

GUARDINI S. et al. - Performance values of Non-Destructive Assay (NDA) techniques applied to safeguards, the 1993 evaluation by the ESARDA-NDA working group, Proc. of 15th ESARDA Symposium, Rome (I), May 1993 - ORA/PRO 37451

MATTHES W. - Montecarlo simulation of neutron coincidence counting techniques; Proc. of 15th ESARDA Symposium, Rome(I), May 1993 - ORA/PRO 37603

GUARDINI S. - Results and conclusions of the international workshop on plutonium and tritium calorimetry; Proc. of 15th ESARDA Symposium, Rome(I), May 1993 - ORA/PRO 37450

FOGGI C., HUNT B.A. - The TAME laboratory installation, at the JRC Ispra Site of the CEC; Proc. of ESARDA Symposium, Rome(I), May 1993 - ORA/PRO 37561

FRANKLIN M. et al. - Unattended monitoring and measurement for safeguards; Proc. of ESARDA Symposium, Rome (I), May 1993 - ORA/PRO 37448

CUYPERS M., DWORSCHAK H., GUARDINI S. et al. - Verification technology in an evolving nuclear environment; Proc. of ESARDA Symposium Rome (I), May 1993

LU M.S., TEICHMANN T., VOCINO V., VERRECCHIA G.P.D., CHARE P. - Fissile Mass-Multiplication Factor Correlation for Pu Measurements; ESARDA, May 1993 - ORA/PRO 37449

HAGE W., PEDERSEN B., VOCINO V. - Development state of the triple neutron correlation technique by the factorial moment method, at JRC Ispra; ESARDA International Workshop on passive neutron coincidence counting, April 1993

GUARDINI S. et al. - Results of the ESARDA international workshop on passive neutron counting, Proc. of 34th INMM annual meeting, Scottdale (Arizona, USA), July 1993 - ORA 37617

FRANKLIN M. - A comparison of different 'D' statistic approaches; Proc. of 34th INMM annual meeting, Scottdale (Arizona, USA), July 1993

KRAEMER R., BESSERER U., JOURDAN G. HOUSIADAS C., VASSALLO G., PERUJO A. - Common Tritium Control Methodology Proposed for Two Civil Tritium Facilities ETHEL and TKL; Proceedings of the 15th ESARDA Symposium, 11-13 May 1993, Roma (I), Kluwer Acad. Publ., C. Foggi (Ed.), EUR 15214/EN, 1993, pp 147-151 - ORA/PRO 37604

GUARDINI S. - Non-Destructive Assay on Uranium and Plutonium Materials in Safeguards: Lecture at the Institute for Atomic Energy, 25 January 1993, Beijing (China) - ORA 37306

DIERCKX R., NONNEMAN S., SCHILLEBEECKX P., FAVERO L. - Spectrum Modification: Calculation and Experimental Verification; 8th ASTM/Euratom Symposium, 29 August - 3 September 1993, Vail, Co. (USA) - ORA 37646

BRANCATI U., TINAGLI F., VENTURUZZO M. - Qualifica Sismica di Strutture Esistenti Destinati ad Ospitare Nuovi Laboratori presso il Centro Comune di Ricerca di Ispra della Commissione delle Comunità Europee; 6. Convegno Nazionale "L'Ingegneria Sismica in Italia", 13-15 Ottobre 1993, Perugia (I) - ORA 37736

GUARDINI S. - Summary and Conclusions of the ESARDA Passive Neutron Workshop; Proceedings of the Intern. Workshop on Passive Neutron Counting, 20-23 April 1993, Ispra (I) - ORA/PRO 37772

TECHNICAL NOTES*

BINDA F., DIERCKX R., DONGIOVANNI S., GRITTI R., REMORINI B. - JRC Ispra, Technical Note IST/NFC NE 40.1800.A.001

VOCINO V., MAUCQ T. - Experiments on Neutron Coincidence Counting, Technical Note I.93.44, April 1993

VOCINO V., MAUCQ T. - Setting up of the Neutron Electronic Chain Used for the HLNCC Family, Technical Note I.93.45, April 1993

VOCINO V., FARESE N., MAUCQ T. - PECC Algorithms and Procedures, Technical Note I.93.46, April 1993

VOCINO V., FARESE N., MAUCQ T., CALDON L. - Plutonium Pin Assay (PUPA), Technical Note I.93.43, April 1993

VOCINO V., MAUCQ T. - Pulse Interval Analysis (PIA), Technical Note I.93.47, April 1993

HAGE W., PEDERSEN B., VOCINO V. - Development State of the Triple Neutron Correlation Technique by the Factorial Moment Method at JRC Ispra - Technical Note I.93.31

BERNDT R. - Plutonium Content and Activity of Nuclear Fuel after Short-Term Irradiation - Technical Note I.93.42

HAGE W. - Multivariate Characteristic Functions for Correlated Function Type Signals - Technical Note I.93.48

WENG U. - MTR Gamma Scanner: Software Documentation - Technical Note I.93.136

SPECIAL PUBLICATIONS

GUARDINI S. (Ed.) - PERLA, Training and Technology Transfer, S.P./I.93.17

Fusion technology and safety

CONTRIBUTIONS TO PERIODICALS AND MONOGRAPHS

FORCEY K.S., PERUJO A., REITER F., LOLLI-CERONI P.L. - The Formation of Tritium Permeation Barriers by CVD; Journal of Nuclear Materials, Vol. 200 (1993), pp 417-420

REITER F., ALBERICI S., CAMPOSILVAN J., SERRA E.,FORCEY K.S., PERUJO A. - Diffusivity and Solubility of Hydrogen Isotopes in the Martensitic Steel DIN 1.4914 (MANET) after Thermal Exposure at 900 K, Zeitschrift für Physikalische Chemie - ART 41248

FORCEY K.S., PERUJO A., REITER F., LOLLI-CERONI P.L. - The Permeability, Diffusivity and Solubility of Deuterium in TZM, Journal of Nuclear Materials, Vol. 203 (1993), pp 36 - 42 - ART 41322

VASSALLO G., VAN DEN BERGH R., FORCEY K.S., PERUJO A. - Improved Permeation Barriers for Tritiated Waste Packaging; Fusion Technology - ART 41910

TECHNICAL EUR REPORTS

KRAEMER R., BESSERER U., JOURDAN G., HOUSIADAS C., PERUJO A., VASSALLO G. - Proceedings of the 15th Annual Symposium on Safeguards and Nuclear Material Management, Rome, Italy, 11-13 May, 1993, EUR 15214 EN, pp 147-151

REITER F., FORCE K.S., GERVASINI G. - A Compilation of Tritium Material Interaction Parameters in Fusion Reactor Materials, EUR 15217 EN

REITER F., ALBERICI S., CAMPOSILVAN J., CUERONI G.B., DOUGLAS K., FORCEY K.S., GERVASINI G., LOLLI-CERONI P.L., PERUJO A., SERRA E., TOMINETTI, S. - Hydrogen Isotopes- Material Interaction Studies at JRC-Ispra, EUR 15269 EN

MANNONE F. (Ed.) - Safety in Tritium Handling Technology; Proceedings of the EUROCOURSE, Ispra (I), 28-30 April 1993 - EUR 15144/EN, 1993

CONTRIBUTIONS TO CONFERENCES

CONRAD R., FÜTTERER, M., GIANCARLI R., MAY R., PERUJO A., SAMPLE T. - LIBRETTO 3: Performance of Tritium Permeation Barriers under Irradiation at the HFR Petten, presented at the ICFRM-6, Stresa, Italy 27/9 - 1/10, 1993

REITER F., FORCEY K.S., GERVASINI G. - Tritium-Material Interaction Properties in Fusion Reactor Materials; Proc. XII Conf. on Vacuum Science and Technology, Bolzano, 23-26 March 1993

MALARA C., MENCARELLI T., PIERINI G., RICAPITO I., TOCI F.- Determination of Multicomponent Adsorption Equilibria on Microporous Adsorbent; Paper presented at 3rd International Symposium on Separation Technology, Antwerpen (Belgium), August 22-27, 1993

HOUSIADAS C., TINAGLI F., VASSALLO G. - Estimates of Routine Tritium Discharges from ETHEL; Technical Committee on Developments in Fusion Safety, IAEA, 7-11 June 1993, Toronto, Ontario (CAN), Journal of Fusion Energy - ORA/ART 37581

HOUSIADAS C., PERUJO A., VASSALLO G. - The Control of Tritium in ETHEL; Technical Committee on Developments in Fusion Safety, IAEA, 7-11 June 1993, Toronto, Ontario (CAN), Journal of Fusion Energy - ORA/ART 37582

GERVASINI G., REITER F. - Hydrogen Isotopes Transport in Fusion Reactor First Wall Materials; Sixth Intern. Conference on Fusion Reactor Materials, CEC - JRC, 27 September - 1 October 1993, Stresa (I), Journal of Nuclear Materials - ORA/ART 37855

PERUJO A., DOUGLAS K., AGOSTINI P., CALDWELL-NICHOLS C. - Tritium Permeation through Engineering Components: JET Bellows Experiment; Proceedings of the 17th Symposium on Fusion Technology, ENEA, 14-18 September 1992, Roma (I), Elsevier Sc. Publs., C. Ferro, M. Gasparotto, H. Knöpfel (Eds.), 1993, pp 1201-1205 - ORA /PRO 36996

DWORSCHAK H. - The Experimental Programme in ETHEL: Developments in Fusion Safety, IAEA, 7-11 June 1993, Toronto, Ontario (CAN) - ORA 37583

MODICA G., EDWARDS R. - A Reactor-Permeator for Reduction of Tritium Oxide on Iron; Proceedings of the Workshop on Physics and Technology of Tritium for Fusion Reactors, Intern. School of Plasma Physics, 6-14 September 1993, Varenna, CO, (I) - ORA/PRO 37784

VIOLA A., TOCI F. - Actual Perspectives of Hydrogen Isotope Separation Systems; Proceedings of the Workshop on Physics and Technology of Tritium for Fusion Reactors, Intern. School of Plasma Physics, 6-14 September 1993, Varenna, CO, (I) - ORA/PRO 37785

VASSALLO G., ENGELMANN U. - A Review of General Tritium Accountancy Techniques; Proceedings of the Workshop on Physics and Technology of Tritium for Fusion Reactors, Intern. School of Plasma Physics, 6-14 September 1993, Varenna, CO, (I) - ORA/PRO 37939

REITER F., FORCEY K.S., GERVASINI G. - Tritium-Material Interaction Properties in Fusion Reactor Materials; XII National Conference on Vacuum Science and Technology, AIV, 23-26 March 1993, Bolzano (I), Vuoto - Scienza e Tecnologia - ORA/ART 37495

TECHNICAL NOTES*

DOUGLAS K., PERUJO A., AGOSTINI P. - Tritium Permeation Through Inconel 625 Bellows: The Jet Bellows Experiment, Technical Note I.93.72

HOUSIADAS C., PERUJO A., VASSALLO G. - Tritium Control in ETHEL, Contribution of JRC-STI to the 3rd TLK/ETHEL Workshop, Karlsruhe, May 24-25, 1993, edited by H. Dworschak, Technical Note I.93.78

PERUJO A., TOMINETTI S., CAMPOSILVAN J., LOLLI-CERONI P.L., CUERONI G.B. - Recycling of Hydrogen Isotopes from Fusion Reactor First Wall Materials under ITER Conditions, Contribution of JRC-STI to the 3rd TLK/ETHEL Workshop, Karlsruhe, May 24-25, 1993, edited by H. Dworschak, Technical Note I.93.78

FORCEY K.S., PERUJO A., REITER F., LOLLI-CERONI P.L. - Tritium Permeation Barriers for Fusion Applications; Contribution of JRC-STI to the 3rd TLK/ETHEL Workshop, Karlsruhe, May 24-25, 1993, edited by H. Dworschak, Technical Note I.93.78

DOUGLAS K., PERUJO A. - Tritium Permeation Through Inconel 625 Bellows: The Jet Bellows Experiment; Contribution of JRC-STI to the 3rd TLK/ETHEL Workshop, Karlsruhe, May 24-25, 1993, edited by H. Dworschak, Technical Note I.93.78

THORNTON M., GRASSI G., VASSALLO G. - Tritium Calorimetry in ETHEL; Contribution of JRC-STI to the 3rd TLK/ETHEL Workshop, Karlsruhe, May 24-25, 1993, edited by H. Dworschak, Technical Note I.93.78

VASSALLO G. et al. - Progress of ETHEL; Contribution of JRC-STI to the 3rd TLK/ETHEL Workshop, Karlsruhe, May 24-25, 1993, edited by H. Dworschak, Technical Note I.93.78

VASSALLO G. et al - ETHEL-002: Large-Scale Gaseous Detritiation; Contribution of JRC-STI to the 3rd TLK/ETHEL Workshop, Karlsruhe, May 24-25, 1993, edited by H. Dworschak, Technical Note I.93.78

MALARA C., PIERINI G., RICAPITO I., TOCI F. - Multicomponent Adsorption Equilibria on Microporous Adsorbents; Contribution of JRC-STI to the 3rd TLK/ETHEL Workshop, Karlsruhe, May 24-25, 1993, edited by H. Dworschak, Technical Note I.93.78

VIOLA A., GIONA M., MALARA C. - Mathematical Modelling for a Gas-Solid Process Unit; Contribution of JRC-STI to the 3rd TLK/ETHEL Workshop, Karlsruhe, May 24-25, 1993, edited by H. Dworschak, Technical Note I.93.78

MALARA C., PIERINI G., RICAPITO I., SPELTA B., TOCI F., VIOLA A. - Progress in Quantitative Analysis of Hydrogen Isotopes; Contribution of JRC-STI to the 3rd TLK/ETHEL Workshop, Karlsruhe, May 24-25, 1993, edited by H. Dworschak, Technical Note I.93.78

RICAPITO I., MALARA C., PIERINI G., SPELTA B. - Near Real-Time Diagnostic Analysis of Hydrogen Isotopes by Gas-Chromatography; Contribution of JRC-STI to the 3rd TLK/ETHEL Workshop, Karlsruhe, May 24-25, 1993, edited by H. Dworschak, Technical Note I.93.78

CARAVATI G., D'ADAMO D. - Remote Use of Primary Standard - Technical Note I.93.73

DWORSCHAK H. - Contribution of the JRC-STI to the 3rd TLK/ETHEL Workshop, Karlsruhe, May 24-25, 1993 - Technical Note I.93.78

BESSERER U., JOURDAN G. KRÄMER R., HOUSIDIAS C., PERUJO A., VASSALLO G. - Common Tritium Control Methodology Proposed for Two Civil Tritium Facilities, ETHEL and TLK - Technical Note I.93.84

SPECIAL PUBLICATIONS

PERUJO A., CAMPOSILVAN J., AGOSTINI P., REITER F. - ETHEL-001: Recycling and Outgassing of Tritium from First Wall Materials under NET/ITER Conditions, in Proc. of the Second ETHEL-TLK Workshop on Tritium Technology and Safety in Thermonuclear Fusion, Ispra, Italy, February 6-7, 1992, Ed. by F. Mannone and R.D. Penzhorn, S.P.I. 93.12

DOUGLAS K., PERUJO A. - Tritium Permeation Through Engineering Components: Jet Bellows Experiment, in Proc. of the Second ETHEL-TLK Workshop on Tritium Technology and Safety in Thermonuclear Fusion, Ispra, Italy, February 6-7, 1992, Ed. by F. Mannone and R.D. Penzhorn, S.P.I. 93.12

FORCEY K., PERUJO A., LOLLI-CERONI P.L., REITER F. - Tritium Permeation Barriers: The Hydrogen Prototype and ETHEL-004; Proc. of the Second ETHEL-TLK Workshop on Tritium Technology and Safety in Thermonuclear Fusion, Ispra, Italy, February 6-7, 1992, Ed. by F. Mannone and R.D. Penzhorn, S.P.I. 93.12

MODICA G., PERUJO A., MANNONE F. - ETHEL-006: Tritium Recovery from Waste Materials; Proc. of the Second ETHEL-TLK Workshop on Tritium Technology and Safety in Thermonuclear Fusion, Ispra, Italy, February 6-7, 1992, Ed. by F. Mannone and R.D. Penzhorn, S.P.I. 93.12

REITER F., ALBERICI S., CAMPOSILVAN J., FORCEY K., PERUJO A., SERRA E. - Diffusivity and Solubility of Hydrogen Isotopes in the Martensitic Steel MANET; Proc. of the Second ETHEL-TLK Workshop on Tritium Technology and Safety in Thermonuclear Fusion, Ispra, Italy, February 6-7, 1992, Ed. by F. Mannone and R.D. Penzhorn, S.P.I. 93.12

MANNONE F. (Ed.) - Proceedings of the Second ETHEL-TLK Workshop on Safety Technology in Nuclear Fusion, 6-7 February 1992, Ispra, Italy - S.P./I.93.12

Industrial hazards

CONTRIBUTION TO PERIODICALS AND MONOGRAPHS

BENUZZI A. - Le reazioni "runaway": misure di prevenzione e protezione, Prevenzione - Dossier; N. 5, pp 7-10, Aprile 1993 - ART 40840

HERNANDEZ H., ZALDIVAR J.M., BARCONS C. - Development of a Mathematical Model and a Numerical Simulator for the Analysis and Optimisation of Batch Reactors, Computer Chem. Engng. 17S, pp 45-50, 1993

ZALDIVAR J.M., HERNANDEZ H., NIEMAN H., MOLGA E., BASSANI C. - The FIRES project: Experimental study of thermal runaway due to agitation problems during toluene nitration, J. Loss Prev. Process Ind. 6, pp 319-326, 1993 - ART 41427

MOLGA E., BARCONS C., ZALDIVAR J.M. - Mononitration of Toluene and Quantitative Determination of the Isomer Distribution by Gas Chromatography, Afinidad 50, pp 15-20, 1993

KRÜGER G.J., HAUPT J., WEISS R. - A nuclear magnetic resonance method for the investigation of two-phase flow - Measuring techniques in gas-liquid two-phase flows, IUTAM Symposium Nancy, Francez, 1983, pp. 435-454, DELHAYE J.M., COGNET G., Eds. Springer, Berlin Heidelberg, 1984

ANDRONOPOULOS S., BARTZIS J.G., WÜRTZ J., ASI-MAKOPOULOS D. - Simulation of the Thorney Island Dense Gas Trial No.8 Using the Code ADREA-HF, Process Safety Progress Vol.12, No.1, January 1993

STATHARAS J.C., BARTZIS J.G., VENETSANOS A., WÜRTZ J. - Prediction of Ammonia Releases Using the ADREA-HF Code, Process Safety Progress, Vol. 12, No. 2, April 1993 - ART 41617

CARISSIMO B., ANDRONOPOULOS S., BARTZIS J.G., WÜRTZ J. - Intercomparison on Heavy Gas Dispersion Between the Three Dimensional Models MERCURE and ADREA, Part II: Instantaneous Release with a Semi-Circular Wall, EdF Report HE-33/93-05, 1993

DUFFIELD J.S., FRIZ G., NIJSING R. - Critical flow in a chemically reacting two-phase multicomponent mixture; Accepted: International Journal of Mutliphase Flow, 1993 - ART 40492

SKOULOUDIS A. - Benchmark Exercises on the Emergency Venting of Vessels Journal of Loss Prevention - ART 40558

ANDRONOPOULOS S., BARTZIS J.G., WÜRTZ J., ASI-MAKOPOULOS D. - Modelling the Effects of Obstacles on the Dispersion of Denser-than-Air Gases; Journal of Hazardous Materials - ART 41616

STATHARAS J.C., BARTZIS J.G., VENETSANOS A., W?URTZ J. - Prediction of Ammonia Releases Using the ADREA-HF Code, Process Safety Progress, Vol. 12, No. 2, 1993, pp 118-122 - ART 4167

MOUSSAS C., BITSORIS G. - Generalised One-Step-Ahead Control Subject to Input Constraints: A Linear Time-Varying System Approach; Control-Theory and Advanced Technology (C-TAT) - ART 41611

TECHNICAL EUR REPORTS

WÜRTZ J. - A Transient One-Dimensional Shallow Layer Model for Dispersion of Denser-than-Air Gases in Obstructed Terrains under Non-Isothermal Conditions, EUR 15342 EN, 1993

CONTRIBUTIONS TO CONFERENCES

MORRIS S.D. - The new venting facilities at JRC Ispra: DRACULA and COLUMBUS, European DIERS Users Group Meeting, Lyon, France, 4/5 May 1993

MORRIS S.D. - The DRACULA venting facility: design of the relief system; US DIERS Users Group Meeting, Albuquerque, USA, 11/13 May 1993

MORRIS S.D. - A venting test with a high-viscosity foamy fluid; European DIERS Users Group Meeting, Lyon, France, 4/5 May 1993

MORRIS S.D. - Maximum void fraction in vessel: some comments and further developments; European DIERS Users Group Meeting, Lyon, France, 4/5 May 1993

MORRIS S.D. - Luviskol Round-Robin problem; US DIERS Users Group Meeting, Albuquerque, USA, 11/13 May 1993

MORRIS S.D., KUHN H.G. - Some simplified design equations for gas vent sizing; US DIERS Users Group Meeting, Albuquerque, USA, 11/13 May 1993

MORRIS S.D. - 4P6 safety valve Round-Robin problem; US DIERS Users Group Meeting, Albuquerque, USA, 11/13 May 1993

MORRIS S.D. - The bubbly flow model, European DIERS Users Group Meeting, The Hague, Netherlands, 14/15 October 1993

NIEMAN H., ZALDIVAR J.M., HERNANDEZ H., BASSANI C. - The J.R.C. FIRES project for investigations on runaway reactions; Proceedings of the 11th International Congress of Chemical Engineering, Chemical Equipment Design and Automation, Praha (Czech Republic), 1993

MOUSSAS C., BITSORIS G. - Adaptive Constrained Control subject to both Input-Amplitude and Input-Velocity Constraints; IEEE Systems, Man and Cybernetics Conference, 17-20 October, Touquet (F), 1993

ZALDIVAR J.M., BARCONS C., HERNANDEZ H., MOLGA E. - Safety Aspects of Aromatic Nitrations by mixed acid in discontinuous reactors; Proceedings of the 11th International Congress of Chemical Engineering, Chemical Equipment Design and Automation, Praha (Czech Republic), 1993

ZALDIVAR J.M., HERNANDEZ H., MOLGA E., GALVAN I.M.,PANETSOS F. - The use of neural networks for the identification of complex reactions; Proc. of ESCAPE-3, Graz (A), pp 42-46, 1993 - ORA/PRO 37615

STÄDTKE H., WORTH B. - Numerical Simulation of Two-phase Flow based on Hyperbolic Flow Equations; Sixth International Topical Meeting on Nuclear Thermal Hydraulics, NURETH-6, Grenoble, October 5-8, 1993 - ORA/PRO 37358

TECHNICAL NOTES*

ZALDIVAR J.M., HERNANDEZ H., MOLGA E., ALOS M.A. - Mathematical Modelling and Simulation of Aromatic Nitrations by Mixed Acid in discontinuous reactors, Part I: Slow Liquid-Liquid reactions, JRC Ispra, Technical Note I.93.162, 1993

RUEL F., SORIA A. - A Semi-Implicit Solution of the Multicomponent Euler Equations in Subsonic Regime, JRC-Ispra, Technical Note No. I.93.76, June 1993

HULD T. - Numerical Simulation of Reacting Gas Flows: Explicit and Implicit Solvers for Diffusive Processes, JRC-Ispra, Technical Note No. I.93.104, July 1993

PETER G. - DIGLIB: A Device Independent Graphics Library, JRC-Ispra, Technical Note I.93.102, July 1993

ZALDIVAR J.M., HERNANDEZ H., MOLGA E., ALOS M.A. -Mathematical Modelling and Simulation of Aromatic Nitrations by Mixed Acid in Discontinuous Reactors, Part I: Slow Liquid-Liquid Reactions - Technical Note I.93.162

HAMMANS W. - Auxiliary Tools for Use with the Software Package ISPRAMIX - Technical Note I.93.57

Reference methods for the evaluation of structural reliability

CONTRIBUTIONS TO PERIODICALS AND MONOGRAPHS

DONEA J. VERZELETTI G., JONES P. PINTO A. - ELSA: European Laboratory for Structural Assessment (Reaction-Wall Facility) of the JRC Ispra; Proceedings of the 10th World Conference on Earthquake Engineering - ART 40943

HUERTA A., CASADEI F. - New ALE Applications in Non-Linear Fast-Transient Solid Dynamics; Intern. Journal for Computer-Aided Engineering and Software: Engineering Computations - ART 40247

GUTIERREZ E., MAGONETTE G., VERZELETTI G. - Experimental Studies of Loading Rate Effects on Reinforced Concrete Columns, Journal of Engineering Mechanics, vol. 119, No 5, pp 887-904, May 1993 - ART 40732

DONEA J. - Méthodes d'Eléments Finis pour les Problèmes de Convection-Diffusion; Revue Européenne des Eléments Finis - ART 40906

SORIA A., PEGON P. - An Arc Length Control Procedure to Solve Parabolic Problems Computer Methods; Applied Mechanics & Engineering - ART 41226

TECHNICAL EUR REPORTS

SORIA A., PEGON P. - Semi-Implicit Conservative Upwind Schemes for Transient Compressible Flows, EUR 14986 EN, 1993

PEGON P., SORIA A., LAVAL A. - Review of Finite Element Solvers for the Compressible Navier-Stokes Equations, EUR 14987 EN, 1993

CONTRIBUTIONS TO CONFERENCES

DONEA J., RUEL F., SORIA A. - On the Numerical Solution of Hyperbolic Problems; Actos del II. Congreso Metodos Numéricos en Ingeniera, 7-11 June 1993, La Coruña (E), Comunicaciones del II Congreso SEMNI, F. Navarrina, M. Casteleiro (Eds.) - ORA/PRO 37584

GUTIERREZ E., MAGONETTE G. VERZELETTI G. - Experimental Studies of Loading Rate Effects on Reinforced Concrete Columns; ASCE, Vol. 119, No. 5, pp 887-904, May 1993 - ORA/PRO 37464

GUTIERREZ E., VERZELETTI G. - Possibilities of Vibration Isolation Testing at the ELSA Laboratory of the Joint Research Centre; Proc. International Post-SMIRT Conference on Isolation, Energy Dissipation and Control of Vibrations of Structures, Capri, August 1993 - ORA/PRO 37821

PINTO A.V., NEGRO P., PEGON P., AREDE A. - Analysis of the 4 Storey R/C Building to be Tested in the ELSA Laboratory (2nd Phase), Cooperative Research on Seismic Response of Reinforced Concrete Structures, Contract n. 4504 - 91-10 ED ISP P, E.C. Carvalho (Ed.), proc. 135/11/10778, LNEC, Lisbon, 1993

RENDA V., BELLORINI S., PAPA L. - Extension of the Pseudo-Dynamic Method to Test Structures with Distributed Mass; Proceedings of Symposium on Structural Mechanics in Reactor Technology (SMIRT 12), 15-20 August 1993, Stuttgart (D) - ORA/PRO 37326

PEGON P., COMBESCURE D. - Impact of Experimental Errors on the PSD Method; Workshop on Pseudo-dynamic Test Method, ELSA, July 1993

ALBERTINI C., DEL GRANDE A., DELZANO C., KIEFER R., MONTAGNANI M., MURAROTTO M., PIZZINATO E.V., RODIS A., SCHNABEL W. - New Approach to Crash-Worthiness Studies of Automotive and Aerospace Thin Sheet Metal Structures by a Large Hopkinson Bar Method; Proceedings of EURDYN 1993, Norwegian Inst. of Technology, 21-23 June 1993, Trondheim (N), Balkema Publs. - ORA/PRO 37589

ALBERTINI C., DELZANO C., PIZZINATO E.V., RODIS A. - Dynamic Mechanical Properties of Ductile Steel to Base Failure Criteria of Advanced Containment Shells; Proceedings of the 12th SMIRT Symposium, 15-20 August 1993, Stuttgart (D) - ORA/PRO 37462

ALBERTINI C., DELZANO C., MONTAGNANI M., RODIS A. - Large Hopkinson's Bar Method for Advanced Impact Testing of Structural Containment Components in Steel and Concrete; Proceedings of the 12th SMIRT Symposium, 15-20 August 1993, Stuttgart (D) - ORA/PRO 37463

ALBERTINI C., MONTAGNANI M., RODIS A., MARIOTTI P., PALUFFI A., PAZIENZA G. - Influence of Strain Rate, Biaxial Loading and Deformation Mode on Fracture Criteria of Ductile Steels; Porceeding of the 8th Conference on the Realtionship between Microstructure and Dynamic Properties of Metals, Alloys and MMC, DYMAT, 12-13 October 1993, Ispra (I) - ORA/PRO 37865

CASADEI F., HALLEUX J.P. - Fluid-Structure Sliding in Complex Transient Dynamic Problems; EUROMECH 306 Colloquium on Mechanics of Contact Impact, 7-9 September 1993, Prague (CS) - ORA 37786

ALBERTINI C., PIZZINATO E.V., RODIS A. - Large Hopkinson Bar Experiments for the Validation of Numerical Crash Computations of Car and Road Safety Structures; Proceedings of the 26th Intern. Symposium on Automative Technology and Automation (26th ISATA), 13-17 September 1993, Aachen (D) - ORA/PRO 37788

DONEA J. - A Review of Upwind Finite Elements; Proceedings of the VIII Intern. Conference on Finite Elements in Fluids, Univ. Polit. Catalunya, 20-24 September 1993, Barcelona (E) - ORA/PRO 37800

TECHNICAL NOTES*

PEGON P. - A Timoshenko simple beam element in CASTEM 2000, JRC-Technical Note I.93.05, 1993

CASADEI F. - PLEXIS-3C Solutions to a Shock Tube Problem, Technical Note I.93.33, March 1993

CASADEI F. - A Non-linear 3-D Shell Finite Element Implementation for Transient Problems, Technical Note I.93.41, April 1993

CASADEI F. - Considerations about a Data Management and Document Production System for AMU, Technical Note N. I.93.55, April 1993

CASADEI F., HALLEUX J.P. (Eds.) - PLEXIS-3C User's Manual (Preliminary Version), Technical Note I.93.83, June 1993

CASADEI F. - Implementation of Compressible Fluid Models in PLEXIS-3C, Part I - Models, Technical Note I.93.86, June 1993

CASADEI F. - Implementation of 3-D Degenerated Shell Elements in PLEXIS-3C, Technical Note I.93.88, July 1993

CASADEI F. - Generalisation of a Two-Dimensional Rectilinear Beam/Conical Shell Element to Large Membrane Strains, Part I - Theory, Technical Note I.93.89, July 1993

CASADEI F. - A Miscellanea of New Models in PLEXIS-3C, Technical Note I.93.90, July 1993

CASADEI F. - Treatment of Essential Boundary Conditions in PLEXIS-3C, Technical Note I.93.91, July 1993

CASADEI F. - A Triangular Plate Element for the Non-linear Dynamic Analysis of Thin 3-D Structural Components, Technical Note I.93.92, July 1993

CASADEI F. - Implementation of ALE Fluid-Structure Interaction Models in PLEXIS-3C, Technical Note I.93.139, November 1993

CASADEI F. - Simulation of a gas explosion in a reactor containment by PLEXIS-3C, Technical Note I.93.148, November 1993

CASADEI F. - Simulation of a gas explosion in an underground cell by PLEXIS-3C, Technical Note I.93.149, November 1993

CASADEI F. - Post-processing of PLEXIS-3C calculated results by CASTEM 2000, Technical Note I.93.150, November 1993

RODIS A., DEL GRANDE A., PIZZINATO E.V., SCHNABEL W., ALBERTINI C. - Progetto di Barra di Hopkinson per lo Studio delle Proprietà Meccaniche in Tensione Taglio: ad Alta Velocità di Deformazione, di Acciai, Materiali Compositi e Ceramiche - Technical Note I.93.113

RODIS A., DEL GRANDE A., PIZZINATO E.V., SCHNABEL W., ALBERTINI C. - Mechanical Properties of Zircaloy-2 under Dynamic Uniaxial Tensile Testing Plate Type Specimens - Technical Note I.93.71

RODIS A., DEL GRANDE A., PIZZINATO E.V., SCHNABEL W., ALBERTINI C. - Mechanical Properties of Austenitic Stainless Steel (SUS 304) and Nickel Alloy (NI 201) under Dynamic Uniaxial Tensile Testing Using Plate Type Specimens - Technical Note I.93.61

Working environment

CONTRIBUTION TO CONFERENCES

NGUYEN H. - A Petrov-Galerkin least squares finite element algorithm for prediction of room air motion; Indoor Air '93, Int. Conf., Helsinki-Finland, July 1993 - ORA/PRO 37612

TECHNICAL NOTES*

DONEA J., GIULIANI S. - A proposed strategy for the numerical simulation of thermal discharges into coastal waters of the sea, Technical Note I.89.84, August 1993

NGUYEN H. - Finite element calculations of incompressible turbulent flows, Technical Note I.93.170, December 1993

AL-KHUDHAIRY D. - Particle Dispersion in two-dimensional confined turbulent flows: A survey of models, Technical Note I.93.152, November 1993

Support to Community policies

Safeguards

CONTRIBUTION TO CONFERENCES

VERRECCHIA G.P.D. et al. - Calibration of the neutron coincidence collar for the assay of fuel assemblies contianing thermal neutron poison, 13th ESARDA Symposium on safeguards and nuclear material management, Avignon, France, 16-16 May 1991

FOGGI C., HUNT B.A. - The TAME laboratory installation at the JRC Ispra site of the CEC; 15th annual symposium on safeguards and nuclear material management, ESARDA, Rome, Italy, 11-13 May 1993

FOGGI C., HUNT B.A. - R&D on the volume mesurements of liquids in the TAME laboratory; 34th Annual Meeting of the Institute of Nuclear Material Management, Phoenix, USA, July 1993

FRANKLIN M. - A Comparison of D Statistic Approaches; Proc. of 34th Annual Meeting of the Institute of Nuclear Materials Management, Phoenix, USA, July 1993

TECHNICAL NOTES*

VOCINO V. et al. - PECC Algorithms and Procedures, Technical Note I.93.46, April 1993

FRANKLIN M. - Implementation of Difference Statistics in Safeguards, JRC Ispra, Technical Note I.93.103

Exploratory research

CONTRIBUTION TO CONFERENCES

RIEF H., TAKAHASHI H. - Control of Accelerator Driven Subcritical Systems Fuelled by Actinides; Technical Committee Meeting on Safety and Environmental Aspects of Partitioning and Transmutation of Actinides and Fission Products, IAEA, Vienna, Nov. 29 - Dec. 2, 1993

FRANKLIN M. et al. - Unattended monitoring and measurement for safeguards; Proc. of ESARDA Symposium, Roma (I), May 1993

Large test facilities

CONTRIBUTION TO CONFERENCES

2nd International Working Group Meeting on R&D on Volume and Mass Determination of Liquids in Tanks used at Nuclear Materials Processing Installations, Ispra, 6-7th October, 1993

TECHNICAL EUR REPORTS

FASOLI-STELLA P., KRISCHER W. (Ed.) - Annual Report 1992 of the Safety Technology Institute, Joint Research Centre Ispra, EUR 15055 EN, 1993

7.2 MEETINGS

Reactor safety

ESTER workshop - users club meeting

A Workshop was held at Ispra on 7-9 June 1993, on the European Source Term Evaluation Research (ESTER) system code. This second ESTER Workshop was combined with a training for beginners on the use of the RSYGAL tools and with the Users' Club Meeting. The objectives of the meeting were to promote ESTER to a wider rang of users, to train the users and potential ESTER developers to the use of the tools and to receive feedback for future developments of the system code. The meeting was attended by 16 participants from 7 European countries and 8 participants from the STI Institute of Ispra. Two new users have been registered during 1993.

First STORM meeting

The first meeting on the STORM Project was held in Ispra on the 21st and 22nd April 1993, organised by the Safety Technology Institute (STI). The main purpose of the meeting was to present the STORM Project to national experts on Source Term. The meeting was also a forum for discussing the present and future trends of the various national research activities on severe accidents and, in particular, the interest for an involvement in the STORM Project. 36 experts of 15 different organisations from seven countries attended the meeting. Several institutions declared their interest for active collaboration with the analytical or the measurement programme.

Second STORM meeting

The second meeting on the STORM Project was held in Ispra on the 15th December 1993. The main purpose of the meeting was to launch code benchmarks concerning the aerosol transport, deposition and resuspension as well as the thermo-hydraulics in the STORM facility. 42 experts from 17 organisations participated and they expressed their consensus on the proposal to carry out benchmarks. The results obtained from different codes will be compared amongst each other and to the measured experimental data at the next STORM Meeting which is foreseen on 4th of July 1994.

LOBI data users club meeting

The members of the LOBI Data Users' Club were convened for their second meeting at JRC-Ispra on November 12, 1993. The meeting was attended by representatives of several research organisations from EC as well as east-european countries. The meeting offered an opportunity to scientists involved in LOBI post-test analysis for an exchange of information and expertise on the use of the data and on related code assessment activities. The third meeting of the club will be held in Budapest/Hungary in October 1994, hosted by the Hungarian KFKI Atomic Energy Research Institute.

Safeguards and fissile material management

International workshop on passive neutron assay

The JRC organized jointly with ESARDA (European Safeguards R&D Association) an International Workshop on Passive Neutron Counting at PERLA on 20-23 April 1993. Developers and users of passive neutron assay techniques and instruments, together with EURATOM and IAEA inspectors and facility operators, 35 participants in total, attended a one-week workshop on passive neutron assay of plutonium bearing materials. The Proceedings of the Workshop were published in EUR 14102 EN/1993.

Second meeting on use of TAME laboratory

On 6-7 October 1993 a second TAME Users' meeting was held in Ispra to define the future tasks and programme of the TAnk MEasurement laboratory. Around 30 experts were present, from EC countries, Japan, USA and from the IAEA, to discuss problems associated with volume/mass measurements in large-scale nuclear plants.

Fusion technology and safety

3rd ETHEL/TLK workshop

This was the 3rd of the annual workshops held between ETHEL Ispra and the TLK Karlsruhe. The meeting took place in Karlsruhe on 24 and 25th May 1993 with 23 representatives from KfK and 20

from Ispra. The workshop on titrium technology and safety in the thermonuclear fusion concentrated on operational and safety aspects of the laboratories as well as research activities. The proceedings were published as a KfK report.

Course on safety in tritium handling technology

This was a Euro-Course based on lectures given by invited tritium experts. The lectures were presented in Ispra on 28 - 30th April 1993 with 9 participants from external organisations and 31 from Ispra. The course on safety tritium handling technology concentrated on tritium biological hazard, dosimetry, radiological protection and environmental safety with particular attention on implications for tritium plant operators and the general public. The lectures were published in book form.

Reference methods for the evaluation of structural reliability

EUROCODE 8 network

Following the acceptance in November 1992 of the proposed Human Capital and Mobility network on prenormative research in support of Eurocode 8, three meetings were organised at the ELSA laboratory on March 11-12, July 22-23 and October 22 to finalize the work programme and distribute the experimental and numerical tasks among the 18 laboratories participating in the network.

COST-C1

COST-C1 is an international project intended to study the behaviour of semi-rigid structural connections. A member of the ELSA staff has been nominated chairman of the "Seismic Behaviour/Design" working group of COST-C1. Two meetings of this working group have taken place in 1993, the first at Ispra in June and the second in Lausanne in December.

Workshop on pseudo-dynamic testing

This workshop, organised at Ispra on July 13, 1993, provided an opportunity to review ongoing research on the pseudo-dynamic test method in Europe and the United States. More than 20 participants, mainly from laboratories in the European Association of Structural Mechanics Laboratories, attended the meeting. A major topic in the discussions was the development and implementation of implicit schemes for numerical time integration of the equations of motion for the test structures. The meeting was attended by Prof. Benson Shing from the University of Colorado, Boulder, a pioneer of implicit pseudo-dynamic schemes.

DYMAT conference

DYMAT is a non-profit Association founded in 1983 at the initiative of a group of French Scientists who shared an interest in promoting the study of the dynamic behaviour of materials. The 8th DYMAT technical conference, organised at Ispra on October 12-13, 1993, was attended by more than 60 participants from all over Europe. The conference provided an opportunity to exchange information and share experiences on the relationship between microstructure and dynamic properties of structural materials, as well as on the behaviour of structures under transient dynamic loading. Detailed visits to the ELSA and LDTF facilities were organised at the occasion of the DYMAT Conference.

8 LIST OF TABLES AND FIGURES

8.1 TABLES

Reactor safety

Management and storage of radioactive waste

Safeguards and fissile material management

Fusion technology and safety

Reference methods for the evaluation of structural reliability

Safeguards

Exploratory research

Human resources

The ELSA reaction-wall facility

8.2 FIGURES

Reactor safety

Management and storage of radioactive waste

Safeguards and fissile material management

Fusion technology and safety

Industrial hazards

Reference methods for the evaluation of structural reliability

Working environment

Safeguards

Association of laboratories

Exploratory research

Human resources

The ELSA reaction-wall facility

The FARO facility

PERLA

ETHEL

TAME

9 INDEX OF AUTHORS

Editors

Reactor Safety

Safeguards and Waste Management

Fusion Technology and Safety

Industrial Hazards

Reference Methods for the Evaluation of Structural Reliability

Working Environment

Support to Community Policies

Association of Laboratories

Exploratory Research

Decommissioning

Large Test Facilities

Acknowledgements

The editors would like to thank Mrs C. Kind, Mrs K. Faber and Mrs H. Van Paemel for text editing, the Public Relations and Publications Office for its assistance and, in particular, Mrs M. Magermans for the graphical layout.

10 GLOSSARY OF ACRONYMS AND ABBREVIATIONS

ACE	Advanced Containment Experiments
ACCU	ACCUmulator
AEA	Atomic Energy Agency (UK)
AECC	Active Euratom Coincidence Counter
AECL	Atomic Energy of Canada Laboratory
AFW	Auxiliary Feed Water
AGCM	Atmospheric General Circulation Model
AIB	Association Industrielle Belge
ALE	Arbitrary Lagrangian - Eulerian
ALPO	ALumino PhOsphate
AMU	Applied Mechanics Unit
AN	ANtech Technology Ascot
ANOVA	ANalysis Of VAriance
ANS	American Nuclear Society
a.o.	amonst others
ASCII	American Standard Code for Information Interchange
ATWS	Anticipated Transient Without Scram
AWCC	Active Well Coincidence Counter
BAM	BundesAnstalt für Materialforschung (D)
BCT	Base Case Test
BETHSY	Boucle d'Etudes THermohydrauliques SYstème (CEA)
BNCT	Boron Neutron Capture Therapy
BNFL	British Nuclear Fuel Ltd.
BNL	Brookhaven National Laboratory (USA)
BR	Belgian Reactor
BWR	Boiling Water Reactor
CAD	Computed Aided Design
CAL	CALorimetry
CASTEM	(2000) finite element system for structural analysis (CEA-Saclay)
CBNM	Central Bureau for Nuclear Measurements (JRC)
CCF	Counter Current Flow
CE	Centre d'Etudes
CEA	Commissariat à l'Energie Atomique (F)
CEC	Commission of the European Communities
CECILE	Cellule d'Examen et de Contrôle de l'Iode et de Lotissement des Echantillons
CEN	Comité Européen de Normalisation
CEU	Commission of the European Union
CGC	Comité de Gestion et Coordination (CEU)
CIEMAT	Centro de Investigaciones Energeticas Medio-Ambientales y Tecnologicas, Madrid (E)
CISI	Compagnie Internationale Services Informatiques (F)
CL	Cold Line (leg)
CNR	Comitato Nazionale delle Ricerche (ENEA)
COLUMBUS	venting of long horizontal vessels facility
COMETA	COre MElt Thermal-hydraulic Analysis code
CORA	Complex Out-of-pile Rod bundle Assembly
COST-C1	European Concerted Action on control of semi-rigid behaviour of civil engineering connections
CPA	Computational Process Analysis (STI-Sector)
CPT	Counter-Part Test
CPU	ComPUter
CRIS	Centro di Ricerca Idraulica e Strutturale (ENEA)
CRTN	Centro di Ricerca Termica e Nucleare (ENEL)
C/S	Containment/Suveillance
CSCS	Centro Svizzero di Calcolo Scientifico, Manno
CSNI	Committee on Safety Nuclear Installations
CVD	Chemical Vapour Deposition
DA	Destructive Analysis
DAS	Data Acquisition System
DCS	Direction Contrôle de Sécurité
DDA	Differential Die-Away method
DEA	Diplôme d'Etudes Approfondies
DEC	Digital Equipment Company
DEDA	type of waste container
DEVAP	DEpositon of VAPours (CEA experiment)
DG	Directorate General
DIERS	Design Institute for Emergency Relief Systems
DIGLIB	Device Independent Graphics LIBrary
DISP	DIrezione Sicurezza Nucleare e Protezione Sanitaria (ENEA)
DOE	Department Of Energy (USA)
DoF	Degree of Freedom
DOS	Disk Operating System
DRACULA	Depressurization, Relief And Containment Using Large Apparatus
DSC	Differential Scanning Calorimetry
DSP	Digital Signal Processors
DTG	Differential Thermal Gravimetry
DYMAT	DYnamic behaviour of MATerials
EASML	European Association of Structural Mechanics Laboratories
EBR-1	Experimental Breeder Reactor N° 1
EC	European Communities
EC8	EuroCode N° 8
ECCS	Emergency Core Cooling System
ECO	Expérience Critique Orgel, Ispra
ECMWF	European Center for Medium range Weather Forecasts
ECP	Ecole Centrale de Paris
EdF	Electricité de France
EDF	Experimental Data File

EEDF	ELSA Experimental Data Files
EERI	Earthquake Engineering Research Institute
EFL	Explosion and Flame Laboratory of the Health and Safety Executive
EFTA	European Free Trade Association
EI	Environment Institute (JRC)
ELSA	European Laboratory for Structural Assessment, Ispra
ENEA	Energia Nucleare ed Energie Alternative
ENEL	Ente Nazionale per l'Energia Elettrica (I)
ENUSA	Empresa Nacional de Urano S.A. (E)
EPRI	Electric Power Research Institute (USA)
ERCOFTAC	European Research COmmunity for Flow, Turbulence And Combustion
ESARDA	European SAfeguards R and D Association
ESD	Euratom Safeguards Directorate
ESSOR	ESSai ORgel (organique eau lourde) - Ispra
ESTER	European Source Term Evaluation Research
ETHEL	European Tritium Handling Experimental Laboratory, Ispra
EU	European Union
EURATOM	EURopäische Gemeinschaft für *ATOM*energie
FAL	FALcon
FARO	Fuel melting And Release Oven
FBFC	Franco-Belge Fabrication Combustible
FCI	Fuel Coolant Interaction
FE	Finite Element
FIRES	Facility for Investigating Runaway Events Safely
FISIM	FIRES SIMulator
FLADIS	two-phase FLAshing releases DISpersion
FP	Fission Product
FPGA	Field Programmable Gate Arrays
FPT	Fission Product Test
FVS	Flux Vector Splitting
FWP	FrameWork Programme
FZR	Forschungs-Zentrum Rossendorf (D)
GC	Gas Chromatography
GCM	General Circulation Model
GdF	Gaz de France
GRS	Gesellschaft für Reaktor-Sicherheit (D)
HB	High Burn-up
HCM	Human Capital and Mobility
HDPE	High Density PolyEthylene
HETP	Height Equivalent to a Theoretical Plate
HEU	Highly Enriched Uranium
HEXNODYN	HEXagonal NODal DYNamic code
HL	Hot Line (leg)
HFR	High Flux Reactor
HLNCC	High Level Neutron Coincidence Counter
HIAS	Heterogeneous Ideal Adsorbed Solution
HIP-BN	High-Isostatic Pressed - Boron Nitride
HP	High Purity or Hewlett Packard
HPIS	High Pressure Injection System
HRGS	High Resolution Gamma Spectrometry
HRT	Heater Rod Temperature
IAEA	International Atomic Energy Agency
IAM	Institute of Advanced Materials
IAS	Ideal Adsorbed Solution
IBM	International Business Machines
ICE	Implicit Continuous Eulerian method
ICFRM	International Conference on Fusion Reactor Materials
IF	fast neutron Induced Fission
IFCI	Integrated Fuel Coolant Interaction
IKE	Institut für Kerntechnik und Energiesysteme (D)
INMM	Institute of Nuclear Material Mesurements
INRS	Institut National de Recherche et de Sécurité (F)
INTEL	Hardware Company (USA)
IPSN	Institut de Protection et de Sûreté Nucléaire (F)
IPU	Impianto PlUtonio
IR	InfraRed
IRSA	Institute of Remote Sensing Applications (JRC)
ISCC	Inventory Sample Coincidence Counter
ISEI	Institute for Systems Engineering and Informatics (JRC)
ISO	International Standards Organisation
ISOLDA	Interactive System for On-Line Data Animation
ISP	International Standard Problem
ITER	International Thermonuclear Experimental Reactor
IUTAM	International Union of Theoretical and Applied Mechanics
JAERI	Japan Atomic Energy Research Institute
JBL	Jet Break-up Length
JET	Joint European Torus
JRC	Joint Research Centre (EU)
KfK	Kernforschungszentrum Karlsruhe (D)
KFKI	Hungarian Central Research Institute for Physics
KROTOS	small-scale steam explosion facility, Ispra
KWU	KernkraftWerks-Union Siemens (D)
LACE	LWR Aerosol Containment Experiments
LAM	Limited-Area Model
LAMS	Low Activation Martensitic Steels
LAN	Local Area Network

LANL	Los Alamos National Laboratory (USA)
LB	Low Burn-up
LCFS	Last Closed magnetic Flux Surface
LDTF	Large Dynamic Test Facility, Ispra
LER	Laboratory for Exploratory Research
LEU	Low Enriched Uranium
LIBRETTO	LIquid BReeder Experiment with Tritium Transport Option
LLNL	Lawrence Livermoore National Laboratory (USA)
LMA	Laboratorio di Media Attività, Ispra
LMB	Liquid Metal Blanket
LMFBR	Liquid Metal Fast Breeder Reactor
LNEC	Laboratorio Nacional de Engenharia Civil (P)
LOAF	Loss-Of-All Feedwater
LOBI	LWR Off-normal Behaviour Investigations, Ispra
LOCA	Loss Of Coolant Accident
LOF	Loss Of Flow
LOFT	Loss Of Flow Test
LOFW	Loss Of Feed Water
LONOP	Loss Of Normal Onsite Power
LP	Large Port
LPIS	Low Pressure Injection System
LSTF	Large-Scale Test Facility
LVDT	Linear Variation Displacement Transducer
LWR	Light Water Reactor
MANET	MArtensitic for NET
MCCI	Molten Core - Concrete Interaction
MCNP	MonteCarlo Neutron Photon transport code
MCP	Main Coolant Pump
MeAPO	Metallo AluminioPhOsphate
MFCI	Molten Fuel Coolant Interaction
MGA	Multi-Group Analysis
MOX	Mixed OXide
m.p.	melting point
MP	Melting Progression
MPMC	MultiPhase-MultiComponent
MS	MicroSoft
MTC	MATEC Milano (I)
MTR	Material Testing Reactor
MUSCL	Monotonic Upwind Scheme for Conservative Laws
NCC	Neutron Coincidence Counting
NDA	Non Destructive Assay
NEA	Nuclear Energy Agency
NEACRP	Nuclear Energy Agency Committee on Reactor Physics
NED	Nuclear Experiment Division
NEGACA	NEutrons GAmma CAlorimeter
NET	Next European Torus
NFC	Nuclear Fuel Cycle
NISEE	National Information Service for Earthquake Engineering
NMA	Nuclear Material Accountancy
NMR	Nuclear Magnetic Resonance
NPT	Non - Proliferation Treaty
NUPEC	NUclear Power Engineering Centre, Japan
OD	Outer Diameter
OECD	Organisation for Economic Cooperation and Development
OGCM	Oceanic General Circulation Model
OH	Ontario Hydro (CAN)
OLIWA	On-LIne WArning
ORNL	Oak Ridge National Laboratorium (USA)
OS	Operator-Splitting method
PBF	Power Burst Facility (USA)
PC	Personal Computer
PCS	Primary Cooling System
PDTM	Pseudo-Dynamic Test Method
PEC	Poste d'Examen et de Contrôle
PECC	Passive Euratom Coincidence Counter
PED	Process Engineering Division (STI)
PERLA	PERformance LAboratory for safeguards, Ispra
PETRA	Plant for Evaluation and Testing of Radwaste management Alternatives, Ispra
PHONID	PHOto-Neutron Interrogation Device
PIA	Pulse Interval Acquisition
PIE	Post-Irradiation Examination
PILC	Pillared Inter-Layer Clay
PIV	Physical Inventory Verification
PLC	Programmable Logic Controller
PNC	Passive Neutron Counting
PREC8	Prenormative Research for EuroCode N° 8
PS	Primary System
PSD	PSeudo-Dynamic
PSI	Paul Scherrer Institut (CH)
PTA	Post-Test Analysis
PTB	Physikalisch-Technische Bundesanstalt (D)
PTS	Pressurizer Thermal Shock
PUPA	PlUtonium Pin Assay
PVM	Parallel Virtual Machine
PVT	Pressure-Volume-Temperature
PWR	Pressurized Water Reactor
QA	Quality Assessment
QC	Quality Control
QT	Quenching Test
RAS	Real Adsorbed Solution

RBU	Reaktor Brennelement Union Siemens (D)
RC	Reaction Calorimeter
R/C	Reinforced Concrete
RCA	Reinforced Concerted Action
RCWG	R/C Working Group
R & D	Research and Development
RDF	Reduced Degree of Freedom
Ref.	Reference
RELIEF	design venting systems code
REPF	REservoir Produits Fission
Rev.	Revision
r.f.	radio frequency
RF	Resolution Factor
RPC	Remote Procedure Calls
RSYGAL	portmanteau acronym from two database systems: RSYST and SIGAL
SANGRIA	System for Automatic Non-structured GRId Adaptation
SAPO	Silico-Alumino-PhOsphate
SAWG	Scientific Analysis Working Group (Phebus-FP)
SCA	Shared Cost Action
SD	Standard Deviation
SEMAR	Service d'Etudes et de Modelisation d'Accidents de Réacteurs (CEA/IPSN)
SF	Spontaneous Fission or Separation Factor
SFD	Severe Fuel Damage
SG	Steam Generator
SGTR	Steam Generator Tube Rupture
SIO	Società Italiana Ossigeno
SNL	Sandia National Laboratories (USA)
SOAR	State-Of-the-Art Report
SOL	Scrape-Off Layer
SPECTRA	Safeguards PErla Centre for TRAining
SS	Stainless Steel
SSN	Sistema Salvataggio Nocciolo
ST	Scoping Test
STEP	Science and Technology for Environmental Protection
STI	Safety Technology Institute (JRC)
STORM	Simplified Tests On Resuspension Mechanism
STP	Standard Temperature and Pressure: 273 K, 100 kPa
SUN	Micro-Systems Computer Corporation
TAME	TAnk MEasurement laboratory, Ispra
T & C	Testing and Commissioning
TCA	Time Correlation Analyser
TD	Derandomizing Time
TeX	public domain typesetting program
TG	Technical Group (Phebus-FP)
THORP	THermal Oxide Reprocessing Plant
TLK	Tritium Laboratory Karlsruhe (D)
TOP	Transient Over-Power accident
TRG	TRainInG
TRSS	Tritium Receipt and Storage System
TSTA	Tritium System Test Assembly
TTL	Transistor-Transistor Logic
TUBA	TUBe Aerosol experiment (CEA)
TUI	TransUran Institut (JRC)
TURCOM	TURbulent COMbustion
TVD	Total Variation Diminishing scheme
TZM	molybdenum alloy
UCLA	University of California at Los Angeles (USA)
UHV	Ultra-High Vacuum
UIA	UnIversity of Antwerpen (B)
UIUC	University of Illinois at Urbana - Champaign (USA)
UK	United Kingdom
UKAEA	United Kingdom Atomic Energy Authority
UMS	Unattended Monitoring System
UNIX	UNiplexed Information and Computing System
UPC	Universitat Politecnica de Catalunya (E)
UPM	Universidad Politecnica de Madrid (E)
US	United States
USNRC	United States Nuclear Regulatory Commission
UTS	Ultrasonic Temperature Sensor
UV	UltraViolet
VAX	Virtual Access memory: DEC computer architecture
VCR	Video Casette Recorder
VDC	Variable Deadtime Counter
VENUS	Belgian nuclear facility
VME	VERSA Module Europe
WG	Working Group
wt	weight

APPENDIX

A LARGE TEST FACILITIES

A.1 THE ELSA REACTION-WALL FACILITY

In 1992, the Safety Technology Institute has completed the construction of a structural assessment laboratory based on a 16m high, 21m wide reaction wall (*Fig. A1.1*). This new facility, now named ELSA (European Laboratory for Structural Assessment), will make it possible to study how large-scale models of complex civil engineering structures react when subjected to severe static or dynamic loading. Designed to resist the huge forces, typically several hundred tonnes, which are necessary to deform and seriously damage full-scale test models of structures, the ELSA reaction-wall is actually one of the largest facilities of its type in the world, only exceeded by Japan.

In addition to static and cyclic tests on large structures and components, the facility is equipped to perform the so-called pseudo-dynamic (PSD) test technique, enabling for example, the simulation of earthquake loading on full-scale buildings.

Fig. A1.1 Testing of a three-storey steel frame (left) and of a four-storey reinforced concrete frame (right) at the ELSA reaction-wall

Basis of the pseudo-dynamic test method

Fig. A1.2 illustrates the method schematically as applied to an earthquake simulation test of a civil engineering structure. A record of an actual or artificially generated earthquake ground acceleration history is given as input data to the computer and the horizontal displacements of the floors (the levels at which the mass of the building can be considered to be concentrated) are calculated for a small time-step. These displacements are then applied to the structure by servo-controlled hydraulic actuators attached to

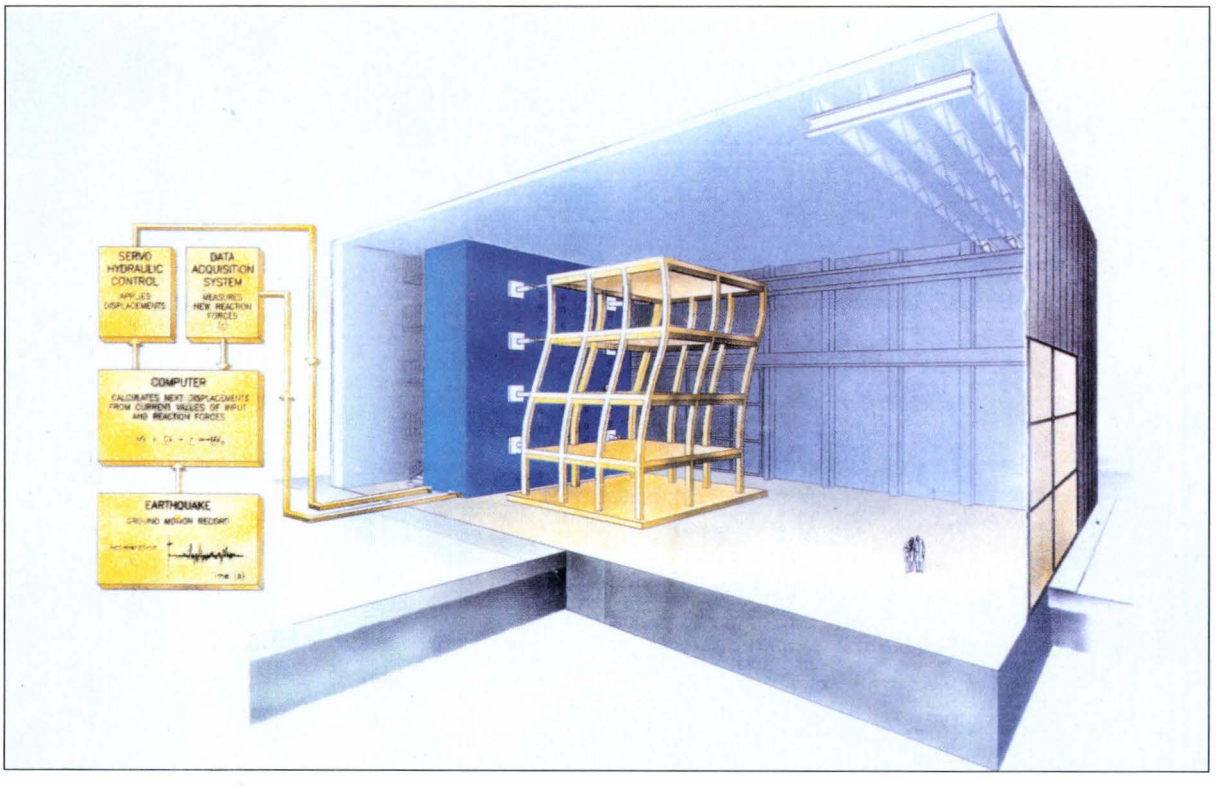

Fig. A1.2 Pseudo-dynamic test (schematic)

the reaction wall. Load-cells on the actuators measure the forces necessary to achieve the required deformation (the structural restoring forces) and these are then used in the next step of the calculation. A more detailed description of the PSD method is given in the STI Annual Report 1992 [1], Appendix 1.

Technical data for the reaction-wall system

The details of the reaction-wall/ strong-floor system are given in *Fig. A1.3* and *Table A1.1* below. The dimensions allow the testing of full-scale buildings up to five-storeys high either quasi-statically or pseudo-dynamically. Real-time dynamic tests can also be performed on lighter models such as, for example, piping systems. There is a large area of testing floor and an extended specimen preparation area which can also be employed in testing very large components.

The hydraulic pumping station has a maximum capacity of 1500l/m and is equipped with six LINDE constant pressure piston pumps. The oil distribution system is entirely made from type 304 stainless steel, including the reservoir, and the total volume is 5 m^3. Currently there are 12 electro-hydraulic actuators which can be used under either load or displacement control. These are all of 500kN capacity, 4 have a stroke of ± 0.5m, 8 have a ± 0.25m stroke.

Each actuator is driven via a digital controller based on an INTEL 386 microprocessor. All the controllers are connected in a local area network (LAN) through an optical fibre to the main computers (three INTEL 486's) running the pseudo-dynamic test algorithm (capable of using explicit or implicit methods of time integration).

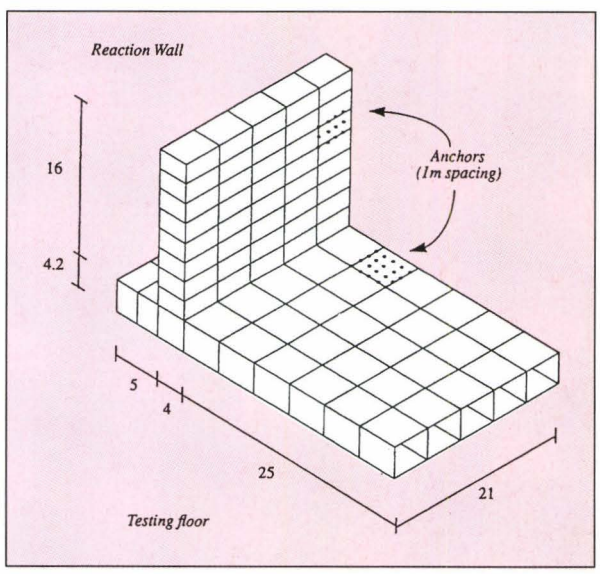

Fig. A1.3 Dimensions (m) of the reaction-wall/strong-floor system

The deformation of the test structure is monitored primarily by fifty LVDT's covering a range from 1 to 200mm, thirty of which have built-in amplifiers. The laboratory also has a long experience in strain-gauge systems and related instrumentation. The data acquisition system is able to record up to 200 channels (distributed on 6 PC's) having a 12 bit resolution and a maximum sampling frequency of 10 kHz global throughput.

References

[1] Safety Technology Institute, Annual Report 1992, Joint Research Centre Ispra, EUR 15055 EN

Table A1.1 Parameters of the ELSA reaction-wall system

Load Capacity	Reaction Wall	Bending Moment.....200 MNm Base Shear.....20 MN	
	Reaction Floor	Bending Moment.....240 MNm	
	Anchor Load Capacity	Axial Force.....500 kN	
Hydraulics Characteristics	Flow	1500 l/min	
	Pressure	210 bar	
	Actuators	Load (MN) Stroke (m)	0.5 ±0.25 – ±0.5

A.2 THE FARO FACILITY

The JRC-Ispra FARO plant is a large multi-purpose test facility in which phenomena related to severe accidents in Nuclear Reactors can be simulated out-of-pile. From 1987 to 1990, the plant was used for LMFBR safety problems such as melt relocation and molten fuel/sodium interaction. The programme was entirely funded by the Commission. During this campaign experience was acquired in producing, handling and cooling large masses of UO_2 melts.

Following the recommendations of the EU-Member States experts, a change to LWR Severe Accident problems was decided in 1990. A first series of corium meltwater quenching experiments was launched in September 1990 in collaboration with the United States Nuclear Regulatory Commission (US-NRC), the Electric Power Research Institute (EPRI) and the Ente Nazionale per l'Energia Elettrica (ENEL). This test series is part of the 1992-1994 CEU Framework Programme.

The objective of the present test series is to determine, for different initial pressures, bottom vessel geometries and number of jets: the steam generation rate associated with the melt quenching and the hydrogen production associated with the zirconium oxidation, the thermal load on the bottom structures and the debris structure. The data are used to understand the physical processes that govern quenching and to validate computer models.

The FARO plant is located within the containment shield of the former ECO (Experience Critique Orgel) reactor in building 42 of JRC-Ispra. Basically, a maximum quantity of the order of 150 kg of oxide fuel type melts (up to 3273K) can be produced in the FARO furnace, possibly mixed with metallic components and delivered to a test section of interest (containers up to 1.6 m^3, 10 MPa and 573K are available). The TERMOS test vessel is used to perform MFCI experiments.

Fig. A2.1 shows a schematic view of the test facility and a typical experimental arrangement is illustrated in *Fig. A2.2*. The interaction vessel TERMOS is connected to the FARO furnace via the release tube, the intersection valves SO1 and SO2 and the release vessel. The melt is first released from the furnace to the release vessel and then delivered to the water contained in the TERMOS test vessel.

The FARO furnace (see *Fig. A2.3*) is located at the upper level of the containment shield. It consists of a pressure container (10 MPa), a fuel container, two

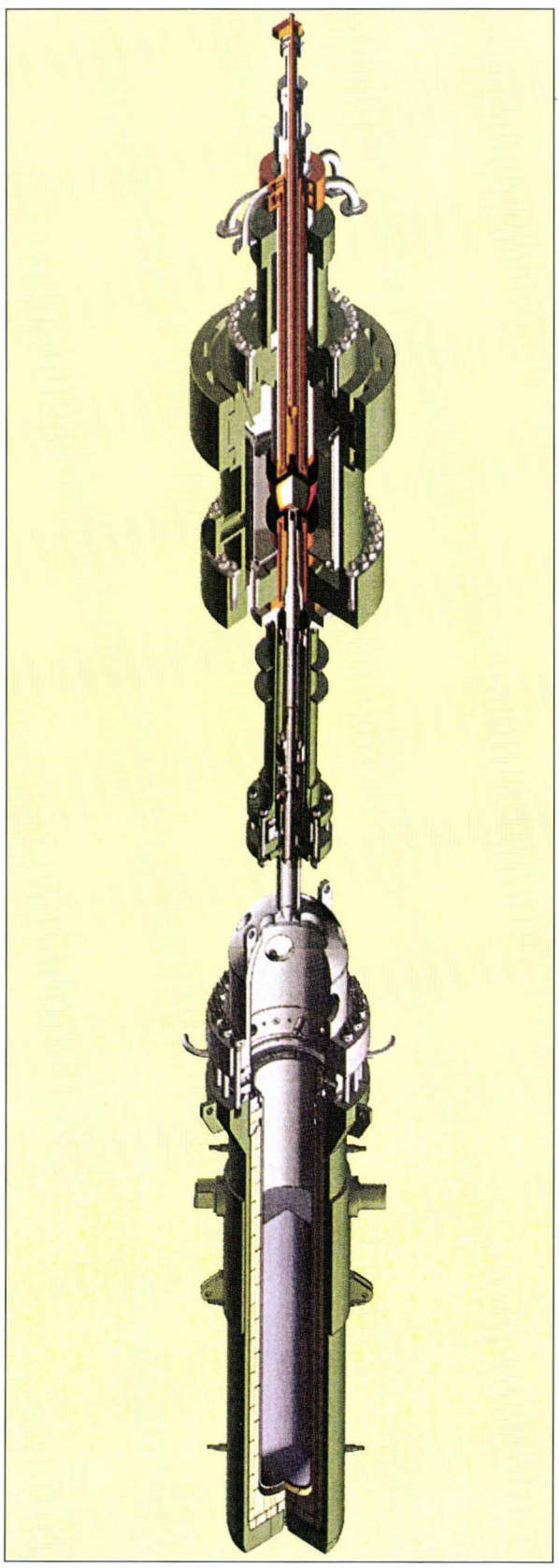

Fig. A2.1 Schematic view of the FARO facility

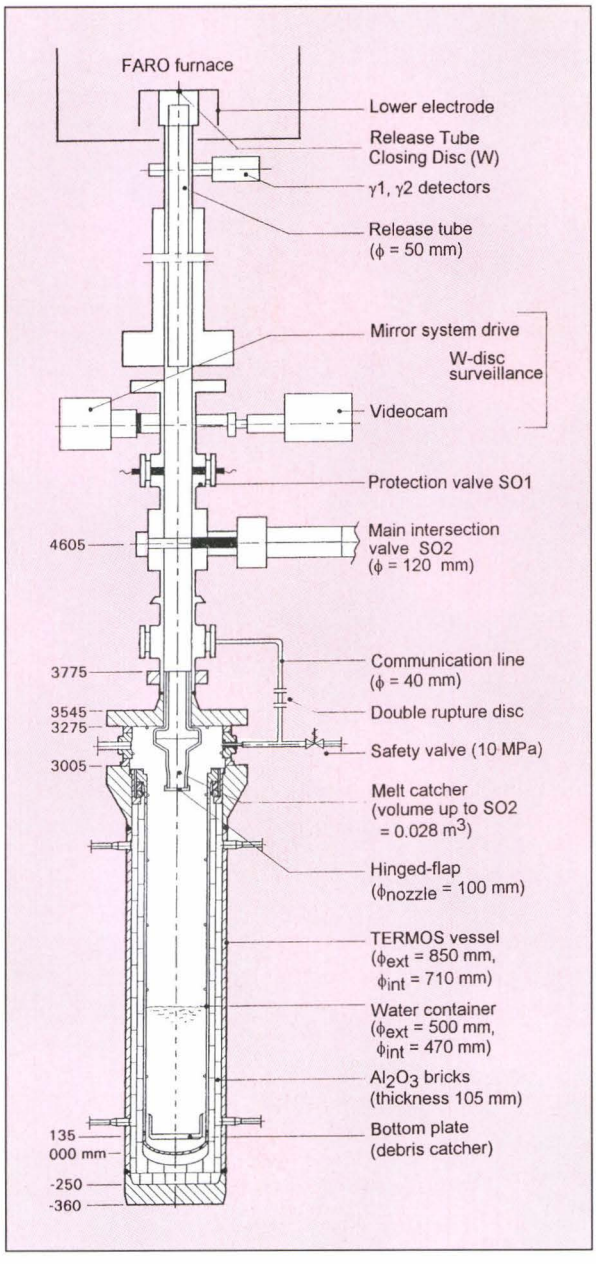

Fig. A2.2 Scoping test arrangement

Fig. A2.3 View of the FARO furnace

copper electrodes and a release tube. Pure UO_2 or UO_2-ZrO_2 mixtures are melted by direct heating of a granulate compacted between the electrodes. Four power supplies are used successively to heat up and melt the corium: 30 000 VDC/0.2 A, 3000 VDC/2 A, 400 VAC/150 A, 60 VDC/15 000 A. The release opening in the centre of the lower electrode is closed by a tungsten disc fitted on the graphite cap which protects the copper electrode. For releasing the melt to the release vessel, this disc is pushed up into the pool by the pneumatic operated release tube.

The release vessel is located inside the TERMOS vessel. Its function is to hold the melt just for the time necessary to isolate the furnace from the test vessel (SO2 closing) and balance the pressure above the melt to the TERMOS pressure, maintained initially at about 5 MPa in the current experiments. It acts as a lock-chamber between the furnace (the corium is melted at low pressure) and TERMOS. It may contain a certain amount of metal (zirconium, stainless steel, ... up to 10 kg) which melts upon contact with the oxidic melt to produce a corium including a metallic phase.

The TERMOS vessel (see ***Fig. A2.4***) is located at the lower level of the containment shield. It is a container of a height of 3 m and of an internal diameter of 0.71 m, designed for sustaining 10 MPa at 573K. It allows simulating prototypical water depth (up to 2 m). A flat lid as shown in ***Fig. A2.2*** can be used. Alternatively, a dome shaped cover can be mounted, increasing the overall height to 4.6 m and the volume to 1.6 m^3. A debris catcher is installed on the

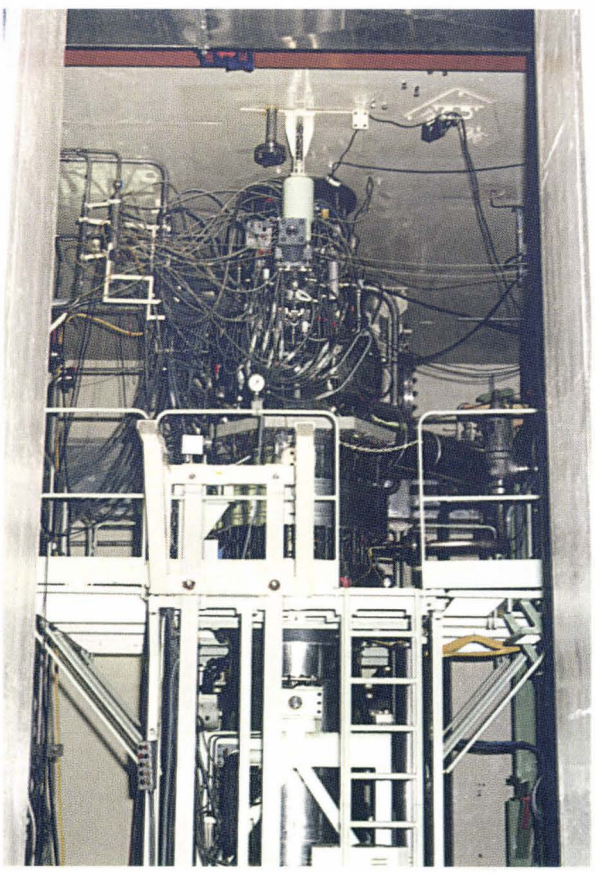

Fig. A2.4 TERMOS test section

bottom of the vessel and collects the corium after interaction. The heating of the vessel is provided by trace heaters located on the outer wall and below the debris catcher. The vessel is thermally insulated.

For melt/water interaction tests, the TERMOS vessel may be connected to a venting unit. The purpose of this unit is to vent and condense part of the steam produced during the quenching, should the pressure in the TERMOS interaction vessel TERMOS exceed a set point (maximum 10 MPa). It includes a high pressure steam/water separator capable of retaining 200 kg of water, five relief valves and a 4-m^3-low-pressure (0.8 MPa) condenser capable of condensing 200 kg of steam at 1 bar at a rate of 30 kg/s. Non-condensable gases (such as the hydrogen produced by metal oxidation) can be stored up to 0.8 MPa in the 2.5 m^3 free volume of the condenser.

The principal quantities measured during a test are the initial melt temperature by tungsten ultrasonic sensors, pressures and temperatures in TERMOS and in various places of the venting unit, water level swell in TERMOS, hydrogen production due to the metallic phase oxidation. A data acquisition system using workstations and PCs allows to record more than 200 measurement signals for each experiment at various frequencies and time intervals. The data are elaborated for analysis and documentation by means of modern graphics software.

The FARO experimental capabilities are being expanded for future tests employing prototypical corium up to 350 kg of melt containing approximatively 50% of metallic components. For these tests the feasibility of sustained heating of the corium is also being explored in order to investigate ex-vessel phenomena during severe accidents.

A.3 PERLA

The PERformance LAboratory (PERLA) is a complex of different laboratories located at the JRC in the Nuclear Island of STI. The decision to set-up PERLA was taken by the JRC Directorate in conformity with the obligations of subsidiarity required by the Commission of European Union.

The basic aim of PERLA is to improve technology transfer from laboratory development to the application of safeguards instruments and techniques in an industrial environment.

Safeguard laboratory and plant operators either from inside or outside the Union as well as from national and international inspectorates can find in PERLA a suitable location and adequate tools to calibrate their instruments, to follow training courses and to assess the performances of their techniques.

The main tasks of PERLA are currently:

- Performance evaluation of Non-Destructive Assay (NDA) techniques,
- Preparation and characterisation of standards for NDA,
- Development of customer oriented systems and software,
- Training and technology transfer,
- Basic research.

From 1987 to 1992 the above tasks were carried out in the PRE-PERLA laboratory which was realised prior to the construction of PERLA (*Fig. A3.1*).

The PERLA licensing tests started beginning 1992. Combined tests of ventilation, physical protection and health physics systems have been performed by the Nuclear Experiment Division (NED) licensing and operative groups, under the supervision of the Italian Licensing Authority (ENEA-DISP). The nuclear tests have been carried out in July 1992. The facility has started operation in August 1992. During 1993 PERLA has carried out on its R&D tasks on safeguards and in support to the Commission. Eleven courses have been given to ESD and IAEA inspectors. In addition, an International Workshop on passive neutron counting techniques has been held in April at the PERLA laboratory. A more detailed description of PERLA has already been given in the annual report 1991 [1], Appendix A2.

References

[1] Safety Technology Institute, Annual Report 1991, Joint Research Centre Ispra, EUR 14803 EN

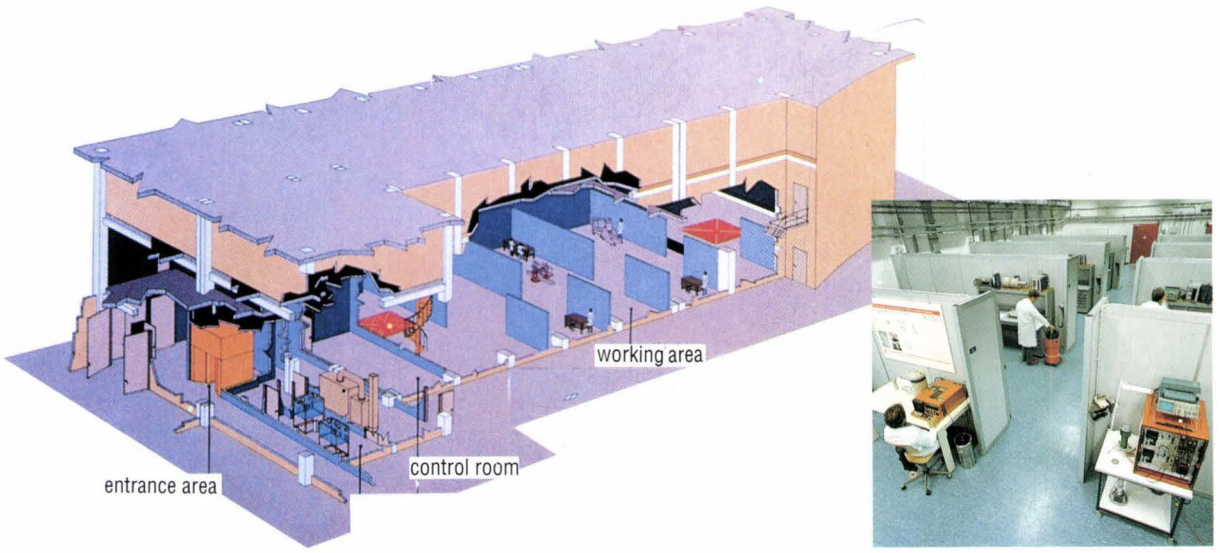

Fig. A3.1 View of the new-PERLA facility showing the internal layout

A4 ETHEL

The European Tritium Handling Experimental Laboratory (ETHEL) is a new tritium research facility located at the JRC-Ispra in the Nuclear Island of STI. The laboratory, envisaged to be licensed for 37 PBq (1 MCi or 100 g) of tritium and commissioned with tritium in mid-1994, embraces a volume of approximately 1300m^3 and can host a total of about 25 persons.

The operation of the laboratory itself and the future experimental activities planned represent a direct contribution of the European Union to the European Fusion Programme and ultimately to the worldwide efforts in the frame of the ITER project.

A detailed description of systems for managing, containing and processing tritium in ETHEL as well as for conditioning and storing ETHEL tritiated wastes has already been presented in Appendix A3 of ref. [1]. *Fig. A4.1* gives a photographic view of the ETHEL building.

References

[1] Safety Technology Institute, Annual Report 1991, Joint Research Centre Ispra, EUR 14803 EN

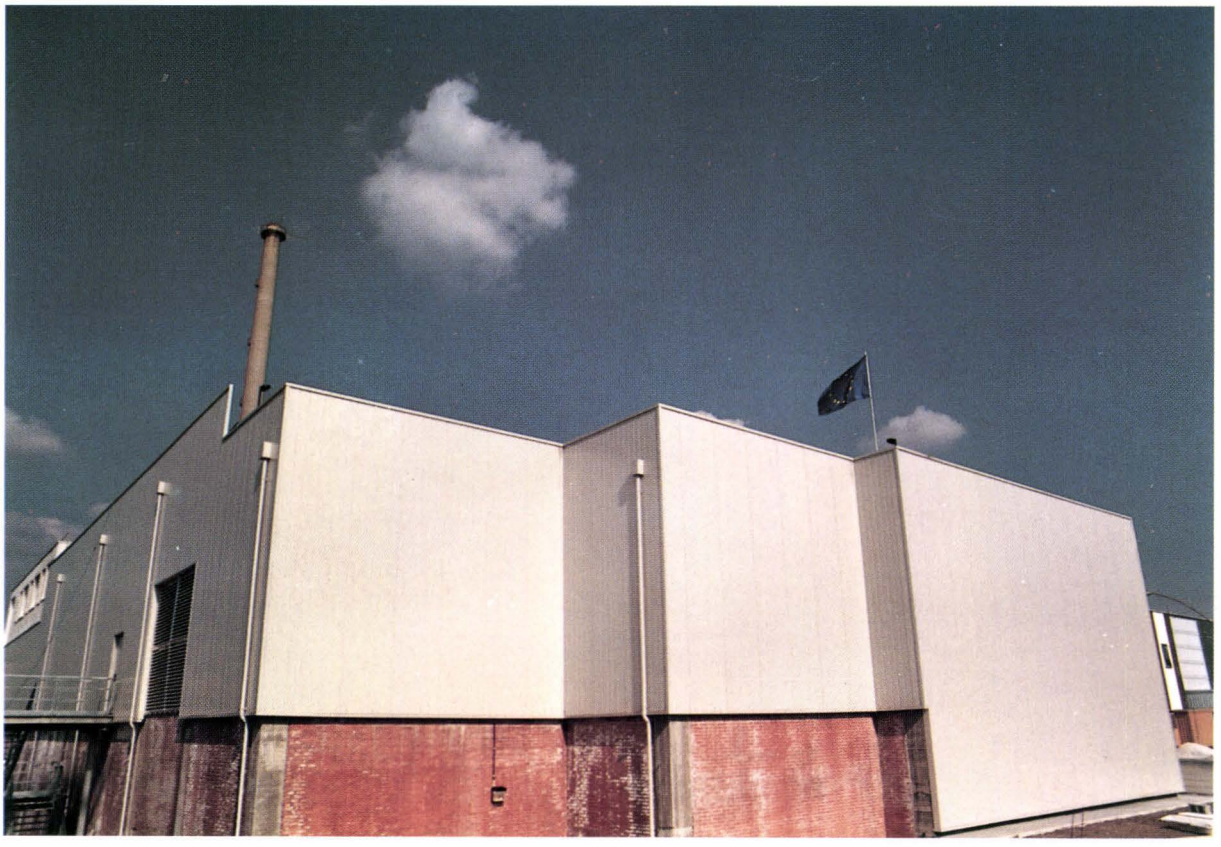

Fig. A4.1 View of the ETHEL building

A.5 TAME LABORATORY

The TAME (TAnk MEasurement) Laboratory is a new facility which has been commissioned at the JRC-Ispra for studying the problems related to the mass and volume determination of liquids in tanks used at nuclear materials processing installations. The facility is equipped with several real-size tanks and shapes, the largest of which has a capacity of 12m^3 with the whole structure resting on a surface area of 10m by 10m and reaching to a height of 15m. The objectives proposed for the laboratory [*Ref. 1 & 2*] are the development and performance assessment of tank measurement methods; testing and assessment of homogenisation, sampling, measurement and data evaluation procedures; calibration of measurement systems and the training of the safeguards inspectorates and plant operators in the application of mass determination techniques and procedures.

Fig. A5.1 Input accountancy tank showing load cells and Paar densitometer (0 meter level)

Safeguarding nuclear material received an ever increasing importance over recent years and above all concerning the back-end area of the nuclear fuel cycle. Here, the construction and operation of large throughput industrial reprocessing plants, including large volume input (10 to 70m^3) and output (700dm^3) tanks proposes a new challenge to the performances of weighing and volume measurement techniques. These measurements are the basis for process control, quality control of intermediate and final products and for material accountancy and its verification. Applications of such techniques are seen to be used in the parts of the nuclear fuel cycle which have a very high strategic importance and where the measurement uncertainty has to be low. These techniques, however, have not received the same attention in the safeguards framework as have DA and NDA techniques. One reason for this is that, because bulk measurement instrumentation is built into the plant design and operating procedures, testing and evaluating the methods and performance of such systems has, in the past been difficult and

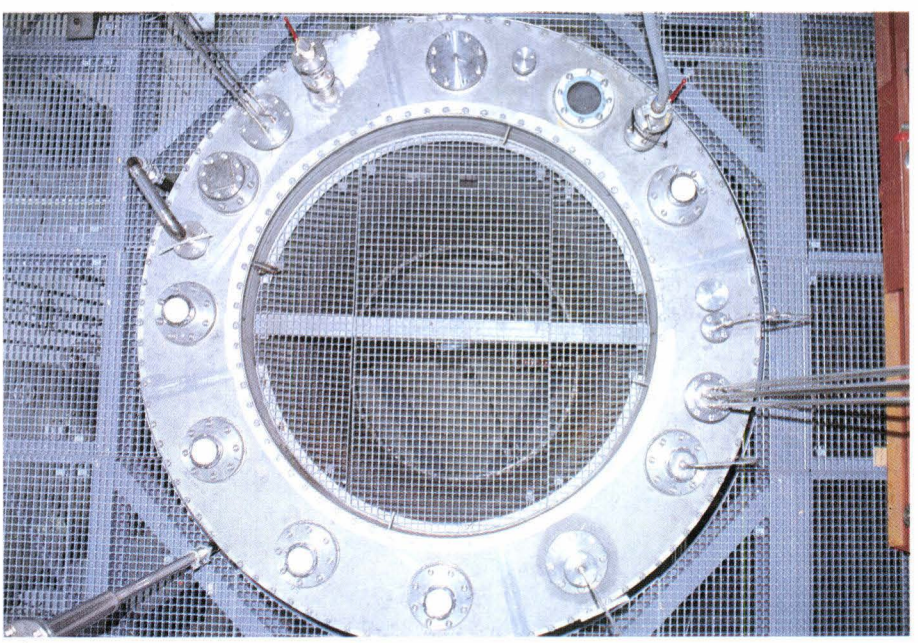

Fig. A5.2 Top view of the input accountancy tank (+5 meter level) showing feed line top right, bundle of dip-tubes lower right, ejector air-lift sampling tubes top left and off-gas line lower left

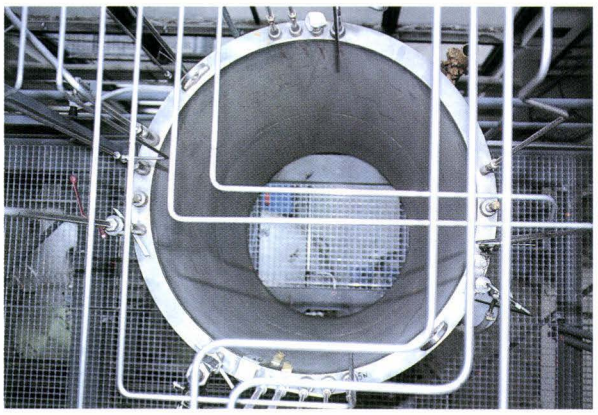

Fig. A5.3 Top view of the output product tank of 250 litres (+7 meter level)

disruptive of plant operations. Another reason is that carrying out these measurements was assumed to be straightforward and well known, despite the fact that verification of the calibration of in-plant systems is one of the most challenging tasks in safeguards. The Safeguards Inspectorates are indeed facing increasing safeguards responsibilities at a time when resources are limited. It is important therefore that the performance of measurement techniques are assessed. The Inspectorates need the verification capability to maintain an effective safeguards role. The problems are many and varied but are generally linked to phenomena affecting verification accuracy, instruments and equipments, calibrations, data acquisition, analysis and evaluation. One way of tackling these problems is to establish a capability for mass measurement research, development, testing and analysis on a continuous basis. This presupposes the availability a tank calibration facility, incorporating tanks representative of those in current and future reprocessing facilities. This concept was therefore the driving force, coupled with the experience already gained in the "pre-PERLA" and subsequent "PERLA" facilities, which persuaded the JRC Ispra Establishment to set up a large tank measurement laboratory.

The main components of the TAME laboratory are:

- input accountancy tank of 12.5 m^3 resting on 3 load cells (see ***Figs. A5.1*** and ***A.5.2***);
- output product vessel of 250 dm^3 (***Fig. A.5.3*** shows a top view which gives an indication of the geometry, circular slab vessel of thickness 51 mm for criticality reasons, which can be compared with ***Fig. 5.2*** of a slab thickness 400 mm but which contains much more dilute fissile material concentrations);
- "mini" TAME, which is the ex-IAEA facility and already operational at Ispra, consisting of a 200 dm^3 vessel and associated equipment for volume/mass determinations;
- dosing station capable of operating in a continuous or batch mode with a maximum flowrate of 2500 dm^3/hr in the former mode and 40 dm^3/batch (increasing after modification to 140 dm^3/batch) in the latter mode. ***Fig. A.5.4*** shows the dosing station located at the 9 m level.

3 storage feed vessels of combined volume 14 m^3. These are connected to the circuitry via 2 pumps and an overhead tank of 250 dm^3 capacity which provides a constant water feed head to the tank being calibrated;

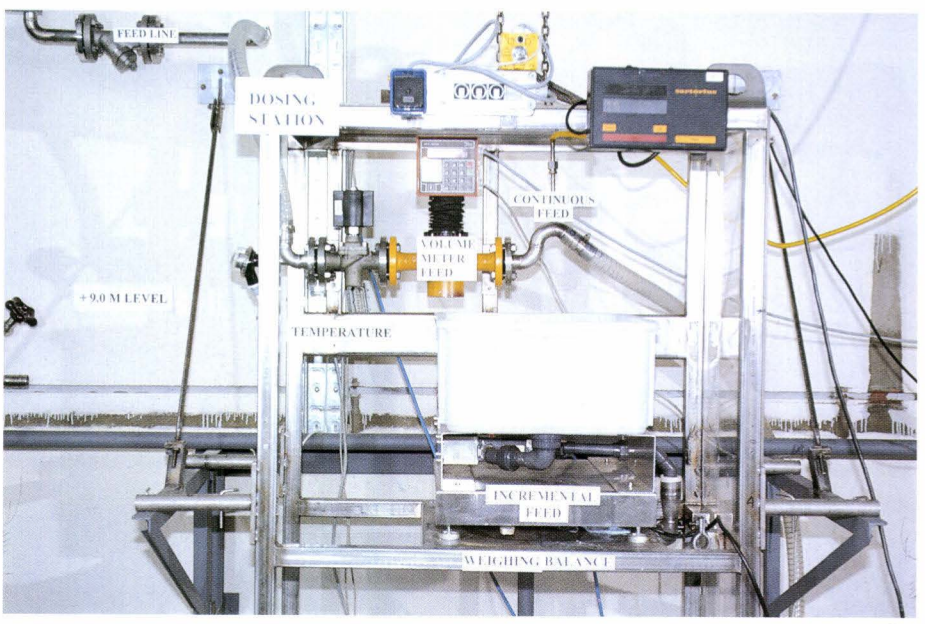

Fig. A5.4 View of the dosing station at the +9 meter level showing the volume meter feed, weighing balance and feed line

- output product storage vessel in the form of a "D" (harp tank) vessel of volume 400 dm^3, equipped with dip-tubes and weighing scales.

The activities of TAME are, based on the detailed discussions forthcoming from two international workshops held in 1992 and 1993 at Ispra and in collaboration with the IAEA tasks, have been identified which can be summarised as follows:

- performance evaluation of instruments and their characteristics used in the input and output accountancy tanks;
- comparison of the precision and accuracy achievable with different operating procedures (incremental vs. continuous tank calibration, temperature effects, density, vented vs. closed pipes, dip-tube flow rate, homogenisation and sampling procedures);
- phyiscal effects of operating and environmental parameters (evaporation losses, unmeasurable inventories- dead volumes in tank and piping);
- phyiscal effects of equipment layout (instruments location, homogenisation system layout, sampling method adopted);
- authentication of measurements, data and samples;
- use of tracers for tank calibration;
- data collection, treatment and interpretation;
- nuclear material solution accountancy and verification training.

References

[1] 1st International Working Group Meeting on R&D on Volume and Mass Determination of Liquids in Tanks used at Nuclear Materials Processing Installations - Working Document, SP1 92-26, Ispra, Italy, 25-27th March 1992

[2] 2nd International Working Group Meeting on R&D on Volume and Mass Determination of Liquids in Tanks used at Nuclear Materials Processing Installations, Ispra, 6-7th October, 1993

European Commission

EUR 15669 – Safety Technology Institute - Annual Report 1993

Editors: P. Fasoli-Stella, W. Krischer

Luxembourg: Office for Official Publications of the European Communities

1994 – V, 254 pp. – 21.0 x 29.7 cm

Scientific and Technical Research series

CL-NA-15669-EN-C

The first part of the report briefly outlines the content and the main results of research work performed in 1993 by the Safety Technology Institute (STI) in the Specific Programmes: Reactor Safety, Waste, Safeguards, Fusion, Industrial Hazards, Reference Methods for Evaluation of Structural Reliability and Working Environment.

In the Reactor Safety area the research is mainly devoted to the study of severe accident phenomena with the FARO programme and the participation in the PHEBUS-FP in-pile tests. Research on other aspects of the nuclear energy developes around the laboratories of the Nuclear Island: PETRA, PERLA and TAME for waste and safeguards and ETHEL for fusion.

The programme on Industrial Hazards is focused on experimental and theoretical studies and relates to runaway reactions, accidental release of products from industrial plants and their deflagration/detonation.

Concerning the area of Reference Methods for the Evaluation of Structure Reliability the Reaction-Wall facility ELSA has been employed to test a full-scale three-storey steel and a four-storey reinforced concrete frame.

The second part of the report illustrates the activities performed by the Institute in support of the Commissions policies and gives information on other initiatives of the Institute, like on the exploratory research programme.